ISBN: 978-3-95450-194-6 ISSN: 2226-0366 doi:10.18429/JACoW-LINAC2018-MO1A01

CSNS FRONT END AND LINAC COMMISSIONING

S.N.Fu[1,2†], H.F.Ouyang[1], H.C.Liu[1], J.Li[1], J. Peng[1], S.Wang[1]
[1] Dongguan Campus, Institute of High Energy Physics, 523803 Dongguan China
[2]University of Chinese Academy of Science, 100049 Beijing China

Abstract

The China Spallation Neutron Source (CSNS) accelerator systems is designed to deliver a 1.6GeV, 100kW proton beam to a solid metal target for neutron scattering research. The accelerator consists of a front end, an 80MeV DTL linac, and a 1.6GeV Rapid Cycling Synchrotron (RCS). In August 2017 the first 1.6GeV proton beam hit on the tungsten target and production neutrons were monitored. This paper will report the major steps and results of the machine commissioning and beam commissioning of the CSNS front end and linac. In the first section, a brief introduction of the CSNS accelerator design and present status will be presented. Then, we will share our commissioning experience in the front end and the DTL linac in the following sections. Finally, a brief introduction to the linac energy upgrade design options are presented.

INTRODUCTION

After 6.5 years construction [1], the CSNS completed its project construction in March 2018. The bird view of the CSNS campus is shown in Fig. 1. In this photo, from right to left we can see the buildings of klystron gallery for the linac, target station and synchrotron hall.



Figure 1: CSNS site bird view.

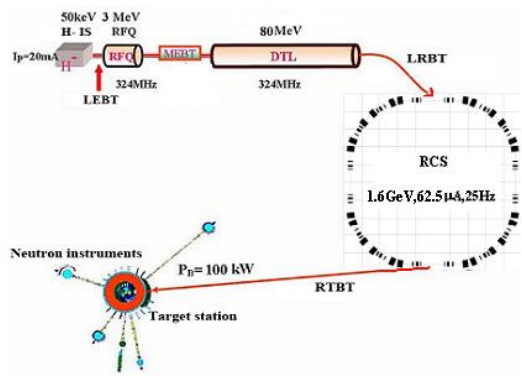


Figure 2: CSNS facility layout.

CSNS accelerator is designed with a beam power of 100kW in the phase-1 and reserved capability to upgrade the beam power to 500kW in Phase-2. The accelerator complex consists of an 80MeV H^- linac and a rapid cycling synchrotron of 1.6GeV at 25Hz repetition rate. CSNS facility layout is schematically plotted in Figure 2. Whole machine complex has been commissioned in the second half of 2017, with the first beam on the target in August 2017. Now the facility has been put into user operation at 20kW beam power. We are going to raise the power to 100kW within two years. This means the beam commissioning work will continue along with some user time about 7000 hours during the two years. As soon as we hit this target, phase-2 program for accelerator power upgrade to 500kW will be hopefully launched. For injecting 5-times more beam current into the RCS, it is necessary to raise linac beam energy to compensate for the space charge tune shift in the ring. The CSNS linac tunnel reserve a space of 80m long in the LRBT beam line for installing additional linac cavities for up to 300MeV output beam. Both RT and SC cavity are our present options for the linac section from 80MeV to 300MeV.

The present 80MeV linac consists of a Penning H^- ion source, a LEBT, a 3MeV RFQ powered by two tetrodes at 324MHz, a MEBT and a DTL linac with 4 tanks driven by 4 klystrons at 324MHz, as shown in Fig. 3.

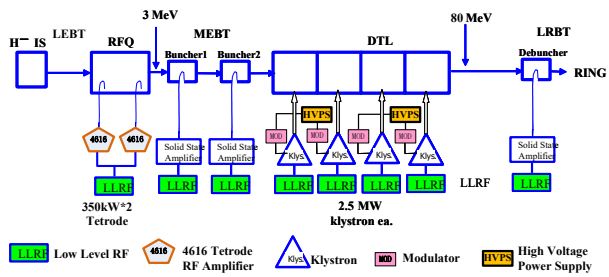


Figure3: Schematics of CSNS linac.

Beam chop at 50%-70% rate is performed by an electrostatic chopper at the end of the LEBT with space charge neutralization. There is no further chopping in the MEBT.

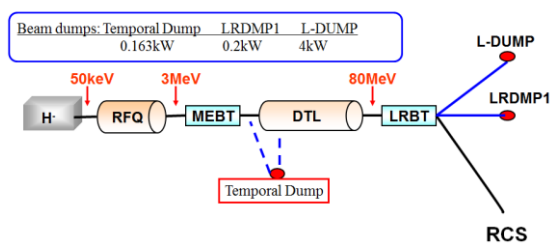


Figure 4: Linac beam dumps for beam commissioning.

† email address: fusn@ihep.ac.cn

Content from this work may be used under the terms of the CC BY 3.0 licence (© 2018). Any distribution of this work must maintain attribution to the author(s), title of the work, publisher, and DOI.

ISBN: 978-3-95450-194-6 ISSN: 2226-0366 doi:10.18429/JACoW-LINAC2018-MO1A02

AN OVERVIEW OF RECENT DEVELOPMENTS IN SRF TECHNOLOGY

R.E. Laxdal, TRIUMF, Vancouver, Canada, V6T 2A3

Abstract

Superconducting Radio-Frequency (SRF) is now the technology of choice for both large and small linac projects. Several challenging projects are in progress or planned that are pushing SRF technology and/or are enabled by SRF technology. This paper gives an overview of the present status of the field.

INTRODUCTION

Present research has been focussed on the key projects of the day, namely LCLS-II, FRIB, ESS as well as preparing for near term future projects ERLs, RISP, EIC and ILC. As LCLS-II represents a cw electron project, much of the elliptical cavity research focus has been on achieving, and maintaining, high Q in a cryomodule environment. The holy grail of projects is still the ILC. Here research is focussed on reliably increasing gradient and quality factor in an effort to reduce costs. Researchers are also pursuing thin films and new materials in order to either reduce the cost of Nb or increase the performance or operating temperature.

SRF BASICS

A characteristic of superconductors is that below some critical temperature, T_c, the DC resistance vanishes, allowing lossless transmission of electrical current. The rf surface resistance does not drop to zero, but still decreases dramatically. SRF technology offers a reduction of ~5 orders of magnitude in rf surface resistance compared to room temperature Cu that, after considering Carnot efficiency of cryogen production, still improves electrical efficiency by more than a factor of 100.

SRF Surface Resistance

The SRF surface resistance is typically described as the sum of a strongly temperature dependent component called the BCS resistance, and a second term called the 'residual resistance' (Fig. 1a).

$$R_s = R_{BCS}(\omega,T) + R_0 \quad \text{with} \quad R_{BCS} = \frac{A(\ell)}{T}\omega^2 e^{-\Delta/kT} \qquad (1)$$

The operating temperature is chosen so that R_{BCS} is reduced to an economically tolerable value for cryogenic losses with higher frequency cavities requiring colder operating temperatures. The A term depends on material parameters of the superconductor: the London penetration depth (λ_L), the coherence length (ξ_0) and the electron mean free path (ℓ). For a given temperature and rf frequency R_{BCS} can be optimized by modifications of the mean free path within the first 100nm of the surface and finds an optimum between shorter (dirty) and longer (clean) mean free paths (Fig. 1b).

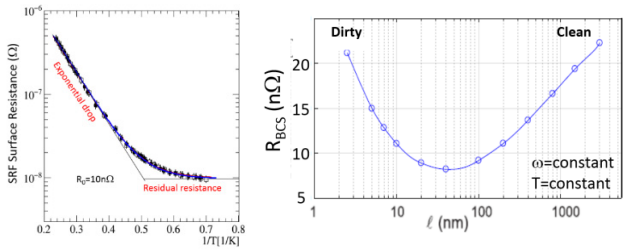


Figure 1: (a) RF surface resistance vs. temperature, and (b) BCS surface resistance as a function of mean free path for constant rf frequency and temperature.

The two most important features of an rf cavity are the accelerating gradient and the quality factor; the first impacts linac length (infrastructure cost) and the second impacts the cryogenic load (operating costs). Note that since the cavity quality factor is roughly proportional to the inverse of the average surface resistance

$$Q_0 = \frac{G}{R_s} = \frac{\omega_0 U}{P_c} \quad \text{and} \quad P_c = \frac{(E_a L)^2}{\frac{R_{sh}}{Q_0}Q_0} \qquad (2)$$

then a reduction of surface resistance by four can allow a doubling of the gradient for the same cryogenic load.

Meissner Effect

Niobium is a weak Type-II superconductor. Raising the applied field past a critical value H_{c1} leads to a mixed state (also known as the vortex state) in which an increasing amount of magnetic flux penetrates the material in quantized flux vortices. At a second critical field strength, H_{c2}, superconductivity is destroyed. However, above H_{c1} a metastable state persists up to the superheating field H_{sh} allowed by a surface energy barrier that inhibits vortex nucleation. As rf fields increase in amplitude magnetic vortices with normal cores can nucleate in the near surface and rf losses, hence surface heating occurs. For high gradient performance we need a material that can withstand vortex penetration up to a high peak magnetic field.

Present Performance

SRF research and development [1] have targeted limitations on cavity performance. Extrinsic sources include multi-pacting, field emission, surface residues, trapped magnetic flux, and surface defects. Multipacting is combated with new cavity shapes, better simulation codes and pre-test bake. Field emission has largely been controlled by high pressure water rinse (HPWR) and clean assembly techniques to eliminate particulate contamination. Defects that could cause quench (local heating) are reduced by choosing pure material with high thermal conductivity (RRR>250) and maintaining the purity through fabrication with EB welding and care. A final material removal by electro-polish (EP) or buffered chemical polish (BCP) of

Content from this work may be used under the terms of the CC BY 3.0 licence (© 2018). Any distribution of this work must maintain attribution to the author(s), title of the work, publisher, and DOI.

ISBN: 978-3-95450-194-6 ISSN: 2226-0366 doi:10.18429/JACoW-LINAC2018-MO2A03

TECHNOLOGY DEVELOPMENTS OF ELI-NP GAMMA BEAM SYSTEM

L. Piersanti*, D. Alesini, A. Battisti, M. Bellaveglia, S. Bini, F. Cardelli, R. Di Raddo, A. Falone, A. Gallo, V. Lollo, L. Pellegrino, S. Pioli, S. Tomassini, A. Variola INFN-LNF, Frascati, Italy
L. Ficcadenti, M. Migliorati[1], A. Mostacci[1], L. Palumbo[1], V. Pettinacci INFN-Roma, Rome, Italy
D. T. Palmer, L. Serafini INFN-Sezione di Milano
K. Cassou, D. Douillet, K. Dupraz, T. Le Barillec, A. Martens, C. F. Ndiaye, Y. Peinaud, F. Zomer LAL, CNRS/IN2P3 Université Paris Sud - France
N. Beaugerard, B. Lacrampe, H. Rocipon, ALSYOM/SEIV-ALCEN, France
[1]also at Sapienza University of Rome, SBAI Department Rome, Italy

Abstract

The ELI-NP gamma beam system (GBS) is a linac based gamma-source in construction in Magurele (RO) by the European consortium EuroGammaS led by INFN. Photons with tunable energy, from 0.2 to 19.5 MeV, and with intensity and brilliance beyond the state of the art, will be produced by Compton back-scattering between a high quality electron beam (up to 740 MeV) and an intense laser pulse at 100 Hz repetition rate. Production of very intense photon flux with narrow bandwidth requires multi-bunch operation and laser recirculation at the interaction point. In this paper, the main technological developments carried out by the EuroGammaS consortium for the generation of the ELI-NP gamma beam will be described with a special emphasis on the electron linac technology, such as: RF-gun and C-band accelerating structures design fabrication and tests; low level RF (LLRF) and synchronization systems specifications and development. Finally, the laser recirculation apparatus design is briefly described and first results reported.

INTRODUCTION

An advanced source of gamma-ray photons will be built in Magurele in the framework of the ELI-NP project [1, 2] by the EuroGammaS consortium. The gamma-rays will be generated by a high quality electron beam colliding with a high power laser pulse (200 mJ, 3.5 ps, 515 nm) recirculated 32 times at the interaction point. The machine is expected to produce photons with tunable energy between 0.2 and 19.5 MeV with a narrow bandwidth (< 0.5 %) and a high spectral density ($0.8\text{-}4 \times 10^4$ ph/s eV) [3].

The accelerator layout is based on a C-band (5712 MHz) RF linac, with a S-band (2856 MHz) photo-injector similar to that of SPARC_LAB at LNF-INFN (Frascati, Italy) [4], able to deliver a high phase space density electron beam in the 300-740 MeV energy range. The repetition rate is 100 Hz and, in order to reach the required photon flux, the machine is foreseen to work in multi-bunch mode (fitting 32 electron bunches spaced by 16 ns in each RF pulse), thus with an effective repetition rate of 3.2 kHz. The main electron beam parameters of the ELI-NP-GBS, together with the description of the complete RF system have been reported in [2, 5].

* luca.piersanti@lnf.infn.it

LINAC OVERVIEW

ELI-NP-GBS photo-injector comprises a 1.6 cell S-band RF-gun, which has been manufactured with a new fabrication technique which does not require copper brazing [6–9], and two S-band 3 m long SLAC-type TW constant gradient accelerating structures. The S-band system comprises also two deflecting cavities used for longitudinal beam diagnostics. The linac booster is made of 12 travelling wave (TW) C-band disk loaded accelerating structures. Moreover, a waveguide high order mode (HOM) damping system that employs 4 SiC RF absorbers for each cell [10–13] has been included in the design, to avoid beam break up instabilities that may arise due to multi-bunch operation.

In order to reduce bunch-by-bunch energy spread due to structure beam loading (BL), a tailored pulse shaping compensation has to be provided to the klystrons by the LLRF systems [5]. Moreover, since the use of pulse compressors would make the pulse shaping even more critical, each accelerating section is individually driven by a dedicated power station (with the exception of the last 4 TW sections that are fed by 2 klystrons). A sketch of the linac has been reported in Figure 1.

S-BAND RF-GUN DESIGN, LOW AND HIGH POWER TESTS

RF photo-guns find several type of applications including high brightness electron sources for free-electron lasers, energy recovery linacs, Compton/Thomson photon sources. Being the achievable beam brightness proportional to the peak field at the cathode, in the last generation of RF guns a great effort has been put to increase the field amplitude while reducing, at the same time, the breakdown phenomena. Moreover, modern RF guns must be able to withstand high repetition rate operation (of the order of 100 Hz) with a reasonable realization cost. Currently the standard fabrication process relies on copper brazing. However, this technique requires large vacuum furnaces, it is expensive and has a non-negligible risk of failure. Furthermore, studies carried out on X-band prototypes indicated that it is possible to reduce the breakdown probability if copper thermal stress is avoided [14]. For all these reasons, a new brazing-free fabrication method based on the use of special RF-vacuum gaskets has been recently developed at LNF-INFN [7], and

Content from this work may be used under the terms of the CC BY 3.0 licence (© 2018). Any distribution of this work must maintain attribution to the author(s), title of the work, publisher, and DOI.

ISBN: 978-3-95450-194-6 ISSN: 2226-0366 doi:10.18429/JACoW-LINAC2018-MO2A04

COMPACT SRF LINAC FOR HIGH BRILLIANCE INVERSE COMPTON SCATTERING LIGHT SOURCE

K. E. Deitrick*, G. A. Krafft[1], B. Terzić, J. R. Delayen[1],
Center for Accelerator Science, Old Dominion University, Norfolk, VA, 23529, USA
[1]also at Thomas Jefferson National Accelerator Facility, Newport News, VA 23606, USA

Abstract

New designs for compact SRF linacs can produce micron-size electron beams. These can be used for inverse Compton scattering light sources of exceptional flux and brilliance.

INTRODUCTION

Currently, there exist many x-ray techniques which are used in several different fields, including material science, cultural heritage, medicine, national security, and basic research in biology, chemistry, and physics. While a number of light source facilities around the world produce very high quality X-ray beams, there is a significant gap between this performance and the one most X-ray users experience from their laboratory-scale sources.

Increasing research over recent years has been aimed at bridging this gap through compact inverse Compton light sources (ICLSs). One of the significant benefits of this type of source is their production of narrow bandwidth x-ray beams, which is not a feature of most typical small-scale sources, but is required for a number of techniques. In the most general description, the target specifications for these compact ICLS designs has been for high average flux, high average brilliance x-rays - while keeping the requisite electron accelerator compact in size and cost. The design presented here, shown in Fig. 1, has the highest anticipated performance to date among compact Inverse Compton Light Source (ICLS) designs.

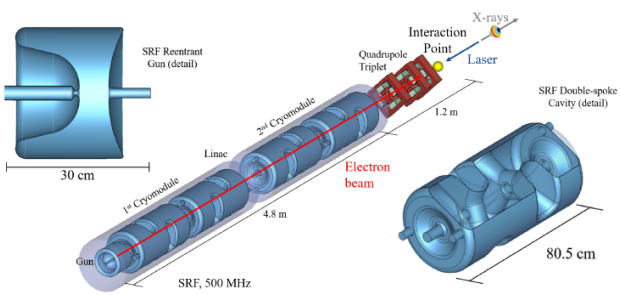


Figure 1: A schematic of the entire design. The first cryomodule contains the gun and two double-spoke cavities, the second contains the last two double-spoke cavities. Three quadrupole magnets follow the linac, before the interaction point. Detailed images of the gun and the double-spoke cavity are shown in the top left and bottom right, respectively.

* kdeit001@odu.edu; deitrick@jlab.org

INVERSE COMPTON SCATTERING

Compton scattering is the process of scattering a photon off of an electron at rest. Inverse Compton scattering (ICS) is the process of scattering a photon off a moving electron, leading the electron losing energy in the process. This collision between electron beam and incident laser occurs at the interaction point (IP).

For this compact ICLS design, we operate in a regime where the Thomson formula is a good approximation - the energy of the incident laser in the beam frame is significantly less than the rest mass of the electron. Consequently, the energy of the x-rays produced in the collision are given by

$$E_x(\Phi,\theta) \approx E_{\text{laser}} \frac{1-\beta\cos\Phi}{1-\beta\cos\theta}, \tag{1}$$

where Φ is the angle between the electron beam and scattering laser, θ is the angle between the electron beam and generated x-rays, E_{laser} is the energy of the incident scattering laser, and β is the relativistic factor v_z/c of the electron beam. For a head-on collision, the highest energy x-rays are those scattered in the same direction as the electron beam is traveling; this is the case shown in Fig. 1. The energy of these x-rays is given by $E_x(\Phi=\pi,\theta=0) \approx \gamma^2(1+\beta)^2 E_{\text{laser}} \approx 4\gamma^2 E_{\text{laser}}$, where γ is the typical relativistic factor for the electron beam and is significantly greater than 1.

The number of scattered x-rays from this collision is given by

$$N_x = \sigma_T \frac{N_e N_{\text{laser}}}{2\pi(\sigma_e^2+\sigma_{\text{laser}}^2)}, \tag{2}$$

where σ_T is the Thomson cross section, N_e is the number of electrons in the bunch, N_{laser} is the number of photons in the scattering laser, σ_e is the *rms* size of the electron beam, and σ_{laser} is the *rms* size of the laser. The assumption behind this formula and those following is that the distribution of both the electron and laser beams are Gaussian. The number of x-rays within a 0.1% bandwidth at the highest possible x-ray energy is $N_{0.1\%} = 1.5\times10^{-3}N_x$, so it follows that the flux into this bandwidth is $\mathcal{F}_{0.1\%} = 1.5\times10^{-3}\dot{N}_x$. For high frequency repetitive sources, $\dot{N}_x = fN_x$, where f is the repetition rate.

The spectral brightness or brilliance of an x-ray beam is the density of x-rays in the six-dimensional phase space containing the beam. The general formula for the brilliance of an x-ray beam into a 0.1% bandwidth is

$$\mathcal{B} = \frac{\mathcal{F}_{0.1\%}}{4\pi^2\sigma_{\gamma,x}\sigma_{\gamma,x'}\sigma_{\gamma,y}\sigma_{\gamma,y'}} \tag{3}$$

Content from this work may be used under the terms of the CC BY 3.0 licence (© 2018). Any distribution of this work must maintain attribution to the author(s), title of the work, publisher, and DOI.

ISBN: 978-3-95450-194-6 ISSN: 2226-0366 doi:10.18429/JACoW-LINAC2018-MO1P01

STATUS OF THE SNS PROTON POWER UPGRADE PROJECT *

J. Galambos†, M. Champion, M. Connell, M. Howell, S. Kim, J. Moss, M. Plum, B. Riemer, W. Steffey, K. White, Oak Ridge National Laboratory, 37831 Oak Ridge TN, USA

Abstract

The Proton Power Upgrade (PPU) project [1,2,3] will double the accelerator power capability at Spallation Neutron Source (SNS) [4], from 1.4 to 2.8 MW. This project received initial funding in 2018, and plans have been formulated to complete equipment installation and begin beam commissioning in 2024. The project plans and status, with an emphasis on recent progress, are summarized for the different sub-systems.

INTRODUCTION

The SNS is a short pulse neutron scattering facility with a 1.4 MW capable accelerator powering the neutron source. The SNS accelerator complex includes a linear accelerator, an accumulator ring and transport lines. This accelerator complex was constructed with built-in upgrade provisions, and these are being exploited to double the power capability to 2.8 MW. High level parameters are shown in Table 1, indicating the strategy to double the power by increasing the beam energy by 30% and the linac beam current by ~ 50%. The higher power will allow new science capabilities and will also increase capacity by increasing beamline throughput [5].

The PPU project is organized into primary subsystems of Superconducting RF cryomodules, RF equipment, Ring systems, Conventional Facilities, and Target systems. Controls efforts are distributed throughout these systems. Much of the project upgrade is focused in the SNS linac and consists of providing additional equipment similar to presently operating equipment (for example, RF equipment and superconducting cryomodules). This aspect reduces project risks and permits early movement on the design and procurement of some linac associated equipment. The sections below describe the upgrade approaches in the PPU sub-systems, and recent progress.

PPU SUB-SYSTEMS

Superconducting Linac (SCL)

The increased beam energy will be provided by the addition of 7 new cryo-modules in existing empty slots at the high energy end of the linac [6]. These cryo-modules will be similar to a spare cryomodule built at SNS, installed and operated since 2012, and has demonstrated the required PPU gradient level [7]. This cryomodule is shown in Fig. 1. The cryomodules will be fabricated by Thomas Jefferson Accelerator Facility, through a partnership. SNS will oversee the cavity fabrication, and this is part of a recently initiated Long Lead Procurement strategy to minimize schedule risk. The cryomodules will be installed in seven of the nine available empty slots.

Table 1: PPU High Level Parameters

Parameter	Present operation	PPU
Beam power (MW)	1.4	2.8
Beam energy (GeV)	1.0	1.3
Average linac current (mA)	1.6	2.3
Linac macropulse current (mA)	25	39
Beam repetition rate (Hz)	60	60
Linac pulse length (ms)	1	1
Medium beta cryomodules	11	11
High beta cryomodules	12	19
High beta cavities	48	76

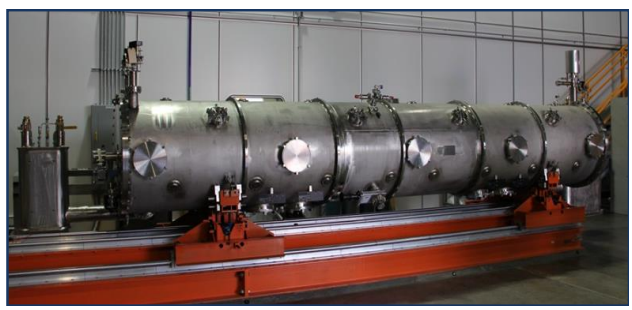


Figure 1. The spare SNS cryomodule, in operation since 2012 and demonstrating PPU gradient.

Key changes in the PPU cryomodules from the operational high beta cryomodules already installed in the SNS linac are: improved Nb material quality for the cavity end groups, higher power capability for the RF couplers, and elimination of the Higher Order Mode couplers. A prototype cavity with high quality end groups and no HOM coupler was recently fabricated and tested, and successfully demonstrated gradients required for PPU (see Fig. 2.)

* ORNL is managed by UT-Battelle, LLC, under contract DE-AC05-00OR22725 for the U.S. Department of Energy. This research was supported by the DOE Office of Science, Basic Energy Science, Scientific User Facilities.
† jdg@ornl.gov

Content from this work may be used under the terms of the CC BY 3.0 licence (© 2018). Any distribution of this work must maintain attribution to the author(s), title of the work, publisher, and DOI.

ISBN: 978-3-95450-194-6 ISSN: 2226-0366 doi:10.18429/JACoW-LINAC2018-MO1P02

APPROACHES TO HIGH POWER OPERATION OF J-PARC ACCELERATOR

Hidetomo Oguri, JAEA/J-PARC, 319-1195 Tokai-mura, Japan

Abstract

The J-PARC linac started beam operation with an energy of 181 MeV in 2006. To realize the nominal performance of 1 MW at a 3 GeV Rapid Cycling Synchrotron (RCS) and 0.75 MW at a Main Ring synchrotron (MR), the linac beam energy was increased to 400 MeV and the beam current was also increased from 30 to 50 mA. After the upgrade, the RCS demonstrated 1 MW equivalent beam operation and currently operates 500 kW for the Material and Life Science Facility. The MR beam power is also increasing and it recently achieved the beam operation of 490 kW for the Neutrino experiment and 51 kW for the Hadron experiment, respectively. At present, we are considering two further upgrade plans increasing the RCS beam power to 1.5 MW and duplation the linac repetition rate to 50 Hz for the planned Transmutation Experimental Facility. To achieve 1.5 MW from the RCS, it is necessary to increase both the beam current and the pulse length about 20% at the linac.

INTRODUCTION

A layout of the J-PARC facilities is shown in Fig. 1. The J-PARC facilities consist of the linac, the 3-GeV Rapid Cycling Synchrotron (RCS), the Main ring Synchrotron (MR) and three experimental facilities of the Material and Life Science Facility (MLF), the Hadron Experimental Facility (HD) and the Neutrino Facility (NU). Construction of a Transmutation Experimental Facility (TEF) is planned in phase-II in the near future. The goal of the J-PARC project in phase-I is to achieve a 1-MW beam power at the RCS and a 0.75-MW beam power at the MR [1].

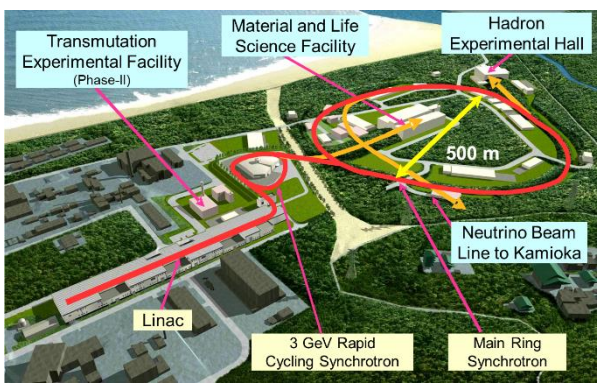


Figure 1: A layout of J-PARC facilities.

In 2006, the J-PARC linac started beam operation with an output energy of 181 MeV and a designed peak current of 30 mA. Thereby, we could reach an RCS output beam power of 600 kW in principle. The space charge effect in the RCS injection is increased with the beam intensity upgrade, and it limits the obtainable beam power. To suppress the space-charge effect to a tolerable level, it was necessary to increase the injection energy. Therefore, we conducted both the energy and the intensity upgrade of the linac. For the intensity upgrade, we replaced a front-end system, which consists of an ion source, a radio frequency quadrupole linac (RFQ) and a beam chopper system to deliver a peak current of 50 mA. For the energy upgrade, the linac output energy was increased to 400 MeV by adding an annular-ring coupled structure linac (ACS) after the separated drift tube linac (SDTL). A layout of the linac before and after upgraded is shown in Fig. 2.

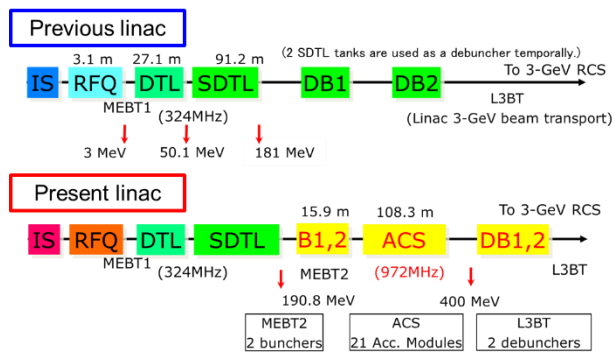


Figure 2: A layout of previous and present linac.

Two further upgrade plans of 1.5-MW beam power at the RCS and construction of the TEF are now in consideration. To achieve the 1.5-MW beam, it is necessary to increase both the peak beam current and the beam pulse length about 20% at the linac. For the TEF, duplation the linac repetition rate to 50 Hz is necessary. The detail process in the past upgrade and the possibility for further upgrade at the linac are presented in this paper.

BEAM INTENSITY UPGRADE

High Intensity Negative Hydrogen Ion Source

A cesium-free negative hydrogen ion source driven with a lanthanum hexaboride (LaB_6) filament was used since linac operation started in 2006 [2]. Although it satisfied the J-PARC's initial stage requirements of 30 mA, it was confirmed that the current level did not increase by cesiation and the life time of the filament of approximately 500 h was insufficient for the desired life of 2000 h at least. In order to satisfy linac upgrade requirements, a cesiated RF-driven negative hydrogen ion source has been developed. A schematic of the RF-driven ion source is shown in Fig. 3. An internal antenna that was developed at Spallation Neutron Source at Oak Ridge National Laboratory [3] is used for the source of plasma. The RF-driven ion source was tested on an off-line test stand for about five years, and it was found to satisfy the requirements. The RF-driven ion source was installed in the summer of 2014.

Content from this work may be used under the terms of the CC BY 3.0 licence (© 2018). Any distribution of this work must maintain attribution to the author(s), title of the work, publisher, and DOI.

ISBN: 978-3-95450-194-6 ISSN: 2226-0366 doi:10.18429/JACoW-LINAC2018-MO1P03

STATUS OF THE ESS LINAC

A. Sunesson†, R. Garoby, M. Lindroos, M. Jensen, C. Martins, T. Shea, J. Weisend,
P. Arnold, A. Nordt, S. Birch, European Spallation Source ERIC, 22100, Lund, Sweden

Abstract

The European Spallation Source (ESS) under construction in Lund (Sweden) uses a 2 GeV-5 MW pulsed superconducting linac as proton driver. Normal conducting accelerating structures are used up to 90 MeV and superconducting structures up to 2 GeV. Most linac components are designed and procured as in-kind contributions by institutes/laboratories in the partner countries in Europe. Installation of the Ion source delivered by INFN-Catania started January 2018. Installation of more components and infrastructure progresses at a high pace. Commissioning of the normal conducting linac section will take place in parallel with installation of the superconducting section. Beam commissioning of the superconducting section will start in 2021, interlaced with the installation of additional high beta cryomodules. Beam will be sent to the target in 2022, initially at an energy of 1.3 GeV. Start of the User Program is scheduled in 2023, when some neutron instruments will be ready and end of construction is in 2025, with the full set of instruments operational. This paper reports the status of linac components construction, the progress with installation on site, and the overall project schedule.

INTRODUCTION

ESS will be a long pulse neutron source of the next generation with performance exceeding all similar existing and planned facilities world-wide [1]. The ESS superconducting proton linac is a key ingredient for that purpose, with a beam power of 5 MW at 2 GeV delivered in 2.86 ms pulses at a 14 Hz rate. ESS is being built north of the University town of Lund in the south of Sweden. The site layout can be seen in Fig. 1. The facility is presently (2018) under construction, with the start of user operations planned to late 2023. At the end of construction, in 2025, ESS will operate 15 instruments for neutron users.

A facility of ESS size and scope is a major undertaking both cost and scope-wise, and even more when starting from a green field. The project in general and the accelerator in particular are therefore extensively relying on knowledge and competences throughout Europe, provided as in-kind contributions. For the accelerator project, partners and contributions are listed in [1].

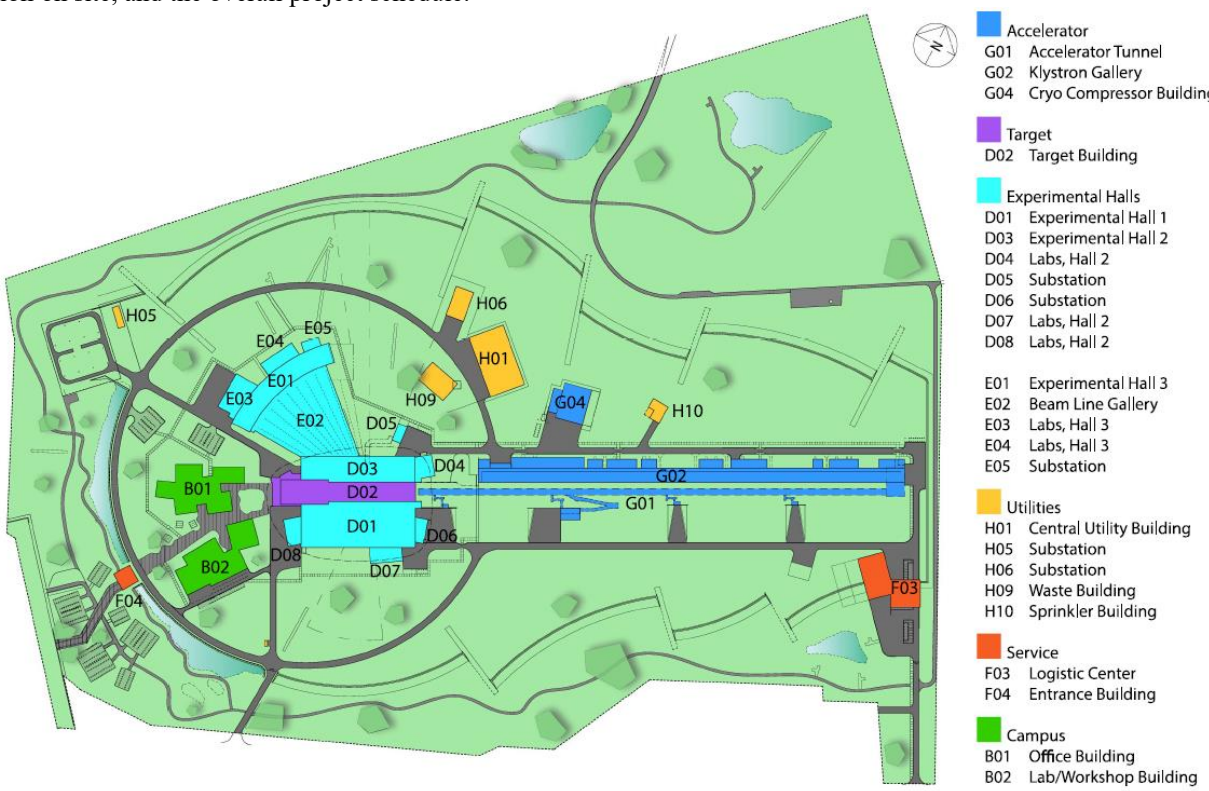


Figure 1: ESS site layout.

† anders.sunesson@esss.se

Content from this work may be used under the terms of the CC BY 3.0 licence (© 2018). Any distribution of this work must maintain attribution to the author(s), title of the work, publisher, and DOI.

ISBN: 978-3-95450-194-6 ISSN: 2226-0366 doi:10.18429/JACoW-LINAC2018-MOPO004

COMMISSIONING OF SRF BOOSTER CAVITY FOR LEReC*

Wencan Xu†, A. Fedotov, T. Hayes, D. Holmes, G. McIntyre, K. Mernick, S. Seberg, K. Smith, F. Severino, R. Than, Q. Wu, B. Xiao, T. Xin, A. Zaltsman
Collider-Accelerator Department, Brookhaven National Laboratory, Upton, NY 11790, USA

Abstract

One important component for LEReC project is a 704 MHz booster cavity, which was modified from the BNL ERL 704 MHz SRF gun cavity. Within one and half year, the modification completed. The booster cavity cryomodule was successfully commissioned in mid-October 2017, and it was moved to LEReC location at RHIC tunnel 2 O'clock, where it has been serving routine operation since March 2018. This paper will report the configuration of the new cryomodule and its commissioning results.

INTRODUCTION

Low Energy RHIC Electron Cooling (LEReC) [1] aims to improve luminosity lifetime by counteracting Intra-Beam Scattering (IBS). The Energy scan of interest are 7.7, 9.1, 11.5, 14.6, 19.6 GeV, which requires corresponding kinetic energy of electron beam to be 1.6 – 2.6 MV. The energy gain is provided by SRF booster and a 400 kV DC gun. The 704 MHz SRF booster cavity introduces an energy chirp that causes ballistic stretching of the bunch as it drifts down the beam line. Additional RF systems (2.1 GHz, 704 MHz warm RF cavity, 9 MHz warm cavity) are employed to remove the energy chirp, longitudianl bunch curvature and bunch-by-bunch energy variation. Figure 1 shows the beamline layout LEReC.

The 704 MHz SRF booster cavity was converted from ERL SRF gun cavity [1]. The major conversion includes 1) convertion of the choke-joint cathode support to a beampipe, 2) retracting FPC for optimum coupling, 3) improvement of cryogenic plumbing for microphonics suppression, 4) change of beampipe HOM damper to coaxial line HOM damper, etc. This paper will describe the convertion of booster cavity and cryomodule, vertical test, commissioning results, and operation status of the booster cavity.

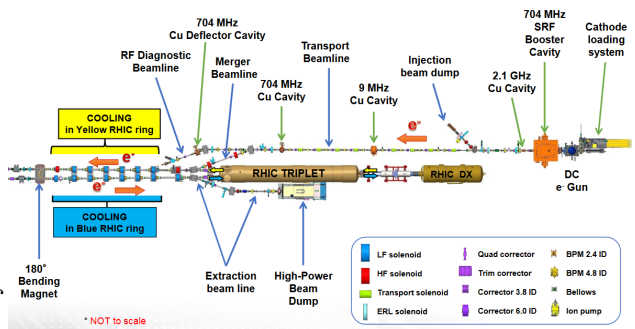


Figure 1: LEReC layout.

704 MHz SRF GUN CAVITY REVIEW

Before describing the modification, it is necessary to review the performance of the booster cavity as a gun cavity. Figure 2 shows the high current SRF gun cavity configuration. Two high power fundamental power coupler were used to deliver up to 1 MW RF power to the cavity. A choke-joint structure was used for photocathode support. Beam commissioning with this gun was carried out during end of 2014 to mid. 2015, which one can find more detail about the commission in reference [2]. One important point about the commission is that the cavity without cathode was able to reach CW 2.3 MV (although a lot of radiation), as shown in Figure 3. However, it kept quenching at around 1.6 MV after commissioning with cathode stalk a few month, which we believe that is due to cavity (near the cathode area) contamination by the either cathode stalk (Cu) or cathode (K_2CsSb). Due to tight schedule of LEReC and as the cavity reached 2.3 MV (shown in Figure 3), which is higher than the requirement of LEReC, we had sufficient confidence to convert the gun to LEReC booster.

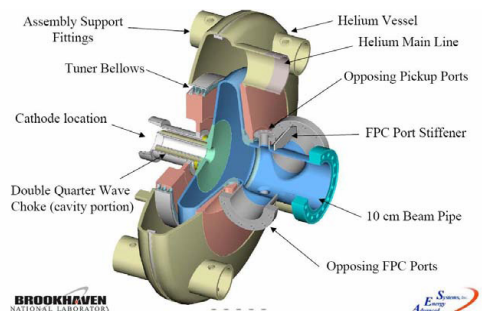


Figure 2: 704 MHz SRF gun cavity.

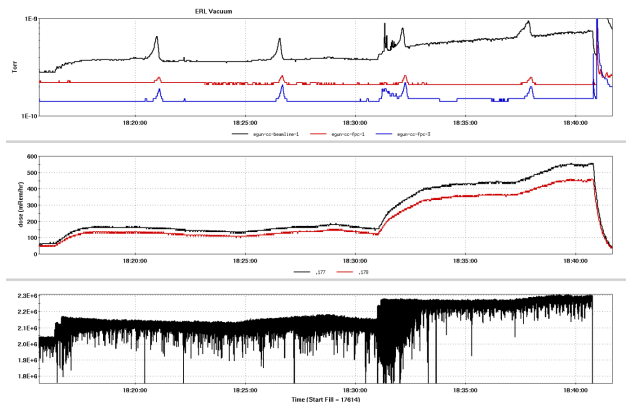


Figure 3: 704 MHz SRF gun cavity reached 2.3 MV prior to cathode commissioning.

* Work supported by LDRD program of Brookhaven Science Associates, LLC under Contract No. DE-AC02-98CH10886 with the U.S. DOE.
† email: wxu@bnl.gov

Content from this work may be used under the terms of the CC BY 3.0 licence (© 2018). Any distribution of this work must maintain attribution to the author(s), title of the work, publisher, and DOI.

ISBN: 978-3-95450-194-6 ISSN: 2226-0366 doi:10.18429/JACoW-LINAC2018-MOPO005

COMMISSIONING OF THE NORMAL CONDUCTING CAVITIES FOR LEReC PROJECT*

Binping Xiao†, K. Mernick, F. Severino, K. Smith, Tianmu Xin, A. Zaltsman
Brookhaven National Laboratory, Upton, New York 11973-5000, USA

Abstract

To improve RHIC luminosity for heavy ion beam energies below 10 GeV/nucleon, the Low Energy RHIC electron Cooler (LEReC) is designed and is currently under commissioning at BNL. The linac of LEReC consists of a DC photoemission gun, a 704 MHz superconducting radio frequency (SRF) booster cavity, a three-cell 2.1 GHz third harmonic cavity for RF curvature correction, a single-cell 704 MHz cavity for energy de-chirping and a 704 MHz deflecting cavity for diagnostic line. In this paper, we present the commissioning of three normal conducting cavities mentioned above.

INTRODUCTION

A bunched beam electron cooler called LEReC [1] has been designed and is under construction at the Relativistic Heavy Ion Collider (RHIC) to significantly improve the collider luminosity at energies below 10 GeV/nucleon to map the QCD phase diagram, especially to search the QCD critical point.

The electron linac of LEReC consists of a DC photoemission gun, one 704 MHz SRF booster cavity [2], and four normal conducting cavities: a 2.1 GHz third harmonic cavity, a 704 MHz cavity [3-5], a 9 MHz cavity, and a 704 MHz deflecting cavity on the beam diagnose line for longitudinal energy spread measurement. The 704 MHz SRF booster cavity accelerates 400 keV bunches from the DC gun near the top of the RF wave, with an accelerating voltage up to 2.2 MV. The booster also introduces an energy chirp for ballistic stretching of the bunches in a beam transport section. The remaining curvature of the bunch in longitudinal phase space is then corrected by decelerating the beam in the 2.1 GHz third harmonic cavity, so that the bunch is nearly linear in phase space. After the 30-meter long transport section, the bunch is still short enough so that the energy chirp can be removed with the normal conducting 704 MHz cavity.[6]

The 2.1 GHz cavity is a three-cell cavity operating at 2.112 GHz. It delivers an accelerating voltage up to 250 kV, at 9 kW power dissipation in the cavity walls, and 21.2 kW maximum power from the beam (decelerating). The 704 MHz cavity is a single-cell structure operating at 704.0 MHz that delivers a voltage up to 251 kV, at 9.5 kW power dissipation in the cavity walls, and 13.4 kW maximum power to the beam (accelerating). The 704 MHz deflecting cavity is a single-cell structure operating at 704.0 MHz that delivers a voltage up to 50 kV, at 150 W power dissipation in the cavity walls, and the power goes to the beam can be ignored since it works at zero phase and only limited number of electron bunches go into the diagnose line per second. In this paper, we describe the commissioning of these three normal conducting cavities.

CAVITY COMMISSIONING

The 2.1 GHz cavity was measured using network analyzer. At 2.1127 GHz, cavity unloaded Q was at 2.0e4, FPC Q_{ext} was at 2.0e4, critically coupled to the cavity. Pickup coupler 1 Q_{ext} was at 1.25e8 and pickup coupler 2 Q_{ext} was at 2.71e7. Cavity R/Q was calculated to be 175.1 Ω in circuit definition.

The RF window was first tested at JLab using 12.1 kW amplifier at 1.5 GHz. An IR camera was used to monitor the temperature on the ceramic, and 8 thermal sensors were attached outside the RF window to monitor the temperature on the stainless-steel frame. The highest temperature on the ceramic was 161.6 °C, and on the stainless-steel was 109.6 °C. The RF window was installed on a JLab530 to WR430 transition piece with two knobs so that it can be tuned to match the new working frequency at 2.112 GHz. The S-parameter results with optimized knob locations are shown in Figure 1.

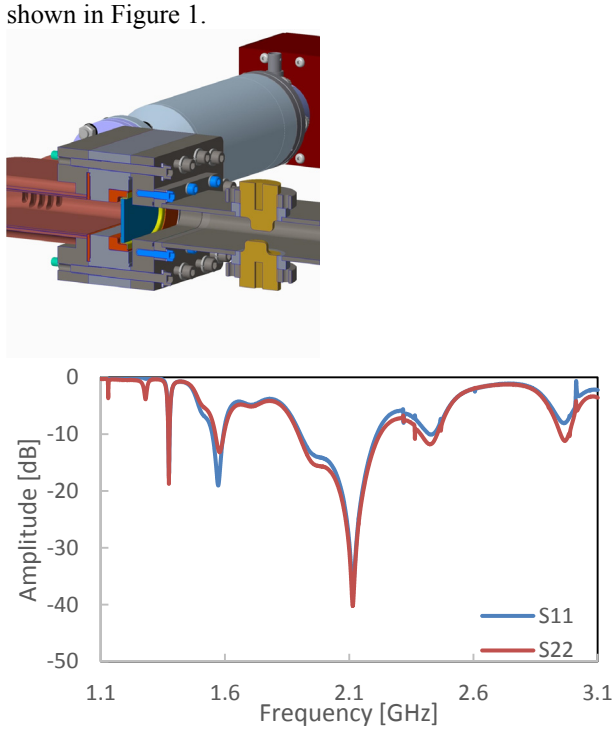


Figure 1: (top) RF window with two tuning knobs (yellow) to tune the frequency from 1.5 GHz to 2.1 GHz; (bottom) S-parameter of the JLab530 RF window with tuning knobs.

* Work is supported by Brookhaven Science Associates, LLC under contract No. DE-AC02-98CH10886 with the US DOE.
†binping@bnl.gov

Content from this work may be used under the terms of the CC BY 3.0 licence (© 2018). Any distribution of this work must maintain attribution to the author(s), title of the work, publisher, and DOI.

ISBN: 978-3-95450-194-6 ISSN: 2226-0366 doi:10.18429/JACoW-LINAC2018-MOPO006

CROSSTALK EFFECT IN THE LEREC BOOSTER CAVITY*

Binping Xiao†, K. Mernick, F. Severino, K. Smith, Tianmu Xin, Wencan Xu, A. Zaltsman
Brookhaven National Laboratory, Upton, New York 11973-5000, USA

Abstract

The Linac of the Low Energy RHIC electron Cooler (LEReC) is designed to deliver a 1.6 MeV to 2.6 MeV electron beam, with peak-to-peak *dp/p* less than ±7e-4. The booster cavity is the major accelerating component in LEReC, which is a 0.4 cell cavity operating at 2 K, with a maximum energy gain of 2.2 MeV. It is modified from the Energy Recovery Linac (ERL) photocathode gun, with fundamental power couplers (FPCs), pickup (PU) couplers and HOM coupler located close to each other. Crosstalk effects in this cavity are simulated and measured. A correction method is proposed to meet the energy spread requirement.

INTRODUCTION

The LEReC design is a non-magnetized cooling scheme that uses electron bunches at kinetic energies between 1.6 MeV and 2.6 MeV that match the ion beam velocity, with peak-to-peak *dp/p* less than ±7e-4, to cool RHIC ion bunches [1]. The electron linac of LEReC consists of a DC photoemission gun, a 704 MHz SRF booster cavity, and three normal conducting cavities [2, 3]. The 704 MHz SRF booster cavity accelerates 400 keV bunches from the DC gun, near crest with an accelerating voltage up to 2.2 MV. It is modified from the ERL photocathode gun [4]. It has two FPCs, two PUs, and one HOM coupler, with a PU (HOMPU) on the HOM coupler. All couplers are on the same side of the cavity, shown in Figure 1. Please note the second PU is located opposite to the one shown in the figure.

Typically, the FPC and the PU are positioned on different sides of the cavity, and thus isolated by the cavity with no direct coupling (normally capacitive) between them. In an SRF gun, however, one side of the cavity is reserved for photocathode with its stalk, thus the FPC and PU are installed on the same side of the cavity that is opposite to the photocathode. The only exception so far is the 112 MHz SRF gun for the Coherent electron Cooler (CeC) experiment at BNL, in which the PU is on the same side of the photocathode, and the FPC is on the other side of the cavity. In that design the coupling strength (Q_{ext}) of the PU in the 112 MHz gun varies with the insertion depth of the photocathode, thus calibration is required every time after cathode installation.

With FPC and PU on the same side of the cavity, the direct coupling between FPC and PU causes distortion of the RF response, the so-called crosstalk effect. This effect was first studied by Zhao at BNL using an equivalent circuit model of the cavity with couplers, by applying an additional capacitor between FPC and PU [5]. Later He at PKU proposed a simple method to extract the resonance frequency and loaded quality factor Q from the RF response with crosstalk [6]. As pointed out by both Zhao and He, the crosstalk effect severely distorts the RF response (S-parameter) between FPC and PU when the cavity is at room temperature, and makes it difficult to measure the resonance frequency and Q. While in the superconducting state, the distortion of the RF response is insignificant.

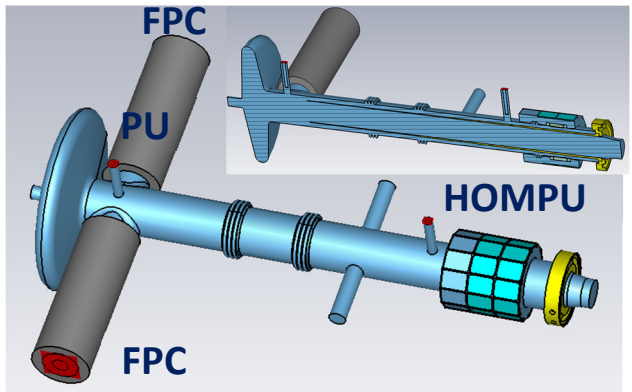


Figure 1. LEReC booster cavity with cross-section view (top-left).

In the LEReC booster cavity, however, the crosstalk effect is important, and its effect needs to be corrected. During operation, due to the limited life time of the main tuner, a "dead band" is applied to limit total tuner motion. Within this dead band, the cavity resonant frequency is allowed to vary, and LLRF feedback loops must stabilize the cavity voltage and phase (V_{pu}) using available RF power. It is found that there is a ±1000 Hz slow frequency drift, and a ±100 Hz frequency shift due to microphonics, with its source yet to be identified during operation. These frequency shifts cause a deviation between amplifier's output frequency and cavity's resonance frequency. Since the S-parameter is slightly distorted by the crosstalk effect in superconducting state, it is no longer in Lorentz form. With V_{pu} fixed, the cavity accelerating voltage V_{acc} deviates from the reference accelerating voltage without crosstalk effect, $V_{acc\text{-}ref}$. With the tight *dp/p* requirement, at 1.6 MeV, the voltage fluctuation should be within ±1.12 kV for the whole LEReC system, the fluctuation from V_{acc} should be a small portion of this number. Even though the crosstalk effect insignificantly distorts resonance frequency and Q, the voltage fluctuation caused by it might not be tolerable. In this paper the crosstalk effect in the LEReC booster cavity is analyzed. A method of correction is proposed so that the design specification can be met.

* Work is supported by Brookhaven Science Associates, LLC under contract No. DE-AC02-98CH10886 with the US DOE.
† binping@bnl.gov

Content from this work may be used under the terms of the CC BY 3.0 licence (© 2018). Any distribution of this work must maintain attribution to the author(s), title of the work, publisher, and DOI.

ISBN: 978-3-95450-194-6 ISSN: 2226-0366 doi:10.18429/JACoW-LINAC2018-MOPO007

THE DEVELOPING OF THE BEAM INJECTION SECTION WITH LASER SOURCE AND S-BAND ELECTRON RF GUN FOR SUPERKEKB PROJECT

Xiangyu Zhou†, Mitsuhiro Yoshida, Rui Zhang, Yujiro Ogawa, High Energy Accelerator Research Organization (KEK/SOKENDAI), 305-0801, Tsukuba, Ibaraki, Japan

Abstract

For the beam injection at Linac accelerator of the SuperKEKB project, the s-band RF gun needs to provide low-emittance high-charge electron bunches. A photocathode RF gun system with an advanced RF cavity structure (quasi-travelling side-coupled structure, cut disk structure), a new photocathode material (Ir_5Ce cathode) and a hybrid laser system (Yb fiber and Nd:YAG hybrid system) have been developing in the SuperKEKB injector Linac. Furthermore, many monitors and remote controls program were built to increase the stability of operation. By the injection system, the required charge and emittance for Phase-II commissioning were achieved.

INTRODUCTION

KEK injector Linac has delivered electrons and positrons source for high energy accelerator research, particle physics and photon science experiments for more than 30 years. Then, KEKB is being upgraded towards the SuperKEKB which is an asymmetric energy of 7-GeV electron and 4-GeV positron double-ring collider [1]. Full-energy, high-charge and low-emittance beams are necessary in order to achieve a design luminosity of 8×10^{35} $cm^{-2}s^{-1}$ for the study of the flavour physics of elementary particles. The injector continues to deliver various beams to SuperKEKB and light source rings such as PF and PF-AR.

In the positron beam, new Flux Concentrator (FC) and capture section was developed for efficient positron generation. Since generated positron beam has large emittance, new damping ring (DR) has been constructed to reduce beam emittance. Therefore, the thermionic electron gun was reinstalled for positron beam generation with the charge of 10 nC [2].

For the injector upgrade, the electron beams with a charge of several nC and a normalized emittance of less than 10 μm are expected to be generated in the electron gun. A thermal cathode DC gun had been used for KEKB. Because the DC gun could not make low-emittance beam, a quasi-traveling wave side couple (QTWSC) RF gun which has two side coupled standing wave field was developed [3]. This gun has a strong focusing field at the cathode and the acceleration field distribution also has a focusing effect. In addition another cut disk structure (CDS) RF gun was installed to 90 degree injection line. These guns have been used for electron beam study.

A multi-crystalline iridium cerium (Ir_5Ce) compound is used as a photoemitter of a high charge and low emittance RF gun [4]. The quantum efficiency (QE) is approximately 9.1×10^{-4} with 219 nm laser source at room temperature, which has the long lifetime (>LaB_6).

For the laser source, an Ytterbium-doped (Yb-doped) fiber and Ytterbium-doped YAG (Yb:YAG) hybrid laser system was development. 30 ps, mJ-class, 257 nm ultraviolet (UV) pulse was provided and injected to the photocathode [5].

The Phase I beam commissioning successfully ended in the June of 2016. The electron beam and positron beam with the bunch charge of around 0.7 nC is successfully delivered to the end of beam transport line.

Table 1: Requirements for Linac in SuperKEKB Phase II

	Electron HER 7 GeV	Positron LER 4 GeV
Normalized emittance $\gamma\beta\varepsilon_x$ / $\gamma\beta\varepsilon_y$	150 / 150 [μm]	200 / 40 [μm] with damping ring
Energy spread σ_δ	0.10 [%]	0.16 [%]
Bunch charge at injection point	1.0 [nC]	0.5 [nC]

Towards Phase-II beam commissioning, the high-charge and low-emittance beam development is going on for the higher requirement (Table. 1). The mainly improvement is the laser source. An Ytterbium/Neodymium (Yb/Nd) hybrid laser system was developed. With the synthetic crystalline material Neodymium-doped YAG (Nd:YAG), high reliability of the laser source is realized. The layout of the electron guns and laser system is shown in Fig.1. The transport line between the laser and RF gun was restored with the backup line and remote control system.

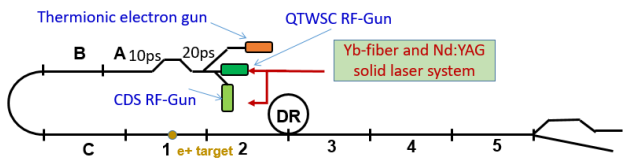


Figure 1: Layout of Linac.

Yb/Nd DOPED HIBRID LASER SYSTEM OF RF GUN

Based phase-I commissioning, the laser system for RF gun consisted Yb-doped fiber oscillator, Yb-doped fiber amplifiers and Yb:YAG thin-disk laser amplifiers. Yb:YAG crystal has large absorption bandwidth to reduce thermal management requirements for diode lasers, a

† email address : xiangyu.zhou@kek.jp

Content from this work may be used under the terms of the CC BY 3.0 licence (© 2018). Any distribution of this work must maintain attribution to the author(s), title of the work, publisher, and DOI.

ISBN: 978-3-95450-194-6 ISSN: 2226-0366 doi:10.18429/JACoW-LINAC2018-MOPO008

THE RF GUN ADOPTING THE DIELECTRIC ASSIST ACCELERATING STRUCTURE

Shingo Mori*, Mitsuhiro Yoshida†, KEK, Tsukuba, Japan
Daisuke Satoh‡, National Institute of Advanced Industrial Science and Technology, Tsukuba, Japan

Abstract

We apply the dielectric assist accelerating (DAA) structure to the RF gun, which is a candidate for a high average current and high brightness electron source. The DAA structure consists of ultralow-loss dielectric cylinders and disks which are periodically arranged in a metallic enclosure. Due to the high quality factor and the high shunt impedance of the DAA cavity, the RF gun adopting the DAA cavity can be a high-duty electron beam source at room temperature. We provide design work for RF gun adopting the DAA structure.

INTRODUCTION

The RF photoinjectors have been widely used as a source of high-quality beam. The electron beam of low emittance and high beam current are now considered as the electron sources for the x-ray free electron laser (FEL) which requires lower emittance to obtain shorter wavelengths and high peak current to obtain good gain, and linear colliders to meet the requirement of a complex pulse structure and to provide small emittance flat beam [1].

The first use of the RF photoinjector was done by Fraser et al. [2] in 1985 at LANL for the application to the FEL. The idea to combine a photocathode and a laser system with an RF cavity that supports a standing-wave field has many advantages. First, the electron bunch length is determined by the laser pulse without the following buncher section and provides narrow energy spread. Second, the electron beam is immediately accelerated up to relativistic energy by high RF field on the cathode within the first cell, which can decrease the space-charge growth of the emittance when the electrons are non-relativistic. Third, the quite low emittance beams can be produced by decreasing the laser spot size at the photocathode [3] which can reach as small emittance as 0.1 mm · mrad with relatively small bunch charge $>$ 0.1 nC. The electron beam dynamics after generation from the cathode is well understood analytically [4, 5] and numerically. The emittance of the beam produced by the RF electron gun is determined by three contributions: the emittance as the bunch emerges from the cathode; the electromagnetic interaction among the non-relativistic electrons called as the space charge effect; nonlinear radial dependence of the transverse components of RF.

In most cases, the RF photoinjector operates at a low duty factor and have relatively low average current. The first photoinjector with a duty factor of 25% was designed by Boeing in 1992 [6]. Currently, a collaboration between LANL and AES is developing a normal conducting photoinjector, which works in the CW mode. In the CW mode operation of a normal conducting photoinjector, the large amount of RF power loss causes cooling problems and bounds the gradient, e.g. 7 MV/m in ref. [6], which becomes drawbacks in the emittance. While superconducting RF photoinjectors also provides CW mode operation with high average current, with low emittance $O(1)$ mm · mrad due to the moderate gradient 20-50 MV/m.

A dielectric assist accelerating (DAA) structure [7, 8] is promising in power efficiency and could be a new candidate of photoinjector with CW mode operation, because it provides high efficiency $Q \sim O(10^5)$ at room temperature. Due to the structures of the dielectrics and the use of the ultra-low-loss dielectric material [8], the five cell DAA cavity provides the Q-value, $Q = O(10^5)$, and the shunt impedance $Z_{sh} \simeq 650$ MΩ/m. We have constructed the test stand for the DAA test cavity whose design frequency is 5712 MHz. In the tentative high voltage test, we found the gradient can reach up to multi-MV/m. This test cavity is planned to examine the main cavity to accelerate a relativistic electron beam which is generated from the RF photoinjector. In order to examine the possibility of the high-duty operation of the DAA main cavity, it is reasonable to construct the RF photoinjector which applies the DAA structure as well.

In order to investigate the possibility of the DAA structure as an RF photoinjector, we carry out the numerical calculation of the electromagnetic field in the cavity and the coupler, and the dynamics of an electron bunch generated by the photocathode.

This paper is organized as follows. In Sec.2, the dielectric cell of the DAA structure is introduced and we discuss the boundary problem which appear when the beam hole opens. In Sec.3, we introduce the novel structure of the end cell to avoid the boundary problem. In Sec.4, we will show the numerical result of the RF photoinjector based on the DAA structure. In Sec.5, we will summarize our result.

THE DAA STRUCTURE AND THE BOUNDARY PROBLEM

In this section, we will review the concept of the DAA structure and its boundary effect.

The basic structure of the DAA cavity is periodic, which is composed of the cylindrical waveguide made of metal and a cell called regular cell. Figure 1 shows the distribution of the electric force line calculated using *SUPERFISH* in the pillbox cavity which contains a regular cell. We call the

* smori@post.kek.jp
† mitsuhiro.yoshida@kek.jp
‡ dai-satou@aist.go.jp

Content from this work may be used under the terms of the CC BY 3.0 licence (© 2018). Any distribution of this work must maintain attribution to the author(s), title of the work, publisher, and DOI.

ISBN: 978-3-95450-194-6 ISSN: 2226-0366 doi:10.18429/JACoW-LINAC2018-MOPO009

ELI-NP GAMMA BEAM SYSTEM – CURRENT PROJECT STATUS

Piotr Tracz†#
ELI-NP/IFIN-HH, RO-077125, Bucharest-Magurele, Romania

Abstract

The Gamma Beam System at the ELI-NP (Extreme Light Infrastructure – Nuclear Physics) under construction in Bucharest-Magurele, Romania, aims at producing high brilliance gamma-rays, based on the laser Compton backscattering, up to 3.5 and 19.5 MeV out of two interaction chambers. The design of a warm radio frequency linac is optimized to meet a unique source specification i.e. high brilliance, small relative bandwidth, tunable energy, and high spectral density. Together with the technological development in the field of high energy/high quality lasers it will open new opportunities for nuclear physics research in fields like nuclear photonics, nuclear astrophysics, photofission, and production of exotic nuclei, applications in industry, medicine, and space science. The S-band laser driven RF gun and two accelerating sections constitute the injector. Then the beam is accelerated by C-band linac up to 350 and 720 MeV. The GBS was designed and is being constructed by the EuroGammaS Association – a consortium of European academic and research institutions and industrial partners.

This paper gives an overview of the facility, describes the linac system and summarizes the project status.

INTRODUCTION

The Gamma Beam System (GBS) at ELI-NP was designed to provide gamma beam with unprecedented features: continuous tunable γ-ray energy over a broad range from 0.2 to 19.5MeV, high spectral density about 10^4photons/sec/eV, small relative bandwidth $< 0.5\%$, high degree of polarization $> 95\%$, and high peak brilliance $10^{20} \div 10^{23}$ N_{ph}/sec mm^2 mrad^2 0.1% [1].

The high brightness electron beam will be provided by a warm multi-bunch RF linear accelerator, operating with repetition rate 100 Hz. Electrons will be formed in trains of 32 micro-bunches of 250pC each, separated at 16ns from each other, repeating every 10ms. To achieve small emittance with low energy spread a particular care was paid to a damping of higher-order modes to reduce the beam break-up effects and beam loading effects of the cavities due to the short-time separation between the electron micro-bunches [2, 3]. The expected parameters of the electron beam at the high energy interaction point are given in the Table 1 [1].

The experimental activities with gamma beams at ELI-NP are evolving on three main lines of research: fundamental research, applied physics and gamma beam diagnostic tools development. In Fig. 1 the location of the GBS in the ELI-NP building is illustrated. The main experimental halls dedicated to measurements with gamma beams are indicated on the figure.

Table 1: Electron Beam Parameters at High Energy Interaction Point [1]

Energy	720MeV
Bunch charge	250 pC
Bunch length	1 ps
Norm. transverse emittance	0.4 mm·mrad
Bunch energy spread	0.04÷0.1 %
Energy variation along macro-bunch	0.1%
Energy jitter shot to shot	0.1%
Time arrival jitter	< 0.5 ps
Pointing jitter	1 μm
Focal spot size	~ 15 μm
Number of bunches per RF pulse	32
Bunch-to-bunch distance	16 ns
RF pulse repetition rate	100 Hz

The ELI-NP facility covers an area of approx. 33 000m^2. It will be a user facility. The civil construction comprised office building, a guest house and a canteen. ELI-NP is hosted by the Horia Hulubei National Institute of Physics and Nuclear Engineering (IFIN-HH) [4].

GBS DESCRIPTION

A schematic view of the GBS layout is shown in Fig. 2. The electron source is a 1.6 cell gun BNL/SLAC/UCLA type. Nevertheless it was fabricated with a new technique developed at LNF-INFN that does not involve brazing and, consequently, avoiding a thermal stress on copper. Several other improvements were implemented to increase the peak field at the cathode but reducing the break down rate probability [5]. The gun is equipped with a copper photocathode and there is a focusing solenoid at the exit of the gun for emittance compensation due to the space charge effects. The accelerating field at the cathode is 120MV/m and energy gain is 5.7MeV. The S-band TW accelerating sections will act as a bunch compressor decreasing the bunch length from 10 to 1ps in the velocity bunching process. There are twelve independent coils mounted on the first S-band section. The S-band sections will be driven by independent klystrons. A separate klystron will feed the RF gun and two S-band transverse deflecting structures, for the measurement of the longitudinal charge profile, located after injector and at the entrance of the high energy linac.

The C-band linac is divided into two segments – the low energy linac (LEL) and the high energy linac (HEL)

†piotr.tracz@eli-np.ro
#For the ELI-NP team

Content from this work may be used under the terms of the CC BY 3.0 licence (© 2018). Any distribution of this work must maintain attribution to the author(s), title of the work, publisher, and DOI.

ISBN: 978-3-95450-194-6 ISSN: 2226-0366 doi:10.18429/JACoW-LINAC2018-MOPO010

JINR PHOTOCATHODE RESEARCH: STATUS AND PLANS

M. A. Nozdrin*, N. I. Balalykin, V. F. Minashkin, G. D. Shirkov, JINR, Dubna, Russia
E. I. Gacheva, A.K. Potemkin, V. V. Zelenogorskii, IAP RAS, Nizhny Novgorod, Russia
J. Huran[1], IEE SAS, Bratislava, Slovakia
[1]also at JINR, Dubna, Russia

Abstract

Photocathode research in the frame of the "transmission" photocathode conception (backside illuminated cathode based on a quartz/sapphire plate or a metal mesh which is a substrate for thin film made of a photomaterial) is being conducted in the Veksler and Baldin Laboratory of High Energy physics (LHEP) of the Joint Institute for Nuclear Research (JINR). Status of the 30-kev DC Photogun test bench and recent results of the extremely thin carbon film based cathodes research are described. Progress in the full-scale photoinjector prototype (max electron energy of 400 keV) is given. Startup of the photoinjector was performed, 70 keV electrons were extracted (650 pC).

INTRODUCTION

Initial beam quality is of high importance for contemporary and future electron accelerators. Photoinjector sources provide beams of unexcelled quality.

Two main material types for photocathodes are metals and semiconductors. Latter have high quantum efficiency (>10% for CsTe at UV [1]), but have relatively small operational lifetimes and are sensitive to environment [2]. Metals are robust but have low quantum efficiency [3]. Also, GaAs should be mentioned for its ability to produce polarized electrons [4].

Diamond films are considered as promising photo emission cathodes because of their low threshold field as well as high thermal conductivity, high breakdown field and chemical inertness.

Quantum efficiency of diamond films can be additionally increased (up to 14% [5] or even up to 47% [6]) by hydrogenation and usage of the vacuum ultraviolet laser (140 nm).

A new concept of photocathode design was proposed at JINR [7]: a backside-illuminated "transmission" photocathode — an optically polished quartz/sapphire plate or a metal mesh (copper or stainless steel, 40×40 µm cell size, 30 µm wire diameter). This plate or mesh is a substrate for thin film made of a photomaterial. The metal mesh can also work as a photocathode without any coating. Such cathode geometry permits an increase in quantum efficiency due to the vectorial photoeffect. Furthermore, intrinsic emittance reduction is expected for the transmission mode operation [8].

EQUIPMENT

Photocathode research at JINR is being conducted at two benches: Photogun and Photoinjector.

* nozdrin@jinr.ru

Photogun Bench

Photogun bench is the main research instrument so far. It consists of the DC photogun (max anode voltage 30 kV), industrial single-pulse driver laser by LOTIS TII, focusing magnet with correction windings and various diagnostics (Faraday cup, laser energy meter, CCD camera for beam imaging). Main laser model is LS-2134 (wavelength 266 nm, pulse length 15 ns, pulse energy 15 mJ). This year second beamline was assembled (Fig. 1). It is based at LS-2132UTF laser (wavelength 266 nm, pulse length 8 ns, pulse energy 45 mJ) with a fifth harmonic external assembly which allows 213-nm laser beam generation.



Figure 1: 213-nm photogun bench setup.

Photoinjector Bench

Photoinjector bench is the photogun bench development. It features the full scale accelerating structure (triode type gun with forced resistive potential distribution which can provide electron beam with an energy of up to 400 keV) and the unique laser driver by IAP RAS (Table 1).

Table 1: Photoinjector Laser Driver Parameters

Parameter	Value
Wavelength	262 nm
Bunch train repetition rate	10 Hz
Bunch train duration	800 µs
Bunches in the train	8000
Bunch duration	10 ps
Bunch energy	1.5 µJ

First electron beam at the bench was obtained in April 2017. Bunch trains with 650 pC total charge were registered, what corresponds to current of 8 mA in the bunch, 0.8 µA in the bunch train and 6.5 nA average current(10 Hz repetition rate). Copper mesh photocathode (40×40 µm cell size,

Content from this work may be used under the terms of the CC BY 3.0 licence (© 2018). Any distribution of this work must maintain attribution to the author(s), title of the work, publisher, and DOI.

ISBN: 978-3-95450-194-6 ISSN: 2226-0366 doi:10.18429/JACoW-LINAC2018-MOPO016

NARROWBAND-FREQUENCY TERAHERTZ GENERATION FROM BEAM PIPE WITH HELIX WIRES

D. Wang†, Y. Liang, Q. Tian, Y. Du, L. Yan‡, W. Huang, C. Tang
Department of Engineering Physics, Tsinghua University, Beijing, China

Abstract

We studied through analysis and numerical simulations the use of a relativistic electron bunch to drive a metallic beam pipe with helix wire inside, for the purpose of generating narrowband-frequency terahertz radiation. We have shown that the frequency is related to the radius of the pipe and that of the wire, thus one can generate a narrow-band radiation pulse with frequency tunable through this scheme with different pipes and wires. The total energy of a few milli-Joules. The pulse length tends to be on the order of hundreds of picoseconds. We have also shown that, if the pipe radius is tapered along its length, the generated pulse will end up with a frequency chirp.

INTRODUCTION

The development of an accelerator-based Terahertz (THz) source could represent a real advancement for the scientific community [1], with important perspectives in different areas of fundamental research and applied physics, including applications in medical imaging, spectroscopy of solids and liquids, and chemical and security identification [2].

To generate THz radiation, the electron beam has to pass through a slow-wave structure, such as a corrugated metallic waveguide and a dielectric-loaded waveguide. The relativistic electron bunch generates radiation that follows the beam, which is also referred to as wakefield. The electron beam excites only modes with phase velocity equal to the velocity of beam, i.e., close to the speed of light c. With a sufficiently short (rms bunch length σ_z less than a radiation wavelength λ) driving beam, the radiation from the electron bunch is coherent [3].

In a recent experiment at FACET, a metallic beam pipe with round bore and small, rectangular corrugations is used to generate narrow-band radiation at 0.4 THz, with depth of corrugation $\delta = 60\mu$m and pipe radius $a = 1$mm the corrugated structure is 50 mm long, a 50 pC electron beam with $\sigma_z = 50\ \mu m$ has passed through the structure and transferred 1.2 uJ energy into the THz radiation [4]. Another example is a W-band flat metallic corrugated structure at around 0.1 THz driven by AWA bunch train, few millijoules of pulse energy with MW peak power was generated with 3 sub-bunches of 75 MeV, 500 μm long, 2 nC electron beam passing through a 12-cm long structure [5].

In this report, we design a simpler layout of a THz wakefield structure, which we call it as helix-wire pipe structure (HWP). This structure can be taken as a corrugated structure, with the wire diameter $2r$ is equivalent to the peak to peak depth of corrugation δ. Therefore, similar analytical estimates in corrugated structure can be applied for the HWP [6]. For the simulations, we employ electromagnetic design and analysis program CST, which computes the fields generated by an ultra-relativistic bunch in a structure in the time domain [7]. Simulations agree well with the theoretical analysis, which show that a 50-mm long HWP structure is able to generate mJ energy at THz freqeuncy when driven by 1nC electron beam, the gradient is in order of 100MV/m, and THz power is 10 MW The frequency from HWP is narrow-band frequency is tunable with wire diameter and pipe diameter We have also shown that, if the pipe radius is tapered along its length, the generated pulse will end up with a frequency chirp.

BASIC DESIGN OF THE STRUCTURE

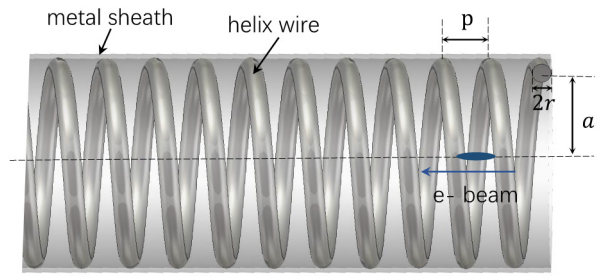


Figure 1: Basic design of the helix-wire pipe (HWP) structure, which is a helix wire inserted into a metal round pipe, the whole serves as a high impedance THz wakefield structure, parameters of the structure is listed in Table 1.

In our study, a metal round pipe with helix wire inside serves as the THz wakefield structure, the parameters are helix period p, wire diameter $2r$, pipe radius a and total length of the structure L_s, which are list in Table 1.

Table 1: Parameters of HWP Structure

parameter	DLW No.1
a	1.0 mm
r	0.1 mm
p	0.5 mm
L_s	50 mm

The wire diameter $2r$ in HWP is equivalent to the peak to peak depth of corrugation δ. Similar analytical estimates is applicable. Analytical formulas as following: the frequency $f = \frac{c}{\pi\sqrt{2ar}}$=0.2 [THz] only depends on the wire diameter and the pipe radius, while the group velocity v_g is also highly depend on the helix wire period parameter p,

†wangdan16@mail.tsinghua.edu.cn
‡ yanlx@mail.tsinghua.edu.cn

Content from this work may be used under the terms of the CC BY 3.0 licence (© 2018). Any distribution of this work must maintain attribution to the author(s), title of the work, publisher, and DOI.

ISBN: 978-3-95450-194-6 ISSN: 2226-0366 doi:10.18429/JACoW-LINAC2018-MOPO018

DEVELOPMENT OF AN IMPROVED CAPTURE SECTION FOR THE S-DALINAC INJECTOR*

S. Weih#, M. Arnold, J. Enders, N. Pietralla,
Institut für Kernphysik, TU Darmstadt, Germany
D. Bazyl, W.F.O. Müller, H. De Gersem,
Institut für Theorie Elektromagnetischer Felder, TU Darmstadt, Germany

Abstract

For the injector of the superconducting Darmstadt electron linear accelerator S-DALINAC, the design of a new capture cavity was recently completed. This beta-reduced structure will optimize the capture of low-energy electron bunches from the gun section and therefore improve the longitudinal beam quality of the injector beam, as simulations have shown. The existing cryomodule of the injector has to be modified for the installation of the new cavity. These modifications include adaptions of the tuner frame as well as modifications of other surrounding parts. To improve the diagnostics in the low-energy section, an energy-spread measurement setup is currently also under development. In this contribution the cryomodule modifications as well as simulation results for the longitudinal beam dynamics are presented.

INTRODUCTION

The injector of the superconducting Darmstadt linear accelerator S-DALINAC [1] provides electrons with a kinetic energy of up to 10 MeV. It consists of a normal conducting section where the beam is prepared for RF acceleration and two cryomodules containing superconducting elliptical Nb accelerator structures (Fig. 1). The injector is driven by a 250 keV thermionic gun, the also existing spin-polarized gun [2] is currently being prepared for an upgrade to 200 keV [3]. In its present state, the superconducting part of the injector features a five-cell capture cavity and two 20-cell cavities similar to the structures used in the main LINAC. All cavities are operated at 3 GHz and designed for a β of 1. However, the 250 keV beam from the thermionic gun corresponds to a relativistic β of only 0.74, introducing significant phase slippage effects as the low-energy bunch travels through the current five-cell cavity. In order to increase the efficiency of the electron capture and the longitudinal beam quality of the beam after injection it is therefore intended to replace the five-cell structure with a new dedicated capture cavity. The design of the new capture structure, a 6-cell cavity with a reduced β of 0.86, has been recently completed [4,5] and its construction will start in the near future.

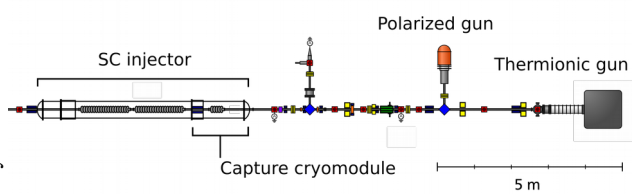


Figure 1: Overview of the S-DALINAC injector. Main subject of this project is the capture cryomodule which is part of the superconducting (SC) injector. It currently houses a 5-cell β=1 cavity.

MECHANICAL MODIFICATIONS

Inside the liquid helium vessel of the cryostat, the cavity is surrounded by its input and output RF coupler as well as the tuner system. It was already decided in the early stage of the project to keep the overall cavity length fixed, enabling the re-use of the couplers and the cryostat. However, the tuner frame has to be adapted. First CAD models of the tuner system were created in order to apply the necessary modifications. Figure 2 shows the finished tuner frame model. The tuner frame is fixed at the cavity cutoff tubes with aluminum plates (grey), which can be re-used from the existing 5-cell frame. Since the overall length of the cavity cell region will be increased by 8 mm, the tuner frame length has to be adapted. A shorter cutoff-tube at the output coupler side will compensate this additional length. However, due to the longer cell region, the titanium fixation rods (yellow), which stabilize the frame and guide the cavity, have to be modified. The piezo tuner system for microphonics compensation is

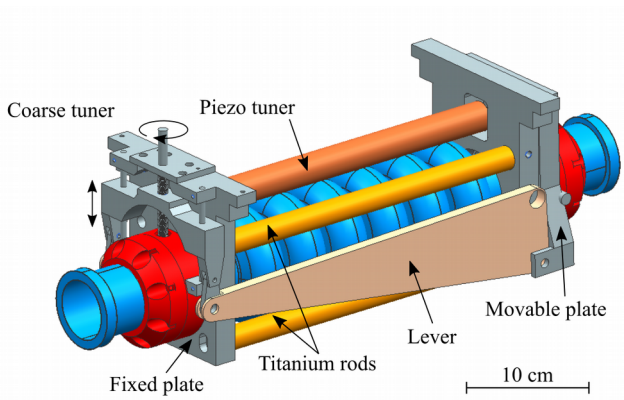


Figure 2: Trimetric view of the tuner frame CAD model with the applied modifications for the new capture cavity. The grey parts will be re-used from the existing setup, the piezo tuner and the support rods (orange and yellow) as well as the lever (pink) have to be adapted according to the increased length of the cell region. The cavity fixation rings shown in red have to be increased in diameter to adapt to the larger wall thickness of the cavity.

* Work supported by DFG (GRK 2128).
sweih@ikp.tu-darmstadt.de

Content from this work may be used under the terms of the CC BY 3.0 licence (© 2018). Any distribution of this work must maintain attribution to the author(s), title of the work, publisher, and DOI.

ISBN: 978-3-95450-194-6 ISSN: 2226-0366 doi:10.18429/JACoW-LINAC2018-MOPO019

STUDY ON CLEANING OF COPPER PLATED BELLOWS FOR LCLS-II*

L. Zhao†, E. Daly, K. Davis, G. Eremeev, T. Reilly, A-M. Valente-Feliciano, K. Wilson
Thomas Jefferson National Accelerator Facility, Newport News, Virginia, USA

Abstract

Inter-cavity copper plated bellows are part of the LCLS-II cryomodule beamline components. Since the bellows are close to superconducting radio frequency (SRF) cavities during accelerator operation, it is desirable that these bellows have similar cleanliness as SRF cavities. Studies have been done to help evaluate bellows interior cleanliness after the standard bellows cleaning procedure at Jefferson Lab.

BACKGROUND

LCLS-II cryomodule design includes copper plated bellows between each cavity, similar to that of the European XFEL [1, 2]. During string assembly at JLab, bellows are assembled to the cavity vertically as part of the cavity sub-assembly. Connections made on the rail were done horizontally [3]. Bellows are cleaned in a manner similar to the standard hardware cleaning processes except that lower solution temperature and expedited drying are applied. Bellows present some challenges for cleaning, for example, the convoluted shape is more difficult to clean and dry, the adhesion quality of the plating added concerns during processing [4]. To help confirm our horizontal assembly practice as well as understanding bellows cleanliness, three cavities were tested with a bellows assembled to the top of each cavity. Particle samples were collected from one of the three cavity-bellows assembly after vertical testing for further study.

EXPERIMENTS

Processing of Cavities and Bellows

Bellows were cleaned in an ultrasonic tank with ultrapure water and Citranox®, thoroughly rinsed with ultrapure water, dipped in acetone, and blown dry with nitrogen. Previously field-emission-free cavities were selected for this experiment. CAV0116: cleaned bellows were assembled horizontally onto cavity; cavity was pumped down, and then attached to the test stand with bellows on the top. After vertical test, the bellows were stretched and squeezed 0.5 inch while staying on top of the cavity before the next vertical test. CAV0278 and CAV0286: Bellows were assembled vertically onto the cavity; the cavity was flipped and received the final HPR with the bellows on the top; after final assembly (the bellows were still wet), the cavity was pumped down and attached to the test stand with bellows on the top.

Vertical RF Test

The three cavities were tested vertically at 2.0 K to see if there was any early field emission onset. The cavity configuration during vertical testing is shown in Fig. 1.

Sampling of Bellows and Cavity

After vertical test, the interior of CAV0278 and bellows 2068 were sampled to help understand the source of field emitters. Sampling was performed by two operators using two types of tooling, to allow comparison of findings from the two sampling process. Particles found in both sampling processes are likely from the surface of interest, while those found in only one sampling process could be introduced by the sampling process. In the first method (L series), a cleaned Gore-Tex (Teflon, or PTFE) piece was used to sample the surface of interest and transfer any particles onto a carbon tape, and the carbon tape was preserved carefully until SEM analysis. Two samples were collected at each of three locations: the flat region and inside of one convolution of the bellows (L1, L2), the cavity beam tube next to the bellows (L3, L4), and the cavity beam tube on the other end (L5, L6). In the second method (S series), a piece of isopropanol soaked cleanroom wipe (TX®1082 QuanSat, polyester) was used to sample the surface of interest and transfer the sample to a carbon tape, which was preserved inside a commercially available standard SEM sample case [5]. Sample locations are shown in Figure 1. One sample was collected at each of eight locations: bellows top flat region (S0456), inside top first convolution (S0457), several iris (S0458), inside bottom first convolution (S0459), bottom flat region (S0460), shaking of bellows (S0461), cavity top beam tube (S0462), and cavity bottom beam tube (S0463).

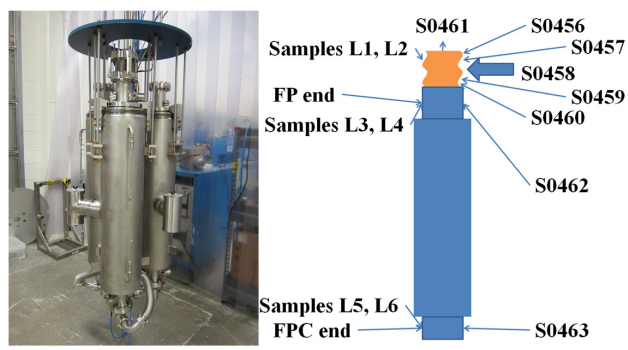


Figure 1: Bellows attached cavity on a test stand waiting to be loaded into the Dewar (left). Sampling locations on CAV0278-Bellows 2068 (right).

* Authored by Jefferson Science Associates, LLC under U.S. DOE Contracts DE-AC05-06OR23177 and DE-AC02-76SF00515 for the LCLS-II Project.
† lzhao@jlab.org

Content from this work may be used under the terms of the CC BY 3.0 licence (© 2018). Any distribution of this work must maintain attribution to the author(s), title of the work, publisher, and DOI.

ISBN: 978-3-95450-194-6 ISSN: 2226-0366 doi:10.18429/JACoW-LINAC2018-MOPO020

BEAM DYNAMICS STUDIES AND INSTRUMENTATION TESTS FOR BUNCH LENGTH MEASUREMENTS AT CLEAR

L. Garolfi*, S.Doebert, M. Bergamaschi, R. Corsini, A. Curcio,
W. Farabolini[1], D. Gamba, I. Gorgysian, CERN, Geneva, Switzerland
C. Bruni, P. Lepercq, H. Purwar, C. Vallerand, LAL, Orsay, France
[1]also at CEA/DSM/IRFU, Saclay, France

Abstract

A new CERN Linear Electron Accelerator for Research (named CLEAR) has been installed as a general-purpose user facility to study novel accelerating techniques, high-gradient structures, instrumentation and irradiation experiments. CLEAR is a flexible accelerator that can provide high quality bunched electron beams with a wide range of beam parameters up to an energy of 220 MeV, offering several testing capabilities. Among all the potential applications, novel accelerating techniques, such as plasma acceleration and THz generation are considered. These applications require shorter bunches, down to the 100 fs level. This paper reports on beam dynamics studies and instrumentation tests to establish a bunch length of this order in CLEAR. The short bunches are generated using adiabatic bunching in the first accelerating structure. For bunch length diagnostic, CLEAR is equipped with a streak camera and a transverse deflecting cavity. Alternatively, a phase-scan of the last accelerating structure could be used as well to estimate the bunch length. The experimental results with respect to these different techniques are presented and compared with simulations.

INTRODUCTION

CALIFES (Concept d'Accélérateur LInéaire pour Faisceau d'Electron Sonde) [1] represented the electron probe beam injector for the CLIC Test Facility 3 (CTF3) [2] at CERN. Recently, this accelerator has been refurbished as a new general-purpose user facility for accelerator R&D and components tests for existing and future accelerator applications. CLEAR [3, 4] can provide high quality bunched electron beams from 60 to 220 MeV in single or multi-bunch configuration with a bunch spacing of 1.5 GHz. The test accelerator exhibits a broad range of capabilities, such as prototyping and validation of accelerator components (for the Large Hadron Collider upgrade and its injector), high-gradient acceleration studies (normal-conducting X-band structures), irradiation of electronic components and medical applications. Furthermore, novel concepts as plasma acceleration and THz generation [5] could profit from the CLEAR beam line optimized for short bunches and low emittance beyond the current performances achieved by the CALIFES photo-injector, in the past. The improvement of the electron bunches quality in terms of length and emittance would also be beneficial to AWAKE (Advanced WAKEfield Experiment) [6], which will need a new short-pulse electron source in view of the "Run 2" phase. Therefore, beam dynamics studies and instrumentation tests have been performed for both determining an accelerator injection configuration that allows bunch lengths less than 1 ps and its subsequent experimental measure.

CLEAR LAYOUT AND DIAGNOSTICS

The accelerator is composed of the CALIFES injector (around 25 meters-long), which provides the electron beam to a subsequent 16 meters-long diagnostics and test lines. The electron photo-injector is composed of a 2.5-cell S-band RF gun [7] where the electrons are extracted and accelerated from a Cs_2Te cathode when illuminated by laser pulses. Two solenoids surround the gun for space charge emittance compensation. The RF gun is able to provide electron bunches with an energy of around 6 MeV, then three S-band LIL (LEP Injector Linac) [8] accelerating sections allow to boost the beam energy up to 220 MeV. An Integrated Current Transformer (ICT) [9] and a ceramic screen are installed right after the RF gun, for beam diagnostics. The first structure can be used to compress the bunch by using the velocity bunching technique. A matching section with a quadrupole triplet and a spectrometer line complete the accelerator. An S-band RF deflecting cavity is also installed along the beam line (Fig. 1). Bunch length measurements are possible by streak camera measurements [10] of Optical Transition Radiation (OTR) or by using an S-band RF deflecting cavity [11]. A transverse beam profile monitor [12] equipped with a Yttrium Aluminium Garnet (YAG) scintillator and an OTR screen is installed before the spectrometer. An additional ICT and YAG screen in the spectrometer line complete the longitudinal beam diagnostic capabilities. The beam-line ends about 20 cm after the spectrometer dipole with a 100 μm-thickness aluminium window, leaving about 1 meter-long in-air test stand. This area hosts the main THz radiation diagnostics [13].

BEAM DYNAMICS MODEL

A train of laser pulses, each one a few ps length spacing, impinges the photocathode. The number of pulses that constitutes the train can be controlled remotely. The number of pulses in the train was set to two, for most of the measurements. The RF gun is surrounded by two solenoids, the focusing and bucking coils. Three dimensional simulations have been performed using the Opera-3D FEA software. The latter allows to obtain the on-axis longitudinal magnetic field profile along the beam axis. The right current values

* luca.garolfi@cern.ch

Content from this work may be used under the terms of the CC BY 3.0 licence (© 2018). Any distribution of this work must maintain attribution to the author(s), title of the work, publisher, and DOI.

ISBN: 978-3-95450-194-6 ISSN: 2226-0366 doi:10.18429/JACoW-LINAC2018-MOPO024

DEVELOPMENT OF HIGH POWER COHERENT TERAHERTZ WAVE SOURCES AT LEBRA 125MeV LINAC IN NIHON UNIVERSITY*

T. Sakai†, T. Tanaka, Y. Hayakawa, Y. Sumitomo, K. Hayakawa, Y. Takahashi, K. Nogami,
LEBRA, Nihon University, Funabashi, Japan
N. Sei, H. Ogawa, AIST, Tsukuba, Japan

Abstract

Development of a high performance electron linac for the generation of FEL, Parametric X-ray Radiation (PXR) and THz waves has been continued at the Laboratory for Electron Beam Research and Application (LEBRA) of Nihon University as a joint research with KEK and National Institute of Advanced Industrial Science and Technology. The transport systems of the THz wave were installed in the vacuum chamber on the downstream side of the bending magnet of the PXR and FEL beam-line. The CER and the CSR are generated by the bending magnet each of the beam line. In addition, the CTR using thin metal foil is also generated. The average power of the CTR wave was measured approximately 1 mJ/macro-pulse (pulse width 4.5 μs) near the CTR wave beam source point in the frequency range of 0.1 - 2.5 THz. In addition, the energy of the CER as high as 0.5 mJ/macro-pulse were achieved with the experimental room. Furthermore, CER of the generated the FEL beam line can also be guided from the bending magnet on the downstream side of the undulator without disturbing the FEL oscillations. THz transport beam-lines and the characteristics of the THz waves are discussed in this report.

INTRODUCTION

Research and development of a high performance electron linac for the generation of the infrared Free Electron Laser (FEL), Parametric X-ray Radiation (PXR) and THz waves has been continued at the Laboratory for Electron Beam Research and Application (LEBRA) of Nihon University as a joint research with the High Energy Accelerator Research Organization (KEK) and National Institute of Advanced Industrial Science and Technology (AIST) [1-3].

The LEBRA linac consists mainly of the -100 kV DC electron gun, the pre-buncher, the buncher and the three 4 m long traveling wave accelerating tubes. The electron-beam energy is freely adjustable from 40 to 100 MeV according to the purpose of use. The RF power sources has been powered by two S-band klystrons (Mitsubishi Electric Corporation, PV-3030A1, the peak output power of 20 MW, the repetition rate of 2 ~ 12.5 Hz and the pulse duration of 5 ~ 20 μs).

The saturated FEL lasing has been obtained in the wavelength region of 0.4 ~ 6 μm [4]. The PXR generator covers the X-ray energies from 4 to 34 keV by using Si(111) and Si(220) planes as the target and the second crystals [5]. CSR-THz wave source development in the FEL Beam line has been carried out since 2011 [6]. Based on the results of the CSR-THz wave source development in the FEL line, higher power CTR-THz and CER-THz wave sources line has been constructed in the PXR line since 2016. In addition to these, the new high power CER-THz wave transportation line have been constructed between the downstream bending magnet in the FEL undulator section and the downstream optical cavity mirror since 2017.

CER-THZ WAVE SOURCE OF FEL BEAM LINE

Measurements of the spectrum of coherent radiation generated by the electron bunch are well suited for monitoring the condition of the electron beam. Therefore, based on the results of the CSR-THz wave source

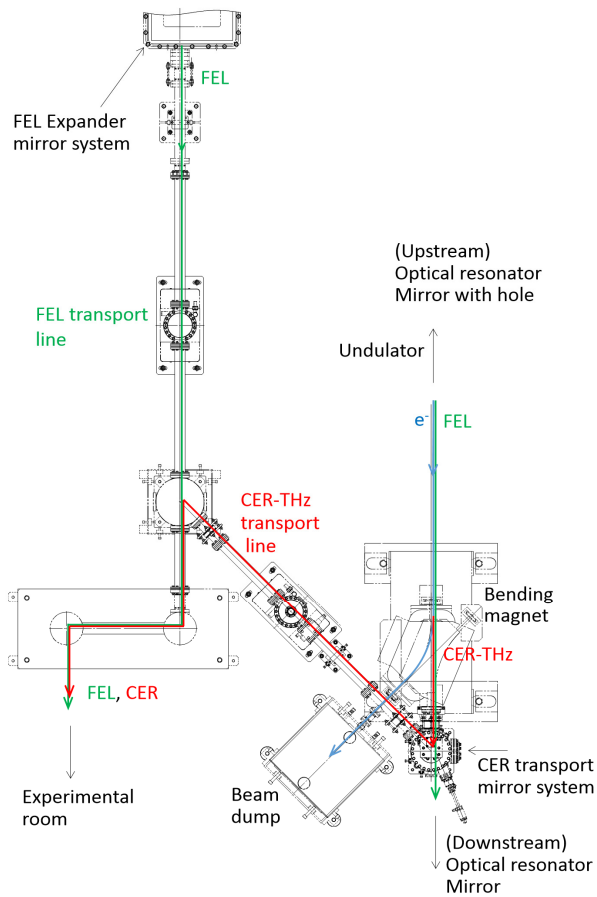


Figure 1: FEL beam line, CER-THz transport line and CER-THz wave transport concave mirrors system.

* This work was supported by JSPS KAKENHI (Grant-in-Aid for Young Scientists (B)) Grant Number JP16K17539.
† sakai@lebra.nihon-u.ac.jp

Content from this work may be used under the terms of the CC BY 3.0 licence (© 2018). Any distribution of this work must maintain attribution to the author(s), title of the work, publisher, and DOI.

ISBN: 978-3-95450-194-6 ISSN: 2226-0366 doi:10.18429/JACoW-LINAC2018-MOPO026

THE RESONANCE FREQUENCY SHIFT AFTER APPLYING THE COOLING SYSTEM FOR A SIDE COUPLED STANDING WAVE LINAC

Masoud Mohseni Kejani†, Fereydoon Abbasi Davani, Shahid Beheshti University, Tehran, Iran
Sasan Ahmadiannamin, Iranian Light Source Facility (ILSF), Tehran, Iran
Farshad Ghasemi, Sara Zarei, Nuclear Science and Technology Research (NSTRI), Tehran, Iran

Abstract

A radio frequency accelerator tube used in linear medical accelerators includes three main sections of the radio frequency cavity, an electron gun and the X-ray target, which is vacuumed by a pump inside it. The electromagnetic energy loss in the structure of the cavity can increase the temperature of the tube, resulting in changes in the geometric dimensions and then changes in some of the cavity characteristics, such as the resonance frequency. A cooling system is required to prevent excessive change in the resonant frequency due to thermal loss. Also, it is necessary to perform some computer simulations to stabilize the cavity's performance in the presence of electromagnetic energy thermal dissipation and the cooling system. In this paper, the simulation results of resonant frequency shifts after applying the cooling system have been reported.

INTRODUCTION

As we know, in terms of the accelerating structure, essentially electron linear accelerators are divided into traveling wave and standing wave structures. The design and construction of standing wave cavities are more complicated than standing wave cavities. On the other hand, the stability of the cavity's performance plays an important role in the characteristics of the outlet beam. In medical applications, the stability of cavities is more important [1]. By changing the nominal frequency of the cavity, the impedance matching of the transmission line and the accelerating cavity are changed and a large part of the power is reflected. Due to the high quality factor of standing wave cavities (about 17000), and 1.23 coupling constant, the cavity bandwidth (FWHM) will be about 400 kHz. It means that, by varying the frequency of 200 kHz, the input power to the cavity will halved and the output energy will be 4.28 MeV instead of 6MeV. The acceptable frequency shift of the cavity applied by using the cooling system, depends on the ability of the automatic frequency control system (AFC) [2]. The operation of the automatic frequency control system is determined by the two factors of the linear behavior and the response rate of the system relative to the radiofrequency pulse repetition rate [3, 4]. In the conventional analog frequency regulator system used in medical linear accelerators, the frequency correcting range in about 0.9 MHz with 300 pulse per second repetition rate. Therefore, the maximum frequency shift of the cavity after applying the water cooling system should not exceed 450 kHz. That can be easily stabilized by the automatic frequency control system [3].

GEOMETRY AND COOLING SYSTEM DESIGN

The geometrical parameters of RF cavity were optimized for operation in 2998.5 MHz in coupled cells configuration. The cavity will be operated with 2.6 MW input power with 5 μs beam length and 150, 200 and 300 Hz repetition rate. The loss of each accelerating cell will be calculated for mentioned repetition rate equal to 250, 350 and 500 watts for each accelerating cell for beam current of 100 mA by dividing to number of accelerating cells respectively. For this cavity, three types of cooling systems were investigated. The first type is the cooling system with tangential circular cross section, the second type is the cooling system with tangential rectangular cross section, and the third type is internal cooling system with circular cross-section. The inner diameter of the circular cross-section pipes is 8mm and the internal dimensions for the rectangular cross-section is 7mm*5mm. The inlet water velocity and temperature for all three types is 2m/s and 20, 22, 25°C respectively. The thermal calculations and total deformation of the cavities after applying of the cooling system have been reported in another paper [5]. Figure 1 illustrates the cooling system designs and Table 1 shows the temperature comparison for them.

† Masoud.mohseni.kejani@gmail.com

Content from this work may be used under the terms of the CC BY 3.0 licence (© 2018). Any distribution of this work must maintain attribution to the author(s), title of the work, publisher, and DOI.

ISBN: 978-3-95450-194-6 ISSN: 2226-0366 doi:10.18429/JACoW-LINAC2018-MOPO027

PHOTOCATHODE LASER PULSE SHAPING FOR IMPROVED EMITTANCE

M. Kotur*, J. Andersson, M. Brandin, J. Björklund Svensson, F. Curbis, F. Lindau, R. Lindvall, E. Mansten, L. Isaksson, R. Svärd, S. Thorin, S. Werin
MAX IV Laboratory, Lund University, Lund, Sweden

Abstract

We present a setup for producing and characterizing picosecond ultraviolet laser pulses for use in the MAX IV photocathode electron gun preinjector. Frequency-tripled laser pulses from a commercial laser system are shaped directly in the ultraviolet domain using a Fourier-domain pulse shaper. The pulses were characterized using a transient grating FROG. We discuss a proposed upgrade of the pulse shaper, as well as its limitations.

INTRODUCTION AND MOTIVATION

The MAX IV Laboratory is a synchrotron radiation facility. Its two storage rings reach electron energies of 1.5 and 3 GeV. In addition to the rings, the lab operates a short pulse facility [1], while a design study for a soft X-ray free electron laser (FEL) at 1-5nm is currently in progress. Both rings are injected by a full energy linac at 3 GeV [2]. The linac can use either a thermionic or a photocathode gun as a source of electrons, but only the photocathode gun can deliver the short electron bunches required for the short pulse facility and the possible future FEL. Our 1.6-cell, normal-conducting, BNL/SLAC-type photocathode gun [3] is operated at 2.9985 GHz. We make use of a polished copper cathode. An emittance-compensating solenoid is installed directly following the gun. The emittance requirement for the short pulse facility of 10 μm has already been met. The more stringent requirement for the free electron laser, of 0.4 μm, at a charge of 40 pC is likely to necessitate developments of both the gun laser and the electron gun itself. Preliminary simulations conducted in Astra [4] indicate that the emittance of a spatially relatively uniform electron bunch is dependent on the shape of the photocathode laser pulse. In the case of a flat-top pulse shape with a finite rise-time, decreasing the rise time was predicted to reduce the emittance by up to 25%.

Our laser pulses are produced by a commercial laser system, which is capable of outputting 9 mJ infrared pulses at 790 nm, with a bandwidth of 25 nm. The laser system specifications have been summarized in Table 1. The infrared pulses are frequency tripled in a pair of β-BBO crystals, yielding ultraviolet pulses at 262 nm, with a photon energy of 4.7 eV, and a spectral bandwidth of 1.6 nm. Table 2 lists the UV pulse properties. These pulses are normally stretched to a duration of about 1.4 ps using a prism stretcher, and subsequently stacked to a final pulse duration of either 3ps or 6ps using birefringent α-BBO crystals [5]. The pulse energy is about 100 µJ on cathode. The laser setup is described in more detail in [6].

Table 1: IR Pulse Specifications

Parameter	Value
Central wavelength	790 nm
Bandwidth	25 nm
Pulse energy	9 mJ
Repetition rate	100 Hz

Table 2: UV Pulse Specifications

Parameter	Value
Central wavelength	262 nm
Bandwidth	1.6 nm
Pulse energy	1 mJ
Repetition rate	20 Hz

The stacked pulses are characterized using two-color cross-correlation, where the picosecond UV pulses are gated using the IR pulses that are left over from the tripling, whose duration is about 100 fs. The IR pulses thenselves are independently characterized in a second harmonic generation frequency resolved optical gating (SHG FROG). The pulses have a double Gaussian longitudinal profile, with a rise time of about 1 ps.

In order to produce picosecond pulses with a closer to a flat-top shape, we direct our pulses through a 4-f pulse shaper (Fig. 1). The pulse is first spectrally dispersed using a diffraction grating. A lens is placed a focal f length away from the grating (g=3846 mm^{-1}), collimating the dispersed beam, and focusing it in the Fourier plane a distance f away. A double knife edge in the Fourier plane can be used to cut out some of the spectral components, and acts as a simple amplitude mask. After the Fourier plane the setup is reversed, so the beam is first collimated by another lens and finally the spectral components are overlapped again using another

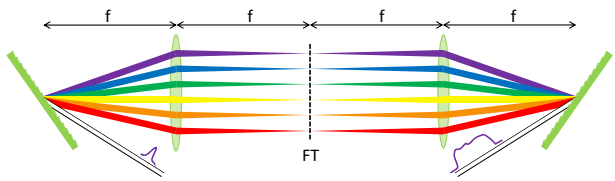


Figure 1: The principle of Fourier domain pulse shaping.

* marija.kotur@maxiv.lu.se

Content from this work may be used under the terms of the CC BY 3.0 licence (© 2018). Any distribution of this work must maintain attribution to the author(s), title of the work, publisher, and DOI.

ISBN: 978-3-95450-194-6 ISSN: 2226-0366 doi:10.18429/JACoW-LINAC2018-MOPO028

SURVEY AND ALIGNMENT SYSTEM OF 100 MeV/100 kW ELECTRON LINEAR ACCELERATOR

O. Bezditko, A. Zelinsky, I. Karnaukhov, M. Moisieienko, A. Mytsykov,
NSC KIPT, Kharkov, Ukraine

Abstract

For successful operation and working of electron linear accelerator of "NEUTRON SOURCE" driver it is necessary that all the acceleration sections, the quadrupole triplets, the quadrupole lenses, the dipole magnets, the scanning magnets and the chicane should be installed in design position according design parameters. Accuracies of all electromagnetic elements installation are 150 mkm for all three rotation freedom. The whole process, fiducialization and developing of survey net, alignment is controlled by laser tracker Leica AT 401.

INTRODUCTION

According to the design, to provide required electron beam parameters at the target, accuracies of NSC KIPT 100 MeV/100 kW electron linear accelerator electromagnetic element installations are 150 mkm in the transverse coordinate, 200 mkm in the longitudinal coordinate and 200 mrad for all three rotation freedom. The whole installation and alignment process is controlled by Leica Absolute Tracker AT401 [1]. The electromagnetic system of the linear accelerator consists of quadrupole lenses, quadrupole triplets, bending magnets and scanning magnets.

Leica Absolute Tracker AT401 is a portable coordinate measuring machine (CMM) that allows extreme precision over ultra large distances. The Leica Absolute Tracker AT401 are shown in Fig. 1.

All accuracies are specified with Leica Geosystems precision 1.5" Red Ring Reflectors and a measurement mode of 2 seconds per point under stable environmental conditions.

Full range is specified as 1.5 to 80 meters away from the laser tracker within a vertical range of +/- 45˚. All accuracies are stated in maximum permissible error (MPE).

Absolute Angular Performance:

Resolution: 0.07 arc Seconds

1. Accuracy (MPE): +/- 15 μm + 6 μm/m (+/- 0.0006" + 0.00007″/ft);
2. Repeatability (MPE): +/- 7.5 μm + 3 μm/m (+/- 0.0003″ + 0.00004″/ft);
3. Inclination Setting Accuracy (2σ): +/- 1 arc second.

Absolute Distance Performance:

1. Resolution: 0.1 μm;
2. Accuracy (MPE): +/- 10 μm (+/- 0.00039″).



Figure 1: The Leica Absolute Tracker AT401.

ACCELERATOR COORDINATE NET

For linear accelerator electromagnetic element installations a survey coordinate net was developed. The coordinate net was formed by 23 survey targets, that were installed on the walls and in the floor of accelerator tunnel and 4 survey targets were installed in the experimental hall. 23 survey target design is like nest with magnet for the red ring reflector installation. To develop the coordinate net it is necessary to identify and fix the coordinates of all survey targets along the accelerator tunnel in vertical plane considering the electron beam reference orbit as a longitudinal horizontal coordinate axis. The vertical coordinate axis is axis of the electron beam and the neutron-generating target interaction.The process of the survey targets coordinate measurements and fixations was carried out by the laser tracker with move station method. The move station method was used between every two neighbouring sections consist of at least 3 (or more) survey targets. Measuring coordinates of 3 survey targets in the previous group is necessary and sufficient for the transition to the measurement of the positions of the targets in the new group. Taking into account the number of survey targets (23) NSC KIPT 100 MeV/100 kW has 7 sets of target for the move station method. The process of coordinate determinations is shown Fig. 2.

Content from this work may be used under the terms of the CC BY 3.0 licence (© 2018). Any distribution of this work must maintain attribution to the author(s), title of the work, publisher, and DOI.

ISBN: 978-3-95450-194-6 ISSN: 2226-0366 doi:10.18429/JACoW-LINAC2018-MOPO029

PHYSICS DESIGN AND DYNAMIC SIMULATION OF A C-BAND PHOTOCATHODE ELECTRON GUN FOR UEM*

T.J. Chen, Y.J. Pei#, Z.X. Tang, W.M. Li
NSRL, University of Science and Technology of China, Hefei, China

Abstract

For discovering structure at atomic scale and getting more details of chemical material and biological tissue, an ultrafast electron microscopy (UEM) has been developed and applied in plenty of subjects and studies. This paper described a C-band photocathode electron gun which will be working at 5712 MHz to produce ultrashort electron beams with better dynamic parameters. The RF gun is using coaxial coupler to decrease the size of the gun and keep better symmetry of the field in the photocathode gun so that the beam emittance and energy spread can be reduce a lot. The photocathode rf gun will be an important part of the ultrafast electron microscopy (UEM). Using CST MWS and superfish code to simulate design the gun. After dynamic simulation, the beam parameters as the following: Energy is of 3MeV, Normal emittance of 0.12mm-mrad in both direction, energy spread is of 5.8×10^{-4}, which are better enough for an UEM.

INTRODUCTION

The electron microscope is a kind of useful experimental instrument for observing structure of chemical material and biological tissue and studying the composition of them at small length scale. The electron gun, which provides electron beams with high energy to probe materials, is the most important part in electron microscope and also determines the quality of projective images [1, 2]. Photocathode gun, field-emission gun and thermal emission gun are the most common kinds used in electron microscopes as the electron source. Photocathode gun, which could provide electron beams with much higher energy and better dynamic properties, is suitable for ultrafast electron microscope (UEM).

The UEM, which differs from the traditional electron microscope, uses ultrafast electron beams with higher energy from hundreds of keV to several MeV level as a probe to discover molecule structure. Besides, the ultrafast electron beams with short pulse of femtosecond level, could also be used to observe the dynamic process with high temporal resolution.

Due to breakdown limit, electron gun using direct current could only accelerate electrons to hundreds of keV, which would cause the expansion of dimension due to space charge effect [3-5]. Thus, radio frequency gun (RF gun) is chosen to be used to get electron beams with higher energy of MeV. With RF gun, the electron beams will be accelerated rapidly to near realistic speed, which will decrease space charge effect.

* Supported by National High-tech R&D Program (No.na8211009b).
Corresponding author (email: yjpei@ustc.edu.cn)

A solenoid magnet is used at the downstream of accelerating cavity to focus the electron beams and compensate the emittance of the electron beams so that the dynamic parameters of the exit beam of the photocathode gun will be improving. With emittance compensation, the emittance of both x and y plane would be decreased to the desired value [6].

In this research, CST Microwave Studio is used to simulate the 1.6-cell C-band gun cavity and optimize the structure of coaxial coupler. With smaller radius due to coaxial coupling, the solenoid could produce stronger magnetic field and will compensate the emittance much better. The magnetic field of solenoid is simulated and optimized to keep the dimension of electron beams and compensate emittance by using Parmela code. The dynamic parameters after optimization are calculated at the exit of the photocathode gun.

PHYSICS DESIGN OF THE PHOTOCATHODE

The photocathode gun consists of two parts: 1.6-cell accelerating cavity and waveguide coupler. The 1.6-cell cavity is designed and simulated by superfish code and CST MWS. Radius and shape of iris and length of cells are mainly optimized to get higher shunt impedance and cavity radius of half-cell and full-cell is adjusted to tune the frequency to working frequency of 5712 MHz. The result of 2D pi-mode field is calculated in superfish and the electric field along z-axis is showed in Fig. 1, which is used to accelerate electron beams.

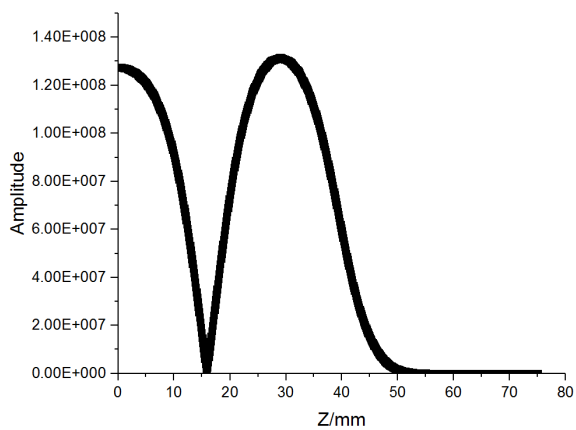


Figure 1: Ez of pi-mode along axis.

The coaxial coupler is adopted in this C-band gun to keep symmetry of field and decrease the radius of gun cavity to save space for solenoid in order to compensate emittance better. The coaxial coupler connects two rectangular waveguides and a coaxial transmission line.

Content from this work may be used under the terms of the CC BY 3.0 licence (© 2018). Any distribution of this work must maintain attribution to the author(s), title of the work, publisher, and DOI.

ISBN: 978-3-95450-194-6 ISSN: 2226-0366 doi:10.18429/JACoW-LINAC2018-MOPO034

DIELECTRIC WAVEGUIDE BASED THz RADIATOR STUDY FOR SwissFEL*

L. Shi†, F. Marcellini, S. Reiche, R. Ischebeck, A. Mittelbach,
S. Bettoni, V. Thominet, B. Hermann, E. Ferrari, M. Dehler
Paul Scherrer Institut, 5232 Villigen PSI, Switzerland

Abstract

THz pulses have many unique properties in terms of radiation matter interaction. In particular, their non-ionizing excitation of phonons in matter makes them a preferred pump for pump-probe studies at free-electron laser facilities. Among many THz generation techniques, the one based on dielectric lined waveguide and electron beam is emerging as a compact and powerful means for the THz generation. We will investigate the feasibility of this technique to produce narrowband pulses of 1-20 THz with above 100 µJ per pulse for SwissFEL. As a first step, we focus on the proof of principle experiments. This paper overviews the project with a focus on the numerical study of the dielectric lined waveguide, in terms of mode structure, energy, pulse length etc, which are essential parameters for the pump-probe experiments. These waveguides will be fabricated and tested in the near future at SwissFEL.

INTRODUCTION

THz radiations, which lie between approximately 1 and 20 THz, have multiple properties in terms of radiation matter interaction due to the unique spectroscopic signatures for a wide range of phenomena. In particular, their non-ionizing excitation of phonons in matter, which is important to understand the physiochemical as well as biological processes of condensed matter [1]. The dynamics of the excited states can be probed by the high brightness, ultrashort X-ray pulses available at free electron laser facilities [2].

Due to the appealing characteristics and the great potential applications of the THz radiation, there are ever-increasing efforts in generating THz [3], including but not limited to the methods based on the solid state oscillators, the quantum cascaded laser, the laser pumped solid state devices and accelerators etc. In this paper, we report on a THz radiator study based on a relativistic electron beam and a dielectric lined waveguide (DLW) [4]. Many experiments have been performed in the field in order to show the validity of this means of high power generation but they are normally limited to a few tens or hundreds GHz due to the quality and the length of the electron beam. We aim to demonstrate the generation of narrowband pulses in the range of 1-20 THz, which will require a rather small vacuum aperture for the electron beam to traverse. If demonstrated successfully, this narrowband THz source can be a strong candidate for the pump-probe setup aforementioned. Especially, the high power of these THz pulses would open new possibilities of experiments for the photon beamline users at SwissFEL (Swiss Free Electron Laser) [5].

SwissFEL is a less than one kilometer long free electron laser facility based on normal conducting RF technique as schematically shown in Fig. 1. It is able to generate ultrashort and ultra-bright soft and hard X-ray pulses simultaneously in the two undulator lines Athos and Aramis, respectively [5]. These are driven by the electron bunches from an RF injector followed by S and C-band RF accelerating structures.

To demonstrate the plausibility of the THz generation based on this method, the proof of principle beam test of the DLW will be carried out in the ACHIP vacuum chamber [6] in the switchyard of the Athos beamline. If this DLW based THz source can provide above 100 µJ per pulse, less than 10% bandwidth in the frequency range of 1-20 THz, we then plan to investigate further to propose a possible design implementation of such a DLW based device for the THz generation. By exploiting the electron bunches after the Aramis undulator right before the electron beam dump as indicated in Fig. 1 , the THz could be generated together with a DLW device without too much complication. This is essentially due to the insensitivity to the energy spread of the otherwise still bright blow-up electron beam. The THz could be transported to the ATHOS station before the soft X-ray pulse to form a pump-probe experiment setup.

THE DLW BASED THZ RADIATOR

An electromagnetic field is excited when a relativistic electron bunch traverses a DLW. The electromagnetic fields can be decomposed in multipole expansion into orthogonal modes. Among these modes, the monopole transverse magnetic modes, showing azimuthal symmetry, are of particular interest due to the strong coupling between the electron beam and its longitudinal field. By tailoring the geometry size of the DLW, radiation in the THz can be obtained. The mode can be guided out of the DLW and is the principal source of the THz radiation.

A sample DLW is shown in Fig. 2 and it consists of a vacuum channel ($0 < r < a$) for the electron bunch passage, and a dielectric layer ($a < r < b$), characterized by the relative permitivity ε_r, for slowing down the phase velocity of the mode to match it with the velocity of the electron bunch. The outer side of the DLW is coated with metallic material to enclose the radiation and to form a set of discrete electromagnetic modes. The total length L of the DLW governs the bandwidth and power of the THz pulses. In

* Work supported by Marie Curie Action H2020
† liangliang.shi@psi.ch

Content from this work may be used under the terms of the CC BY 3.0 licence (© 2018). Any distribution of this work must maintain attribution to the author(s), title of the work, publisher, and DOI.

ISBN: 978-3-95450-194-6 ISSN: 2226-0366 doi:10.18429/JACoW-LINAC2018-MOPO035

STATUS OF CLARA FRONT END COMMISSIONING

D. Angal-Kalinin[1†], A. D. Brynes[1], S. Buckley[1], R. Cash, R. F. Clarke, P. Corlett[1], L. S. Cowie[1], G. Cox, K. Dumbell[1], D. J. Dunning[1], C. Hodgkinson, P. Hornickel[1], F. Jackson[1], J. K. Jones[1], J. W. McKenzie[1], B. L. Militsyn[1], A. J. Moss[1], J. Murphy[1], T. C. Q. Noakes[1], M. D. Roper[1], D. J. Scott[1], B. J. A. Shepherd[1], R. J. Smith[1], E. Snedden[1], N. R. Thompson[1], C. Tollervey[1], D. A. Walsh[1], T. Weston[1], A. E. Wheelhouse[1], J. T. G. Wilson
STFC, Sci-Tech Daresbury, UK, also at [1]Cockcroft Institute, Sci-Tech Daresbury, Warrington, UK

Abstract

CLARA (Compact Linear Accelerator for Research and Applications) is a Free Electron Laser (FEL) test facility under development at Daresbury Laboratory. The progress in commissioning of the CLARA front end focussing on recent investigations into photoinjector (PI) drive laser transport and development/commissioning of high level software scripts are presented.

INTRODUCTION

CLARA is a proposed 250 MeV FEL test facility [1] based at Daresbury Laboratory. The test facility has been designed to test advanced FEL concepts and capabilities for next generation X-ray FELs as well as to provide high brightness beam to academic and industrial users. CLARA is intimately linked to the VELA facility based on the RF photocathode gun, which was commissioned in 2013 and successfully delivered beam to academic and industrial users from 2013-2015 [2]. During 2016-2017, the Front End of CLARA has been installed in the accelerator hall. This consists of a 10 Hz S-band RF gun [3] and a S-band Linear accelerator Linac1. An S-bend incorporating the spectrometer dipole, a quadrupole triplet and a Lozenge dipole transports high energy beam from CLARA FE to the existing VELA beam line. The 10 Hz RF gun, earlier used on VELA is now installed on the CLARA beam line. First results of CLARA Front End commissioning were reported at IPAC18 [4]. This paper gives an update since May 2018 on investigations into PI laser transport and future plans as well as problems in linac wave guide and the remedial actions taken. The progress in commissioning of high level software scripts with beam is presented.

PHOTOINJECTOR LASER TRANSPORT INVESTIGATIONS AND PLANS

Systematic investigation of the laser system (10 mJ Ti:Sapphire, 80 fs @ 10 Hz; frequency tripling from 800 to 266 nm through harmonic generation in consecutive BBO crystals) and transport have been performed with three primary goals: 1) to increase the total UV pulse energy reaching the photocathode and facilitate >100 pC charge extraction from the Cu photocathode; 2) understand and mitigate factors responsible for deterioration of the laser transverse profile (nominally Gaussian); and 3) replace a number of contaminated and damaged optics along the UV transport line.

After optimisation the third harmonic generator at saturation now yields 850 μJ pulse energy at 266 nm. An additional 20% gain in transport efficiency has been obtained by moving the pulse energy control from the UV directly (previously performed using a UV half-wave plate and pair of Brewster polarisers for rejection) to the near infrared (NIR) by exploiting the polarisation sensitivity of the sum-frequency generation process.

Visible contamination of exit face of the sum frequency crystal and first four mirrors in the UV transport line is responsible for a significant decrease in transport efficiency (as much as 40%). The mirror contamination is largely reversible through standard cleaning procedures which must be performed weekly to maintain reasonable transport efficiency. Surface analysis of the contamination reveals primarily hydrocarbon components, likely formed through UV-induced breakdown.

Laser transport consists of relay imaging of a truncated Gaussian beam from an aperture in the Photoinjector Laser Laboratory to the cathode. Investigations have revealed damage to optics in the transport plane due to hot spots in the UV beam profile. These hot spots are generated at source and are not a function of the transport optics. We believe these hot spots originate due to variation in the NIR profile following single-pass amplification (as a result of damage to the Ti:Sapphire crystal), which is then effectively amplified through harmonic generation.

To mitigate damage due to hot spots and improve the transverse profile, a UV-based vacuum spatial filter has been designed with a view to implementation early 2019. With the hot spots removed, an aspheric lens beam shaper will be used to generate a flat-top transverse profile as required for CLARA beam physics.

ISSUES WITH LINAC WAVEGUIDE

Linac1 is a two meter S-band travelling wave linac, and has been in operation on CLARA since November 2017. The waveguide system is operated with 3 bar of SF6 and has a circulator after the klystron. The waveguide is sealed with CPR flat and grooved flanges which seal on a rubber gasket. The klystron power for the system is 35 MW, giving 45 MeV/c of measured momentum gain from the linac. In June 2018 the beam momentum jitter measured on CLARA increased dramatically, and the forward power pulse measured just before the linac was discov-

† deepa.angal-kalinin@stfc.ac.uk

Content from this work may be used under the terms of the CC BY 3.0 licence (© 2018). Any distribution of this work must maintain attribution to the author(s), title of the work, publisher, and DOI.

ISBN: 978-3-95450-194-6 ISSN: 2226-0366 doi:10.18429/JACoW-LINAC2018-MOPO036

STATUS OF THE 10MW MBKS DURING COMMISSIONING OF THE EUROPEAN XFEL IN DESY

Vladimir Vogel, Lukasz Butkowski, Stefan Choroba, Andrey Cherepenko and Jens Hartung
DESY, 22607 Hamburg, Germany

Abstract

At present 26 RF stations for European XFEL are in operation. Each RF station consists of a HV modulator located in a separate building on the DESY campus, up to 1600 m long 10 kV HV cables that connect the modulator and the HV pulse transformer located in the underground tunnel, 120kV, 3 m long HV cable connecting the HV pulse transformer and the connection module (CM) of the horizontal multi-beam klystron (MBK). The klystron can produce RF power up to 10 MW, at a RF frequency of 1.3 GHz, 1.5 ms pulse length and 10 Hz repetition rate. Two RF stations of the injector have already got about 24000 hours of operation, RF stations of the XFEL bunch compressor area have operated up to 13000 hours and the klystrons in the XFEL main linac already have about 11000 hours of operation (Status August 2018). To increase the lifetime of the klystrons, we use a fast protection system (KLM) that is based on the comparison of the actual RF shape and the expected RF shape. In the case of a difference exceeding a certain margin, for example, in the case of RF breakdown in a klystron or RF breakdown in a waveguide system (WGS), the KLM quickly, shorter than 800 ns, switches off the input RF signal. Thus, it does prevent the vacuum level in the klystron worsen too much or it minimizes the RF overvoltage time at the output windows of the klystron in case of breakdown in WGS. In this article we will give a summary of the present klystron status including the numbers of HV klystron gun and RF arcs in the klystrons.

INTRODUCTION

The European X-ray Free-Electron Laser (XFEL) [1] can be operated up to energy of 17.5 GeV (July 2018). Currently up to 300 coherent laser pulses per second with duration of less than 100 fs and with photon energy up to 19.1keV are delivered to the experiments. In future the number of pulses will increase to the design value of 27000 per second. For the production of these laser pulses, electrons have to be accelerated using a 2 km long accelerator based on superconducting radio frequency (RF) technology. For the XFEL project for a source of RF power of 26 RF stations were chosen the series horizontal MBKs made by two companies: MBK TH1802 from "Thales" [2 and 3] and MBK E3736H from "Toshiba" [4 and 5]. Both types of MBKs were equipped with CMs [6 and 7] and 3 meter long HV cables, and then they were tested on DESY MBK test stands [8]. The test was done with full RF power of 10 MW, full RF pulse length of 1.5 mS and with repetition rate of 10 Hz. Two types of HV cables and HV connectors were tested. Big advantages of using CM and HV cable connection between MBK and HV transformer are that we don't have to work with the open transformer oil during MBK installation in the tunnel and that MBK and WGS can be easy connected together. CM has monitors for the measurement of klystron voltage and cathode current. Figure 1 shows the one of 24 RF stations in the XFEL tunnel.



Figure 1: XFEL tunnel view.

Since 2013 the commissioning of the first RF station for XFEL injector has been started. In 2015 the second RF station started operation for the first cold AC module and since 2016 the commissioning of the main part of linac has been started.

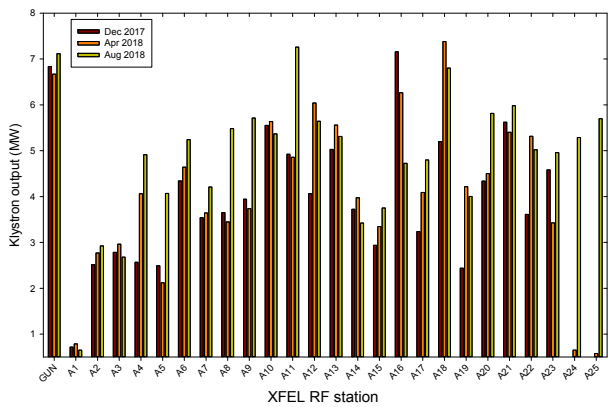


Figure 2: Output power for each of MBK.

In beginning of 2018 the commissioning of last two RF stations was done and in July 2018 the XFEL reached the design energy of 17.5 GeV. Figure 2 shows the output RF power for each of RF station. The average power from one MBK is 4.87 MW, but for several of RF stations the level of output power are more than 7 MW. Figure 3 shows the high voltage level for each of RF stations. In average the high voltage is 104.5 kV. For the moment we don't have any limitation for XFEL operation from RF

Content from this work may be used under the terms of the CC BY 3.0 licence (© 2018). Any distribution of this work must maintain attribution to the author(s), title of the work, publisher, and DOI.

ISBN: 978-3-95450-194-6 ISSN: 2226-0366 doi:10.18429/JACoW-LINAC2018-MOPO037

SRF GUN DEVELOPMENT AT DESY

Elmar Vogel, Jacek Sekutowicz, Serena Barbanotti, Ingmar Hartl, Kay Jensch, Daniel Klinke, Denis Kostin, Wolf-Dietrich Moeller, Manuela Schmoekel, Sven Sievers, Nicolai Steinhau-Kuehl, Alexey Sulimov, Jan-Hendrik Thie, Birte van der Horst, Hans Weise, Lutz Winkelmann, DESY, Hamburg, Germany
John Smedley, BNL, Upton, Long Island, NY, USA
Jochen Teichert, HZDR, Dresden, Germany
Mateusz Wiencek, IFJ-PAN, Kraków, Poland
Jerzy Andrzej Lorkiewicz, Robert Nietubyc, NCBJ, Świerk/Otwock, Poland

Abstract

A future upgrade of the European XFEL (E-XFEL) foresees an additional CW operation mode, which will increase the flexibility in the photon beam time structure [1–3]. One of the challenges of this operational mode is the need for a CW operating photo injector. We believe that using an SRF gun is the preferred approach as the beam parameters of normal conducting pulsed guns can be potentially met by SRF guns operating CW. For more than a decade DESY, in collaboration with TJNAF, NCBJ, BNL, HZB and HZDR, has performed R&D to develop an all superconducting RF gun with a lead cathode. In the frame of E-XFEL CW upgrade feasibility studies, the SRF-gun R&D program gained more attention and support. Within the next few years we would like to demonstrate the performance of the all superconducting injector required for the E-XFEL upgrade. The selected approach offers advantages w.r.t. the cleanliness of the superconducting surface, but requires a complete disassembly of a cryostat and stripping the gun cavity in a clean room to exchange the cathode. Thus it is practical only when the life time of the cathode is at least several months. In this paper we present the actual status of the R&D program, next steps and the longer term plans.

INTRODUCTION

At present, the high brightness beams required for the E-XFEL are reliably generated by normal conducting (NC) pulsed RF gun technology [4]. The NC CW gun technology developed by LBNL has been chosen as baseline for LCLS-II, operating CW, because SRF guns have not yet demonstrated reliable operation [5]. In contrast to LCLS-II the schedule of the future upgrade of the E-XFEL permits some development time to demonstrate reliable operation of SRF guns. Table 1 contains a comparison of the basic parameters of the three technologies.

ALL SUPERCONDUCTING GUN

RF guns are commonly first installed and aligned to the subsequent accelerator components before inserting cathodes via cathode insertion systems. This approach permits a quick exchange of cathodes but faces challenges at ultra-clean superconducting (SC) cavities w.r.t. cathode heating, cathode lifetime, field emission and multipacting. R&D is still required and ongoing, e.g. performed at HZDR [6–8] and HZB [9–11]. Work on SRF guns performed elsewhere can be found in [12].

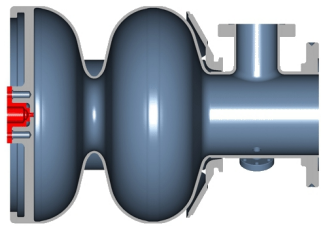


Figure 1: All superconducting gun with a plug (red) with lead cathode screwed into a hole on the cavity backside.

Since more than a decade DESY in collaboration with TJNAF, NCBJ, BNL, HZB and HZDR performs R&D to develop an all superconducting RF gun, e.g. see [13–17]. The recent design foresees a plug with a lead cathode screwed in a clean room into a hole on the cavity backside and sealed with indium, Fig. 1. Doing so, the cavity can be cleaned after the cathode insertion, and possibly lost cathode particles should not heat and quench the cavity, as they are all superconducting. In contrast to setups with cathode insertion systems, exchanging cathodes requires a complete disassembly of the cryostat and bringing the gun cavity back into the clean room. Consequently, this approach requires reasonable long cathode lifetimes above 100 days.

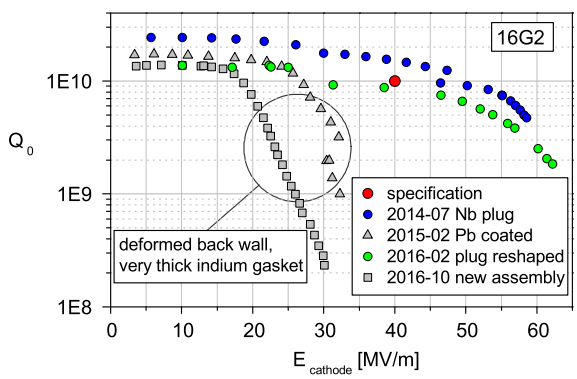


Figure 2: Promising vertical test results of the first prototypes of an all superconducting gun.

Content from this work may be used under the terms of the CC BY 3.0 licence (© 2018). Any distribution of this work must maintain attribution to the author(s), title of the work, publisher, and DOI.

ISBN: 978-3-95450-194-6 ISSN: 2226-0366 doi:10.18429/JACoW-LINAC2018-MOPO038

RF OPERATION EXPERIENCE AT THE EUROPEAN XFEL

J. Branlard†, V. Ayvazyan, Ł. Butkowski, M. Grecki, M. Hierholzer, Mar. Hoffmann, Mat. Hoffmann, M. Killenberg, D. Kostin, T. Lamb, L. Lilje, U. Mavrič, M. Omet, S. Pfeiffer, R. Rybaniec, H. Schlarb, C. Schmidt, N. Shehzad, V. Vogel, N. Walker, DESY, Hamburg, Germany

Abstract

After its successful commissioning during the first half of 2017, the European X-ray free electron laser is now in regular operation delivering photons to users since September 2017.

This contribution presents an overview on the experience gathered during the first couple of years of operation. In particular, the focus is set on RF operation, advanced commissioning and RF related machine studies.

INTRODUCTION

The European X-ray free electron laser (XFEL) is a user facility delivering ultra-short hard and soft X-ray flashes with the highest brilliance worldwide, through 3 undulator lines and serving up to 6 experiments. It is based on a 10 Hz pulsed 17.5 GeV superconducting linac, commissioned since 2017. The first self-amplified spontaneous emission (SASE) light was demonstrated in May 2017, the first user run took place in September 2017 delivering photons at a wavelength of 1.3 Å. After a month shutdown in April 2018, the last 2 RF stations were commissioned. In May 2018, lasing was demonstrated simultaneously in all 3 beam lines (SASE 1, 2 and 3). A total of 1600 hours are devoted to user programs in 2018; this number should increase to 4800 hours in 2019. A summary on the machine commissioning and its highlights is given in [1, 2]. In this contribution, the focus is set on the experience gathered during the first operation years of the XFEL, in particular the commissioning of the LLRF system beyond its basic functionality, reported in the following section and an insight on a couple of dedicated machine studies is given in the subsequent section.

LLRF ADVANCED COMMISSIONING

The LLRF commissioning procedure was first presented in [3], and the accelerator operation and performance was reported in [4]. These commissioning steps guaranteed the proper operation of all RF stations, controlling the RF field inside the superconducting cavities and accelerating the beam to the desired energy. The advanced LLRF commissioning covers taking into operation LLRF subsystems related to performance optimization such as the drift compensation module [4], or modules related to more advanced exception handling mechanism such as the klystron lifetime management system (KLM) [5]. Figure 1 gives an example of this protection mechanism where a sudden increase in reflected power (P_{REFL}) was observed on one arm of the 10 MW klystron. This anomaly was detected within 200 nsec and resulted in switching off the drive 600 nsec later, preventing a high reflected waveform potentially harmful for the klystron. The increase in P_{REFL} is likely due to waveguide sparking, which started appearing when operating the klystron above 7 MW.

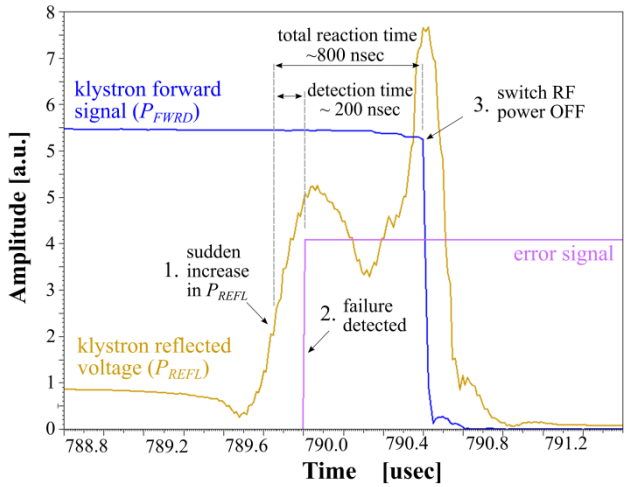


Figure 1: Event observed on August 29th 2018 at station A6. A sudden increase of the reflected power (1) triggered the klystron management system (2) to stop the klystron drive (3).

During this advanced commissioning phase, servers to monitor and service LLRF auxiliary modules were also deployed and commissioned (modules responsible for the local oscillator and clock generation, for the power supplies, for the remote controllable fuse and relay submodules or for the piezo driver for example). During this phase, firmware and server updates were deployed to improve the performance of the LLRF system. One can cite the toroid-based beam loading compensation algorithm as an example [6]. The optical RF synchronization (REFM-OPT) module was also taken into operation. This module synchronizes the 1.3 GHz RF reference distributed along the accelerator with respect to sub-fs stabilised optical links. Based on a Mach-Zender modulator, the REFM-OPT compares the phases of the optical link and RF signals and corrects for any drifts taking place in the RF distribution chain [7]. The re-synchronized RF is distributed locally to the nearest RF stations. The plot in Fig. 2 shows the temperature drift measured in the Linacs 1, 2 and 3 and the corresponding phase corrections applied by the different REFM-OPT units along the accelerator. Although there were no temperature data available for the injector, the tighter ambient temperature regulation in the injector directly translates into smaller reference phase corrections required from the injector REFM-OPT.

† julien.branlard@desy.de

Content from this work may be used under the terms of the CC BY 3.0 licence (© 2018). Any distribution of this work must maintain attribution to the author(s), title of the work, publisher, and DOI.

ISBN: 978-3-95450-194-6 ISSN: 2226-0366 doi:10.18429/JACoW-LINAC2018-MOPO039

STATUS UPDATE OF THE FAST ENERGY CORRECTOR CAVITY AT FLASH*

S. Pfeiffer†, J. Branlard, Ł. Butkowski, M. Hierholzer, M. Hoffmann, K. Honkavaara, H. Schlarb, C. Schmidt, S. Schreiber, M. Vogt, J. Zemella, DESY, 22607 Hamburg, Germany
M. Fakhari, Department of Physics, Universität Hamburg, 20355 Hamburg Germany

Abstract

Linear accelerator facilities driving a free-electron laser require femtosecond precision synchronization between external laser systems and the electron beam. Such high precision is required for pump-probe experiments and also for example for the electron bunch injection into a plasma bubble for laser plasma acceleration. An upgrade of the fast intra-train beam-based feedback system is planned at the Free-Electron Laser FLASH in Hamburg, Germany. This linear accelerator is based on superconducting (SRF) technology operating with pulse trains of maximum 1 MHz bunch repetition rate. Arrival time fluctuations of the electron beam are correctable by introducing small energy modulations prior to the magnetic bunch compressor. This contribution focuses on the design and the characterization of a normal-conducting RF (NRF) cavity with large bandwidth, mandatory to correct fast arrival time fluctuations. The cavity has recently been installed in the FLASH beamline. First measurements with the new cavity will be presented.

INTRODUCTION

The Free Electron LASer at Hamburg (FLASH) is a facility for research with tunable laser light in the X-ray range [1]. It delivers to its users a pulsed light with tunable wavelength down to 4.2 nm generated by SASE processes. Electron bunch trains of variable length and frequency with a repetition rate of 10 Hz are accelerated to a maximum energy of 1.2 GeV. Each pulse is enabled for about 1.4 ms while up to 800 bunches with a repetition rate of 1 MHz are injected. Providing stable and reproducible photon pulses needs a precise acceleration field control. During the last years additional control strategies were developed and included in the LLRF controller. This includes RF-field control and its superposition with beam-based information using the bunch arrival time and bunch compression information, [2–4]. By this the stability of the bunch arrival time at the end of the main accelerator could be improved, highly important e.g. for the precise synchronization between an external laser system and the electron beam [5]. To further improve the arrival time a fast energy corrector cavity prior to the bunch compressor is needed. This corrector cavity should be operated in the upper kHz bandwidth. The technical design and specifications for the fast corrector cavity named BACCA (Bunch Arrival Corrector CAvity) are given in [6].

DESIGN OF THE CAVITY

The basis for the design was the buncher cavity at the *Relativistic Electron Gun for Atomic Exploration* (REGAE) accelerator facility [7]. The main difference is the power coupling to the cavity. Due to longitudinal space constraints for the installation at FLASH this is realized by magnetic coupling, i.e. coupling loop instead of coaxial coupler. Figure 1 shows the first 3D drawing of the cavity with the beamline connection and the feedthroughs hosting the loops for magnetic coupling.

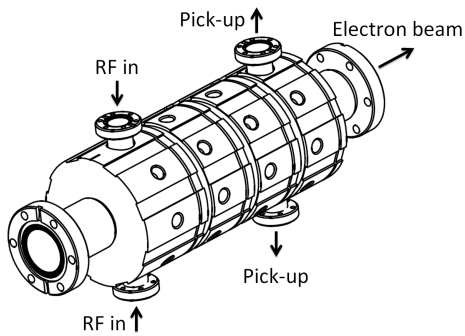


Figure 1: Technical design of the 4-cell fast corrector cavity with the 2 beamline flanges and the 4 feedthroughs for RF input and output loops/pickup.

The main design requirements are given as maximum energy correction of about 50 keV, a maximum feedback loop latency of 700 ns and a corrector cavity half bandwidth of 500 kHz. Furthermore, longitudinal and transverse wakefields as well as orbit changes for multi bunch operation should not occur during operation.

There is a trade-off between the accelerating voltage and the bandwidth of the corrector cavity as a function of the coupling constant [8]. The thermal stress to the input loop has been simulated justifying the power distribution with 2 input loops, [9]. Two output loops, i.e. the probe pickups, are used for symmetry reasons. The NRF cavity cells were produced at the Hansa Press- und Maschinenbau GmbH in Hamburg, Germany. Its assembly and the soldering of all parts were done at DESY. The assembled corrector cavity is shown in Fig. 2 with its 4 feedthroughs; 2 for in-coupling and 2 for the pick-up antennas.

CHARACTERIZATION OF THE CAVITY

The corrector cavity has been characterized and tuned for resonance after production. First we were driving the cavity with a test signal from the network analyzer via the input loop

* The work is part of EuCARD-2, partly funded by the European Commission, GA 312453.
† sven.pfeiffer@desy.de

Content from this work may be used under the terms of the CC BY 3.0 licence (© 2018). Any distribution of this work must maintain attribution to the author(s), title of the work, publisher, and DOI.

ISBN: 978-3-95450-194-6 ISSN: 2226-0366 doi:10.18429/JACoW-LINAC2018-MOPO040

COHERENT SYNCHROTRON RADIATION MONITOR FOR MICROBUNCHING INSTABILITY IN XFEL

J. H. Ko, I. S. Ko, POSTECH, Pohang, Korea
G. J. Kim, C. Kim, H. -S. Kang, Pohang Accelerator Laboratory, Pohang, Korea

Abstract

The microbunching instability is an important issue in an X-ray Free Electron Laser (XFEL) [1-4]. In Pohang Accelerator Laboratory X-ray Free Electron Laser (PAL-XFEL), the CCD camera installed in the accelerator tunnel at Coherent Radiation Monitor. The CCD camera measured the Coherent Synchrotron Radiation which made from the electron bunch compressor. This facility is called the Coherent Synchrotron Radiation (CSR) monitor. The CSR monitor measured the CSR and used for the microbunching instability measurement tool.

INTRODUCTION

The X-ray Free Electron Laser of the Pohang Accelerator Laboratory (PAL-XFEL) can produce a 0.1 nm wavelength XFEL [5]. The electron beam of the 150 pC charge is generated in the photo-cathode RF gun with an ultraviolet (UV) laser pulse. The generated electron bunch is accelerated by the 4 accelerating columns, and the electron bunch accelerated to 10 GeV energy. Moreover, four magnetic bunch compressor installed next to the accelerating column 1, 2, and 3 and soft x-ray part. Each electron bunch compressor has the coherent radiation monitor (CRM). The coherent radiation generated by the dipole magnet of the bunch compressor. They are synchrotron radiation and edge radiation. Also, another coherent radiation produced by a mirror with a hole in the middle which is called the diffraction radiation [6,7]. The PAL-XFEL structure is shown in Fig. 1. In the CRM, the pyro-electric detector is installed to detect the THz range coherent radiation. Using the pyro-electric detector, we can measure the THz range of coherent radiation, and it related with the electron bunch length. However, the measurement result of the pyro-electric detector in the very short electron bunch length range shows the saturation result. So, we need shorter electron bunch length range measurement tool. For this purpose, we installed the CCD camera in the CRM. In the CRM, we installed the moving stage then we can choose the CCD camera and pyro-electric detector. The CRM structure is shown in Fig. 2.

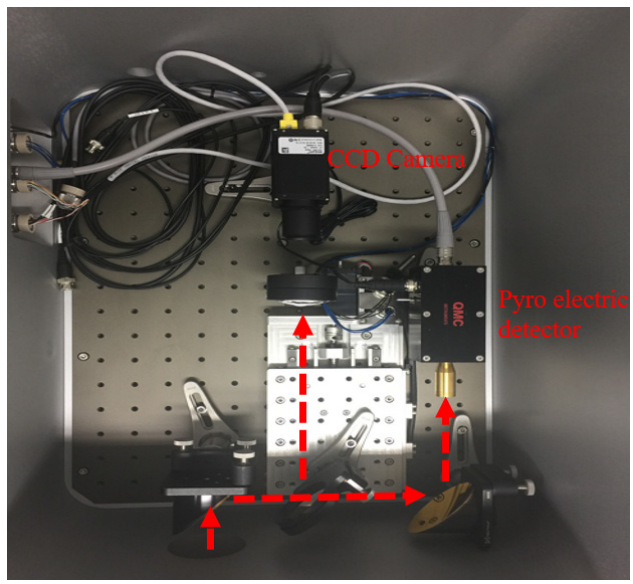


Figure 2: CRM structure.

The CCD camera is called the coherent synchrotron radiation (CSR) monitor, and it is detected the visible range radiation. The detecting radiation image is shown in Fig. 3. The visible range radiation made from the shorter longitudinal structure than the longitudinal structure of the THz radiation range. So, we can conclude that the visible radiation is related to small longitudinal structure such as the microbunching state.

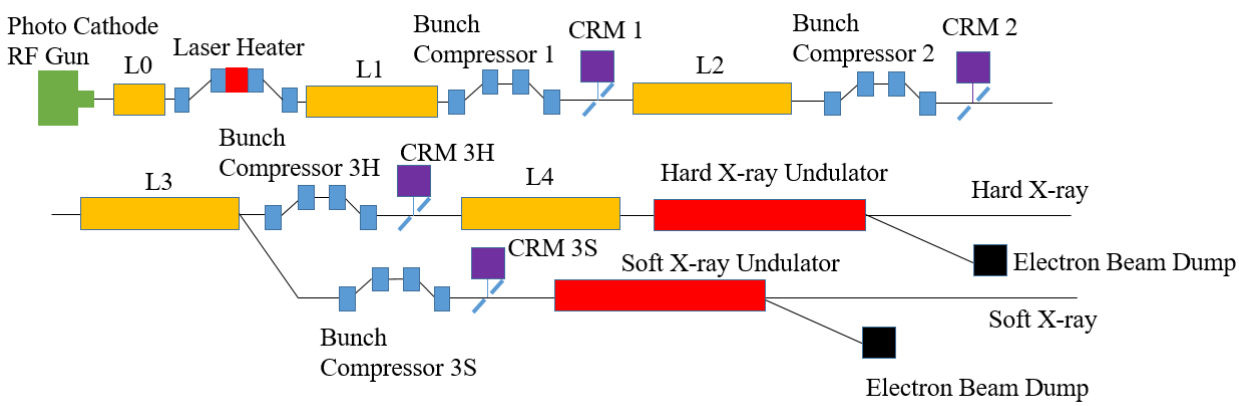


Figure 1: Schematic structure of PAL X-FEL.

Content from this work may be used under the terms of the CC BY 3.0 licence (© 2018). Any distribution of this work must maintain attribution to the author(s), title of the work, publisher, and DOI.

ISBN: 978-3-95450-194-6 ISSN: 2226-0366 doi:10.18429/JACoW-LINAC2018-MOPO041

PERFORMANCE TEST RESULTS OF MAGNET POWER SUPPLY*

K. H. Park†, S. H. Jeong, Y. G. Jung, D. E. Kim, H. S. Suh, H. G. Lee, S. B. Lee, B.G. Oh, M. J. Kim and J. H. Han, PAL, POSTECH, Pohang, Korea

Abstract

A high stable magnet power supply (MPS) was developed, which was a bipolar type with 200 A of the output current at the 36 V of output voltage. The MPS has been implemented by the digital signal processing technology using the DSP, FPGA, ADCs and so on. The output current stability of the MPS showed about 6 ppm peak-to-peak in a short term experiment at its full 200 A output current. The long term stability was shown in 15 ppm peak-to-peak for 10 hours at 200 A. And the others experimental results about the MPS were shown in this paper.

INTRODUCTION

The particle accelerator needs a highly stable magnet power supply (MPS) to assure the stable beam dynamics. A MPS must provide high-stability output current, fast response, high reliability, etc. It should also be easy to maintain. The stability and accuracy of the MPS are very important specifications because they directly affect the beam dynamics of the accelerator operation. Nowadays the MPS is developed by switching mode type using FET or IGBT devices that are controlled by a digital signal processor (DSP). This design is efficient, small, light-weight, and has good dynamic response but switching-mode MPS generates electrical noises whenever switching devices are turning on or turning off because of their generally high switching voltage and current. The short-term stability of the MPS is affected by the several causes which come from the control loop responses, surrounding switching noise, analog signal processing including ADC circuits, and so on [1]. Ripple components of the input rectifier are also one of the sources which make MPS stability worse [2]. The one of the cause of the long-term stability of the MPS comes from the temperature drift of components in MPS. Improper ground configurations can provide the path on which noise can propagate from its source point to all over the system. These components are very small but can degrade the performances of an analog-to-digital converter (ADC) circuits with the fine voltage fluctuation.

This paper describes the design schemes of the MPS. The results of the various experiments such as short term stability, long term stability, repeatability and step responses were showed.

SYSTEM CONFIGURATION

The developed MPS was divided into three parts as shown in the Fig. 1. The first is a rectifier to make DC link voltage. The second is the two power stacks which has the current driving capacity of 100 A, respectively. Thus two power stacks are operated in parallel to increase the current driving capability. The last is digital controller configured with DSP TMS320F28335 from TI [3].

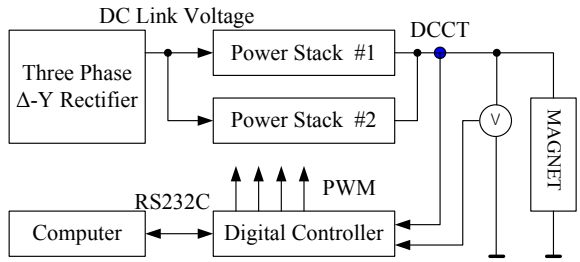


Figure 1: The block diagram of the developed MPS.

The rectifier to make DC link voltage with low ripple components was assembled. The primary winding of the transformer was configured with three phase in Wye configuration for AC 380 V. The secondary winding is consisted of two configurations of the Wye and Delta. The output voltage of the each winding on the secondary side is 33 V, respectively. They are fully rectified by the twelve diodes and connected in series to make DC link voltage of 66 V. Two diode modules of SEMIX341D16s from SEMICRON Co. were assembled on the water cooled aluminium plate. The input rectifier has an inductor of 1 mH to compose the input filter with the capacitor bank, 12000 μF x 4, in two power converter modules, respectively.

The performances of the ADC were very important part for the high stable MPS. The circuits of around ADCs for the MPS should have a good signal to noise ratio. The major specifications when the ADC was chosen were the throughput, resolution, input range, interface, DC accuracy, and so on [4]. Two different types of ADCs were tested to confirm their performances under the same conditions. The first one is the AD7690 from Analog Devices that is 18-bit resolution. The tested effective resolution of this ADC showed only 10-bit. The 8-bit in 18-bit was meaningless. The last one is the AD977 from also Analog Devices showed the effective resolution of 12-bit in spite of the 16-bit resolution in the given specification. These test results showed sometimes worse resolution than that of the datasheets. It might be depended on design scheme of the ADC and the conditions around circuits such as reference voltage source type, supply voltage and ground conditions, etc. The higher resolution than 16-bit in ADC may be meaningless because the ground thickness was about 1mV in general analog and digital mixed circuits. It was corresponding to nearly 1-bit at 10 V reference voltage.

Two types of ADC daughter boards for the MPS were developed as in the Fig. 2. The type 1 ADC board was to

*Work supported by Ministry of Science and ICT
†pkh@postech.ac.kr

Content from this work may be used under the terms of the CC BY 3.0 licence (© 2018). Any distribution of this work must maintain attribution to the author(s), title of the work, publisher, and DOI.

ISBN: 978-3-95450-194-6 ISSN: 2226-0366 doi:10.18429/JACoW-LINAC2018-MOPO042

EVOLUTIONARY MANY-OBJECTIVE OPTIMIZATION ALGORITHM FOR LARGE-BANDWIDTH FREE-ELECTRON-LASER GENERATION

J. W. Yan[1,2], H. X. Deng[1*],
[1]Shanghai Institute of Applied Physics, Chinese Academy of Sciences, Shanghai 201800, China
[2]University of Chinese Academy of Sciences, Beijing 100049, China

Abstract

X-ray free-electron lasers (XFELs) are leading-edge instruments in a wide range of research fields. Besides pursuing narrow bandwidth FEL pulses, the large-bandwidth XFEL pulses are very useful in various spectroscopy experiments, multi-wavelength anomalous diffraction, and X-ray crystallography. Overcompression operation scheme can be utilized to generate electron beams with large energy chirp which is benefit for bandwidth broadening. Recently, an evolutionary many-objective (having four or more objectives) algorithm, NSGA-III, was used to optimize the electron beam parameters in the overcompression including energy chirp, energy spread, current profile, peak current, and projected emittance. In this paper, combining with the Xie's semianalytical estimate formula, the NSGA-III is utilized to find an optimal working point of linac by optimizing the XFEL pulse properties directly. Start-to-end numerical simulations based on the Shanghai soft X-ray Free-Electron Laser user facility parameters demonstrate that a full bandwidth of 4.75% can be generated.

INTRODUCTION

X-ray free electron lasers (XFEL) are capable of providing x-ray pulses with high peak brightness, narrow bandwidth spectrum and ultra-fast time structure. Besides pursuing narrow bandwidth XFEL pulses, large-bandwidth XFEL pulses are demanded for several certain types experiments such as X-ray absorption spectroscopy, multi-wavelength anomalous diffraction and X-ray crystallography.

The FEL wavelength is decided by the resonance condition [1]:

$$\lambda = \frac{\lambda_u}{2\gamma^2}(1 + \frac{K^2}{2}), \quad (1)$$

where λ_u is the undulator period length, γ is the mean Lorentz factor of the electrons, and K is the undulator field parameter. Therefore, the XFEL bandwidth is related to the electron beam energy chirp and the undulator field parameters. In principle, making different parts of a transverse tilted electron beam experience different magnetic fields [2, 3] or utilizing an energy-chirped electron beam can broaden the XFEL bandwidth. While the beam tilt always needs additional hardware elements like the transverse deflecting structure or de-chirper device. The beam energy chirp can be achieved by just changing operation parameters of the acceleration sections. One natural way to obtain energy chirp is to let the electron bunch be accelerated at the off-crest phase, however, it at the cost of the beam energy. Overcompression [4–7] is a promising scheme to increase correlated energy spread of electron beams. In this scheme, electron bunches are overcompressed in one bunch compressor and the sign of the energy chirp of the electron bunches are changed. Therefore, the wakefields of the subsequent rf structures will increase the beam energy chirp. One of the crucial problem for the overcompression scheme is how to find an optimal working point of the linac where electron beams can generate XFEL pulses with large bandwidth while other properties like pulse energy and power profile can be maintain. The recent paper [7] utilized an evolutionary many-objective algorithm, NSGA-III [8], to optimization electron beam parameters and analyze the dependencies between these parameters. However, the optimization of the electron beam is difficult to analyze the relations between radiation pulse properties, which is also important for exploring the limitations of an operation scheme. As an extended work, in the following sections, based on the Shanghai soft x-ray free-electron laser (SXFEL) user facility [9] parameters, the NSGA-III is used to optimize the XFEL pulse properties directly.

OPTIMIZATION STRATEGY

The SXFEL user facility is under construction at Shanghai, which is the first X-ray FEL in China. The SXFEL user facility consists of a two-stage seeded FEL line and a SASE line. This optimization is to design the large-bandwidth mode for the SASE line. The layout of the SXFEL user facility linac and the SASE line are presented in Fig. 1. 0.5 nC electron beams are generted and accelerated to 130 MeV in the injector. Downstream of the injector are the main linac including one S-band (L1), one X-band (LX), and two C-band (L2, L3) accelerating sections. And there are two magnetic chicanes between these accelerating sections to further compress the electron bunches. To let the overcompressed electron beam be accelerated in more rf structures, turning off the second bunch compressor and utilizing single bunch compressor are considered in this optimization. To produce high qualities XFEL pulses, angle of the first bunch compressor, phases and voltage of the L1 and LX are selected as optimization variables. The corresponding optimization objectives are pulse energy, bandwidth, and power distribution.

In this optimization, the ASTRA and ELEGANT are used to tracking electron beams in the injector and main linac separately. The calculation of the objectives are based on the ELEGANT simulations where one hundred thousand

* denghaixiao@sinap.ac.cn

Content from this work may be used under the terms of the CC BY 3.0 licence (© 2018). Any distribution of this work must maintain attribution to the author(s), title of the work, publisher, and DOI.

ISBN: 978-3-95450-194-6 ISSN: 2226-0366 doi:10.18429/JACoW-LINAC2018-MOPO058

INDUSTRIAL ELECTRON LINEAR ACCELERATOR R&D IN CIAE

Jinghe Yang †, Guolong Yu, Zhibin Zhu, Ziqiang Zeng,China Institute of Atomic Energy, Beijing, China

Abstract

Electron linear accelerator(E-LINAC) is a vital accelerator type for accelerator applications, which widely applied in industry, agriculture and medical industry. The paper introduces R&D of industrial E-LINAC in China Institute of Atomic Energy (CIAE), including electron gun, modulator, accelerating tube, assembling and testing. Based on these R&D results, the GT series for non-destructive test (NDT) and FZ series for radiation processing are developed successfully. At present these E-LINACs play important roles in pressure vessel inspection, food preservation, sterilization and material modification, promoting the E-LINACs application as well as economic development in China.

INTRODUCTION

Accelerator-based high energy X-ray source and accelerator-based high energy electron source are two kinds of important instruments for NDT and electron beam (EB) radiation processing. Both the first NDT accelerator and the first 10MeV/20kW EB processing accelerator in China were developed successfully by CIAE about 20 years ago and 10 years ago respectively [1]. After a long-term development and improvement, the NDT accelerators form a series of accelerator, so called GT series, which can generate X ray with energy ranging from 1 MeV to 12MeV. 10MeV/20kW EB accelerator for radiation processing has been widely applied in China.

NDT ACCELERATOR

The GT series is used for NDT. See Table 1.

Table 1: The GT Series Accelerator for NDT

Model No.	X-ray energy	X-ray dose rate
GT-2/200	2MeV	200cGy/min.m
GT-2D/200	1MeV/2MeV	200cGy/min.m
GT-4/500	4MeV	500cGy/min.m
GT-4D/500	2MeV/4MeV	500cGy/min.m
GT-6/1000	6MeV	1000cGy/min.m
GT-6D/1000	4MeV/6MeV	1000cGy/min.m
GT-9/3000	9MeV	3000cGy/min.m
GT-9D/3000	6MeV/9MeV	3000cGy/min.m
GT-12/5000	12MeV	5000cGy/min.m
GT-12D/5000	9MeV/12MeV	5000cGy/min.m

The letter “D” in the model No. stands for Dual-energy type.

NDT accelerator consist of modulator [2]., X-ray head, cooling unit and control system [3]. This parts are connected by cables including electric power cable, Ethernet cable, signal cable and so on. See Fig. 1.

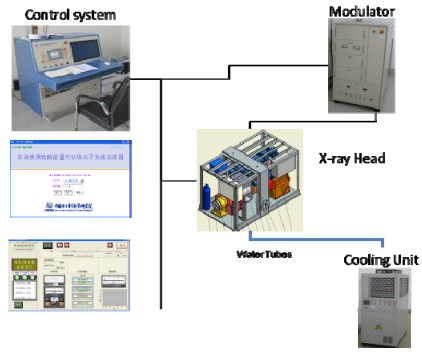


Figure 1: NDT accelerator sketch.

NDT accelerator can be used as a high energy X ray source for film imaging (see Fig. 2) and industrial CT.

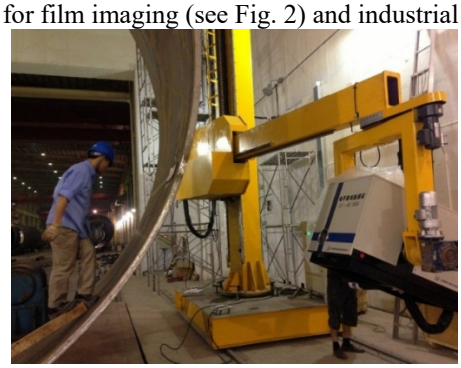


Figure 2: NDT accelerator on duty.

RADIATION PROCESSING ACCELERATOR

The FZ series is used for radiation processing. See Table 2.

Table 2: The FZ Series Accelerator

Model No.	EB energy	Avg. beam power
FZ-10/20	10MeV	20kW
FZ-2/1	2MeV	1kW

10MeV/20kW accelerator is applied in EB radiation processing including sterilization, material modification and so on. 2MeV/1kW accelerator is applied in mail sterilization, radiation curing because of short penetration depth.

High Voltage Pulse Modulator

The line-type modulator is used for 10MeV/20kW to generate 130kV/90A pulse to drive the klystron. The IGBT is used for charging unit and hydrogen thyratron is used for discharging unit. The pulse forming net (PFN) generate 16 μs pulse width. The duty factor is 9‰.

† 13811486349@163.com

Content from this work may be used under the terms of the CC BY 3.0 licence (© 2018). Any distribution of this work must maintain attribution to the author(s), title of the work, publisher, and DOI.

ISBN: 978-3-95450-194-6 ISSN: 2226-0366 doi:10.18429/JACoW-LINAC2018-MOPO059

CHOKE-TYPE RESONATOR FOR A COMPACT STORAGE RING

L. Ovchinnikova*[1], V.I. Shvedunov[1], Skobeltsyn Institute of Nuclear Physics,
Lomonosov Moscow State University (SINP MSU), 119991 Moscow, Russia
A.D. Ryabov, Institute for High Energy Physics (IHEP), 142281 Protvino, Russia
[1]also at Laboratory of Electron Accelerators MSU Ltd (LEA MSU), 119234 Moscow, Russia

Abstract

We present the results of calculations and measurements of the electrodynamic characteristics of the operating and high order modes of a choke-type resonator, intended for a 35–50 MeV storage ring, which is part of the Thomson X-ray generator.

INTRODUCTION

In [1] a variant of a normally conducting choke type RF resonator [2] was proposed (Fig. 1) for a compact storage ring X-ray source [3]. The resonator operates continuously at a frequency of 2856 MHz, has an effective shunt impedance of 3.8 MΩ, and quality factor of 14,000. The nominal voltage at the gap of the resonator is 300 kV while the level of RF power losses in the walls is 24 kW. With the use of the choke structure, the field of the operating mode is effectively isolated from the outer area of the resonator, where the energy of the higher order modes is absorbed.

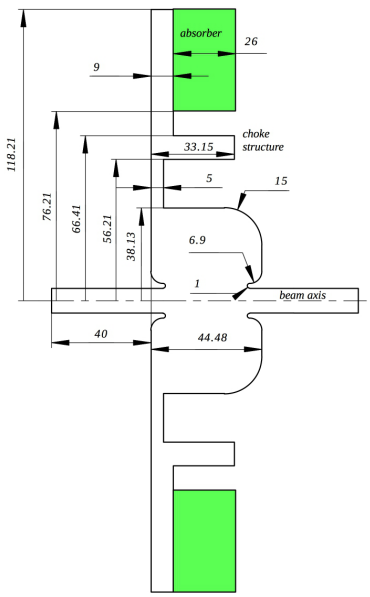


Figure 1: Geometry of the RF resonator.

In this paper we describe the design of a two cavities resonator fed through a 3-dB coupler, which allows to significantly reduce the RF power consumption and get rid of the ferrite isolator in the RF power supply system. The results of calculation of the RF coupler and of cavities thermal conditions with CST [4] and ANSYS [5] codes, as well as the results of measurements of characteristics of higher order modes performed for an aluminum prototype of the RF cavity are presented.

TWO CAVITIES RESONATOR

The presence of sufficient free space in the orbit of our Thomson generator storage ring [3] allows, with the aim of reducing the RF power consumption, to install resonator comprising two RF cavities fed from a single RF source.

The supply of the two cavities from a single RF source can be realized in several ways. For example, a structure comprising two cavities coupled by a magnetic field, which operates at π-mode, or uncoupled cavities fed through a 3-dB coupler [6] can be used. We chose the second solution, since it allows to get rid of the ferrite isolator in high power RF system, and, as it follows from our calculations, requires less RF power to achieve a given effective voltage at the accelerating gap. The design of the two cavities resonator fed through a 3-dB coupler is shown in Fig. 2.

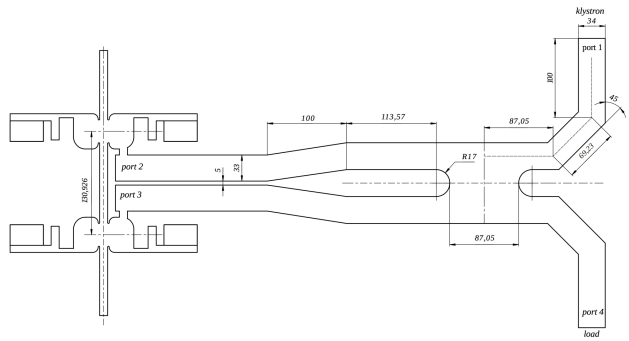


Figure 2: The design of the two cavities resonator fed through a 3-dB coupler.

The two cavities resonator operates as follows. An RF signal from the klystron is fed to port 1 of the 3-dB coupler, this signal is divided equally with the phase difference of 90° between ports 2 and 3, to which the cavities are connected. The signals reflected from the cavities enter port 4 with a phase difference of 180° compensating each other, due to which the klystron is protected from the reflected RF power.

In the chosen design, the RF power is transferred to the cavity via a coupling window cut at the side wall. The cavity coupling window dimensions were tuned to provide coupling factor 1 by adjusting the angle of the window (Fig. 3, parameter a_{sh}); the quality factor of the cavity decreased by 14% due to cutting window, which resulted in a corresponding increase in the RF power consumption. The total RF power consumption for generating effective voltage of

* lub.ovch@yandex.ru

Content from this work may be used under the terms of the CC BY 3.0 licence (© 2018). Any distribution of this work must maintain attribution to the author(s), title of the work, publisher, and DOI.

ISBN: 978-3-95450-194-6 ISSN: 2226-0366 doi:10.18429/JACoW-LINAC2018-MOPO060

LINACS FOR INDUSTRY, CARGO INSPECTION AND MEDICINE DESIGNED BY MOSCOW UNIVERSITY*

A.N. Ermakov†[1], A.S. Alimov[1], L.Yu. Ovchinnikova[1], A.N. Kamanin[1], V.V. Khankin[1], N.I. Pakhomov[1], N.V. Shvedunov[1], V.I. Shvedunov[1], D.S. Yurov[1], Skobeltsyn Institute of Nuclear Physics Lomonosov Moscow State University, 119991, Moscow, Russia
[1]also at Laboratory of Electron Accelerators MSU Ltd., 119992, Moscow, Russia
I.V. Shvedunov, A.S. Simonov, Laboratory of Electron Accelerators MSU Ltd., 119992, Moscow, Russia

Abstract

The report presents the results of development of applied linear electron accelerators with an energy of up to 10 MeV, performed by the Laboratory of Electron Accelerators MSU. We describe linear accelerators for mobile, stationary and train cargo inspection systems with interlaced energies and pulse repetition rate up to 2 kHz, accelerators for radiography, a sterilization accelerator with beam parameters that are adjustable over a wide range, and an accelerator for a radiotherapy complex.

INTRODUCTION

Laboratory of Electron Accelerators MSU Ltd. (LEA MSU) was established on the base of Skobeltsyn Institute of Nuclear Physics Lomonosov Moscow State University (SINP MSU) in 2013. Within five years we have designed six different types of linear accelerators for security, industry and medicine and supplied customers with more than 20 units. The customer of accelerators for security systems is the co-founder of the LEA MSU - Scantronic Systems LLC, which developed a number of cargo inspection systems, including stationary, train and mobile [1]. LEA MSU closely cooperates with the JSC "SPE" Toriy" [2] - enterprise that produces the powerful vacuum RF devices. We use in our accelerators the multi-beam klystrons, accelerating structures and electron guns manufactured by "Toriy" and carry out joint deliveries of accelerators. Our accelerators operate in S-band (2856 MHz) and C-band (5712 MHz). Examples of klystrons and sealed accelerating systems are shown in Figs. 1-2.

The accelerators designed by LEA MSU are equipped with a control system based on specialized controllers - each controller is responsible for a separate accelerator system [3]. The control system allows remote monitoring of the accelerator operation while saving the accelerator regime and beam parameters on the server. The control system allows changing the parameters of the accelerated beam within wide limits in accordance with the requirements of the technological process.

An important part of the RF system of our accelerators is a fast digital AFC system, permitting to reach stable beam energy and dose rate for a time of less than 1 s after start.

* Work supported in part by Ministry of Education and Science of Russia Grant # RFMEFI58217X0011
† email address a_ermak1978@mail.ru.

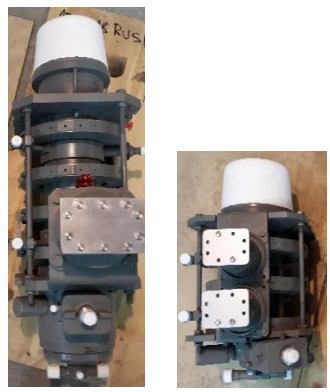


Figure 1: S-band (left) KIU-168 and C-band KIU-271 klystrons [2].

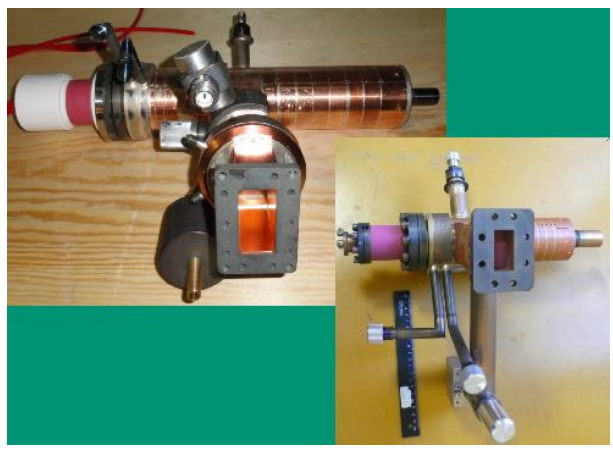


Figure 2: S-band (upper) and C-band accelerating systems.

Preliminary information about LEA MSU accelerators was given in [4-5].

CARGO INSPECTION

We have designed and manufacture accelerators for three types of cargo inspection systems: stationary, train and mobile. All these accelerators operate in interlaced energies mode with beam energy switching between 3.5 and 6 MeV. The beam spot size at the placed in vacuum, liquid cooled bremsstrahlung target is less than 1.5 mm for low energy and less than 1 mm for high. Accelerators are equipped with a local radiation shielding with a narrow gap collimator. Pulse to pulse beam energy stability is about 0.6 % rms. Some additional parameters are given in Table 1, accelerators photo are in Fig. 3. High repetition rate

Content from this work may be used under the terms of the CC BY 3.0 licence (© 2018). Any distribution of this work must maintain attribution to the author(s), title of the work, publisher, and DOI.

ISBN: 978-3-95450-194-6 ISSN: 2226-0366 doi:10.18429/JACoW-LINAC2018-MOPO061

BEAM PARAMETERS MEASUREMENT OF C-BAND 6 MeV LINEAR ELECTRON ACCELERATOR*

D. S. Yurov[1], A. S. Alimov[1], A. N. Ermakov[1], V. V. Khankin[1], L. Yu. Ovchinnikova[1], N. V. Shvedunov[1], V. I. Shvedunov[1], A. S. Simonov, Laboratory of Electron Accelerators MSU Ltd., Moscow, Russia
[1]also at Skobeltsyn Institute of Nuclear Physics, Lomonosov Moscow State University, Moscow, Russia

Abstract

The new linear electron accelerator with beam energy varied in the range of 2-6 MeV with dual-energy option has been designed by Laboratory of Electron Accelerators MSU Ltd. Linac is based on compact high gradient standing wave C-band accelerating structure fed by multi-beam klystron and is used in the cargo inspection and cancer therapy complexes. In the report, we present the results of electron beam parameters measurements at special stand.

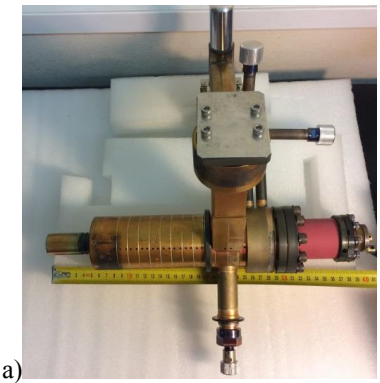
INTRODUCTION

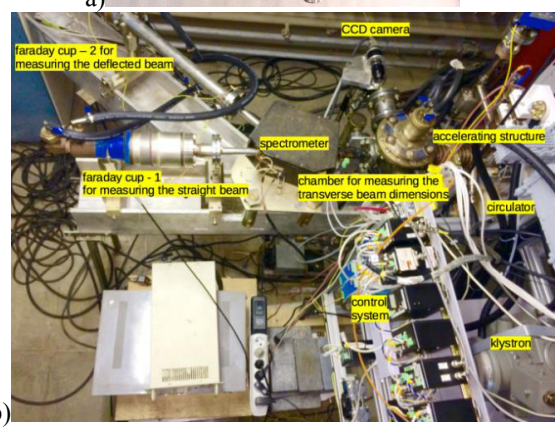
We have developed an accelerating system based on C-band on-axis coupled bi-periodic standing wave accelerating structure (AS) connected to a three-electrodes electron gun [1] for electron accelerators designed for cargo inspection and radiation therapy systems. The above application areas require narrow energy spectrum of the beam and ability to control its energy in the range of 2-6 MeV. In order to measure beam parameters and select an optimal operating mode, a prototype of the accelerating system without the bremsstrahlung target has been built and installed on a special stand. The paper provides a description of the stand and gives the measurement results.

EXPERIMENTAL SETUP

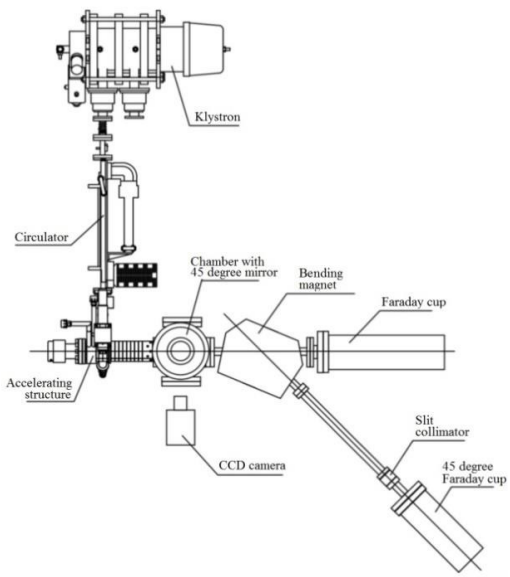
Photo and layout of the stand are given in Fig. 1.

The accelerating system that includes an AS, electron gun, feeding waveguide with vacuum RF window and antenna installed in the coupler cell is connected to a vacuum chamber with a viewing window and a movable screen made of titanium foil mounted at 45^0-angle to the beam axis. The screen is intended to measure transverse charge distribution of accelerated beam by registering generated at foil transition radiation by the CCD camera. A spectrometer based on 45^0 magnet with Faraday cups (FC) located at 0^0 and 45^0 is installed at the output of the vacuum chamber. A slit collimator with the slit width of 3 mm is placed at the 45^0 FC input. 0^0 FC signal comes to an oscilloscope for measuring amplitude of pulsed current of accelerated beam, and 45^0 FC signal is measured with ADC through an integrating chain or sent to an oscilloscope as well. Power supply of the AS is provided by multi-beam klystron KIU-273 with operating frequency of 5712 MHz and maximum pulsed RF power of 3.5 MW [2].


a)



b)



c)

Figure 1: Photo of a) the accelerating system and b) the stand. c) Stand layout.

* Work supported in part by Grant of the Ministry of Education and Science of the Russian Federation #RFMEFI58217X0011

Content from this work may be used under the terms of the CC BY 3.0 licence (© 2018). Any distribution of this work must maintain attribution to the author(s), title of the work, publisher, and DOI.

ISBN: 978-3-95450-194-6 ISSN: 2226-0366 doi:10.18429/JACoW-LINAC2018-MOPO062

LINEAR ELECTRON ACCELERATOR FOR RADIATION TECHNOLOGIES WITH BEAM PARAMETERS VARIED IN WIDE RANGE

V.V. Khankin†, A.S. Alimov, A.N. Ermakov, A.N. Kamanin, A.S. Kurilik, N.I. Pakhomov, N.V. Shvedunov, V.I. Shvedunov, D.S. Yurov, Skobeltsyn Institute of Nuclear Physics, MSU, Moscow, Russia and Laboratory of Electron Accelerators MSU, Ltd., Moscow, Russia.
I.V. Shvedunov, A.S. Simonov, Laboratory of Electron Accelerators MSU, Ltd., Moscow, Russia.

Abstract

We present the overview and beam parameters measurements results as well as the operational experience with the S-band pulsed linear electron accelerator with beam energy in the range of 5-10 MeV and maximum beam power of up to 15 kW. The possibility of adjusting the beam parameters in a wide range, provided by the design and control system of the accelerator, allows to use the accelerator in a wide variety of radiation technologies.

INTRODUCTION

Linear electron accelerators with the energy up to 10 MeV and beam power up to 50 kW are widely used in various radiation technologies. In the cases, when the specifications of the products being processed making use of the same installation are significantly changed, in order to optimize the radiation process it is necessary to have the possibility of on-line adjustment of the accelerated beam parameters. For example, during the radiation processing of the food products the mass-per-unit-area thickness of the products and the required dose can vary multi-fold; this requires for the several-fold change of beam power and value of dose for one beam pulse. The adjustment of the accelerated beam power with respect to the mass-per-unit-area thickness of the products enables not only to ensure the required uniformity of the dose distribution by the depth, but also to save the electric power to the considerable extent with proper design of the accelerator RF power supply system. The adjustment of dose being delivered to the products per one beam pulse enables to change the dose from hundreds of Grays to tens of kilo Grays with ensuring the uniformity of dose distribution along the surface and with high efficiency of the process.

ACCELERATOR DESCRIPTION

The linear accelerator described earlier in [1] has been installed in the centre for antimicrobial processing of products of vegetable and animal origin by the stream of accelerated electrons [2]. The photo and schematic view of the accelerator are given in Fig. 1, main parameters are presented in table 1.

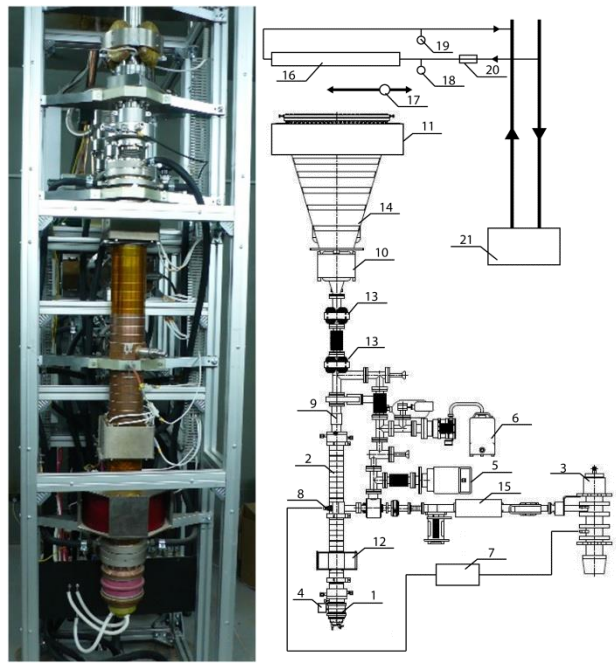


Figure 1: Photo and schematic view of the accelerator. 1 – electron gun, 2 – accelerating structure, 3 – klystron, 4, 5, 6 – vacuum pumps, 7 – low power RF unit, 8 – RF antenna, 9 – beam current monitor, 10 – scanning magnet, 11 – correcting magnet, 12 – solenoid, 13 – quadrupole lenses, 14 – scanning chamber, 15 – circulator, 16 – beam absorber 1, 17 – beam absorber 2, 18, 19 – temperature sensors, 20 – flow meter, 21 – chiller.

Table 1: Accelerator Parameters

Range of beam energy regulation	5-10 MeV
Pulsed beam current	400 mA
Range of beam power regulation	1-15 kV
Range of pulse duration regulation	4-12 μs
Range of pulse repetition rate regulation	50-400 Hz
Range of beam scanning width regulation	40-60 cm
Range of scanning frequency regulation	1-30 Hz
Operating frequency	2856 MHz
Maximum power of klyastron, pulse/average	6 MW/25 kW
Wall plug efficiency	>20%

† v-k32@yandex.ru

Content from this work may be used under the terms of the CC BY 3.0 licence (© 2018). Any distribution of this work must maintain attribution to the author(s), title of the work, publisher, and DOI.

ISBN: 978-3-95450-194-6 ISSN: 2226-0366 doi:10.18429/JACoW-LINAC2018-MOPO063

DEVELOPMENT OF SIDE COUPLED X-BAND MEDICAL LINEAR ACCELERATOR FOR RADIOTHERAPY*

Y. S. Lee†, G. J. Kim, S. H. Kim, J. H. Lee, I. S. Kim, Y. W. Choi, J. I. Kim††,
Medical Device Research Center, Korea Electrotechnology Research Institute, Ansan 15588, Republic of Korea
J. H. Hwang[1,2], A.R Kim[1,2], J. N. Kim[1,2], J. S. Shin[1,2], Y. J. Seol[1,2], T. G. Oh[1,2], Y. A. Oh[2], Y. N. Kang[2,3]
[1]Department of Biomedicine & Health Sciences, The Catholic University of Korea, Seoul 06591, Republic of Korea
[2]Advanced Institute for Radiation Fusion Medical Technology, College of Medicine, The Catholic University of Korea, Seoul 06591, Republic of Korea
[3]Department of Radiation Oncology, Seoul St. Mary's Hospital, College of Medicine, The Catholic University of Korea, Seoul 06591, Republic of Korea

Abstract

Recently, LINAC-based radiotherapy equipment are being developed by combining with imaging devices such as CT or MRI, so that it is possible to precisely focus high dose radiation on tumor tissues while minimizing the normal tissue damage. In order to place the diagnostic and treatment devices simultaneously in a confined space, constraints related to interference and volume between the subsystems must be considered. To meet these requirements, the size and weight of the LINAC system need to be reduced, which can be achieved by applying X-band technology. For the purpose of use in IMRT based on image guided radiotherapy, we developed a 9.3 GHz X-band medical LINAC using side-coupled structure. The LINAC is designed to have the accelerating field strength of 16.8 MV/m, and the beam current transmission efficiency of 26 % at the end of accelerating cell when the supplied RF power is at 1.7 MW. Therefore, it can accelerate the electron beam up to 6.2 MeV with having about 90 mA beam current. We plan to carry out the performance test using beam diagnostics system and X-ray measurement system, and the details of design and experimental results of LINAC will be described in this paper.

DESIGN OF X-BAND LINAC

RF Cavity Structure

The developed 9.3 GHz X-band LINAC system accelerates electron beam and finally produce high energy X-rays and, the specifications are shown in Table 1. The RF cavity include 4 bunching cells, 20 accelerating cells, coupler port and vacuum port (see Fig. 1). The side coupling method is applied to distribute RF energy supplied from magnetron, which is an external RF source, to each cell inside cavity. The advantage of the side coupling method is higher acceleration efficiency per unit length, so it is possible to make the LINAC length shorter. In addition, since the cavity operate with π/2 mode which has the largest mode spacing comparing with other mode, it has advantage related to the performance and stability [1].



Figure 1: X-band RF cavity.

The total length of the RF cavity is 42 cm, which includes the flange for assembly. When 1.7 MW of RF power is supplied from the magnetron to the LINAC system, the RF loss is occurred in the coupler port and the RF module such as 4-port circulator and directional coupler, so the 1.58 MW of RF power is actually transmitted to the RF cavity. In this RF condition, the LINAC system is designed to generate the 90 mA electron beam 6.2 MeV.

Electron Gun Type

For the radiation therapy, the triode e-gun is mainly used, because it is essential to precisely control the beam current

* This research was supported by the KERI Primary Research Program of MSIT/NST (No. 18-12-N0101-42)
†yongseok@keri.re.kr
††sky@keri.re.kr

Content from this work may be used under the terms of the CC BY 3.0 licence (© 2018). Any distribution of this work must maintain attribution to the author(s), title of the work, publisher, and DOI.

ISBN: 978-3-95450-194-6 ISSN: 2226-0366 doi:10.18429/JACoW-LINAC2018-MOPO064

O-ARM MOUNTED X-BAND LINEAR ACCELERATOR SYSTEM FOR RADIOTHERAPY*

S. Kim†, G. J. Kim, Y. S. Lee, J. H. Lee, I. S. Kim, Y. W. Choi, and J. I. Kim‡
Medical Device Research Center, Korea Electrotechnology Research Institute, Ansan 15588, Republic of Korea
J. Hwang[1,2], A. Kim[1,2], J. Kim[1,2], J. S. Shin[1,2], Y. Seol[1,2], T. Oh[1,2], Y. Oh[2], Y. N. Kang[2,3]
[1]Department of Biomedicine & Health Sciences, The Catholic University of Korea, Seoul 06591, Republic of Korea
[2]Advanced Institute for Radiation Fusion Medical Technology, College of Medicine, The Catholic University of Korea, Seoul 06591, Republic of Korea
[3]Department of Radiation Oncology, Seoul St. Mary's Hospital, College of Medicine, The Catholic University of Korea, Seoul 06591, Republic of Korea

Abstract

Current advances in radiotherapy are based on the precise imaging techniques, and there is a pressing need for the development of techniques capable of visualizing cancer tissues in real time in conjunction with radiotherapy. Indeed, the image-guided radiotherapy systems in which conventional diagnostic tools such as CT and MRI are combined with the linear accelerator (LINAC)-based radiotherapy have been extensively studied. In this work, we mounted 9.3 GHz X-band LINAC system designed by KERI on the 360 degree-rotatable O-arm system, which allows efficient integration of a diagnostic tool with the radiotherapy equipment. After mounting, the X-ray profile and percentage depth dose were measured by following the quality assurance using the AAPM TG-51, 142 protocol. The beam profile symmetry was estimated to be 102.44% with ± 3% tolerance. The X-ray dose was also measured by rotating the O-arm gantry system to confirm the stable operation of the mounted X-band LINAC. As a result, the standard deviation of the X-ray dose was 0.016 while rotating. Therefore, we demonstrate the operational stability of our O-arm mounted X-band LINAC system for use in highly effective radiotherapy combined with simultaneous Computerized Tomography image guidance.

INTRODUCTION

Radiotherapy is preferred as a common choice in the management of patients with cancers as treatment outcomes (i.e. patients' survival or quality of life) are importantly considered. It is moving towards image-guided radiotherapy (or combined radiotherapy) that allows delivering highly precise radiotherapy with periodic image guidance before and/or during each treatment. A core technology in such radiotherapy lies with LINAC devices that generate high energy radiation required for both imaging and treatment. Although the S-band LINAC is widely used, it is not suitable for the compact radiotherapy system. On the other hand the X-band LINAC is fits into small space, thereby reducing the costs of the system [1]. The X-band LINAC system recently developed by Korea Electrotechnology Research Institute (KERI) could reduce the overall device size by about 2/3 compared to the current S-band LINAC system [2]. In this study, we developed a compact X-band LINAC system and integrated into the O-arm computed tomography (CT) diagnostic system for image guided radiotherapy. We confirmed the normal operation of the developed O-arm CT-LINAC by mechanical analysis and ensured its stability and maintainability with the optimized quality assurance (QA) tests.

O-ARM BASED X-BAND LINAC

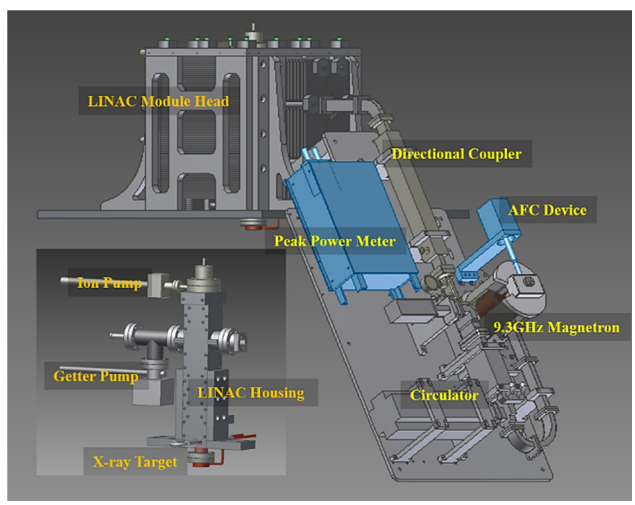


Figure 1: Compact X-band LINAC system.

Miniaturization and reduction in the weight of the LINAC are highly required for combined radiotherapy. In comparison with the 3.0 GHz S-band LINAC system, the 9.3 GHz X-band LINAC produces the same level of X-ray output while reducing the size and weight of the system. Therefore, we designed a compact LINAC system (LINAC module & RF Module) by mounting the X-band LINAC on the O-arm gantry (see Fig. 1). LINAC module consists of a triode type of the electron gun, a side-coupled structure

* Work supported by MSIT/NST (No. 16-11-N0101-06, 18-12-N0101-42)
† skim428@keri.re.kr
‡ sky@keri.re.kr

Content from this work may be used under the terms of the CC BY 3.0 licence (© 2018). Any distribution of this work must maintain attribution to the author(s), title of the work, publisher, and DOI.

ISBN: 978-3-95450-194-6 ISSN: 2226-0366 doi:10.18429/JACoW-LINAC2018-MOPO066

SIMULATION OF THE TRANSITIONAL PROCESS IN ACCELERATING SECTIONS BY EQUIVALENT CIRCUIT METHOD

S. V. Matsievskiy*, V. I. Kaminskiy, Ya. V. Shashkov
National Research Nuclear University MEPhI , Moscow, Russia

Abstract

Nowadays linac accelerating RF systems design is usually done by the finite difference method. It provides high accuracy of calculations and freedom in topology choosing, but may draw considerable amounts of computer resources with long calculation times. Alternative to this method, equivalent circuit method exists. The basic idea of this method is to build a lumped element circuit, which with certain approximation acts as an original accelerating cell. It drastically reduces the number of equations to solve. This method is long known but usually only used for the particular accelerating structures when speed of calculation is a key-factor. Present paper describes a way to numerically simulate transition processes in arbitrary coupled accelerating cells using the equivalent circuit method. This approach allows simulating transitional processes in accelerating structures significantly faster and allows doing so for structures with high quality factor and many cells – a hard task for conventional transient solvers based on the finite difference method.

CALCULATION MODEL

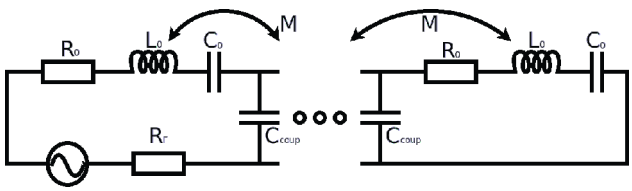


Figure 1: Equivalent circuit of the accelerating structure.

Equivalent Circuit

In Fig. 1 the equivalent circuit of the accelerating structure is presented. In it distributed parameters of the accelerating structure are substituted with the lumped elements. This circuit may be used to simulate accelerating RF structures with electric and magnetic coupling between cells. It appropriately represents structures operating on TM_{01} and TM_{11} wave modes, which covers most types of accelerating cells for the electron accelerators [1, 2]. Depending on the generator and load positions, standing and travelling wave structures may be simulated.

Usually accelerating cells are connected in serial manner but it's possible to simulate more complex connection topologies by introducing additional C_{coup} and M components between non-adjacent cells to the circuit 1.

Equations

Each circuit contour is described by the Kirchhoff Equation (1).

$$L\frac{di}{dt} + \frac{1}{C}\int idt + (R + R_G + R_L)i + \\ + \sum_{n=1}^{N} \frac{1}{C_n^{coup}} \int (i - i_n)dt + \sum_{n=1}^{N} M_n \frac{di_n}{dt} = e_n \quad (1)$$

It has been shown that for serial connected cells analytical solution of the system of Equations (1) may be presented in a recurrent form [3]. However, for the cases with more complex coupling topologies, in which the matrix of the Laplacian transformations is not tridiagonal, obtaining analytical solution may become problematic.

Solution of the system of Equations (1) may be obtained using classical or operator methods. For the operator method, numerical solution of the algebraic system of Laplacian transformations is straightforward. Several algorithms are available for the numeric calculation of the inverse Laplace transformation. In this paper the classical method of direct solution of the system of DAE equations will be described.

After substituting lumped element parameters with electrodynamic parameters and getting rid of second derivatives, equation takes the form 2.

$$\begin{cases} \frac{dx}{dt} = \hat{x} \\ \frac{d\hat{x}}{dt} + \sum_{n=1}^{N} -\frac{K_n^H}{2}\frac{f}{f_n}\frac{d\hat{x}_n}{dt} = \sum_{n=1}^{N} 2\pi^2 f^2 K_n^E x_n - \\ -(1 + \chi_G + \chi_L)\frac{2\pi f}{Q}\hat{x} + 4\pi f^2 x + \\ + \sqrt{\frac{4\chi_G P_g}{\pi f_G Q}} \cos(2\pi f_G t + \varphi) \end{cases} \quad (2)$$

Which, written in matrix form, looks like this:

$$\begin{cases} |\dot{X}| = |\hat{X}| \\ |K^H||\dot{\hat{X}}| = |K^e||g(t, \hat{x}, x)| \end{cases} \quad (3)$$

Here, $|\dot{X}|$, $|\hat{X}|$ and $|\dot{\hat{X}}|$ are the vectors of normalised amplitudes of electric field and its derivatives. $|g(t, \hat{x}, x)|$ is the vector of functions, independent of the adjacent cells parameters. $|K^H|$ and $|K^E|$ are the matrices of magnetic and electrical connection between cells respectively.

Finally, for numerical solution of the system, only derivative vectors should remain on the left part of equations.

$$\begin{cases} |\dot{X}| = |\hat{X}| \\ |\dot{\hat{X}}| = |K^H|^{-1}|K^e||g(t, \hat{x}, x)| \end{cases} \quad (4)$$

* MatsievsliySV@gmail.com

Content from this work may be used under the terms of the CC BY 3.0 licence (© 2018). Any distribution of this work must maintain attribution to the author(s), title of the work, publisher, and DOI.

ISBN: 978-3-95450-194-6 ISSN: 2226-0366 doi:10.18429/JACoW-LINAC2018-MOPO069

NUCLEAR AND MECHANICAL BASIC DESIGN OF TARGET FOR Mo-99 PRODUCTION USING HIGH POWER ELECTRON LINAC

H. Khalafi, Atomic Energy Organization of Iran (AEOI), Thran, Iran
A. T. Khotbeh-Sara†, F. Rahmani, Department of Physics, K. N. Toosi University of Technology, Thran, Iran
M. M. Kejani, F. Ghasemi, Nuclear Science and Technology Research Institute (NSTRI), Thran, Iran

Abstract

Today providing enough supplies of ^{99m}Tc / ^{99}Mo as a most applicable radioisotope in diagnostic nuclear medicine for the world demand is an important challenge. One of the proofed ways to access reliable source of this radioisotopes is the production using e-Linac [1]. In this investigation it has been tried to find the simple and the optimized design of ^{99}Mo production target based on photoneutron reaction using e- Linac. Based on the Monte-Carlo calculation for radiation transport and finite element thermal analysis, 9 thin plates of enriched ^{100}Mo has been suggested. Equal distance between plates has been considered for cooling to prevent target melting. The main target includes only ^{100}Mo in one-stage approach method to increase production rate in comparison with two-stage approach [2]. Applying 2.5 m/s for inlet velocity of cooling water provides suitable cooling process with maximum temperature of target about 900 ˚C.

INTRODUCTION

The most widely used diagnostic radioisotope in clinical practice of nuclear medicine is ^{99m}Tc, which covering 35 million diagnostic imaging process annually [3]. Its short half-life limits the distribution process to long distances, so suppliers generally try to produce ^{99}Mo, which transforms into ^{99m}Tc nucleus in β decay mode ($t_{1/2}$= 66 h).

Production of ^{99}Mo using e-Linac is a common method with two main approaches. Two-stage approach is a general method (W target as a photon converter and ^{100}Mo as a photoneutron target). In one-stage approach, the Mo target is electron-photon converter as well as the photoneutron target simultaneously, so self-absorption of photons in electron-photon converter will be prevented and produced photons participate directly in photoneutron reactions. In this study, the one-stage approach has been selected.

The maximum cross section of ^{99}Mo production reaction is on 14 MeV and by considering of logarithmic bremsstrahlung spectrum, the beam with energies between 30 to 45 MeV is desired. So 30 MeV e-beam has been selected for irradiation the target. It should be mentioned that this energy is edge of commercial high power e-Linacs abilities [4].

The different geometries for target has been investigated that reported in ref. [5]. According to it, the hemispherical target is efficient than other geometries. But due to the thermal and mechanical challenges in construction, it is decided to use simplest geometry. To achieve better results of cooling, the scanning e-beam on long ^{100}Mo plates has been considered.

NUCLEAR SIMULATION

Molybdenum is a dense metal that can be used as an electron-photon converter. Of course the photon flux of molybdenum is not as high as the produced photon flux in tungsten, but in two-stage approach, some portion of photons are absorbed in tungsten before they can be able to participate in photoneutron reaction in ^{100}Mo target. So using ^{100}Mo target as an electron-photon converter and an isotope production target simultaneously, resolves this problem.

The peak forward direction of bremsstrahlung photons are in the limited conical shape area [2], but since these photons creation happen rarely in the angles of 0, 90 and 180 degrees (relative to e-beam direction), photons population is minimum in these areas. Figure 1 shows the distribution of particles in volume of massive cylindrical target.

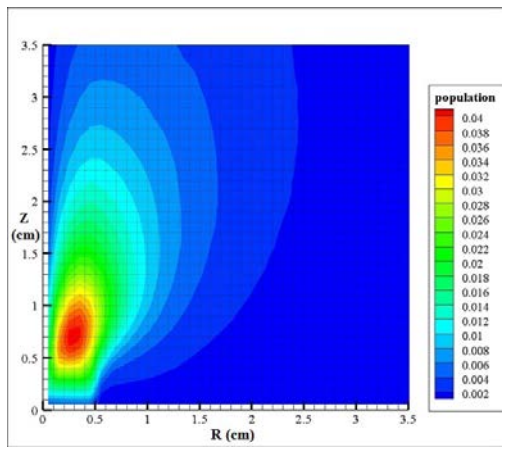


Figure 1: Distribution of photons population in volume unit of each mesh, per one incident electron.

In ^{100}Mo(γ,n)^{99}Mo reaction, the created photoneutrons during this reaction, is corresponded with produced ^{99}Mo. So the photoneutron production rate is equal to ^{99}Mo production rate. The distribution of neutrons population is shown in Fig. 2.

† khotbesara@email.kntu.ac.ir

Content from this work may be used under the terms of the CC BY 3.0 licence (© 2018). Any distribution of this work must maintain attribution to the author(s), title of the work, publisher, and DOI.

ISBN: 978-3-95450-194-6 ISSN: 2226-0366 doi:10.18429/JACoW-LINAC2018-MOPO070

CONSTRUCTION OF THE SIDE-COUPLED STANDING-WAVE e-LINAC

S. Zarei, F. Ghasemi†, Nuclear Science and Technology Research Institute (NSTRI), Tehran, Iran
M. Lamehi Rachti, M. Bahrami, Iranian Light Source Facility (IPM), Tehran, Iran
F. Abbasi Davani, Shahid Beheshti University, Tehran, Iran

Abstract

Due to Iran's growing need for accelerators in various applications, NSTRI electron linear accelerator project has been defined for medical and inspection applications. This accelerator is a 6 MeV side-coupled standing-wave that operate is π /2 mode in the frequency of 2998.5 MHz.

In this paper the construction and measurement results of the tube of this accelerator are presented. The prototype tube was constructed from aluminum and was clamped with bolts. By using a network analyzer, electric and magnetic probes and a side-coupled cavity tuning method and a bead-pull measurement technique, RF measurements were carried out. The resonant frequency and quality factor have been achieved 2998.5 MHz and 7940 respectively

INTRODUCTION

In Iran, a project has been started in Nuclear Science and Technology Research Institute to build an electron linear accelerator for medical and inspection applications.

For this accelerator, a side-coupled standing-wave accelerating tube was selected that the main specifications of it are given in Table 1 and also a layout of it is given in Fig. 1.

Table 1: The Desirable Tube Specifications

Parameters	Value
RF frequency	2998.5 MHz
Input beam energy	30 keV
Output beam energy	6 MeV
Operating mode	π/2
Maximum RF power	2.6 MW

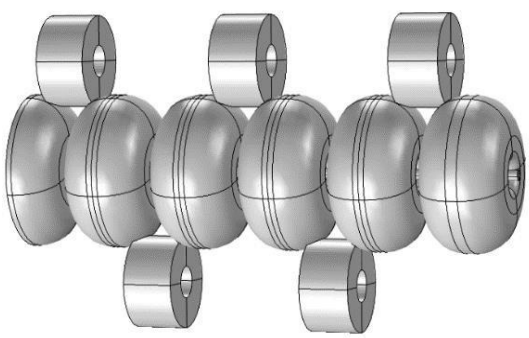


Figure 1: The layout of the entire accelerating tube.

Electromagnetic design, beam dynamics studies and thermal and mechanical simulations of the tube have been carried out by using COMSOL [1], ASTRA [2] and ANSYS [3] respectively [4-6]. After the design was completed, construction and RF measurement of the porotype aluminum tube carried out that the results of them are presented in this paper.

CONSTRUCTION

The design of the tube has been carried out and the mechanical drawings of the tube have been prepared, then each cavity of the tube was machined and polished. The exploded view drawing of the prototype tube is shown in Fig. 2.

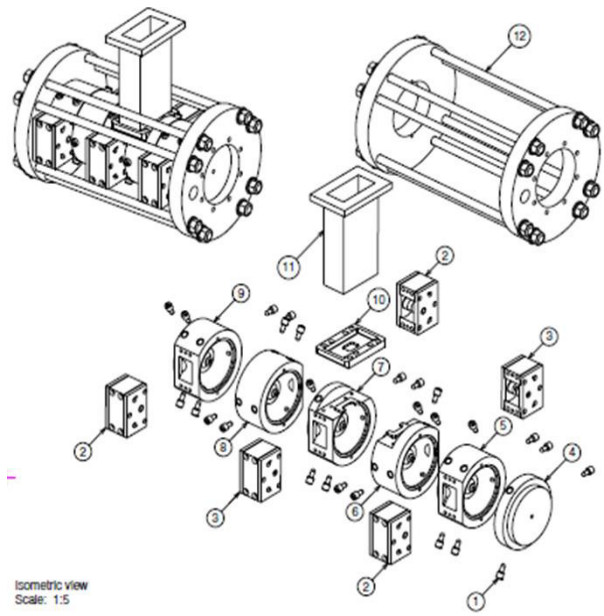


Figure 2: The exploded view drawing of the entire tube.

The first prototype tube was built from aluminium. The cavities were machined and polished and the bolts clamp the cavities in place. We have created six holes on the accelerating cavities wall and one hole on the coupling cavities wall for frequency tuning. The constructed tube is shown in Fig. 3.

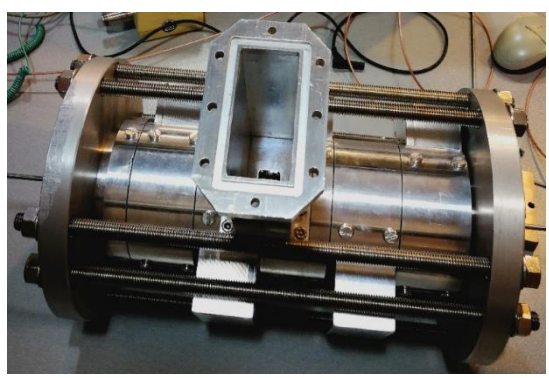


Figure 3: The constructed tube.

Content from this work may be used under the terms of the CC BY 3.0 licence (© 2018). Any distribution of this work must maintain attribution to the author(s), title of the work, publisher, and DOI.

ISBN: 978-3-95450-194-6 ISSN: 2226-0366 doi:10.18429/JACoW-LINAC2018-MOPO073

COHERENT EDGE RADIATION SOURCES IN LINAC-BASED INFRARED FREE-ELECTRON LASER FACILITIES

N. Sei†, H. Ogawa, Research Institute for Measurement and Analytical Instrumentation, National Institute of Advanced Industrial Science and Technology, 1-1-1 Umezono, Tsukuba, Ibaraki 305-8568, Japan
T. Tanaka, Y. Hayakawa, T. Sakai, Y. Sumitomo, K. Hayakawa, K. Nogami, Laboratory for Electron Beam Research and Application, Nihon University, 7-24-1 Narashinodai, Funabashi, 274-8501, Japan.
H. Ohgaki, H. Zen, Institute of Advanced Energy, Kyoto University, Gokasho, Uji, Kyoto 611-0011, Japan

Abstract

National Institute of Advanced Industrial Science and Technology has been studied far-infrared coherent radiation at Linac-based infrared free-electron laser (FEL) facilities in collabo-ration with Nihon University and Kyoto University. Generally, it is possible to extract information about the electron bunch by observing the coherent radiation. To clarify the relationship between the FEL interaction and the coherent radiation, we developed coherent edge radiation, from which the bunch length could be evaluated, in FEL straight sections.

INTRODUCTION

In order to oscillate an FEL, it is necessary to estimate characteristics of an electron beam in a straight section in which an undulator is installed. The bunch length of the electron beam related to the electron density is a significant parameter which characterizes behavior of the FEL. The bunch length influences not only the gain but also the pulse width of the FEL and the cavity-length detuning curve [1]. Observing the behavior of the bunch length in the straight section with the undulator is useful for understanding the FEL physics.

Observations of spectra of coherent radiation generated by the electron bunch are suitable for monitoring the bunch length of a short-pulse electron beam. However, FEL pulses exist on the electron-beam orbit in the straight section with the undulator. A target for transition radiation cannot be inserted into the straight section. Hence, the transition radiation cannot be used to generate coherent radiation. The usage of synchrotron radiation is unlikely because the radiation power becomes week away from the axis of the electron-beam orbit. Diffraction radiation can be extracted for the spectral measurement without losing the FEL oscillations. However, the spectrum of the diffraction radiation depends on the aperture diameter of the diffraction element. Because it is necessary to enlarge the aperture for long-wavelength FELs, conditions in which the diffraction radiation can be applied for a bunch length measurement are limited. Therefore, we used the coherent edge radiation (CER) generated by the downstream bending magnet in the FEL straight section. Because edge radiation has an annular shape distribution as the asymmetric first-order Laguerre-Gaussian (LG_{01}) mode [2], the CER can be extracted from the optical cavity without a diffraction loss of the FEL beam. In the terahertz (THz) region, where the edge radiation becomes coherent, the intensity of the edge radiation is much higher than that of the synchrotron radiation. In this paper, CER sources at Kyoto University Free Electron Laser (KU-FEL) [3] and at Laboratory for Electron Beam Research and Application (LEBRA) in Nihon University [4] are discussed.

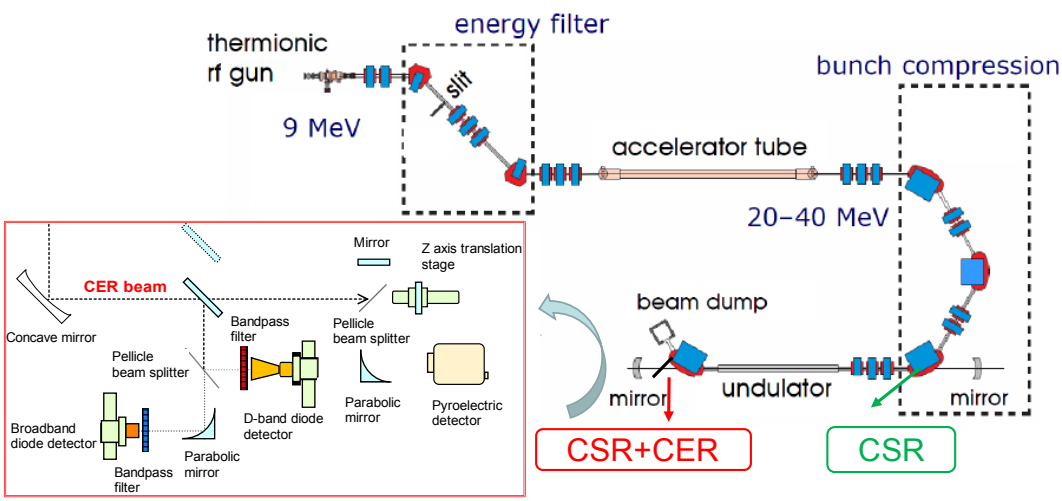


Figure 1: Schematic layout of the CER source and the measurement system at KU-FEL.

Content from this work may be used under the terms of the CC BY 3.0 licence (© 2018). Any distribution of this work must maintain attribution to the author(s), title of the work, publisher, and DOI.

ISBN: 978-3-95450-194-6 ISSN: 2226-0366 doi:10.18429/JACoW-LINAC2018-MOPO076

STUDY ON GENERATION OF VARIABLE POLARIZED COHERENT THz RADIATION USING A CROSSED UNDULATOR

Hirotoshi Saito†, Hiroyuki Hama, Fujio Hinode, Ken Kanomata, Shigeru Kashiwagi, Sadao Miura, Toshiya Muto, Ikurou Nagasawa, Ken-ichi Nanbu, Shingo Ninomiya, Ken Takahashi, Research Center for Electron Photon Science, Tohoku University, Sendai, Japan

Abstract

A variable polarized THz radiation source using a crossed undulator system has been developed at Tohoku University. In this scheme, two coherent undulator radiations from an extremely short electron bunch are used to control the polarization. They are linearly polarized radiations orthogonal to each other. Polarization of superimposed radiation is controlled by adjusting a relative phase between them. A compact planar undulator with seven periods has been designed for an experiment at our facility. The radiation frequency is 2.06 THz for electron beam energy of 22 MeV. The opening angle of the crossed undulator radiation was estimated to be 34 mrad (FWHM). Since the polarization state of the crossed undulator depends on observation angle, its angular dependence was evaluated. It was found that ideal polarization control is realized only in the angle range of 2.5 mrad, which is quite smaller than that of the radiation itself.

INTRODUCTION

Coherent THz light sources based on an accelerator have been developed at Research Center for Electron Photon Science, Tohoku University. A test accelerator called t-ACTS (test Accelerator as Coherent THz Source) has been constructed for generating coherent THz radiation from an extremely short electron bunch. It consists of a thermionic rf gun, an alpha magnet with an energy filter and 3 m long accelerating structure. An electron bunch is compressed down to shorter than 100 fs by means of a velocity bunching scheme in the traveling wave accelerating structure. Coherent transition radiation of a frequency range up to about 4 THz and coherent undulator radiation from 2.6 to 3.6 THz have been successfully observed [1].

At present, we are considering a variable polarized THz light source using a crossed undulator system. In order to carry out a demonstration experiment of its polarization control at t-ACTS, design consideration of the crossed undulator system and an investigation of its polarization properties are underway.

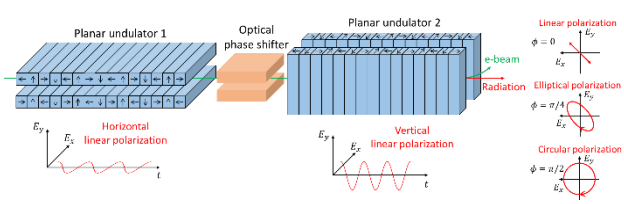


Figure 1: Concept of a crossed undulator.

† hsaito@lns.tohoku.ac.jp

CONCEPT OF A CROSSED UNDULATOR

Concept of the crossed undulator system is shown in Fig. 1. It consists of two planar undulators and an optical phase shifter between them. The undulators are arranged so that polarization direction of each radiation is orthogonal. Two linearly polarized coherent radiations are generated from an extremely short electron bunch passing through the undulators. They are superimposed both spatially and temporally by delaying the first radiation in the optical phase shifter using mirrors. Polarization is controlled by changing the optical path length in the phase shifter and adjusting phase difference between the two radiations.

PLANAR UNDULATOR

In order to carry out a demonstration experiment, the crossed undulator system must be designed considering some constrains and beam conditions at t-ACTS. Total length of each planar undulator must be shorter than 1 m because of a constraint of the experimental space. Radiation frequency must be lower than 3 THz because of beam conditions of the bunch compression mode of t-ACTS, namely, the electron energy of 22 MeV and the bunch length of approximately 80 fs. A planar undulator was designed taking these requirements into account. The undulator parameters are shown in Table 1. Block dimensions 60 mm, 30 mm and 20 mm are width, height and thickness, respectively.

Electric field radiated from an electric charge q is calculated from the Lienard-Wiechert potential. Its radiation field term is expressed as [2]

$$\vec{E}(\vec{r},t) = \frac{q}{4\pi\varepsilon_0}\left[\frac{\vec{n}\times\left\{\left(\vec{n}-\vec{\beta}\right)\times\dot{\vec{\beta}}\right\}}{Rc\left(1-\vec{n}\cdot\vec{\beta}\right)^3}\right]_{\mathrm{ret}}, \qquad (1)$$

where ε_0 is the dielectric constant of vacuum, R the observation distance, c the speed of light, $\vec{\beta}$ the velocity vector normalized by c and $\vec{n}$ the unit vector in the observation direction. The bracket $[\ ]_{\mathrm{ret}}$ denotes that values inside it are evaluated at the retarded time. A frequency spectrum of the radiation field can be calculated by the Fourier transformation.

Angular distribution of the undulator radiation can be derived by changing observation point and calculating radiation field Eq. (1) emitted from an electron passing through the magnetic field in the undulator. The angular spread is 34 mrad in the x direction (the electron oscillation direction) and 96 mrad in the y direction in FWHM.

Content from this work may be used under the terms of the CC BY 3.0 licence (© 2018). Any distribution of this work must maintain attribution to the author(s), title of the work, publisher, and DOI.

ISBN: 978-3-95450-194-6 ISSN: 2226-0366 doi:10.18429/JACoW-LINAC2018-MOPO077

DESIGN OF THE HIGH GRADIENT NEGATIVE HARMONIC STRUCTURE FOR COMPACT ION THERAPY LINAC*

S.V. Kutsaev[1], R. Agustsson[1], A. Barcikowski[2], R. Fischer[2],
B. Mustapha[2], A.Yu. Smirnov[1], A. Verma[1],
[1]RadiaBeam Systems, LLC, Santa Monica, CA, 90404, USA
[2]Argonne National Laboratory, Lemont, IL, 60439, USA

Abstract

A novel concept for an Advanced Compact Carbon Ion Linac (ACCIL) that will deliver up to 1 pnA of carbon ions with variable energy from 45 MeV/u to 450 MeV/u in a 45m footprint, has been developed by Argonne National Laboratory (ANL) in collaboration with RadiaBeam. The ACCIL will have a 35 MV/m real-estate accelerating gradients that became possible to achieve with the development of novel S-band high-gradient structures, capable of providing 50 MV/m accelerating gradients for particles with β>0.3. In particular, a β=0.3 structure based on the novel approach of operation at the first negative spatial harmonic with the increased distance between the accelerating gaps will be presented. This is the first attempt to reach such high gradients at such small velocities. RadiaBeam and ANL have demonstrated the feasibility of building this structure for accelerating carbon ions by means of advanced computer simulations and are currently working towards the fabrication of this structure for high power tests.

INTRODUCTION

A usable device for cancer therapy needs to produce up to 200-250 MeV protons or/and up to 400-450 MeV/u carbon ions [1]. Both cyclotrons and synchrotrons that are currently used for these purposes are expensive and bulky constructions with large magnets and have significant limitations with rapid and efficient energy adjustment [2].

Within hadron therapy, proton therapy is the most common [3], although studies indicate that carbon ion therapy offers additional advantages [4], and combined proton and carbon therapy could achieve the most precise dose confinement to the tumor volume [5], while sparing healthy tissues.

Argonne National Laboratory and RadiaBeam are seriously considering the development of an ultra-high gradient linear accelerator, named ACCIL, for the full energy range from ion source to 450 MeV/u for $^{12}C^{6+}$ and 250 MeV for protons [6], which includes the following main sections: a radiofrequency quadrupole (RFQ) accelerator operating at a sub-harmonic of the S-band frequency, a conventional DTL section followed by a CCDTL section up to 45 MeV/u, and a high-energy section made of high-gradient structures for the energy range from ~45 MeV/u to ~450 MeV/u.

The compact footprint of ACCIL (8x45m) can be achieved by the development of accelerating structures capable of providing 50 MV/m for the particles with beta from 0.3 to 0.7. Such a high accelerating gradient for the ACCIL linac is possible due to the operation at high frequency, 2856 MHz, at very low duty cycle <0.06% and very short <0.5 μs beam pulses.

There are several ongoing projects worldwide [7,8] pursuing the development of S-band high gradient structures. Among the proposed structures only TULIP's backward-traveling wave structure (BTW) provides parameters close to ACCIL requirement. However, the direct scaling of BTW cells design from β=0.38 to β=0.3 beam velocities lead to unacceptably high peak fields (>220 MV/m) or dramatically lower power efficiencies.

ACCELERATING STRUCURE

To work around this issue, we have designed a cavity where the beam is synchronous with the higher spatial harmonic (NHS) [9]. The structure was designed to operate at the -1st harmonic, capable of producing 50 MV/m gradient at peak field levels of <160 MV/m with 50% higher shunt impedance than the β=0.3 structure scaled from TULIP's fundamental harmonic BTW. However, the NHS design had mechanical stresses of ~60 MPa as shown in Fig.1, left, which is slightly above the yield stress of the annealed copper.

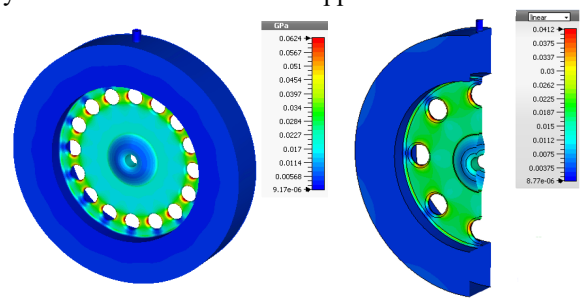


Figure 1: Mechanical stress maps in NHS with 16 (left) and 8 (right) coupling holes.

To reduce peak stresses, we investigated several approaches. Since the location of these stresses is the coupling hole, the strategy to reduce them is by reinforcing the iris part between the holes. The first obvious approach was to reduce the number of coupling holes, and thus increase the distance between them. The simulation results, shown in Fig.1, right, demonstrate that lesser number of holes makes the structure more rigid and improves thermal conductance at the cost of the group velocity, which can be compensated by increasing the hole diameter. The optimal number of holes is eight since

* This work was supported by the U.S. Department of Energy, Office of High Energy Physics, under Accelerator Stewardship Grant, Proposal No. 0000219678 and STTR grant DE-SC0015717

Content from this work may be used under the terms of the CC BY 3.0 licence (© 2018). Any distribution of this work must maintain attribution to the author(s), title of the work, publisher, and DOI.

ISBN: 978-3-95450-194-6 ISSN: 2226-0366 doi:10.18429/JACoW-LINAC2018-MOPO079

CAVITY DESIGN OF A 7MeV 325MHz PROTON APF IH-DTL FOR A COMPACT INJECTOR*

X. Li[1], Y.H. Pu†, X.C. Xie, M.H. Zhao, Shanghai Institute of Applied Physics, Chinese Academy of Sciences, Shanghai, China
F. Yang, Shanghai APACTRON Particle Equipment Co., Ltd, Shanghai, China
[1]also at University of Chinese Academy of Sciences, Beijing, China

Abstract

An Interdigit H-mode Drift-Tube-Linac (IH-DTL) with Alternating-Phase-Focusing (APF) method working at 325 MHz was designed. With the RF field established properly in the cavity, protons can be accelerated from 3 MeV to 7 MeV successfully. In this paper, the process of designing such an APF IH-DTL cavity is going to be presented. Also, the characteristics of the cavity and parameters studying of RF are going to be demonstrated.

INTRODUCTION

Over the recent decades, with the development of particle accelerator physics and related technologies, using energetic particles such as protons, electrons provided from them to treat cancers is more and more efficient and practical. Because of protons' unique Bragg peak, proton accelerators attract a lot of attention.

As a key member, Shanghai Institute of Applied Physics (SINAP) work together with other two members to establish a joint company named Shanghai APACTRON Particle Equipment Co., Ltd to manufacture the Advance Proton Therapy Facilities. To be competitive, we are going to improve the facility in many aspects. A 7 MeV injector is one of main components which are being improved by us now.

Usually, this typical injector consists of a compact Electron-Cyclotron-Resonance Ion Source (ECRIS), a Radio-Frequency-quadrupole (RFQ) and a Drift-Tube-Linac (DTL), the RFQ and DTL accelerates protons from 40keV to 3 MeV and then to 7 MeV respectively. Traditional DTL is quite bulky, heavy, high-cost and difficult-to-maintain which limits its popularization as an injector for medical facility.

IH-DTL working with APF have the advantages of compact, cost-efficient and easy-to-maintain, so we adopt it as a candidate for our compact injector. Interdigit H-mode as an idea was first proposed in the 1950s by J. P. Blewett [1]. High shunt impedance is one of its main features, so this type of structure's RF power consumption is much lower than that of a conventional Alvarez-type DTL with energy lower than 10 MeV. Unfortunately, due to the slow development of three-dimensional(3D) electromagnetic (EM) field solver and rather complicated cavity structure, this advanced structure didn't have a good development over the past decades.

Entering the 21st century, well-developed 3D EM solvers like CST, HFSS, etc. make it practical to get the precise field distribution and optimize the cavity dimensions and RF characteristics [2]. Also, we exported the 3D RF field from CST microwave studio and got rather good results using a third-part code TraceWin [3].

In the following sections, a latest design of the APF IH-DTL for a compact injector is going to be presented. It concludes considerations of the cavity, the RF characteristics and geometric dimensions, the comparison between the calculated-voltages and required-voltages from beam dynamics.

APF IH-DTL

There are several linear accelerators adopting APF IH-DTL cavities [4-6]. Regarding to the principle of APF, A sequence of negative and positive phases alternatively appear between adjacent two electrodes(tubes). When the particles go through these different gaps and the tubes along the longitudinal axis, the negative phases they meet will focus the particle bunches longitudinally but defocus them radially. Conversely, the positive phases will focus the particles bunches radially but defocus them longitudinally. After several sinusoidal like periods of the phase sequence, we can get the particles focused successfully both in longitudinally and radially. Figure 1 shows the principle of APF [7]. Then the additional focusing elements in the case of conventional DTL can be saved in the APF LINACs. These features can significantly reduce the construction and maintenance cost of the radio therapy facilities adopting APF IH-DTL as its injector.

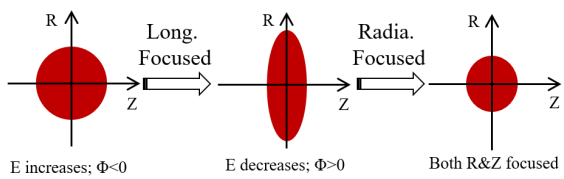


Figure 1: Demonstration of focusing principle of APF.

Unlike TM_{010} mode in the conventional DTL, TE_{111} mode is excited in an IH-DTL cavity. Alternatively introducing tubes supported by the stem connecting to the opposite wall, we can get the longitudinal accelerating E-field at π mode in Fig. 2.

† corresponding author: Tel: +86 130 6260 1189
E-mail address: puyuehu@sinap.ac.cn

Content from this work may be used under the terms of the CC BY 3.0 licence (© 2018). Any distribution of this work must maintain attribution to the author(s), title of the work, publisher, and DOI.

ISBN: 978-3-95450-194-6 ISSN: 2226-0366 doi:10.18429/JACoW-LINAC2018-MOPO080

THE MANUFACTURING OF THE CSNS DTL TANK

X. L. Wu[1,†], H. C. Liu[1], K. Y. Gong, H. Song, S. M. Liu[1], L. Dong, T. Luo[1], Institute of High Energy Physics, Chinese Academy of Sciences (CAS), 100049 Beijing, China
[1]also at Dongguan Neutron Science Center, 523803 Dongguan, China

Abstract

The DTL tank is a crucial component of the China Spallation Neutron Source (CSNS) linear accelerator (LINAC), which mainly use the technology of oxygen-free copper (OFC) electroplating on the inner surface of the 20# carbon steel tube. It is the first time to perform OFC electroplating with high electrical conductivity in the high intensity beam accelerator in China. In the process of cavity manufacturing, problems such as machining deformation, plating surface nodule and plating peeling are encountered. In this project, based on pre-research and information from literature, the formula of acid solution was improved to construct a stable pickling process protocol. The manufacturing process of DTL tank and the measurement details are introduced in this paper.

INTRODUCTION

The CSNS DTL tank is approximately 36m long and contains 4 RF cavities. A total of 153 drift tubes are installed on the top of the cavities. Each RF cavity is equipped with 12 fixed tuners evenly distributed at the bottom of cavity, these tuners are used to compensate for the frequency shift caused by machining errors. 2 movable tuners are also used to modulate local frequency disturbances caused by high frequency heating. The high frequency power is fed by an iris waveguide coupler mounted in the middle of the cavity. There are 12 water cooling channels embedded into the tank out-wall. The tank will operate in a sufficiently high vacuum for RF environment by using 3 turbo molecular pumps and 9 ion pumps per RF cavity [1].

For ease of manufacturing, transportation and installation, each RF cavity is divided into 3 unit sections which can be bolted together [2]. The inner diameter of the unit section is about 566mm, and the length ranges from 2760mm to 3100mm. The manufacturing precision is high, and the key technical indicators are shown in Table 1.

The cavity manufacturing mainly include machining, electroplating, pickling and measuring. The machining factory that cooperated during the pre-research period is replaced by two new manufacturers. The electroplating process is also changed, which must be re-explored. The manufacturing and test details are presented in this paper.

Table 1: Key Technical Indicators of DTL Tank

Indicators	Tolerance
Length (before plating)	-0.30~-0.10 (mm)
Inner diameter (before plating)	± 0.10 mm
Side holes position (before plating)	± 0.10 mm
Plating thickness	0.15 ± 0.05 (mm)
Surface roughness	0.8 um
Plating adhesion	No peeling after baking
Vacuum	≤ 1.0 E-5 Pa

MACHINING

The cavity has a large size, a large number of side holes, and requires high precision. There are 15 key processes in machining, including turning, welding, benching, heat treatment, milling, boring, grinding, measuring, etc. The cylindricity of the cavity 1# machined by manufacturer A is out of tolerance (0.50mm>0.10mm). The precision of milling machine in the manufacturer B is low (the worktable moves 3000mm, its displacement deviation is -0.36mm; the reset deviation is -0.22mm, after the worktable moves 3000mm)，which results in difficulty in fine boring of the side holes on the cavity 2#.

It's analyzed that the reason for the deviation of the cavity 1# is because the process has been reversed between turning the inner surface of the cavity and milling cooling sink around the out-wall. In order to solve the problem, we strengthened communication with manufacturers, reconfirmed the process route, and required manufacturers to strictly implement the process. Offset value is offered by the laser tracker before the fine boring of the side holes on the cavity 2#. Our colleagues were stationed in factories to track the quality of machining at the critical stage of the processing. Finally, we successfully completed the machining of all cavities. The key indicators are shown in Fig.1.

The length precision is partially out of tolerance (Max ΔX=0.13mm), which can meet the design requirements (after plating) by controlling the plating thickness on the end plate. The inner diameter precision of all cavities meets the requirements. The position of all 153 drift tube holes is measured and only 3 out of tolerance (Max ΔX=0.02mm), which we considered to meet the installation requirements.

† wuxiaolei@ihep.ac.cn

Content from this work may be used under the terms of the CC BY 3.0 licence (© 2018). Any distribution of this work must maintain attribution to the author(s), title of the work, publisher, and DOI.

ISBN: 978-3-95450-194-6 ISSN: 2226-0366 doi:10.18429/JACoW-LINAC2018-MOPO081

LIGHT PROTON THERAPY LINAC LLRF SYSTEM DEVELOPMENT

B. Baricevic, A. Bardorfer, R. Cerne, Instrumentation Technologies, Solkan, Slovenia
G. De Michele, Y. Ivanisenko, AVO-ADAM, Meyrin, Switzerland

Abstract

Proton cancer therapy is a state-of-the-art medical treatment technique based on an accelerator beam production facility. The LIGHT linear accelerator design by AVO-ADAM offers a modular compact solution for precise control of the treatment dose delivery, both position and energy wise. Proton energy can be modulated at up to 200 Hz in a range from 70 to 230 MeV by varying the gradient of the accelerating structures. The normal conducting LINAC RF system is based on a 750 MHz RFQ and 12 S-band stations individually controlled. A customized LLRF system is being developed on the Libera LLRF platform for the LIGHT project. The paper is describing the required cavity field control functionality and the other subsystems such as master oscillator reference, cavity tuning, real-time control, data acquisition, control system and synchronization interfaces.

INTRODUCTION

The LIGHT (Linac for Image Guided Hadron Therapy) proton cancer therapy LINAC, designed by AVO-ADAM, is based on 13 normal conducting RF station modular design, conceived to modulate independently the RF power at 200 Hz, at the level of each high-power station. Together with low emittance it allows accurate dose delivery within the tumour volume and longitudinal layer switching on pulse-to-pulse basis. Moreover this feature opens up the highly desirable possibility to implement image-guided adaptive radiation therapy with protons, which is a unique property of the LIGHT system [1].

The compact LIGHT LINAC design consists of:

- a proton source at 40 keV providing currents up to 300 uA with pulses up to 20 us at 200 Hz repetition rate.
- an RFQ (Radio Frequency Quadrupole) at 749.48 MHz accelerating the protons up to 5 MeV, operated at the forth sub-harmonic of the 2997.92 MHz LINAC frequency. The RFQ RF system provides to the LLRF system, 4 cavity probe signals and 4 pairs of directional coupler forward and reflected signals.
- Two SCDTL (Side Coupled Drift Tube LINAC) high power RF units at 2997.92 MHz, delivering the beam at 37.5 MeV. Each SCDTL RF station provides 4 cavity probe signals and 3 pairs of directional coupler forward and reflected signals, as the klystron amplifier output is split between two accelerating structures.
- Ten CCL (Coupled Cavity LINAC) high power RF units at 2997.92 MHz accelerating beam up to 230 MeV. Five CCL units provide 2 RF probe signals and 2 pairs of directional coupler forward and reflected signals. In the other five CCL RF stations, 4 probes and 3 pairs of directional coupler signals are provided as the high-power drive is split among two accelerating structures.

In Figure 1 a scheme of the LIGHT proton accelerator compact design is presented. The total peak RF power required by the structures would therefore be 400 kW, 8 MW and 45 MW, respectively for the RFQ, SCDTL and CCL structures [2,3].

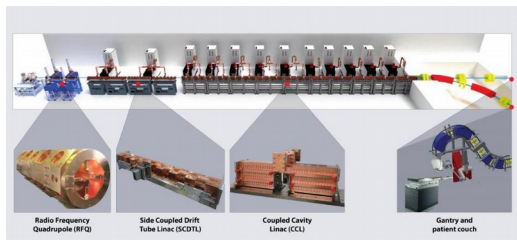


Figure 1: A scheme of the LIGHT proton accelerator.

THE LLRF SYSTEM REQUIREMENTS

To control the proton acceleration, it's required that all the 13 RF stations are tightly synchronized to the Master Oscillator (MO) and the LLRF system provides field control at the level of individual RF stations. Moreover, the LLRF system must apply the RF pulses of specific shape at nominal RF pulse length 20 μs and 7μs for the RFQ and the S-band structures respectively. Parameters defining RF pulse shape, it's amplitude and phase, must be provided to the LLRF system in real-time at 200 Hz rate in order modulate the proton energy according to the programmed treatment plan.

For cavity conditioning purpose, it's further required that the LLRF system has the ability to drive the cavity in a frequency range of 749.38 ± 1 MHz and 2997.92 ± 4 MHz. The LLRF system is also designed to automatically track the cavity resonant frequency within the range.

For the purpose of proton energy modulation, it is required that the LLRF system is operated in a 20 dB dynamic range, where also amplitude and phase stability requirements are specified (Table 1) [4].

To avoid the transmission of the reference MO signal over distance, it's required that the LLRF units controlling the RF stations are tightly synchronized to a common MO source to be installed at the same location of the LLRF units. The required stability for the MO signal distribution shall be within ±0.1°.

Content from this work may be used under the terms of the CC BY 3.0 licence (© 2018). Any distribution of this work must maintain attribution to the author(s), title of the work, publisher, and DOI.

ISBN: 978-3-95450-194-6 ISSN: 2226-0366 doi:10.18429/JACoW-LINAC2018-MOPO082

COMMISSIONIG STATUS OF THE LINAC FOR THE iBNCT PROJECT

M. Sato†, Z. Fang, M. Fukuda, Y. Fukui, K. Futatsukawa, Y. Honda, K. Ikegami, H. Kobayashi, C. Kubota, T. Kurihara, T. Miura, T. Miyajima, F. Naito, K. Nanmo, T. Obina, T. Shibata, T. Sugimura, A. Takagi, E. Takasaki, High Energy Accelerator Research Organization (KEK), 305-0801 Tsukuba, Japan
H. Kumada, Y. Matsumoto, T. Ohnishi, S. Tanaka, University of Tsukuba, 305-8577 Tsukuba, Japan
N. Nagura, T. Ohba, Nippon Advanced Technology 319-1112 Tokai, Japan
T. Ouchi, H. Sakuryama, ATOX Co., Ltd., 319-1112 Tokai, Japan
K. Hasegawa, Japan Atomic Energy Agency, 319-1195 Tokai, Japan

Abstract

For a new type of cancer therapy, the accelerator-based boron neutron capture therapy (BNCT) has been attracted renewed interest. The basic concept of BNCT is to utilize secondary products from a neutron capture reaction on boron medicaments locally-implanted into cancer cells. It has been originally studied with neutrons from nuclear reactors for a long time, meanwhile many activities have been recently projected with accelerator-based neutron generation techniques. In the iBNCT (Ibaraki BNCT) project, the accelerator is consisted with RFQ and Alvarez DTL. We have started the beam commissioning of the accelerator from the end of 2016, and an acceptably-stable operation was achieved with beam repetition of 50 Hz, which is equivalent of the average current of 1.4 mA at the target. This current makes the project possible to proceed to non-clinical bench test toward a first-phase clinical trial study. Further beam commissioning will be performed toward higher beam current. In this paper, a present status of the iBNCT linac and its future prospect will be reported.

INTRODUCTION

An academic-industrial collaborative project for BNCT, Ibaraki-Boron Neutron Capture Therapy (iBNCT) project, has been started in the year of 2010. It is a collaboration with High Energy Accelerator Research Organization (KEK) for an accelerator part, Tsukuba University for a medical part and supportive works by neighbouring companies and Ibaraki prefecture in Japan [1].

BNCT has been originally studied with neutrons generated from a nuclear reactor, but the recently many activities have been started with accelerator-based neutron generation methods. In the iBNCT project, the accelerator is consisted of an RFQ and Alvarez DTL, whose configuration was based on that in J-PARC linac. Primary 50-keV protons extracted from an ECR ion source are accelerated by RFQ and DTL up to 3 MeV and 8 MeV, respectively, and bombarded onto a beryllium target to generate neutrons by the ^{9}Be(p, n) reaction. The most significant difference from J-PARC one is the higher duty factor, more than 5 %, is necessary to have a sufficiently-strong epithermal neutron flux for BNCT. Detailed parameters of RFQ and DTL are found in Ref. [2]. One of the features of the iBNCT project is to take aim for BNCT to become a popular cancer therapy not to need specific irradiation facilities. Thus, iBNCT makes compact the whole size of the components to be enable to install inside hospitals.

We have confirmed the first 8-MeV proton beam and neutron generation from the target in 2014 and 2015, respectively. The beam commissioning for higher beam current has been started since 2016. After that, the iBNCT accelerator has been officially certificated as a radiation generator facility since Jan. 2017. In this paper, recent commissioning status will be reported

INSTABILITY OF RFQ AND ITS IMPROVEMENTS

In the former half of 2017, instability of the beam operation caused by an RF interlock followed by a failure in its recovery made difficult to keep the operation for 1 hour which is required for a typical medical-treatment time of BNCT. A discharge inside RFQ frequently occurred and it stopped the RF pulse for the machine protection system of the cavity. In a normal situation, we can quickly re-input RF after the stop (Quick-Recovery) within 1 second. However, a success rate of this Quick-Recovery functionality is not so high due to a problem on RFQ cooling water system described later. Another problem is a pressure in RFQ. A hydrogen gas flow from the ion source increases the pressure in RFQ during the beam operation. It was obviously shortage of the pumping power for the 1-hour operation. Therefore, we first tried to improve these two issues, and details are described in the following sections.

Reinforcement of the Vacuum System

In the beam operation with 50 Hz repetition, due to the hydrogen gas flow from the ion source, the pressure in RFQ gradually increased and sometimes came up to the interlock level. For the beam operation longer than 1 hour, it is necessary that the reinforcement of the vacuum system of RFQ. Originally, 2 cryo-pumps, 10 ion pumps and 2 NEG pumps were equipped to RFQ. We newly installed turbo molecular pumps (TMP). To have enough compulsivity to hydrogen, two TMPs with evacuation

† email address masaharu.sato@kek.jp

Content from this work may be used under the terms of the CC BY 3.0 licence (© 2018). Any distribution of this work must maintain attribution to the author(s), title of the work, publisher, and DOI.

ISBN: 978-3-95450-194-6 ISSN: 2226-0366 doi:10.18429/JACoW-LINAC2018-MOPO084

THE SIMULATION AND MANUFACTURE OF THE ROOM TEMPERATURE CH-DTL*

Jinhai Li†, Chunguang Li, Guangwen Han, China Institute of Atomic Energy, Beijing,China
Zhihui Li, Institute of Nuclear Science and Technology, Sichuan University, Chengdu,China

Abstract

The room temperature Cross-bar H Type Drift Tube Linac (CH-DTL) is one of the candidate acceleration structures working in CW mode. In order to optimize the parameters, the 3 dimensional electromagnetic field of the CH-DTL cavity is simulated. The method of parameter sweeping with constraint variable is better than the method of parameter sweeping with only one variable during the optimization. In order to simplify the manufacture, the drift tube surface can be designed as spherical shape. The CH-DTL cavity has been manufactured and tested.

INTRODUCTION

An Accelerator Driven transmutation System (ADS) [1, 2], currently under development in China, will be used to reduce both the toxicity and half-life of the long-lived radioactive nuclear waste created in light-water reactors to a controllable level [3]. An industrial scale ADS will require an average beam current of≥10 mA. In 2010, the Institute of High Energy Physics (IHEP) and the Institute of Modern Physics (IMP) are both developing superconducting accelerating structures which would follow an RFQ [4].

Although low power consumption and a large aperture favor superconducting structures following a 2-3.5MeV RFQ, normal-conducting accelerating structures have some advantages [5, 6]. Normal-conducting structures in the energy range from 2 to a few tens of MeV are more compcter and can obtain high acceleration gradient than the superconducting ones and, when located downstream of the RFQ, they can serve as a beam filter to reduce the potential for beam loss at higher energies. The CH structure, initially proposed by IAP [7, 8], belongs to the π-mode family of accelerating structures and is typically characterized by high shunt impedance, low stored energy and stable geometry that is relatively easy to cool. This structure is evaluated as a potential candidate for CW operation. In this paper it is presented the results of geometry optimization of the CH structure using the method of parameter sweeping with constraint variable (PSCV) [9].

THE METHOD OF PARAMETER SWEEPING WITH CONSTRAINT VARIABLE

The parameters of a single cell are shown in Fig. 1. The outer drift tube radius (TR) and the radius of the drift tube aperture (HR) are fixed during the optimization. Typically a single parameter was swept while monitoring the cavity's RF properties. However, by changing the length of the drift tube, the resonant frequency changes. Our objective is to optimize the cavity geometry at a fixed frequency (325 MHz). If the frequency changes during the optimization, the optimized value of the swept parameter will differ from the value corresponding to the correct frequency as shown in Fig.2 and Table1. In Fig. 2 the radius of the drift-tube stem base (R2) was swept while fixing the cavity radius (CR). It can be seen that the effective shunt impedance decreases with increasing R2 while the resonant frequency increases from 321.7 to 333.5 MHz. It is convenient to use the cavity radius (CR) as a "constraint variable" to fix the resonant frequency to 325 MHz as shown in Table1. By doing so, it can be found that the maximum effective shunt impedance at the correct frequency occurs at R2=22. This method can be named after "parameter sweeping with constraint variables" (PSCV). Other parameters can be selected as constraint variables, but it is found that the resonant frequency is more sensitive to cavity radius than it is to other geometrical parameters.

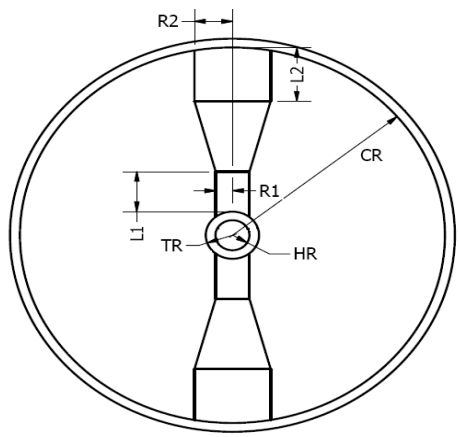


Figure 1: Geometry of a CH single cell.

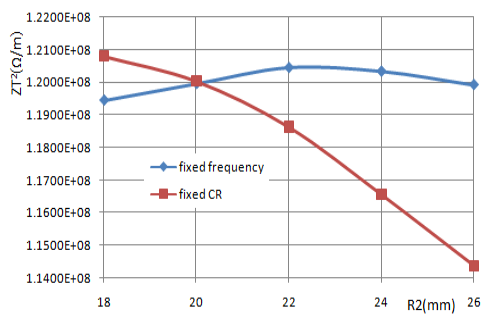


Figure 2: Shunt impedance as a function of outer stem radius using two methods of parameter sweeping.

* Work supported by the National Natural Science Foundation of China (NSFC)
† email address:13661338455@163.com

Content from this work may be used under the terms of the CC BY 3.0 licence (© 2018). Any distribution of this work must maintain attribution to the author(s), title of the work, publisher, and DOI.

ISBN: 978-3-95450-194-6 ISSN: 2226-0366 doi:10.18429/JACoW-LINAC2018-MOPO085

PROTOTYPE OF AN INTER-DIGITAL H-MODE DRIFT-TUBE LINAC FOR MUON LINAC

Y. Nakazawa*, H. Iinuma, Ibaraki University, Mito, Ibaraki, Japan
Y. Iwata, National Institute of Radiological Sciences, Chiba, Japan
Y. Iwashita, Kyoto University, Kyoto, Japan
M. Otani, N. Kawamura, T. Mibe, T. Yamazaki, M Yoshida, KEK ,Tsukuba, Ibaraki, Japan
R. Kitamura, H. Yasuda, University of Tokyo, Hongo, Tokyo, Japan
Y. Kondo, K. Hasegawa, T. Morishita, JAEA, Tokai, Naka, Ibaraki, Japan
N. Saito, J-PARC center, Tokai, Naka, Ibaraki, Japan
Y. Sue, Nagoya University, Nagoya, Japan
N. Hayashizaki, Tokyo Institute of Technology, Tokyo, Japan

Abstract

An inter-digital H-mode (IH) drift-tube linac (DTL) is developed for a low velocity part in a muon linac at the J-PARC E34 experiment. It will accelerate muons from $\beta = 0.08$ to 0.28 at an operational frequency of 324 MHz. In order to achieve higher acceleration efficiency and make cost lower, an alternative phase focusing (APF) scheme is adopted. A prototype with 6 cells of 0.45 m length was manufactured. The prototype accelerates muons from $\beta = 0.08$ to 0.15 stage. We conducted frequency measurement and bead-pull measurement as a low-power measurement, in order to evaluate the prototype product. In this paper, the results of the low-power measurement for prototype cavity will be presented.

INTRODUCTION

The muon anomalous magnetic moment (g-2) is the one of the promising signals of beyond the Standard Model. The E821 experiment at Brookhaven National Laboratory found the 3.7σ discrepancy between the SM theoretical calculation and the measurement of the muon g-2 [1, 2]. The muon beam in the E821 experiment was produced by in-flight pion decay with large emittance, which requires electric quadrupoles to keep the muon beam inside of the beam pipe. In order to avoid muon precession in the electric field, the muon beam should be well adjusted to the fixed value (magic momentum).

In the case of J-PARC experiment (J-PARC E34), we plan to measure muon g-2 and EDM (Electric Dipole Moment) with new technique [3]. We will provide a low emittance muon beam for high precision measurement from the stopping pion decay and their reacceleration steps [4]. In this method, electric field is not needed in storage ring, and the systematic error is reduced.

Figure 1 shows the schematic image of muon linac. μ^+ with a kinetic energy of 30meV called ultra slow muon (USM) is accelerated by muon linac. The muon linac is composed of a radio frequency quadrupole (RFQ) linac, the IH-DTL, a disc and washer coupled cavity linac (DAW-CCL), and a disc loaded structure (DLS). The USM is accelerated to 212 MeV. The IH-DTL is employed during the particle velocity $\beta = 0.08$ to 0.28 stage with an operational frequency of 324 MHz.

In this paper, we describe the result of the low-power measurement of the prototype cavity. The paper is structured as follows. First the prototype design is described. Next, the results and discussion of frequency measurement and bead-pull measurement is presented. Finally, the summary is presented.

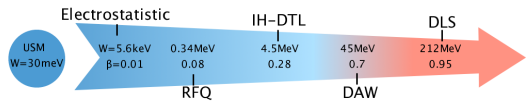


Figure 1: Schematic image of muon linac.

APF IH-DTL

H-mode DTL is installed hollow conducting drift tube along the beam axis. The drift tube is supported by stems attached to the outer wall. In time variation, the magnetic fields at the surface of the stems induce current. The structure of IH-DTL prototype is shown in Fig. 2. The IH cavity consists of two ridges arranged on both the top and bottom sides of the cavity. Five drift tubes are arranged alternately on the top and bottom via stems on the ridges, in order to excite TE_{11}-mode. The beams are accelerated by the longitudinal electric field with the gap.

The focusing section is necessary for linac to suppress the beam dispersion. The usual focusing method is provided by a quadrupole magnet and a permanent magnet. However, our IH-DTL employs the alternating phase focusing (APF) method [5, 6]. In APF method, the focusing or divergence of beam is controlled with the RF field only by optimizing synchronous phase of gap. Thus, the IH structure is simplification and is able to be fabricated at lower cost.

The motion equation of the longitudinal and transverse focusing in RF field are expressed as

$$z'' - \frac{\pi e E_0 T \sin\phi}{2 m_0 c^2 \beta^3 \gamma^3 \lambda} z = 0 \qquad (1)$$

* 18nm021f@vc.ibaraki.ac.jp

Content from this work may be used under the terms of the CC BY 3.0 licence (© 2018). Any distribution of this work must maintain attribution to the author(s), title of the work, publisher, and DOI.

ISBN: 978-3-95450-194-6 ISSN: 2226-0366 doi:10.18429/JACoW-LINAC2018-MOPO087

COLD TEST OF HYBRID RFQ PROTOTYPE

P.Y. Yu †, B. Zhang, C.X. Li, F.F. Wang, Z.J. Wang, Y. He
Institute of Modern Physics, Chinese Academy of Sciences, Lan Zhou 730000, China

Abstract

Hybrid RFQ is proposed as a potential good choice at the low-energy range of linear accelerator, which is combined by four-vane RFQ structure and CH-DTL structure. It has higher energy gain rate compared to conventional RFQ, and it is more compact than traditional DTL. In order to research on the RF performance and process exploration of this structure, an aluminium prototype is developed. The cold test of Hybrid RFQ prototype is completed. This paper will present the results and analysis of the test.

INTRODUCTION

Hybrid RFQ is a spatially periodic structure with RF quadrupoles [1, 2], which is combined by alternating CH-DTL sections and four-vane RFQ sections. It has higher accelerating efficiency than traditional RFQ, and shows stronger focusing strength than magnetic focusing DTL, especially when accelerating low r/q ions [3]. The results of beam dynamics and RF simulation of the Hybrid RFQ operated at 81.25 MHz show that the structure has a good performance to accelerate $^{238}U^{34+}$ from 0.38 MeV/u to 1.33 MeV/u [4].

In order to verify the RF performance and the mechanical structure (see Fig. 1) of Hybrid RFQ, as well as to explore the machine processing, an aluminium prototype is developed. The frequency is chosen as 325 MHz to reduce the size of cavity. The length is 1m, and the diameter is approximately 0.3m. The mechanical structure of Hybrid RFQ is complicated. Thus on the one hand, it requires high precision for machining. On the other hand, it is difficult to assemble [5]. The manufacture and cold test of Hybrid RFQ are completed; the results and analysis will be presented.

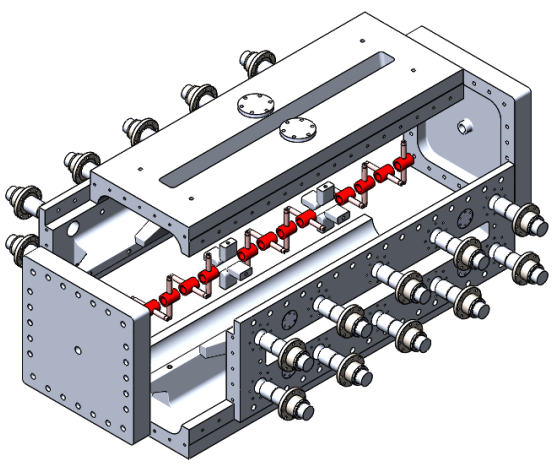


Figure 1: The overall mechanical model of Hybrid RFQ.

† email address: peiyanyu@impcas.ac.cn

RF MEASUREMENT

Measurement Instrument

According to the resonator perturbation theory, the cold test of Hybrid RFQ is conducted using the bead-pull measurement system. During the progress of the C-ADS project, a motion control and data acquisition system for bead-pull measurement has been fabricated [6]. The system including equipment is shown in Fig. 2. The computer controls the motor to drive the wire to move the bead through the cavity, and records the motion steps of the motor. The Vector Network Analyzer transports the frequency or phase signal to the computer.



Figure 2: Bead-pull measurement system.

Measurement of Frequency and Q Value

The frequency and Q value are measured at first after processing. The measured frequency is 326.72 MHz with each penetration depth of 20 tuners is 20 mm. It's 1.72 MHz higher than designed frequency, which is in the adjustable range of tuners. In consideration of the measured size of the parts of cavity, it shows that the main reason of this frequency deviation is the lack of constant temperature condition while processing. The ambient temperature is high when machining, while the measurement is conducted in low temperature. The shrinkage of size leads to the increase of frequency. Furthermore, this point needs verification by simulation. The measured unloaded Q value is 7198. Compared with the calculated value 9083, the measurement value reaches 79.2% of it. Considering there is no RF sealing in the aluminium cavity, this result is acceptable.

The RF measurement of Hybrid RFQ is performed to verify the accuracy of processing and assembly. It includes two parts, one is the measurement of the accelerating field of central axis, and the other is the measurement of the quadrupole field at the RFQ section. The measurement results are compared with the theoretical results which are simulated using CST software. The perturbation body is chosen as a plastic sphere bead with a diame-

Content from this work may be used under the terms of the CC BY 3.0 licence (© 2018). Any distribution of this work must maintain attribution to the author(s), title of the work, publisher, and DOI.

ISBN: 978-3-95450-194-6 ISSN: 2226-0366 doi:10.18429/JACoW-LINAC2018-MOPO088

STUDY ON A 325MHz HOM DRIFT TUBE LINAC*

L. Lu†, C. C. Xing[1], T. He[1], L. Yang[1], X. B. Xu, L. B. Shi, L. P. Sun, J. Li[1], Q. X. Xia[1], Z. C. Gao
Institute of Modern Physics (IMP), CAS, 730000 Lanzhou, China
[1] also at University of Chinese Academy of Sciences, 100049 Beijing, China

Abstract

Normally, drift tube linacs (DTL) are used following RFQ linacs for beam acceleration in middle and high beam energy region. but acceleration efficiency of DTLs is decreasing with beam energy increasing. Using resonated higher order mode (HOM) of cavity, DTL can get higher effective shunt impedance. we proposed a 325MHz DTL with TE_{115} mode. In this paper, the dynamics calculation and electromagnetic design of the HOM-DTL will be reported.

INTRODUCTION

Shown in Fig. 1, in the low energy region, because the Interdigital-H (IH) type drift tube linacs (DTLs) have a higher shunt impedance and suitable accelerating structure for heavy ion acceleration, the DTLs operated in TE111 mode are normal used following the RFQ type linac [1-3]. However, in the medium and high energy region, the Alvarez type DTLs operated in TM010 mode are normally used although its shunt impedance reduces rapidly [4-5], shown in Fig. 2, because its higher shunt impedance is higher than the IH-DTLs in those energy regions.

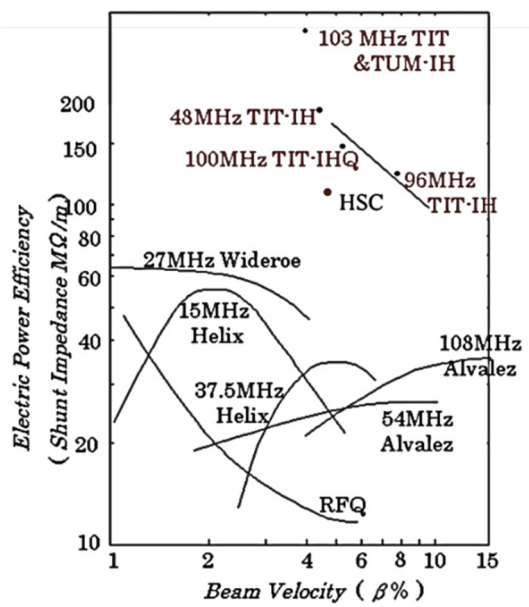


Figure 1: The shunt impedance of the low beta linacs.

Since the DTLs operated in TE11n mode of the higher order mode have a property which is suitable to accelerate ions in medium and high energy region [6], we proposed a 325MHz DTL operated in TE115 mode. Our proposed HOM-DTL is designed as a prototype buncher and its structure is shown in Fig. 3.

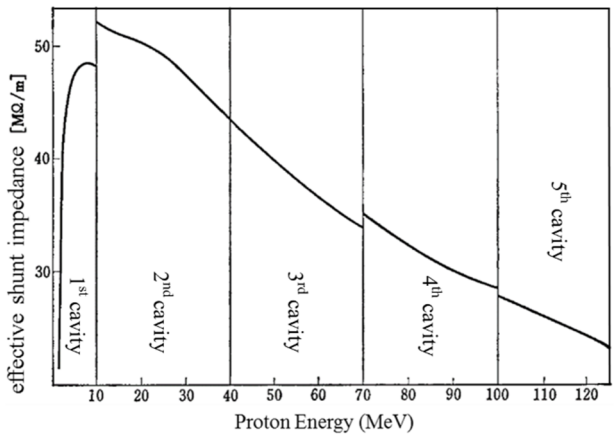


Figure 2: The shunt impedance changing of the Alvarez type DTLs.

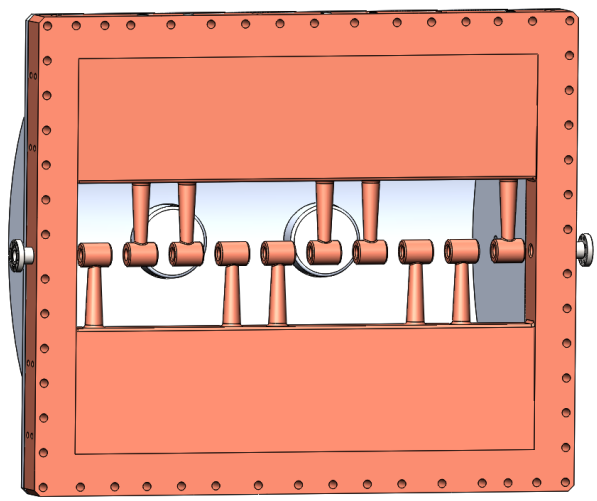


Figure 3: The inner structure of proposed HOM-DTL.

ELECTROMAGNETIC DESIGN

The frequency of proposed HOM-DTL is 325MHz which is 4th harmonic of the frequency of 81.25MHz. This HOM-DTL is a prototype research for future heavy ion buncher. The estimated peak voltage is rather high as several mega-voltages (MV). The Microwave Studio (MWS) code and ANSYS code are used to calculate the cavity electromagnetic simulation and mechanical simulation [7-8].

*Work supported by NSFC under Grant No. 11427904, No. 11475232 and No. 11535016
† luliang@impcas.ac.cn

Content from this work may be used under the terms of the CC BY 3.0 licence (© 2018). Any distribution of this work must maintain attribution to the author(s), title of the work, publisher, and DOI.

ISBN: 978-3-95450-194-6 ISSN: 2226-0366 doi:10.18429/JACoW-LINAC2018-MOPO089

DESIGN DETAILS OF THE EUROPEAN SPALLATION SOURCE DRIFT TUBE LINAC

P. Mereu*, M. Mezzano, C. Mingioni, M. Nenni, INFN-TO, Torino, Italy
F. Grespan, A. Pisent, INFN-LNL, Legnaro, Italy
G. Cibinetto, INFN-FE, Ferrara, Italy

Abstract

The Drift Tube Linac (DTL) of the European Spallation Source (ESS) is designed to operate at 352.2 MHz with a duty cycle of 4% (3 ms pulse length, 14 Hz repetition period) and will accelerate a proton beam of 62.5 mA pulse peak current from 3.62 to 90 MeV. This paper gives a detailed overview of the ESS-DTL current mechanical design, and the related driving criteria. It presents also an outlook of the main aspects of the assembly and installation, with related equipments, tooling and procedures.

DTL GENERAL DESIGN

In the ESS accelerator the initial warm linac section is composed by the Ion Source, Low Energy Beam Transport line (LEBT), Radio Frequency Quadrupole (RFQ), Medium Energy Beam Transport line (MEBT) and DTL [1].

The DTL has a partially similar design to the CERN LINAC4: it is a 38.8 m long system, divided in five cylindrical RF cavities (Tanks) [2]. Each tank is a standalone structure composed by four 2 m long modules, made of AISI 304L stainless steel with copper plating on internal surfaces. The Drift Tubes are positioned in the girder, a precisely machined aluminium alloy structure housed in the upper part of each module [3].

The tank is closed at both ends by a closing cover with a half DT on the inner side. Each tank is individually supported by an isostatic mechanical support, which provide also the fine alignment of the tank on the beam line. The space between two consecutive tanks, Inter-Tank (IT), is taken up by a vacuum valve and a stain-less steel vacuum chamber, which houses diagnostic instrumentation such as Faraday Cup (FC), Wire Scanner (WS) and non-invasive Profile Monitor (PM).

COVER DESIGN

The tank covers are composed mainly by an AISI 304L circular plate and a half DT on the inner wall. Depending on the position along the beam line, the cover houses a Permanent Magnet Quadrupole (PMQ) or a Beam Current Monitor (BCM).

The steel plate is 30 mm thick and is copper plated on the inner surface facing the RF cavity. It houses 8 V-shaped cooling channels, 10 mm offset from the inner wall, each one obtained by intersecting two ⌀6 mm holes deep-drilled in the thickness of the material. Two additional ⌀8 mm channels provide the inlet and outlet for the DT cooling circuit.

The half DT is made by an external copper profile and an internal steel sleeve, both vacuum brazed on the steel plate. The DT cooling circuit is obtained by machining a circumferential channel on the sleeve, in a single or double loop depending on the DT length.

In the cover with PMQ (Fig. 1) the magnets assembly is housed inside the sleeve, while in the BCM version a current transformer is placed in a seat on the outer wall of the cover; in both cases the components are fixed by a flange on the outer side.

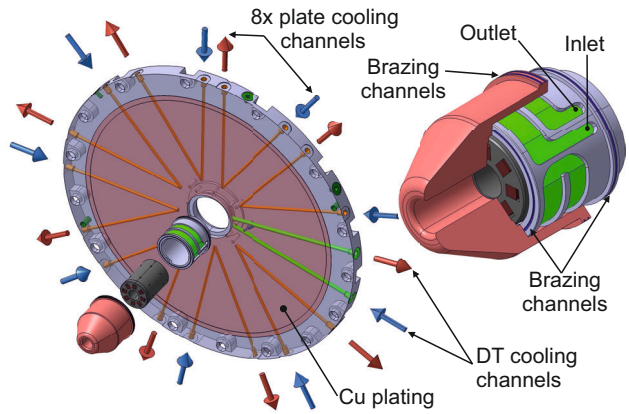


Figure 1: Layout of the cover with PMQ. Plate cooling channels coloured in orange, DT cooling circuit in green, brazing channels in blue.

Table 1: Boundary conditions and results of CFD simulation: inlet mass flow rate ($\dot{m}$) and temperature (T_{in}), average convective heat-flux coefficient (h) and pressure drop (Δp)

Circuit	$\dot{m}$ [kg/s]	T_{in} [°C]	h [W/m^{2}K]	Δp [bar]
DT channel	0.11	30	7350	0.41
Plate channel	0.05	30	6500	0.12

Computational Fluid Dynamics (CFD) and Finite Element Method (FEM) simulations were carried out to validate the design of the cover. For those analysis the maximum thermal load, corresponding to the last cover in tank 5, was set at 3869 W/m^2 on the cover wall facing the RF, and spanning from 154 W/m^2 and 23 520 W/m^2 on the DT (depending on the position). First a CFD simulation was performed in Ansys Fluent on a simplified geometry, in order to evaluate the convective heat-flux coefficient and pressure loss on both DT and plate channels (see Table 1) [4]. On this bases, a FEM thermo-structural analysis was performed in Ansys Mechanical. Figure 2 shows the results obtained from the

* paolo.mereu@to.infn.it

Content from this work may be used under the terms of the CC BY 3.0 licence (© 2018). Any distribution of this work must maintain attribution to the author(s), title of the work, publisher, and DOI.

ISBN: 978-3-95450-194-6 ISSN: 2226-0366 doi:10.18429/JACoW-LINAC2018-MOPO090

STATUS OF THE MYRRHA CH CAVITIES

K. Kümpel, S. Lamprecht, P Müller, N. F. Petry, H. Podlech, S. Zimmermann
IAP, Goethe Universität Frankfurt, Germany

Abstract

The MYRRHA (Multi-purpose hYbrid Research Reactor for High-tech Applications) project is a planned accelerator driven system (ADS) for the transmutation of long-living radioactive waste [1]. A critical passage for the beam quality and especially for the emittance is the injector, which for the MYRRHA project consists of a 4-rod RFQ, two Quarter Wave Rebunchers (QWR) and a total of 16 normal conducting CH-DTL cavities [2]. The first installment of the MYRRHA injector in Louvein-La-Neuve (Belgium) will include an ion source, a RFQ, the QWRs and the first seven CH cavities.

This paper will report on the status of the first tests of CH 1 and 2 as well as on further developments on CH 8 to 15.

THE CH SECTION OF THE MYRRHA INJECTOR

The CH section of the MYRRHA injector (see Figure 1) consists of 15 room temperature CH cavities and accelerates the proton beam from 1.5 MeV up to 16.6 MeV while using a constant phase configuration.

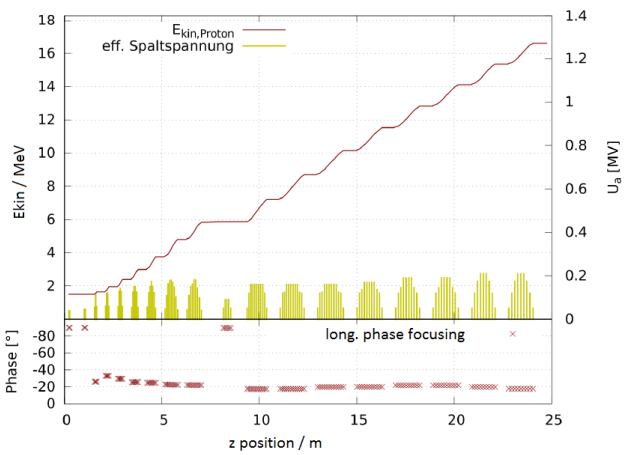


Figure 1: The estimated proton energy after the RFQ is 1.5 MeV [3] and increases up to 16.6 MeV at the end of CH 15 (upper graph in red). The effective voltages of the gaps are plotted in yellow. The lower graph shows the constant phase configuration of the CH cavities. An additional 5-gap CH Rebuncher (CHR) can be seen between CH 7 and CH 8.

Table 1: The Number of Gaps and Shunt Impedances of the CH Structures. The shunt impedances have been simulated with CST Microwave Studio [4].

Cavity	Number of Gaps	Shunt impedance [MΩ/m]
CH 1	3	22.18
CH 2	4	36.18
CH 3	5	48.38
CH 4	6	56.91
CH 5	7	61.50
CH 6	9	65.06
CH 7	9	61.06
CH 8	11	56.6
CH 9	12	53.3
CH 10	12	49.4
CH 11	11	47.8
CH 12	10	43.1
CH 13	10	41.5
CH 14	9	40.1
CH 15	9	38.8

STATUS OF CH 1

The CH 1 has been manufactured by NTG (Gelnhausen, Germany), it was copper plated at Galvano-T (Windeck, Germany) and is now in the experimental hall of the IAP (see Figure 2).

Both after production and after copper plating, measurements of the resonance frequency could be carried out and compared with the simulation result of the STEP model of the cavity (without copper plating) made with CST Microwave Studio (see Table 2).

Table 2: The Resonance Frequency f_0 of the CH 1 Simulated with CST (left), Measured Before (Middle) and After Copper Plating (right).

f_0 (simulation model) [MHz]	f_0 (before copper plating) [MHz]	f_0 (after copper plating) [MHz]
177.296	177.251	176.536

Content from this work may be used under the terms of the CC BY 3.0 licence (© 2018). Any distribution of this work must maintain attribution to the author(s), title of the work, publisher, and DOI.

ISBN: 978-3-95450-194-6 ISSN: 2226-0366 doi:10.18429/JACoW-LINAC2018-MOPO092

A 3-GAP BOOSTER CAVITY TO MATCH ION SOURCE POTENTIAL TO RFQ ACCEPTANCE

R.E. Laxdal†, ZT Ang, T. Au, S. Kiy, S. Rädel, O. Shelbaya, V. Zvyagintsev TRIUMF, Vancouver, Canada

Abstract

The ISAC RFQ can accelerate ions with A/Q ration from 1 to 30 and requires an input energy of 2.04keV/u. The harsh environment of the ISAC on-line ISOL target facility is challenged to meet the energy for the heaviest masses. For these cases we have designed and installed a short three gap device that accelerates the beams produced at source potential to match the required energy for RFQ acceptance. The booster cavity operates at 11.7MHz the RF frequency of the pre-buncher and delivers up to 9.8kV to the beam. The device can also be used as a second buncher to augment the acceptance in the RFQ or to improve the acceptance of higher space charge beams.

INTRODUCTION

The Isotope Separator and ACcelerator (ISAC) at TRIUMF produces rare-isotope beams (RIB) for studies in astrophysics, nuclear structure and reactions, electroweak interactions and material science [1]. A variety of radioisotope beams, below the space charge regime, can be generated and accelerated to a high energy area in ISAC-I or to the superconducting linac (SCL) in ISAC-II. In both cases the first accelerator in ISAC-I is a 35.4MHz split ring, four vane Radio Frequency Quadrupole (RFQ), designed without a gentle buncher or buncher section. The RFQ focusses and accelerates RIB from 2.04 keV/u (β= 0.0021) to 153 keV/u with a mass-to-charge ratio of $1 \leq A/Q \leq 30$ [2]. The source must extract ions with a bias voltage of up to about ~60 kV, depending on A/Q. Current ISAC target modules have issues holding biases beyond V_s = 52 kV. Thus for charge to mass ratios of $A/Q \geq 25$ a boost in energy is required for successful RFQ injection.

The pre-bunching of the beam allows the use of an RF device to match the beam energy to the RFQ acceptance. An RF Booster was designed, providing a voltage kick of up to10 kV to compensate for the target module issues to achieve matching to the RFQ energy acceptance of 2.04 keV/u. The booster has been designed as a three gap RF device, with an aperture large enough to avoid interference with the existing beam envelop. Fig. 1 depicts a schematic of the booster and its position in ISAC-I located between the RFQ and the three harmonic 11.8MHz pre-buncher. The required booster voltage V_b is determined by the ion's mass-to-charge ratio A/Q and the target module's extraction voltage V_s:

$$V_b[\mathrm{kV}] = 2.04[\mathrm{keV/u}]\frac{A}{Q} - V_s \quad . \qquad (1)$$

In this paper we present test results of the booster cavity as an energy compensation device and as a supplemental buncher. The relationship between bunch current and space charge is investigated for the bunching case.

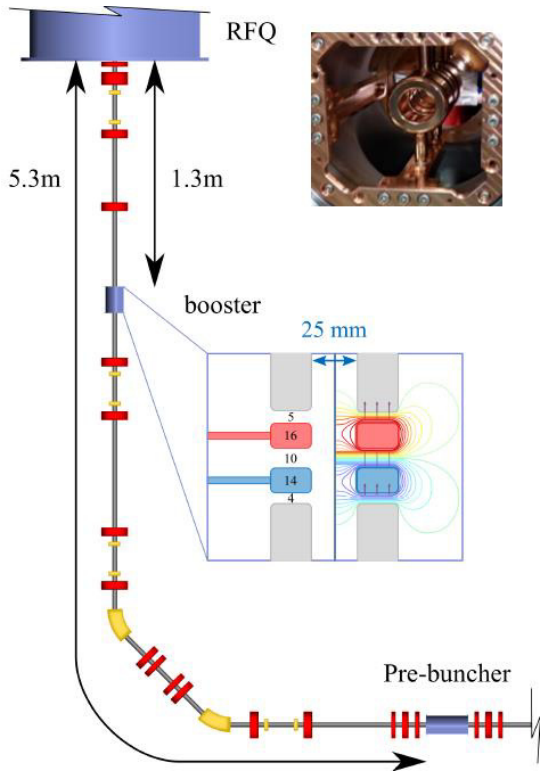


Figure 1: Pre-buncher, booster (inlay photo) and RFQ location at ISAC-I.

BOOSTER DESIGN FEATURES

An efficient design for the booster is a three gap RF device driven by an external lumped circuit. The booster drift tubes operate in a π-mode at 11.8MHz, the pre-buncher's fundamental frequency. An initial variant was described in [3]. The initial device was tested to V_{eff}=7kV and then modified to allow a power increase. The Macor used to support the drift tubes was found to be too lossy and was replaced with a small Teflon brace to support the HV feedlines to the two central drift tubes (Fig. 2).

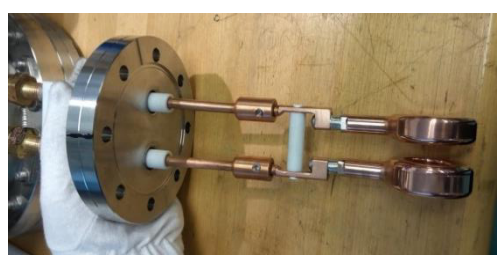


Figure 2: Booster central drift tubes and voltage feed.

Content from this work may be used under the terms of the CC BY 3.0 licence (© 2018). Any distribution of this work must maintain attribution to the author(s), title of the work, publisher, and DOI.

ISBN: 978-3-95450-194-6 ISSN: 2226-0366 doi:10.18429/JACoW-LINAC2018-MOPO093

A STUDY OF A COOLING CONFIGURATION FOR AN OFHC COPPER REBUNCHER

O. Mazor, M. Bukai, D. Nusbaum, J. Rodnizki†, Soreq NRC, Yavne, Israel
G. Ziskind, Ben-Gurion University in the Negev, Beer Sheva, Israel
E. Dyunin, Ariel University, Ariel, Israel

Abstract

A four gap OFHC copper rebuncher is developed at SNRC as a research study and a risk reduction for the MEBT of SARAF Phase II proton/ deuteron linac. The rebuncher is designed to bunch a 5 mA CW beam at 176 MHz. The required cavity voltage according to beam dynamics evaluation is 150 kV with a beam aperture diameter of 40 mm, beam energy of 1.3 MeV/u with a Q value of 8000. Considering utilizing this cavity for enhancing the beam energy, the cooling configuration is explored for a cavity voltage of 300 kV, consuming 20 kW dissipated power, at a peak electric field of 14 MV/m, equivalent to the Kilpatrick limit. The electromagnetic study conducted with the CST MW Studio was reproduced at ANSYS HFSS. The simulated dissipated power was assigned to the ANSYS Fluent model to explore the resulted temperature map. Several evolved cooling configurations were studied, including cooling of the drift tubes. In this configuration the temperature rise along the cavity is in the range of 30 K. A detailed design of the four gap rebuncher is following this study.

INTRODUCTION

An Oxygen Free High Conductivity (OFHC) copper 4 gap rebuncher is developed for the proton/ deuteron 5 mA Continues Wave (CW) SARAF linac at 176 MHz. The rebuncher beam energy is 1.3 MeV/u (beam $\beta = 0.053$) [1-3]. The required cavity voltage according to beam dynamics simulation is 150 kV with an aperture diameter of 40 mm with a Q value of 8000 [4]. We consider applying this cavity for enhancing the beam energy in order to reduce the ion velocity mismatch upstream the RFQ. In this case the peak electric field on the cavity surface is 14 MV/m (1 Kilpatrick Criterion) and the expected cavity voltage and dissipated power are 300 kV and 20 kW respectively. For normal functioning as a rebuncher the maximum field is 50% and, thus, the dissipated power is 25%. The rebuncher cooling configuration for 20 kW dissipated power is explored in this study.

MODEL ANALYSIS

The rebuncher configuration is shown in Fig. 1. The main components are: the RF cavity chamber, the upper fork with two drift tubes and the base cone with a drift tube. All these elements are made from OFHC copper. The electro-magnetic properties were simulated with CST MW Studio using the eigenmode solver (Fig. 2).

The next stage of the research was to simulate the 20 kW injected power regime. The coupler (Port 1) and the pickup antenna (Port 2) were introduced into the CST MW Studio and HFSS designs. The driven modal HFSS solver (Fig. 3) reproduced the similar results pattern that was generated by the CST eigenmode and driven modal solvers.

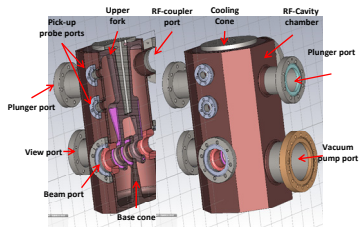


Figure 1: The rebuncher design.

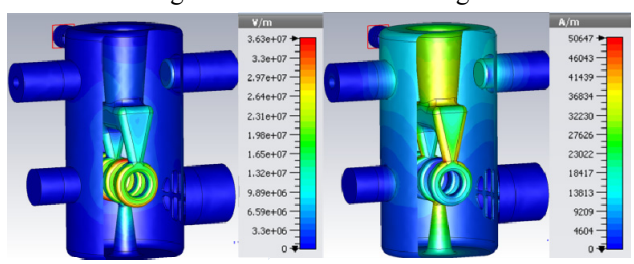


Figure 2: The induced eigenmode surface electric field (left) and magnetic field (right) at 176 MHz normalized for a 1 Joule rebuncher stored energy received from CST MW studio.

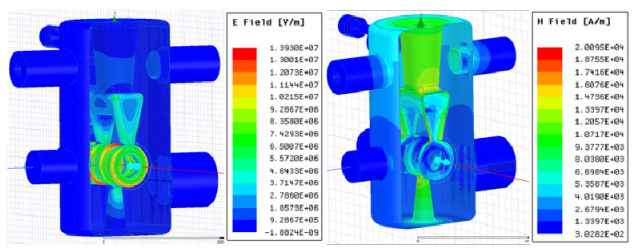


Figure 3: The induced surface electric field (left) and magnetic field (right) for 20 kW input power received with the driven modal HFSS solver.

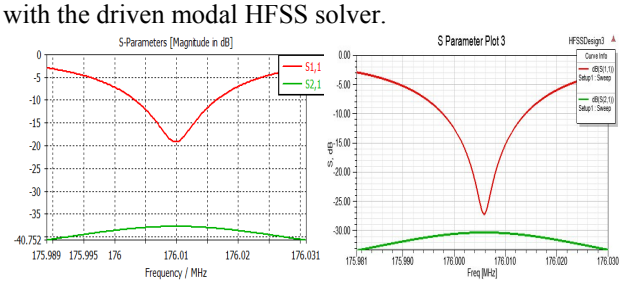


Figure 4: S-parameters of the rebuncher results from driven modal solvers of CST (left plot) and HFSS (right plot) - S11 (red curve) and S21 (green curve). The frequency range is the FWHM value (S21 -3dB level).

† jacob@soreq.gov.il

Content from this work may be used under the terms of the CC BY 3.0 licence (© 2018). Any distribution of this work must maintain attribution to the author(s), title of the work, publisher, and DOI.

ISBN: 978-3-95450-194-6 ISSN: 2226-0366 doi:10.18429/JACoW-LINAC2018-MOPO094

RF STABILITY TEST OF RFQ CAVITY WITH PROTOTYPE LOW-LEVEL RADIO FREQUENCY IN RAON

Doyoon Lee†, Bonghyuk Choi, Ohryong Choi, Kitaek Son, Hyojae Jang and Hoechun Jung
Rare Isotope Science Project, Institude for Basic Science, Daejeon 34047, Republic of Korea

Abstract

RAON is a heavy ion accelerator of the Institute for Basic Sciences (IBS) in Korea. The prototype Low-Level Radio Frequency (LLRF) operated at 81.25 MHz has been designed and fabricated for a prototype Radio Frequency Quadrupole (RFQ) cavity in RAON. Stabilities of ±1 % in amplitude and ±1 degree in phase are required for specifications of the RFQ system. The prototype LLRF controls the RF amplitude and phase in the cavity by PID feedback loop. The prototype LLRF has been tested with one RFQ cavity and stabilities have been measured. In this paper, we present the design and results of stability test.

INTRODUCTION

Prototype LLRF for RFQ cavity is designed to maintain the stability of amplitude and phase of RF power in the cavity at 81.25 MHz frequency within ±1 % and ±1 degree through PID feedback control. Table 1 shows parameter of 81.25 MHz LLRF. The prototype LLRF has one reference clock, two RF input channels and one output channel. The reference clock input channel operates with a reference signal of -15 to 0 dBm and the sampling frequency is generated by using a clock signal down-converted to 4/5 times. The operating frequency range is 81.25 ±1 MHz. The RFQ pick-up signal is put into the RF input channel and feedback control is performed. The RF power from the output channel is used as the input drive power for the SSPA (solid state power amplifier). The LLRF controller based on EPICS OPI (operator interface) communicates with the LLRF module via ethernet. It is responsible for controlling the RF field of the RFQ cavity, interlocking, monitoring and data archiving. Feedback on-off is applied independently to amplitude and phase. User can set the target values of amplitude and phase and the PID coefficients. The RF output power limiter is equipped for SSPA protection. The LLRF module consists of RF module and FPGA board as shown in Fig. 1.

Table 1: Parameter of 81.25 MHz LLRF

Parameter	Value
Frequency Range	81.25 ± 1 MHz
Amplitude Stability	< ± 1 %
Phase Stability	< ± 1 degree
Operating Mode	CW, Pulse
RF Input	Ref. : -15 ~ 0 dBm Ch 1, 2 : -40 ~ 0 dBm
RF Output	-40 ~ 0 dBm
I/O Impedance	50 ohm

† dylee@ibs.re.kr

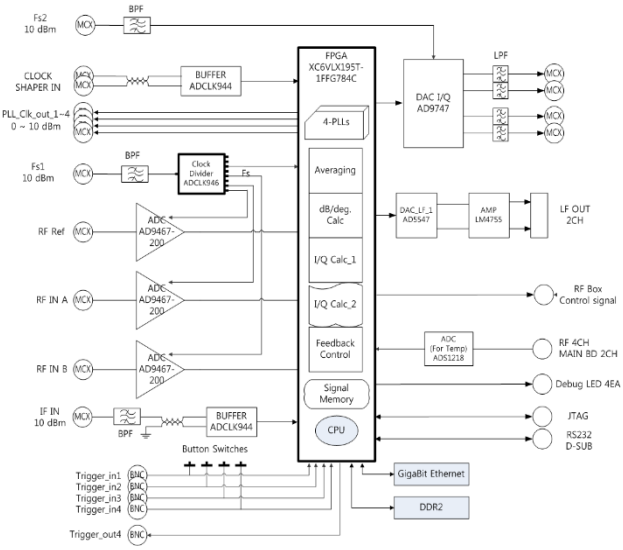


Figure 1: Block diagram of 81.25 MHz LLRF module.

STABILITY TEST

We set up the test bench with 81.25 MHz LLRF, 15 kW SSPA and RFQ cavity as shown in Fig. 2. The block diagram of the test bench for stability test is shown in Fig. 3.

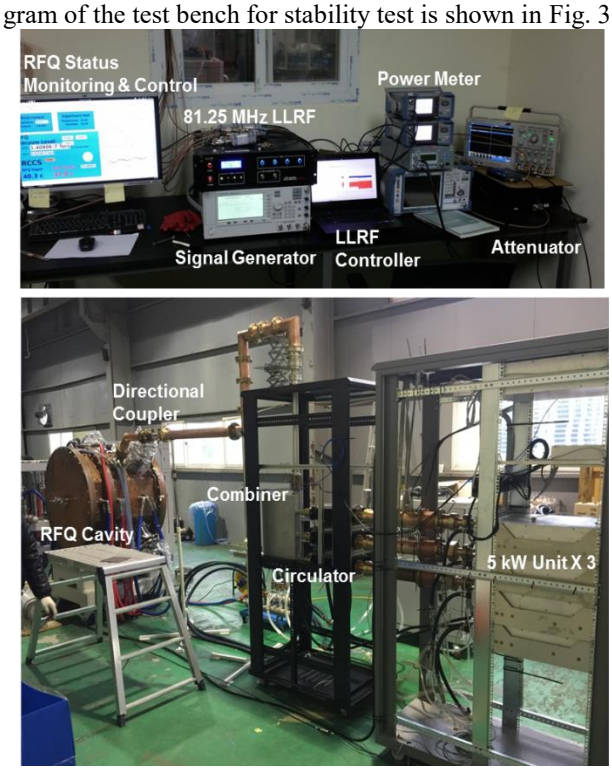


Figure 2: Test setup with 81.25 MHz LLRF,15 kW SSPA and RFQ cavity.

Content from this work may be used under the terms of the CC BY 3.0 licence (© 2018). Any distribution of this work must maintain attribution to the author(s), title of the work, publisher, and DOI.

ISBN: 978-3-95450-194-6 ISSN: 2226-0366 doi:10.18429/JACoW-LINAC2018-MOPO095

A RISK BASED APPROACH TO IMPROVING BEAM AVAILABILITY AT AN ACCELERATOR FACILITY*

W. C. Barkley†, M. J. Borden, R. W. Garnett, M. S. Gulley, E. L. Kerstiens, M. Pieck, D. E. Rees, F. E. Shelley, B. G. Smith, Los Alamos National Laboratory, Los Alamos, NM 87545, USA

Abstract

This paper describes a risk-based approach to improving beam availability at an accelerator facility. Los Alamos Neutron Science Center (LANSCE), like many other accelerator facilities, was built many years ago and has been repurposed when new missions were adopted. Many of the upgrades to the accelerator and beamlines allowed partial improvements but large-scale, system-wide improvements were never accomplished. Because of this, the facility operates with a mix of old and new equipment of varying conditions. Limited budgets have constrained spending for spare part procurement making it vital to prioritize those items predicted to have the highest impact to availability, should they fail. A systematic approach is described where equipment is inventoried, condition assessed, rated for potential failure and finally compiled into a risk-based priority list.

Introduction

The LANSCE facility operates a proton accelerator originally built in the late 60s and early 70s to deliver beam to five experimental areas. The facility has done very well over the years delivering beam at an overall 80-85% availability [1] even as the original mission has changed and expanded by several other Experimental Areas (EAs). Accelerator availability is a measure of uptime divided by total time so the Mean-Time-To-Repair (MTTR) metric lowers available beam time to each of the EAs. The Availability metric is calculated weekly during production runs to each EA and then combined into an overall total for the accelerator.

It is the objective of Accelerator Operations and Technology (AOT) Division management, the organization operating and maintaining LANSCE, to improve the availability metric to 90% or greater using a risk-based approach for identifying and purchasing adequate operational spares to lower the unscheduled down time (MTTR). To achieve this goal, risks of failure shall be identified and prioritized from the top level down, from systems to structures to components (SSCs). Downtime (MTTR) data for the past history of failures along with the trends associated with particular equipment has already been captured for the availability metric. By mining this data, performing equipment assessments and assigning risk by subject matter experts, the most appropriate spares procurement list can be created.

* Work supported by the United States Department of Energy, National Nuclear Security Agency, under contract DE-AC52-06NA25396
† barkley@lanl.gov

Unscheduled Down Time

An intricate set of systems operate in unison to produce and deliver particle beam to EAs at LANSCE. In fact, AOT division is organized such that key disciplines are grouped according to areas of specialty. Each of these AOT groups is populated with Subject Matter Experts (SMEs) that are intimately familiar with the details of their respective systems and can troubleshoot and repair issues arising that cause unscheduled downtime. The key to dealing with the unscheduled downtime lies in the recognition that the systems have single point failures that will turn off all or part of the entire machine if not functional. These single point failures are partially depicted, at a high level, in Fig. 1:

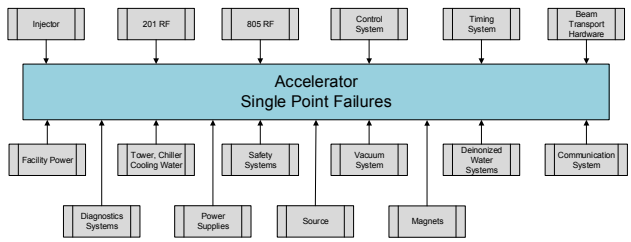


Figure 1: Single point failure diagram of the LANSCE accelerator.

As a 24 hour, 7 day a week operation, the LANSCE accelerator is attended by an excellent Operations staff that resolves many of the unscheduled downtime issues themselves with only small impacts to MTTR. For issues beyond their expertise or knowledge base, staff rotate on-call schedules to address the more difficult or complex issues that arise. The use of on-call staff affects the availability metric in terms of wait time for personnel to arrive on site, of proper diagnosis of the problem and whether the right person or persons have been called. These times contribute to the MTTR metric.

Maintainability

The maintainability for LANSCE is measured as the Mean Time to Repair [2]:

$$MTTR_i = RT + AD + LD \quad (1)$$

where RT is the repair time, AD is the administrative delay and LD is the logistical delay or lead time waiting for parts and/or people. Repair times for unscheduled events have been mined from the Operator Logs and categorized into specific SSCs that caused the failure. The

Content from this work may be used under the terms of the CC BY 3.0 licence (© 2018). Any distribution of this work must maintain attribution to the author(s), title of the work, publisher, and DOI.

ISBN: 978-3-95450-194-6 ISSN: 2226-0366 doi:10.18429/JACoW-LINAC2018-MOPO096

REALISTIC MODELING OF MEBT FOR THE NEW LANSCE RFQ INJECTOR

S.S. Kurennoy, LANL, Los Alamos, NM 87545, USA

Abstract

The new RFQ-based proton injector at LANSCE requires a specialized medium-energy beam transfer (MEBT) after the RFQ at 750 keV due to a following long (~3 m) existing common transfer line that also transports H^- beams to the DTL entrance. The horizontal space for MEBT elements is limited because two beam lines merge at 18-degree angle. The MEBT includes two compact quarter-wave RF bunchers and four short quadrupoles with steerers, all within the length of about 1 m. The beam size in the MEBT is large, comparable to the beam-pipe aperture, hence non-linear 3D fields at large radii and field-overlap effects become important. With CST Studio codes, we calculate buncher RF fields and quadrupole and steerer magnetic fields, and use them for particle-in-cell beam dynamics modeling of MEBT with realistic beam distributions from the RFQ. Our results indicate a significant emittance growth in MEBT not predicted by the standard beam dynamics codes. Its origin is traced mainly to the quadrupole edge fields; the buncher RF fields also contribute noticeably. Proposed design modifications improve the MEBT performance.

INTRODUCTION

A modern front end for the LANSCE linac is under development: the aging Cockcroft-Walton based injectors will be replaced by modern RFQ-based ones [1]. Now two lines, one for H^+ (proton) and the other for H^- ions, produce 750-keV beams that merge into a common transport, which goes to the entrance of the first DTL tank. The proton injector will be upgraded first, but the existing common transport line for different beam species creates significant constrains for the injector line design. The first challenge is a very long distance from the proton RFQ exit to the DTL entrance, almost 4 m. Second, because the two beam lines merge at 18-degree angle, the horizontal space for proton-line elements is limited by the existing hardware near the merging area. Therefore, a specialized medium-energy beam transfer (MEBT) after the new proton RFQ at 750 keV was developed [2] with envelope codes, and the beam dynamics in MEBT was modeled using Parmila [3]. The MEBT shapes the RFQ output beam to transfer it through the long existing common transport to the DTL with minimal losses. The MEBT includes four electromagnetic (EM) quadrupole magnets and two buncher cavities [2], all within about 0.9 m along the beam line, followed by a 0.5-m long drift to the merging point of the common transport line, which continues for ~2.6 m to the DTL entrance. The beam pipe in the injector line has inner diameter (ID) 1.875" (aperture radius $a \approx 2.381$ cm) and outer diameter 2"; the pipe wall thickness is 1/16" (≈ 0.159 cm).

The proton beam size in the MEBT is large, comparable to the beam-pipe aperture; therefore, non-linear 3D field effects at large radii become important, both in bunchers and quadrupoles. We calculated buncher RF fields and quadrupole and steerer magnetic fields with CST Studio codes [4], and applied them in particle-in-cell (PIC) beam dynamics modeling of MEBT [5]. The beam transverse emittances increase after MEBT significantly more than predicted by design [2]. Here we study the effects of MEBT element modifications and the beam transport to DTL using PIC simulations with CST Particle Studio (PS).

MEBT AND TRANSPORT TO DTL

The main MEBT elements are two compact quarter-wave (QW, $\lambda/4$) 201.25-MHz RF cavity bunchers and four short EM quadrupole magnets with additional windings for beam steering. Both elements have a small footprint on the beamline, shorter than 8 cm. The QW buncher is a coaxial resonator with two gaps separated by distance $\beta\lambda/2 = 2.98$ cm for $\beta = 0.04$ [5, 6]. The bunchers (B) and quadrupoles (Q) are arranged in the MEBT in the following order: Q_1, B_1, Q_2, Q_3, Q_4, and B_2. The buncher and quadrupole EM parameters and fields were calculated in CST MicroWave and EM Studios, see details in [6]. The maximal effective voltage of QW buncher in the design [2] is $V_{\text{eff}} = 25$ kV (12.5 kV per gap). The quad effective length is 7.6 cm with gradients G from 7.1 to 10.8 T/m.

The beam envelopes in the MEBT and transport to DTL corresponding to the design [2] are shown in Fig. 1. The MEBT includes elements 1-12 in Fig. 1. The proton and H^- beams merge in the bending dipole (elements 14-16), then pass through the main buncher (20) and a long drift (21-36) with 4 tuning quadrupoles to the DTL entrance. The main buncher (MB) is a single-gap reentrant 201.25-MHz cavity with a narrow aperture of 1-cm radius.

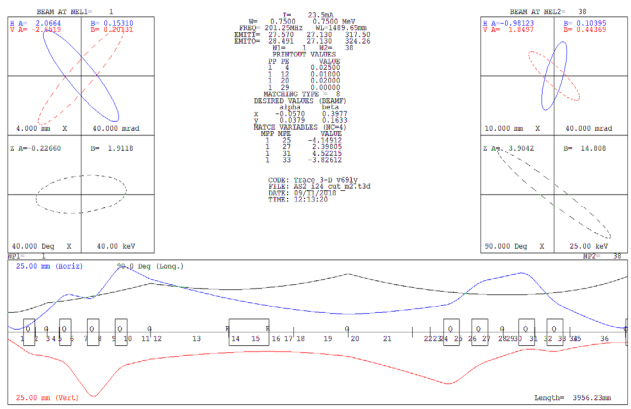


Figure 1: Trace 3D beam envelopes in the proton RFQ MEBT and common transport line to DTL.

Content from this work may be used under the terms of the CC BY 3.0 licence (© 2018). Any distribution of this work must maintain attribution to the author(s), title of the work, publisher, and DOI.

ISBN: 978-3-95450-194-6 ISSN: 2226-0366 doi:10.18429/JACoW-LINAC2018-MOPO100

DOUBLY STRIPPED PROTON CAUSING VACUUM LEAK AT BROOKHAVEN 200 MeV LINAC COMPLEX*

D. Raparia†, G. Atoian, T. Lehn, V. Lodestro, M. Mapes, A. McNerney, J. Ritter, A. Zelenski
Brookhaven National Laboratory, P. O. Box 5000, Upton, NY 11973, USA

Abstract

Doubly stripped protons in the low energy transport are captured at 180 degree apart in RF of RFQ and accelerated to the full energies. These protons are bend in the opposite direction of the H^- after 200 MeV drift tube linac and caused a vacuum leak. A new beam dump and a faraday cup for these stripped protons are planned.

INTRODUCTION

The Brookhaven National Laboratory (BNL) 200 MeV drift tube linac (DTL) provides H^- beam at 6.67 Hz, 200 MeV for the polarized proton program of Relativistic Heavy Ion Collider (RHIC) and 66-200 MeV for Brookhaven Linac Isotope Production (BLIP) [1-5]. The RHIC polarized proton program needs 2 pulses every super cycle (~4 sec), one for injection into booster and other for polarization measurement at 200 MeV-polarimeter located in the high-energy transport line (HEBT). The rest of the pulses go to BLIP. BNL 200 MeV H^- linac consists of a 35 keV high intensity (magnetron) ion source [6], polarized source (optically pumped polarized H^- ion source, OPPIS) [7], low energy beam transport (LEBT), a 750 keV radio frequency quadrupole accelerator (RFQ), medium energy beam transport (MEBT) and 200 MeV drift tube linac. Space charge effects are most severe at low energy i.e. in the LEBT where the H^- energy is 35 keV and current excess of 100 mA. To overcome space charge effects in the LEBT, different gases are used to charge neutralize the H^- beam.

LOW ENERGY BEAM TRSPORT (LEBT)

LEBT connects RFQ to two ion sources, namely high intensity magnetron ion source (source-1) and OPPIS. Figure 1 shows layout of LEBT. A 45-degrees pulse dipole magnet connects these two ion sources to RFQ. High intensity part of LEBT consists of two solenoids, two quadrupoles, and two set of steering magnets in each horizontal and vertical plane, a beam chopper, a beam stop, a cryopump, and two gate valves. First gate valve is located just after the first solenoid and second gate valve is located just before the RFQ. Base pressure in LEBT is about $2x10^{-7}$ Torr with ion source gate valve closed and with ion source gate valve open, pressure is about $1x10^{-6}$ Torr.

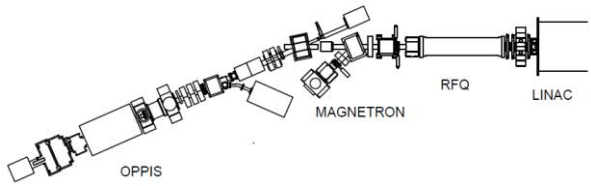


Figure 1: LEBT layout showing OPPIS and Magnetron source.

Cryopump is located under chopper box and equipped with two gate valves, one pneumatic and other hand operated gate valve. There is a provision to inlet various gas via needle valves at two places, first in ion source gate valve and second in chopper box.

Last year (Run 2018), no polarized protons were needed for RHIC program; a second magnetron source (source-2), a solenoid and two steering magnets were installed by replacing spin-solenoid and diagnostic box in OPPIS line before the 45-degree dipole magnet. Second source was installed for source development and as back-up source for BLIP. Source-2 is at 0 degrees with RFQ. Source-2 is bit different than source-1; it has smaller vacuum chamber and smaller turbo pump. It operates at little higher pressure ($8x10^{-6}$ Torr) than source-1; it has better gas injection pulse valve, ion source body temperature control, better electric connection etc.

DOUBLY STRIPPED H^-

H^- can be can be converted to protons via two channels, (1) stripping two electrons H^- => P and (2) two step process (a) H^- => H^0 (b) H^0=> P. Cross-sections for these processes at 35 keV and Hydrogen & Nitrogen as background gases are given in Table 1 [8, 9].

Table 1: Summary of 35 keV H- Cross Sections Used in Calculations.

Gas	σ_{-10} (10^{-16} cm^2)	σ_{-11} (10^{-16} cm^2)	σ_{01} (10^{-16} cm^2)
Hydrogen	7.3	0.43	*2.4
Nitrogen	13.2	1.7	*4.4

* Scaled

For source-1, doubly stripped protons generated between 45-degree dipole and RFQ are captured and accelerated by RFQ. For source-2, doubly stripped protons generated between source-2 and RFQ are captured and accelerated by RFQ. Nitrogen gas was injected at the chopper camber, which is located after the 45-degree dipole magnet in LEBT, to optimize the average beam current at the BLIP target. For both sources, optimized pressure in LEBT was about $3x10^{-6}$ Torr. Transmissions

*Work performed under Contract Number DE-AC02-98CH10886 with the auspices of the US Department of Energy
†raparia@bnl.gov

Content from this work may be used under the terms of the CC BY 3.0 licence (© 2018). Any distribution of this work must maintain attribution to the author(s), title of the work, publisher, and DOI.

ISBN: 978-3-95450-194-6 ISSN: 2226-0366 doi:10.18429/JACoW-LINAC2018-MOPO101

LINAC-MULTITOOL – AN OPEN SOURCE JAVA-TOOLKIT*

M. Schwarz†, D. Bade, J. Corbet, H. Podlech
IAP, Goethe University, Frankfurt am Main, Germany

Abstract

Dedicating more precious time to advanced research instead of spending it towards time-consuming routine tasks is a desirable goal in particle accelerator simulation and development. Requirements engineering was started at IAP in order to identify routine processes at our institute's R&D that can be automated or simplified. Results indicated that there were several areas to consider: Bead pull measurements, data processing and visualization for the beam dynamics code LORASR, CST field map processing for the use with TraceWin, conversion between different particle distribution data formats and more. Subsequently development of the LINAC-Multitool started to rationalize these processes and replace preexisting scripts also to ensure consistency of results and increase transparency and reliability of computation. In order to guarantee maintainability, expandability and platform independence, LINAC-Multitool is programmed using Java and will be open source. This contribution presents the current state of development.

SOFTWARE ARCHITECTURE

In preparation of choosing an appropriate platform (programming language, GUI toolkit, other libraries) three key factors emerged: Ease of use, maintainability and expandability. In conclusion Java, the probably most widely used programming language for the development of desktop applications, was chosen. It offers a convenient GUI toolkit (JavaFX [1]), which is bound to be supported for a long time by Oracle but still enables us to integrate all the features one would expect from a modern UI. The same goes for Java as a programming language and has been proven in the past as code that was written years ago can still be used. Other languages which sparked our interest however have undergone design changes in their past which broke source code compatibility and therefore were not as suitable as Java. In addition, we profited from the availability of a competent plotting framework – JFreeChart [2], which allowed us to introduce advanced features like data selection into our graphs and proved to be a stable base. As a team of two students and one supervisor kicked off this project, we chose to part the program along the lines of frontend and backend. The backend part includes all the parsing of files and most of the computational aspects for bead–pull measurements while the frontend part focuses on GUI, handling 3d field maps as well as particle distributions and better visualizations for LORASR-computations [3] in order to minimize friction and overall improve efficiency of implementation. In order to maximize our throughput we chose to minimize our reliance on expensive computational libraries wherever we could come up with more resource-conservative ideas. Figure 1 depicts an excerpt of the program architecture whose classes and functions can be categorized on the whole as *read*, *parse*, *analyze* and *visualize*.

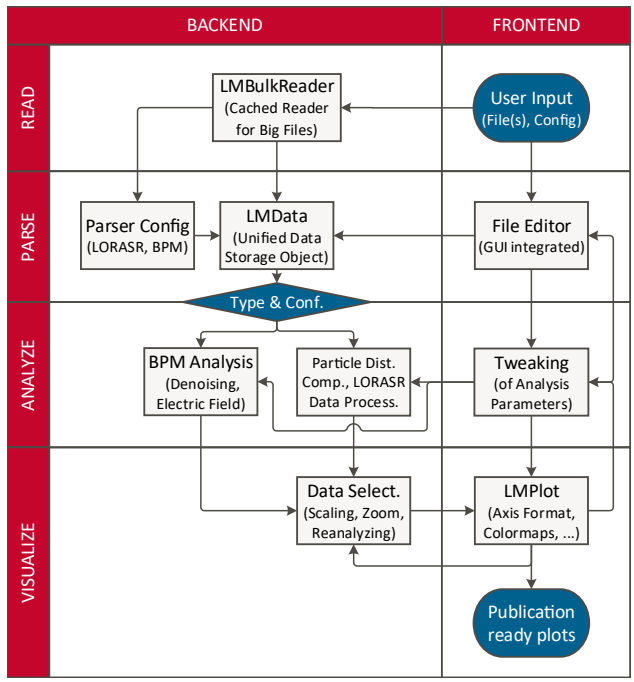


Figure 1: Schematic layout of the program architecture.

RANGE OF FUNCTIONS

An overview of the planned features for the LINAC-Multitool is given in Fig. 2. Up to now they can be divided into four parts: *LORASR*, *Bead Pull Measurement*, *Particle Distributions* and *CST Field Maps*. Finally, they will be documented in detail both in the source code and the user manual. The initial features are given in the following:

LORASR LORASR is a multi-particle tracking code for the beam dynamics design for all kind of DTLs, optimized for the "Combined Zero Degree Structure (KONUS)" lattices [4–8]. The code has been used for the beam dynamics design of many linacs in operation or under construction like GSI-HLI, -HSI and -pLINAC, CERN Linac 3, TRIUMF ISAC-I, HIT, MedAustron, HILac/NICA and MYRRHA. As its first code version was already developed in the late 80s, the possibilities for graphical user interactions were and are still not very wide-ranging. Nevertheless, the code has been significantly improved in the past decades with better gap field representation, a PIC space charge routine, error study

* Work supported by BMBF contr. No. 05P15RFRBA and HIC for FAIR.
† schwarz@iap.uni-frankfurt.de

Content from this work may be used under the terms of the CC BY 3.0 licence (© 2018). Any distribution of this work must maintain attribution to the author(s), title of the work, publisher, and DOI.

ISBN: 978-3-95450-194-6 ISSN: 2226-0366 doi:10.18429/JACoW-LINAC2018-MOPO102

PROGRESS OF MicroTCA.4 BASED LLRF SYSTEM OF TARLA

C. Gumus*, M. Hierholzer, H. Schlarb, C. Schmidt, DESY, Hamburg, Germany
O. F. Elcim, A. Aksoy, A. Aydin, C. Kaya, Ankara University, Ankara, Turkey

Abstract

The Turkish Accelerator and Radiation Laboratory in Ankara (TARLA) is constructing a 40 MeV Free Electron Laser with continuous wave (CW) RF operation. In order to control and monitor the RF field inside four superconducting (SC) 9-cell TESLA type cavities as well as the two normal conducting (NC) buncher cavities, a MicroTCA.4 based LLRF system is foreseen. This highly modular system is also used in resonance control of the cavities via piezo actuators and mechanical motor tuners. This paper gives brief overview on hardware and software components of LLRF control of TARLA, as well as updates of the ongoing integration tests at DESY.

PROJECT OVERVIEW

TARLA facility, located in Ankara, will be the first particle accelerator of Turkey with the Free Electron Laser (FEL) of operating at 3–250 μm wavelength. Other usages will be the Bremsstrahlung radiation and the fixed target experiments [1]. The MicroTCA Technology Lab (A Helmholtz Innovation Lab) of DESY is responsible for delivering a turn-key system for Low Level Radio Frequency (LLRF) control to TARLA. There are six cavities that need to be controlled by LLRF system. Four of these cavities are TESLA type 1.3 GHz superconducting whereas others are normal conducting buncher cavities operating with 1.3 GHz and 260 MHz respectively. The RF operation will be continuous wave (CW) with the expected maximum total beam energy of 40 MeV. Main parameters of the accelerator are shown in Table 1.

Main design of the accelerator is quite similar to Electron linac for beams with high brilliance and low emittance (ELBE) in HZDR-Dresden / Germany where difference is that TARLA uses additional piezos for resonance control. Since ELBE is also in the process of switching their control system to MicroTCA.4 standard, parallel development is ongoing [2]. The main construction on TARLA facility has been finished and accelerator modules have been delivered.

Apart from the hardware delivery and the commissioning of the complete system, DESY is also cooperating with TARLA to train personnel in order to make sure that know-how is transferred.

Table 1: Machine and Beam Parameters

Parameter	Unit	Base Value	Upgraded Value
Beam Energy	MeV	0 - 40	0 - 40
Max. Bunch Charge	pC	77	115
Max. Average Beam Current	mA	1	1.5
Horizantal Emittance	mm mrad	<15	<15
Vertical Emittance	mm mrad	<12	<12
Longitudinal Emittance	keV ps	<85	<85
Bunch Length	ps	0.4 – 6	0.3 - 6
Bunch Repetition	MHz	13	0.001 – 52
Macro Pulse Duration	μs	10 – CW	10 – CW
Macro Pulse Repetition	Hz	1 – CW	1 - CW

LLRF DESIGN

MicroTCA.4 Standard Overview

Using the MicroTCA.4 technology standard, each cavity's RF regulation is controlled by a pair of Advanced Mezzanine Card (AMC) in which FPGA holds the controller and digital signal processing and Rear Transition Module (RTM) card which has the analog RF circuitry to provide the down converted cavity signals over the Z3 connection. On the same crate CPU-AMC board communicates with digitizer AMCs with PCIe lanes using the backplane. Remote access is established through Ethernet via MicroTCA Carrier Hub where crate management takes place [3].

LLRF System Architecture

The LLRF system for TARLA consists of 6 RF station controls and the corresponding resonance control components. In additional to RF and mechanical tuning of the cavities, additional drift compensation modules (DCM) will be installed to the rack in order to compensate the slow drifts on RF signal paths caused by humidity and temperature.

The RF amplification of the drive signal on LLRF system is realized by Solid State Power Amplifiers (SSPA). As for the control system environment, EPICS will be used on the LLRF system.

* cagil.guemues@desy.de

Content from this work may be used under the terms of the CC BY 3.0 licence (© 2018). Any distribution of this work must maintain attribution to the author(s), title of the work, publisher, and DOI.

ISBN: 978-3-95450-194-6 ISSN: 2226-0366 doi:10.18429/JACoW-LINAC2018-MOPO104

LLRF R&D TOWARDS CW OPERATION OF THE EUROPEAN XFEL

A. Bellandi*, V. Ayvazyan, J. Branlard, C. Gümüs, S. Pfeiffer, K. Przygoda, R. Rybaniec, H. Schlarb, C. Schmidt, J. Sekutowicz, DESY, Hamburg, 22607 Hamburg, Germany
W. Cichalewski, TUL-DMCS, Łódź, Poland

Abstract

The ever growing request for machines with a higher average beam pulse rate and also with a relaxed (< 1 MHz) pulse separation calls for superconducting linacs that operate in Long Pulse (LP) or Continuous Wave (CW) mode. For this purpose the European X-ray Free Electron Laser (European XFEL) could be upgraded to add the ability to run in CW/LP mode. Cryo Module Test Bench (CMTB) is a facility used to perform tests on superconducting cavity cryomodules. Because of the interest [1] in upgrading European XFEL to a CW machine, CMTB is now used to perform studies on XM-3 [2], a 1.3 GHz European XFEL-like cryomodule with modified coupling that is able to run with very high quality factor ($Q_L = 10^7 ... 10^8$) values. The RF power source allows running the cavities at gradients larger than 16 MV/m. Because of the Q_L and gradient values involved in these tests, detuning effects like mechanical resonances and microphonics became more challenging to regulate. The goal is then to determine the appropriate set of parameters for the LLRF control system to keep the error to be less than 0.01° in phase and 0.01% in amplitude.

A POSSIBLE CW UPGRADE AT EUROPEAN XFEL

XFELs are important tools of discovery that allow unprecedented brightness and spectral purity. In 2017 the European XFEL came into operation, producing the brightest and hardest X-ray FEL light in the world. At the moment European XFEL can produce a maximum of 2700 pulses with a temporal distance of 220 ns and a repetition rate of 10 Hz. Because of the advantage (from the experimental point of view) of having a bigger temporal separation between the pulses and simultaneously increasing the average number of pulses per seconds, a CW upgrade of European XFEL could be made. For such upgrade the duty cycle would change from the actual value of 1.4% at 17.5 GeV for Short Pulse (SP) to a maximum value of 100% at 8.6 GeV, for CW, or 10% to 50% at 12.8 GeV for LP [1]. For CW/LP operations, IOT amplifiers, along with the existing klystrons, will be installed in European XFEL tunnel to allow both SP (high gradient) and CW/LP (reduced gradient) with minimum downtime between the switch of the two modes. To limit the required RF power, the Q_L could be increased to values higher than 10^7. To meet the field quality requirements inside the cavities with an increased Q_L and to decide the optimal set of parameters of the Low Level RF (LLRF) controller, further studies have to be done both on European XFEL and dedicated test facilities.

* andrea.bellandi@desy.de

CHALLENGES OF CW OPERATION

Increasing the Q_L from the current European XFEL value of $4.6 \cdot 10^6$ to values bigger than 10^7 results in a full bandwidth less than 100 Hz that will make the cavities more susceptible to detuning effects. In order to keep the cavities on resonance with the required field stability but, at the same time, to limit the required peak RF power, these effects must be canceled out using a LLRF control system that acts on the fast piezoelectric tuners.

Lorentz Force Detuning

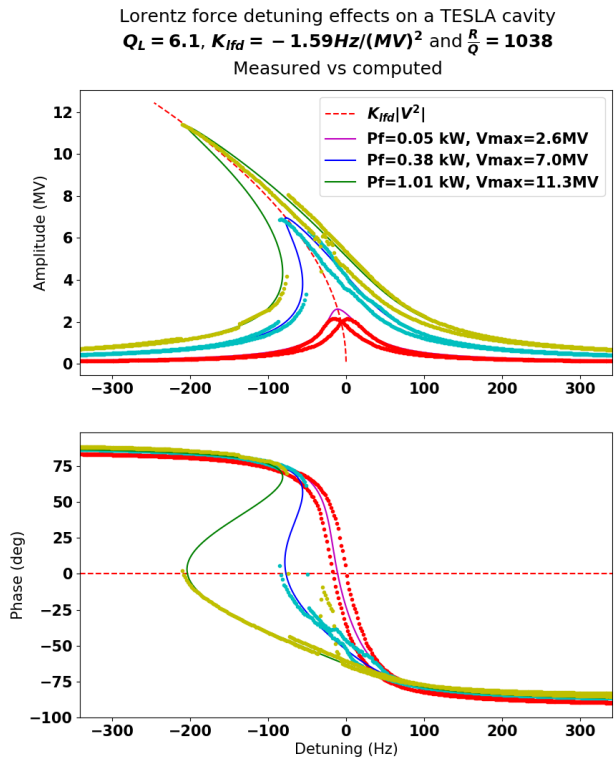


Figure 1: Resonance scan of a TESLA-like superconducting cavity at different values of the forward power using piezoelectric actuators. Computed (lines) vs. measured (points) values are shown. Tests were taken on cavity 2 of XM-3 module.

Lorentz Force Detuning (LFD) is a detuning effect that arises from the electromagnetic pressure that the accelerating field exerts on cavity walls. The detuning produced by LFD is proportional to the square value of the field.

$$\Delta f_{lfd} = K_{lfd} \cdot (\Delta V)^2$$

Content from this work may be used under the terms of the CC BY 3.0 licence (© 2018). Any distribution of this work must maintain attribution to the author(s), title of the work, publisher, and DOI.

ISBN: 978-3-95450-194-6 ISSN: 2226-0366 doi:10.18429/JACoW-LINAC2018-MOPO106

NEW DIGITAL LLRF SYSTEM FOR HIT

E. Feldmeier, Th. Haberer, A. Peters, HIT, Heidelberg, Germany

Abstract

The Heidelberg Ion Therapy Center HIT is in clinical operation since 2009. The accelerator complex consists of a linear accelerator and a synchrotron to provide carbon ions and protons for clinical use as well as helium and oxygen ions. The analog LLRF system for the linac should be replaced after more than 10 years of continuous operation. In its life-time the LLRF caused no interruption of the clinical operation with a downtime of more than 15 minutes. In order to keep the reliability in the next 10 years at least as high, a new digital LLRF system is planned. Further difficulties for the installation of a new system are due to the clinical full time usage of the accelerator and the short maintenance slots of only two days in series.

INTRODUCTION

The layout of the accelerator of the Heidelberg Ion Therapy Center HIT [1] includes three ECR ion sources, a 7 MeV/u injector linac, a 6.5 Tm synchrotron and a high energy beam transport line to deliver beam for the four target places: Two treatment rooms with a horizontally fixed beam-line, the worlds first heavy ion gantry and an experimental area.



Figure 1: The accelerator of the Heidelberg Ion-Beam Therapy Center (HIT) with three ion sources, the LINAC (7 MeV/u) consisting of a 4-rod-RFQ and a IH-DTL, the synchrotron (48-430 MeV/u), the beam lines to the treatment rooms and the experimental area and the heavy ion gantry [2].

The ECR ion sources produce proton, helium, carbon and oxygen beam, of which the protons and the carbon ions are used for the medical treatment of localized tumors.

In the injector linac, beams with an AoQ of 1-3 can be accelerated to 7 MeV/u. The synchrotron accelerates the beam to an energy of up to 430 MeV/u for carbon ions.

LINAC AND RF SYSTEMS

The LINAC RF system shown in Fig. 2 supplies three RF cavities in front of the Synchrotron to accelerate and form the beam from the ion sources. A 4-rod-RFQ is used to accelerate the beam to 400 keV/u, focus the beam and form bunches. The following IH-DTL accelerates the beam to 7 MeV/u and the Debuncher spreads the bunches longitudinal to match the acceptance of the synchrotron. The cavities are operated at 216.816 MHz. For a beam with an $AoQ = 3$ a power for the RFQ of 200 kW, for the IH-DTL of 900 kW and for the Debuncher of 1.2 kW is needed.

The RF system (Fig. 2) consists of a common master oscillator providing the frequency. A amplifier and splitter is used to distribute the RF signal to the three power amplifiers. The RFQ has a 8 kW transistor preamplifier and a 250 kW tube final stage. The IH-DTL has a 4 kW transistor preamplifier, a 120 kW tube stage and a 1.4 MW tube final stage. The RF system for the Debuncher only uses a 4 kW transistor amplifier.

The analog PI-controller for each system corrects the amplitude and the phase of the decoupled cavity signal.

The RF system was designed by GSI in Darmstadt, Germany and build by Bertronix in Munich, Germany and Ampegon in Turgi, Switzerland.

LLRF SYSTEM

The requirements for the new digital LLRF system are based on the current analog LLRF system. Even there are new advantages with digital systems the great useability of the given system with its various possibilities for fault diagnostics and well-thought-out features must not be reduced. The preferred solution is a ready to use system with a lot of flexibility and free to program. Whether projects like microTCA [3] [4] or Libera [5] [6] can be used has to be proven. Otherwise a complete new system has to be developed.

In the following section the most important features will be discussed.

Master Oscillator

The HIT Linac works at 216.816 MHz and needs a frequency stability of better than 10^{-6}. The master oscillator can be set up separately and needs 4 or more output ports for the 3 rf systems and for the diagnostics. The phase stability of $< 0.1°$ is required.

Content from this work may be used under the terms of the CC BY 3.0 licence (© 2018). Any distribution of this work must maintain attribution to the author(s), title of the work, publisher, and DOI.

ISBN: 978-3-95450-194-6 ISSN: 2226-0366 doi:10.18429/JACoW-LINAC2018-MOPO107

PERFORMANCE EVALUATION OF THE RF REFERENCE PHASE STABILIZATION SYSTEM ON FIBER-OPTICAL LINK FOR KEK e-/e+ INJECTOR LINAC

N. Liu†,1, T. Miura1,2, T. Matsumoto1,2, F. Qiu1,2, D. Arakawa2, H. Katagiri2, Y. Yano2, S. Michizono1,2, B.T. Du1, 1SOKENDAI, Kanagawa 240-0193, Japan, 2KEK, Ibaraki 305-0801, Japan

Abstract

The KEK e-/e+ injector is the 600 m J-shaped LINAC, which has 8 RF sectors. Stabilization of the RF phase reference for long distance transmission is necessary for stable RF operation. In the present system, single-mode fiber-optical links without feedback control are used from sector 2 to 5. The long-term phase drift of the reference phase at sector 5 was observed for more than 10° over 7 days. For SuperKEKB injector LINAC, the phase stability requirement is estimated to be 0.2° rms corresponding to 195 fs at 2856 MHz including short-term jitter and long-term phase drift. A more stable RF phase reference is necessary for the improvement of the phase stability. An RF reference phase stabilization system using a pair of wavelength division multiplexing (WDM) devices and a variable optical delay line (VODL) is constructed for the evaluation of the system's performance. The temperature and humidity characteristics of the electric and optical components, in addition to the phase stabilized optical fiber (PSOF) with different wavelengths are measured. In this paper, the performance of the proposed phase stabilization system will be evaluated.

INTRODUCTION

The KEK e-/e+ injector LINAC comprises of 124.8 m long and 488.3 m long straight beam lines, which consist of 8 sectors (sector A-C and 1-5) [1]. The Master Oscillator (MO, 571 MHz) system generates a 2856 MHz reference signal, which is delivered to sector A-C, 1 by coaxial cables and to sector 2 to 5 by optical links. During the long-distance transmission, the RF reference phase drifts due to the effect of temperature and humidity fluctuations on the propagation medium (coaxial cables and optical fiber) and the electric/optical components, especially for the S-band signal. The phase stability of the RF reference will contribute to the beam arrival jitter and influence the beam quality accordingly. In this paper, we focus on the phase stabilization system of the optical fiber link.

The phase stability of the RF reference depends on the short-term RF jitter and the long-term phase drift. The RMS jitter of the RF reference transmitted signal was found to be 100-200 fs for each sector [2]. In addition, the long-term phase drift of the reference phase at sector 5 was observed to be more than 10° for 7 days by the phase monitoring system, as shown in Fig. 1.

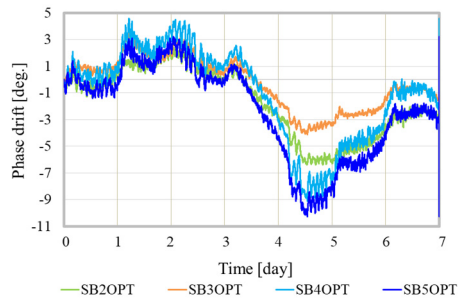


Figure 1: Phase drift of the optical link from sector 2-5 at injector LINAC.

In order to stabilize the RF reference phase, a phase stabilization system using a pair of wavelength division multiplexing (WDM) device and variable optical delay line (VODL) is implemented in the laboratory in order to evaluate the system's performance. In this paper, the temperature and humidity characteristics of the phase stabilized optical fiber (PSOF) are measured with different wavelengths (1310 nm, 1550 nm) and the performance of the phase stabilization system is evaluated.

OVERVIEW OF RF REFERENCE PHASE STABILIZATION SYSTEM

A similar feedback system to [3-5] is considered according to the current status of the injector LINAC. Figure 2 shows a schematic diagram of the proposed phase stabilization system for performance evaluation in the laboratory. The 2856 MHz electric RF signal is generated by a signal generator (SG) as the reference signal (REF). This signal is subsequently converted into an optical signal with a wavelength of 1310 nm (λ_1) using an optical transmitter (E/O). The optical signal is then transmitted by the single-mode phase-stabilized optical fiber (PSOF) and converted into an electrical signal (transmitted signal) by an optical receiver (O/E). In order to stabilize the transmitted signal, it is sent back using the same PSOF but at a different wavelength 1550 nm (λ_2) with a pair of WDM devices and another pair of E/O and O/E. All the S-band signals (REF, transmitted signal and returned signal) are down-converted to the intermediate frequency (IF, 14.28 MHz) by a local oscillator (LO, 2870 MHz). The phase difference (feedback phase) between the returned signal and REF is used for the feedback control. The transmitted signal is monitored in order to evaluate the performance of the feedback system.

† liuna@post.kek.jp

Content from this work may be used under the terms of the CC BY 3.0 licence (© 2018). Any distribution of this work must maintain attribution to the author(s), title of the work, publisher, and DOI.

ISBN: 978-3-95450-194-6 ISSN: 2226-0366 doi:10.18429/JACoW-LINAC2018-MOPO111

DEVELOPMENT OF NEW LLRF SYSTEM AT THE J-PARC LINAC

K. Futatsukawa*, Z. Fang, Y. Fukui, KEK, Ibaraki, Japan
S. Shinozaki, JAEA, Ibaraki, Japan
Y .Sato Nippon Advanced Technology Co.,Ltd., Ibaraki, Japan

Abstract

In the Low-Level RF (LLRF) system of the J-PARC linac, the digital feedback (DFB) and the digital feedforward (DFF) were adopted to meet the requirement of amplitude and phase stabilities. Almost all modules of the LLRF system were operated without serious problems. However, those for the 324 MHz LLRF system have been used since the beginning of the J-PARC linac and it is concerned about increasing the failure rates. It is difficult to maintain the exact same system because some boards of the present one were discontinued. In addition, the OS and the software to develop FPGA, DSP and the server of this system are too old to be purchased. Therefore, we are starting to study the new LLRF system of the next generation. The digital board of the LLRF system with the Zynq FPGA on the µTCA.4 platform was produced and its basic performance meets the requirement.

INTRODUCTION

In the J-PARC linac, the energy of the beam injected to RCS was upgraded and the front-end was improved to achieve the design power of 1 MW [1, 2].

The twenty-four 324 MHz LLRF systems were installed to accelerate the H^- beam to 191 MeV using RFQ, DTL, and SDTL. The twenty-five 972 MHz LLRF ones were used to drive the ACS cavities of the normal-conducting and the beam is accelerated to 400 MeV for the injection to RCS. These two types of th LLRF system have the functions of DFB and DFF using the Vertex-II FPGA to satisfy the requirement of amplitude and phase stabilities (less than ±1%, less than ±1 deg. at peak-to-peak) [3–5]. However, almost all modules of the 324 MHz LLRF system, which were developed more than ten years ago, have been used since the beginning of the J-PARC linac. Therefore it is concerned about increasing the failure rates.

In the present system of DFB and DFF, the cPCI platform have been adopted and the five modules of cPCI have been used. The three digital modules consist of a FPGA/DSP board, an IO, and a CPU. The two analog ones correspond to a RF&CLK board and a Mixer&IQ-modulator. However, some of the digital boards are already discontinued and the software and the OS to develop FPGA and DSP for this system are too old to be purchased. Table 1 shows the discontinued boards and too old development environment on the LLRF system of the J-PARC linac.

Therefore, we are starting to study the new LLRF system of the next generation.

Table 1: Agenda of the Problems and Too Old Development Environment on the J-PARC LLRF System

FPGA module	discontinued
DSP module	discontinued
CPU module	discontinued, but fungible
FPGA	Xilinx ISE Ver 6.2i
DSP	TI Code Composer Studio Ver 2.1
Host program	Redhat 8.0 gcc compiler Ver 3.2
Application	python2.4, wxPython 2.6

PROTOTYPE BOARD

In the first step, a new digitizer instead of the present three digital modules of cPCI are being developed. The µTCA.4 AMC and RTM is adopted as the platform in the consideration of the future. The feature of this prototype board in Table 2.

Table 2: Feature of the New Prototype Board

platform	µTCA.4 AMC, µTCA.4 RTM
FPGA	Zynq XC7Z045-1FFG900C, QSPI FLASH-ROM 16MB, SD-card Remote Update
RAM	DDR3-SDRAM 1GB×2 (PL, PS)
OS	Xilinx Linux (EPICS-IOC)
ADC	8 ch, 16 bit, 370 MSPS (max.), BW: 800 MHz
DAC	2 ch, 16 bit, 500 MSPS
SFP	2 ports

The AMC board having Zynq FPGA, 16bit-370MSPS ADC, and 16bit-370MSPS DAC is specialized to use the bus of the µTCA.4 standard. The number of ADC becomes eight channels from four of the present system. In addition, two SFPs are mounted for the future expansions and we will be planning to be applied to acquire the all macro-pulse data and to take the J-PARC event-tag.

The RTM board has the PLL and the multiplicity of the clock using VCO. The frequency of the input TTL signal is 48 MHz and the 96 MHz clock to use in FPGA, ADC, and DAC is generated. Whether the clock is inputted from the front panel of the RTM module or from the RF-backplane of µTCA.4 can be selected by the jumper pin. The eight input channels just go through to the µTCA.4 AMC ADCs.

The shelf of µTCA.4 with the bus and the RF-backplane is not used in the first step and the µTCA.4 AMC and RTM are installed to a box with a power supply. The ARM on the Zynq FPGA with linux installed is used as the communication tools instead of a CPU board. Figure 1 shows the block

* kenta.futatsukawa@kek.jp

Content from this work may be used under the terms of the CC BY 3.0 licence (© 2018). Any distribution of this work must maintain attribution to the author(s), title of the work, publisher, and DOI.

ISBN: 978-3-95450-194-6 ISSN: 2226-0366 doi:10.18429/JACoW-LINAC2018-MOPO115

CEBAF PHOTO GUN RF SYSTEM*

T. Plawski†, R. Bachimanchi, M. Diaz, S. Higgins, C. Hovater, C. Mounts, D. Seidman,
Jefferson Lab, Newport News 23606, VA, USA

Abstract

During the CEBAF 12 GeV Upgrade at Jefferson Lab, a fourth experimental hall, "D", was added to the existing three halls. To produce four beams and deliver them to all halls concurrently requires new frequencies and a new timing pattern of the electron bunches. Since a photo-gun is used to produce electron bunches, the gun's drive laser pulses need to be synchronized with the required bunch rate frequencies of 499 MHz or 249.5 MHz. To meet these new operational requirements, a new RF system has been proposed.

Very specific requirement of dual frequency operation prohibited us from using a typical LLRF system. Limited budget and time forced us to use commercial off-the-shelf digital platforms. The commercial boards we chose include, the Texas Instruments FPGA board, the high-speed 8-Channel, 14-Bit ADC board, and a 4-Channel, 16-Bit DAC board. The DAC board includes the clock generator for clocking ADCs, DACs and the FPGA. A custom designed RF transceiver section provides the RF to the digitizer and vice versa for the DACs. The Gun Laser RF system has been designed, built, and recently commissioned in the CEBAF Injector. This paper will detail the design and report on commissioning activities.

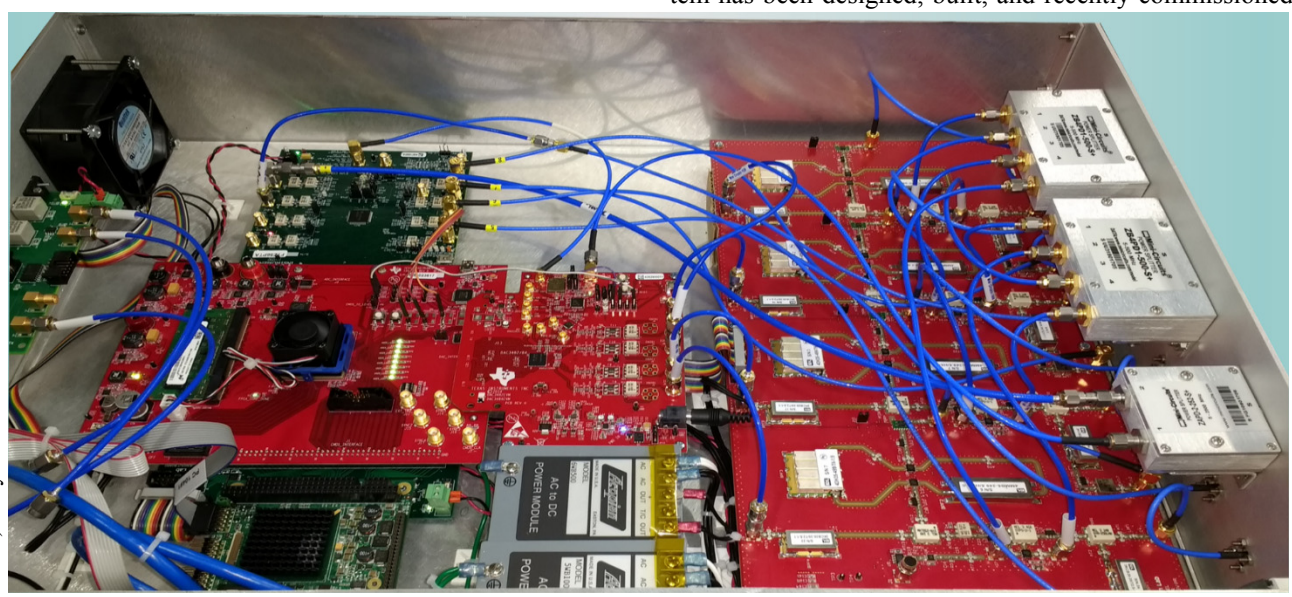


Figure 1: LLRF Chassis.

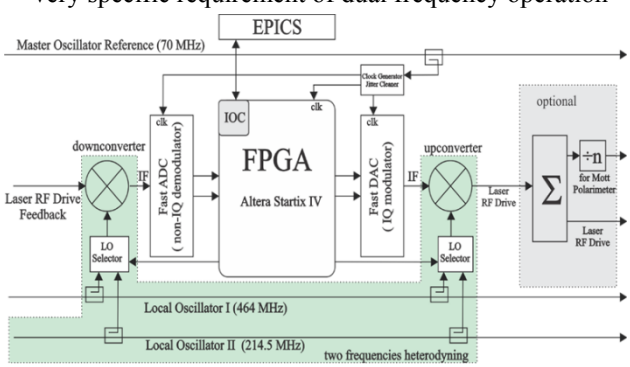


Figure 2: One channel of the Laser LLRF.

SYSTEM DESCRIPTION

Laser RF System consists of four RF receivers and four RF transmitters (see Fig. 1) allowing independent operation of four RF driven lasers [1]. The RF front-end section uses heterodyning in order to obtain 35 MHz IF signal (see Fig. 2). Depending on the required frequency of operation (499 MHz or 249.5 MHz), one of the two local oscillator (LO) frequencies (464 MHz or 214.5 MHz) can be selected. The digital section of the system contains an Altera Stratix IV FPGA, 1 GB memory and support up to 1.5 GSPS LVDS I/O rates for both ADCs and DACs (see Fig. 3). This board was built by Texas Instrument as a pattern generator/data capture system, and is compatible with multiple ADC and DAC boards from this manufacturer.

The ADS5294EVM board is an eight-channel, 14-bit serial LVDS interface, analog-to-digital converter with sampling speeds up to 80 MSPSs. that can be connected directly to the FPGA board. The DAC3484EVM is a DAC board that allows a user to operate a four-channel, ultra-

*Authored by JSA, LLC under U.S. DOE Contract DE-AC05- 06OR23177 and DE-SC0005264
† email: plawski@jlab.org

Content from this work may be used under the terms of the CC BY 3.0 licence (© 2018). Any distribution of this work must maintain attribution to the author(s), title of the work, publisher, and DOI.

ISBN: 978-3-95450-194-6 ISSN: 2226-0366 doi:10.18429/JACoW-LINAC2018-MOPO116

STUDY ON THE CONTROL TECHNOLOGY OF LARGE–LOAD TIME CONSTANT ACCELERATOR MAGNET POWER SUPPLY*

X. Wang†, F. L. Long, Institute of High Energy Physics, CAS, Beijing, China

Abstract

With the increasing application of power supply to industrial system, digital control system has become the mainstream of modern industrial control system. The wide application of digital control system has also led to the rapid development of digital controller. In the field of accelerator magnet power supply, the adoption of digital closed-loop control has become a trend in recent years. Due to the system's tracking and regulation characteristics, the output current will slowly track the change of the given value in the course of the given current gradually rising. When the system reaches steady state, the disturbance of the system requires the regulator to adjust at a faster rate to correct the impact of the disturbance on the system. Today's digital power supply control method mainly reflected in when load time constant is large, interference or load change, the power output is prone to overshoot or adjust the time is long, so the tracking and adjustment features cannot be met simultaneously. Therefore, this paper will study the power supply digital control technology for large - load time constant and the independent control method of tracking and regulating.

INTRODUCTION

The control algorithm of digital controller is one of the key factors that affect the performance of digital power supply. Compared to the traditional analogy power and digital power supply has the short design cycle, flexible control method, is easy to realize the modular management, to eliminate instability caused by discrete components and the characteristics of electronic jamming, so digital power source is a development trend of accelerator magnet power supply. Digital power supply control module has a great influence on the performance of the digital power supply, if digital control technology want to get further development in the digital power supply, depends on whether can achieve what we need in accelerator magnet power supply control algorithm.

Due to the tracking and regulation characteristics of the system, the output current will slowly track the change of a given value in the course of a given current. When the system reaches steady state, the disturbance of the system requires the regulator to be adjusted at a faster rate to correct the influence of the disturbance on the system. Today's digital power supply control method generally uses the traditional digital PID control algorithm [1], but poor dynamic performance of traditional PID algorithm, mainly reflected in when load time constant is large, there is interference or load change, the power output is prone to overshoot, or adjust the time is long, the tracking and adjusting performance cannot be consideration. This topic makes it possible to obtain the desired tracking behaviour (following the reference) independent of the desired regulation behaviour (rejection of a disturbance).

LOAD TIME CONSTANT

For any accelerator magnet power supply, its load characteristics are the basis of power closed-loop control. For the normal temperature magnetic we generally adopt, for example, digital proportional integral differential (PID) control as a closed loop control algorithm, and the design of the core of current loop integral time constant will be set mainly depends on the load time constant. This research institute is aimed at the load of a special kind of accelerator magnet power supply, namely the superconducting magnet load with very large time constant.

High energy particle accelerator technology has led the rapid development of superconducting technology in the past 30 years. The Fermi national accelerator laboratory (Fermi lab) in the 1980s of the construction of the TEVATRON collider particles, using the 774 for the first time in the world based on the technology of titanium niobium NbTi superconducting accelerator dipole magnets, applying NbTi superconducting technology from the laboratory into the industrialization level, to promote this technology in the civilian fields such as medical nuclear magnetic spectrometer (MRI) and so on a wide range of applications. Compared with the normal temperature magnet, the superconducting magnet can achieve the super high field strength that ordinary magnet cannot reach with a smaller volume. At the same time, due to the superconductivity of the load, its resistance is almost zero, which can greatly reduce the output voltage demand of the excitation power supply and reduce the operating cost of the accelerator excitation power system.

For example, BEPCII quadrupole magnet power supply (normal temperature magnet) and the LHC's diode of superconducting magnet power supply load [2], the time constant of the different types of load ratio on the following: time constant has the difference of several orders of magnitude. For different loads, the bandwidth and algorithm of the current closed-loop of digital controller will be different.

BEPCII quadrupole power supply load: Resistance =0.266Ω, Inductance=0.14H and Time constant τ =L/R=0.14/0.266 = 525ms.

LHC diode load: Resistance=0.8mΩ, Inductance=18H and Time constant τ=L/R=18/0.0008=22500=6.25 h.

Taking the future circular collider CEPC-SPPC project as an example, In order to deflect and focus on high-energy proton beams, the SPPC needs to install thousands of high field strong diodes and quadrupole magnets in a 100-kilometer circular tunnel in order to deflect and focus

* Work supported by IHEP
† wangxu@ihep.ac.cn

Content from this work may be used under the terms of the CC BY 3.0 licence (© 2018). Any distribution of this work must maintain attribution to the author(s), title of the work, publisher, and DOI.

ISBN: 978-3-95450-194-6 ISSN: 2226-0366 doi:10.18429/JACoW-LINAC2018-MOPO118

OPTIMIZED DESIGN FOR A COMPACT LINAC WITH COLLINEAR ABSORBING LOADS AT THE HUST FEL-THz

J. Jiang, T. N. Hu*, G.Y. Feng, Y. Lu, X. D. Tu, Y. Q. Xiong,
Huazhong University of Science & Technology, 430074 Wuhan, China
Y. J. Pei, National Synchrotron Radiation Laboratory, USTC, Hefei, China

Abstract

To meet the requirement of miniaturization for high power THz radiation in the field of commercial and civil use, RF Linacs have been applied widely as beam injectors, and the Linac with collinear absorbing loads reveals the potential to achieve a tradeoff between performance and compactness. Under overall consideration of systematic conflicts, optimization choices for such Linacs involving power absorbing ability, accelerating efficiency, as well as beamline length were described in this context. Meanwhile, cold testing has been conducted to verify design parameters for the collinear absorbing loads. Furthermore, elaborated calculation of thermal power loss and integrated helical water channel cooling has been performed for the 14MeV Linac with collinear absorbing loads installed on the HUST FEL-THz, and online experiments demonstrated that both the accelerating efficiency and the water cooling performance fulfilled operation demands.

INTRODUCTION

In recent decades, a lot of attention has been paid on compact high-power free-electron laser (FEL)-based terahertz (THz) radiation sources, which can be applied to the fields of security, communications and other scientific fields [1,2]. Since Linac-based FEL can provide above megawatt (MW) peak power radiation with the spectrum covering entire THz band [3,4], efforts have been made to reduce the facility scale and simplify peripheral systems.

Huazhong University of Science and Technology has built a porotype of compact FEL-THz facility [5], which has chosen a room-temperature accelerator to provide high-quality electron beams. Similar as typical beam injectors, the HUST-FEL-THz injector consists of a RF gun and a Linac, and the latter is set to boost the beam extracted by the RF gun to an energy of 14MeV. In order to absorb remnant RF power, an output coupler is commonly installed at the termination of the Linac. Since collinear load instead of traditional waveguide load is advanced for Linac miniaturization [6] and field symmetry, design of the beam injector based on the acceleration section with collinear loads, which aim at implementing layout compactness and high performance, will be introduced in this context.

DESIGN FOR THE LINAC WITH COLLINEAR LOAD

The HUST-FEL-THz Injector

At the HUST-FEL-THz, the booster Linac, which aims at accelerating the beams and driving them out of space-charge-dominated range, has been designed around disk-loaded constant gradient travelling-wave structures. According to the design demands of THz radiation [5], the driving beams should have the energy of about 14 MeV, so that a normal SLAC-like Linac has been adopted to provide adequate acceleration fields. Furthermore, since the beams extracted by the RF gun is still subject to space-charge effects before and in the Linac, as a common solution for emittance compensation, magnetic coils have wrapped around the Linac to provide focusing fields. According to the beam dynamic simulation in physical design of the HUST-FEL-THz injector [7], to obtain sufficient magnetic field strength and adjustment flexibility, a short lens has been placed downstream of the RF gun, and seven pancake-like solenoids cast with epoxy resin have surrounded the Linac. As suggested by Ref. 6, the collinear load based on FeSiAl material has been applied at the Linac to absorb the remnant RF power, so that the sizes of the focusing coils can be reduced. Moreover, comparing with traditional output coupler and waveguide absorbing load, the collinear load is perfectly symmetric which avoids transverse excitation of the beam and intrinsically does not contribute to any emittance growth.

According to the required THz radiation power of the HUST-FEL-THz, the injector must have the ability to work under the beam energy of 14 MeV, the repetition frequency of 50 Hz and the macro-pulse width of 4 μs. In order to accelerate the beam to 14 MeV within a distance as short as possible, a 19-cell Linac with the constant gradient of about 20.77 MV/m in each cell has been adopted, and a 4-cell collinear load has been set subsequently. Thus, the peak value of input RF power should be 16 MW. For a single load cavity, the input power (P_{in}) and transmitted power (P_{out}) is related by the following relation

$$P_{out} = P_{in} \cdot e^{-2\alpha D} \tag{1}$$

where α is attenuation constant, D is cavity length.

Since the calculated remnant power at the termination of the 14 MeV Linac is 12.10 MW and 5.54 MW with the beam turned-off and turned-on respectively. According to the principle of distribution of average power, to make the

*Corresponding author.
E-mail addresses: TongningHu@hust.edu.cn (T.N. Hu)

Content from this work may be used under the terms of the CC BY 3.0 licence (© 2018). Any distribution of this work must maintain attribution to the author(s), title of the work, publisher, and DOI.

ISBN: 978-3-95450-194-6 ISSN: 2226-0366 doi:10.18429/JACoW-LINAC2018-MOPO119

Content from this work may be used under the terms of the CC BY 3.0 licence (© 2018). Any distribution of this work must maintain attribution to the author(s), title of the work, publisher, and DOI.

DESIGN OF A FULLY AUTOMATED TEST BENCH FOR MESURING THE FIELD DISTRIBUTION OF STANDING WAVE CAVITY*

Y. Lu, T. N. Hu, G. Y. Feng, J. Jiang, X. D. Tu, Y. Q. Xiong
School of Electrical and Electronic Engineering,
Huazhong University of Science and Technology, Wuhan, China

Abstract

The resonant cavity plays a great role in the linear accelerator. An accurate measurement of the cavity field distribution is very important to design linear accelerators. A fully computer controlled bench for the electric field distribution has been developed in this context. Based on the perturbation theory, the acquisition of the resonant frequency shift is proportional to the square of E (electric field). In order to verify the reliability of the test bench, a standard cylindrical cavity has been tested in this measurement system. The simulation by HFSS (High Frequency Structure Simulator) and the practice will be both presented in this paper. And the result demonstrates that, because of its high concentricity, the automated test bench achieves high precision in measuring the distribution of electric field.

INTRODUCTION

RF cavities can support various electromagnetic fields. When designing a cavity to accelerate electrons, the field distribution should be calculated analytically. Bead pulling method based on perturbation theory is the most common technique to measure the field distribution in the cavity. This paper describes that a fully automated test bench that has been applied to detect the electric field distribution. The test bench has a compact structure, but realizes an accurate measurement and costs a little time to complete measurement due to automated measurement system.

BASIC PERTURBATION THEORY

The perturbation theory describes that the presence of a small volume of dielectric sample in the resonant cavity can make a slight change in resonant frequency and perturb the electromagnetic field [1]. The frequency shift is related to the intensity of electric field and magnetic field where the dielectric sample exists. According to Maxwell equations, the equation between frequency shift and electromagnetic parameters can be given as

$$\frac{\omega-\omega_0}{\omega_0} \approx -\frac{\int_{\Delta V}(\Delta\varepsilon|\boldsymbol{E_0}|^2+\Delta\mu|\boldsymbol{H_0}|^2)\mathrm{d}\Delta V}{\int_V(\varepsilon|\boldsymbol{E_0}|^2+\mu|\boldsymbol{H_0}|^2)\mathrm{d}V} \quad (1)$$

The volume of resonant cavity is V. In the unperturbed state, let the relative permittivity and the magnetic permeability be ε and μ. The electric field and magnetic field are $\boldsymbol{E_0}$ and $\boldsymbol{H_0}$, and the resonant frequency is ω_0. After placing a conductor sample whose volume is ΔV in the cavity, the electric field, the magnetic field and the resonant frequency become $\boldsymbol{E}$, $\boldsymbol{H}$ and ω. Let the relative permittivity and the magnetic permeability of the bead be $(\varepsilon+\Delta\varepsilon)$ and $(\mu+\Delta\mu)$.

For cylindrical accelerating cavities work at the TM010 mode, the magnetic field on the central axis is zero, namely $\boldsymbol{H}=0$ at $r=0$, where r is the radial position in the cavities. So if the dielectric sample is placed on the central axis, in the region of the sample, the equation (1) can be simplified as

$$\frac{\omega-\omega_0}{\omega_0} \approx -\frac{\int_{\Delta V}(\Delta\varepsilon|\boldsymbol{E_0}|^2)\mathrm{d}\Delta V}{\int_V(\varepsilon|\boldsymbol{E_0}|^2+\mu|\boldsymbol{H_0}|^2)\mathrm{d}V} \quad (2)$$

Hence,

$$E_z(r=0,z) \propto \sqrt{\Delta f(z)} \quad (3)$$

Therefore, it's feasible to get the distribution of axial electric field by moving the dielectric sample along the central axis and measuring the resonant frequency point by point.

MEASUREMENT PROCEDURE OF THE TEST BENCH

According to the perturbation theory, the axial electric field is acquired by measuring the resonant frequency when a metallic conductor sample is displaced through the cavity. In the design of automated test bench, a small bead is used as a small conductor sample and it is moved by the bead displacement system which consists of a wire, a stepper motor and several pulleys. The bead gets accurate position along the central axis by a stepper motor, which is controlled by a computer over a LAN(Local Area Network). Besides the resonant frequency of cavity could be measured by the VNA(Vector Network Analyzer) with the same control method. An agilent E5061B VNA measures the S11 transmission coefficient through the cavity and find the resonant frequency [2, 3]. And it offers an excellent stability and accuracy, and an easy control via LAN.

Thus, the data collection and processing are achieved automatically. The design of automated measurement system, shown in Figure 1, could obtain the distribution of the axial electric field by perturbation method. The components of the measurement system: a computer, a VNA, a cylindrical cavity excited by a probe, a stepper motor and several pulleys.

ISBN: 978-3-95450-194-6 ISSN: 2226-0366 doi:10.18429/JACoW-LINAC2018-MOPO120

IMPROVEMENT OF THE LINEAR PART IN THE TUNER SYSTEM OF ADS 25 MeV LINAC

L. Zhang†, F.F. Wang, L.B. Liu, Z. Gao, B. Zhang
Institute of Modern Physics, Chinese Academy of Science, Lanzhou, China

Abstract

Tuner system is the indispensable part of ADS high current proton superconducting linac. It influences the working frequency of superconducting cavity of particle accelerator. To completely understand the working situation of the tuner system and analyses the problems existing in it, experiments of linear part were fully conducted.

INTRODUCTION

The tuner system of ADS 25 MeV Linac (Fig. 1) built in CM1, CM2 and CM3 consists of 17 tuners[1], and every tuner consists of two parts – linear part and tuning implement unit. Linear part is mainly composed of step motor, reduction box, screw-nut and coupler (Fig. 2). To learn about the working conditions and structure characteristics, the linear parts of 17 tuners were tested and the CM1-2, CM2-3 and CM3-1 were chosen as representatives to give a brief introduction of test procedure and results. Through the analysis of the problem, the linear part was improved and tested again, and the effect was remarkable.

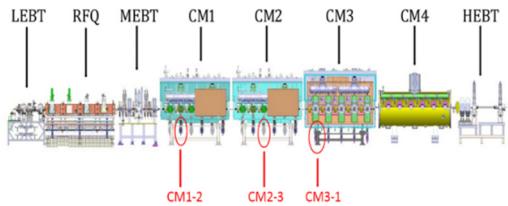


Figure 1: The layout of ADS 25MeV linac.

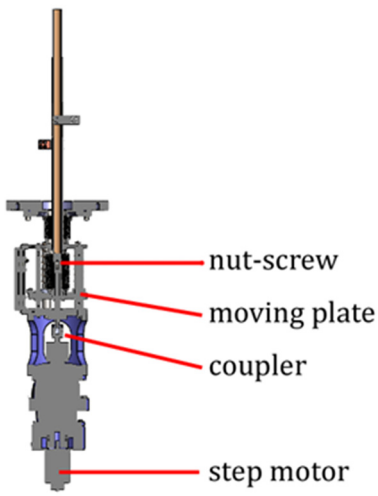


Figure 2: The sectional view of the tuner linear part.

THE TEST OF LINEAR PART

The linear part of tuners was tested at 300 K as shown in Fig. 3. The moving plate was adjusted to a suitable position to ensure enough space to move up and down. Then the dial indicator was fixed on the bracket and was properly set at an indication that later we took as the center. With 200 steps at a time, the step motor was made to move 25 times in the direction where the moving plate rose and fell respectively. Positions of every movement were recorded by the dial indicator.

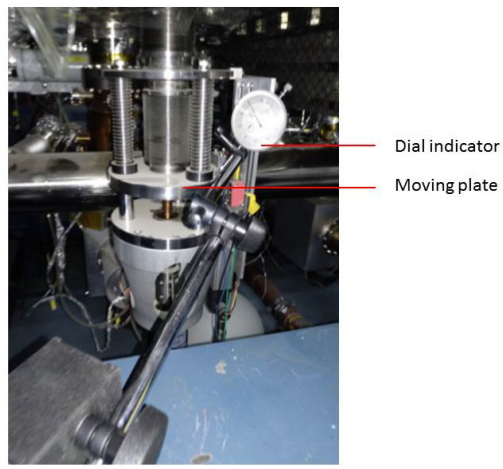


Figure 3: The test of the linear part.

The result of CM1-2 tuner linear driving part (Fig. 4) test shows that the plate tends to move linearly and is barely influenced by hysteresis, which shows the linear drive part works well and meets the requirement of tuners.

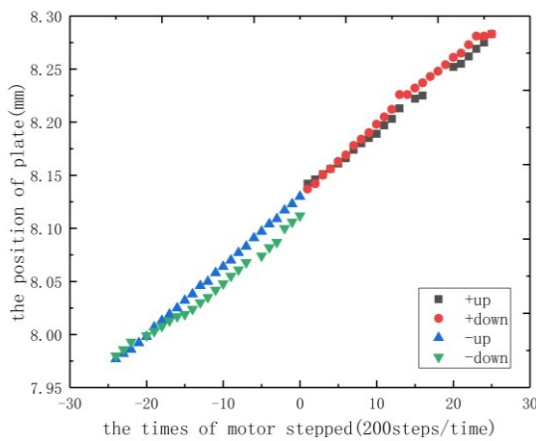


Figure 4: The curve of the line part test in CM1-2.

† zhanglei@impcas.ac.cn

Content from this work may be used under the terms of the CC BY 3.0 licence (© 2018). Any distribution of this work must maintain attribution to the author(s), title of the work, publisher, and DOI.

ISBN: 978-3-95450-194-6 ISSN: 2226-0366 doi:10.18429/JACoW-LINAC2018-MOPO121

LARGE-SCALE OPTICAL SYNCHRONIZATION SYSTEM OF THE EUROPEAN XFEL

J. Müller*, M. Felber, T. Kozak, T. Lamb, S. Schulz, C. Sydlo,
M. Titberidze, F. Zummack, and H. Schlarb
Deutsches Elektronen-Synchrotron (DESY), Notkestraße 85, 22607 Hamburg, Germany

Abstract

At the European XFEL, a facility-wide optical synchronization system providing a femtosecond-stable timing reference at more than 40 end-stations had been developed and installed. The system is based on an ultra-stable, low-noise laser oscillator, whose signals are distributed via actively length-stabilized optical fibers to the different locations across the accelerator and experimental areas. There, it is used to locally re-synchronize radio frequency signals, to precisely measure the arrival time of the electron beam for fast beam-based feedbacks, and to phase-lock optical laser systems for electron bunch generation, beam diagnostics and user pump-probe experiments with femtosecond temporal resolution. In this paper, we present the system's architecture and discuss design choices to realize an extensible, large-scale synchronization infrastructure for accelerators that meets reliability, maintainability as well as the performance requirements. Furthermore, the latest performance result of an all-optically synchronized laser oscillator is shown.

INTRODUCTION

The European X-ray Free-Electron Laser (XFEL) is a fourth-generation linac-based light source being capable of producing X-ray pulses with a duration of only a few to tens of femtoseconds. In particular for time-resolved pump-probe experiments it is crucial to achieve a synchronization between the FEL and the pump-probe laser systems with an accuracy on the same timescale. Accordingly, the synchronization system for the European XFEL was designed and built [1] to achieve a point-to-point timing jitter of 10 fs.

The foundation of the system is a low-noise laser oscillator synchronized to the master radio-frequency (RF) oscillator (MO) of the facility to provide a long- and short-term stable timing reference to critical subsystems using optical fiber links (see Fig. 1). For this, an active fiber length stabilization scheme [2] is employed to compensate optical path length changes, and by this keeping the laser pulse arrival time at the fiber link end stable with a jitter of less than 1 fs (rms) [3]. Since in a large-scale accelerator like the European XFEL the radio-frequency signals, which are the reference signals for the accelerating modules, are distributed over kilometers of cables and amplified several times, phase drift and jitter contributions can add up significantly. To achieve low-drift and low-timing jitter FEL performance, optical reference modules ("REFM-OPT") are installed along the accelerator to re-synchronize the degraded LLRF signals. These modules provide a femtosecond-precise, low-drift and amplitude-insensitive laser-to-RF phase detection based on an integrated Mach-Zehnder interferometer [4]. Another end-station type is the electron bunch arrival-time monitor [5] which, with it's femtosecond temporal resolution, is used for diagnostic purposes as well as within a fast feedback loop on the electron arrival time. In addition to a well stabilized accelerator and thus low-timing jitter X-ray pulses, external laser systems are required to be synchronized with femtosecond precision for time-resolved pump-probe user experiments. Therefore, an all-optical scheme based on two-color balanced optical cross-correlation [6] is applied to precisely measure the timing error between two pulsed laser sources and keep their relative timing jitter at a minimum.

Key requirement for all subsystems relevant for operation of the European XFEL as a facility with over 8000 hours yearly for user experiments is reliability and high availability to ensure minimum amount of downtime. Therefore, strong focus had been laid on development of mechanically, electronically and optically robust systems with large amount of automation, monitoring and redundancy [7, 8].

OPTICAL REFERENCE DISTRIBUTION

Master Laser Oscillator

A commercial, passively mode-locked SESAM-based master laser oscillator (MLO) with a repetition rate of 216.7 MHz (one-sixth of the main RF cavity resonance frequency of 1.3 GHz) provides the main optical reference pulse train. The laser is synchronized to the MO at the 7th harmonic of its repetition rate (1516.7 MHz) in a PLL-type scheme, such that the phase detection is realized at an intermediate frequency. This kind of down-conversion instead of applying a conventional DC phase detection scheme bypasses problems like DC offsets, electromagnetic interference at low-frequencies as well as $1/f$ noise related jitter contributions. Furthermore, this scheme allows for choosing an arbitrary phase set point and thus enabling the possibility to electronically shift the timing of the laser pulses. To achieve the highest level of availability a second, redundant laser oscillator of the same type is installed while an automatized and fast switching procedure ensures the possibility of an uninterrupted switching in case of a failure. At the same time the MLOs, together with the complete optical synchronization infrastructure and the MO, are connected to an uninterruptible power supply for maximum uptime.

* jost.mueller@desy.de

Content from this work may be used under the terms of the CC BY 3.0 licence (© 2018). Any distribution of this work must maintain attribution to the author(s), title of the work, publisher, and DOI.

ISBN: 978-3-95450-194-6 ISSN: 2226-0366 doi:10.18429/JACoW-LINAC2018-MOPO122

EUROPEAN XFEL COOLING AND VENTILATION SYSTEMS

Jens-Peter Jensen, Andreas Block, Sylke Feuker; DESY, D 22607 Hamburg, Germany

Abstract

The European Xray Free Electron Laser EuXFEL is operating since 2016. The technical systems for cooling and ventilation CV were designed, built and commissioned by the DESY work package WP34. The water cooling systems consists of 3 cooling systems: 30/45°C low conductivity water LCW for klystron, power converter and magnet cooling; 20/30°C LCW for tunnel rack cooling and 8/14°C for air conditioning and for air-drying. The ventilations of the tunnels are connected to a serial ventilation system. The air flow starts from the experimental hall in opposite direction of the beams until to the injector. The series ventilation system of the tunnels saves costs for air treatment like cooling, heating and air-drying. The tunnel walls are a good heat storage that increases the air temperature stability by a factor of ten. The advantages of this concept will be described.

INTRODUCTION

The European XFEL starts on the DESY premises and ends after 3.4 km at the experimental hall in Schenefeld. The beam direction is from east to west. Figure 1 shows the site map of the facility.



Figure 1: Map of the Eu-XFEL in Hamburg.

WATER COOLING SYSTEM OF XFEL

The water cooling system is divided in 2 sections since the tunnels are about 3.5 km long from the gun to the experimental hall XHEXP1.

- XHM Pump House:

The XHM pump house (Fig. 2) is located on the DESY premises and serves the injector in DESY-Bahrenfeld and the 2 km long XTL tunnel until the first separation shaft XS1 in Osdorfer Born. That is why the main cooling demands are in the linac tunnel XTL for the RF stations, the electronic racks and the normal conducting magnets.

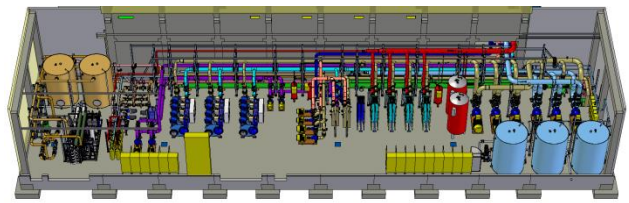


Figure 2: XHM pump house DESY Bahrenfeld, 3D model.

Figure 2 shows the 3D model of the pump house with its piping, pumps, chillers, water storage tanks and control cabinets. Figure 3 is a photo of the final installation.



Figure 3: XHM pump house installation.



Figure 4: XHM cooling towers for dry and wet cooling.

Figure 4 shows the hybrid cooling towers. Each tower has a rated power of 2 MW. The water temperature is controlled by variable speed fans. If the air temperature

Content from this work may be used under the terms of the CC BY 3.0 licence (© 2018). Any distribution of this work must maintain attribution to the author(s), title of the work, publisher, and DOI.

ISBN: 978-3-95450-194-6 ISSN: 2226-0366 doi:10.18429/JACoW-LINAC2018-MOPO124

DETAILS OF THE MANUFACTURING PROCESSES OF THE ESS-DTL COMPONENTS

P. Mereu*, F. Borotto Dalla Vecchia, C. Mingioni, M. Nenni, R. Panero, INFN, Torino, Italy
A. Battistello, P. Bottin, D. Conventi, L. Ferrari, A. Colombo, F. Grespan, A. Pisent, INFN-LNL, Italy

Abstract

The Drift Tube Linac (DTL) of the European Spallation Source (ESS) is designed to operate at 352.2 MHz with a duty cycle of 4% (3 ms pulse length,14 Hz repetition period) and will accelerate a proton beam of 62.5 mA pulse peak current from 3.62 to 90 MeV. This paper presents the details of the manufacturing processes with quality control reports reports of the components of the DTL.

DTL DESIGN

In the ESS accelerator the initial warm linac section is composed by Ion Source, Low Energy Beam Transport line (LEBT), Radio Frequency Quadrupole (RFQ), Medium Energy Beam Transport line (MEBT) and DTL [1]. The ESS-DTL is a 38.8 m long system, divided in five tanks [2]; each tank is a stand-alone structure, composed of four 2 m long modules made of AISI 304L stainless steel with internal copper electro-deposition. The nominal position of the 168 DTs is demanded to the girder, a precisely machined aluminium alloy structure, which is housed in the upper part of each module. The DTL comprises 4 types of DTs, depending on the beam components integrated in the body: Permanent Magnet Quadrupole (PMQ), Beam Position Monitor (BPM), Electro-Magnetic Dipole (EMD) and Empty body [3]. Figure 1 indicates the main components of a typical DT. The DTs are made by a Cu-OFE body and an AISI 304L Cu-plated stem; internally there are machined steel components which provide the proper cooling water flow around the DT body. DTs are assembled by Vacuum Brazing (VB) and Electro Beam Welding (EBW).

DRIFT TUBES MANUFACTURING

The DT production and assembly, apart the EBW and all DTs-BPM, is made internally at INFN, in Torino (Tanks 1, 2) and in Legnaro (Tanks 3, 4, 5). The production of one typical DT is made of different phases, summarized as follows:

1) Machining of Body, Cover, Stem and internal steel components.
2) Copper plating of stem surfaces, housed in the RF cavity of the DTL.
3) VB of body with stem and relative internal components.
4) For the DT-BPM and DT-EMD, inner-pipe welding on the sleeve (see Brazing section in the following).
5) Machining of the coupling references in the stem for the integration in the girder and laser tracker housing.
6) For DT-PMQ, machining of the references surfaces of the PMQ housing.
7) Integration of the internal beam components (PMQ, EMD, BPM).
8) Sealing of the DT cover with EBW. For BPM and EMD, EBW of the Beam-Pipe on both ends of the DT.
9) Machining to the definitive external profile, by removing the EBW allowance at the Beam-Pipe interfaces with the DT.

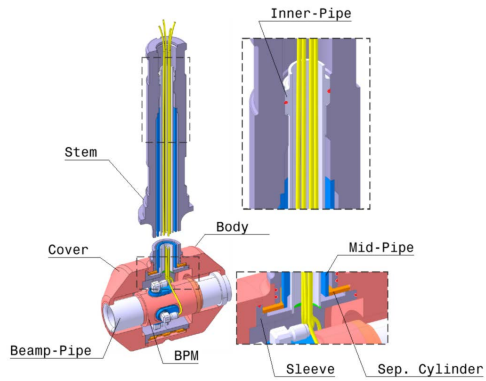


Figure 1: Main components of a DT-BPM. Details show the brazing channels (in red) and press-fit interfaces.

PART PRODUCTION

Mechanical production of bodies and cover is made of different phases, (each one involving different machines and thus different alignment). Referring to Figure 2:

1) Initial rough milling.
2) Lathing of the internal profile. The part is fixed with a classic bracket claw with no pre-alignment.
3) Milling of 90 mm external cylinder. Pre-alignment is made measuring the internal datum plane B and consequently compensating the machine.
4) Milling of 28 mm cylinder for stem integration. Pre-alignment is made with a dedicated alignment block.
5) Lathing of external profile of the angular cone, along with the "nose" plane. The part is fixed on the inner profile with a dedicated alignment as in second picture.

The procedure was continuously improved, in term of production rate, also using feedback from metrology results.

QUALITY CONTROL AND METROLOGY

INFN has developed a quality system in which every single part is designed, producing an executive drawing for each one, then machined and finally measured. This work-flow

* paolo.mereu@to.infn.it

Content from this work may be used under the terms of the CC BY 3.0 licence (© 2018). Any distribution of this work must maintain attribution to the author(s), title of the work, publisher, and DOI.

ISBN: 978-3-95450-194-6 ISSN: 2226-0366 doi:10.18429/JACoW-LINAC2018-MOPO125

STEERING MAGNETS WITH PERMANENT MAGNETS

Y. Iwashita†, M. Abe, T. Yako, ICR, Kyoto Univ., 611-0011, Uji, Kyoto, Japan
Y. Fuwa, KURNS, Kyoto Univ., 590-0494, Osaka, Japan
N. Terunuma, KEK, 305-0801, Tsukuba, Japan

Abstract

Steering magnets with permanent magnets are investigated. They need to generate both polarities of magnetic fields, which can be realized by rotating permanent magnet rods. Such a magnet system will reduce not only electricity but also maintenance cost. The structure and the field adjustment scheme of a trial conceptual design will be discussed.

INTRODUCTION

Electromagnets, which are widely used as optics elements for beam handling, may be replaced by permanent magnets. In addition to reductions of the electricity for coil excitation and cooling, thick electric cabling and water piping, power supply and their maintenance cost-down are also expected. Among optics elements, steering magnets need to generate bipolar magnetic fields, which can be realized by rotating permanent magnet rods [1].

One demand for such a device comes from Ring To Main Linac (RTML) beam lines, whose lengths are more than that of the main linac. Another demand comes from ILC Damping Ring (DR), where more than 300 steering magnets will be installed for orbit correction [2]. With permanent magnets, there is no DC power supplies, no cooling water, and then these failures will never happen. Water leaks have been annoying events among maintenance activities, which would also be dramatically reduced if permanent magnets were applied. These items offer cost reductions for both construction and operations.

While many advantages are expected, we need some investigations in applying permanent magnets. At least three subjects have to be considered: temperature dependence of remnant field (Br), adjustability and demagnetization caused by radiation. The temperature coefficient can be compensated by magnetic shunts made of magnetic materials with low Curie temperature, which have large temperature coefficient around their operating temperatures [3]. Although the strength adjustment of magnets made of permanent magnets are not easy compared with electromagnets, there are some methods that can be incorporated. In order to change the magnetic flux density generated in a gap, we rotate permanent magnets in the structure, which enables a bipolar operation and is suitable for correction magnets. The rotating mechanism may also have troubles like a failure of power supply for electromagnet. The permanent magnet system, however, will not lose the deflecting strength but just the adjustability from the current position, which will not prevent the machine operation immediately, since the adjustment is not expected to be so often in a daily operation.

† iwashita@kyticr.kuicr.kyoto-u.ac.jp

CORRECTION MAGNET

Assumed magnet length and beam pipe diameter are about 32 cm and 6 cm, respectively. Eight ferrite permanent magnet rods with about ø50mm diameter can generate enough strength. We assume to use Y30H, whose remnant field Br is about 0.4T. The magnet diameter is chosen from an available magnet ingot size (25.4×100×150 mm). The octagon shaped magnet rod has a slightly larger volume than a cylindrical rod that can be machined from the ingot with the same size. Figure 1 shows a possible bipolar correction magnet, where the magnet rods are rotated by a stepping motor to vary the magnetic field strength (see Fig. 2). The adjacent rods rotate with opposite directions each other so that the mag-

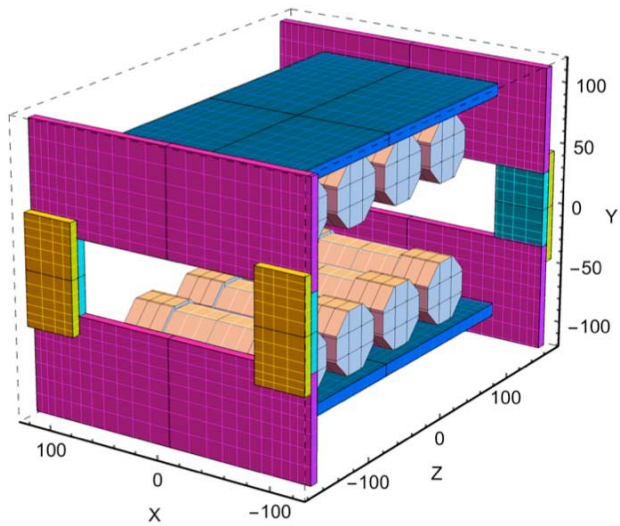


Figure 1: Outline of the permanent steering magnet.

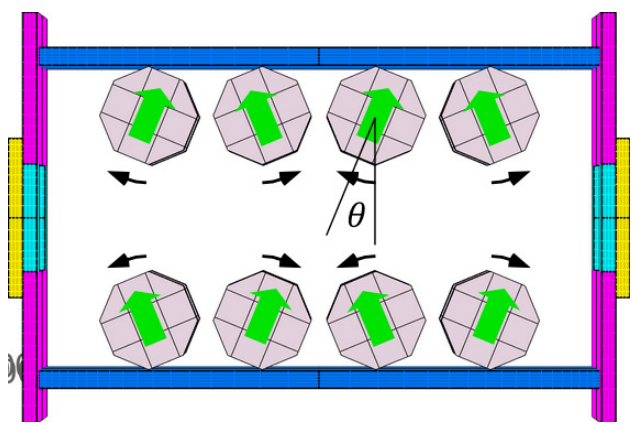


Figure 2: Cut view of the permanent steering magnet. The magnet rods rotate oppositely each other.

Content from this work may be used under the terms of the CC BY 3.0 licence (© 2018). Any distribution of this work must maintain attribution to the author(s), title of the work, publisher, and DOI.

ISBN: 978-3-95450-194-6 ISSN: 2226-0366 doi:10.18429/JACoW-LINAC2018-MOPO127

RECENT RESULTS FROM MICE ON MULTIPLE COULOMB SCATTERING AND ENERGY LOSS*

Jingyu. Tang†, Institute of High Energy Physics, CAS, P. R. China
J. Nugent, University of Glasgow, UK

Abstract

Multiple Coulomb scattering and energy loss are well known phenomena experienced by charged particles as they traverse a material. However, from recent measurements by the MuScat collaboration, available simulation codes (GEANT4, for example) are known to overestimate the scattering of muons in low Z materials. This is of particular interest to the Muon Ionization Cooling Experiment (MICE) collaboration that has the goal of measuring the reduction of the emittance of a muon beam induced by energy loss in low Z absorbers. MICE took data without magnetic field suitable for multiple scattering measurements in the fall of 2015 with the absorber vessel filled with xenon and in the spring of 2016 using a lithium hydride absorber. In the fall of 2016, MICE took data with magnetic fields on and measured the energy loss of muons in a lithium hydride absorber. These data are all compared with the Bethe formula and with the predictions of various models, including the default GEANT4 model.

INTRODUCTION

Muon colliders and neutrino factories will require stored muons with high intensity and low emittance [1]. Muons are produced as tertiary particles ($p + N \rightarrow \pi + X$, $\pi \rightarrow \mu + \nu$) inheriting a large emittance (volume of the beam in the position and momentum phase space). For efficient acceleration, the phase-space volume of these beams must be reduced significantly ("cooled"), in order to be accepted by traditional accelerators. Due to the short muon lifetime, ionization cooling is the only practical and efficient technique to cool muon beams [2]. In ionization cooling, the muon beam loses momentum in all dimensions by ionization energy loss when passing through an absorbing material, reducing the RMS emittance (ε_{RMS}) and increasing its phase space density. Subsequent acceleration by radio-frequency cavities restores longitudinal energy, resulting in a beam with reduced transverse emittance. A factor of 10^5 in reduced 6D emittance has been achieved in simulation with a 970 m long channel [3].

The rate of change of the normalized transverse RMS emittance ε_T is given by the ionization cooling equation [4]:

$$\frac{d\varepsilon_T}{dz} \cong -\frac{\varepsilon_T}{E_\mu \beta^2}\frac{dE_\mu}{dz} + \frac{\beta_\perp}{2mc^2\beta^3}\frac{(13.6\ \text{MeV/c})^2}{E_\mu X_0}, \qquad (1)$$

where E_μ is the muon energy, β the muon velocity, dE_μ/dz the magnitude of the ionization energy loss, m the muon mass, X_0 the radiation length, and $\beta_\perp$ the transverse beta function at the absorber. The first term on the right can be referred as the "cooling" term given by the "Bethe equation", while the second term is the "heating term" that uses the PDG approximation [5] for the multiple Coulomb scattering.

MICE is instrumented with a range of detectors used for particle identification and position-momentum measurements. This includes a scintillating fiber tracker upstream and downstream of the absorber placed in a strong solenoid field to measure the position and the momentum (with a spatial resolution around 0.3 mm). MICE is also equipped with a series of particle identification detectors, including three time-of-flight hodoscopes (ToF0/1/2, with a time resolution around 60 ps), two threshold Cherenkov counters, a pre-shower calorimeter and a fully active scintillator calorimeter. A schematic drawing of MICE Step IV is shown in Fig. 1.

MICE data taking was concluded in December 2017 (in the Step IV configuration) in order to make detailed measurements of multiple Coulomb scattering and energy loss of muon beams at different momenta and channel configurations, with lithium hydride (LiH) and liquid hydrogen (LH_2) absorbers. The collaboration also sought to measure the reduction in normalized transverse emittance [6], comparing the emittance of a sample of muons selected in the upstream tracker with the emittance of the same sample measured in the downstream one, after passing through the absorber.

MEASUREMENTS OF SCATTERING DISTRIBUTIONS

Though multiple Coulomb scattering is a well understood phenomenon, results from MuScat [7-8] indicate that the effect in low Z materials is not well modelled in simulations such as GEANT4 [8]. MICE therefore measured the multiple Coulomb scattering distribution to validate the scattering model and understand the heating term in Eq. (1), in order to make more realistic predictions of the emittance reduction.As MICE was designed to measure the emittance change to 0.1% level, precise measurements on multiple Coulomb scattering are required. Both data with field off and field on in the scintillating fiber tracker are available for MICE. While the field on data is still being analysed, the field off analysis is presented here.

MICE has collected data for muon beams at three different momenta, 172 MeV/c (in order to compare with MuScat), 200 MeV/c and 240 MeV/c with and without the LiH absorber in place (thickness 65 mm, X_0 = 79.62 g/cm^2) and with a full and an empty liquid hydrogen absorber vessel (~22 litre). Here the LiH analysis is presented.

*on behalf of the MICE Collaboration
†tangjy@ihep.ac.cn

Content from this work may be used under the terms of the CC BY 3.0 licence (© 2018). Any distribution of this work must maintain attribution to the author(s), title of the work, publisher, and DOI.

ISBN: 978-3-95450-194-6 ISSN: 2226-0366 doi:10.18429/JACoW-LINAC2018-MOPO129

RECENT RESULTS FROM THE STUDY OF EMITTANCE EVOLUTION AT MICE

V. Blackmore, C. Hunt*, Imperial College London, London, UK
W. B. Liu, Institute of High Energy Physics, CAS, Beijing, China
on behalf of the MICE Collaboration

Abstract

The Muon Ionization Cooling Experiment (MICE) has measured the evolution of emittance due to ionization energy loss. Muons were focused onto an absorber using a large aperture solenoid. Lithium-hydride and liquid hydrogen-absorbers have been studied. Diagnostic devices were placed upstream and downstream of the focus, enabling the phase-space coordinates of individual muons to be reconstructed. By observing the properties of ensembles of muons, the change in beam emittance was measured. Data taken during 2016 and 2017 are currently under study to evaluate the change in emittance due to the absorber for muon beams with various initial emittance, momenta, and settings of the magnetic lattice. The current status and the most recent results of these analyses will be presented.

INTRODUCTION

Low emittance stored muon beams have been proposed as the source of neutrinos at a neutrino factory [1, 2] or as the means to deliver multi-TeV lepton-antilepton collisions at a muon collider [3]. The muons at such a facility originate from the decay of pions and occupy a large volume in phase space (emittance). This must be reduced (cooled) to fit within the acceptance of a storage ring or accelerating structure. The short muon lifetime prohibits existing cooling techniques such as synchrotron or stochastic cooling. Ionisation cooling is the only viable method that can act within the short muon lifetime to reduce phase space volume of a muon beam.

Ionisation cooling occurs when a muon beam passes through an absorber material and ionises atomic electrons, losing both transverse and longitudinal momentum. This reduces the volume in phase space occupied by the beam, and thus reduces the beam emittance. Concurrently, multiple Coulomb scattering within the absorber increases the angular divergence of the beam, increasing the emittance. The interplay of emittance reduction, due to energy loss by ionisation, and emittance growth, through multiple Coulomb scattering, results in a change in normalised RMS emittance, $\varepsilon_\perp$, over a distance, dz, given by [4],

$$\frac{d\varepsilon_\perp}{dz} \approx -\frac{\varepsilon_\perp}{\beta^2 E_\mu}\left\langle\frac{dE}{dz}\right\rangle + \frac{\beta_\perp (13.6MeV/c)^2}{2\beta^3 E_\mu m_\mu X_0} \quad (1)$$

where $\beta_\perp$ is the transverse optical Twiss function, βc, E_μ, and m_μ are a particle's velocity, energy, and mass respectively, and X_0 is radiation length of the absorber material. Maximum emittance reduction is achieved by using absorbers with large radiation lengths such as liquid hydrogen or lithium hydride.

THE MUON IONISATION COOLING EXPERIMENT

The Muon Ionisation Cooling Experiment (MICE) [5] consists of a transfer line that transports particles from the ISIS synchrotron at the Rutherford Appleton Laboratory, UK, to a segment of a cooling lattice. The beam is transported through PID detectors using conventional quadrupole magnets, then by large-aperture superconducting solenoids through the cooling channel operated at up to 3 T. At the centre of the cooling lattice is an absorber material. The beam is measured before and after the absorber in the constant 3 T field of the up- and down- stream spectrometer solenoid modules using scintillating fibre trackers. A schematic drawing of MICE is shown in Fig. 1.

MICE has measured the passage of individual muons through an empty channel, 21 litres of liquid hydrogen contained within an aluminium vessel, and a 65 mm solid lithium hydride disc. These measurements were made with the same magnetic optical configuration to evaluate phase space evolution across a cooling cell and compare the cooling performance of liquid hydrogen and lithium hydride. Individual particle trajectories are measured as they cross the experiment and are assembled offline into analysable particle ensembles. These ensembles consist of particles with: 1) an upstream Time-of-Flight consistent with a muon, 2) a measured total momentum, p, in the range 135–145 MeV/c, 3) a single, good quality track in the upstream tracking detector, and 4) a measured momentum in the upstream tracking detector consistent with the Time-of-Flight. The current status of the analysis of the measured ensembles is presented here.

EMITTANCE EVOLUTION

The measured components of transverse phase space, x, y, p_x, p_y are compared to those of a Monte Carlo simulation, that includes the response of instrumentation, in Fig. 2. The reconstructed data (black, circles) and the reconstructed simulation (filled histogram) show good agreement. Distributions of x, y, p_x, p_y are shown (left) up- and (right) downstream of the liquid hydrogen absorber.

The ensemble's covariance matrix, $\Sigma_\perp$, is calculated from the measured transverse quantities as,

* Christopher.hunt08@imperial.ac.uk

Content from this work may be used under the terms of the CC BY 3.0 licence (© 2018). Any distribution of this work must maintain attribution to the author(s), title of the work, publisher, and DOI.

ISBN: 978-3-95450-194-6 ISSN: 2226-0366 doi:10.18429/JACoW-LINAC2018-MOPO130

MAGNETIC FLUX GENERATED BY THERMAL CURRENT IN CEBAF 5-CELL CAVITY SYSTEM*

R. L. Geng†, S. C. Huang[1], Jefferson Lab, Newport News, VA 23693, USA

Abstract

The unloaded quality factor Q_0 of many 5-cell CEBAF cavities was lowered by a factor of ~2 from their vertical qualification testing to their beam operation in CEBAF tunnels. Causes of this Q_0 degradation were studied previously, including a more recent one addressing static flux arising from magnetic components near these cavities. This paper reports on a preliminary study of the dynamic flux generated by a thermal current, arising from the Seebeck effect and flowing in closed-loops formed by a niobium cavity and its surrounding tuner rods and liquid helium vessel made of stainless-steel. Flux generation in response to various thermal profiles in a 5-cell CEBAF cavity with integrated tuner rods were studied through varied cool-down cycles in a vertical dewar at JLAB. One outcome of this study is a proposed cool-down procedure for eliminating the thermal current generated magnetic flux around 5-cell cavities placed in CEBAF tunnels. This procedure may be useful for improving cavity Q_0 in a cost-effective manner, which in turn saves cryogenic expenditures for more efficient CEBAF operation.

INTRODUCTION

The unloaded quality factor of an RF cavity Q_0 can be described by $Q_0 = {}^{G}/_{R_s}$, where G is the geometry factor determined solely by the cavity geometry and resonating mode, R_s is the RF surface resistance which consists of the BCS term R_{BCS} and residual term R_{res}. The Q_0 values of many original 5-cell cavities placed in the CEBAF tunnels were degraded by a factor of ~2 as compared to that measured during their vertical qualification testing. The origin of this Q_0 degradation is attributed to an increase of R_{res}. Magnetic flux trapped in the RF penetration layer of an SRF cavity during its cool-down crossing Tc contribute to R_{res}, as it has been well established. Sources of magnetic flux include *static* ones, such as the remaining earth magnetic field inside the magnetic shielding, magnetized components enclosed in the inner magnetic shield, and *dynamic* ones such as thermal current generated magnetic flux. A recent prior work revealed large remnant magnetic fields in various magnetic components being near a cavity yet enclosed inside the inner magnetic shield [1]. That work led to a change in CEBAF cryomodule refurbishing practice. Non-magnetic strut springs made of 316L stainless-steel (SS) replaced their magnetic counterparts starting at the 11th rework module C50-11, eliminating one source of static magnetic flux that was enclosed in the inner magnetic shield. In the best case for C50-11, the cavity Q_0 at 5 MV/m measured in cryomodule was preserved at 88% of the value measured during its vertical qualification. However in the worst case, the preservation was still poor, at 40% level, begging additional effort.

More recently, systematic measurements of an original CEBAF cavity in a vertical cryostat with progressively added cryomodule components were carried out with an effort of degaussing the remaining magnetic components enclosed in the inner magnetic shield [2]. That work led to a new change in refurbishment practice starting at C50-12. The tuner components and helium vessel were all degaussed with a surface demagnetizer. In the best case for C50-12, the cavity Q_0 at 5 MV/m measured in cryomodule was preserved at 100% of the value measured during its vertical qualification. However in the worst case, the preservation was still ~ 60%, despite the static magnetic flux having fallen into the specification of ±10 mG for that cavity when measured in the tunnel.

Aiming for CEBAF operation with improved energy efficiency, the effort is continuing at JLAB, in pursuit of origin and remediation of the low Q_0 observed in original and refurbished 5-cell cavity cryomodules placed in linac tunnels. In this contribution, we report on preliminary studies of a *dynamic* source for magnetic flux, arising from the thermal-electric effect. Similar effects were observed in 9-cell cavities jacketed with titanium helium vessels [3]. Through these elementary studies, we seek ways for thermal-current elimination and raising Q_0 [4].

5-CELL CAVITY SYSTEM

As completed in 1994, the original CEBAF accelerator was consisted of 338 L-band (1497 MHz) 5-cell SRF niobium cavities hosted in 42 8-cavity cryomodules plus an additional 2-cavity cryomodule. The basic building block is a cryo-unit as shown in Fig. 1. Two 5-cell cavities are connected back-to-back, which in turn are enclosed in a 610 mm diameter liquid helium vessel made of SS. Each end of the unit is isolated by a gate valve (not shown in Fig. 1). The overall length of this unit is about 1778 mm.

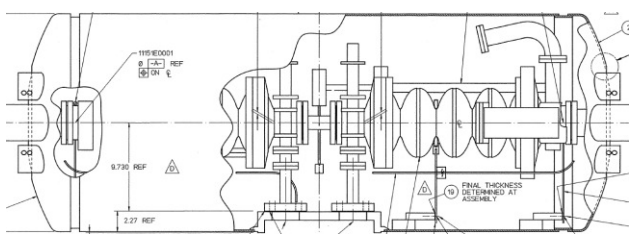


Figure 1: CEBAF Cryo-unit. Each cryomodule consists of four of such cryo-units.

* Authored by Jefferson Science Associates, LLC under U.S. DOE Contract No. DE-AC05-06OR23177.
†geng@jlab.org.
[1] former graduate student, presently at IMP, CAS.

Content from this work may be used under the terms of the CC BY 3.0 licence (© 2018). Any distribution of this work must maintain attribution to the author(s), title of the work, publisher, and DOI.

ISBN: 978-3-95450-194-6 ISSN: 2226-0366 doi:10.18429/JACoW-LINAC2018-MOPO132

THE 7 MeV APF DTL FOR PROTON THERAPY

Xiucui Xie, Yuehu Pu[1], Jian Qiao, Fan Yang[1], Xuan Li, Deming Li, Minghua Zhao, Zhentang Zhao
Shanghai Institute of Applied Physics, Chinese Academy of Sciences, Shanghai 201800, China
[1] also at Shanghai APACTRON Particle Equipment Co.Ltd, Shanghai, China

Abstract

A 7 MeV alternating phase focused (APF) drift tube linear (DTL) for proton therapy has been designed, and a design code has been developed based on a sinusoidal synchronous phase formula and a linearly increasing electrode voltage assumption. The design procedure includes the radio frequency quadrupole (RFQ) to drift tube linac (DTL) matching, and end-to-end simulation that conducted by Trace Win. Moreover, a cutting method has been performed to correct the integral electric field deviation of RF gaps.

INTRODUCTION

The Advance Proton Therapy Facility APTRON is a dedicated proton therapy facility located in Shanghai, China. The facility made up by a linac injector and a synchrotron of 24.6 m circumference, providing proton beam from 70 MeV to 250 MeV. Two fixed beam treatment rooms and one rotating gantry room is located downstream of the accelerator. A schematic layout of the facility is shown in Figure 1.

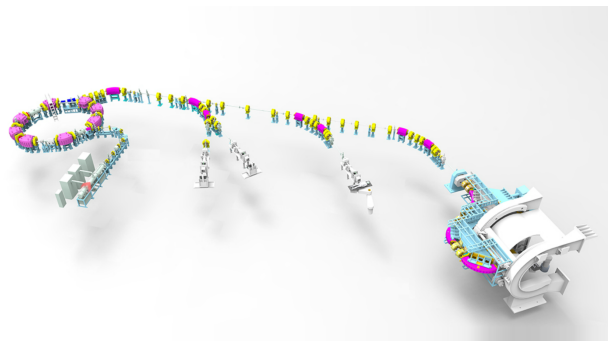


Figure 1: The bird's eye schematic view of the APTRON facility.

The alternating phase focused (APF) drift tube linac (DTL), together with a radio frequency quadrupole (RFQ), has been developed as the injector of the synchrotron ring. With its advantages of dimensions compactness and cost effectiveness, the APF DTL is an ideal choice for proton therapy facilities.

THE APF DESIGN CODE

The beam dynamics of the APF is solely depends on the electromagnetic field of the RF gaps, which determined by the synchronous phase sequence. In the past decades, several APF schemes has been proposed and developed. According to solid theoretical considerations as well as empirical rules, we choose the phase variation scheme that proposed by Yoshiyuki Iwata. In this scheme, the synchronous phase sequence is described by the following Equation (1) [1]:

$$\phi_s(n) = \phi_0 e^{-a \cdot n} sin\left(\frac{n - n_0}{b \cdot e^{c \cdot n}}\right), \quad (1)$$

where n is the number of the acceleration gaps; ϕ_0, a, b, c, and n_0 are free parameters.

Moreover, we add two hypotheses to our design strategy:

1. The potential of the electrodes are increasing monotonically and linearly.
2. The average electric field of the accelerating gaps is maintained.

Therefore, two extra parameter VE_0 and ΔVE, which stands for the voltage of the first electrode and the voltage growth of the successive electrode, together with the five Iwata formula parameters, could determine the structure of the APF.

Therefore, we developed the design code with the Iwata formula and the hypothesis to optimize the APF parameters automatically. The beam dynamics code is based on the BEAMPATH [2], and the parameters optimization algorithm is based on the nonlinear correlated stacking optimization method:

1. Estimate a set of initial parameters, generate the structure of the accelerator by the matrix transport method, feed the structure data into the BEAMPATH code, calculate the beam dynamics and evaluate the obtained results by a cost function.
2. Change two of the seven structural parameters described above to generate a new structure, feed the new structure data into the BEAMPATH and simulate the acceleration process. Compare the new results to the preceding results until all the possible parameter combinations have been considered and the best combination will be found.

THE APF DTL

The injection beam parameters for designing the APF DTL are obtained from the simulation results of a four-vane RFQ which serves as a pre-accelerator. Because the beam that extract from RFQ diverges horizontally but converges vertically while the horizontal and vertical focusing forces of the APF structure is totally identical, therefore a matching section is typically required to convert the injection beam from the RFQ into a symmetric one with symmetric properties in both the X and Y directions.

The injection and extraction energy of the APF is 3 MeV and 7 MeV, respectively. The cell number is 32 and the working frequency is 325 MHz; the on-axis acceleration field is 8.9 MV/m, corresponding to 0.5 times the Kilpatric limit.

Content from this work may be used under the terms of the CC BY 3.0 licence (© 2018). Any distribution of this work must maintain attribution to the author(s), title of the work, publisher, and DOI.

ISBN: 978-3-95450-194-6 ISSN: 2226-0366 doi:10.18429/JACoW-LINAC2018-TU1A01

CHALLENGES IN SUPERCONDUCTING ACCELERATING MODULE DESIGN AND CONSTRUCTION FOR HIGH POWER PROTON ACCELERATORS

C. Madec†, CEA, Saclay, France

Abstract

CEA is engaged in the construction of the Linear IFMIF-Prototype Accelerator (LIPAc), SARAF and ESS superconducting linacs and in particular in the design and production of their accelerating cryomodules: 1 for LIPAc composed of low-beta half-wave 175 MHz resonators, 4 half-wave 176 MHz resonators for SARAF and 32 medium and high-beta elliptical cavity resonators for ESS. The developments of these RF cryomodules, although at various stages, are led in parallel by the cryomodule team at CEA-Saclay, including all RF, mechanical, thermal, cryogenic, integration and QA-QC aspects in a global approach which attempts to optimise synergies and lessons learnt between these projects. A status report will be presented describing the common approaches and methods, and the systemic particularities of each project.

INTRODUCTION

CEA is designing, building, testing, installing and commissioning accelerator (or part of them) for others labs since 20 years : 352MHz cryomodule for SOLEIL, 88 MHz QWR cryomodules for SPIRAL2, 1.3 GHz cryomodules for XFEL, 175 MHz cryomodule for LIPAC [1] and SARAF [2], 704MHz cryomodules for ESS [3]. Among those cryomodules, SOLEIL and XFEL are operating; SPIRAL2 is under commissioning; LIPAC is under construction; ESS is under prototyping, SARAF is finishing its design. The development of last three cryomodules (CM) are led in parallel by the cryomodule CEA team. This talk will highlight the challenges faced and fruitfully used for the other next projects.

The LIPAC, SARAF and ESS will serve various applications (material study for fusion, nuclear science, production of radiopharmaceuticals, neutrons production for physics studies) and their overview is presented below.

PROJECTS OVERVIEW

The International Fusion Materials Irradiation Facility (LIPAC) aims at producing intense neutron fluxes so as to characterize materials envisioned for future fusion reactors. To this end, two identical Linacs, each accelerating a continuous-wave 125-mA deuteron beam at the final energy of 40 MeV, would be necessary to produce by break-up interactions of the D+ beam with the Li target the required 10^{17} neutrons per seconds with the appropriate energy. Because the accelerators have to reach unprecedented performances, the feasibility is being tested through the design, manufacturing, installation, commissioning and testing activities of a 1:1-scale prototype accelerator from the injector to the first cryomodule [4]. The cryomodule (Figure 1) is one of CEA Saclay's contribution, the others being the injector, the cryoplant and some beam diagnostics.

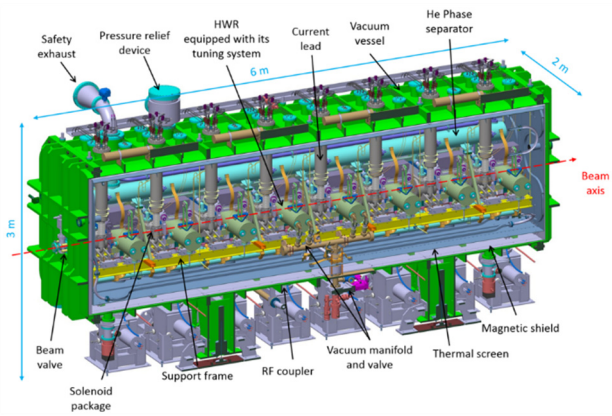


Figure 1 : LIPAC/IFMIF cryomodule.

The European Spallation Source (ESS) will bring new insights to the grand challenges of science and innovation in fields as diverse as material and life sciences, energy, environmental technology, cultural heritage, solid-state and fundamental physics. A 2GeV, long pulse proton accelerator is used to reach this goal. The pulsed length is 2.86 ms and the repetition frequency is 14 Hz (4 % duty cycle). The protons beam is accelerated in a superconducting linac [5] composed of one section of spoke cavity cryomodules and two sections of elliptical cavity cryomodules (Figure 2). These cryomodules, under CEA responsibility, contain elliptical cavities operating at 2 K.

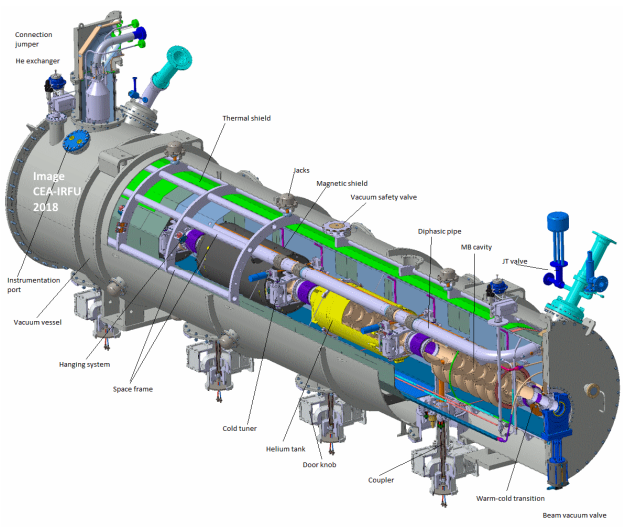


Figure 2 : ESS cryomodule.

Content from this work may be used under the terms of the CC BY 3.0 licence (© 2018). Any distribution of this work must maintain attribution to the author(s), title of the work, publisher, and DOI.

ISBN: 978-3-95450-194-6 ISSN: 2226-0366 doi:10.18429/JACoW-LINAC2018-TU1A03

STATUS AND ISSUES (MICROPHONICS, LFD, MPS) WITH TRIUMF ARIEL e-LINAC COMMISSIONING

S. R. Koscielniak†, T. Planche, S. Radel, Y. Ma, M. Alcorta, B. Humphries, F. Ames, E. Chapman, K. Fong, O. Kester, D. Kishi, R. Laxdal, M. Rowe, V. Verzilov, Z. Yao
TRIUMF, V6T 2A3, Vancouver, B.C., Canada

Abstract

The ARIEL electron linac (e-linac) is designed to generate cw beams of up to 30 MeV and 10 mA for delivery to a photo-convertor. Bremsstrahlung induced fission of a production target yields neutron-rich rare isotope beams to be supplied to the ISAC experimental facilities. The beam power will eventually reach 300 kW, and a machine protection system (MPS) with 10 μs rapidity is essential. The e-linac, which adopts 1.3 GHz, 2K SRF technology, is composed of a 10 MeV single-cavity injector cryomodule (EINJ) and a 20 MeV two-cavity accelerator cryomodule (EACA). The latter has vector-sum control of two cavities driven from a single klystron. Beam commissioning of these systems is ongoing since 2016. The magnetic optics and MPS commissioning to 10 MeV is reported herein. Beam has been accelerated up to 25 MeV, and threaded to the high energy dump (EHD). A campaign to investigate microphonics driving terms, LN2 disturbances, and a ponderomotive instability in the EACA, is underway.

INTRODUCTION

The ARIEL* facility for rare isotope nuclear science was proposed in 2008 [1]. The facility and science program are described in [2, 3]. ARIEL-I Funding emerged in 2010, plans solidified in 2011 [4], leading to a mature linac design 2012 [5], construction of the EINJ in collaboration with VECC, Kolkota [6], and installation of EACA, with a single 9-cell cavity, was completed 2014.

Figure 1 shows the main sections of the e-linac and their naming. TRANSOPTR is adopted as the online beamline modeling and optimization tool [7] in the control room, and is used throughout the e-linac from source to beam dump.

Commissioning of the 300 keV low energy beam transport (ELBT/D) up to 1 kW beam power is reported in Refs. [7, 8]. Rudimentary beam tests on EINJ at 10 MeV and on EACA at 23 MeV each equipped with a single RF cavity were reported in 2014 [9] and 2015 [8], respectively. Preparation of the EACA for two-cavity operation is reported in [10, 11, 12, 13].

Throughout 2016 and 2017, attempts to commission the injector and medium energy transport were compromised by RF phase and amplitude jitter. Therefore, the 2018 campaign includes two objectives: commission magnetic optics, and identify (and abate) RF jitter sources. Further, by mutual agreement with the regulatory authority, e-linac operations at ≥ 10 MeV are not permitted above 100 W beam power until the machine protection is commissioned.

ELECTRON GUN

Operation of the thermionic electron gun (EGUN) is reported in Ref. [14]. Performance of the gun itself has been excellent. After overhaul of the high-voltage power supply by Glassman in 2016, the HVPS has also proven reliable.

For >10 MeV commissioning it is critical that the EGUN supports a duty factor ranging from 0.01% to cw so that beamline components are subjected to low average power during beam threading if there is accidental beam loss.

Stable Duty Factor Parameters

The HVPS is nominally a DC supply, but we pulse it. Stable combinations of repetition rate and pulse length have been measured. At 100 μA peak, the combinations of 50 Hz to 10 kHz and 5-200 μs are stable. At 10 mA, the combinations 100 Hz to 2 kHz and 5-50 μs are verified stable duty factors [15].

Measured Beam Energy Stability

Results from ELBD with high-dispersion optics confirm the energy stability of the HVPS at 0.01%. Contrastingly, the sum signal from the first beam position monitor (BPM) after the gun show a 60 Hz phase jitter ~ 0.2° at 650 MHz.

OPTICS COMMISSIONING

Polarity Check

Prior to beam tests, the polarity of every magnetic element was checked using a Hall probe. This proved to be a worthwhile time saver as the polarity of several steerers and quadrupoles was found to be incorrect.

Optics Commissioning with Beam

Beam commissioning began at very low average power (< 10 W). All magnetic elements were tested individually:

- Steerers by their effect at downstream beam position monitors (BPM).
- Quadrupoles by searching for the setting which achieves minimum beam size on a fluorescent screen, and by comparing this setting with our optics model.

All magnetic elements performed precisely as expected.

RF Commissioning with Beam

The injector optics design is given in Ref. [16]. The gun emits 650 MHz bunches; these are energy modulated, head-to-tail, by a 1.3 GHz buncher cavity [6] to prepare them for the EINJ 9-cell cavity acceptance at 300 keV.

* ARIEL is funded by the Canada Foundation for Innovation, the Provinces AB, BC, MA, ON, QC, and TRIUMF. TRIUMF receives funding via a contribution agreement with the National Research Council of Canada.
† shane@triumf.ca.

Content from this work may be used under the terms of the CC BY 3.0 licence (© 2018). Any distribution of this work must maintain attribution to the author(s), title of the work, publisher, and DOI.

ISBN: 978-3-95450-194-6 ISSN: 2226-0366 doi:10.18429/JACoW-LINAC2018-TU1A05

SEAMLESS QUARTER WAVE RESONATORS FOR HIE ISOLDE

W. Venturini Delsolaro†, A. Miyazaki[1]
CERN, 1211 Geneva, Switzerland
[1]also at Manchester University, M13 9SPL, Manchester, United Kingdom

Abstract

The HIE-ISOLDE post accelerator consists of 4 cryomodules with 5 niobium-coated Quarter Wave Resonators (QWR) each. The standard manufacturing technique was to machine the inner and outer conductor separately, to shrink-fit the 2 pieces and to apply an electron beam welding at the interface. Due to micro cracks, observed on some of the cavities around the welds, we took the decision to explore the possibility of a seamless design. First cavities became available in late 2017 and were then cold-tested in the vertical cryostat. These seamless coated quarter wave resonators have shown some of the highest Q-values of all HIE-ISOLDE cavities in the acceptance tests. Furthermore, we studied the cavity performance with different compensations of the earth magnetic field and different temperature gradients upon cool down. These tests have demonstrated record-breaking RF surface fields for the Nb/Cu technology. This paper reviews the design and fabrication, and reports on the cold tests results of seamless quarter wave resonators. Possible future applications are briefly illustrated.

INTRODUCTION

The HIE-ISOLDE post accelerator is in operation at CERN since 2015, delivering a rich physics program to the community of users. The project was staged, and the high beta section of the machine was completed in spring 2018 with the addition of the fourth cryomodule. The backbone of the accelerator are the niobium sputter coated QWR,realized at CERN using copper cavity substrates done in industry. The early cavity development is documented in [1]. During the production phase, we faced performance degradations, which could be traced back to defects on the copper substrates, in proximity of the electron beam weld. In response to this issue, a seamless design was developed, as reported in [2]. In this paper we report more results, including the performance with beam. Cavities of the new design are labelled QSS, as opposed to the old QS type.

SEAMLESS QWR DESIGN

The main rationale for a seamless design was in our case to remove the possible source of defects in the copper substrates, represented by the electron beam weld, which was located close to the peak magnetic field. Small cracks on the copper substrate can trap fluids during the chemical polishing phases, which then contaminate the niobium layer. However, there are more advantages: the fabrication is simpler and cost effective with respect to the old design. Also, removing the weld allowed to greatly increasing the cross section for the heat path between the lower portion of the resonator and the heat sink in the inner conductor, with beneficial effects on the cooling, both during coating and in operation. This is because in the old design an annular gap remains above the weld, as the required mechanical tolerances for the mating pieces are more easily achieved over a short length. In Fig. 1 the seamless QWR is compared to the welded design.

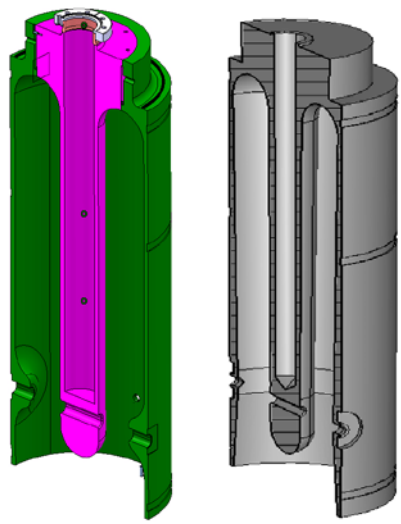


Figure 1: Welded and seamless HIE-ISOLDE QWRs.

In order to make possible the use of a lathe, and avoid milling, the cavity had to be axially symmetric. However, the removal of the cavity “noses” posed a difficulty as it severely decreased the R/Q and thinned the cavity wall, with consequent potential risk of RF leakage. We adopted a double conical shape mainly to recover R/Q.

RF leakage was suppressed by changing the beam port aperture from a racetrack to a circle with a diameter reduction of 2 mm, and by extending the cut-off length in a matching piece, which is made to support the cavity in the cryomodule, as shown in Fig. 2.

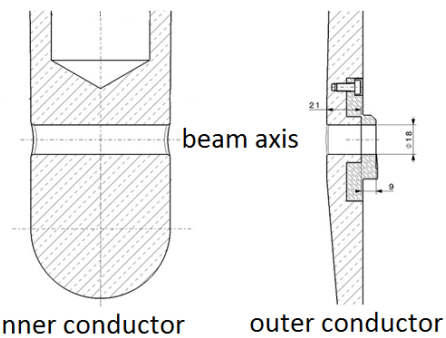


Figure 2: Beam port of the seamless HIE-ISOLDE QWR.

† walter.venturini@cern.ch

Content from this work may be used under the terms of the CC BY 3.0 licence (© 2018). Any distribution of this work must maintain attribution to the author(s), title of the work, publisher, and DOI.

ISBN: 978-3-95450-194-6 ISSN: 2226-0366 doi:10.18429/JACoW-LINAC2018-TU2A01

FIRST ACCELERATION OF HEAVY ION BEAMS WITH A SUPERCONDUCTING CONTINOUS WAVE HIM/GSI CW-LINAC

W. Barth†,1,2, K. Aulenbacher1,3, M. Basten4, M. Busch4, F. Dziuba1, V. Gettmann1, M. Heilmann2, T. Kürzeder1, M. Miski-Oglu1, H. Podlech4, A. Rubin2, A. Schnase2, M. Schwarz4, S. Yaramyshev2
[1] Helmholtz Institute Mainz, Germany
[2] GSI Helmholtzzentrum für Schwerionenforschung, Darmstadt, Germany
[3] Johannes Gutenberg-Universität Mainz, Mainz, Germany
[4] IAP Goethe-Universität Frankfurt, Frankfurt, Germany

Abstract

First acceleration of heavy ion beams with a superconducting continuous wave HIM/GSI cw-Linac. After successful RF-testing of a new superconducting Linac RF-cavity at GSI Helmholtzzentrum für Schwerionenforschung and a short commissioning and ramp up time of some days, this 15-gaps Crossbar H-cavity accelerated first time heavy ion beams with full transmission up to the design beam energy. The design acceleration gain of 3.5 MV inside a length of less than 70 cm has been verified with heavy ion beam of up to 1.5 pμA. The measured beam parameters show a nice beam quality. The machine commissioning with beam is a milestone of the R&D work of Helmholtz Institute Mainz (HIM) and GSI in collaboration with IAP Goethe-University Frankfurt in development of the superconducting heavy ion continuous wave linear accelerator cw-Linac.

INTRODUCTION

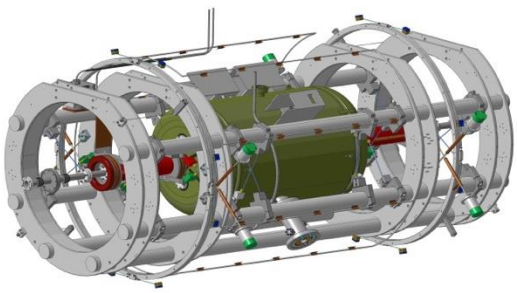


Figure 1: Demonstrator CH-cavity (CH0) with two sc-solenoids inside the support frame.

The design and construction of cw high intensity Linacs is a crucial goal of worldwide accelerator technology development [1]. Above all, compactness of a particle accelerator is a beneficial demand for the development of high intensity cw proton and ion Linacs [2]. In the low- and medium-energy range cw-Linacs can be used for several applications, as boron-neutron capture therapy, high productivity isotope generation and material science. A high-energy Linac is an integrated and essential part of several large scale research facilities, as spallation neutron sources or accelerator driven systems. Thus the study and investigation of the design, operation and optimization of a cw-Linac, as well as progress in elaboration of the superconducting technology [3] is of high relevance.

For the HIM/GSI cw-Linac HELIAC (HElmholtz LInear ACcelerator) several superconducting CH cavities operated at 217 MHz should provide for ion acceleration to beam energies between 3.5 MeV/u and 7.3 MeV/u, while the energy spread should be kept smaller than ±3 keV/u. The cw-Linac allows the acceleration of highly charged ions with a mass to charge ratio of up to 6. For proper beam focusing superconducting solenoids have to be mounted between the CH cavities. The general parameters are listed in Table 1 [4]. R&D and prototyping (demonstrator project) [5] in preparation of the proposed HELIAC is assigned to a collaboration of GSI, HIM and GUF. The demonstrator setup is located in straightforward direction of the GSI–High Charge State Injector (HLI).

Table 1: Design Parameters of the cw-Linac

Mass/charge		6
Frequency	MHz	216.816
Max. beam current	mA	1
Injection energy	MeV/u	1.4
Output energy	MeV/u	3.5 – 7.3
Output energy spread	keV/u	±3
Length of acceleration	m	12.7
Sc CH-cavities	#	9
Sc solenoids	#	7

The demonstrator comprises a 15 gap sc CH-cavity (CH0) embedded by two superconducting solenoids; all three components are mounted on a common support frame (see Fig. 1) [6]. The beam focusing solenoids provide maximum fields of 9.3 T, the free beam aperture is 30 mm. A configuration of one main Nb_3Sn-coil and two compensation coils made from NbTi shields the maximum magnetic field of 9.3 T within a longitudinal distance of 10 cm down to 30 mT. The solenoids are connected to LHe ports inside the cryostat by copper tapes allowing dry cooling. The sc CH structure CH0 is the key component and offers a variety of research and development [7].

*Work supported by the BMBF, project number 05P15RFBA, MYRTE which is funded by the European Commission under Project-ID 662186 and Helmholtz International Center for FAIR.
†w.barth@gsi.de

Content from this work may be used under the terms of the CC BY 3.0 licence (© 2018). Any distribution of this work must maintain attribution to the author(s), title of the work, publisher, and DOI.

ISBN: 978-3-95450-194-6 ISSN: 2226-0366 doi:10.18429/JACoW-LINAC2018-TU2A03

THE NEW FAIR POST-STRIPPER DTL - ALVAREZ 2.0

Sascha Mickat, Norbert Bönsch, Xiaonan Du, Peter Gerhard, Jens Holluba, Lars Groening, Manuel Heilmann, Stefan Jagsch, Michael Kaiser, Eberhard Merz, Carsten Mühle, Markus Romig, Marcel Rosan, Anna Rubin, Vaishnavi Srinivasan, Wilfried Sturm, Stephan Teich

GSI Helmholtzzentrum für Schwerionenforschung GmbH, Planckstraße 1, 64291 Darmstadt, GER

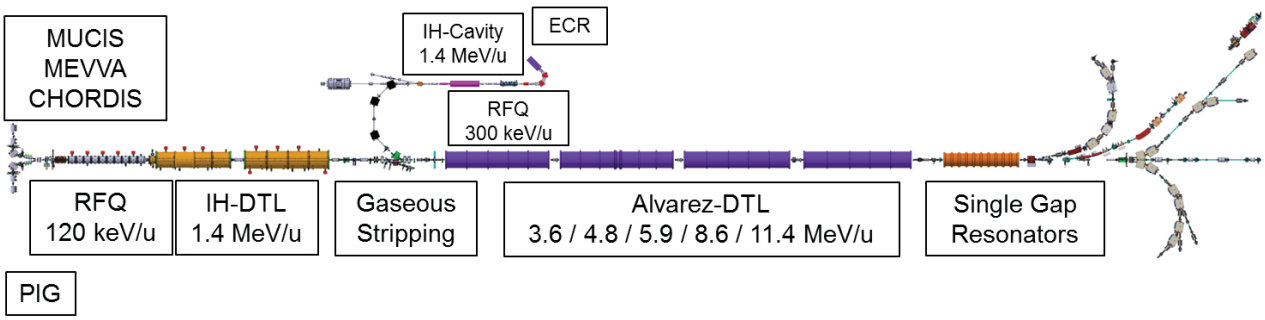
Abstract

The existing GSI accelerator facility, comprising both the UNILAC and the SIS18, is assigned to be the dedicated injector chain for FAIR. Two aspects require the substitution of the existing post-stripper section of the UNILAC, which is an Alvarez type drift tube linac (DTL).

- With respect to its beam dynamic design the existing Alvarez DTL does not cover high current applications for heavy ions as required for FAIR. This will limit the performance of FAIR from the middle 2020's on.
- The existing Alvarez DTL is in regular operation since 1978. An increase in failures due to material fatigue is observable and can be avoided in parts just by an out of scale maintenance effort. A new Alvarez DTL will minimize the operational risk for FAIR commissioning from the middle 2020's.

THE UNILAC POST-STRIPPER DTL

Since the commissioning of the original UNILAC in 1978 the facility was adapted to the demands of its users and to its present expansion (Fig. 1). A complex technical system has grown comprising technologies of different decades. Within this context next to the performance upgrades for reaching the FAIR design parameters, the upgrades aiming at operation reliability have to be considered also. Sections like the existing Alvarez (DTL), the section behind the gaseous stripper (post-stripper), are over 40 years in operation, which is far beyond of its expected lifetime of about 20 years.



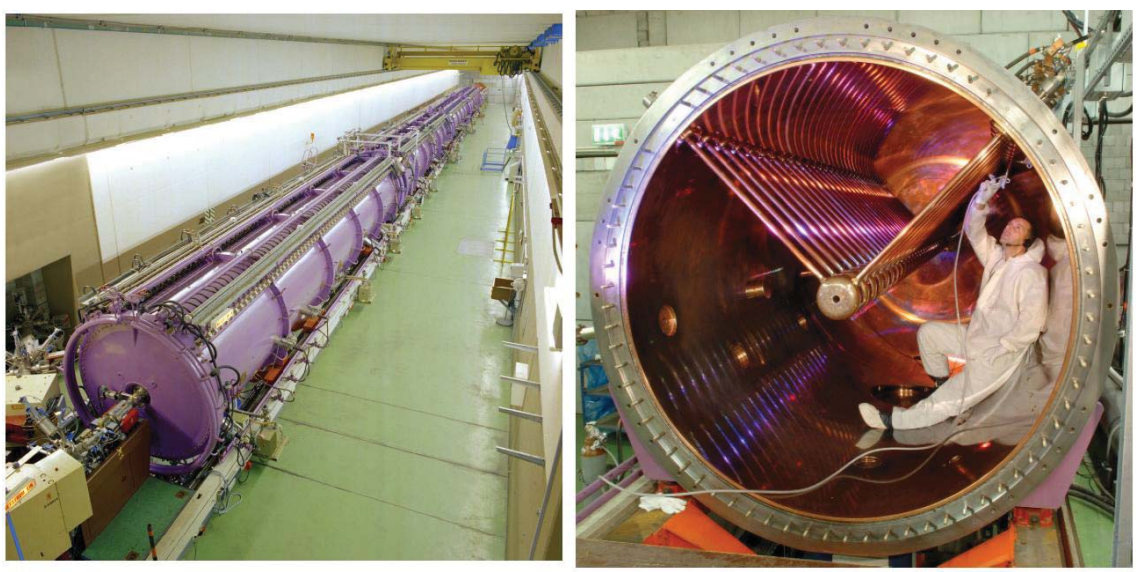


Figure 1: Top: Overview of the existing UNILAC. Left: View into the UNILAC tunnel along the 55 metres long post-stripper. Right: View into the Alvarez DTL cavity during maintenance.

Content from this work may be used under the terms of the CC BY 3.0 licence (© 2018). Any distribution of this work must maintain attribution to the author(s), title of the work, publisher, and DOI.

ISBN: 978-3-95450-194-6 ISSN: 2226-0366 doi:10.18429/JACoW-LINAC2018-TU2A04

PROGRESS REPORT ON LIPAC*

M. Sugimoto†, T. Akagi, T. Ebisawa, Y. Hirata, R. Ichimiya, A. Kasugai, K. Kondo, S. Maebara, K. Sakamoto, T. Shinya, QST, 039-3212 Rokkasho, Japan
P. Abbon, N. Bazin, B. Bolzon, N. Chauvin, S. Chel, R. Gobin, J. Marroncle, B. Renard, CEA/IRFU, 91191 Gif-sur-Yvette, France
D. Jimenez-Rey, D. Gavela, I. Kirpitchev, P. Méndez, J. Molla, C. de la Morena, I. Podadera, D. Regidor, R. Varela, M. Weber, CIEMAT, 28040 Madrid, Spain
G. Pruneri, Consorzio RFX, 35127 Padova, Italy
J. Knaster, Fusion for Energy, 13067 Saint Paul lez Durance Cedex, France
P.-Y. Beauvais, H. Dzitko, D. Gex, R. Heidinger, A. Jokinen, A. Marqueta, I. Moya, G. Phillips, Fusion for Energy, Garching, D-85748 Germany
P. Cara, IFMIF/EVEDA, 039-3212 Rokkasho, Japan
L. Antoniazzi, L. Bellan, D. Bortolato, M. Comunian, E. Fagotti, F. Grespan, M. Montis, A. Palmieri, A. Pisent, F. Scantamburlo, INFN/LNL, 35020 Legnaro (PD), Italy

Abstract

LIPAc (Linear IFMIF Prototype Accelerator) for challenging the technical validation of the low energy section up to 9 MeV of the IFMIF accelerator, consisting of 2 units of 40 MeV, 125 mA CW deuteron accelerator, is under construction and staged commissioning is ongoing in QST Rokkasho, Japan. The injector commissioning was completed in summer 2017 and the latest results of the beam characteristics showed good emittance acceptable for RFQ injection. The installation and checkout of 5 MeV deuteron RFQ, beam transport & instrumentation, temporary beam dump and RF power system were finished in early 2018 including the RF conditioning of RFQ in low duty pulsed mode. At the initial beam commissioning of RFQ in June 2018, the 50 keV proton beam with <30 mA and 0.3 ms pulse was used for simulating the 100 keV deuteron beam acceleration in RFQ and transport up to beam dump, without a risk of activation. The good transmission around 93% was observed for input beam current of 8–30 mA. The installation work for the final configuration of LIPAc with a superconducting RF linac is continuing and ready to start by end of 2018.

INTRODUCTION

The Engineering Validation and Engineering Design Activities for the International Fusion Materials Irradiation Facility (IFMIF/EVEDA) project is underway as one of three projects of the Broader Approach (BA) agreement between the Japanese government and EURATOM [1]. The concept of the IFMIF was matured through the activities under the IEA's Fusion Materials Technology Collaboration Program over 10 years since 1994 [2]. The mission of IFMIF is to provide an accelerator-based, D-Li neutron source to produce high energy neutrons at sufficient intensity and irradiation volume to test samples of candidate materials up to about a full lifetime of anticipated use in fusion energy reactors. IFMIF would also provide calibration and validation of data from fission reactor and other accelerator-based irradiation tests. It would generate an engineering base of material-specific activation and radiological property data, and support the analysis of materials for use in safety, maintenance, recycling, decommissioning, and waste disposal systems.

The mission of the IFMIF/EVEDA project is to provide the detailed engineering design of the IFMIF and to validate the technological challenges on the major components. One of the major technological challenges is the demonstration of the low energy section of one of two accelerators of the IFMIF called as LIPAc (Linear IFMIF Prototype Accelerator) to accelerate the 125 mA CW D+ beam up to 9 MeV, while the IFMIF accelerator is a 40 MeV linac (see Fig. 1 for full IFMIF linac design in 2013 [3]).

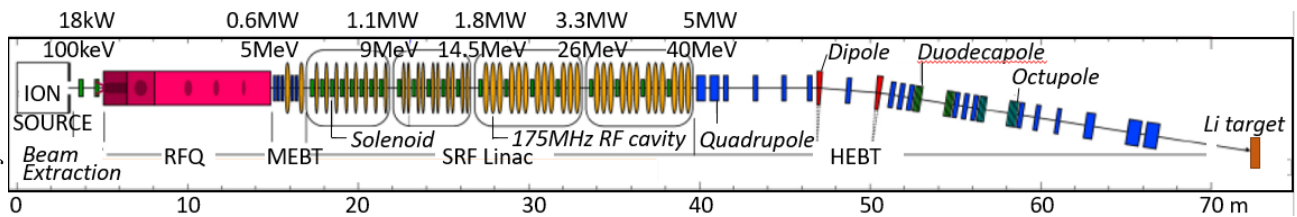


Figure 1: Schematic representation of IFMIF linac. LIPAc is a prototype up to 9 MeV including the first SRF linac.

As show in in Fig. 2, the LIPAc plant consists of the following subsystems:

* Work undertaken under the Broader Approach Agreement between the European Atomic Energy Community and the Government of Japan. The views and opinions expressed herein do not necessarily state or reflect those of the Parties to this Agreement.
† email address sugimoto.masayoshi@qst.go.p

Content from this work may be used under the terms of the CC BY 3.0 licence (© 2018). Any distribution of this work must maintain attribution to the author(s), title of the work, publisher, and DOI.

ISBN: 978-3-95450-194-6 ISSN: 2226-0366 doi:10.18429/JACoW-LINAC2018-TU1P01

EXTREME HIGH BRIGHTNESS ELECTRON BEAM GENERATION IN A SPACE CHARGE REGIME

A. Bacci, L. Faillace, M. Rossetti Conti* INFN-Mi, 20133 Milano, Italy
*also at Università degli Studi di Milano, 20133 Milano, Italy

Abstract

The generation of ultra-short, low emittance and low energy spread electron bunches is nowadays a critical requirement for accelerators in plasma wave or for femtosecond light sources. A new longitudinal compression scheme, based on velocity and ballistic bunching techniques in presence of space charge forces, allows to enter in a peculiar regime, so-called laminar bunching (LB). In this regime, the bunch is longitudinally compressed, at the expense of its transverse size, and the over-bunching is forbidden by the laminarity: going to the minimal longitudinal dimension the bunch is adiabatically frozen and transversally refocused. Furthermore, this technique heats slightly the uncorrelated energy spread resulting in electron distributions that, in case of bending paths, does not require Laser Heater devices.

INTRODUCTION

In the last decade the production of ultra-short electron bunches has become a major item in many fields that are related to accelerating machines. One of the main application interested in such kind of beams is the Free Electron Lasers (FELs) with the aim to produce ultra-short light pulses, femtosecond orders, to explore ultra-fast phenomena like chemical reactions or phase transitions. A typical example is the study of the water splitting in the photosynthesis that ranges from 1 up to 100 fs [1]. Other technologies pursuing ultra-short electron bunches are the plasma wave acceleration [2-5], the femtosecond electron diffraction FED [6] and the coherent THz transition radiation [7].

There are many techniques to longitudinally compress electron bunches. Basically all these techniques are based on a linearly correlated energy spread (linear chirp) given along the distribution and accordingly on the velocity differences of the particles which return in to the compression effect. The compression is performed along a drift in terms of time of flight (ballistic bunching [8, 9]) or along a dispersive line, in terms of different paths length (magnetic chicanes) [10]. An alternative compression technique, named Velocity Bunching (VB) [11], occurs inside a traveling wave (TW) accelerating cavity, where the beam is accelerated and chirped at the same time. The VB technique operates at low energies, typically electron guns exit energies which are lower than 7 MeV. In order to prevent the emittance degradation, the laminarity of the beam, which permits to damp the emittance oscillations during the compression, has to be preserved. This laminarity beam condition is kept propagating the beam as close as possible to an equilibrium invariant envelope, representing an exact solution of the envelope equation, that is obtained by the following conditions: inject in to the compressor with a laminar envelope waist ($\sigma' = 0$), a compression factor that scale linearly with the acceleration $I = \frac{\gamma}{\gamma_0} I_0$ where I stands for the current, γ for the relativistic factor and the index 0 for values before the compression.

The VB is a technique used, or tested, worldwide in different labs and nowadays it is a reference technique to compress electron beams at low energy. Typical VB performances, easily reached, are peak beam currents approaching, or overcoming, 1 kA and emittance values lower than 1 mm-mrad for bunch charge of few hundreds of pico-coulombs and final energies of 80-100 MeV [12]. These high brightness bunches generated by VB show the common characteristics to have a spike current on the bunch head, where most of the charge is stacked and a long low charge tail. The beam quality of the tail is usually poor, shown a very high energy spread, which is a peculiarity of the VB itself where the compression is obtained at the expense of the energy spread, then damped by the acceleration.

In this work is presented a new compression technique that permits to compress an electron bunch in an almost uniform way, if compared to the VB and, at the same time, to quasi fully compensate the bunch energy spread. This method takes advantage from a space-charge dominated regime and because most of the compression happens along a drift, where the bunch is laminar, under the effect of its only field, it has been named laminar bunching LB. In the following paragraph is presented an ideal machine layout to perform the LB and discussed it beam dynamics, considering the longitudinal and the transversal envelop equations. At the end of the proceeding is presented a comparison between the VB and the LB from simulations point of view and from the different evolutions of the envelope equation self-fields terms.

LAMINAR BUNCHING

The LB machine layout presented in this work is as follows (Fig. 1): 1.6 cells s-band photoinjector coupled to a solenoid for the emittance compensation; a drift of about 1.3 meters; a x-band TW 9 cells accelerating cavity, which is used in decelerating mode; a s-band 3 m long, SLAC type, accelerating cavity embedded into a solenoids array; a quite long drift, about 3 m long, where the electron bunch enters into the LB; a couple of equal TW c-band accelerating cavities, 114 cells, 2 meters long, that boost the beam.

For sake of a better LB beam dynamics understanding let us start analyzing transverse and longitudinal envelope equation, respectively Equations (1) and (2):

Content from this work may be used under the terms of the CC BY 3.0 licence (© 2018). Any distribution of this work must maintain attribution to the author(s), title of the work, publisher, and DOI.

ISBN: 978-3-95450-194-6 ISSN: 2226-0366 doi:10.18429/JACoW-LINAC2018-TUPO001

ABOUT THE LIMITS FOR THE ACCELERATED BEAM CURRENT IN THE LUE-200 LINAC OF THE IREN FACILITY

A.P. Sumbaev †, JINR, 141980, Dubna, Russia
A. Barnyakov, A. Levichev, Budker INP, 630090, Novosibirsk, Russia

Abstract

The beam current loading of the accelerating fields is discussed for the linear accelerator LUE-200 of the IREN facility (a neutron source at Frank Laboratory of Neutron Physics JINR). The LUE-200 electron linac consists of two disk loaded travelling wave accelerating structure with the operating frequency of 2856 MHz and power compression SLED-type system. The limits by the accelerated beam current are defined for different pulse durations of the beam current and RF power. The calculated results are discussed and compared with the measurements.

INTRODUCTION

The IREN facility [1, 2] of the Joint Institute for Nuclear Research (JINR) is the ADS neutron source (**a**ccelerator **d**riving **s**ystem). It is known that for electron beams with energy more than 20-25 MeV the integral photoneutron yield from a target is directly proportional to energy of electrons. The beam energy is limited by the beam current loading effect. Therefore, analysis of the properties of the accelerating structure and search of the optimum parameters of the acceleration is very actual problem for LUE-200 linac.

In the current work calculations for a beam accelerated in one accelerating section, powered by klystrons of three types have been carried out: 5045 SLAC (the maximum pulse power 63 MW), E3730A Toshiba (the maximum pulse power 50 MW) and TH2129 Thomson (the maximum pulse power 20 MW) taking into account the use of SLED - system.

BEAM LOADING EFFECT FOR THE CZ ACCELERATING STRUCTURE

In a stationary regime the accelerating field of the wave travelling along the z axis of the constant impedance (CZ) structure can be described by the superposition of two equations [3]:

$$E_z(z) = E_0 e^{-\alpha z} - I_0 R_{sh}(1 - e^{-\alpha z}) \quad (1)$$

The first term of the right side of equation is caused by an external generator field: $E_0 = \sqrt{2\alpha R_{sh} P_0}$, where P_0 - power of the generator, R_{sh} - shunt impedance of structure, α - loss factor in the structure. The second term defines the field induced by an electron beam with an average current of I_0. It is supposed that the beam consists of dot bunches with length of much less than that of a wave which follow with frequency of own working mode of structure $f_0 = \omega_0/2\,\pi$.

By means of (1) it is possible to receive additional beam potential which the beam will obtain at the acceleration:

$$U(z) = \int_0^z E_z(z)dz = (E_0 + I_0 R_{sh})\frac{1-e^{-\alpha z}}{\alpha} - I_0 R_{sh} z. \quad (2)$$

From (2) it is visible that there is a beam current I_{cr} at which the average growth of energy in CZ structure of L length will be equal to zero:

$$I_{cr} = \sqrt{\frac{2\alpha P_0}{R_{sh}}}\frac{1-e^{-\alpha L}}{\alpha L-(1-e^{-\alpha L})}. \quad (3)$$

In a nonstationary regime, changing of the beam potential will be defined by changing of the generator power $P_0(t)$ and of the beam induced field by the following equation [4]:

$$\Delta U_b(\tau) = -R_{sh} L I_0 \left\{\left(1 - \frac{\tau_{0A}}{T_f}\right)\left[1 - e^{-\tau/\tau_{a0}}\right] + \frac{\tau}{T_f} e^{-\tau/\tau_{a0}}\right\}. \quad (4)$$

Here τ - time from the injection start in accelerating structure of the first bunch ($0 \le \tau \le \tau_b$, where τ_b – beam current duration), $\tau_{a0} = 2Q_{a0}/\omega_0$ –time constant of the accelerating structure, Q_{a0} – quality factor of structure, $T_f = L/V_{gr}$ – filling time of structure, V_{gr} – wave group velocity of an accelerating field. The beam full potential will compose of the potential obtained from the external generator field without a beam and from the field, induced by a beam (4). For a case when the beam flies in the accelerating structure already completely filled with the RF power at $\tau \ge T_f$, it is possible to write down:

$$U(\tau) = U_m + \Delta U_b(\tau), \quad (5)$$

where $U_m = E_0(1\text{-}e^{-\alpha z})/\alpha$. Thus, the beam particles energy spread-out is defined by a beam current and its duration.

In case of using of SLED system [4] RF power gained from the generator is nonstationary in time. Let normalized pulse amplitude of an input signal is defined by the dependence shown in Fig. 1. The condition normalizing is expression for power $P(t) = P_o E^2(t)$, where P_0 - power of the generator.

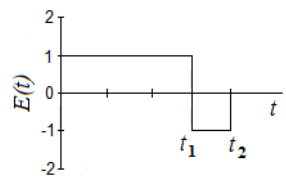


Figure 1: The RF power signal coming at the input of SLED system.

The phase inversion is carried out at the moment of time t_1 and lasts till time t_2. In this case, the wave amplitude

† sumbaev@nf.jinr.ru

Content from this work may be used under the terms of the CC BY 3.0 licence (© 2018). Any distribution of this work must maintain attribution to the author(s), title of the work, publisher, and DOI.

ISBN: 978-3-95450-194-6 ISSN: 2226-0366 doi:10.18429/JACoW-LINAC2018-TUPO002

ELECTRON GUN FOR 100 MeV / 100 kW LINEAR ACCELERATOR OF ELECTRONS AS THE DRIVER OF NUCLEAR SUBCRITICAL ASSEMBLY NEUTRONS SOURSE

M. Moisieienko, O. Bezditko, I. Karnaukhov, A. Mytsykov, A. Zelinsky

NSC KIPT, Kharkov, Ukraine

Abstract

100 MeV / 100 kW linear electron accelerator of The NSC KIPT "Neutron Source" nuclear subcritical assembly uses the 120 kV triode electron gun as the primary source of electrons. The gun was designed, manufactured and tested at IHEP, Beijing, China. At present, the gun was installed and are under testing. The maximum pulse current of the gun is equal to 2 A. In design operation, the pulse current of the gun should be equal to 0.55 A. The report describes the design of the 120 kV triode electron gun, the results of testing and test operation.

INTRODUCTION

100 MeV/100 kW electron linear accelerator that is a driver of the ADS NSC KIPT Neutron Source was design and manufactured in IHEP, Beijing, China and assembled in NSC KIPT, Kharkov, Ukraine during 2010-2014 [1] .

In 2015 and 2016 the accelerator technological systems commissioning and beam commissioning were started in Spring 2017 the design value of pulse electron beam current was obtained in the end of the accelerator horizontal part. During the last year the main task of the accelerator commissioning was to optimize the technological system parameters and improve the accelerator performance in accordance with basic design parameters listed in Tab. 1 [2].

Table 1: Main KIPT Linac Parameters

Parameter	Value
RF frequency	2856 MHz
Beam energy	100 MeV
Pulse beam current	0-0.6 A
Average beam power	0.005 – 100 kW
Energy spread (1)	2 %
Emittance (1)	$5x10^{-7}$ m-rad
Beam pulse length	2.7 μs
RF pulse duration	3 μs
Pulse repetition rate	2 - 625 Hz
Gun voltage	~120 kV

The electron gun is a triode-type gun, which consists of an anode, cathode, and grid. The electron gun system consists of an electron gun body, a high voltage power supply, a high voltage deck, a pulser and a control unit. The gun should be able to operate in long beam pulse mode to generate the electron beam. The electron gun includes the following systems:

- electron gun cathode manufactured by EIMAC Y824;
- high-voltage power supply unit of the electron gun manufactured by GLASSMAN LT150N10;
- high-voltage station of GloryMV Electronics Limited, China;
- control system of the electron gun;
- Switching power supply of the electrode gun control grid developed at IHEP Institute of High Energy Physics, Beijing, China;
- electron gun protection and interlock system;
- vacuum system of the electron gun.

The main parameters of the electron gun are shown in Tab. 2.

Table 2: Main Electron Gun Parameters

Items	Value
Type	Triode
Beam Current （max） A	2
Anode Voltage kV	~120
Filament Voltage V	6.4
Filament Current A	5.5
Grid Bias V	50~ 500
Bunch length μs	3.0
Repetition Rate (max) Hz	625

GUN BODY

A planar triode electron gun, the EIMAC Y824 shown in Fig 1 with 150 kV (maximum) GLASSMAN high-voltage deck, is used with a fast pulser cathode driver. The acceleration voltage is 120 kV, the maximum extraction current is 2 A (normal operation is about 0.6 A) with minimum pulse width of less than 3.0 μs. The gun pulser system contains a driving circuit. A 3.0 μs FWHM pulser is used to drive the cathode for long pulse operation. The gun structure and the gun beam pulse form are shown in Fig. 2, 3.

Content from this work may be used under the terms of the CC BY 3.0 licence (© 2018). Any distribution of this work must maintain attribution to the author(s), title of the work, publisher, and DOI.

ISBN: 978-3-95450-194-6 ISSN: 2226-0366 doi:10.18429/JACoW-LINAC2018-TUPO003

DEVELOPMENT OF CW HEAVY ION LINAC AT IMP*

X. J. Yin†, Y. J. Yuan, J.W. Xia, Y. He, H.W. Zhao, H. Du, Z. S. Li, X. N. Li, K. D. Wang, Q. Y. Kong, Y. Q. Yang, P. Jin, C. Qian, L.Z. Ma, J. X. Wu, Z. Xu, L.T. Sun, W. Zhang, X. Z. Zhang, J. Meng, W. J. Xie, Z. Z. Zhou, Q.G. Yao, S. M. Wang, X. W. Xu, H. N. Wang, Y. Zhang,
Institute of Modern Physics, Chinese Academy of Sciences, Lanzhou, China
Y. R. Lu, K. Zhu, G. Liu, X. Q. Yan, S. L. Gao, Z. Wang, and J. E. Chen,
State Key Laboratory of Nuclear Physics and Technology, Peking University, Beijing, China

Abstract

A new heavy ion linac as the injector for the Separated Sector Cyclotron (SSC), named SSC-Linac [1], is being under constructed at the national laboratory Heavy Ion Research Facility in Lanzhou (HIRFL). The SSC-Linac mainly consists of a 4-rod RFQ and three IH-DTL cavities which can accelerate ion of $A/q \leq 7$ from 3.73 keV/u to 1.025 MeV/u. Both of them operating at 53.667MHz had been developed. In the commissioning, ions were successfully accelerated to 0.295 MeV/u by IH-DTL1. The beam commissioning of the IH-DTL2 which can accelerate the ion to 0.586 MeV/u will come soon. In this paper, the recent R&D progress of the SSC-Linac including the development of key components and the beam commissioning results are presented.

INTRODUCTION

As the main part of the upgrade project of Heavy Ion Research Facility in Lanzhou (HIRFL), a new heavy-ion linac which operated at Continuous Wave (CW) mode was designed and constructed as the injector for the separated-sector cyclotron (SSC).The design parameters of SSC-Linac were listed in Table 1.There are two stages for the energy upgrade project. In the first stage, the ion particles will be accelerated to 0.586 MeV/u using two IH-DTL cavities. And then they will be further injected and accelerated to 6 MeV/u by the SSC facility. In the second stage, the particle will be accelerated to 1.025 MeV/u by adding the DTL3.

Table 1: Design Parameters of SSC-Linac

Parameters	Values
Design ion	$^{238}U^{34+}$
ECR ion source	
Extraction voltage	25 kV
Max. axial injection field	2.3 T
Frequency	18 GHz
RFQ Type	4-rod
Input /Output energy	3.73/143 keV /u
Inter-electrode voltage	70 kV
Max.current	200.0 eμA
IH-DTLs	
Input /Output energy	0.143/1.025 MeV/u

*Work supported by National Natural Science Foundation of China (10635090, 11375243)
†yinxj@impcas.ac.cn

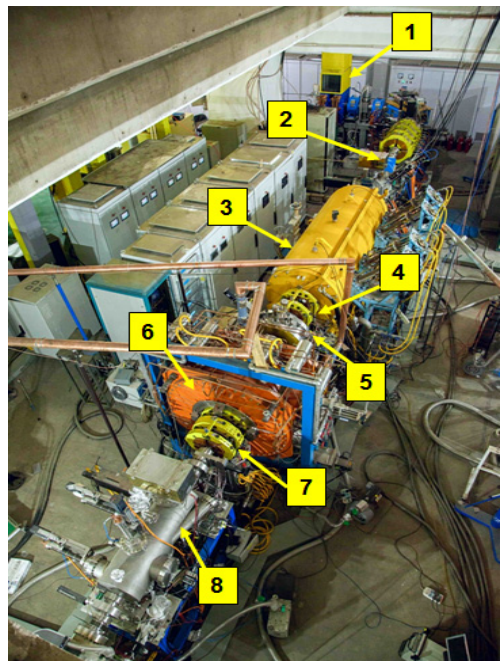


Figure 1: General view of the SSC-Linac. 1-ECR ion source; 2-LEBT section; 3-RFQ; 4-MEBT section; 5- Rebuncher cavity; 6- IH-DTL1; 7-Foucsing triplets; 8-Beam diagnostics system.

Finally, the particles will be accelerated to 10.7 MeV/u also by the SSC facility. Figure 1 shows the layout of the front end section of the SSC-Linac.

ION SOURCE&LEBT

The high charge state room temperature ECR ion source had been successfully constructed. This source magnet coils were cooled through evaporative cooling technology. The maximum mirror field was 2.3 T (with iron plug) and the effective plasma chamber volume was Ø76 mm×260 mm. The commissioning test of ECR ion source had been performed continually from 2014. Various specie ion beams had been successfully delivered for the linac commissioning.

With 0.1 kW RF injection power and 11.92 kV extraction voltage, 200 eμA of $^{16}O^{5+}$ was produced. The transverse emittances were measured by the emittance scanners located at the downstream of the analysing magnet. As shown in the Fig. 2, the measured normalized rms emittances at 200 eμA beam current for $^{16}O^{5+}$ were 0.22π mm.mrad and 0.15π mm.mrad in horizontal and vertical plane, respectively.

Content from this work may be used under the terms of the CC BY 3.0 licence (© 2018). Any distribution of this work must maintain attribution to the author(s), title of the work, publisher, and DOI.

ISBN: 978-3-95450-194-6 ISSN: 2226-0366 doi:10.18429/JACoW-LINAC2018-TUPO004

RF DESIGN AND COLD MODEL MEASUREMENT OF AN IH-DTL FOR HIMM INJECTOR*

H. Du†,1, X. J. Yin[1], Z. S. Li[1], K. D. Wang, Q. Y. Kong,Institute of Modern Physics, Chinese Academy of Sciences, 730000 Lanzhou, China
[1]also at Huizhou Research Center of Ion Sciences, 516003 Huizhou, Guangdong, China

Abstract

An interdigital H-mode drift tube linac (IH-DTL) will be constructed as a postinjector linac for the Heavy Ion Medical Machine (HIMM). Its resonant frequency, injection and final energies are determined from beam dynamics and hardware parameters considerations of the entire machine to be 162.5MHz, 600keV/u and 4MeV/u, respectively. The beam duty cycle of the injector linac is less than 0.1% based on the injection requirements of the synchrotron. Beam dynamics and RF structure design and optimize of the IH-DTL has been finished. The maximum surface electric field is less than 2.0-times the Kilpatric limit for accelerating C^{4+} beam. This IH-DTL contains 41 accelerating gaps and two focusing quadrupole triplets. In order to examine the field distribution of the IH-DTL which reaches the length of 3.17m, an aluminium alloy 1:1 cold model cavity with 4 moveable tuners and 2 empty focusing magnet shell was constructed. The relative intertube-distance errors are less than ±0.05mm. The measurements show that the gap voltage values can match the CST-MWS simulating results within relative difference of ±3% by adjusting the 4 moveable tuners.

INTRODUCTION

To improve the performance and reduce the cost of the Heavy Ion Medical Machine (HIMM), Institute of Modern Physics designed a compact C^{4+} linac injector to replace the C^{5+} cyclotron injector [1,2]. This linac injector mainly contains an ECR ion source, a RFQ, an IH-DTL, two buncher cavity and several beam lines. KONUS beam dynamics design of the IH-DTL has been reported in the previous paper [3]. This IH-DTL cavity with a resonant frequency of 162.5MHz and a length of 3.17m will be constructed as the main accelerating section for the HIMM linac injector. Its total integral gap voltage on the beam axis is above than 10MV, which is fairly high as a normal conducting cavity. In general, it is difficult to design fabricate a long IH-DTL which contains several focusing quadrupole triplets. In the cavity design process, on-axis electric field distribution is tuned carefully by adjusting the cavity structure. On the other hand, nearest mode problem of a long IH-DTL cavity must be considered. In order to examine the on- axis electric field distribution and the nearest mode of such a long IH-DTL cavity, a cold model cavity of the IH-DTL has been constructed. The measurement results of this cold model will be discussed in this proceeding.

* Work supported by National Natural Science Foundation of China (11375243, 11405237) and Guangdong Innovative and Entrepreneurial Research Team Program (2016ZT06G373).
† duheng@impcas.ac.cn

RF STRUCTURE DESIGN OF IH-DTL

CST-MWS code [4] has been used to make the RF structure design and simulation. The optimized 3D RF structure is shown in Fig. 1. To make the on-axis electric field match with the dynamics requirement, end cut tuner, lens coupling tuner and local volume tuner are used and fine adjusted. Four movable plunger tuners are installed in the IH-DTL cavity, which has totally 0.9 MHz frequency tuning range. Remove the 4 plunger tuners, the H_{110} mode (operation mode) resonance frequency, Q0 value and RF power loss for C^{4+} is 163.0MHz, 14200 and 332kW respective. For the H_{111} mode (nearest mode), the resonance frequency and Q0 value is 165.4MHz and 12400. The on-axis electric field distribution compare between the H_{110} and H_{111} mode is shown in Fig. 2.

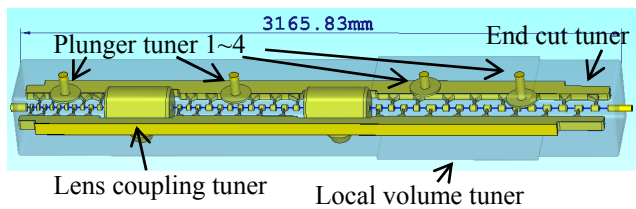


Figure 1: CST-MWS 3D model.

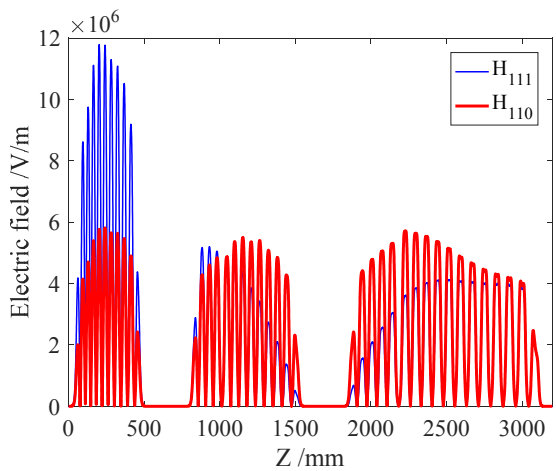


Figure 2: The on-axis electric field distribution compare between the H_{110} and H_{111} mode.

To avoid stimulating the H_{111} mode, the magnetic field distributions of both the operation and nearest mode are studied. As shown in Fig. 3, the magnetic field distributions are different between these two modes at the second focusing lens, so we can locate the power coupler here. When the coupler is tuned to the critical coupling for the H_{110}

Content from this work may be used under the terms of the CC BY 3.0 licence (© 2018). Any distribution of this work must maintain attribution to the author(s), title of the work, publisher, and DOI.

ISBN: 978-3-95450-194-6 ISSN: 2226-0366 doi:10.18429/JACoW-LINAC2018-TUPO005

INITIAL BEAM COMMISSIONING OF LEAF AT IMP*

Y. Yang†, Y. H. Zhai, L. T. Sun, L. Lu, H. Jia, W. P. Dou, X. Fang, L. Jing, Y. Wei, W. Ma, L. P. Sun, W. Lu, Y. H. Guo, X. J. Liu, H. W. Zhao, IMP/CAS, Lanzhou, China

Abstract

A Low Energy intense-highly-charged ion Accelerator Facility (LEAF), which mainly includes an ECR ion source, LEBT and an 81.25 MHz RFQ, was designed to produce and accelerate heavy ions, from helium to uranium with A/Q between 2 and 7, to the energy of 0.5 MeV/u. The typical beam intensity is designed up to 2 emA CW for the uranium beam. The facility has been successfully commissioned with He^{+} (A/Q=4) and N^{2+} (A/Q=7) beams and accelerated the beams in the CW regime to the designed energy of 0.5 MeV/u. Beam properties and transmission efficiencies were measured, indicating a good consistency with simulated data. After having briefly recalled the project scope and parameters, this paper describes the beam commissioning strategy and detailed commissioning results.

INTRODUCTION

A Low Energy intense-highly-charged ion Accelerator Facility (LEAF) was launched at IMP in 2015 for researches of irradiation material, highly charged atomic physics, low energy nuclear astrophysics, *et. al*. Meanwhile, this facility can be a prototype of the frontend of HIAF project [1] which is a new national project proposed by IMP and officially approved for heavy ion related researches. LEAF is mainly composed of a superconducting ECR ion source, a LEBT line and a RFQ. The ion source, a so-called 4th generation ECR ion source with 45 GHz microwave hearting, FECR, is expected to be able to provide 2 emA U^{34+} beam. The RFQ, operating at 81.25 MHz, is a 4-vane structure cavity designed to accelerate various heavy ion beams from 14 keV/u to 0.5 MeV/u, in CW mode. The layout of LEAF is shown in Fig. 1. DC beam produced by the ECR ion sources is bunched and matched to the RFQ acceptance by an external Multi-Harmonic Buncher (MHB) located in the LEBT upstream of the RFQ. The MHB helps to produce a smaller longitudinal output emittance and reduce the length of the RFQ since the starting synchronous phase of the RFQ is set to -45 degree and therefore the RFQ should only accept the well-bunched central part of the distribution containing more than 80% of the particles. Table 1 shows the main RFQ parameters.

The RFQ was assembled in Dec. 2017 and the cavity RF conditioning finished in Feb. 2018. The conditioning in CW mode up to 75 kW (1.1 times the required maximum RF power) went smoothly, consuming only 44 hours. The whole complex installation was finished in May 2018, and the beam commissioning started soon after that. However, the 45 GHz superconducting ECR source and MHB are still under development. In the initial beam commissioning, we use a 14.5 GHz room-temperature ECR source as a proxy and DC beam injection into RFQ. The facility has been successfully commissioned with A/Q=4 ion He^{+} and A/Q=7 ion N^{2+}. This paper will present the beam commissioning details and characteristics.

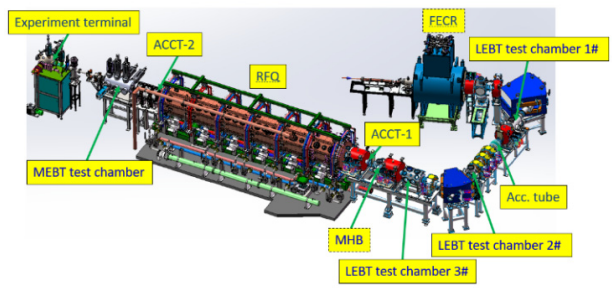


Figure 1: Layout of LEAF.

Table 1. Basic Design Specifications of LEAF-RFQ

Duty cycle	100%
Operating frequency	81.25 MHz
Resonant cavity	4-vane
Input particle energy	14 keV/u
Output particle energy	500 keV/u
Max. Vane voltage	70 kV (U^{34+})
CW RF power	67 kW (U^{34+})
Peak field at electrode surface	1.67 Kilpatrick units
Length of the RFQ vane	~596.4 cm

BEAM COMMISSIONING

Diagnostics

Diagnostic devices were installed in both LEBT and MEBT lines to validate the facility performances and measure the following beam characteristics:

- ✧ LEBT Test Chamber 1# (LTC 1#):
  - ➢ Intensity with Faraday cup (FC).
  - ➢ Transverse emittance with Allison scanners.
  - ➢ Beam transverse profile with fluorescent target.
- ✧ LEBT Test Chamber 2# (LTC 2#):
  - ➢ Intensity with Faraday cup.
  - ➢ Beam transverse profile with fluorescent target.
- ✧ LEBT Test Chamber 3# (LTC 3#):
  - ➢ Intensity with FC.
  - ➢ Transverse emittance with Allison scanners.
  - ➢ Beam transverse profile with fluorescent target.

* This work is supported by the National Nature Science Foundation of China (contract No. 11427904 and 11575265).

† yangyao@impcas.ac.cn.

Content from this work may be used under the terms of the CC BY 3.0 licence (© 2018). Any distribution of this work must maintain attribution to the author(s), title of the work, publisher, and DOI.

ISBN: 978-3-95450-194-6 ISSN: 2226-0366 doi:10.18429/JACoW-LINAC2018-TUPO007

FRIB FAST MACHINE PROTECTION SYSTEM: CHOPPER MONITOR SYSTEM DESIGN *

ZhiYong Li†, D. Chabot, R. C. Webber, S.M. Lidia, S. Cogan,
Facility for Rare Isotope Beams, East Lansing, Michigan, USA

Abstract

The Facility for Rare Isotope Beams tunes the beam power from 0 to 400KW by chopping the beam current with a beam chopper in the Low Energy Beam Transport. A chopper monitoring system is employed to verify proper chopper operation to avoid delivery of undesired high-powered beam and to inhibit beam for machine protection purposes. The system monitors the incoming beam gate time structure, the chopper switch high voltage pulses, the chopper electrode charge/discharge currents, and the status of machine protection system. It is designed to switch off the beam within tens of nanoseconds of a detected fault. Challenges include a dynamic beam gate pulse structure with pulse lengths as short as 0.6 μs and high voltage power supply current pulses of ~25 ns. A high speed "integrate and hold circuit with reset", Field Programmable Gate Array based digital control circuit and high speed ADC circuit were developed to fulfil the required functions. Design approach, simulation, and test results with the beam are the focus of this paper.

INTRODUCTION

The average beam power in Facility for Rare Isotope Beams (FRIB) [1-3] is determined by the instantaneous beam current and the duty factor. When beam is requested, the duty factor is determined solely by the beam chopper in the Low Energy Beam Transport (LEBT). Therefore, chopper is actually a fast-acting, 0-400 kW control knob on the beam power. The FRIB chopper control devices, displayed in Fig. 1, include an Event Receiver (EVR) providing the beam gate signal, positive and negative high voltage (HV) power supplies providing 0-4kV and -4kV-0V respectively, and positive and negative HV switches to drive the chopper electrodes in the beam line. The chopper monitor system serves the ultimate purposes of preventing delivery of undesired high-powered beam and inhibiting beam for machine protection purposes [4]. The system is designed to receive the beam gate signal from the EVR, verify its acceptability for the current beam mode, drive the HV switch inputs, monitor the high voltage output pulses, monitor the chopper charge/discharge current, monitor the status of Fast machine Protection System (FPS) [4], and to inhibit the beam within tens of nanoseconds of a fault. The beam gate can exhibit a dynamic structure to ramp up beam power in a few seconds and the pulse lengths can range from 0.6 μs to nearly 10 ms. It is an engineering challenge to monitor every pulse of this ramp up process with a set of configurable parameters. The high voltage pulses exhibit rise and fall times ≤25 ns which poses difficulty for accurately measuring the charge and discharge currents. A Field Programmable Gate Array (FPGA) based digital control circuit, high speed "integrate and hold circuit with reset", and high speed ADC are employed to fulfil the required functions. Design approach, architecture, simulation, test results to meet these challenges are discussed in the following sections.

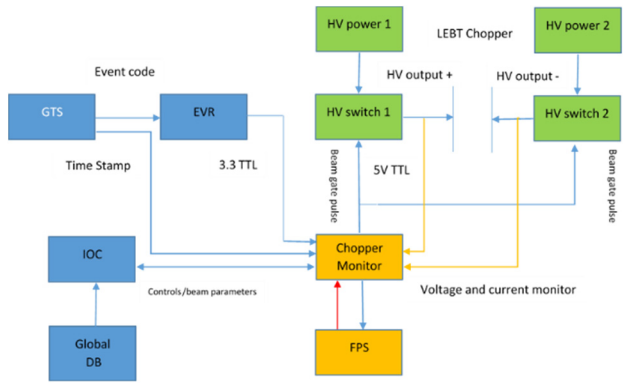


Figure 1: FRIB Chopper Control and Monitor System block diagram.

DESIGN

The chopper monitor system consists of chopper monitor chassis, Input Output Controller (IOC), and Operator Interface (OPI). The IOC/OPI serves to establish the chopper operational state, configure the chopper monitor for checking the beam pulse pattern for various beam modes, and provide the threshold values necessary for checking the amplitudes of each HV pulse and charge/discharge current. The chopper monitor system hardware consists of an FRIB General Purpose Digital Board (FGPDB) [4], the chopper monitor ADC board, and required power supplies. The chopper monitor ADC board interfaces to the MPS, the beam gate signal from the EVR, the control inputs to the HV switches, and the HV switch output voltage and current monitor signals (V_{mon} and I_{mon}). The I_{mon} signal is integrated by a high speed integrator circuit. A 14 bit, 125 Msps low power quad ADC, the LTC2175, is used to digitize the V_{mon} and integrated I_{mon} signals. The ADC board also contains a high speed DAC circuit to calibrate the ADC circuit and a circuit to monitor the board power. The FGPDB controls the DAC circuits, resets the integrator, initializes the ADC, and reads ADC outputs. The core of the FGPDB is a Spartan-6 XC6SLX150T-2FGG900C FPGA [4].

The FPGA firmware architecture includes a Micro-Blaze System to manage the circular buffers of ADC waveform data, EPICS communication and other management functions. It also includes a chopper monitor logic which consists of an embedded EVR, MPS-related logic, pulse

*Work supported the U.S. Dept. of Energy Office of Science under Cooperative Agreement DE-SC0000661.
†liz@fnib.msu.edu

Content from this work may be used under the terms of the CC BY 3.0 licence (© 2018). Any distribution of this work must maintain attribution to the author(s), title of the work, publisher, and DOI.

ISBN: 978-3-95450-194-6 ISSN: 2226-0366 doi:10.18429/JACoW-LINAC2018-TUPO009

HEAT TREATMENT FOR A PROTOTYPE HALF-WAVE RESONATOR CAVITY*

Yoochul Jung† Junwoo Lee, Sangbeen Lee, Juwan Kim, Bonghyuk Choi,
Heetae Kim, Jongdae Joo, Youngkwon Kim, Hoechun Jung
RISP, IBS, Daejeon, South Korea

Abstract

Performance of a superconducting cavity, which is made of niobium, tends to be degraded easily depending on the surface resistance. Surface residual resistance of the cavity can be increased during the cavity fabrication process such as pressing, cutting and welding, because these multiple steps can lower the crystallinity of the cavity surface not only by disordering the lattice atoms but also by supplying lattice atoms with impurity atoms. Among the impurity atoms, hydrogen is a well-known impurity that lowers the cavity performance in the form of Q-disease. High temperature heat treatment was performed to remove impurity gas (mainly hydrogen) from the surface of a cavity, and to anneal the cavity to increase the crystllinity. Optical images of the heat treated niobium sample were investigated. Crystallinity was improved after the heat treatment by investigating X-ray diffraction (XRD), thus it confirmed that the annealing was successfully carried out. The residual gas analysis (RGA) was investigated and it confirmed that hydrogen was removed successfully during the heat treatment.

INTRODUCTION

For a LINAC, called "RAON" adopts four types of superconducting cavities: quarter-wave (81.25 MHz), half-wave (162.5 MHz), and two different single-spoke resonators. All the superconducting cavities operate with an alternating current of high frequency; thus, the surface resistance must be extremely low to maintain the superconductivity. Superconductivity will vanish easily if the temperature of any part in the cavity reaches a critical temperature (Nb_{T_c} is around 9.2K).

The temperature-dependent BCS resistance decreases as the temperature goes down but the residual resistance is independent of the temperature [1]. The residual resistance due to the imperfection of a raw superconducting material is almost fixed during the production. However, multiple steps for fabricating cavities can inevitably increase the residual resistance additionally by creating other sources such as a dislocation, a vacancy and a grain boundary. Therefore, the cavity fabrication must be carefully processed not to have additional surface resistance [2, 3].

One of the surface treatments to improve the surface resistance, the high temperature baking is well known for both annealing the cavity and removing hydrogen from the surface of the cavity. In case of annealing, it is for recovering the crystallinity of the cavity by moving disordered atoms to their original lattice points. In case of removing hydrogen, it is for outgassing impurity gas, which acts as a potential scattering center as a form of hydride at low temperatures.

From the earlier studies, hydrogen, which is easily introduced into the cavity surface during the chemical etching, is well known for deteriorating cavity performance in the form of Q-disease [4]. The residual gas analysis (RGA) and the X-ray analysis were performed after the heat treatment to check the baking effect. In this study, we report how the heat treatment process was carried out. Furthermore, we discuss the results along with the cavity performance in terms of the residual gas and X-ray analyses.

FURNACE SETUP & EXPERIMENTAL

Specifications of a vacuum furnace for the heat treatment are listed Table 1. Figure 1 shows the vacuum furnace.

Table 1: Specifications of Vacuum Furnace

Items	Specification	Unit
Dimension	1 × 1 × 3 (W×L× H)	Meter
Vacuum	10^{-6}@650°C, 10^{-8}@25°C	Torr
Temperature	Max. 1400°C,	Celsius
Heating element	Molybdenum	Mo



Figure 1: Vacuum furnace for heat treatment:cavity is loaded horizontally.

And Fig. 2 shows the horizontally loaded half-wave resonator cavity (HWR) with a titanium box in the furnace. HWR cavity is in contact with the titanium box through alumina (Al_2O_3) frame in order to avoid the chemical reaction between the cavity and the titanium box, as shown in Fig. 2. Two thermocouple wires are connected to titanium box, and two additional thermocouple wires are connected to cavity flanges, which are made of SUS316L.

* This work was supported by the Rare Isotope Science Project of Institute for Basic Science funded by the Ministry of Science, ICT and Future Planning (MSIP) and the National Research Foundation (NRF) of the Republic of Korea under Contract 2013M7A1A1075764
† sulsiin@ibs.re.kr

Content from this work may be used under the terms of the CC BY 3.0 licence (© 2018). Any distribution of this work must maintain attribution to the author(s), title of the work, publisher, and DOI.

ISBN: 978-3-95450-194-6 ISSN: 2226-0366 doi:10.18429/JACoW-LINAC2018-TUPO010

MUON ACCELERATION TEST WITH THE RFQ TOWARDS THE DEVELOPMENT OF THE MUON LINAC

R. Kitamura*, S. Li, University of Tokyo, Hongo, Tokyo, Japan
M. Otani, Y. Fukao, K. Futatsukawa, N. Kawamura, T. Mibe, Y. Miyake, T. Yamazaki, KEK, Tsukuba, Ibaraki, Japan
Y. Kondo, K. Hasegawa, T. Morishita, JAEA, Tokai, Naka, Ibaraki, Japan
S. Bae, B. Kim, S. Choi, SNU, Seoul, Korea
T. Iijima, Y. Sue, Nagoya Univ., Chikusa-ku, Nagoya, Japan
H. Iinuma, Y. Nakazawa, Ibaraki Univ., Mito, Ibaraki, Japan
K. Ishida, RIKEN, Wako, Saitama, Japan
G. Razuvaev, BINP SB RAS, Novosibirsk, Novosibirsk State Univ., Novosibirsk 630090 and Pulkovo Observatory, St. Petersburg, 196140, Russia
N. Saito, J-PARC center, Tokai, Naka, Ibaraki, Japan

Abstract

The muon linac is planned at the Japan Proton Accelerator Research Complex (J-PARC) for the precision measurement of the muon dipole moments. However, the muon acceleration with an radio-frequency (RF) accelerator was not carried out yet. Then, the first muon RF acceleration experiment using an radio-frequency quadrupole (RFQ) linac was carried out in the J-PARC. The incident positive muon was cooled using the production of the negative muonium ion (Mu^-) before the accelaration. Subsequently, the Mu^- was accelerated to 89 keV with the RFQ. Thanks to the pulsed muon beam in the J-PARC, the accelerated Mu^- was clearly identified with the Time-Of-Flight measurement after the momentum selection with the bending magnet. The measured event rate of the accelerated Mu^- was consistent with the expectation using the simulation and the result of the Mu^- production experiment as the preparatory experiment of the acceleration experiment. The first muon RF acceleration was successful.

INTRODUCTION

A muon anomalous magnetic moment $(g-2)_\mu$ is one of the quantities theoretically predicted with the high precision. The E821 experiment at the Brookhaven National Laboratory (BNL) measured $(g-2)_\mu$ with the precision of the 0.54 ppm and reported a discrepancy of more than three standard deviations between the experimental value and the prediction with the standard model (SM) of the particle physics [1]. Since the $(g-2)_\mu$ includes contributions from the physics beyond the SM via quantum loop effects, this discrepancy may imply the evidence of the new physics (NP). As one possibility, the non-zero small muon electric dipole moment (EDM) may contribute the discrepancy of the $(g-2)_\mu$ [2] [3]. Therefore, a more precise and independent measurement of the $(g-2)_\mu$ and the muon EDM than the BNL E821 has been desired to search the NP.

The new precision measurement of the $(g-2)_\mu$ and the muon EDM, the E34 experiment is proposed at the Japan Proton Accelerator Research Complex (J-PARC) using the low-emittance muon beam [4]. Final goals of the J-PARC E34 are 0.1 ppm for the $(g-2)_\mu$ and 10^{-21} e·cm for the muon EDM, respectively. One of the key components is the low-emittance muon beam produced using the low-energy muon source and the muon linac [5]. However, the muon acceleration with the radio-frequency (RF) accelerator was not carried out yet. Therefore, the demonstration of the muon RF acceleration should be carried out to develop the method of the measurement for the accelerated muon beam towards the construction of the muon linac. The first muon RF acceleration using an radio-frequency quadrupole (RFQ) linac was demonstrated at the J-PARC Material and Life science experimental Facility (MLF) [6] [7]. This paper reports the result of the first muon RF acceleration in the world.

PRODUCTION OF THE NEGATIVE MUONIUM ION

To accelerate muons using the RFQ, the muons should be cooled to match the input energy of 5.6 keV for the RFQ, because the kinetic energy of the high-intensity muon beam supplied at the J-PARC MLF is about 4 MeV. When the positive muon penetrates through a thin aluminum foil target (Al target), the negative muonium ion (Mu^-) is produced [8] [9]. The Mu^- is in the bound state of a positive muon and two electrons. Since the mean initial kinetic energy of the Mu^- is in vicinity of 0.2 keV, the Mu^- production can be used as the cooling method for the muon RF acceleration.

The Mu^- production was carried out to estimate the event rate of the accelerated Mu^- in the muon acceleration experiment. Figure 1 shows the experimental setup of the Mu^- production experiment as the preparatory experiment of the muon acceleration experiment [10].

Both of this Mu^- production experiment and the muon acceleration experiment were carried out at the Muon D-

* rkita@post.kek.jp

Content from this work may be used under the terms of the CC BY 3.0 licence (© 2018). Any distribution of this work must maintain attribution to the author(s), title of the work, publisher, and DOI.

ISBN: 978-3-95450-194-6 ISSN: 2226-0366 doi:10.18429/JACoW-LINAC2018-TUPO011

UPGRADE OF HEAVY ION INJECTOR I-3 AT ITEP

N. N. Alexeev, P. N. Alekseev, V. A. Andreev, T. V. Kulevoy, A. D. Milyachenko, V. I. Nikolaev, Yu. A. Satov, A. V. Shumshurov, A. B. Zarubin
ITEP, B. Cheremushkinskaya 25, 117218 Moscow, Russia

Abstract

Heavy ion injector I-3 represents two-gap 2.5 MHz resonator with accelerating voltage 2x2 MV. It's used with laser ion source (LIS) for acceleration of ions in wide range of charge to mass ratio. As a result of modernization, injector structure will be supplemented by the second two-gap resonator, RF voltage will be increased to 3x4 MV and accelerated beam structure has to be improved by increasing accelerating frequency to 5 MHz. Design features of upgraded linac I-3M and peculiarity of beam dynamics for different types of ions are presented.

INTRODUCTION

Linac I-3 with laser ion source LIS100, constructed on the base of 100 J CO_2 laser, had been used many years as the ion injector for booster synchrotron UK of proton-ion accelerator-accumulator facility ITEP-TWAC [1, 2]. Generated at the output of injector I-3 ion, such as C^{4+}, Al^{11+}, Si^{10+}, Fe^{16+}, Cu^{17+}, Ag^{19+} etc., with energy of 4Z MeV had been accelerated in UK ring up to the energy of several hundred MeV per nucleon with intensity limited by high charge density of 2 MHz bunch structure of injected beam. Upgraded structure of I-3M is optimized for acceleration of heavy ions with A/Z in the range from 3 to 10. For acceleration of protons and light ions, injectors I-2 [3, 4] and I-4 [5] are used. The energy of accelerated in I-3M ions increased by factor of three at some improvement of beam density uniformity will allow to raise the intensity of accelerated in booster ring beam by more than an order of magnitude.

Increasing of accelerating voltage in I-3M is achieved by optimizing the configuration of accelerating electrodes, which will reduce the maximum electric field strength on the surfaces of electrodes that will allow to raise by half the amplitude of operating voltage on the accelerating gaps to 3 MV. The structure of two two-gap phased resonators allows having an accelerated voltage close to maximum of up to 12 MV for ions with variable charge-to-mass ratio.

OPTIMIZATION OF ACCELERATING ELECTRODES CONFIGURATION

Maximum amplitude of voltage 2 MV on the accelerating gaps in existing construction of resonator is limited by electric field strength on the localized areas of the electrode surfaces. Maximum electric field strength on the surface of electrodes as the function of relevant parameters shown in Figure 1 allows optimizing the shape of electrodes providing to reduce electric field strength on the surface of electrodes at a given voltage value at the accelerating gap. The optimum shape of the electrodes, providing extreme voltage value on the accelerating gap, is characterized by a minimum radius of surface curvature of 60 mm at the electrode diameter value of 600 mm.

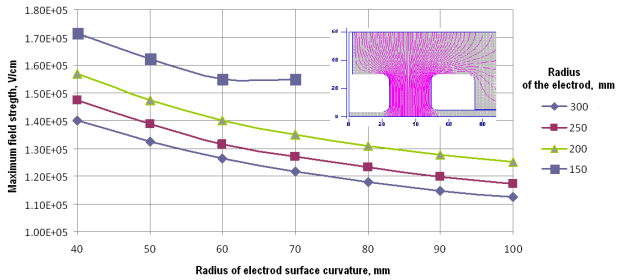


Figure 1: Maximum electric field strength on the surface of electrodes as the function of relevant parameters.

ACCELERATING STRUCTURE

Layout of the injector I-3M accelerating structure is shown in Figure 2, comparison parameters of both I-3 and I-3M injectors are given in Table 1. The length of drift tubes 0.5 m and 1.4 m in resonators is optimized for acceleration of heavy ions with A/Z=6.

The initial beam is formed at the output of the 50 kV gap that breaks the laser plasma generated in the target chamber of LIS100. In the matching channel of I-3M, the beam is focused by three electrostatic lenses and bunched at the input of the first accelerating resonator using the 10x2 kV, 5 MHz, two-gap buncher. Additional transverse focusing of the bunched beam of high charge density is provided in the first accelerating gap by optimized configuration of axially symmetric nonlinear RF field.

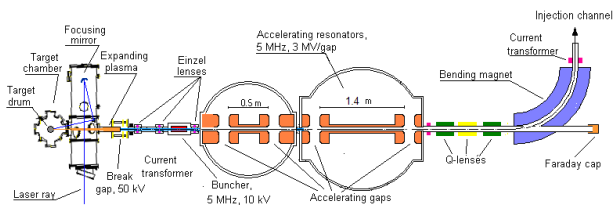


Figure 2: Acceleration structure of I-3M.

Table 1: Comparison Parameters of I-3 and I-3M

Injector	I-3	I-3M
Accelerating frequency, MHz	2.5	5.0
Number of resonators	1	2
Accelerating gaps	2	4
Accelerating voltage, MV	4	12
Bunching voltage, kV	10x2	
Accelerating ions. A/Z	2÷5	3÷10
Injection energy, kV	50	
Trans. acceptance, π mm mrad	>1000	
Momentum spread, Δp/p, %	up to ±2.5	
Transmission factor, %	~50	

Content from this work may be used under the terms of the CC BY 3.0 licence (© 2018). Any distribution of this work must maintain attribution to the author(s), title of the work, publisher, and DOI.

ISBN: 978-3-95450-194-6 ISSN: 2226-0366 doi:10.18429/JACoW-LINAC2018-TUPO012

COMPACT MULTIPURPOSE FACILITY - BELA

T. Kulevoy[1,2,§], R. Fatkullin[2], A. Kozlov, G. Kropachev, D. Seleznev, A. Semennikov, A. Sitnikov
NRC Kurchatov institute - ITEP, 117218, Moscow, Russia
[1]also at NRC Kurchatov institute , 123182, Moscow, Russia
[2]also at NRNU MEPhI, 115409, Moscow, Russia

Abstract

In ITEP the project of multidiscipline facility Based on ECR ion source and Linear Accelerator (BELA) is started. The injector part of facility is based on combinations of ECR ion source and dc H^+ and He^+ source will provide the multi beams irradiation of the reactor materials for modeling experiments. The cw RFQ and following DTL will enable the set of experimental activity both for fundamental physics and for practical applications.

INTRODUCTION

After long time the mega science project NICA (Nucotron-based ion Collider fAcility) based on the modern accelerator technologies is under development in Russia [1]. In framework of this project national research center "Kurchatov institute" – Institute for Theoretical and Experimental Physics (ITEP) developed the new RFQ for polarized ion program which is inder operation for more than two years [2]. Several other mega-science projects are under discussion in Russia. In Dubna that is the DERICA project (Dubna Electron-Radioactive Ion Collider fAcility). DERICA is proposed as the next step rare isotope beam facility. From the accelerator point of view DERICA will include the driver LINAC-100 (energy up to 100 MeV/u) with the operating mode close to CW, the fragment separator, the re-accelerator LINAC-30 (energy up to 30 MeV/u), the fast ramping ring (energy <300 AMeV), the collector ring and the electron storage ring with an injector. DERICA general concept and first results of LINAC-100 and LINAC-30 general layout is presented in [3]. Another project which is under discussion now is a Spallation Source for neutron generation. The need for a next-generation neutron source is evidenced by the analysis of a specially established ESFRI Physical Sciences and Engineering Strategy Working Group [4]. Several neutron generator is either under operation (IPNS [5], Los Alamos Neutron Science Center [6], ISIS [7], SNS [8] and JPARC [9]) or under construction (ESS [10]).

The NEPTUN project where the high intensity linac and the target from neptunium are used for neutron beam generation is under discussion as a Russian Spallation Source [11].

The main trend of the ion linac are the development of (i) cw RFQ and DTL up to 3-10 MeV/n, (ii) different types of superconducting RF cavities (SCRF) and solid state RF amplifiers (SSA).

§kulevoy@itep.ru

Development of cw RFQ and DTL enables the construction of compact devices both for physical researches and industrial application. Today several projects based on compact linacs are under development. First of all it is the IFMIF-EVEDA neutron generator for fission reactor material investigation. The facility is under commissioning in Rokkasho (Japan) [12]. As well it can be mentioned SARAF in Israel [13] , FRANZ [14] in Germany, MUNES in Italy [15] and others.

The project of multidiscipline facility **B**ased on **E**CR ion source and **L**inear **A**ccelerator (BELA) is under development in ITEP. Taking into account the current research activity the facility will provide the experiments for fission and fusion reactor materials investigation, β-nuclear magnetic resonance and semiconductor device modification by ion beams. The technologies developed in framework of this project will be used for serial production of compact facilities based on cw linac for PET, as well as compact neutron generators for BNCT and activation analysis. The further development of the project will lead to construction of Spallation Source and RIB complexes in Russia.

GENERAL LAY-OUT

The general layout of the BELA project is shown in Fig. 1. It consists of injector complex (pos. 1 and 2), proton RFQ, several bunchers and 3-gap DTLs. Such structure enables the material science with ion beams from hydrogen to uranium at injector complex and the semiconductor irradiation by proton beams with variable energy. After the output energy of linac reach the 3 Mev level the neutron generation from lithium target will be started for BNCT and neutron experiments.

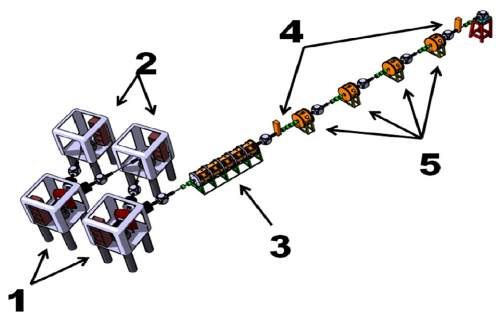


Figure 1: General layout of BELA.

INJECTORS COMPLEX

Injector complex includes several high voltage platforms (HVP) and beam lines connecting them. At HVPs two ECR ion sources are located (pos 1, Fig. 1) and targets (pos. 2, Fig. 1). Ion sources are located at the HVP

Content from this work may be used under the terms of the CC BY 3.0 licence (© 2018). Any distribution of this work must maintain attribution to the author(s), title of the work, publisher, and DOI.

ISBN: 978-3-95450-194-6 ISSN: 2226-0366 doi:10.18429/JACoW-LINAC2018-TUPO013

COMMISSIONING STATUS OF THE LIGHT DEVELOPMENT MACHINE

G. De Michele†, J. Adam, D. Aguilera Murciano, A. Benot-Morell, R. Bonomi, M. Breitenfeldt, F. Cabaleiro Magallanes, M. Caldara, S. Candolfi, G. Castorina, M. Cerv, G. D'Auria[1], A. Degiovanni, V. A. Dimov, M. Esposito, S. Fanella, D. Fazio, D. A. Fink, Y. Fusco, S. Gibson, M. Gonzalez, P. Gradassi, Y. Ivanisenko, A. Jeff, V. Khan, L. Kobzeva, G. Levy, S. Magnoni, G. Magrin, A. Marraffa, A. Milla, R. Moser, P. Nadig, L. Navarro Quirante, G. Nuessle, A. Patino-Revuelta, H. Pavetits, P. Paz Neira, T. Rutter, F. Salveter, A. Samochkine, A. Sanchez Gonzalez, D. Guillen Soriano, P. Stabile, K. Stachyra, M. Torreira Gallas, A. Valloni, L. Wallet, C. Zannini
ADAM, Meyrin, Switzerland,
[1]also at Elettra-Sincrotrone Trieste S.C.p.A., Trieste, Italy

Abstract

ADAM (Application of Detectors and Accelerators to Medicine) is a CERN spin-off company currently working on the construction and testing of the LIGHT (Linac for Image-Guided Hadron Therapy) machine. LIGHT is an innovative high-frequency linac based proton therapy system designed to accelerate protons up to 230 MeV: it consists of three different linac sections i.e. a 750 MHz Radio Frequency Quadrupole (RFQ) accelerating the beam up to 5 MeV; a 3 GHz Side Coupled Drift Tube Linac (SCDTL) up to 37.5 MeV; and a 3 GHz Coupled Cavity Linac (CCL) section up to 230 MeV. The compact and modular design is based on cutting edge technologies developed for particle colliders and adapted to the needs of hadron therapy beams. The LIGHT development machine is currently being built at CERN and this paper describes its design aspects and its different stages of installation and commissioning.

INTRODUCTION

The LIGHT solution is a unique technology based on years of research at ADAM. There are several advantages of such machine w.r.t. accelerators currently used in proton therapy such as cyclotrons and synchrotrons: among others the fast beam energy change, a smaller beam emittance, reduced losses allowing for less shielding, and modularity that allows an easy installation and fit in already built infrastructures.

This paper is a continuation of the previous report [1].

THE LIGHT DEVELOPMENT MACHINE

The LIGHT development machine is being built and commissioned by ADAM at CERN. It consists of a proton injector assembly (PIA), a high frequency RFQ [2], a four modules SCDTL structure and a four modules CCL structure, designed to deliver a proton beam at 70 MeV. The latter proton energy will suffice to prove the LIGHT technology and that all sub-components (PIA, RFQ, SCDTL, CCL) will work as an embedded system.

General Layout

The details of the lattice of the LIGHT development machine to reach up to 7.5 MeV protons are described in [1]. Figure 1 shows the current status of the installation with all four SCDTL modules on beam line. Another substantial difference w.r.t. the previous commissioning stage [1] is the introduction of the new movable diagnostic test-bench, described in [3], that replaces the spectrometer dipole with a combination of Time-of-Flight (ToF) and multi-layer Faraday cup measurements.

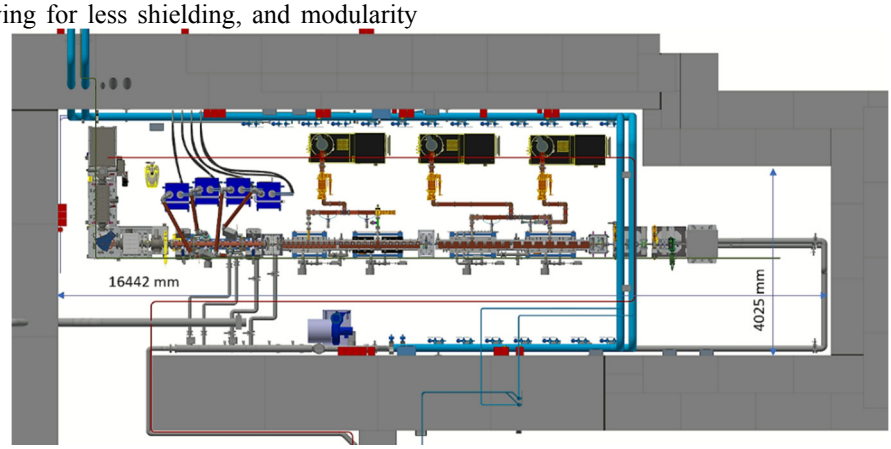


Figure 1: Top view of the current LIGHT development machine. From left to right: the L-shape PIA, the RFQ, four SCDTL modules and the medium energy diagnostic test bench without spectrometer.

† giovanni.demichele@avo-adam.com

Content from this work may be used under the terms of the CC BY 3.0 licence (© 2018). Any distribution of this work must maintain attribution to the author(s), title of the work, publisher, and DOI.

ISBN: 978-3-95450-194-6 ISSN: 2226-0366 doi:10.18429/JACoW-LINAC2018-TUPO014

TRIUMF ISAC LINAC DEVELOPMENTS and UPGRADES

Z. T. Ang†, T. Au, Y. Bylinski, K. Fong, J. Keir, D. Lang, R. Laxdal, R. Leewe, B. Waraich, Z. Yao, Q. Zheng, V. Zvyagintsev

TRIUMF, 4004 Wesbrook Mall, Vancouver V6T 2A3, BC, Canada

Abstract

TRIUMF ISAC accelerator complex is in consists of ISAC-I room temperature linac and ISAC-II superconducting linac structure [1]. ISAC-I linac has seventeen RF systems in operation for about twenty years, and ISAC-II linac has forty superconducting QWR. The SRF cavities in operation for some about ten years. To match beam energy to RFQ, a small booster 3-gap structure at 11.78 MHz has been designed and installed in upstream of RFQ. A sliding mode extremum seeking control for LLRF control was developed and implemented in operation. Test results demonstrated very stable and reliable performs. Six of DTL systems have been working in the control mode. RFQ, two more DTL systems, HEBT and DSB bunchers, Rotator systems will be upgraded in the sliding mode control soon. The amplifiers for twenty ISAC-II QWR superconducting cavity SCB were developed and upgraded from YV-229 triode tube amplifier into a solid-state amplifier (SSA). The prototype and other four SSAs have been commissioned in 2017 and in operation over one year faithfully. The rest of 16 SSAs has been tested on bench at beginning of 2018. All twenty are in operation this year.

INTRODUCTION

The ISAC Linac of radioactive ions beams facility at TRIUMF have been in successfully operation for experiments many years. RFQ at 35.36 MHz to accelerate ions beam with A/Q≤30 from 2.03 keV/u to 153 keV/u and variable energy draft tube linac (DTL) at 106 MHz to accelerate the stripped ions beam of A/Q≤7 between 153 keV/u and 1.53 MeV/u. The designed capacity of beams energy for DTL to accelerate ions from 153 keV/u to 1.5 MeV/u with A/Q≤6. To meet the experiment requirements, some upgrades were done in DTL Tank number 3, number 4 and 5 in the RF power transmission line and final RF power amplifiers. The Tank 3 power amplifier outputs was increased to 20 kW from 16 kW after changing HCA 158-50 J coaxial semi-rigid transmission line to SPX communication technology 3-1/8'' copper rigid transmission line. Tank 5 amplifier's high voltage transformer has been upgraded to 51 KVA from 36.6 KVA, which output power increased from 20.5 kW to 28 kW. Tank 4 amplifier's specified power level increased to 22 kW from 19 kW after retuning amplifiers setup limit trip points. The temperatures of the tuners and RF coupler windows are monitored, and the coarse tuners were setup to meet fine tuner working distances for all power levels. Table 1 shows the DTL amplifiers upgrading results:

†Email address: zang@triumf.ca

Table 1: DTL Amplifiers Output Power

System	Before	After upgrading
Tank 3	16 (KW)	19 (KW)
Tank 4	19 (KW)	22 (KW)
Tank 5	20.5 (KW)	28 (KW)

After the above upgrading for DTL RF systems there are more variable ions beams and beam energies could be delivered for experiments at TRIUMF.

RF BOOSTER

The 35.36 MHz RFQ is designed to accelerate beams with A/Q≤30 in CW. A three harmonic pre-buncher, located 5m upstream of the RFQ, operates with a fundamental frequency of 11.78 MHz so that one of every three RFQ buckets is filled with beams. The RFQ requires a beam injection energy at 2.03 keV/u for about 60% beam transmission. The injection energy acceptance of the RFQ requires that the ions beam must be extracted from a source at an electric potential up to about 60 kV. The ISOL target modules operate in a grim environment that can limit the source bias. Presently the ISAC target modules cannot hold higher than 54 kV and this value can degrade with time so that to schedule experiments for ions with A>25 has a risk.

In order to accelerate high mass beams and to mitigate against further source bias degradation a small 3-gap RF structure cavity has been installed at upstream of RFQ. The effective voltage for the booster was specified 16 KV. A 7 KV effective voltage has been achieved for beam experiments. 2 KV, 4 KV and 6 KV effective voltage for ions beams of Carbon and Nitrogen have been tuned through RFQ at the designed transmissions respectively. Table 2 shows the effective voltages with RF power feeding to the primary coil in the RF circuit box. A stable operation could not be approached while effective voltages applied to beams higher than 8 KV.

Before we installed the RF structure and RF circuitry box in beam line, we powered the system to 150 W RF power through primary coils in RF Lab driven from a 300 watts CW amplifier. The forward and reflected RF powers were monitored. A stable RF performs off line tests gave us a confident to install it for beam test. Instead of real RF structure and feedthrough, we used two capacitors with equal capacitances to the feedthrough and draft tubes for the test and tuning resonance frequency. However, when we installed the structure in beam line to test with beams in vacuum, the effective voltage to beam is much lower from simulations and bench tests.

Content from this work may be used under the terms of the CC BY 3.0 licence (© 2018). Any distribution of this work must maintain attribution to the author(s), title of the work, publisher, and DOI.

ISBN: 978-3-95450-194-6 ISSN: 2226-0366 doi:10.18429/JACoW-LINAC2018-TUPO016

HIGH FREQUENCY RFQ DESIGN AND LEBT MATCHING FOR THE CERN TWINEBIS ION SOURCE

V. Bencini*, M. Breitenfeldt, J.B. Lallement, A.M. Lombardi, H. Pahl, J. Pitters, A. Pikin, F. Wenander
CERN, Geneva, Switzerland

Abstract

An Electron Beam Ion Source (EBIS) is being developed at CERN [1] for production of highly charged ions, for instance fully stripped ^{12}C. The focus has so far been on the electron gun design, aiming for a high current compression, which results in a rapid ionisation process and thereby high repetition rate. Initial commissioning tests of such an electron gun, the so-called MEDeGUN [2], have already been performed and we are now in the process of designing a multi-purpose ion extraction and diagnostics line. The Low Energy Beam Transport (LEBT) line will transport the ions into the downstream Radio Frequency Quadrupole (RFQ) with a nominal energy of 15 keV/u. The 750 MHz RFQ is designed to accelerate ions from 15 keV/u up to the final energy of 2.5 MeV/u. After the RFQ design was finalized and its acceptance calculated, the beam matching to the RFQ was studied, finding a set of parameters for the LEBT that maximize the transmission through the RFQ. Details of the RFQ design, of the LEBT matching procedure and its final results are illustrated in this paper.

INTRODUCTION

After the design, construction and successful commissioning of a 750 MHz Radio Frequency Quadrupole for the acceleration of protons from 40 keV to 5 MeV in the space of 2 meters, we have studied a potential extension of the beam dynamics concept from protons to ions. In the framework of the strategy paper for medical applications [3] the layout of a linac-based carbon ion accelerator for medicine is a key ingredient of a potential future study involving other partners. Besides, the availability of a fully stripped carbon ion beam at the energy of 15keV/u in the framework of MEDeGUN allowed for a perfect synergy between the endeavors on the LEBT and the RFQ design. The result of this study is two-fold. First, we have detailed an RFQ designed for fully stripped carbon and tailored to the beam characteristics of the source and LEBT of MEDeGUN that could be used as such as a pre-injector of a linac-based medical facility. Second, we have studied the variation of critical parameters, exploring the trade-off between length, RF power needs, beam throughput and machinability for a standalone RFQ that could accelerate carbon ions as well as alpha particles and could be used for other purposes.

LEBT MATCHING

The LEBT has been designed to transport the ion beam from the TwinEBIS source, set at 30 kV, to the RFQ (at the matching plane). The ion distribution used for the matching is the result of simulations that reproduce the physics of the ion production in the source [4]. The resulting beam is extracted by a 17 kV extractor electrode and accelerated up to 6.5 keV/u. It then travels into a set of nine accelerating rings set between 27 kV and ground voltage that boost the energy up to 15 keV/u. Between the extractor and the accelerating gaps an additional 'adaptor' electrode was added to keep the beam focused. The particles at their final energy are then focused and matched to the RFQ by two gridded lenses and one Einzel lens. The aim of the matching is to maximise the number of particles that fall into the RFQ acceptance, defined as the biggest ellipse in the transverse phase space that can be accelerated and transported through the RFQ with nominal transmission. The matching technique is explained in [4] and consists of finding the optimal set of voltages applied to the focusing elements (the adaptor, the two gridded lenses and the Einzel lens).

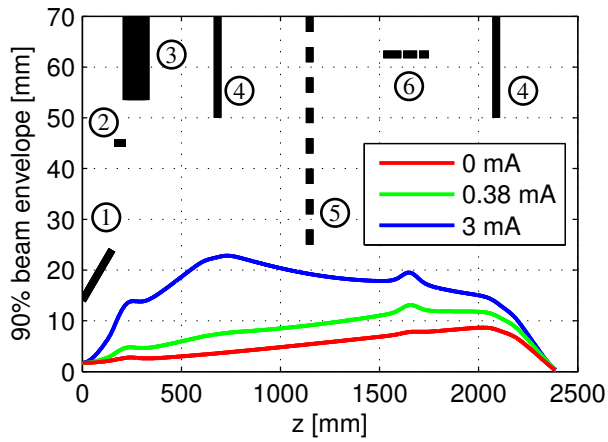


Figure 1: Plot showing the envelope of the matched beam for a current of 0 mA, 1 mA and 3 mA. The apertures of the relevant optical components are indicated: (1) Extractor, (2) adaptor, (3) accelerating gaps, (4) gridded lenses, (5) horizontal collimator, (6) Einzel lens.

The matching was performed for three input currents. 3 mA, corresponding to the maximum theoretical current that can be generated by the TwinEBIS, 0 mA, representing the case without space charge, and 0.38 mA (corresponding to $1{\cdot}10^9$ $^{12}C^{6+}$ ions in a 5 µs pulse), the current that could be extracted by the EBIS source in the present configuration. All the extracted beams are composed of 50% of $^{12}C^{6+}$ and of 50% of other charge states.

In Figure 1 a sketch of the main elements of the LEBT, together with the 90% beam envelopes are showed. The

* vittorio.bencini@cern.ch

Content from this work may be used under the terms of the CC BY 3.0 licence (© 2018). Any distribution of this work must maintain attribution to the author(s), title of the work, publisher, and DOI.

ISBN: 978-3-95450-194-6 ISSN: 2226-0366 doi:10.18429/JACoW-LINAC2018-TUPO017

THE NEW LIGHT ION INJECTOR FOR NICA

B. Koubek*, M. Basten, H. Höltermann, H. Podlech, U. Ratzinger,
A. Schempp, R. Tiede, Bevatech GmbH, Frankfurt am Main, Germany
A. Butenko, A. Govorov, B. Golovenskiy, D. Donets, K. Levterov, D. Lyuosev, A. Martynov,
V. Monchinskiy, D. Ponkin, K. Shevchenko, I. Shirikov, E. Syresin, JINR, Dubna, Russia
C. Kampmeyer, H. Schlarb, DESY, Hamburg, Germany

Abstract

Within the upgrade scheme of the injection complex of the NICA project and after a successful beam commissioning of a heavy ion linac, Bevatech GmbH will build a first part of a new light ion linac as an injector for the Nuclotron ring. The linac will provide a beam of polarised protons and light ions with a mass to charge ratio up to 3 and an energy of 7 MeV/u. The mandate of the Linac does not only include the hardware for the accelerating structures, focusing magnets and beam diagnostic devices, but also the LLRF control soft- and hardware based on the MicroTCA.4 standard in collaboration with the MicroTCA Technology Lab at DESY. An overview of the Linac is presented in this paper.

INTRODUCTION

In the frame of the NICA ion collider upgrade [1] a new light ion frontend Linac (LILac) for polarised particles, protons and ions with a mass to charge ration of up to 3 will be built. Behind the ion source and LEBT, LILac will consist of 3 parts:

1. a normal conducting Linac up to 7 MeV/u
2. a normal conducting energy upgrade up to 13 MeV/u
3. a superconducting section from 13 MeV/u up to a final energy to be determined

In this paper only the Part 1 of LILac up to 7 MeV/u is discussed. This normal conducting Linac will be built in collaboration between JINR and Bevatech GmbH.

The Linac will be located in LU20 hall at JINR and provides a beam energy of 7 MeV/u to be injected into the Nuclotron ring for further acceleration as a first stage of the project. Protons and light ions up to a mass to charge ratio of up to 3 will be used for either fixed target experiments to study baryonic matter or will be injected into the NICA collider ring for hadron matter and its phase transition experiments and to study spin physics on polarised particles.

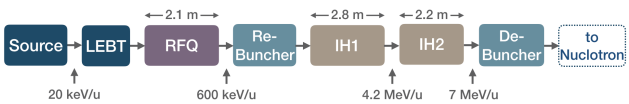


Figure 1: Scheme of the LILac cavities.

* benjamin.koubek@bevatech.com

The Linac consists of 5 cavities, an RFQ followed by a rebuncher, 2 IH-DTL structures and a de-buncher as shown in Fig. 1. It is operating at 162.5 MHz with a beam repetition rate of 5 Hz and a duty cycle of 0.15 % [2]. The main parameters of the LILac are summarised in Table 1. The length of the Linac comprising the cavities, the beam diagnostic devices and focusing magnets but excluding the de-buncher will be realised within a length of 9 m. A scheme of the LILac cavities is shown in Table1.

Table 1: LILac Main Parameters

Parameter	Protons	C^{4+}
Mass to Charge Ratio	1	3
Injection Energy	20 keV	60 keV
Exit Energy	7 MeV	21 MeV
Beam Current	5 mA	15 mA
Repetition Rate Limit	≤5 Hz	
Current Pulse Duration	30 μs	
RF Pulse Length	200 μs	
RF Frequency	162.5 MHz	
Transmission	≥80 %	
Full Length of the Linac	<9 m	

Each cavity will be fed by a dedicated high power solid state amplifier to provide the corresponding power for the accelerating fields in the cavities. The LLRF control soft- and hardware based on the MicroTCA.4 standard will be developed together with Bevatech and the MicroTCA Technology Lab at DESY.

ARCHITECTURE

Ion Source and LEBT

At the LILac two different ion sources, a laser ion source (LIS) and a source of polarised ions (SPI), will be used. From the LIS it is planned to receive light ions, while the SPI will generate polarised and non-polarised protons [3]. The ion sources are placed on a high-voltage terminal (up to 150 kV) [4]. The LEBT channel with a length of about 1.8 m is split into two main parts. The first part is an electrostatic section with ion optics and an electrostatic tube, and the second part uses two magnetic solenoids with a maximum magnetic field of 1.2 T. This channel will be similar to the existing which works at the LU-20 pre-injector.

Content from this work may be used under the terms of the CC BY 3.0 licence (© 2018). Any distribution of this work must maintain attribution to the author(s), title of the work, publisher, and DOI.

ISBN: 978-3-95450-194-6 ISSN: 2226-0366 doi:10.18429/JACoW-LINAC2018-TUPO019

SPIRAL2 CRYOGENIC SYSTEM THERMODYNAMIC BEHAVIOUR PREDICTION THROUGH DYNAMIC MODELING

A. Vassal*, P.E. Bernaudin, A. Ghribi, GANIL, 14000 Caen, France
P. Bonnay, F. Bonne, F. Millet, CEA/INAC/SBT, 38000 Grenoble, France

Abstract

SPIRAL 2 (Caen, France) is a state of the art superconducting linear accelerator composed of 26 quarter wave accelerating cavities. Each cavity is plunged in a liquid helium bath at 4.4 K itself surrounded by a thermal shield at 70 K. In this paper, a dynamic model of the cryogenic system of the LINAC is proposed. This model simulates the dynamic behaviour of the 19 cryomodules and their respective valves box connected through the cryodistribution. Model accuracy is evaluated through a comparison between simulation and experimental data. Using the model we should be able to predict the behaviour of the cryogenic system for different beam operating conditions of the accelerator. The model also highlights the link between the cryogenic system and the cavity RF losses through a dynamic estimator of those RF losses in the cavity walls. The latter could be used as a rough estimator of the quality factor of a cavity.

INTRODUCTION

SPIRAL2 accelerator aims at delivering high intensity beams for research in the nuclear fields [1]. It is built around a LINAC (LINear ACcelerator) composed of 26 quarter wave accelerating cavities. Because they are made of bulk niobium, each cavity is plunged in a liquid helium bath. The whole formed by the cavity and its helium bath is called a cryomodule. Liquid helium production and routing is ensured by a complex cryogenic system [2]. To provide the best operating condition for the LINAC it is necessary to understand the behaviour of this cryogenic system. To do so we model the overall SPIRAL2 cryogenic system. Model accuracy is evaluated through experimental comparison. A dynamic estimator of the radio frequency (RF) losses is also proposed as a direct use of the model.

MATERIALS AND METHOD

The oveall cryogenic system of SPIRAL2 is modeled using the Simcryogenics [3] library on MATLAB/SIMSCAPE environment. The model is designed to be control oriented and to allow fast simulation. It means that only the macroscopic physical behaviour (e.g., pressure variation) are considered and not the microscopic ones (e.g., flow distribution in piping). Only two sub-systems of the cryogenic system are considered in this paper: the cryomodules and the cryodistribution. An RF losses estimator is also presented as a direct use of the model.

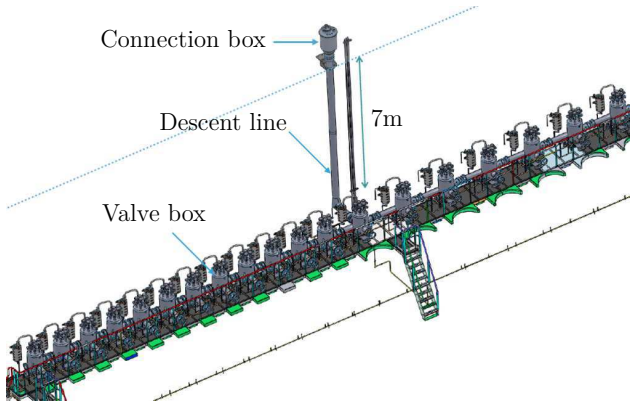


Figure 1: View of the SPIRAL2 cryodistribution without the cryomodules.

The Cryodistribution

The cryodistribution represents the link between the cryoplant and the cryomodules (see Fig. 1). It is composed of four lines: two for the cryomodule bath (supply and return) and two others for the cryomodule shield (also supply and return). The cryodistribution can be seen as multiple pipes connected together as shown in Fig. 2

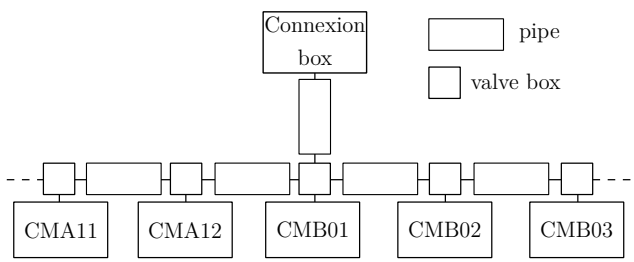


Figure 2: Decomposition of the cryodistribution in multiple pipes - *CMAi represents type A cryomodule whereas CMBi represents type B cryomodule*

To model the flow of helium in those pipes, three physical phenomena are considered:

- Friction: when a fluid is flowing in a pipe, it generates friction between the fluid and the pipe. This friction results in a pressure drop calculated through the Darcy-Weisbach equation: $\Delta P = f_D \frac{L}{D_h} \rho \frac{V^2}{2}$ with ΔP the pressure drop due to pipe friction, f_D the friction factor calculated with the Haaland approximation, L

* adrien.vassal@ganil.fr

Content from this work may be used under the terms of the CC BY 3.0 licence (© 2018). Any distribution of this work must maintain attribution to the author(s), title of the work, publisher, and DOI.

ISBN: 978-3-95450-194-6 ISSN: 2226-0366 doi:10.18429/JACoW-LINAC2018-TUPO020

MICROPHONICS INVESTIGATION OF ARIEL e-LINAC CRYOMODULES

Yanyun Ma†, K. Fong, M. Keikha, J. Keir, D. Kishi, S.R. Koscielniak, D. Lang, R.E. Laxdal, R. Nagimov, Z.Y. Yao, Q.W. Zheng, V. Zvyagintsev
TRIUMF, 4004 Wesbrook Mall, Vancouver, BC, Canada
Lutz Lilje, DESY, Notkestrasse 85, D-22607 Hamburg, Germany

Abstract

Now the stage of the 30 MeV portion of ARIEL (The Advanced Rare Isotope Laboratory) e-Linac is under commissioning which includes an injector cryomodule (ICM) and the 1st accelerator cryomodule (ACM1) with two cavities configuration. In this paper, the progress of the microphonics investigation and suppression of ICM and ACM1 is presented.

INTRODUCTION

ARIEL e-Linac is a continuous-wave (CW) electron linear accelerator utilizing superconducting bulk niobium technology at 1.3 GHz. The accelerator is divided into three cryomodules [1, 2]: a single cavity injector cryomodule (ICM) and two accelerating cryomodules (ACM) with two cavities each. The 'Demonstrator' phase of ARIEL was installed for initial technical and beam tests [3]. Then ACM1 cryomodule, high-power RF distribution system and LLRF system were updated for 2 cavities [4]. During commissioning, acoustic noise from the environment vibration generated by cooling water pumps, cryogenic system and vacuum system affect the ACM1 RF performance and final beam energy stability.

PONDERMOTIVE EFFECT

Both ICM and ACM1 are working in phase-locked loop (PLL) self-excited loop (SEL) in CW mode. Unlike the ICM with one cavity and one SEL loop, the two ACM1 cavities are driven by a single klystron with vector-sum control of the two cavity SEL PLL. As such there is no gradient regulation for each individual cavity in the ACM1 [5]. Individual tuner loops are established to maintain the cavity frequency with respect to the established reference phase. Microphonics can excite mechanical resonances in one cavity, perturbing the RF resonant frequency, which can couple to the other cavity via vector-sum regulation. The modulations of the RF field between the two cavities can drive a ponderomotive instability through Lorentz force detuning. The threshold for excitation of this instability is impacted both by ambient microphonic noise that can seed the instability and the precise settings of the two cavity phase loops. The coupled oscillation can deteriorate the e-Linac final energy stability outside specification and needs to be controlled.

During the commissioning, the ACM1 cavities gradients were limited by the ponderomotive effect when the summed voltage was higher than 17 MV. The ACM1 cavities pickup signals showed oscillation in counterphase (Fig. 1) while under vector-sum regulations impacting the energy stability and ultimately the loop stability.

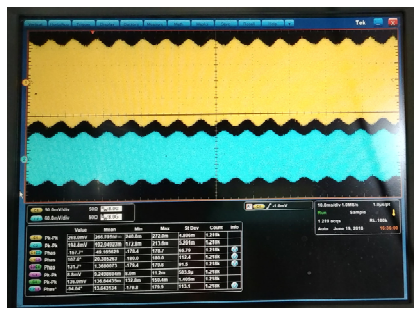


Figure 1: The ponderomotive oscillation of ACM1 pickup signals. The yellow waveform is 1st cavity pickup signal and the green waveform is 2nd cavity pickup signal.

NOISE OF PICKUP SIGNALS

To identify the noise peak for each cavity, the ACM1 was switched from vector-sum mode to single cavity mode and the pickup signals were analysed by phase noise analyser (R&S®FSWP26). Figure 2 shows that there is a noise hump from 10Hz to 400Hz in each pickup signal and indicates the noise sources are universal for all three cavities.

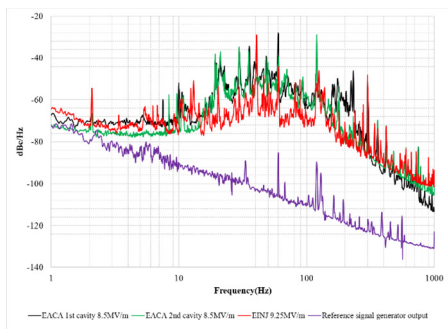


Figure 2: pickup signals noise analyses. During the test the ACM1 was setup in single cavity mode with closed amplitude and phase loop with low proportional gain; the ICM was under operational mode.

The coupling between microphonic noise disturbances and Lorentz force has been measured on ACM1 cavities. Amplitude modulations of various frequencies were added onto the amplitude loop driver while keep the amplitude loop and phase loop closed and fixed tuners position. Both cavities were measured at the similar e-field level. The parameters of the first 5 strongest microphonic disturbances coupling to Lorentz force are listed in Table.1.

† mayanyun@triumf.ca

Content from this work may be used under the terms of the CC BY 3.0 licence (© 2018). Any distribution of this work must maintain attribution to the author(s), title of the work, publisher, and DOI.

ISBN: 978-3-95450-194-6 ISSN: 2226-0366 doi:10.18429/JACoW-LINAC2018-TUPO022

MANUFACTURING OF X-BAND ACCELERATING STRUCTURES: METROLOGY ANALYSIS AND PROCESS CAPABILITY

J. Sauza Bedolla, S. Atieh, N. Catalan Lasheras, CERN, Geneva, Switzerland

Abstract

The fabrication tolerances of RF components are essential for CLIC X-band accelerating structures to perform efficiently. On one hand, the capability of high power accelerating structures depends on the shape accuracy and the asperity of the inner surfaces, when microwaves pass through the cavity. On the other hand, surface flatness and dimensional tolerances are necessary to guarantee a correct assembly process. Hence, the discs that build up the structure require sub-micrometre specifications and, in order to meet all the needs, ultra-precision machining using single crystal diamond tools is mandatory. This paper shows the analysis of the metrology results of the fabrication of 118 discs (4 accelerating structures). Dimensional and form tolerances are studied following the production order to find drifts in the production and to predict the impact on the assembly process. Finally, process capability is evaluated.

INTRODUCTION

The Compact Linear Collider (CLIC) is an international study for a future high-gradient, multi TeV electron-positron linear collider. In order to test CLIC's main parameters, 72 Accelerating Structures (AS) prototypes, of 22 different designs, have been built during the last ten years. Six principal suppliers of five different countries have participated in the production of CLIC components. This paper evaluates the performance of one of these suppliers in the production of four accelerating structures.

The AS baseline design represents a diffusion bonded stack of cylindrical Oxygen Free Electronic copper discs, which are machined to form a cavity of the RF cells. The discs (or cell) geometry and high order modes damping loads had been extensively optimized in order to maximize the RF-to-beam efficiency, and to meet the beam dynamics and high gradient RF constraints [1]. A regular cell disc is described by about ten different parameters that define its geometry. The internal shape and alignment of the cells are crucial for efficient collider operation. The mechanical tolerances of the cells have been defined according to the RF requirements [2] and they are defined in the CLIC Design Report [3]. Sub-micrometre tolerances are needed to reach the accelerating gradient goal of 100 Mv/m if no tuning is applied and if no temperature correction is allowed to the AS [4].

CLIC TD26R1CC PROTOTYPE

In 2015, there was a re-design of the 3 TeV CLIC main linac AS at 12 GHz [5]. This new prototype is a tapered, damped, 26 regular cells with integrated compact couplers. Main changes include a modification on the "nose" of the waveguide from an elliptical geometry to a 4-th order polynomial function. Moreover, the radius at the bottom of the RF waveguide was increased from 0.5 mm to 1 mm to allow the use of bigger milling cutter, and therefore, to reduce the machining cost. Finally, the disc diameter was increased from 74 mm to 83 mm in order to have a more rigid interface between waveguides and the disc stack. This is the biggest disc diameter design in CLIC production history. The most important tolerances were maintained with respect to the previous design.

- Diameter of the disc Ø83 mm: ±1 µm
- Concentricity of iris with respect to the disc diameter: 2 µm
- Cell iris shape accuracy (zone A): 5 µm
- Cell waveguide shape accuracy: 20 µm
- Flatness accuracy: 1 µm
- Cell iris roughness (zone A) Ra 0.025 µm
- Cell waveguide roughness Ra 0.1 µm

MANUFACTURING

The total fabrication included four structures: 98 standard cells plus 20 compact coupler cells (total 118 discs). This quantity represents the biggest amount of discs ever produced in a single order. The contract was adjudicated to one qualified, CERN's member state company. The production of the whole supply took four months. The parts were produced by a combination of Ultra-Precision diamond fly cutting, milling and turning. All discs were manufactured in batches of four in the milling step, while they were individually machined in the fly cutting and turning steps. The parts were measured at the factory with a customized CMM machine (accuracy better than 0.6 µm) for dimensional control and a white light interferometer (non-contact) for roughness measurements. Results were validated at CERN, where no significant differences were found. Furthermore, visual inspection was also performed before accepting the batch (Figure 1).

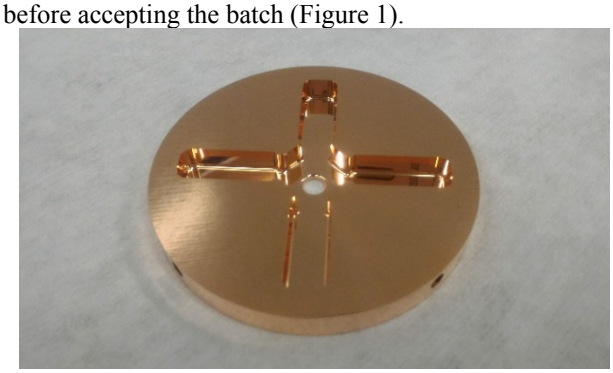


Figure 1: Visual inspection of a standard cell.

Content from this work may be used under the terms of the CC BY 3.0 licence (© 2018). Any distribution of this work must maintain attribution to the author(s), title of the work, publisher, and DOI.

ISBN: 978-3-95450-194-6 ISSN: 2226-0366 doi:10.18429/JACoW-LINAC2018-TUPO023

PRESERVING MICROMETRE TOLERANCES THROUGH THE ASSEMBLY PROCESS OF AN X-BAND ACCELERATING STRUCTURE

N. Catalan Lasheras, A. Grudiev, J. Sauza Bedolla, H. Bursali, A. Solodko, K. T. Szypula, S. Lebet, E. Rodriguez Castro, P. Sobrino Mompean, CERN, Geneva, Switzerland

Abstract

The CLIC structures are designed for operating at X-Band, 2π/3 traveling wave mode with a loaded 100 MV/m gradient. Mechanical tolerances, at the submicron level, are required to satisfy the RF design constraints and beam dynamics and are reachable using ultra-precision diamond machining. However, inherent to the manufacturing process, there is a deviation from the nominal specifications and as a result; incorrect cavity dimensions produce a less efficient linac. Moreover, the assembly process increase the difference from the original geometry. As part of a cost and manufacturability optimization of the structures for mass production, this study aims to identify a correlation between frequency deviations and geometrical errors of the individual discs of the accelerating structures caused by the production process. A sensitivity analysis has been carried out to determine the most critical parameters. Cell frequency deviations have been monitored by bead pull measurements before and after bonding. Several accelerating structure prototypes have been tested to determine our assumptions and to assess if the assembly process preserves the tight tolerances achieved by machining.

INTRODUCTION

CLIC baseline accelerating structure (AS) stack is composed by a variable quantity of discs of the prototype being produced. The cavity formed by the disc represents the RF zone. The geometry of the disc depends on different parameters and each of these parameters contributes differently to satisfy the RF design. Sub-micrometre tolerances are needed to reach the accelerating gradient goal of 100 MV/m if no tuning is applied and if no temperature correction is allowed to the AS [1]. However, the normal variability of the manufacturing processes makes that the disc presents discrepancies with respect to the nominal design. This paper aims at identifying the most critical design parameters through the means of a sensitivity analysis of the geometrical effects on the AS regular cells. For this purpose, six AS of two different prototypes are analysed: T24 N4 and N5 (Figure 1.a) and TD26 N1 to N4 (Figure 1.b).

GEOMETRICAL PARAMETERS

RF designs of both T24 and TD26 discs has been completed by ANSYS High Frequency Structure Simulator (HFSS) software. The T24 prototype consists of 24 undamped cells with a weak tapering of the irises [2]. The geometry of the standard cell is illustrated in Figure 2.a: ***b*** represents the inner radius; ***a*** is the iris aperture and ***h*** the height of the cell. The TD26 prototype also consists of 26 tapered cells with integrated coupling cells [3]. The TD26 cells have more complicated RF design compare to T24 cells because they include damping waveguides as illustrated in Figure 2.b (design with symmetry plane) where ***a***, ***b***, ***L***, ***w*** and ***HW*** represents iris aperture, inner radius, height, width and length of the damping part of the cell.

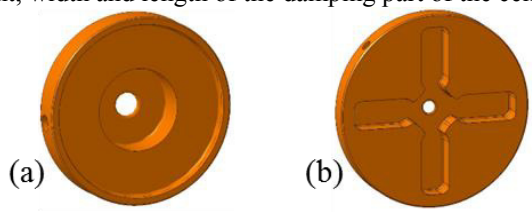


Figure 1: (a) T24 and (b) TD26 regular disc.

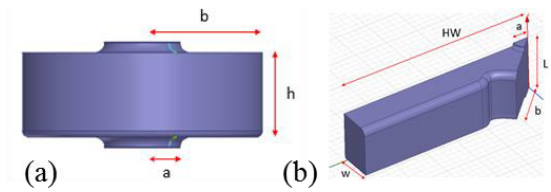


Figure 2: Geometrical parameters of (a) T24 and (b) symmetry plane of TD26.

SENSITIVITY ANALYSIS

In a sensitivity analysis, each geometric parameter is varied slightly around the design value to determine the sensitivity of the return loss to that parameter. The analysis was performed using ANSYS HFSS. The results for both T24 and TD26 included the first, middle and last cells (only first cell is shown) with ±10 µm interval around the nominal design value. According to the simulation results, the most sensitive geometrical parameter to the frequency change is the inner radius ***b*** for T24 cells, followed by the iris diameter **a** (Figure 3).

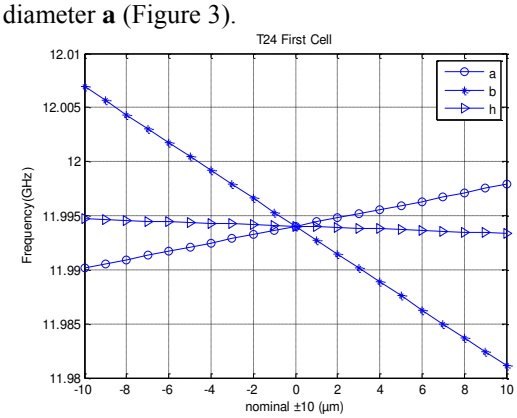


Figure 3: Frequency sensitivity of T24 cell.

The same behaviour of the cell parameters to frequency change is still valid for TD26 cells. The most sensitive geometrical parameter to frequency change is the inner radius ***b*** as T24, followed by the iris diameter (Figure 4).

Content from this work may be used under the terms of the CC BY 3.0 licence (© 2018). Any distribution of this work must maintain attribution to the author(s), title of the work, publisher, and DOI.

ISBN: 978-3-95450-194-6 ISSN: 2226-0366 doi:10.18429/JACoW-LINAC2018-TUPO027

SERIES PRODUCTION OF THE SPECIFIC WAVEGUIDE DISTRIBUTION FOR THE EUROPEAN XFEL AT DESY

B.Yildirim[1], S.Choroba[1], V.Katalev[1], P.Morozov[1], Y.Nachtigal[1], E.Apostolov[2]
[1]DESY, Hamburg, Germany
[2]Technical University of Sofia, Bulgaria

Abstract

The European XFEL uses 100 accelerating cryomodules. One RF station with 10 MW klystron supplies, through a waveguide distribution, four cryomodules with eight cavities each. The RF station operates at 1.3 GHz, 1.37 ms pulse width and 10 Hz repetition rate. The results of the cryomodule test have shown however different maximum gradients for each cavity. The maximum gradient has been measured between 11 MV/m and 31 MV/m, which requires cavity power of 29 kW to 230 kW. To operate with the maximum energy for every cryomodule, it is necessary to supply individual power to the cavity. In this case the weakest cavity problem can be avoided. For this goal, a specific waveguide distribution has been developed. 100 waveguide distributions have been successfully tailored, produced, and tested at the Waveguide Assembly Test Facility (WATF) at DESY and finally assembled to the cryomodules.

We present the series production of the specific waveguide distributions at the WATF.

REQUIREMENTS FOR WAVEGUIDE DISTRIBUTION PRODUCTION

To meet the requirements for measuring such complex waveguide distribution, basically three different test stands have been created for special procedures of measurements at the Waveguide Assembly Test Facility (WATF), binary cell test stand, LLRF test stand and HPRF test. The installation of all test stands had taken a lot of time due to the mechanical control and RF control. In addition, the custom-built test stands needed special equipment to avoid mistakes during measurements.

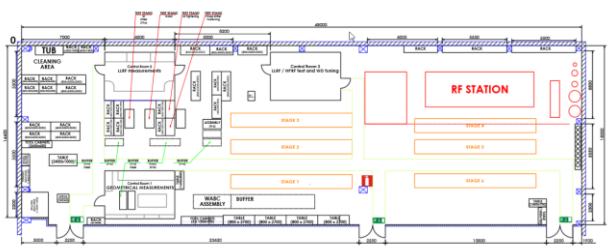


Figure 1: Layout of the WATF.

Fig. 1 shows the 670 m^2 area of the WATF. The WATF includes two RF laboraty for LLRF and HPRF tests of the waveguide distributions. In addition the WATF area has a laboraty for the waveguide components referring to the geometric parameter control. An assembly area with five movable platforms for installation of the waveguide distributions is also part of the WATF. Many auxiliarities systems such as waveguide distribution support hangers, water cooling systems and cable trays are available at the WATF. Furthermore there is a test area for reliability position tests of the movable phase shifters and for pneumatic components. The WATF includes test areas for cooling water leakage, for pressure hydraulic tests and for checking of isolators cooling water flow sensors. In addition there is an area for cleaning, drying and dust hermetically covering of the waveguide components. To avoid problems with logistic time from main store, there is a small area for storing six waveguide distributions.

The working process at the WATF provides a parallel installation of different systems such as waveguide distribution supporting structures, water cooling systems, and flexibility in the assembly activities organization.

More than 150 complex mounting, adjustment, measurement and control operations are performed at the WATF for each waveguide distribution.

The waveguide distribution is based on the tunable binary cells and the tunable asymmetric shunt tees [1]. It consists of several specific waveguide components, which were created precisely to operate with the maximum energy for every cryomodule. On the one hand, the waveguide distribution should have a compact size, on the other hand it should supply high pulse RF power to the individual cryomodule cavities with high flexibility by only one power klystron.

Each RF station of the test facility consists of a 5 MW RF station, with a waveguide distribution. Each waveguide distribution supplies RF power to eight cavities, four pair of cavities as shown in Fig. 2.

In order to satisfy these conditions, specific waveguide components have been developed and integrated in the waveguide distribution for the series production of the specific waveguide distribution.

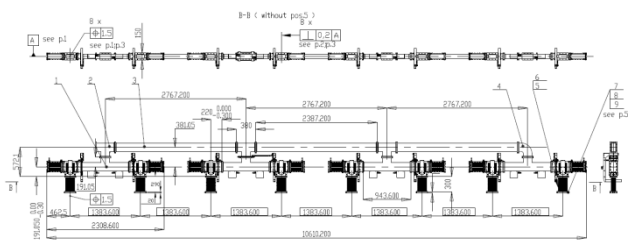


Figure 2: Layout of the XFEL waveguide distribution.

Content from this work may be used under the terms of the CC BY 3.0 licence (© 2018). Any distribution of this work must maintain attribution to the author(s), title of the work, publisher, and DOI.

ISBN: 978-3-95450-194-6 ISSN: 2226-0366 doi:10.18429/JACoW-LINAC2018-TUPO028

RETREATMENT OF EUROPEAN XFEL SERIES CAVITIES AT DESY AS PART OF THE REPAIR OF EUROPEAN XFEL ACCELERATING MODULES

S. Sievers†, N. Krupka, D. Reschke, S. Saegebarth, J. Schaffran, M. Schalwat, P. Schilling, M. Schmoekel, N. Steinhau-Kuehl, B. v. d. Horst, E. Vogel, H. Weise,
Deutsches Elektronen-Synchrotron DESY, 22607 Hamburg, Germany
M. Wiencek, Instytut Fizyki Jądrowej PAN, 31-342 Kraków, Poland

Abstract

For the European XFEL 102 accelerating modules were built and tested. Several accelerating modules had to be reworked due to different kinds of non-conformities. The extent of this rework varied greatly. At the end of production four accelerating modules could not be qualified in time before the tunnel installation was to be finished in September 2016. Meanwhile the cavity strings of two of these accelerating modules have been disassembled in the DESY clean room. The cavities have been retreated at DESY either by additional high pressure water rinsing or BCP flash chemical treatment. All cavities were vertically tested and 15 out of 16 were qualified for the reassembly of the cavity strings. One accelerating module will be reassembled completely and tested until the end of 2018; the other will follow in the first half of 2019. We report on retreatment procedures and performance of these cavities.

INTRODUCTION

The European XFEL was built in a European Collaboration [1] and is located at DESY in Hamburg. The superconducting cavities have been built in industry in Italy [2] and Germany [3] and tested at DESY. From there the cavities were brought to CEA Saclay, France for accelerating module assembly [4,5]. After assembly the accelerating modules were shipped back to DESY for test and tunnel installation.

On 61 of the 102 accelerating modules for the European XFEL, repair actions of different extent have been performed to qualify them for tunnel installation. Four of these accelerating modules did not qualify for tunnel installation in time and had to be further investigated. These accelerating modules (XM8, XM46, XM50 and XM99) are being reworked at DESY in Hamburg [6].

Already during the production phase of the European XFEL, cavities that did not match the acceptance criteria were retreated mostly at DESY [7]. In the same way the cavities of the XFEL accelerating modules XM46 and XM50 have been treated.

RETREATMENT PASSES

For the retreatment of superconducting European XFEL series cavities that did not achieve the approval for string installation, different retreatment passes were specified [8]. During the repair of the accelerating modules XM46 and XM50 only the retreatment passes RP1 and RP2 were applied. The retreatment pass RP1 is mainly an additional high pressure rinsing (HPR), while RP2 is an additional chemical polishing (BCP). The complete retreatment cycles are described in Table 1 and Table 2.

After the retreatment all cavities are vertically tested to determine their usable gradient in the vertical cryostats at the Accelerator Module Test Facility AMTF [9] at DESY.

Table 1: Retreatment Pass - RP1

Cleaning by ultrasonic cleaning and ultra-pure water rinsing to enter ISO 4 cleanroom
Venting to normal pressure with 3 l/min Nitrogen gas flow rate
Dismounting of beam tube flange short side
Six times high pressure rinsing and drying for 12 hours in ISO 4 cleanroom area
Assembly of beam tube flange
Pump down, leak check with standard turbo molecular pumping unit

Table 2: Retreatment Pass – RP2

Cleaning by ultrasonic cleaning and ultra-pure water rinsing to enter ISO 4 cleanroom
Venting to normal pressure with 3 l/min Nitrogen gas flow rate
Dismounting of all cavity accessories
Chemical treatment of maximum removal of 10 µm by BCP, ultra-pure water rinsing and one time HPR.
Drying for 12 hours in ISO 4 cleanroom area
Assembly of accessories and beam tube flanges to cavity, leak check
Dismounting of beam tube flange short side
Six times high pressure rinsing and drying for 12 hours in ISO 4 cleanroom area
Assembly of beam tube flange
Pump down, leak check and residual gas analysis (RGA) with standard standard turbo molecular pumping unit
120°C baking

REWORKED MODULES

On seven accelerating modules beam vacuum leaks were found after the assembly or appeared during the module tests at AMTF. These leaks may affect the cavities directly.

† sven.sievers@desy.de

Content from this work may be used under the terms of the CC BY 3.0 licence (© 2018). Any distribution of this work must maintain attribution to the author(s), title of the work, publisher, and DOI.

ISBN: 978-3-95450-194-6 ISSN: 2226-0366 doi:10.18429/JACoW-LINAC2018-TUPO029

HIGHLIGHTS OF THE XM-3 CRYOMODULE TESTS AT DESY

J. Branlard†, V. Ayvazyan, A. Bellandi, J. Eschke, Ç. Gümüş, D. Kostin, K. Przygoda, H. Schlarb, J. Sekutowicz, DESY, Hamburg, Germany
W. Cichalewski, DMCS, Łódź, Poland

Abstract

To investigate the feasibility of the continuous wave (CW) upgrade [1] of the European X-ray free electron laser (XFEL), on-going tests are performed on XFEL prototype and production cryomodules since 2011. For these studies, DESY's cryomodule test bench (CMTB) has been equipped with a 105 kW CW capable inductive output tube (IOT) in addition to the 10 MW pulsed klystron, making CMTB a very flexible test stand, enabling both CW and pulsed operation. XFEL-like low level radio frequency (LLRF) electronics is used for these tests to stabilize amplitude and phase of the voltage vector sum (VS) of all 8 cavities of the cryomodule under test. The cryomodule most often tested is the pre-series XM-3, unique since it is housing one fine grain niobium and seven large grain niobium cavities. Modified flanges were installed in autumn 2017 on all 8 input couplers to increase the maximum reachable loaded quality factor (Q_L) beyond 2E7. With higher Q_L, up to 6E7 for 6 cavities and 3E7 for 2 cavities, we have investigated the VS stability and SRF-performance of this cryomodule under various conditions of cooling down rate and operation temperature 1.65K, 1.8K and 2K, at gradients up to 21.5 MV/m. The results of these tests are presented in this paper.

INTRODUCTION

The cryomodule test bench at CMTB offers versatile test conditions to investigate superconducting radio frequency (SRF) cryomodules under various conditions. It is equipped with a 10 MW klystron used for pulsed operations and a 105 kW inductive output tube used for continuous wave (CW) or long pulse (LP) operations. Two independent LLRF systems can be used to perform single cavity or vector sum field regulation. The LLRF system includes RF field feedback and resonance control using stepper motors and fast piezo feedback looped around individual cavities [2]. The waveguide distribution system can be adjusted to distribute power according to the different cavity performance. The cryogenic plant, supporting both the free electron laser in Hamburg (FLASH) and CMTB has a cooling capacity of 6.8 kW at 4.3K making it robust to heat load intensive experiments. Since 2011, several test runs have been carried out at CMTB to investigate the challenges associated with CW operation of XFEL-like cryomodules. The dynamic heat load and in particular the impact of end-cell heating was investigated as a function of RF pulse duty factor and gradient in [3].

More recently RF stability measurements for Q_L as high as 1.5E7 were reported in vector sum [4] and for single cavity operation [5]. To investigate issues related to narrow bandwidth and high gradient operations the input power couplers have been modified to reach higher Q_L, as described in section I. The dynamic heat load of individual cavities was measured to estimate the cavity unloaded quality factor (Q_0) as a function of gradient for different cryogenic temperatures. These results are reported in section II. Section III reports on the RF field stability performance demonstrated in CW for various gradient as high as 21.5 MV/m and various Q_L up to 8.2E7. A short summary and perspectives are given in the conclusion.

COUPLER MODIFICATIONS

The eight couplers of the XFEL pre-series cryomodule XM-3 were modified to move the Q_L range towards higher values. This was achieved by inserting a modified iso-vac flange, shown in blue in the figure below, moving the warm part of the coupler 10 mm further away from the 70K window. The motorized coupler allows for an additional 5mm displacement.

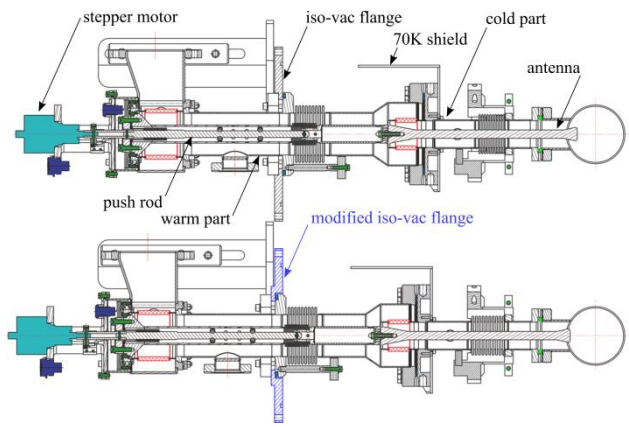


Figure 1: Unmodified XFEL power coupler (top) and with the modified iso-vac flange (bottom), shifting outwards the warm part of the coupler.

The achievable Q_L ranges before and after modification are listed in Table 1. Simulation predicts that a 5 mm displacement induces a Q_L increase from 2E7 to 8E7 which would suffice. In practice this increase in Q_L value was achieved by a 10 mm displacement, due to the fact that the coupling antenna also moved sideways. The improved Q_L range was limited in the case of cavity 7 and 8. This is due to a collision between the coupler 70K shield and the cryomodule 70K shielding cut out appearing after cool down for larger coupler movements on the last cavities (C7 and C8).

† julien.branlard@desy.de

Content from this work may be used under the terms of the CC BY 3.0 licence (© 2018). Any distribution of this work must maintain attribution to the author(s), title of the work, publisher, and DOI.

ISBN: 978-3-95450-194-6 ISSN: 2226-0366 doi:10.18429/JACoW-LINAC2018-TUPO030

PRECISE EVALUATION OF CHARACTERISTIC OF THE MULTILAYER THIN-FILM SUPERCONDUCTOR CONSISTING OF NbN AND INSULATOR ON PURE Nb SUBSTRATE

R. Katayama*, Y. Iwashita, H. Tongu, Kyoto ICR, Uji, Kyoto
A. Four, CEA/DRF/IRFU, Gif-sur-Yvette, C. Z. Antoine, CEA/IRFU, Gif-sur-Yvette
H. Hayano, T. Kubo, T. Saeki, KEK, Ibaraki, Hayato Ito, Sokendai, Ibaraki
R. Ito, T. Nagata, ULVAC, Inc, Chiba
H. Oikawa, Utsunomiya University, Tochigi

Abstract

In recent years, it has been pointed out that the maximum accelerating gradient of a superconducting RF cavity can be pushed up by coating the inner surface of the cavity with a multilayer thin-film structure that consists of alternating insulating and superconducting layers. In this structure, the principal parameter that limits the performance of the cavity is the critical magnetic field or effective H_{C1} at which vortices start penetrating into the superconductor layer, and it is predicted to depend on the combination of the film thickness. We made samples that have NbN/SiO_2 thin-film structure on pure Nb substrate with several thicknesses of NbN film deposited using DC magnetron sputtering method. Here, we report the measurement results of effective H_{C1} of the NbN sample with a thickness of 200 nm by using the third-harmonic voltage method. In addition, we report the preliminary results to evaluate the dependence of the effective H_{C1} on the thickness of the NbN film in the range 50 nm–200 nm.

INTRODUCTION

Recently, it has been pointed out that the effective H_{C1} of a superconducting RF cavity might be pushed up by coating the inner surface of the cavity with a multilayer thin-film structure that consists of alternate insulating and superconducting layers [1–3]. Hereafter, such multilayer structures on pure bulk Nb in superconducting state is referred to as S-I-S (Superconductor-Insulator-Superconductor) structure. Generally, the effective H_{C1} of a superconducting material can be evaluated by applying a sine-wave magnetic field to the material with a small coil and detecting the third-harmonic signal of the coil voltage because the third-harmonic signal occurs when the phase transition from the full Meissner state to the vortex-penetrating state happens. Hereafter, this method is called third harmonic voltage method. C. Antoine already showed that a multilayer structure on a Nb substrate has higher effective H_{C1} than that of the Nb substrate by the third-harmonic voltage method [4]. We also verified that the effective H_{C1} is enhanced for a sample that consists of NbN (200 nm) and SiO_2 (30 nm) formed on pure Nb substrate that has an RRR of >250 [5]. Our measurement result on the third harmonic measurement using AC magnetic fields less than 13 mT are reported in IPAC18 proceedings. This article describes details of the new result to evaluate effective H_{C1} of the NbN(200 nm)/SiO_2(30 nm)/Nb sample using the AC magnetic field of the amplitude up to 44 mT. In addition, in order to evaluate the dependence of effective H_{C1} on the film thickness, this article presents the preliminary result of the measurement of effective H_{C1} of the NbN(50 nm)/SiO_2(30 nm)/Nb sample using the AC magnetic field of the amplitude up to 29 mT.

* katayama@kyticr.kuicr.kyoto-u.ac.jp

THIRD HARMONIC MEASUREMENT

For the third harmonic voltage method, an AC magnetic field at the frequency of 5 kHz is generated by a coil close to the superconducting sample and the third harmonic voltage $v_3(t) = V_3 \sin(3\omega t)$ induced in the coil is simultaneously measured [6]; ω is the frequency of a sinusoidal drive current, $I_0 \sin(\omega t)$ represents the current flowing in the coil, and V_3 is the amplitude of $v_3(t)$. If the temperature of a sample in superconducting state is being raised while amplitude of AC magnetic field H_0 is fixed, V_3 suddenly rises when H_0 exceeds the effective H_{C1} of the sample at a certain temperature. In the measurement performed at Kyoto University, H_0 is controlled by drive current I_0, and the temperature dependence of the effective H_{C1} is estimated from the temperatures at moments when V_3/I_0 suddenly rises. Refer to [5] for details of the measurement setup and flow.

In this study, the coil magnetic field is calibrated with the third harmonic measurement result of pure bulk Nb assuming that the following function $F(T)$ represents the temperature dependence of the effective H_{C1} of pure bulk Nb.

$$F(T) = \begin{cases} 0.18 \times \left(1 - (T/9.2)^2\right) & (T < 9.2\text{K}) \\ 0 & (T > 9.2\text{K}) \end{cases} \quad (1)$$

The calibration curve obtained from this measurement is shown in Fig. 1. The vertical axis is the coil magnetic field, and the horizontal axis is the drive current amplitude I_d derived from the digitized data recorded by our measurement system.

DETAILS OF MEASUREMENT RESULT

We have tested two multilayer samples that consist of NbN and SiO_2 coated on pure bulk Nb. The pure bulk Nb

Content from this work may be used under the terms of the CC BY 3.0 licence (© 2018). Any distribution of this work must maintain attribution to the author(s), title of the work, publisher, and DOI.

ISBN: 978-3-95450-194-6 ISSN: 2226-0366 doi:10.18429/JACoW-LINAC2018-TUPO031

INVESTIGATION OF THE SURFACE RESISTANCE OF NIOBIUM BETWEEN 325 MHz AND 1300 MHz USING A COAXIAL HALF-WAVE CAVITY*

H. Park[1†], J. R. Delayen[1], S. U. De Silva
Center for Accelerator Science, Old Dominion University, Norfolk, VA 23529
[1]also at Jefferson Lab, Newport News, VA 23606, USA

Abstract

The surface resistance of superconductors depends on frequency, temperature, rf field strength, and surface preparation. In particular, a low temperature bake around 100 C has been shown to modify the high-field behavior of the surface resistance. Using a coaxial half-wave resonator operating at 325, 650, 975 and 1300 MHz [1, 2] we have initiated a research program to better understand the role of low temperature heat treatment on the surface resistance of niobium.

INTRODUCTION

The well-known expressions for the surface resistance of superconductors in electromagnetic fields, and its dependence on frequency, temperature, and a few materials parameters, were obtained as a perturbation theory under the assumption that the magnitude of the electromagnetic field is much smaller than the critical field. This resulted in a surface resistance independent of the magnitude of the electromagnetic field.

There have been several attempts at developing theories of the surface resistance at high rf field, up to the critical field [3-5], but, at present, there is no universally accepted consensus on the correct fully self-consistent theory.

So far, the origin of residual resistance is believed to be a result of extrinsic mechanisms such as trapped vortices, metallic suboxide layers at the surface, non-superconducting precipitates (hydrides, etc). The full theory should include residual resistance. Extracting frequency, temperature, rf field dependence will provide significant insight to a better understanding. Because of the statistical nature of multiple materials defect, technological contributions to surface resistance and the lack of reproducibility, it is difficult to extract accurate frequency dependence of the surface resistance when different cavities of different frequencies are tested.

Coaxial half wave resonator provides the frequencies reasonably separated and the same location where the high surface magnetic field is distributed.

FREQUENCY DEPENDENCE

In the low-field limit the BCS surface resistance of superconductors is given by

$$R_{BCS} \cong \frac{\mu_0^2 \omega^2 \lambda^3 \sigma_n \Delta}{k_B T} \ln\left[\frac{C_1 k_B T}{\hbar\omega}\right] \exp\left[-\frac{\Delta}{k_B T}\right] \qquad (1)$$

In real materials, however, the non-isotropy of the gap and the Fermi surface, and the smearing of the gap can produce deviations from Eq. (1).

In the past the frequency dependence of the surface resistance was usually obtained by measurements in different frequencies and, over the range of interest for particle accelerators was of the form $\omega^{1.7\to2}$.

Not included in Eq. (1) also is the so-called residual surface resistance which includes all the sources of power dissipation that do not vanish as $T \to 0$.

Figure 1 shows the temperature dependence of the low-field surface resistance measured in the four lowest TEM modes of the half-wave cavity.

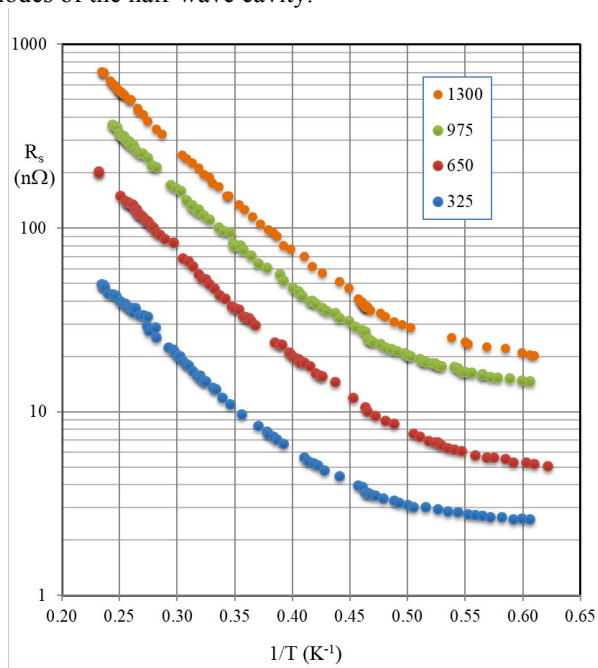


Figure 1: Temperature dependence of the low-field surface resistance of the four lowest TEM modes.

The results of Fig. 1 were obtained after the following surface preparation and treatments.

1. Post fabrication cleaning. Cleaning followed typical UHV cleaning procedure. The cavity was cleaned in a heated ultrasonic tank and triple rinsed with deionized ultra pure water.
2. Bulk BCP. Damaged niobium layer was removed by the chemical composition of HF (48%):HNO_3 (60%):H_3PO_4 (85%) = 1:1:2 inside the clean room. It was aimed to remove 150 microns but the thickness

* Work supported by NSF Award No. PHY-1416051
† hkpark@jlab.org

Content from this work may be used under the terms of the CC BY 3.0 licence (© 2018). Any distribution of this work must maintain attribution to the author(s), title of the work, publisher, and DOI.

ISBN: 978-3-95450-194-6 ISSN: 2226-0366 doi:10.18429/JACoW-LINAC2018-TUPO032

FIRST TEST RESULTS OF SUPERCONDUCTING TWIN AXIS CAVITY FOR ERL APPLICATIONS *

H. Park[1,2#], S. U. De Silva[1], J. R. Delayen[1], F. Marhauser[2], A. Hutton[2]
[1]Center for Accelerator Science, Old Dominion University, Norfolk, VA 23529, USA
[2]Thomas Jefferson National Accelerator Facility, Newport News, VA 23606, USA

Abstract

RF superconducting (SRF) cavities with two beam pipes have been proposed in the past for energy recovery linac applications. The relatively complex geometry of those cavities presented a serious challenge for fabrication and surface processing. The main concerns have now been overcome with the fabrication and successful RF testing of a new elliptical twin-axis cavity proposed by Jefferson Lab (JLab) and optimized by the Center for Accelerator Science (CAS) at Old Dominion University (ODU) in the framework of a DoE accelerator stewardship program. The cavity design provides uniform accelerating or decelerating fields for both beams. This paper describes the cavity design, fabrication experience, and the first cold RF test results and explores potential applications especially for JLab's EIC (JLEIC).

INTRODUCTION

SRF accelerating structures with two beam pipes ('twin axis' cavity) intended for Energy Recovery Linacs (ERLs) applications were proposed a decade ago [1-3]. A seemingly complicated cavity was fabricated by KEK [1] but such a cavity has never been tested and therefore the feasibility has not been proved. ODU CAS designed the new geometry focusing on ease of fabrication and post-processing utilizing today's well-controlled procedures. The design was optimized to minimize the peak RF surface fields, to provide the same longitudinal electric field profile in both beam tubes, and eliminate multipacting [4]. The cavity design also provides a relatively strong cell-to-cell coupling so that several cells can be joined together for a multiple cell cavity design. The fabrication and post-processing followed typical methods used for conventional single beam pipe elliptical SRF cavities [5]. Room temperature measurements and a vertical cold test have been completed. The results prove the feasibility of the twin axis cavity that could be useful for applications such as in the JLEIC cooler ERL [6] or an asymmetric dual axis ERL [7].

DESIGN

The design went through a couple of evolutions to arrive at an optimized RF design, which provides good RF electromagnetic performance properties [4]. The final design is shown in Fig. 1 and its RF properties are summarized in Table 1 [4].

*Work supported by DOE Office of Science via Accelerator Stewardship Test Facility Pilot Program (Proposal No. 0000219731). This work used resources of the NERSC center, which is supported by DOE Office of Science Contract No. DE-AC02-05CH11231.
#hkpark@jlab.org

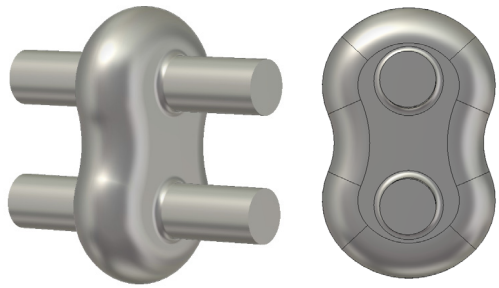


Figure 1: Elliptical-shaped twin axis cavity.

Table 1: Cavity Parameters and rf Properties of the 1497 MHz Single Cell Twin Axis Cavity as Fabricated

Parameter	Value as designed	Unit
Cavity height	202.5	mm
Cavity width	300.0	mm
Cavity length	100.13	mm
Cell length	81.13	mm
Iris curvature	8.0	mm
Beam aperture	60.0	mm
Beam axis separation	136.5	mm
E_p/E_{acc}^*	2.68	-
B_p/E_{acc}^*	5.5	mT/(MV/m)
$[R/Q]$	60.1	Ω
G	320.8	Ω
R_tR_s	1.93×10^4	Ω^2
LOM	1103	MHz
Nearest HOM	1806	MHz

The cavity uses the second TM110 mode as the operating mode. The transverse field components of the operating mode were minimized at the beam pipe centers, and the beam pipes are slightly shifted from the center to cancel the dipole effect [4].

FABRICATION

The fabrication process was comparable to that of typical single beam pipe elliptical cavities. The stamping die set consists of half-cell male and female dies, beam pipe opening punches, and a coining ring with one female

Content from this work may be used under the terms of the CC BY 3.0 licence (© 2018). Any distribution of this work must maintain attribution to the author(s), title of the work, publisher, and DOI.

ISBN: 978-3-95450-194-6 ISSN: 2226-0366 doi:10.18429/JACoW-LINAC2018-TUPO033

CRYOGENIC TEST RESULTS OF THE SPS PROTOTYPE RF-DIPOLE CRABBING CAVITY WITH HIGHER ORDER MODE COUPLERS*

S. U. De Silva[1, †], H. Park[2], J. R. Delayen[1], Z. Li[3]
[1]Old Dominion University, Norfolk, VA, USA
[2]Thomas Jefferson National Accelerator Facility, Newport News, VA 23606, USA
[3]Stanford Linear Accelerator National Laboratory, Menlo Park, CA 94025, USA

Abstract

The rf-dipole crabbing cavity planned for the LHC High Luminosity Upgrade is designed to deliver a transverse kick of 3.34 MV; crabbing the proton beam in the horizontal plane. The proton beams of the LHC machine operating at 7 TeV each sets high impedance thresholds on the crabbing cavity systems. The rf-dipole crabbing cavity is designed with a two higher order mode couplers to suppress those HOMs. The first prototype of the HOM couplers are fabricated at Jefferson Lab. This paper reports the cryogenic test results of the HOM couplers with the SPS prototype rf-dipole cavity.

INTRODUCTION

Crabbing cavity systems are an essential component in the LHC High Luminosity Upgrade in recovering the loss of luminosity due to the crossing angle of the colliding bunches [1]. These crabbing systems allow head-on collision of bunches compensating the loss of luminosity. Novel compact crabbing cavities have been designed to meet the tight dimensional constraints in LHC [2]. The SPS prototype rf-dipole crabbing cavity shown in Fig. 1 is one of the cavities that is being designed and fabricated with all the ancillary components including the fundamental power coupler, higher order mode (HOM) couplers, and tuning and He vessel interfaces.

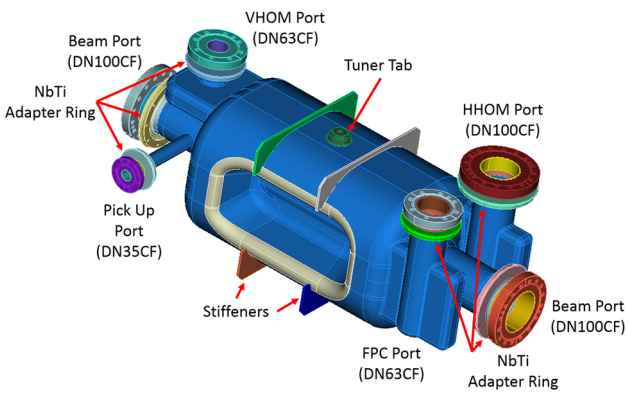


Figure 1: 400 MHz SPS prototype rf-dipole cavity.

The rf-dipole cavity has been designed to operate in a TE_{11}-like mode where the primary contribution to the kick is given by the transverse electric field between the poles [3]. The poles and outer body are optimized to minimize the peak surface field ratios for given transverse kick.

*Work supported by DOE via US LARP Program and by the High Luminosity LHC Project. Work was also supported by DOE Contract No. DE-AC02-76SF00515
†sdesilva@jlab.org

SPS PROTOTYPE RF-DIPOLE CRABBING CAVITY

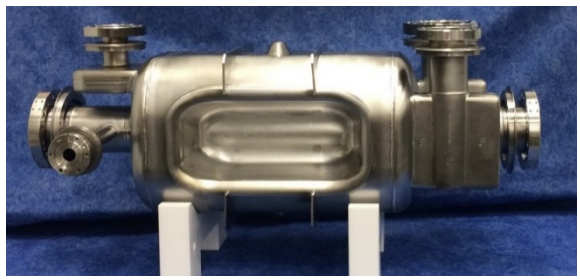


Figure 2: Fabricated Nb rf-dipole cavity.

Two prototype cavities were fabricated by Niowave Inc. and completed at Jefferson Lab under US-LARP. Figure 2 shows the fabricated full prototype rf-dipole crabbing cavity. The cavities were bulk BCPed followed by heat treatment at 600 C for 10 hours. Then the cavities were light BCPed, high pressure rinsed and assembled for rf testing. Prior to rf test the cavity was baked at low temperature of 120 C. The details of the fabrication and cavity processing are given in Ref. [4].

Bare Cavity Test Results

The two cavities were rf tested at Jefferson Lab with performance exceeding the design specifications [5]. Figure 3 shows the measured Q curves of the RFD-CAV-002. The same cavity was rf tested with the HOM couplers following the bare cavity test.

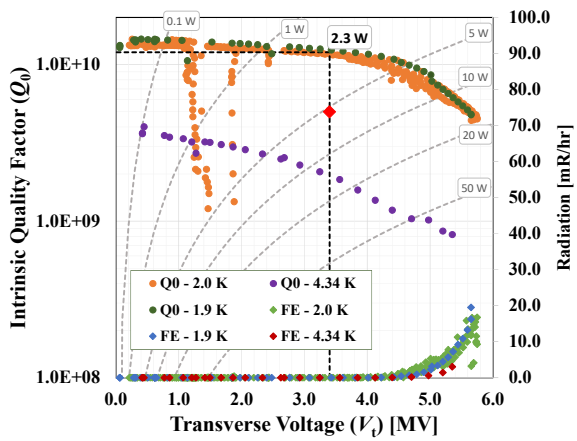


Figure 3: Q curves of the bare RFD-CAV-002.

The cavity achieved a maximum transverse kick of 5.8 MV with peak surface fields of E_p = 56 MV/m and B_p = 96 mT and low field Q_0 is greater than 1.3×10^{10}. The

Content from this work may be used under the terms of the CC BY 3.0 licence (© 2018). Any distribution of this work must maintain attribution to the author(s), title of the work, publisher, and DOI.

ISBN: 978-3-95450-194-6 ISSN: 2226-0366 doi:10.18429/JACoW-LINAC2018-TUPO035

DETERMINATION OF THE FIELD DEPENDENCE OF THE SURFACE RESISTANCE OF SUPERCONDUCTORS FROM CAVITY TESTS*

J. R. Delayen†1, H. Park[1], S. U. De Silva,
Center for Accelerator Science, Old Dominion University, Norfolk, VA 23529
[1]also at Jefferson Lab, Newport News, VA 23606, USA

Abstract

Cryogenic tests of superconducting cavities yield an average surface resistance as a function of the peak surface magnetic field. An analytical formalism has been developed to extract the actual field dependence of the surface resistance from cavity tests and is applied to coaxial cavities and cavities of more complex geometries.

INTRODUCTION

The well-known expressions for the surface resistance of superconductors in electromagnetic fields, and its dependence on frequency, temperature, and a few materials parameters, were obtained as a perturbation theory under the assumption that the magnitude of the electromagnetic field is much smaller than the critical field. This resulted in a surface resistance independent of the magnitude of the electromagnetic field.

There have been several attempts at developing theories of the surface resistance at high rf field, up to the critical field, but, at present, there is no universally accepted consensus on the correct fully self-consistent theory.

Experimentally, cryogenic tests of superconducting cavities developed for particle accelerators have shown that superconductors can display a strong dependence of their surface resistance on the rf field. Furthermore, the field dependence can vary greatly depending on the history of the cavities: chemical treatment, high temperature and low heat treatment, impurity, ambient magnetic field during transition, cooling rate during, and so on.

Traditionally superconductors have shown an increase of their surface resistance with rf field which puts a limit to the accelerating gradients achievable for high-energy accelerators. More recently, processes have been developed that yield a decrease of the surface resistance with medium fields, a great benefit for accelerators operating in cw mode.

A strong dependence of the surface resistance on magnetic field is also often observed in cavities made by sputtering of Nb on Cu or in cavities made of Nb_3Sn on Nb

Developing a full understanding and theory of the rf field dependence of the surface resistance of superconductors will require accurate knowledge of that surface resistance as a function of the rf field, and its dependence on preparation and processing parameters.

Experimentally it has proven difficult to develop techniques where a superconductor was exposed to a uniform electromagnetic field. Until now, in all measurements, either the superconducting sample was exposed to a non-uniform field in a test cavity or, more often, an entire cavity was made of superconducting material that was exposed to a field that ranged from 0 to a maximum value.

In this paper we present a method and formulae that allow determination of the actual dependence of the surface resistance from experiments where an "average" surface resistance is derived from tests of superconducting resonators. An underlying assumption is still that, while the surface resistance has a magnetic field dependence, it does not have a dependence on location. This is not always true as it is known that superconducting cavities can have "hot spots" where the surface resistance is higher and with a stronger field dependence than in the rest of the cavity

ANALYTICAL METHOD

The geometrical factor G of a cavity is defined as

$$G = \omega\mu_0 \frac{\int_V |\mathbf{H}|^2 \, \mathrm{d}V}{\int_S |\mathbf{H}|^2 \, \mathrm{d}S}. \quad (1)$$

If the surface resistance is constant, then $G=QR_s$. If it is not, then $G/Q(H) = \bar{R}_s(H)$ where $\bar{R}_s(H)$ is an "average" surface resistance. It is related to the actual one by

$$\bar{R}_s(H_p)\int_S |\mathbf{H}(\vec{r})|^2 \, \mathrm{d}S = \int_S R_s\left(H(\vec{r})\right)|\mathbf{H}(\vec{r})|^2 \, \mathrm{d}S. \quad (2)$$

We define the function $a(h)$ as the fraction of the total cavity surface where $|H| \le hH_p$. The function $a(h)$ is continuous, monotonically increasing, with $a(0)=0$ and $a(1)=1$. It could also be interpreted as the probability distribution for the surface magnetic field, and its derivative $\mathrm{d}a/\mathrm{d}h$ as the probability density. For normal cavity geometries we also have $\mathrm{d}a/\mathrm{d}h\big|_{a=1} = \infty$.

Because of the continuity and monotonicity of $a(h)$ we can make a change of variable in Eq. (2) and integrate over the magnetic field instead of the area.

$$\bar{R}_s(H) = \int_0^1 (hH)^2 \frac{\mathrm{d}a}{\mathrm{d}h}\mathrm{d}h = \int_0^1 R_s(hH)(hH)^2 \frac{\mathrm{d}a}{\mathrm{d}h}\mathrm{d}h. \quad (3)$$

We assume that the experimentally measured average surface resistance can be modelled by a sum of powers of the magnetic field:

$$\bar{R}_s\left(\frac{H}{H_0}\right) = \bar{R}_0 \sum_{\alpha_i} r_{\alpha_i}\left(\frac{H}{H_0}\right)^{\alpha_i}. \quad (4)$$

* Work supported by NSF Award No. PHY-1416051
† jdelayen@odu.edu

Content from this work may be used under the terms of the CC BY 3.0 licence (© 2018). Any distribution of this work must maintain attribution to the author(s), title of the work, publisher, and DOI.

ISBN: 978-3-95450-194-6 ISSN: 2226-0366 doi:10.18429/JACoW-LINAC2018-TUPO036

VERTICAL TEST RESULTS OF PLASMA IN-SITU CLEANING ON LOW BETA HWR CAVITY*

A.D. Wu†, S.C. Huang, C.F. Hu, C. L. Li, Y. M. Li, L. Yang, F. Pan, X. M. Liu, H. Guo
Y. K. Song, P. R. Xiong, W. M. Yue, C. Zhang, Y. He, S. H. Zhang, H.W. Zhao
Institute of Modern Physics, Chinese Academy of Sciences, Lanzhou, China

Abstract

Field emission occurred in SRF cavity is the major limitation to operate at high gradient with stability. The plasma in-situ cleaning for the low beta HWR cavity was carried out to remove the hydrocarbons contaminants on the inner cavity surface. And the vertical test results indicated that the field emission effect was relieved with the increasing of the quench point and emission set-on point. Thus, oxygen active plasma processing can be an effective method to solve the field emission issues for the low beta HWR cavity.

INTRODUCTION

The Chinese-Accelerator Driven System (C-ADS) has been developing for the treatment of the nuclear wastes at Institute of Modern Physics, Chinese Academy of Sciences. A 25 MeV superconducting proton linac injector has been constructed, and it had been commissioned successfully for the continuous wave proton beams with the current of 170 μA. However, the operation stability of this linac was limited by the trips of the HWR cavities caused by field emission. In order to mitigate the field emission issues in the HWR cavities, the in-situ plasma cleaning technique was proposed at IMP.

For removing the hydrocarbon contaminants covered on the inner surface of the cavity, the inert gas argon was used for the plasma ignition and a few percentage of oxygen gas was mixed as oxidant [1-6].To understand the plasma interaction with niobium surface during the plasma cleaning progress, the characteristics of electron temperature, free electron number density and the vertical test results of HWR cavity by plasma cleaning are presented in this paper.

PLASMA EGNITION IN HWR CAVITY

RF plasma discharge experimental platform for the in-situ plasma cleaning is shown in Fig. 1. It consists of RF system, vacuum system and the optical emission spectrum (OES) system and mass spectrometer.

An HWR015 was used for the plasma discharge experimental study offline. HWR15 was optimized for accelerating protons with a relative speed of light at 0.15, and the fundamental eigen frequency is 162.5 MHz. In order to obtain the similar conditions in cryomodule for HWR015 cavity, the fundamental power coupler (FPC) with dual ceramic windows structure was installed for the cavity, as shown in the Fig. 1.

The Argon and oxygen mixed plasma was ignited in the HWR015, and the glow brightness in three directions at different pressures and oxygen volume ratios is illustrated in Fig. 2. The lower gas pressure and the smaller oxygen volume ratio has the stronger luminance of the plasma light and more uniform distribution of discharge will be achieved in the cavity.

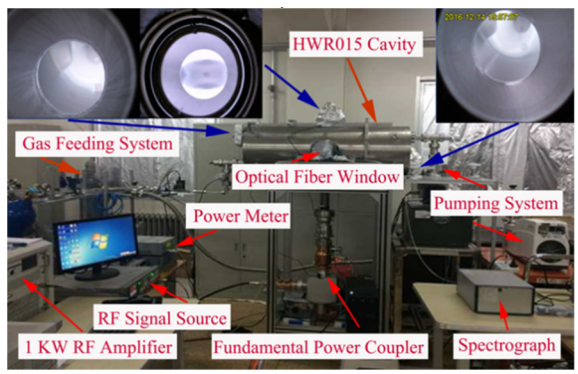


Figure 1: The experimental platform of RF plasma discharge for HWR015 cavity.

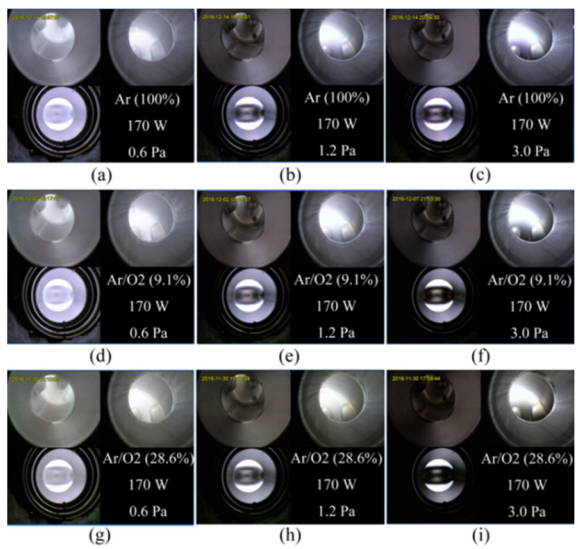


Figure 2: Brightness of the plasma discharge in the HWR015 cavity, at different gas pressures and oxygen volume ratios. The top two cameras were fixed at the two ends of the cavity and the bottom left one was installed at the middle of the cavity.

* Work supported by Major Research Plan of National Natural Science Foundation of China (Grant NO. 91426303) and National Natural Science Foundation for Young Scientists of China (Grant NO. 1150555))
Email address: antonwoo@outlook.com / antonwoo@impcas.ac.cn

Content from this work may be used under the terms of the CC BY 3.0 licence (© 2018). Any distribution of this work must maintain attribution to the author(s), title of the work, publisher, and DOI.

ISBN: 978-3-95450-194-6 ISSN: 2226-0366 doi:10.18429/JACoW-LINAC2018-TUPO038

SEVERAL EXPERIMENTAL PHENOMENA OF Sn NUCLEATION ON Nb SURFACE OBSERVED AT IMP*

Z. Q. Yang, Y. He and F. Pan
Institute of Modern Physics, Chinese Academy of Science, Lanzhou 730000, China

Abstract

Nucleation process is an important step that affects the quality of Nb_3Sn films coated by vapour diffusion method. A uniform distribution of nucleation centres is essential to the uniformity of Nb_3Sn films. In this paper we report several experimental phenomena on the Sn nucleation on Nb surface. Better nucleation in the downstream of the pumping direction was observed. Influence of $SnCl_2$ partial pressure inhomogeneity was studied. Samples with higher $SnCl_2$ partial pressure have denser nucleation, which means homogeneous $SnCl_2$ pressure is a critical factor to the uniform nucleation. Less-nuclear zones, mainly distributed at cracks, grain boundaries and even some whole grain surfaces, were found on the surfaces of all samples. The less-nuclear zones may result in the low tin regions of the Nb_3Sn cavities. The specific solution to the less-nuclear problem was proposed. These studies help to better understanding of the mechanism underlying the nucleation process and will be useful foundation for the follow-up Nb_3Sn/Nb project at IMP.

INTRODUCTION

After many years of worldwide exploration and improvement of the post treatment process, niobium cavities are now approaching their fundamental limits both in terms of maximum accelerating field as well as in terms of surface resistance at typical operating temperatures. To continue to keep up with continually increasing demands of future SRF facilities, there exists urgent demand for the development of new technologies for RF superconductivity.

The A15 superconductor Nb_3Sn is one of the most promising alternative materials to standard niobium for SRF applications not only for its material parameters with obvious advantages [1] but also for the breakthrough performance levels achieved for the vapour diffusion coated 1.3 GHz single cell cavity at Cornell University [2].

One key factor limiting the RF performance of the vapor diffusion coated Nb_3Sn thin film cavities is the heterogeneity of film composition and distribution. An important manifestation of inhomogeneity is the existence of areas with low tin content [2-3]. Presently, the main efforts to further improve the RF performance of the vapour diffusion coated Nb_3Sn thin film cavities is through the optimization of the coating parameters at high temperature, however [2, 4], its effects is not obvious. In the past three years, the RF performance of the Nb_3Sn thin film cavities has not been substantially improved [2, 3, 5].

Whether it is from the growth mechanism of vapour diffusion coated Nb3Sn film, or from the research experience of Siemens AG researchers [6], a uniform distribution of nucleation centres is essential to the uniformity of Nb_3Sn films. Without uniform nucleation, it is difficult to avoid the heterogeneity of Nb_3Sn film composition and distribution even with the optimization of the coating parameters at high temperature. Compared to the optimization of the coating parameters at high temperature, the importance of the nucleation process to break through the limitations of the RF performance of Nb_3Sn cavities has not been paid sufficient attention, and research on nucleation [7] is relatively less.

Under such a background, a thorough study of Sn nucleation on Nb surface was carried out at IMP, which will be useful foundation for the follow-up Nb_3Sn/Nb project at IMP. In this paper, several experimental phenomenon of Sn nucleation on Nb surface will be reported.

EXPERIMENTAL

Sample Preparation

The Nb samples were cut by wire electro-discharge machining (EDM) from the same plate. The samples' treatments were attempted to replicate that of the cavities, which includes polishing smoothly on 1000-grit sandpaper, 150μm heavy BCP (HF: HNO_3: H_3PO_4 =1:1:2), 8000C degas for 3 hours and 20μm light BCP.

Nucleation Experiment

The nucleation experiment of the niobium samples was carried out in a furnace using a high purity quartz tube, taking the advantage of high purity quartz's good thermal and chemical stability at high temperature. The furnace's background pressure is better than 5×10^{-5} Pa, which can meet the requirement of nucleation experiment. The nucleation was accomplished by using the nucleation agent $SnCl_2$. After 24 hours of degasing at 200^0C in high vacuum, the temperature was raised up to 500^0C at a rate of 3.50C/min. Then the samples were kept at 500^0C for 4 hours for nucleation. After which, the furnace was turned off to cool down naturally.

RESULTS

Influence of Pumping Direction

The nucleation was accomplished taking the advantage of $SnCl_2$'s high vapour pressure at relatively low temperature. According to common sense, the $SnCl_2$ molecule moves downstream along the pumping direction. This will possibly cause that the partial pressure of $SnCl_2$ in the downstream of the pumping direction is larger than that of the upstream of the pumping direction, resulting in the difference in the nucleation distribution on the surfac-

Content from this work may be used under the terms of the CC BY 3.0 licence (© 2018). Any distribution of this work must maintain attribution to the author(s), title of the work, publisher, and DOI.

ISBN: 978-3-95450-194-6 ISSN: 2226-0366 doi:10.18429/JACoW-LINAC2018-TUPO039

TESTS OF THE BALLOON SINGLE SPOKE RESONATOR*

Z. Yao†, J. Keir, D. Kishi, D. Lang, R.E. Laxdal, H. Liu, Y. Ma, B. Matheson, B.S. Waraich, Q. Zheng, V. Zvyagintsev, TRIUMF, V6T2A3 Vancouver, Canada

Abstract

A novel balloon variant of the single spoke resonator (SSR) has been designed, fabricated and tested at TRIUMF. The cavity is the β=0.3 325 MHz SSR1 prototype for the Rare Isotope Science Project (RISP) in Korea. The balloon variant is specifically designed to reduce the likelihood of multipacting barriers near the operating point. A systematic multipacting study led to a novel geometry, a spherical cavity with re-entrant irises plus a spoke. The balloon cavity provides competitive RF parameters and a robust mechanical structure. Cold tests demonstrated the principle of the balloon concept. The cold test results will be reported in this paper.

INTRODUCTION

RISP has been proposed as a multi-purpose accelerator facility at the Institute for Basic Science (IBS), Korea, for research in atomic and nuclear physics, material science, bio and medical science, etc. At the heart of RISP is a powerful heavy ion linac [1]. The linac consists of three independently phased superconducting sections. The high energy section SCL2 of the driver linac uses two types of 325 MHz single spoke resonators with geometry β at 0.30 and 0.51 corresponding to SSR1 and SSR2 respectively. TRIUMF has been contracted to design, fabricate and test two of the SSR1 variants.



Figure 1: Bare cavity (left) and jacketed cavity (right) of SSR1 prototype.

The prototype cavity of SSR1 β=0.30 designed by TRIUMF is shown in Fig. 1. The cavity is termed the balloon variant due to the conformal shape of the outer conductor that obviates the need for a central spool. The balloon geometry is proposed to suppress multipacting in the accelerating gradient range of several MV/m [2]. It also provides a more inherently robust mechanical structure. The cavity is designed [3] to operate in continuous wave (CW) mode at 2 K with 35 MV/m peak electric field. The design parameters are listed in Table 1. The SSR1 prototype is fabricated with 3 mm RRR niobium for cavity, and 3 mm 316L stainless steel for flanges and the helium jacket. The details were reported in Ref. [4].

Table 1: Design Parameters of SSR1

Parameters	Value
Frequency	325 MHz
Geometry β	0.30
Geometry factor	93 Ω
R/Q	233 Ω
E_{peak}/E_{acc}	3.84
B_{peak}/E_{acc}	6.07 mT/(Mv/m)
df/dp	-1.6/+1.5 Hz/mbar
Lorentz force detuning	-8.7/-1.4 Hz/$(MV/m)^2$
Tuning sensitivity	467 kHz/mm
Spring constant	14 kN/mm

CAVITY PROCESSING

Cavity was inspected, and leak checked after fabrication. 200 μm surface layer was re-moved by buffer chemical polishing (BCP) in several steps with flipping cavity orientation. The BCP solution is mixed with HNO_3, HF, H_3PO_4 in the volume ratio of 1:1:2. The cavity is fixed on a support frame via stiffener rings on both end shells. The RF ports are positioned up and down during etching. RF ports are used as acid inlet and outlet. The acid temperature was monitored during etching and controlled below 15 ˚C.

High pressure rinsing (HPR) is done through beam ports on the horizontal rinsing stand and each RF port on the vertical rinsing stand. A dedicated nozzle is designed for this cavity. There are two water jets on each direction from 30˚ to 150˚ off the rinsing wand axis with an increment of 30˚. Two additional water jets are 10˚ off the axis on the top. For each cavity assembly, the cavity was rinsed 3.5 hours on the horizontal stand at 80 bar pressure, and 2 hours on vertical stand via each RF port with 45 bar pressure.

The cavity was degassed after an integrated 200 μm BCP. There were obvious signs of hydrogen Q-disease in the pre-degassing tests. Due to concerns about the copper brazing between niobium and stainless-steel flanges, 600 ˚C for 10 hours degassing recipe was selected. The hydrogen partial pressure was monitored with residual gas analyser (RGA) and reduced by 3 orders of magnitude. Additional 20 μm BCP followed by HPR was completed prior to cold test.

Low temperature baking was applied as the last treatment for the hermitic seal cavity before cold test. Two recipes, 50 ˚C for 2 hours and 120 ˚C for 48 hours, were tested to evaluate the effects on BCS resistance and multipacting conditioning. The cavity was actively pumped during the baking procedure. The cavity vacuum was improved by 2 orders of magnitude during the 120 ˚C bake.

* Work supported by RISP – TRIUMF Collaboration
† zyyao@triumf.ca

Content from this work may be used under the terms of the CC BY 3.0 licence (© 2018). Any distribution of this work must maintain attribution to the author(s), title of the work, publisher, and DOI.

ISBN: 978-3-95450-194-6 ISSN: 2226-0366 doi:10.18429/JACoW-LINAC2018-TUPO040

TEST OF MULTI-FREQUENCY COAXIAL RESONATORS*

Z. Yao†, J. Keir, P. Kolb, A. Kong, R.E. Laxdal, B. Matheson, E. Thoeng, B.S. Waraich, Q. Zheng, V. Zvyagintsev, TRIUMF, V6T2A3 Vancouver, Canada

Abstract

A significant issue in low β resonators is the 4K medium field Q-slope (MFQS). To systemically study the field dependence of surface resistance in TEM mode resonators, a quarter-wave resonator (QWR) and a half-wave resonator (HWR) were designed to resonant at integer harmonic frequencies of 200 MHz, and up to 1.6 GHz. A series of cavity treatments were proposed to these cavities. It provides opportunity to investigate the field dependent surface resistance as a function of frequency, temperature, and treatment, including heat treatments and doping. The preparation for the baseline cold test and the preliminary test result will be reported in this paper.

COAXIAL RESONATORS

The resonant frequency of low β cavities, operating in TEM mode, of proton or heavy ions linac applications are normally in the range of 80 MHz to 350 MHz. These frequencies provide opportunity of 4 K operation to reduce the cost of cryogenics system. However, strong Q-slope in the medium field regime reduces cavity performance at the operational field level. To developing systemic study tools for MFQS in low β resonators, two delegated QWR and HWR cavities are designed and fabricated, shown in Fig. 1. The coaxial structure is chosen to represent the common geometry of low β resonators. The RF performances can be measured at different harmonic frequencies in the same cold test cycle. The consistent surface field distributions between various TEM modes mitigate the geometry effect on surface resistance. The role of RF frequency on the field dependent resistance and the optimum treatments for low β resonators can be investigated with these coaxial resonators.



Figure 1: HWR (left) and QWR (right).

The resonators are designed as the 'single cell' for the fundamental R&D programs. To be distinct from acceleration purpose SRF cavities, some common features, such as beam ports and helium jacket, are eliminated to simplify the cavity geometries. In accordance to research proposal, the cavities are required to fit TRIUMF RF induction furnace. The lowest resonant frequency is limited by the cavity length. In addition, four cleaning ports are set at the same end of each cavity. A uniform cylinder inner conductor is chosen to employ a common mobile T-map insert to characterize the local RF heating in addition to the global Q measurement. The detail design of these resonators can be found in [1].

The cavities are fabricated with RRR grade and reactor grade niobium. Reactor grade niobium is used for flanges and the cavity parts at the low magnetic field region, such as bottom plate and port tubes of QWR. Indium seal is required on niobium flange for the hermitic unit assembly. There was not frequency tuning step during manufacture as the absolute resonant frequencies are not critical. The harmonic frequencies at room temperature and atmosphere pressure were measured after received from manufacturer and are shown in Table 1. The To-Be-Tested modes are highlighted in bold and italic. The measurement results are well conformed to the design. The closest TE mode is separated by 37 MHz and its transmission signal is more than 10 dB lower with the same RF couplers. A bandpass filter is required in LLRF for each test mode to eliminates the undesired resonances in cold test.

Table 1: Resonant Frequencies of Coaxial Resonators

QWR	Simu. /MHz	Meas. /MHz
TEM	***217***	***217.4***
TEM	***647***	***647.3***
TE111	892	–
TEM	1055	1054.2
TE112	1103	1100.8/1103.5
HWR	**Simu. /MHz**	**Meas. /MHz**
TEM	***389***	***388.6***
TEM	***778***	***777.4***
TE111	905	901.9/906.6
TE112	1128	1125.4/1129.1
TEM	***1166***	***1166.1***
TE113	1424	1421.9/1424.8
TEM	***1555***	***1554.8***
TE211	1602	1600.7

RF AND CONTROLS

Coaxial resonators are to be tested at the harmonic frequencies of 200 MHz and up to 1.6 GHz. Two wide band

* Work supported by NSERC
† zyyao@triumf.ca

Content from this work may be used under the terms of the CC BY 3.0 licence (© 2018). Any distribution of this work must maintain attribution to the author(s), title of the work, publisher, and DOI.

ISBN: 978-3-95450-194-6 ISSN: 2226-0366 doi:10.18429/JACoW-LINAC2018-TUPO041

LCLS-II CAVITY HIGHER ORDER MODES COUPLER TUNING OPTIMIZATION AND CHALLENGES AT JEFFERSON LAB*

A. Solopova†, D. Forehand, A. Palczewski, Jefferson Lab, 23608, Newport News, VA, USA
T. Khabiboulline, FNAL, 60510, Batavia, IL, USA

Abstract

The Thomas Jefferson National Accelerator Facility is currently engaged, along with several other Department of Energy (DOE) national laboratories, in the Linac Coherent Light Source II project (LCLS II) - a new XFEL linac based on the 1.3 GHz superconducting linear accelerator. Half of the LCLS-II cryomodules are being produced at Jefferson Lab, other half is made at Fermilab. Each cryomodule contains eight 9-cell cavities with two Higher Order Modes (HOM) loop couplers operating at 1.3 GHz. This paper summarizes the HOM filter tuning challenges at Jefferson Lab and describes optimization of the procedure for a 9-cell Tesla type cavity and its integration into a cryomodule production line.

INTRODUCTION

If HOMs are close to the operating mode frequency, they might be excited as well and can disturb the operating mode. HOMs excited in SRF structures by passing beam may deteriorate beam quality and affect beam stability. It is extremely important to properly tune HOM filters, i.e. to minimize RF transmission on the operating mode, to prevent beam breakup and excessive heating of the cavity end group. Capacitive tuning is first done on a single cavity before the vertical test, then checked and adjusted before the cavity string is inserted in the cryomodule vacuum vessel.

CHALLENGES EXPERIENCED

The first production cryomodule (CM02) HOM filters were tuned using the procedure for the Jefferson Lab C100 style cryomodules [1]. CM02 was at the Cryomodule Test Facility in July 2017.

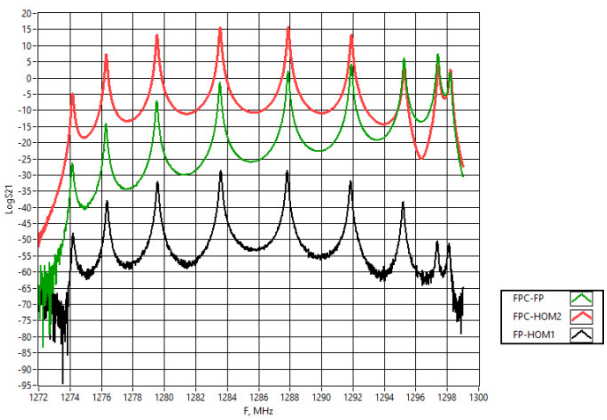


Figure 1: Fundamental mode spectrum of an LCLS-II cavity.

Over a half of the HOMs had a measured quality factor below specification. A plan was developed to asses CM02 and CM03 HOM tuning and HOM heat station connections. Fourteen out of sixteen HOMs accessible through the tuner ports on the CM03 were tuned to the partner laboratory standard notch frequency for a cavity under vacuum, 1297.0 MHz [2].

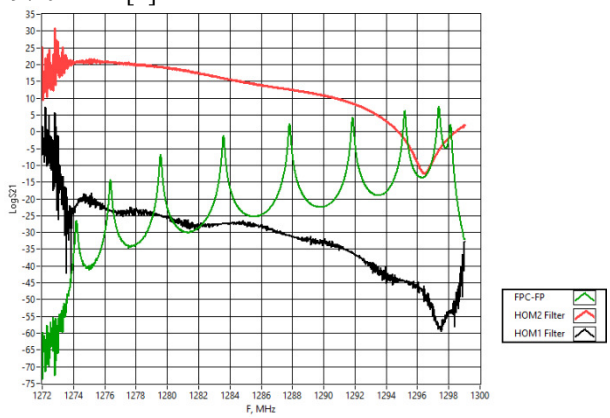


Figure 2: Notch filter view of an LCLS-II cavity spectrum.

We independently discovered that tuning is extremely sensitive to any external manipulation such as tightening cables, assembling magnetic shield covers, tightening of the heat stations. Notch positions were measured multiple times during the process and under several different vacuum conditions, including cavity under vacuum and insulating vacuum at atmosphere, both cavity and insulating vacuum established. Figures 1 and 2 show a typical LCLS-II cavity spectrum and a calculated notch position.

Table 1: Notch Frequency Shift for HOM1

HOM 1 notch atm-vac, MHz	HOM 1 notch vac-vac, MHz	Frequency shift, MHz
1296.7	1297.2	0.5
1297.4	1298.3	0.9
1297.3	1298.0	0.7
1297.3	1298.1	0.8
1297.2	1298.5	1.3
1296.8	1297.4	0.6
1297.4	1297.9	0.5
1296.8	1297.8	1.0

Notch filter position was expected to shift by +0.4MHz [2], observed frequency shift at Jefferson Lab was 0.8MHz for HOM 2, 1 MHz for HOM 1 (Tables 1 and 2). Target notch frequency was lowered to 1296.6 MHz for HOM 1 and to 1296.3 MHz for HOM 2 (Fig. 3 and 4).

*This work was supported by the LCLS-II Project and the U.S. Department of Energy, Contract DE-AC02-76SF00515.
†shabalin@jlab.org

Content from this work may be used under the terms of the CC BY 3.0 licence (© 2018). Any distribution of this work must maintain attribution to the author(s), title of the work, publisher, and DOI.

ISBN: 978-3-95450-194-6 ISSN: 2226-0366 doi:10.18429/JACoW-LINAC2018-TUPO042

RF RESULTS OF Nb COATED SRF ACCELERATOR CAVITIES VIA HIPIMS*

M. Burton, A. Palczewski, L. Phillips, A.M. Valente-Feliciano†, and C. E. Reece
Thomas Jefferson National Accelerator Facility, Newport News, VA, USA
R. A. Lukaszew, The College of William & Mary, Williamsburg, VA, USA

Abstract

Bulk Niobium (Nb) SRF (superconducting radio frequency) cavities are currently the preferred method for acceleration of charged particles at accelerator facilities around the world. However, bulk Nb cavities have poor thermal conductance and impose material and design restrictions on other components of a particle accelerator. Since the SRF phenomena occurs within a shallow depth of 40 nm (for Nb), a proposed solution to this problem has been to deposit a superconducting Nb thin film on the interior of a cavity made of a suitable alternative material such as copper or aluminum. While this approach has been attempted in the past using DC magnetron sputtering (DCMS), such cavities have never performed at the bulk Nb level. However, new energetic condensation techniques for film deposition offer the opportunity to create suitably thick Nb films with improved density, microstructure and adhesion compared to traditional DCMS. One such technique that has been developed somewhat recently is "High Power Impulse Magnetron Sputtering" (HiPIMS). Here we report early results from various thin film coatings carried out on 1.3 GHz Cu cavities, a 1.5 GHz Nb cavity, and small Cu coupon samples coated at Jefferson Lab using HiPIMS.

INTRODUCTION

Superconducting radio frequency (SRF) cavities based on bulk Nb have been used for decades in particle accelerators [1]. In order to truly engineer the active SRF surface, one can take advantage of the shallow RF penetration depth by using an alternative material for the resonant cavity structure with more favorable bulk properties, such as Cu, and coating a ~1 μm Nb thin film as the active SRF surface. One can then optimize the RF response by tuning the various coating parameters available during film growth.

Thin film SRF cavities were first implemented in the 1980's at CERN for LEP II [2], with Nb/Cu thin film cavities deposited with DC magnetron sputtering (DCMS). While these films had good low field Q-values, they exhibited a strong decreasing dependence of the Q-value on RF field, known as the "Q-slope", limiting their applications. To this day, the cause of the Q-slope has not been fully understood and has yet to be overcome.

Many causes proposed for the Q-slope [3-5] can be associated with the low energy film deposition method utilized. DCMS has been shown to yield superconducting films with properties below the bulk material. Energetic condensation methods, such as high-power impulse magnetron sputtering (HiPIMS) promise to create films with enhanced SRF properties [6]. HiPIMS is easily adaptable to coating tri-dimensional shapes and can be implemented on existing DCMS cavity coating systems.

In HiPIMS, the magnetron is pulsed to extremely high-power densities thereby increasing the plasma density by several orders of magnitude and resulting in ionization of a significantly higher fraction of the metal atoms [7, 8], allowing control of the deposition energy by applying a substrate bias. HiPIMS has been shown to yield films with much improved microstructure, density, surface roughness, adhesion and overall quality compared to the low energy DC methods [9-12]. This opens the possibility to produce higher quality films for SRF application.

In order to explore HiPIMS for SRF, a cavity deposition system was designed, built and commissioned at Thomas Jefferson National Accelerator Facility (JLab) [13]. This system offers many benefits such as the ability to mount and unmount cavities while leaving the larger system under vacuum, allowing a higher turn-around cycle and reduced risk of contamination; it also allows deposition of small coupon samples under the same pump down cycle as the cavity through a load-lock and enables conditioning of the magnetron before deposition. A custom built HiPIMS pulser, powering a cylindrical Nb cathode in a Kr atmosphere, is used to deposit Nb films. Here we present early HiPIMS coated cavity results and data from small samples carried out in the same system.

EXPERIMENT

A small sample study of Nb films on Cu substrates was performed in order to investigate the effect of peak pulse power and applied voltage bias on the resulting film properties. The Cu substrates used were polished polycrystalline OFE Cu ultrasonically cleaned in successive acetone and methanol baths. After growth, the structural and surface properties of the samples (lattice parameter, grain size, orientation, roughness…etc.) were determined via X-Ray diffraction (XRD) and Electron Backscatter Diffraction (EBSD), and atomic force microscopy (AFM).

While the ultimate goal is to deposit Nb thin films on Cu cavities, it is important to first understand the film deposition process itself, thus, a known good RF Nb cavity surface was used as first substrate. Prior to the initial baseline RF test, the 1.5 GHz C100 end cell low loss (LL) Nb cavity was exposed to a buffered chemical polish (BCP) etch followed by a high-pressure rinse (HPR). While the 1.3 GHz low surface field (LSF) Cu

* Authored by Jefferson Science Associates, LLC under U.S. DOE Contract No. DE-AC05-06OR23177.
† valente@jlab.org

Content from this work may be used under the terms of the CC BY 3.0 licence (© 2018). Any distribution of this work must maintain attribution to the author(s), title of the work, publisher, and DOI.

ISBN: 978-3-95450-194-6 ISSN: 2226-0366 doi:10.18429/JACoW-LINAC2018-TUPO043

NEW PROGRESS WITH HF-FREE CHEMICAL FINISHING FOR Nb SRF CAVITIES

H. Tian†, B. Straka, J. Carroll, and C. E. Reece, Jefferson Lab, Newport News, VA, USA
T. Hall, R. Radhakrishna, M. Inman, E. J. Taylor, Faraday Technology, Inc., Englewood, OH, USA

Abstract

Jefferson Lab has implemented a bipolar pulsed electropolishing system for final chemical processing of niobium SRF cavities. This FARADAYIC bi-polar electropolishing (BPEP) has been applied to single cells, a 7-cell CEBAF C100 cavity, and to 9-cell TESLA-style cavities [1]. As a mechanistic characterization of the process emerges, the critical role played by the local current density during each cathodic pulse is becoming clear. This influences system and operational parameter refinement. We present current process parameters, removal characterization, and rf performance of the processed cavities. This is the fruit of collaborative work between Jefferson Lab and Faraday Technology, Inc. directed toward the routine commercialization and industrialization of niobium cavity processing. We also present supporting data from controlled-parameter coupon studies.

INTRODUCTION

Bi-polar pulsed electropolishing (BPEP), as an alternative method to treat Nb surfaces, uses anodic pulses to anodize the Nb surface with an HF-free electrolyte and intervening cathodic pulses to erode the oxide via mechanical action of the hydrogen gas bubbles formed at the niobium surface by electrolysis, resulting in a surface leveling polishing [1-3]. This process eliminates the need for HF and/or fluoride salts to remove the Nb surface oxides and is being studied as a safer, greener and more economic method to prepare Nb SRF cavities [4].

BPEP has been used as final chemical processing of niobium SRF cavity recently by Faraday Technology Inc. and Jefferson Lab. Similar work is also being investigated in partnership with KEK and Nomura Plating. The studies demonstrated that bi-polar pulsed electropolishing could effectively polish Nb SRF cavities, and produce a high-quality surface comparable with conventional EP which uses concentrated HF and H_2SO_4 as electrolyte, and provides comparable cavity performance [5-7]. However, optimization of parameters of the BPEP process for improving the removal rate and uniformity, and achieving highly reproducible high RF performance cavities, and utility processing nitrogen "doped" Nb cavities needs further systematic studies.

Jefferson Lab has developed a low cost BPEP control technique and implemented it in a vertical EP processing system. In this study, the systematic mechanistic and surface studies for guiding the design of the BPEP and the optimization of BPEP process for single cells are reported.

EXPERIMENTAL

Cavity processing at JLab by BPEP was performed inside of a closed chemical cabinet where the cavity is mounted on a vertical stand. The mixed metal oxide (MMO)-coated Ti-clad copper rod serving as a counter electrode was inserted coaxially through the cavity. Hydrogen and oxygen generated during BPEP flow back to the solution reservoir where they are diluted and exhausted. The cavity is set as the ground potential; the counter electrode is driven by a custom-designed pulse generator. Figure. 1 is the wiring diagram for the Jefferson Lab pulse generator and controller system, which is under a patent application [8]. Ultrasonic thickness gauges are used to monitor surface removal at different locations of single cell and multi-cell SRF cavities.

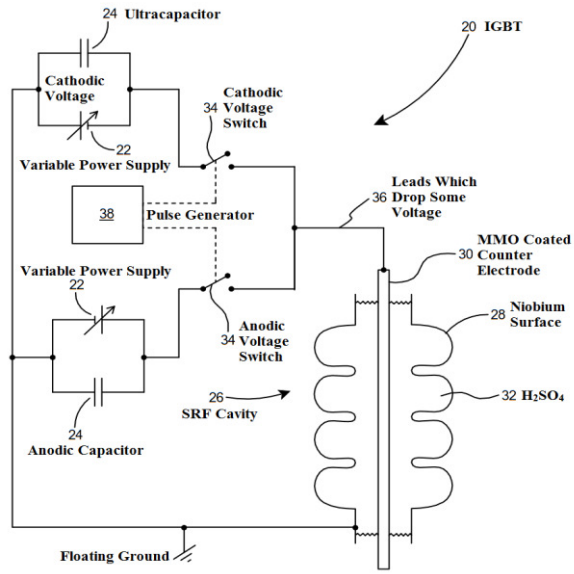


Figure 1: Schematic of the JLab BPEP equipment. [8]

Many standard samples made of high purity niobium with reactive surface of 3.14 cm^2 were fabricated for use exploring process parameters. The counter electrode for such bench-top tests was Ti-clad Cu plate with MMO coating and having reactive surface area of 30 cm^2. The distance between Nb sample and counter electrode was set as 9.8 cm. All the samples underwent 60 µm BCP etching before use. AFM measurements were done on 50 µm × 50 µm areas at three different locations, and the average of root-mean-square roughness (R_q) was calculated for each sample. The surface removal for samples was calculated through loss of mass.

* Authored by Jefferson Science Associates, LLC under U.S. DOE Contract No. DE-AC05-06OR23177.
† huit02@jlab.org

Content from this work may be used under the terms of the CC BY 3.0 licence (© 2018). Any distribution of this work must maintain attribution to the author(s), title of the work, publisher, and DOI.

ISBN: 978-3-95450-194-6 ISSN: 2226-0366 doi:10.18429/JACoW-LINAC2018-TUPO045

OPTIMIZATION OF DUAL AXIS ASYMMETRIC CAVITY FOR ENERGY RECOVERY LINAC

Ya. Shashkov†, A. Bulygin, M. A. Gusarova, National Research Nuclear University MEPhI, 115409, Moscow, Russia
I. V. Konoplev, JAI, Department of Physics, University of Oxford, Oxford, OX1 3RH, UK
F. Marhauser, A. Seryi, Thomas Jefferson National Accelerator Facility, Newport News, VA 23606, USA

Abstract

Optimization of the dual axis asymmetric cavity was performed to minimize the ratio of the peak magnetic and electric fields values to the accelerating voltage, to increase the distance between operating and neighbouring modes as well as to reduce the manufacturing cost of the cavity. To reach the goals several solutions have been suggested bringing the ratios to the acceptable values and leading to simplification of the manufacturing of the structure.

INTRODUCTION

Conceptual design and preliminary RF studies of dual-axis asymmetric RF cavities for energy recovery LINAC has been recently carried out at Oxford and JLab [1-5]. The concept of using two different axes for acceleration and deceleration was known [6,7] but it is only recently the use of asymmetric configuration for acceleration and deceleration of the beam to isolate higher order modes (HOMs) excited in different sections has been suggested [4,8,9]. The objectives were to confine HOMs excited at each pass to either of the axis reducing the feedback between accelerating and decelerating beams and thus increasing BBU start current aiming at creating ERL capable of driving electron beam with an average current above 1 Ampere. The preliminary RF studies at JLab of a single cell dual axis SCRF cavity [1-3] demonstrated very promising results while at Oxford the theoretical and preliminary experimental studies of dual-axis 7 cell cavity had been carried out [4,5].

In this paper we present the results of the theoretical studies carried out to optimise the cavity design and improve the understanding of the cavity parameters on its performance. The overall aim of these studies is to move from the conceptual design to technical drawings enabling the next step – manufacturing and test of SCRF cavity.

ORIGINAL DESIGN OF THE CAVITY AND CHALLENGES

In Fig. 1 the schematic of the original structure made from tesla-type (TT) cells on both axis is presented. The cells on one axis are slightly different than on another. We denote this structure as TT&TT. Recently it was recognised that one of the issues is high picks of the electric (E_p) and magnetic (B_p) fields on the surface (subscript p) of the resonant cell (see Fig. 1), frequency proximity of operating f_0 and nearest parasitic f_p mode with $\Delta f = 0.505$ MHz (Table 1) in pass band and high probability of multipacting discharges due to flat surfaces of the coupling cell.

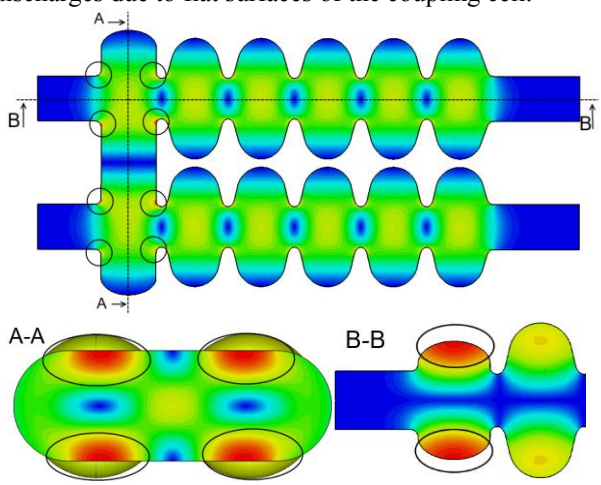


Figure 1: Contour plots of electric (top figure) and magnetic (bottom figure) fields showing the high intensity fields on the surface of the bridge cell.

First we looked at alternative to tesla type (TT) cells. It was suggested that low-loss (LL) cells [10-11] might be a good alternative as they were originally designed to allow high current transportation [11-12] and complete substitution of TT cells with the low-loss cells has been carried out. The substitution led to increase of the field on the surface of the bridge, the distance between modes did not change and the operating field amplitude along the axes became lower. As a result the overall field ratios i.e. field on the surface to the accelerating field on the axis (E_a) have increased $E_p/E_a = 3.22$ and $B_p/E_a = 7.12$ by nearly 20% reaching very high values. Taking this into account the use of solely LL-cells was not persuaded further.

In order to simplify the manufacturing of the structure by reducing the number of forms that are necessary for the machining it was proposed to use a combination of different types of cells (Fig. 2): TT-cells along one axis and LL-cells along second axis (TT&LL). Availability of the forms to stamp the parts, gained experience of making such cells assures relative easiness and quick manufacturing and testing the cells. These features allow minimisation of the cost and research/application risks.

The reported study was funded by RFBR according to the research project № 18-302-00990
† yvshashkov@mephi.ru

Content from this work may be used under the terms of the CC BY 3.0 licence (© 2018). Any distribution of this work must maintain attribution to the author(s), title of the work, publisher, and DOI.

ISBN: 978-3-95450-194-6 ISSN: 2226-0366 doi:10.18429/JACoW-LINAC2018-TUPO048

STUDY PROGRESS OF PULSE LASER ANNEALING FOR NIOBIUM FILM ON COPPER*

Y. J. Yang†, X. Y. Lu, D. T. Xie, W. W. Tan, L. Xiao, D. Y. Yang, B. T. Li
Peking University, Beijing, China

Abstract

The recent studies of laser annealing on niobium films on copper are reported. Annealing is normally used to deal with the surface, reducing defects and even changing the microstructure of the coating film. Short pulse laser can produce a sharp step temperature field on the film thickness scale (μm), which anneals the surface without substrate heated. The laser annealing experiments of niobium thin film sample have been carried out, and according to SEM and FIB results, Nb films melted and recrystallization occurred. Grains growing up can be observed while the power density of laser pulse increased.

INTRODUCTION

Thin film coated copper cavities are a promising alternative for RF superconducting accelerators with better thermal stability, better mechanical stability and low cost compared with bulk niobium cavities, and have been used in many accelerators. Most of Nb sputter-coated copper cavities suffer from obvious Q-slope with increasing accelerating field. There are many factors contributing to Q-slope, such as surface defect, film granularity, film-substrate binding force and roughness. The microstructure of Nb film on copper behaves like a network of superconducting grains coupled by Josephson junctions (the grain boundaries) [1][2], which gives rise to a RF dependent term in the surface resistance. Reducing the number of defects and grain boundaries per unit area should result in the decrease of surface resistance.

The films qualities seriously affect their superconducting performance, and the ultimate goal is to fabricate the bulk-like thin film, which we try to realize both in better fabrication methods and post-treatment.

The common PVD coating method for superconducting cavities including evaporation coating, magnetron sputtering coating, etc. According to the extended SZD (structure zone diagram) proposed by Andre Anders [3] (Fig. 1), the structure of the film is determined by deposition homologous temperature and the pressure. However, for the thin film deposited on copper, the temperature is limited to copper melting point (1083℃), which means it cannot be annealed with traditional heating. To solve this challenge, we are studying the benefits of short pulse laser annealing for niobium films on copper deposited by magnetron sputtering.

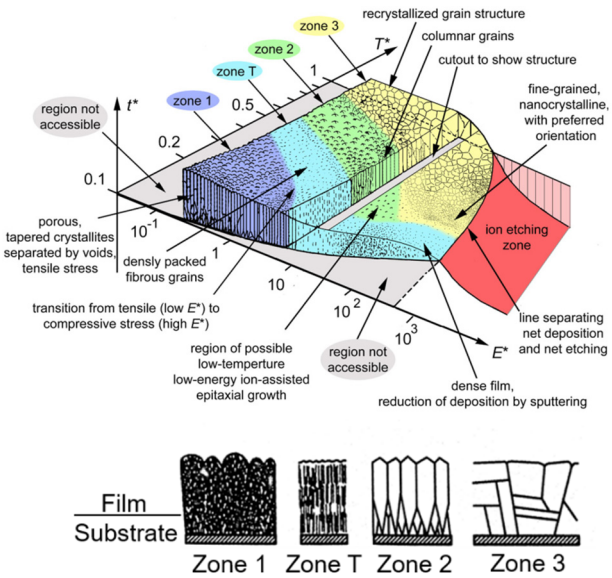


Figure 1: A possible presentation of such extended SZD [3] the figure of different zone. With the increasing temperature and pressure, the film structure changes from zone 1 to zone 3, and the formation of holes and protrusions in grain growth decreases which should make it more similar to bulk material.

EXPERIMENT SET UP AND PROCEDURE

Laser and Sample Preparation

The diffusion of heat generated by laser incident on the film surface satisfies the heat conduction equation, which was simulated by ANSYS first and showed that the pulse width of the incident laser could determine the depth of temperature field distribution. In order to make the heat limited in the film thickness scale, we selected the UV laser pulse of 30ns and changed the voltage and exposure times to explore the proper pulse energy. The simulation results by ANSYS are showed in Fig. 2.

Figure 3 shows the samples we used which were respectively deposited on copper by dcMS (DC magnetron Sputtering) and HIPIMS (High Power Impulse Magnetron Sputtering), both of them have smooth surface and good superconducting performance. The film thickness of the samples is about a few hundred nanometres, while the film of HIPIMS has higher density and compactness, which may benefit the annealing results.

* Work supported by Major Research Plan of National Natural Science Foundation of China (No. 91026001).
† Email address: yangyujia@pku.edu.cn

Content from this work may be used under the terms of the CC BY 3.0 licence (© 2018). Any distribution of this work must maintain attribution to the author(s), title of the work, publisher, and DOI.

ISBN: 978-3-95450-194-6 ISSN: 2226-0366 doi:10.18429/JACoW-LINAC2018-TUPO049

NITROGEN DOPING STUDY WITH 1.3 GHz SINGLE CELL SUPERCONDUCTING CAVITIES *

Shu Chen, Jiankui Hao#, Shengwen Quan, Feng Zhu, Lin Lin, Liwen Feng, Fang Wang, Meng Chen, Kexin Liu
State Key Laboratory of Nuclear Physics and Technology & Institute of Heavy Ion Physics, Peking University, Beijing 100871, China

Abstract

Nitrogen doping studies were carried out at Peking University. A series of 1.3 GHz single cell cavities fabricated with OTIC large grain niobium material were annealed and doped in the furnace of Peking University, and electropolished by a simple EP device. Light doping recipe and heavy doping recipe are both adopted for comparison. The results and analysis are presented in this paper.

INTRODUCTION

Impurity doping has been a hot topic in recent years to increase quality factor Q_0 of superconducting cavity. Especially for nitrogen doping, the effect is much more obviously. Nitrogen doping was discovered by FNAL in 2013 [1], and developed by FNAL, Jlab and Cornell University in the next few years [2]. There are two kinds of doping recipes, light doping and heavy doping. For light doping, the cavity is exposed in nitrogen for 2 minutes and annealed in vacuum for 6 minutes. While for heavy doping, the cavity is exposed in nitrogen for 20 minutes and annealed in vacuum for 30 minutes. Nitrogen doping studies were carried out at Peking University in recent years with 1.3 GHz single cell cavities. The cavities were fabricated with Ningxia OTIC large grain material. After mechanical fabrication, the cavities were eched 250 μm by buffered chemical polishing (BCP) to remove the surface mechanical damage layer. After high pressure rinsing (HPR), the cavities are annealed at 800 °C for 3 hours and nitrogen doping in the high temperature furnace. Following by slightly EP and HPR, the cavities were assembled in clean room and tested in vertical test system.

EXPERIMENTAL SETUP

Nitrogen Doping Furnace

After BCP and HPR, the cavities were annealed and doped in the furnace of Peking University, see Figure 1. The ultimate vacuum of the furnace is 1×10^{-5} Pa. Several 1.3 GHz single cell cavities can be annealed at the same time in the chamber. The cavities were supported by niobium holders and laid on the niobium plate.



Figure 1: High temperature furnace for cavities annealing and three single cell cavities in the chamber before annealing.

The chamber of the furnace is evacuated by cryopump and forepump, including roots pump and screw pump. In operation, the vacuum is reached to 2×10^{-4} Pa from atmospheric pressure in 1 hour. In nitrogen doping procedure, the nitrogen gas was evaporated from liquid nitrogen tank.

Surface Treatment



Figure 2a: Simple EP device.

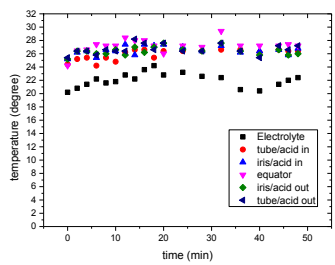


Figure 2b: The temperature in different places of the cavity during the process of EP.

After nitrogen doping, the cavity surface was electropolished with a simple EP device, see Figure 2a. The temperature of electrolyte was controlled under 25 °C. The temperature of the cavity was around 27 °C. Figure 2b shows the temperature in different places of the cavity. The rotation speed was about 1 rpm, and the acid flow rate was about 3 l/min. After EP, high pressure rinsing was used to clean the residual acid at the cavity surface.

*Work supported by National Key Programme for S&T Research and Development (Grant No. 2016YFA0400400) and National Natural Science Foundation of China (Grant No. 11575012)
#E-mail: jkhao@pku.edu.cn

Content from this work may be used under the terms of the CC BY 3.0 licence (© 2018). Any distribution of this work must maintain attribution to the author(s), title of the work, publisher, and DOI.

ISBN: 978-3-95450-194-6 ISSN: 2226-0366 doi:10.18429/JACoW-LINAC2018-TUPO050

CONSTRUCTION OF THIN-FILM COATING SYSTEM TOWARD THE REALIZATION OF SUPERCONDUCTING MULTILAYERED STRUCTURE

R. Ito†, T. Nagata, ULVAC, Inc, 286-0225 Chiba, Japan
H. Hayano, T. Kubo, T. Saeki, KEK, 305-0851 Tsukuba, Ibaraki, Japan
Y. Iwashita, R. Katayama, Kyoto ICR, Kyoto University, 611-0011 Uji, Kyoto, Japan
H. Ito, SOKENDAI, 305-0801 Tsukuba, Ibaraki, Japan
H. Oikawa, Utsunomiya University, 321-8585 Utsunomiya, Tochigi, Japan

Abstract

Although S-I-S (superconductor-insulator-superconductor) multilayered structure is expected to increase the maximum acceleration gradient of SRF cavities, in order for it to function in reality, it is necessary to develop a coating processing that can realize high purity and quality superconducting thin-films. In this study, we prepared several NbN-SiO_2-Nb multilayered samples which have different NbN film thickness to investigate the film thickness dependence of effective H_{c1} of S-I-S multilayered samples. In addition, we launched the co-sputtering system to get Nb_3Sn thin-film samples. The deposition rates of Nb and Sn cathodes were measured, and then the two cathodes were simultaneously sputtered aiming at appropriate composition ratio. Furthermore, we developed another experimental apparatus for coating on the inner surface of the 3 GHz TESLA type small cavities. A cylindrical Nb cathode was fabricated, and glow discharge was confirmed. This paper reports the specification of the two sputtering apparatuses and future experiment plans for demonstration and realizing of S-I-S multilayered cavities.

INTRODUCTION

S-I-S thin-film multilayered structure theory has been proposed to increase vortex penetration field of SRF cavities [1, 2]. According to this theory, the vortex penetration field of multilayered thin-film structures can reach approximately 250 mT when NbN is used for the superconducting layer and approximately 480 mT when Nb_3Sn is used. However, it is not clear whether this calculated value in this theory can really be achieved, in fact, multilayered thin-film cavities which exceed the maximum acceleration gradient of Nb cavities have not been realized. Thus, it is necessary to demonstrate the multilayered thin-film theory and to establish coating techniques for fabricating S-I-S thin-film multilayered cavities.

In order to demonstrate the theory, we firstly aimed to evaluate the effective H_{c1} of S-I-S samples [3, 4]. In previous studies, we have already established the reactive sputtering conditions for obtaining high quality NbN thin-films. Moreover, we have succeeded in preparing S-I-S samples which consist of 200 nm NbN layer, 30 nm SiO_2 layer, and pure Nb substrate. The XRD patterns of these S-I-S samples showed sharp Nb and NbN peaks [5]. In this study, we prepared several NbN-SiO_2-Nb multilayered sample which have different NbN film thickness to investigate the film thickness dependence of effective H_{c1}. Furthermore, we launched an experimental apparatus for co-sputtering of Nb_3Sn. Co-sputtering is a coating method for obtaining alloy thin-films by simultaneously sputtering two or more cathodes. In this method, it is possible to coat Nb_3Sn thin-films which have composition ratio of 3:1 by adjusting the input power ratio of Nb and Sn cathodes.

Table 1: Details of NbN-SiO_2-Nb Multilayered Thin-film Samples

Sample Name	NbN Layer Thickness [nm]	SiO_2 Layer Thickness [nm]
180814-1-A, B	50	30
180814-2-A, B	100	30
180814-3-A, B	150	30
180814-4-A, B	250	30
180814-5-A, B	300	30
180814-6-A, B	400	30

In order to realize S-I-S multilayered cavities, we also launched another experimental apparatus for basic test of the inner sputtering on TESLA type cavities. We will use this apparatus to deposit Nb or NbN on the inner surface of the 3 GHz cavities and evaluate film thickness distribution and the thin-film characteristics such as crystalline orientation.

MULTILAYERED SAMPLE PREPARING

NbN-SiO_2-Nb multilayered thin-film samples were prepared by using in-house sputtering apparatus. The Nb substrates (RRR > 300) were electro polished before NbN-SiO_2 coating. Our sputtering experimental apparatus adopts inter-back system, and a substrate carrier passes in front of Nb cathode (RRR > 300) and two Si cathodes at a regular speed. Therefore, the sputtered elements are uniformly deposited on substrate. The sizes of both Nb and Si cathodes are 5 inches by 18 inches. The base pressure of the sputtering chamber was about 2×10^{-4} Pa. Ar and N_2 (or O_2) gasses were introduced in the sputtering chamber, NbN or SiO_2 thin-films were reactively sputtered. The Nb cathode was powered by DC supply, and the two Si cathodes were powered by AC supply. In NbN coating, DC input power was set constant at 3.0 kW, and Ar partial pressure was 0.3 Pa. On the other hand, in SiO_2 coating, AC input power was set constant at 6.0 kW, and Ar partial pressure

† ryouhei_itou@ulvac.com

Content from this work may be used under the terms of the CC BY 3.0 licence (© 2018). Any distribution of this work must maintain attribution to the author(s), title of the work, publisher, and DOI.

ISBN: 978-3-95450-194-6 ISSN: 2226-0366 doi:10.18429/JACoW-LINAC2018-TUPO051

DESIGN CONSIDERATIONS OF A BALLOON-SHAPED SSR SUPERCONDUCTING CAVITY

H. J. Cha†, J. Y. Yoon, S. W. Jang, K.-R. Kim[1], S. H. Park and E.-S. Kim
Department of Accelerator Science, Korea University Sejong Campus, Sejong, South Korea
[1]also at Pohang Accelerator Laboratory, POSTECH, Gyeongbuk, South Korea

Abstract

We introduce a balloon-shaped SSR superconducting cavity for multipacting mitigation. The electromagnetic modeling of the SSR was made based on the RF parameter optimization. The simulation results show much narrower multipacting bandwidth, compared to those for the traditional spoke cavity. Mechanical analyses with stiffening structure indicate acceptable stresses at the cavity wall.

INTRODUCTION

A single spoke resonator (SSR) having flat or round end walls has broad multipacting (MP) ranges in acceleration gradient, sometimes including operation region. In order to overcome such MP barriers, quite long radio frequency (RF) conditioning is required, which is not cost-effective and disadvantageous for mass production of the superconducting cavities. An alternative cavity with a resonant frequency f of 325 MHz and an optimum beta β_o of 0.3 has been being developed at TRIUMF [1, 2].

An SSR with f = 325 MHz and β_o = 0.51 has been studied at Korea University. Especially, this spoke cavity may be applied to the high-energy superconducting linac sections for a heavy ion accelerator such as RAON [3]. In this study, we introduce a balloon variant of the superconducting SSR which makes the MP mitigation possible due to its structural simplicity, based on its electromagnetic (EM), MP, and mechanical analyses.

ELECTROMAGNETIC SIMULATIONS

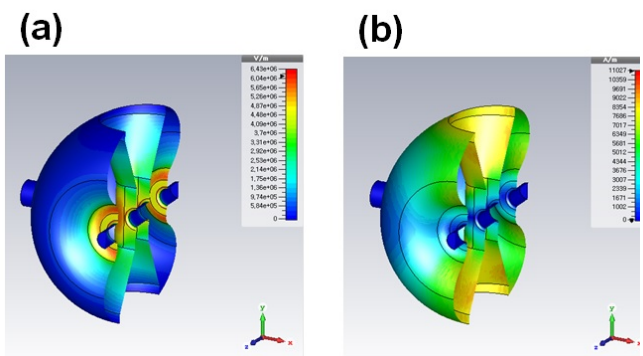


Figure 1: (a) Electric and (b) magnetic field distributions of the balloon-shaped SSR.

Figure 1 shows EM field distributions of the balloon-shaped SSR. The electric fields are mostly distributed at near a beam tunnel and the magnetic fields at loft and base parts of the spoke for the cavity with a transverse electromagnetic (TEM) mode. The horizontal geometric parameters of an EM modeling for the balloon-shaped SSR are based on the definitions from beam dynamics and transit time factor (TTF) studies that an iris-to-iris length L_{iris} is $(2/3)\beta_g\lambda$ and a gap-to-gap length L_{gap} is $\beta_g\lambda/2$, where β_g is a geometric beta ($\approx \beta_o$ of 0.51) and λ a wavelength (~923 mm for 325 MHz). Two (upper and lower) ellipses in a y-z plane were adopted for the balloon-shaped modeling. A view of the balloon-shaped SSR in a x-y plane is nearly circular.

It is well-known that a superconducting cavity should be designed to lower the peak electric field E_{peak} and the peak magnetic field B_{peak} as possible with keeping good RF properties because their increases can limit the acceleration performance by field emission and quench, respectively. In the EM design of the balloon-shaped SSR, we aim the B_{peak} under 80 mT when the E_{peak} is 35 MV/m. The resultant RF parameters are also normalized by 35 MV/m. As the geometric parameters change, we focus on the decrease of E_{peak}/E_{acc} and B_{peak}/E_{acc} and the increase of $G{\cdot}R_{sh}/Q_0$, where E_{acc} is the acceleration gradient, G the geometry factor, R_{sh} the shunt impedance, and Q_0 the unloaded quality factor of the cavity. The surface resistance R_s used for calculating the G (= Q_0R_{sh}) is ~10.64 nΩ from BCS resistance R_{BCS} of 0.64 nΩ at a frequency of 325 MHz and a temperature of 2 K with an assumption of the residual resistance R_{res} of 10 nΩ ($R_s = R_{res} + R_{BCS}$). From proper compromises among simulation results with the geometric parameter sweeps, the final geometry of the balloon-shaped SSR were determined and its RF parameters are summarized in Table 1.

Table 1: EM Simulation Results for the Balloon-shaped SSR.

RF Parameter	Value
Q_0 ($\times 10^9$)	10.7
R_{sh}/Q_0 (Ω)	296
G (Ω)	118
E_{peak} (MV/m)	35
B_{peak} (mT)	75
V_{acc} (MV)	4.2
E_{acc} (MV/m)	9
E_{peak}/E_{acc}	3.9
B_{peak}/E_{acc} (mT/MV/m)	8.4
Stored energy (J)	29.6
Dissipated power (W)	5.6

MULTIPACTING SIMULATIONS

A main advantage of the balloon-shaped SSR is MP suppression due to its simple structure. A traditional spoke

† chahj@korea.ac.kr

Content from this work may be used under the terms of the CC BY 3.0 licence (© 2018). Any distribution of this work must maintain attribution to the author(s), title of the work, publisher, and DOI.

ISBN: 978-3-95450-194-6 ISSN: 2226-0366 doi:10.18429/JACoW-LINAC2018-TUPO052

DESIGN STUDY OF A PROTOTYPE 325MHz RF POWER COUPLER FOR SUPERCONDUCTING CAVITY*

Junyoung Yoon, JungBae Bhang, Chong Shik Park, Hyuk Jin Cha, Si-Won Jang, Kyung-Ryul Kim[1], Seong Hee Park, Eun-San Kim† ,Korea University, Sejong, South Korea
Ilkyoung Shin, Institute for Basic Science, Daejeon, South Korea
Jonghwa Lee, Do Yoon Kim, Vitzrotech, Ansan, South Korea
Eiji Kako, KEK, Tsukuba, Japan
[1]also at Pohang Accelerator Laboratory, Pohang,South Korea

Abstract

We present design studies of a prototype RF input Power Coupler, which provides RF powers to 325MHz cavities up to 18.5kW in CW mode. The prototype power coupler is a coaxial capacitive type with single ceramic window. In order to optimize the RF coupler design, we performed multi-physics simulations, including electromagnetic, thermal, and mechanical analyses.

INTRODUCTION

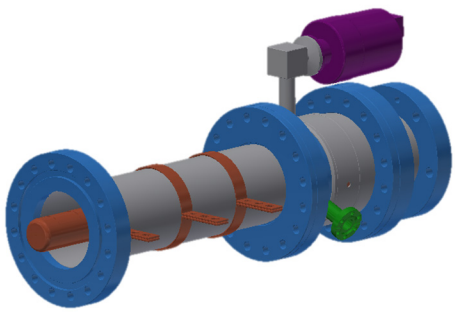


Figure 1: General view of power coupler.

The power coupler is based on conventional 50Ω coaxial transmission line. The prototype coupler has three diagnostic ports for vacuum, arc, and electron pick-ups to prevent RF breakdowns and three thermal interceptors for 4.5K, 40K, and 77K. Figure 1 shows a preliminary design of power coupler and the design requirements are listed in Ta ble 1 [1].

Table 1: Design Requirements of the Input Coupler

Parameters	Values	Unit
Operating frequency	325	MHz
Pass band ($S_{11} < 0.1$)	3	MHz
S_{11} at 325MHz	≤-30	dB
Operating Power	18.5	kW
Q_{ext}	4×10^6	-

SIMULATION

The CST Microwave Studio (MWS) Frequency Domain solver [2] is used for electromagnetic simulations and Ansys Theramal, Structural, Modal solvers were used for the Thermal/Mechanical simulations. [3]

Electromagnetic Simulation

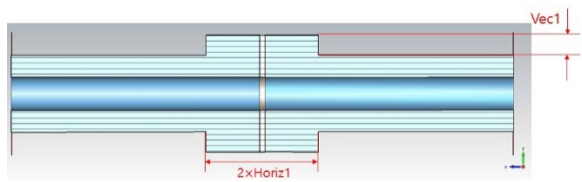


Figure 2: Geometric change of ceramic part.

Figure 2 shows variations of both diameter (Vec1) and length (Horiz1) of the outer conductor at the RF window to minimize reflected powers at 325MHz. We performed simulations to check effects of the diameter change from 8 mm to 10 mm. The optimal values of vertical length were between 8.6 mm to 9 mm shown in Figure 3. Considering engineering and manufacturing errors, we chose the 9 mm variation of the outer diameter at ceramic window.

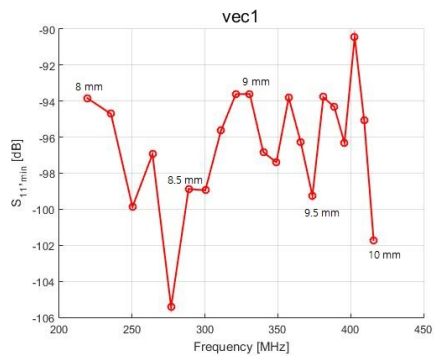


Figure 3: Effect of vertical length change.

The horizontal length change make a small frequency distribution in reflected powers (S_11) at 325MHz. Therefore, we performed the simulation in the narrow range to minimize reflected powers at 325MHz. Figure 4 shows that the optimal horizontal length is 117.2 mm.

† eskim1@korea.ac.kr

Content from this work may be used under the terms of the CC BY 3.0 licence (© 2018). Any distribution of this work must maintain attribution to the author(s), title of the work, publisher, and DOI.

ISBN: 978-3-95450-194-6 ISSN: 2226-0366 doi:10.18429/JACoW-LINAC2018-TUPO053

FABICATION OF Nb MUSHROOM SHAPED CAVITY FOR EVALUATION OF MULTI-LAYER THIN FILM SUPERCONDUCTOR

H. Oikawa†, Utsunomiya University, Utsunomiya Tochigi, Japan
T. Higashiguchi, Center for Optical Research and Education, Utsunomiya, Japan
H. Hayano, H. Inoue, K. Enami, KEK, Tsukuba Ibaraki, Japan

Abstract

The accelerating gradient of the Nb superconducting RF cavity seems to reach the limit due to the RF critical magnetic field of the Nb material. To obtain higher gradient, there has been proposed a method of increasing an RF critical magnetic field of the cavity inner surface by coating of multi-layer thin-film superconductor. It is needed to demonstrate improvement critical magnetic field of the RF cavity coated with multi-layer thin-film superconductor. To optimize thin-film superconductor, sample tests are required. A cavity for sample test is necessary to produce a strong RF magnetic field parallel to the surface of the sample for evaluating RF critical magnetic field. For such a cavity, we designed a mushroom shaped cavity made of Nb which is operated in cryogenic temperature. Input and pick up antenna coupler are also designed electrically and mechanically. The connection design of sample plate and cavity bottom plate in superconducting state is also designed. The Nb mushroom shaped cavity is under fabrication. Fabrication method and status are reported in this paper.

INTRODUCTION

A technique of improving the Q value and acceleration electric field of the cavity by adding a small amount of nitrogen at the time of annealing and by using a method of improving the critical magnetic field leading to a high acceleration electric field by stacking superconducting layers are developing for high performance of the superconducting cavity made of Niobium (Nb) [1, 2]. Those methods improve greatly RF loss and acceleration electric field. In order to optimize each parameter and thin film of the surface treatment, it is necessary to evaluate them repeatedly for manufacturing a cavity having such high performance. However, many cavity evaluations are large-scaled, so that a device for evaluating a test piece subjected to the same treatment is required. Particularly, in the technique using a multilayer thin film structure, it is difficult to form a uniform film from the complicated shape of the cavity and its size. Further, in order to optimize the film forming process, it is necessary to perform film formation many times. Therefore, evaluation with a test piece is desired so that it is smaller than the cavity and easy to form a film, and it is easy to form many times. In this report, in order to evaluate the performance of test piece of multilayer thin film superconductors for superconducting cavity, we report on the design and fabrication of cavities for measuring critical magnetic field at cryogenic temperature.

† oikawah@post.kek.jp

DESIGN, FABRICATION AND EVALUATION OF TEST AL CAVITY

Design and Fabrication of Al Mushroom Shaped Cavity

In evaluating the multi-layer thin-film superconductor for the superconducting cavity, we considered that the following physical quantity evaluation is necessary.

- Superconducting transition temperature (Tc).
- RF surface resistance (Rs).
- critical magnetic field (Hc).

As a device for evaluating these physical quantities, we considered to use a cavity resonator that can replace the test piece repeatedly. This is because excitation of a strong electromagnetic field is possible, the above physical quantity can be measured all at once and it is thought that evaluation of many test pieces becomes easy.

First we started the design with SLAC's 11.4 GHz cavity [3]. The resonance frequency was chosen to 5.2 GHz

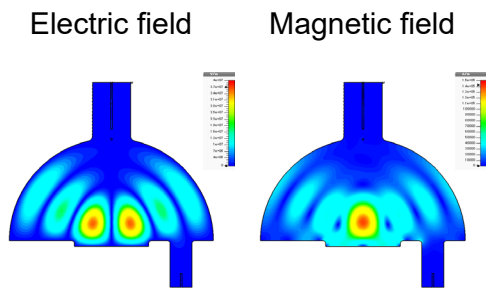


Figure 1: Calculated electromagnetic field in the mushroom-shaped cavity.

and the resonance mode was also chosen to TE_{013}.

Figure 1 shows the electromagnetic field excited in the designed cavity calculated by CST MW STUDIO [4]. As an initial step toward the fabrication of a Nb superconducting cavity, an Al-based cavity was proposed to evaluate the target resonant frequency, the separations of neighboring modes, and the electromagnetic field distribution of the target mode. Figure 2 shows the cross sectional drawing of the aluminum test cavity.

Evaluation of Al Mushroom Shaped Cavity

Figure 3 shows the frequency displacement during bead-pull measurement when a small metal cylinder is inserted into the test cavity and swept. Frequency shift calculated by CST MW STUDIO using perfect conductor cylinder is also inserted. Although there is a difference in frequency deviation along the sweep direction due to the cavity loss and the coupling of the antennas. Since the

Content from this work may be used under the terms of the CC BY 3.0 licence (© 2018). Any distribution of this work must maintain attribution to the author(s), title of the work, publisher, and DOI.

ISBN: 978-3-95450-194-6 ISSN: 2226-0366 doi:10.18429/JACoW-LINAC2018-TUPO054

FUNDAMENTAL STUDIES OF IMPURITY DOPING IN 1.3 GHz AND HIGHER FREQUENCY SRF CAVITIES*

J. T. Maniscalco†, P. N. Koufalis, and M. Liepe
CLASSE, Cornell University, Ithaca, NY 14853, USA

Abstract

As the demand for more powerful, more efficient, and smaller superconducting RF accelerators continues to increase, both impurity doping and high-frequency cavities (>1.3 GHz) have become hot topics for fundamental research because of their potential to significantly decrease surface losses and cost respectively. In this report, we present recent experimental and theoretical results on undoped and nitrogen-doped high-frequency cavities and on alternative doping agents in traditional 1.3 GHz cavities, with a focus on understanding the fundamental science of impurity doping.

"2/6 DOPING" AT 2.6 GHz

Impurity doping is a technique for preparing niobium superconducting radio-frequency (SRF) cavities that can increase the quality factor Q by a factor of two or more at low field and cause an "anti-Q-slope" in which Q rises as the cavity field increases [1–3]. This Q rise has been shown to increase in strength with increasing frequency [4]. At IPAC'18, we presented Cornell's first results of an impurity-doped 2.6 GHz niobium cavity [5, 6]. This ILC/TESLA-shape cavity [7] (B_{pk}/E_{acc} = 4.28 mT/(MV/m)) was treated with the so-called "2/6 doping": a degas step in vacuum for 5 hours, followed by an injection of 40 mTorr (6 Pa) of continuously flowing N_2 gas for 2 minutes, followed by a vacuum anneal step for 6 minutes, all at 800 °C. This is followed by 6 µm of surface removal by vertical electropolish (VEP). In the initial test, the cavity showed a strong field-dependent reduction in the temperature-dependent "BCS" portion of the surface resistance.

In this paper, we present the results of additional study of this cavity, investigating the sensitivity of the temperature-independent "residual" surface resistance R_0 to trapped magnetic flux. This sensitivity has been studied extensively in 1.3 GHz nitrogen-doped cavities, where strongly doped cavities (electron mean free path $\ell < 100$ nm) exhibit up to 5 nΩ of residual resistance per mG of magnetic flux trapped during cooldown [3, 8]. To determine this sensitivity, we record R_0 as a function of field for several different amounts of trapped flux $B_{trapped}$ and subtract the non-flux-dependent R_0 present in a cooldown with no flux trapped (typically a "fast" cooldown with a cross-cavity temperature gradient $\nabla T > 200$ K/m). We then take $R_0/B_{trapped}$ and perform a linear fit over the RF field strength to yield an overall offset sensitivity as well as a field-dependent sensitivity. Previous analyses of 1.3 GHz N-doped cavities largely considered only the offset parameter, *e.g.* the 5 nΩ/mG figure above; analyses of 1.3 GHz Nb_3Sn cavities have included similar two-parameter linear fits [9].

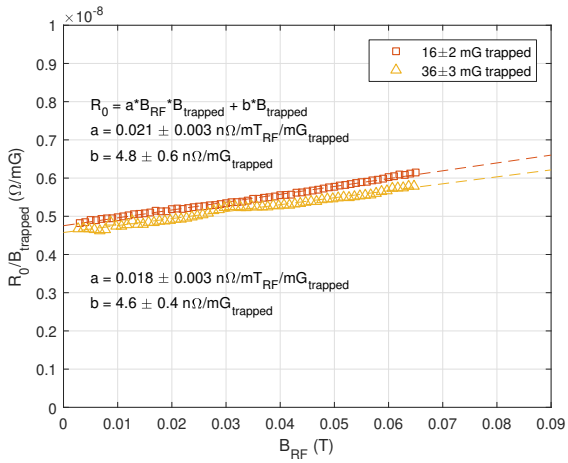


Figure 1: Sensitivity of the residual resistance due to trapped magnetic flux for two cooldowns of a single 2/6-doped 2.6 GHz niobium cavity.

Figure 1 shows these results for two cooldowns of the 2/6-doped 2.6 GHz cavity, which had an $\ell = 46$ nm. The linear fit parameters for both tests (with 16 ± 2 mG and 36 ± 3 mG trapped, respectively) were consistent within uncertainty. Averaging the results yields a sensitivity of $R_0 = aB_{RF}B_{trapped} + bB_{trapped}$ with $a = 0.020 \pm 0.003$ nΩ/mT$_{RF}$/mG$_{trapped}$ and $b = 4.7 \pm 0.5$ nΩ/mG$_{trapped}$.

The offset sensitivity b here is approximately two times larger than the sensitivity we reported at 1.3 GHz for cavities with similar ℓ; in the previously reported model [8], a 1.3 GHz cavity with $\ell = 46$ nm would have sensitivity $b = 2.4$ nΩ/mG$_{trapped}$. This indicates a linear scaling of this effect in 2/6-doped cavities with frequency $b \propto \omega$; other doping protocols may give different scaling. See also [10] for discussion of possible scaling mechanisms.

160 °C "N-INFUSION" AT 2.6 GHz

We also prepared a 2.6 GHz ILC-shape cavity with the "low-temperature dope" or "nitrogen-infusion" procedure, which consists of an 800 °C degas step followed by a ramp down to 160 °C and a 48-hour doping step with 40 mTorr (6 Pa) of continuously flowing N_2 gas. The cavity received no chemical treatment after doping. At 1.3 GHz, this treat-

* This work was supported in part by the U.S. National Science Foundation under Award PHY-1549132, the Center for Bright Beams, and under Award PHY-1734189. This work was also supported by the U.S. Department of Energy and the LCLS-II HE Project.
† jtm288@cornell.edu

Content from this work may be used under the terms of the CC BY 3.0 licence (© 2018). Any distribution of this work must maintain attribution to the author(s), title of the work, publisher, and DOI.

ISBN: 978-3-95450-194-6 ISSN: 2226-0366 doi:10.18429/JACoW-LINAC2018-TUPO055

NEXT GENERATION Nb_3Sn CAVITIES FOR LINEAR ACCELERATORS*

R. D. Porter†, T. Arias, P. Cueva, D. L. Hall, M. Liepe, J. T. Maniscalco, D. A. Muller, N. Sitaraman
Cornell University, Ithaca, NY 14853, USA

Abstract

Niobium-3 Tin (Nb_3Sn) is a very promising alternative material for SRF accelerator cavities. The material can achieve higher quality factors, higher temperature operation and potentially higher accelerating gradients ($E_{acc} \approx 96\,MV/m$) compared to conventional niobium. This material is formed by vaporizing Sn in a high temperature vacuum furnace and letting the Sn absorb into a Nb substrate to form a 2-3 µm Nb_3Sn layer. Current Nb_3Sn cavities produced at Cornell achieve $Q \approx 2 \cdot 10^{10}$ at 4.2 K and $E_{acc} = 17\,MV/m$. Here we present a summary of the current performance of Nb_3Sn cavities at Cornell and recent progress in improving E_{acc}.

INTRODUCTION

Nb_3Sn possesses a high critical temperature (18 K [1]) and superheating field (425 mT [2]) giving it the potential for higher quality factors than Nb, 4.2 K operation, and for accelerating gradients of $\approx 96\,MV/m$. Cornell has a leading program in developing Nb_3Sn accelerator cavities [3–7]. Here we present the current status of the material and review recent progress. In particular we discuss the cause of the low (relative to the maximum possible for this material) quench fields and progress towards raising them.

Nb_3Sn GROWTH PROCESS

Nb_3Sn accelerator cavities cannot be pressed out of a Nb_3Sn sheet as can conventional Nb cavities due to the difficulty of making Nb_3Sn and its brittle nature. Instead, current Nb_3Sn cavity programs use Sn vapor deposition to grow Nb_3Sn on a Nb substrate that is already in the shape of a cavity [8]. In this process an Nb cavity is placed in a high temperature vacuum furnace with a crucible full of Sn and bowl of $SnCl_2$. After a $24 - 48$ hr degas step at 180 °C, the temperature is ramped to 530 °C, and held for 5 hrs while the nucleation agent, $SnCl_2$ vaporizes and decomposes on the Nb leaving behind Sn. The temperature is then raised to ≈ 1150 °C for coating where there is an appreciable Sn vapor pressure. Sn vapor lands on the surface of the cavity where it forms Nb_3Sn. To further increase the Sn vapor pressure the Sn crucible is heated to an even higher temperature. After 1.5 hrs at this temperature the crucible heating is turned off and the surface is allowed to anneal for 1 hr. This process forms a $2-3$ µm Nb_3Sn layer. Figure 1 shows the temperature profile for a Nb_3Sn coating run.

* This work is supported in part by the U.S. National Science Foundation under Award PHY-1549132, the Center for Bright Beams. This work is supported in part by U.S. DOE award DE-SC0008431. This work made use of the Cornell Center for Materials Research Shared Facilities which are supported through the NSF MRSEC program (DMR-1120296).
† rdp98@cornell.edu

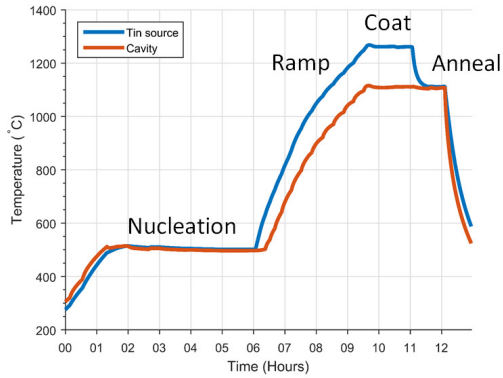


Figure 1: Temperature during Nb_3Sn coating showing both the cavity and the tin source temperatures.

CURRENT PERFORMANCE

Current performance offers transformational quality factors of $2 \cdot 10^{10}$ at 4.2 K and 1.3 GHz (see Fig. 2). This is more than a 20 times improvement in Q over Nb at 4.2 K, allowing 4.2 K operation. In CW operation our Nb_3Sn cavities currently quench around 17 MV/m, capable of meeting accelerator gradient requirement of some current CW LINACs. Pulsed operation (see Fig. 3) sees greater accelerating gradients of up to 26 MV/m [9]. These are usable accelerating gradients, but far below the theoretical maximum of 96 MV/m, giving Nb_3Sn a lot of room for improvement.

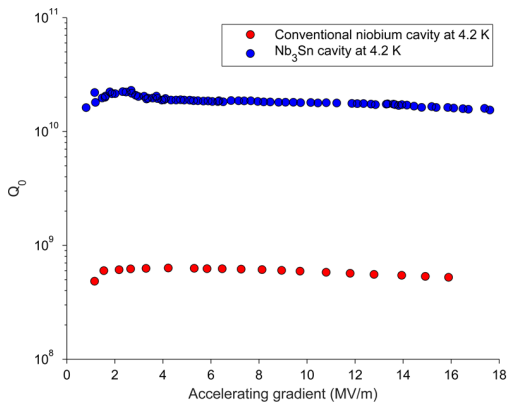


Figure 2: Q versus E performance of a Nb_3Sn cavity versus a Nb cavity at 4.2 K and 1.3 GHz.

THERMOMETRY OF DEFECT

Thermometry (temperature maps) reveal that quench are being caused by heating at some localized defect [10]. The key to raising the quench fields is removing the defect. This requires a firm understanding of what the defect is. To that end Cornell used time resolved thermometry of the quench

Content from this work may be used under the terms of the CC BY 3.0 licence (© 2018). Any distribution of this work must maintain attribution to the author(s), title of the work, publisher, and DOI.

ISBN: 978-3-95450-194-6 ISSN: 2226-0366 doi:10.18429/JACoW-LINAC2018-TUPO057

LOW-TEMPERATURE BAKING AND INFUSION STUDIES FOR HIGH-GRADIENT ILC SRF CAVITIES*

M. Ge†, P. Koufalis, G. Kulina, M. Liepe, J. Maniscalco,
CLASSE, Cornell University, Ithaca, New York, USA

Abstract

Low-temperature infusion has become a hot-topic in SRF researches recently. Past results show that low-temperature infusion can produce high quality factor at medium accelerating fields. Also, 75ºC baking recently has been shown to improve accelerating gradients of SRF cavities. Hence these treatments are very promising for reducing cost of the ILC. In this work, we present latest results of low temperature infusion and baking, showing that these treatments can improve SRF cavities performance.

INTRODUCTION

The proposed International Linear Collider (ILC) is a proposed 200-500GeV linear electron-positron collider, based on 1.3GHz superconducting radio-frequency (SRF) technology [1]. The total cost of the ILC is an important constraint, determining whether the project is feasible or not. As the main part of the linear collider consist of SRF cryomodules, the performances, e.g. quality factor Q_0 and accelerating gradients (E_{acc}), of the SRF cavities are critical to control the cost of the ILC; because high-Q_0 cavities can reduce cryogenic loads, and high-gradient cavities will decrease the total length of the ILC.

The baseline technology of ILC to produce SRF cavities is electropolishing and 120°C baking which can produce a cavity with E_{acc} ~35 MV/m with $Q_0 \sim 8\times10^9$. However, recently new discoveries in SRF field, e.g. low-temperature infusion [2, 3] and 75°C baking [4], could have large potentials to improve quality factor and gradient, and thereby to reduce cost.

CAVITY PREPERATION

We use two 1.3 GHz ILC-type single-cell SRF cavity (LTE1-14 and LTE1-15) for this work. As the baseline treatment, the two cavities had been treated by the ILC baseline recipe [5], i.e. 100 um surface removal by electropolishing (EP), and 900ºC baking for 3 hours, and then 120ºC baking for 48 hours. After the baseline treatment, both cavities have been vertically tested on the Cornell wave-guide insert allowing regular CW and high-power pulse measurement in same cryogenic cycle, as is shown in Fig. 1 [6]. After that, the cavity LET1-14 was baked at 800 ºC for 3 hours then baked at 120ºC under ~40mTorr N_2 for 48 hours. During the baseline treatment and 120ºC infusion, witness samples were baked with the cavities. SIMS data of the samples showed the 120ºC infusion increases the level of nitrogen and carbon, as is shown in Fig. 2. LET1-14 has been tested after the infusion; then the cavity was 75°C baked for 6 hours on the insert and tested again.

LTE1-15 received the 1st 75°C baking for 6 hours on the insert after the baseline test; then the cavity was tested again. After that we did HF rinsing of the cavity, followed by another test. At last, the 2nd 75°C baking was carried out for the cavity on the insert and followed by a final vertical test.

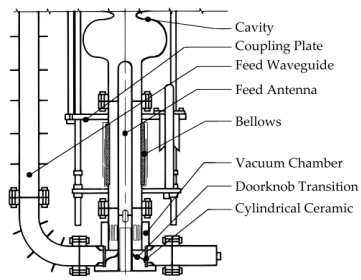
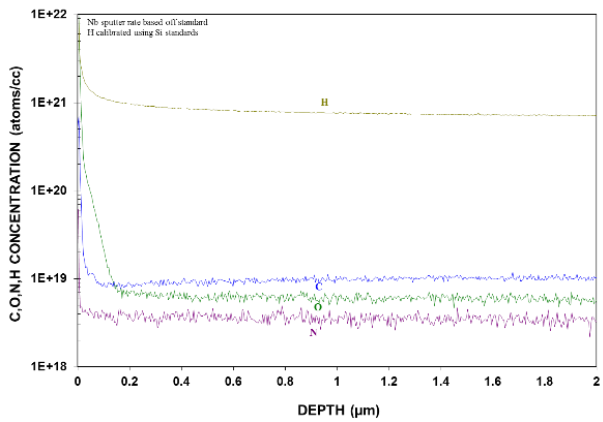
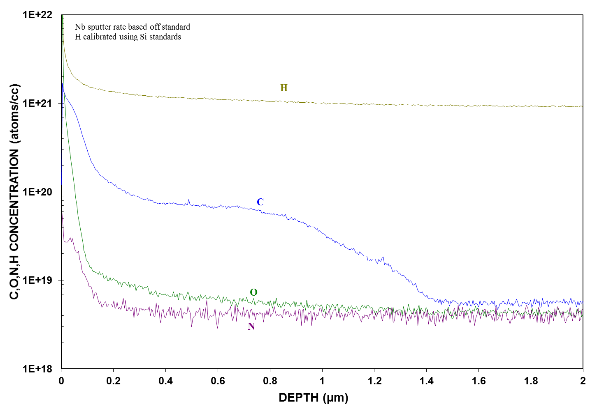


Figure 1: Schematic of wave-guide insert allowing regular CW and high-power pulse measurement in same cryogenic cycle.



(a) SIMS data of samples baked at 120°C under vacuum.



(b) SIMS data of samples baked at 120°C under N_2.

Figure 2: SIMS data comparison between 120°C baking under vacuum and under N_2.

* Work supported by the Department of Energy.
† mg574@cornell.edu.

Content from this work may be used under the terms of the CC BY 3.0 licence (© 2018). Any distribution of this work must maintain attribution to the author(s), title of the work, publisher, and DOI.

ISBN: 978-3-95450-194-6 ISSN: 2226-0366 doi:10.18429/JACoW-LINAC2018-TUPO058

COOL DOWN STUDIES FOR THE LCLS-II PROJECT*

M. Ge†, M. Liepe, J. Sears, CLASSE, Cornell University, Ithaca, New York, USA
D. Gonnella, SLAC National Accelerator Laboratory, Menlo Park, California, USA

Abstract

The quality factor of the nitrogen-doped SRF cavities for the LCLS-II project are strongly impacted by cool down speed. A sufficiently fast cool down speed can produce large thermal gradient across a cavity and sufficiently expel magnetic flux when the cavity wall passes from the normal-conducting to the superconducting state. However, instrumentation in LCLS-II production cryomodules has been kept at a minimum, and additional information during the cool down of the modules is therefore desirable. In this work, we study if and how RF data can be used during cavity cool-down to determine the transition speeds of the individual cavities in the LCLS-II linac.

INTRODUCTION

The LCLS-II project requires an average unloaded quality factory Q_0 for the 1.3 GHz SRF cavities of 2.7×10^{10} at an operating temperature of 2K and accelerating gradient of 16 MV/m [1]. The 2N/6 nitrogen doping recipe (2 min N-doping at 800C followed by a 6 min anneal at 800C) [2, 3] has been chosen for the surface preparation of the LCLS-II SRF cavities, However, the quality factor of nitrogen doped SRF cavities are strongly impacted by cool down speed [4] due to their high sensitivity to losses from trapped magnetic flux [5].

New cool down studies on a single-cell cavity were conducted with the goal of developing a means of measuring cool down rate of SRF cavities using RF methods when temperature sensors are not available, such as in the LCLS-II cryomodules. A single-cell cavity was provided by LCLS-II for these studies. This cavity was reset using EP at Cornell, and then given the standard 2/6 nitrogen-doping that LCLS-II production cavities receive. The cavity was tested at Cornell on a test insert fitted with a variable coupler that could reach Q_{ext} close to 4×10^7, the Q_{ext} required by the LCLS-II project for cavities assembled in cryomodules.

32 cool downs of the cavity were completed in total. The goal of these cool downs was to determine

1. If it is possible to identify cool down rate and/or gradient by means of the transition time of the cavity as measured on a network analyzer
2. If 1. is affirmative, define a model which from a given transition time predicts the cool down rate and/or gradient of a cavity in the cryomodules during linac cooling.

METHOD

A single-cell cavity was cooled in a vertical test Dewar multiple times, with different cool down rates and gradients. A picture of the cavity on the test stand is shown in Figure 1. Temperature sensors were placed on the cavity, two on the equator, and two on each of the irises. The Q_{ext} of the input coupler was set to $\sim4\times10^7$. A network analyzer was connected to the forward and transmitted power connections on the cavity and an S_{21} measurement was taken during cool down. The parameters for the network analyzer measurement are given in Table 1.



Figure 1: Test insert with single-cell cavity and instrumentation.

Table 1: Network Analyzer Parameters

Parameter	Value
Center	Resonance f_0 at starting temp, re-centered after each scan
Span	100 kHz
IF Bandwidth	100 Hz
Forward Power	~10 W

From an S_{21} measurement, the loaded quality factor Q_L of the cavity can be calculated,

$$Q_L = \frac{f_0}{\Delta f}, \quad (1)$$

where f_0 is the resonance frequency of the cavity (peak on the network analyzer) and Δf is the width of the resonance

* Work supported by the US DOE and the LCLS-II project.
† mg574@cornell.edu.

Content from this work may be used under the terms of the CC BY 3.0 licence (© 2018). Any distribution of this work must maintain attribution to the author(s), title of the work, publisher, and DOI.

ISBN: 978-3-95450-194-6 ISSN: 2226-0366 doi:10.18429/JACoW-LINAC2018-TUPO059

LATEST RESULTS OF SALT BASED BIPOLAR ELECTRO-POLISHING R&D AT CORNELL*

M. Ge†, F. Furuta, T. Gruber, J. Kaufman, M. Liepe, R. D. Porter
CLASSE, Cornell University, Ithaca, New York, USA
T. Hall, R. Radhakrishnan, S. Snyder, E. J. Taylor, Faraday Technology, Inc., Clayton, Ohio, USA

Abstract

Acid free electropolishing would be safer to use and friendlier to the environment. A collaboration, supported by the DOE SBIR Phase-II program, between Faraday Technology Inc. and Cornell University focused on salt-based bipolar electropolishing (BEP). In this paper, we present the latest salt-based BEP results. The superconducting performance of a single-cell 1.3GHz cavity has been carefully analyzed, showing that salt-based BEP is promising, but still has large room for improvement.

INTRODUCTION

As superconducting radio-frequency (SRF) technology is increasingly widely used in modern accelerators, the search for an eco-friendly niobium surface process has become an important topic. The objective of this work is finding an alternative to hydrofluoric (HF) and other acids used in the conventional electropolishing process. Acid free electropolishing (EP) uses a near-neutral aqueous salt solution, e.g. $NaNO_3$ or NaCl solution, as electrolyte in bipolar electropolishing [1].

It has been previously reported by Faraday Technology Inc. (Faraday) [1] that the surface roughness of niobium coupons treated with salt-based EP can achieve values as low as 0.05 um, with a material removal rate of ~42 um/hr. The transition from flat coupons to a single-cell cavity requires a more complex set-up, which is based on the bipolar electropolishing system at Faraday. In collaboration with Faraday [2], Cornell tested a 1.3GHz single-cell SRF cavity (LTE1-15) that had been treated by the salt-based bipolar EP at the Faraday EP facility. In the following, we summarize these activities and present results from the single-cell cavity test.

BIPOLAR ELECTROPOLISHING

Bipolar Electropolishing (BEP) applies forward and reverse voltage pulse waveforms on the electrodes, i.e. a cavity and cathode, alternatively, as is shown in Fig. 1. The forward pulse which is positive voltage applied on the cavity enhances mass transport in the EP processing. The reverse pulse is to depassivate the internal surface of the cavity. The off-times are generally inserted between the anodic and catholic pulses to facilitate replenishment of reacting species and removal of by-products and heat. The cathodic pulse eliminates the need for hydrofluoric acid to remove the surface oxide [1]. The bipolar system at Faraday is shown in Fig. 2 [3].

* Work supported by DOE award DE-SC0011235 (1002).
† mg574@cornell.edu

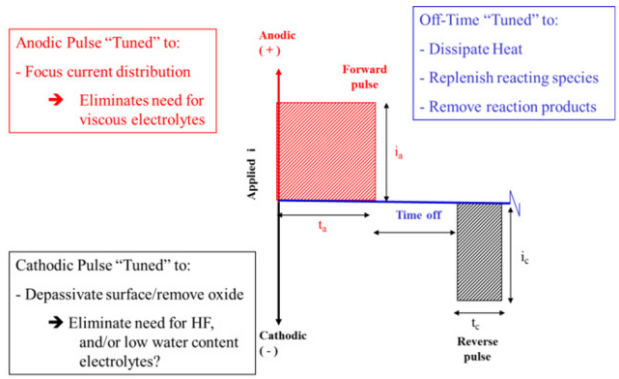


Figure 1: Illustration of the principle of Bipolar EP.



Figure 2: Bipolar EP system at Faraday [3].

SALT ELECTROPOLISHING AND TEST RESULTS

A 1.3GHz ILC-type cavity had been sent to Faraday for the salt-based EP, which was processed in 200 g/L $NaNO_3$ + 19.5 g/L Tris Acid + 1g/L Tris Base mixture. The total removal was ~30um with the polishing rate ~1.6um/hr.

Optical Inspection

After the salt electropolishing, we did optical inspection of the cavity at Cornell [4]. The inner surface of the equator region, shown in Fig. 3, is shiny and looks similar to a surface after conventional EP. However, we observed discoloration on other regions of the cavity wall, as is shown in Fig. 4. These stains are likely thick oxide layers generated in the salt EP processing.

Content from this work may be used under the terms of the CC BY 3.0 licence (© 2018). Any distribution of this work must maintain attribution to the author(s), title of the work, publisher, and DOI.

ISBN: 978-3-95450-194-6 ISSN: 2226-0366 doi:10.18429/JACoW-LINAC2018-TUPO064

PRE-STUDY OF CEPC SRF CAVITY*

P. Sha†, J. Dai, C. Dong, F. S. He, S. Jin, Z. Q. Li, B. Q. Liu, Z. H. Mi,
J. Y. Zhai, X. Y. Zhang, H. J. Zheng,
Key Laboratory of Particle Acceleration Physics and Technology,
Institute of High Energy Physics, CAS, Beijing, China
J. K. Hao, F. Wang, Peking University, Beijing, China

Abstract

CEPC will use 650 MHz cavities for the collider and 1.3 GHz cavities for the Booster. Each booster cryomodule contains eight 1.3 GHz 9-cell cavities, which is similar as LCLS-II, E-XFEL and ILC. Each collider cryomodule contains six 650 MHz 2-cell cavities, which is totally new. Therefore, the pre-study mainly focuses on the 650 MHz 2-cell cavity. N-doping and vertical tests of 650 MHz 1-cell and 2-cell cavities have been carried out at IHEP, which have achieved good results. A test cryomodule, which consists of two 650 MHz 2-cell cavities, has also begun as the first step to the full-scale cryomodule.

INTRODUCTION

Baseline layout and parameters for CEPC Ring SRF system have been public [1]. There're two SRF sections in total, and each one has two SRF stations. There're 10 cryomodules per station, which consist of six 650 MHz 2-cell cavities each. Hence, there're 240 650 MHz 2-cell cavities in total. RF and Mechanical design of these cavities have been completed. And fabrication of prototype cavities has also been finished. The vertical test goal is 4E10@22MV/m, while the horizontal one is2E10@22MV/m. Both these targets are extremely high to reach, so N-doping would be adopted. In recent years, it has been proposed and proven to increase Q of superconducting cavity obviously, which lowers the BCS surface resistance. N-doping research had begun at IHEP since 2015. There've been initial progress, which mainly focused on Nb samples and 650 MHz 1-cell cavities. After N-doping, the Q values of both 650 MHz 1-cell cavities increased at low fields obviously. Besides, prototypes of 650 MHz 2-cell cavities have finished vertical test and the results are quite good.

N-DOPING RESEARCH OF NIOBIUM SAMPLES

Niobium samples were nitrogen doped at OTIC, as Fig. 1 [2, 3]. The furnace in Fig. 1 is equipped with two cryo-pumps in order to keep ultra-clean, which is key for N-doping. Different methods were tried to achieve the best effects. To verify that, experiments of secondary ion mass spectrometry (SIMS), scanning electron microscope (SEM), transmission electron microscope (TEM) and other experiments were carried out.



Figure 1: Furnace for N-doping at OTIC.

Results of SIMS is shown as Fig. 2 and Fig. 3. After N-doping (3Pa@800C for 2 min), intensity of N atom increased obviously, as well as NbN.

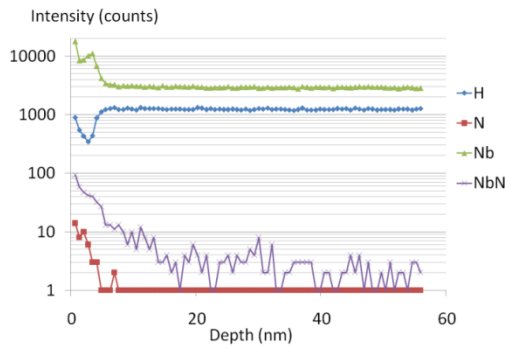


Figure 2: SIMS results before N-doping.

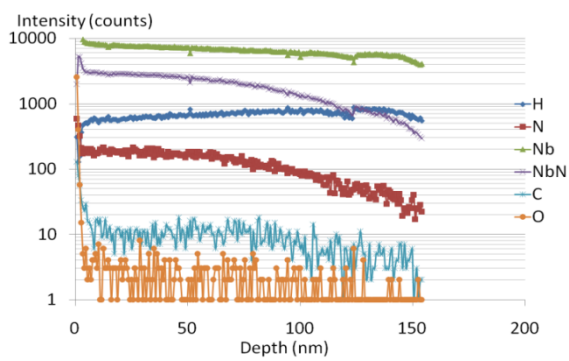


Figure 3: SIMS results after N-doping.

SEM images also show formation of nitride precipitates clearly, as Fig. 4.

*This study was supported by National Key Programme for S&T Research and Development (Grant NO.: 2016YFA0400400)and National Natural Science Foundation of China(Grant NO.:11505197).
#shapeng@ihep.ac.cn

Content from this work may be used under the terms of the CC BY 3.0 licence (© 2018). Any distribution of this work must maintain attribution to the author(s), title of the work, publisher, and DOI.

ISBN: 978-3-95450-194-6 ISSN: 2226-0366 doi:10.18429/JACoW-LINAC2018-TUPO065

IMPROVEMENT OF CAVITY PERFORMANCE BY NITROGEN DOPING AT KEK

T. Okada*[1], Y. Hori[1, 2], E. Kako[1, 2], T. Konomi[1, 2], H. Sakai[1, 2], T. Saeki[1, 2],
K. Umemori[1, 2], Y. Yamamoto[1, 2], T. Dohmae[2], M. Egi[2] J. Kamiya[3], S. Kurosawa[3], K. Takaishi[3],
[1]SOKENDAI, Oho, Tsukuba, Ibarkai, 305-0801, Japan
[2]KEK, Oho, Tsukuba, 305-0801, Japan, [3]JAEA, Tokai, naka, Ibaraki, 319-1195, Japan

Abstract

Reducing loss at the surface of a superconducting cavity is important for reducing the cost of accelerator operation. Nitrogen doping is an effective breakthrough for direct applicaton in High-Q superconducting cavities. At KEK, the nitrogen doping technique is applied to single and three-cell niobium TESLA-like cavities. A J-PARC furnace has a cryopump and three turbopumps, in addition to scroll-pumps, to achieve an oil-free environment. The quality factor of nitrogen doped cavities was improved in comparison with the standard treatment. The temperature dependent resistance decreased with an increase of the accelerating gradients. The nitrogen doping recipe was applied to the single-cell and three-cell cavities applied, and the results of the vertical test are described.

INTRODUCTION

Nitrogen doping is an effective breakthrough in the field of High-Q superconducting cavities [1]. The quality factor Q_0 is represented by $Q = G/R_s$ without field emission. The geometrical factor G is defined by only the shape of the cavity, while R_s represents its surface resistance. The geometrical factor of the TESLA-like cavity is approximately about 280 Ω. The nitrogen doping technique had been investigated at KEK using the large and small furnaces in the mechanical engineering center at KEK. However, this has resulted in the deterioration in the quality factor of the treated cavities [2]. The likely cause of the unsatisfactory results is related to the vacuum system of the furnace. Nitrogen doping and nitrogen infusion were successfully tested using the other furnace at J-PARC which has an oil-free pump system [3].

DOPING PROCEDURE

The oil-free furnace at J-PARC annealed vacuum components as usual. The cryopump was operated at 10000 L/sec. The three turbopumps and scrollpumps have pumping speeds of 3000 L/sec ×3, 500 L/min ×3, respectively. During the introducing of high purity nitrogen gas, the pumps were stopped and the portable pump was used for a deep doping recipe in the single-cell cavity. Durring this process for a light doping, the pumping speed of the turbpumps and scrollpumps were decreased by 50 %. Both the heavy doped and light doped nitrogen doping recipes were applied to the two cavities as shown in Table 1.

Table 1: Nitrogen Doping Applied to the Two Cavities

Cavity	Recipe
Single-cell	800 °C 3 hour + 800 °C for 20 min 2.7 Pa nitrogen + 800 °C for 30 min w/o nitrogen + EP 15 *m*
Three-cell	800 °C 3 hour + 800 °C, 2 min w/3.0 Pa nitrogen, + 800 °C, 6 min w/o nitrogen + EP 5 *m*

The single cavity is the TESLA-like shape and is made of fine grain niobium from Tokyo Denki, with an RRR is approximately about 300. The three-cell cavity is also a TESLA-like shape and is made of fine grain high tantalum niobium from CBMM that was melted twice to yeild an RRR of less than 300 [4]. Figure 1 shows the set-up of the nitrogen dope treatment at J-PARC furnace. Both recipes begin with 3 hours of annealing at 800 degrees after high-pressure rinsing and packing. Figure 2 shows the temperature and pressure data for the nitrogen dope treatment. The pressure was 4.8 Pa during the period when the nitrogen was introduced to the three-cell, and was steadied 3 Pa state then. After treatment, the cavity was packed into a plastic bag and transported to KEK.



Figure 1: The set-up of nitrogen doping using oil-free furnace at J-PARC.

EXPERIMENTAL SET-UP

The cavities were measured at the vertical test stand in KEK [5]. The ambient magnetic field was maintained to less than a few mG using the solenoid coil for the single-cell

* okadat@post.kek.jp

Content from this work may be used under the terms of the CC BY 3.0 licence (© 2018). Any distribution of this work must maintain attribution to the author(s), title of the work, publisher, and DOI.

ISBN: 978-3-95450-194-6 ISSN: 2226-0366 doi:10.18429/JACoW-LINAC2018-TUPO066

LOWER CRITICAL FIELD MEASUREMENT OF THIN FILM SUPERCONDUCTOR

H. Ito†, SOKENDAI, 305-0801 Tsukuba, Ibaraki, Japan
H. Hayano, T. Kubo, T. Saeki, KEK, 305-0801 Tsukuba, Ibaraki, Japan
Y. Iwashita, R. Katayama, H. Tongu, Kyoto ICR, Kyoto University, 611-0011 Uji, Kyoto, Japan
R. Ito, T. Nagata, ULVAC Inc., 286-0225 Chiba, Japan
H. Oikawa, Utsunomiya University, 321-8585, Utsunomiya, Tochigi, Japan
C. Z. Antoine, A. Four, CEA Irfu, F-91191 Gif-sur-Yvette, France

Abstract

The superconducting thin film is the promising technology to increase the performance of SRF cavities. The lower critical field H_{c1}, which is one of the important physical parameters characterizing a superconducting material, will be enhanced by coating Nb with thin film superconductor such as NbN. To measure the H_{c1}, we developed the measurement system using the third harmonic response of applied AC magnetic field from solenoid coil. In order to control the temperature of the sample, we installed heaters and thermal anchors which could be moved by the motor. By this temperature control the sample state can be easily transited from the Meissner state to the mixed state. By raising the temperature of the sample with applying AC magnetic field, H_{c1} and transition temperature, which is point of transition from the Meissner state to the mixed state, can be determined at when the third harmonic response appears in the voltage of solenoid coil. By repeating the measurement for various applied AC magnetic field, the H_{c1} vs temperature can be plotted. In this report, measurement result of the bulk Nb sample and NbN-SiO_2 multilayer thin film sample are presented.

INTRODUCTION

S-I-S (Superconductor-Insulator-Superconductor) thin film multilayer structure has been proposed by Gurevich to enhance the effective H_{c1}, and Kubo made advanced theoretical study [1, 2]. Antoine has measured effective H_{c1} with third harmonic voltage method and shows the possibility of H_{c1} increase [3]. The third harmonic measurement system was also constructed by Iwashita, Katayama, and Tongu in Kyoto University, and improvement of effective H_{c1} has been confirmed by the measurement of NbN-SiO_2 multilayer thin film sample which has been produced by ULVAC, inc. [4-6]. In order to increase H_{c1} measurement capability in our research group and to measure a large number of samples, KEK also set up the third harmonic measurement system. In this report, development status of the measurement system and the measurement result of bulk Nb sample and NbN-SiO_2 multilayer thin film sample are reported.

MEASUREMENT SYSTEM

This experiment is carried out by cooling the sample with liquid helium (LHe) stored in the bottom of cryostat, and LHe is supplied from Helium dewar using transfer tube. The 1kHz AC magnetic field is applied to the superconducting sample using solenoid coil, and the third harmonic components (3 kHz) induced in the solenoid coil when the magnetic field penetrate into the sample is detected. At this time, from the magnetic field strength applied to the sample and the temperature of the sample, the effective H_{c1} of the sample at that temperature (transition temperature) is measured. In addition, by repeating the measurement with various applied magnetic fields, the temperature dependence of H_{c1} is measured.

Sample Stage and Coil Stage

The measurement setup consists of the two copper stages for the sample and the exciting coil. The sample stage has two copper thermal anchors which are equipped with heater for increase sample temperature. The coil stage has also two copper thermal anchors whose bottom ends are immersed in LHe to decrease the sample temperature. By controlling the whole stage position up and down by the vertical mover which movable range is 100 mm, it is possible to control the immersion depth of the copper thermal anchors into the LHe. One of the temperature sensors is directly contact with backside of the sample and the remaining three temperature sensors could monitor the temperature of any part of the stage. The sample put between the two stages. The gap distance of 0.85 mm between sample surface and the coil stage is kept by three small SiN balls embedded in the coil stage (see Figs. 1 and 2).

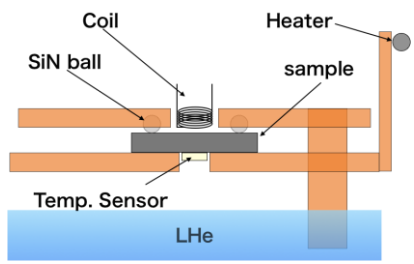


Figure 1: Cross-sectional Schematic of setup.

† hayatoi@post.kek.jp

Content from this work may be used under the terms of the CC BY 3.0 licence (© 2018). Any distribution of this work must maintain attribution to the author(s), title of the work, publisher, and DOI.

ISBN: 978-3-95450-194-6 ISSN: 2226-0366 doi:10.18429/JACoW-LINAC2018-TUPO067

STUDY ON NEW REMOVAL THICKNESS DISTRIBUTION IMPROVEMENT METHODS FOR NIOBIUM 9-CELL CAVITY VERTICAL ELECTROPOLISHING WITH NINJA CATHODE

K.Nii#, V.Chouhan, Y.Ida, T.Yamaguchi, Marui Galvanizing Co., Ltd., Himeji, Japan
H.Hayano, S.Kato, H.Monjushiro, T.Saeki, M.Sawabe, KEK, Tsukuba, Japan

Abstract

Marui Galvanizing Co., Ltd. has been developing niobium 9-cell cavity vertical electropolishing (VEP) technologies with Ninja cathode in collaboration with KEK. Conventional 9-cell cavity VEP had a serious problem, which was asymmetry of removal thickness distribution. Usually removal thickness of upper side became larger than lower side in case of both in-cell and inter-cell. So far, as one solution, we proposed "bubble diffusion prevention" method and proved it was effective for uniform removal. This time, as other new solution, we tried "cavity flip upside down" and "Ninja cathode masking" VEP methods. In this article we will report the purpose, intention and VEP experiment result of these methods.

INTRODUCTION

Marui Galvanizing Co., Ltd. is working on the development of vertical electropolishing (VEP) technology of niobium SRF cavity using Ninja cathode in collaboration with KEK for mass production and cost reduction. In the 9-cell cavity VEP, there was a problem that the removal thickness distribution became non-uniform (upper side is larger than lower side) because of bubble accumulation so far. We have done a lot of experiments working on solving this problem. Divide the flow path of the EP liquid into the inside and the outside of the Ninja cathode and optimally control the respective flow velocities and providing the power off time, it was shown that bubbles are prevented from accumulating in the cavity, and the removal thickness distribution is greatly improved to be uniform [1,2].

Furthermore, in order to understand the 9 cell cavity VEP and approach it for improvement, we aimed to solve the problem of non-uniform removal thickness in another way this time. One method is to invert the upper and lower sides of the cavity during VEP to make the removal thickness uniform (Cavity flip upside down VEP), and the other is using masked cathode to control the removal thickness of each part to make it uniform (Cathode masking VEP). We conducted VEP experiments using these methods and a 9 cell coupon cavity. The results such as removal thickness distribution are reported in this article.

#keisuke_nii@e-maui.jp

CAVITY FLIP UPSIDE DOWN VEP

Cavity flip upside down VEP was performed using dedicated cavity holder. In this holder, motor – cathode connection side is defined as top and the state where the top is on the upper side is called the forward position. The cathode penetration part of top PVC piece was specially sealed to prevent EP acid leakage in case of reverse position. The setup and inversion procedure are shown in Figure 1.



Figure 1: Cavity flip upside down setup and procedure.

Table 1: Conditions of Cavity Flip Upside Down VEP

Parameters	Cavity flip upside down VEP
Voltage	~14V
Current density	20 – 30 mA/cm^2
Cavity surface temperature	20~25 □C
Cathode rotation speed	20 rpm (forward position) 0rpm (reverse position)
Acid flow rate	5~10 L/min
EP time	5min (F-R)+15min (F-R)+20min (F-R)
Average removal thickness	~30um
Cathode	Ninja-v6 (With metallic wings and mesh cover)

Table 1 shows the conditions of cavity flip upside down VEP experiment. For this experiment, a 9cell coupon cavity [3] and Ninja cathode V6 with metal wings and mesh cover were used. The VEP was performed according to the procedure of 5min (forward position) – 5min (reverse position) – 15min (forward position) – 15min (reverse position) – 20min (forward position) – 20min (reverse position). The cathode rotation was carried out in the forward position, however not in reverse position (concerned about EP acid leakage).

Content from this work may be used under the terms of the CC BY 3.0 licence (© 2018). Any distribution of this work must maintain attribution to the author(s), title of the work, publisher, and DOI.

ISBN: 978-3-95450-194-6 ISSN: 2226-0366 doi:10.18429/JACoW-LINAC2018-TUPO068

VERTICAL ELECTROPOLISHIG OF 1.3 GHz NIOBIUM NINE-CELL SRF CAVITY: BULK REMOVAL AND RF PERFORMANCE

V. Chouhan†, Y. Ida, K. Nii, T. Yamaguchi, Marui Galvanizing Co, Ltd, 672-8022 Himeji, Japan
H. Hayano, S. Kato, H. Monjushiro, T. Saeki, M. Sawabe, H. Ito, KEK, 305-0801 Tsukuba, Japan
H. Oikawa, Utsunomiya University, 321-8505, Utsunomiya, Japan
H. Ito, Sokendai, 240-0193, Hayama, Japan

Abstract

Vertical electropolishing (VEP) technique have been successfully developed for 1.3 GHz niobium (Nb) single cell cavity to achieve a smooth surface with uniform removal and better RF performance as achieved after horizontal EP (HEP) process. VEP parameters for 1.3 GHz Nb nine-cell cavities are being studied using a nine-cell coupon cavity and our unique Ninja cathode. The investigated VEP parameters heretofore were applied on a 1.3 GHz Tesla shape nine-cell superconducting RF cavity for bulk removal of 100 µm followed by fine removal of 20 and 10 µm. The interior surface was found to be smooth and shiny after the VEP process. Our recently developed dual flow technique, in which the EP acid is flown separately in the Ninja cathode housing and cavity, yielded lower asymmetry in removal along the cavity length. The cavity was tested in a vertical cryostat after the final VEP process. The cavity achieved 28.3 MV/m at Q_0 value of 6.7×10^9. The cavity performance was almost the same as in the baseline vertical test performed after the HEP process.

INTRODUCTION

Electropolishing (EP) is now a standard method for surface treatment of niobium accelerating cavities where the EP process is carried out with a horizontal EP (HEP) system. As an alternative way, the cavity can be set vertically to perform electropolishing with a so-called vertical EP (VEP) setup which is comparatively simple and cost-effective. However, the VEP method yielded asymmetric removal and bubble traces on the interior surface of the cavity [1]. In our previous studies, we have shown the major cause of asymmetry is an accumulation of H_2 gas bubbles, generated at the aluminum cathode used for EP process, on the cavity surface [2]. We have successfully resolved the issue of the asymmetric removal and rough surface with our patented Ninja cathode and optimized VEP parameters including cathode rotation speed, operational temperature, applied voltage, and current density [3, 4]. The cathode housing covered with a meshed Teflon sheet guides gas bubbles along the cathode and reduces diffusion of bubbles from the cathode housing to the cavity. However, the removal of bubbles from ~1.2 m long nine-cell cavity is quite difficult and the accumulation of bubbles in the upper cells cannot be avoided with the process and parameters applied on the single cell cavity. We have developed a dual flow technique to remove gas bubbles from the cathode housing quickly so as to reduce bubble diffusion from the housing to the cavity. In this technique, the acid is flown separately in the Ninja cathode housing and cavity while keeping a higher flow rate in the cathode housing [5]. Effect of the technique with adequate flow rates has been presented elsewhere [5]. This paper shows the first bulk VEP of a nine-cell cavity with the Ninja cathode, vertical test result, and future work to further improve the VEP technique.

VEP EXPERIMENTS AND RESULTS

A Tesla shape 1.3 GHz Nb nine-cell superconducting RF cavity (TB9-TSB01), which was surface treated earlier with the HEP process and has a baseline vertical test result, was selected for the VEP process. VEP process was performed with our VEP system (see Fig. 1) which is equipped with auto-controlled valves and programmed acid flow direction. The system is equipped with a water spray facility for cavity cooling and a heat exchanger for acid cooling in the acid reservoir. Pure water is uniformly sprayed at the exterior of the cavity during the EP process. As a cathode for the VEP process, the Ninja cathode having 3 insulating blades in each cell of the cavity was used. The acid inlet line was bifurcated in two lines to flow acid in the Ninja cathode housing and the cavity separately. Two flow meters are set on the two lines to measure the flow rates in the cathode housing and cavity.

Three VEP processes have been carried out for the cavity TB9-TSB01 for bulk removal of 100 µm, fine removal of 20 and 10 µm. The removal thickness was calculated from the measured integrated current with a current hour meter. The cavity was annealed at 750 °C after the bulk VEP and 20 µm removal. After each VEP process, the cavity was rinsed with ultrasonic oscillators and at high pressure water rinsing.



Figure 1: VEP system with auto-valves (left) and cavity set at VEP stand (right) for the VEP process.

†vchouhan@e-marui.jp

Content from this work may be used under the terms of the CC BY 3.0 licence (© 2018). Any distribution of this work must maintain attribution to the author(s), title of the work, publisher, and DOI.

ISBN: 978-3-95450-194-6 ISSN: 2226-0366 doi:10.18429/JACoW-LINAC2018-TUPO069

DEVELOPMENT OF VERTICAL ELECTROPOLISHING FACILITY FOR Nb 9-CELL CAVITY (2)

Y.Ida#, V.Chouhan, K.Nii, Marui Galvanizing, Himeji, Japan
H.Hayano, S.Kato, H.Monjushiro, T.Saeki, M.Sawabe, KEK, Tsukuba, Japan
Takao Akabori, Goh Mitoya, Kenich Miyano, Higashinihon Kidenkaihatsu, Morioka, Japan
Yasunori Anetai, Fukumi Takahashi, WING, Kitakami, Japan

Abstract

In IPAC18 (Vancouver, Canada), we reported our first step of development of niobium 9-cell cavity vertical electropolishing (VEP) facility. In this article, we will report the method, system for uniform polishing for niobium 9-cell cavities and the current situation of our 9-cell cavity VEP facility (the result of polishing uniformity, vertical test will be presented in other posters of this conference). In addition, we will show the movie of experiments of VEP-3 with Ninja cathode. This facility aims not only for test VEP but also for mass production and long-time operation.

INTRODUCTION

In May 2018, at the IPAC-18, we made our first historical report regarding our last 5 years of continuous R&D work on vertical electropolishing (VEP). In the last few months, further improvement has been made targeting good VEP results, system automation, and cost-effective mass production. This second report shows these improvements of the VEP facility. The detailed experimental VEP results are reported by Mr. Nii in TUPO067 [1], and Dr. Chouhan in TUPO068 [2].

DEVELOPMENT OF NINJA-VERTICAL EP SYSTEM

VEP system was designed to use it with our unique Ninja cathode. The system includes acid tank, auto-controlled valves, lower chamber for acid flow bifurcation, Ninja rotary system etc. Figure 1 shows the VEP system photos.



Figure 1: Photos of Ninja-vertical EP system.

#yoshiaki_ida@e-marui.jp

ADVANCED ACID TANK

The acid tank is made of clear PVC material and has a 70L capacity. In order to do EP with the least amount of EP solution, the solution is changed every one or two times of VEP process. Make sure the deterioration of the solution doesn't affect the EP finish. The tank is equipped with a niobium heat exchanger for liquid temperature control. The tank also has mesh filters and an ultrasonic oscillator used to remove hydrogen gas bubbles remaining in EP solution. Figure 2 shows the photos of the acid tank.

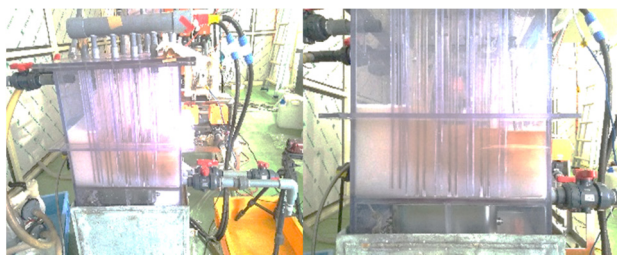


Figure 2: Photos of the acid tank.

AUTOMATIC CONTROLLED VALVES FOR EP SOLUTION CONTROL

For automatic control of EP solution path and direction, electric switching auto valves are used. The operation of valves are controlled with programmed sequences. This allows to select the acid and water flow from bottom to top and vice-versa. The acid and water flow rate can also be remotely controlled with a touch panel screen. Figure 3 shows the touch panel screen and auto valves.

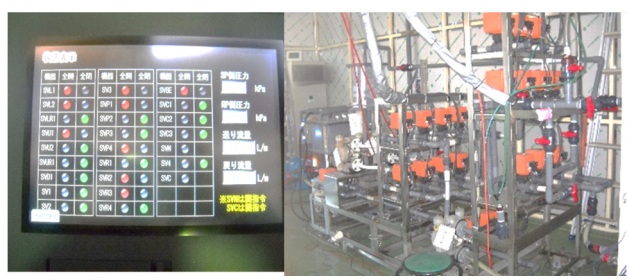


Figure 3: Photos of the touch panel screen and auto valves.

NINJA-VEP SYSTEM

EP solution is inflowed from the lower chamber, and the Ninja cathode is spun. A unique characteristics of the lower chamber is that it can bifurcate the EP solution and allow separate flows in the cathode housing and cavity. This

Content from this work may be used under the terms of the CC BY 3.0 licence (© 2018). Any distribution of this work must maintain attribution to the author(s), title of the work, publisher, and DOI.

ISBN: 978-3-95450-194-6 ISSN: 2226-0366 doi:10.18429/JACoW-LINAC2018-TUPO070

DESIGN AND COMMISIONING OF KEK NEW VACUUM FURNACE FOR SRF CAVITY DEVELOPEMENT*

K. Umemori†[1,2], M. Egi[1], E. Kako[1,2], T. Konomi[1,2], S. Michizono[1,2], H. Sakai[1,2]
[1]KEK/[2]SOKENDAI, 305-0801, Tsukuba, Ibaraki, Japan

Abstract

Recently new techniques such as Nitrogen-doping (N-doping) and Nitrogen-infusion (N-infusion) have been developed to improve performance of SRF (Superconducting RF) cavities. We purchased a new vacuum furnace, which is key to realize these techniques. Cleanness of the furnace is most important issue. The furnace has a cryopump and whole of vacuum system is oil-free system. Target vacuum level after cooling down is 1e-6 Pa. Heater, reflectors and support table were made from Molybdenum to avoid contamination during heat treatment. Metal gaskets are used for all vacuum seals, except big doors. Maximum operation temperature is 1150 degrees. Size is around 1 m diameter and 2m long for a 1.3 GHz 9-cell cavity. Entrance of furnace is covered by a clean booth. The furnace was fabricated, assembled at KEK COI building and commissioned. After several burning runs, target vacuum pressure was achieved after cooling down to room temperature (RT). Design and current status of the furnace is presented.

REQUIREMENT FOR FURNACE

N-doping and N-infusion technique are well known to improve SRF cavity performance [1]. KEK also had carried out R&D studies. Throughout our studies, it was realized that cleanness of furnace is very important issue. In the case of N-doping using a diffusion pump, Q-values always decreased even after removing surface by EP [2]. N-infusion studies using J-PARC furnace, with a cryopump, were much better, but still sometimes we were suffered from Q-degradation due to contaminations from the furnace [3].

"Clean" furnace is essential for current SRF development. What "clean" means are excellent available vacuum pressure and less contaminations, especially from carbons. Pumping system of furnace should be oil-free system. Powerful cryopump is desirable. To achieve good vacuum condition and less contaminant circumference, metallic vacuum seals are basically used and usage of SUS at high temperature region is avoided.

Furthermore, furnace should be surrounded by a clean booth to keep cavity handling clean. Operation of furnace is also important to keep cleanness of furnace, including selection of materials to apply heat treatment.

DESIGN AND CONSTRUCTION

Table 1 shows main design parameters for our new furnace. Size of the furnace is fit to install a L-band 9-cell cavity. Molybdenum was used for the heaters, reflectors and a support table. Heating zones are separated to three divisions. Maximum operating temperature is 1150 degrees. Main vacuum pump is a cryopump with 10000 L/sec for Nitrogen.

Table 1: Design Parameters

Parameters	Design values
Inner size of chamber	ϕ950 x L=2080 mm
Effective heating zone	370 x 370 x 1500 mm
Normal operating temperature	~1100 degree
Maximum temperature	1150 degree
Cryopump (CRYO-U20H)	10000 L/sec (N_2)
Drypump (CR300B)	5000 L/min
Heater	Mo heater
Reflector	6 layers of Mo reflector
Target vacuum pressure	RT: 1e-6 Pa 600 degrees: 1e-5 Pa 1000 degrees: 1e-4 Pa



Figure 1: Construction of the furnace.



Figure 2: (top left) Water-cooled baffle, gate-valve and cryopump. (top right) Inside furnace. (bottom) Completed furnace with clean booth.

† kensei.umemori@kek.jp

Content from this work may be used under the terms of the CC BY 3.0 licence (© 2018). Any distribution of this work must maintain attribution to the author(s), title of the work, publisher, and DOI.

ISBN: 978-3-95450-194-6 ISSN: 2226-0366 doi:10.18429/JACoW-LINAC2018-TUPO071

STUDY ON NITROGEN INFUSION FOR 1.3 GHz SRF CAVITIES USING J-PARC FURNACE*

K. Umemori†[1,3], T. Dohmae[1], M. Egi[1], Y. Hori[1,3], E. Kako[1,3], T. Konomi[1,3], S. Michizono[1,3], T. Saeki[1,3], H. Sakai[1,3], Y. Yamamoto[1,3], [1]KEK, 305-0801, Tsukuba, Ibaraki, Japan
S. Kurosawa[2], K. Takeichi[2], J. Kamiya[2], [2]JAEA, 319-1195, Tokai, Naka, Ibaraki, Japan
T. Okada[3], [3]SOKENDAI, 305-0801, Tsukuba, Ibaraki, Japan

Abstract

Nitrogen infusion (N-infusion) is new surface treatment technique for niobium SRF (Superconducting RF) cavities. After cooling down from 800 degrees heat treatment, a vacuum furnace and cavities are kept 120 degrees, 48 hours with about 3 Pa Nitrogen. Improvement of Q-value and accelerating gradient is expected. We used J-PARC furnace, since N-infusion procedure requires clean vacuum furnace. It has a cryo-pump and turbo molecular pumps and its vacuum system is oil-free system. Six times of N-infusion tests were carried out, while changing vacuum condition, N-infusion temperature, Nitrogen pressure, niobium material and so on. Niobium caps were mounted on cavities to avoid contaminations on inner surfaces. Some of trials were successful and vertical test results showed improvement of Q-values and accelerating gradient. However, some of them were not. Most of failed cases showed degradation of Q-values above 5 MV/m. Details of heat treatment procedure including N-infusion and vertical test results are shown in this presentation.

J-PARC FURNACE

N-infusion technique is recently developed to improve SRF cavity performance for both Eacc (accelerating gradient) and Q-values [1]. KEK also had carried out R&D studies to realize high gradient SRF operations.

Throughout N-doping studies we recognized that cleanness of furnace is most important for Nitrogen treatment [2, 3]. Especially, in case of N-infusion, cleanness of furnace could directly affect to cavity performance, since final EP can not apply to the cavity surface.



Figure 1: J-PARC vacuum furnace.

Therefore, we selected J-PARC furnace for N-infusion studies in Japan. Figure 1 shows the J-PARC furnace. This furnace has oil-free and powerful pumping systems. Right and left of Fig. 1 shows a cryopump with 10000 L/sec and three TMPs with 3000 L/sec (x 3), respectively. Vacuum pressure can be reached to around 1e-6 Pa.

One weak point is that this furnace is not dedicated to SRF cavities, but normally used for degassing of beam-duct and components, made of SUS, Cu, ceramic and so on.

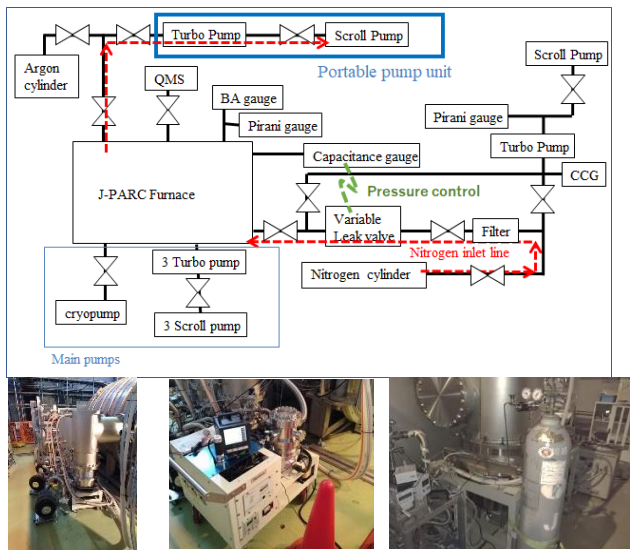


Figure 2: (top) Diagram for N-injection system. (left-bottom) TMPs and scroll pumps. (center-bottom) Portable pumping unit. (right-bottom) N-injection line.

Figure 2 shows Nitrogen-injection (N-injection) system constructed on the J-PARC furnace for the N-infusion study. Nitrogen gas is fed from G1 grade, 99.9999% purity, Nitrogen bombe. Nitrogen pressure in the furnace is controlled by a variable leak valve (right-bottom of Fig. 2). During injection of Nitrogen, the furnace is pumped by pumping system.

At the beginning, a small portable pumping unit (center-bottom of Fig. 2) was used. But we could not maintain clean background condition. Background pressure was estimated to be around 2e-2Pa. After that, we changed to use TMPs with reduced pumping speed. This could improve background pressure to level of 1e-5 Pa.

N-INFUSION PROCEDURE

In order to maintain the furnace as clean as possible, most of case, 950 degrees, 3hours burning runs were carried out, just before N-infusion runs.

Before installing to the furnace, cavities were washed by HPR (High Pressure Rinsing), dried in a cleanroom

† kensei.umemori@kek.jp

Content from this work may be used under the terms of the CC BY 3.0 licence (© 2018). Any distribution of this work must maintain attribution to the author(s), title of the work, publisher, and DOI.

ISBN: 978-3-95450-194-6 ISSN: 2226-0366 doi:10.18429/JACoW-LINAC2018-TUPO072

FIRST TRIAL OF THE IN-SITU NITROGEN INFUSION AT KEK*

T. Konomi†, T. Dohmae, E. Kako, S. Michizono, H. Sakai, K. Umemori, KEK/Sokendai, 305-0801,Tsukuba, Japan
T. Okada, Sokendai, 305-0801, Tsukuba, Japan

Abstract

The nitrogen infusion is the new surface treatment technique for improving the RF loss and the maximum accelerating gradient of superconducting cavity. In this process, it is important to be carried out continuously both the 800 °C annealing in vacuum and 120 °C nitrogen infusion without exposure to the atmosphere. The annealing serves activation process by removing the oxide layer. However, there is a risk of dust particles entrance in to the cavity when the cavity is put in the vacuum furnace. The in-situ nitrogen infusion system was prepared to prevent the dust entrance. The other target is to investigate whether nitrogen infusion effect or something changes happen in the case of applying nitrogen infusion technique without removing the oxide layer. It can only introduce nitrogen into a cavity during 120 °C low temperature baking and transport a cavity to the vertical test system without exposure to the atmosphere. We tried to infuse nitrogen to a single cell by keeping 120 °C and 48 hours with 3 Pa nitrogen. The cavity was annealed in another furnace and applied high pressure rinsing before nitrogen infusion. The vertical test result was same Q as the normal 120 °C baking without nitrogen. It suggests that oxide layer prevents infusion of nitrogen.

NITROGEN TREATMENT

The nitrogen treatment of superconducting niobium cavity is getting a lot of attention as a new technology to improve the performance limit of ILC standard recipe [1]. KEK is studying to apply this technology to ILC. It was applied to 1.3 GHz cavities and confirmed that Q value and accelerating gradient were improved [2,3]. The first step in this procedure at KEK is that the surface is removed by the electropolish to create new niobium surface. The cavity is installed to the vacuum furnace after high pressure rinsing. However, there is a risk of dust particles entrance in to the cavity. We designed the in-situ nitrogen infusion system to prevent the dust particle entrance. The second step is that cavity is annealed at 800 oC for 3 hours, then cooled down to 120 oC and kept in 3.3 Pa nitrogen. It is important not to expose to the atmosphere during heat treatment. The cavity is taken out to the atmosphere and cleaned by high pressure rinsing. Thereafter, cavity is not applied heat treatment such as baking because heat treatment changes the surface condition. The final surface condition is made by 800 oC annealing and 120 oC nitrogen infusion. If additional electropolish is applied to remove defects which limit the maximum field after vertical test, high temperature annealing is required again. We studied whether gradient and Q value change when 120 °C nitrogen infusion applied after exposed the cavity to the atmosphere.

† konomi@post.kek.jp.

IN-SITU NITROGEN INFUSION

The system of the in-situ nitrogen infusion is a modified baking system to control the nitrogen pressure during 120 C baking (Fig. 1). Top and bottom flanges of the cavity each have one vacuum port. The system can be baked before injecting nitrogen into the cavity. Main pump is the turbo molecular pump (HiPace700) which pumping speed is 700 L/min. The pressure reached about 3×10^{-7} Pa after baking. The gas flow can be controlled by the automatic gas regulating valve (RME005) during the nitrogen injecting. The pressure is controlled by monitoring the capacitance gauge mounted at pumping side of the cavity. The purity of the nitrogen cylinder is more than 99.99995 vol.%. This system can keep the same purity of nitrogen gas cylinder in the cavity during nitrogen injection because the base pressure is enough low. The cavity can be transported to the vertical test stand without exposing the inner surface of the cavity to the atmosphere.

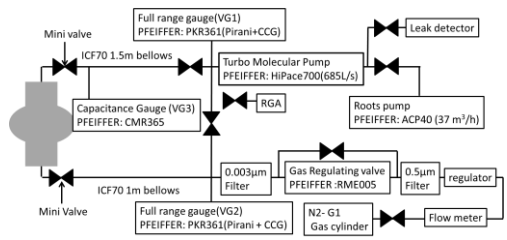


Figure 1: In-situ nitrogen infusion system.

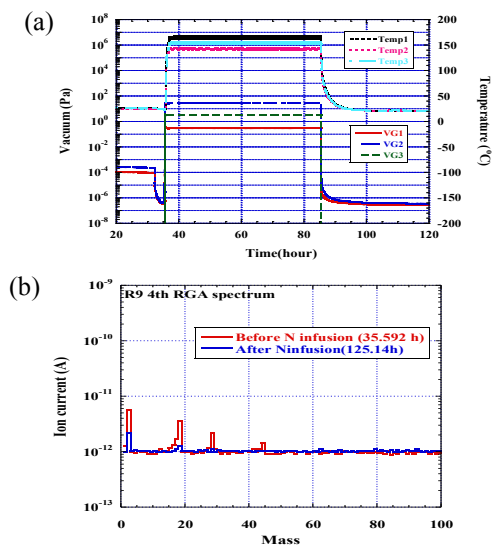


Figure 2: Example of nitrogen infusion. (a) Vacuum and temperature trend. (b) Residual gas spectrum before and after nitrogen infusion.

Content from this work may be used under the terms of the CC BY 3.0 licence (© 2018). Any distribution of this work must maintain attribution to the author(s), title of the work, publisher, and DOI.

ISBN: 978-3-95450-194-6 ISSN: 2226-0366 doi:10.18429/JACoW-LINAC2018-TUPO073

NIOBIUM SAMPLE ANALYSIS FOR NITROGEN INFUSION AND DOPING

T. Konomi†, E. Kako, S. Michizono, H. Sakai, K. Umemori, KEK 305-0801, Tsukuba, Japan
T. Nojima, Tohoku University, 980-8577, Sendai, Japan
T. Nagata, ULVAC Inc., 289-1226, Sammu, Japan

Abstract

KEK has been investigating the better conditions of the heat treatment in nitrogen, which are called as nitrogen doping and nitrogen infusion. We have tried to understand the high gradient performance of the cavity from the analyses of samples which were prepared in the same conditions for the cavity. The main tools are D-SIMS for the depth profile of the elemental concentration, XPS for composition analysis and SQUID magnetometry for the critical DC magnetic field measurement. The difference in the depth profiles of the nitrogen, car-bon and oxygen between the heat treatment conditions, containing the degree of vacuum and furnace temperature of nitrogen injection, was observed by GD-OES, D-SIMS and XPS. Such a difference correlates with the vortex penetration field measured by SQUID. In particular, that of the nitrogen doping sample was greatly degraded, while that of the nitrogen infusion sample was slightly improved. The tendency is consistent with the RF high gradient test results.

NITROGEN TREATMENT AT KEK

The nitrogen heat treatment can improve the performance of superconducting RF (SRF) cavities. There are two ways for nitrogen treatment. One is the nitrogen doping (N-dope), in which the sample is doped with nitrogen heavily during annealing the cavity at a high temperature in the vacuum furnace and then the heavy doped layer is removed by the electropolishing (EP) [1]. The other way is the nitrogen infusion (N-infusion), in which nitrogen is infused into the sample at a low temperature after annealing the cavity without expose the cavity to the air [2]. In both methods, the oxidized surface layer is removed by high temperature annealing before nitrogen treatment. KEK also succeeded in N-dope and N-infusion using the J-PARC furnace which is equipped with oil free pumps [3, 4]. However, N-infusion decreased the Q value in some cases. In order to investi-gate the cause for the decrease in Q, we installed the niobium reference samples to the furnace together with the cavies and analysed them. First, the samples were cut out of the fine grain niobium sheet produced by the Tokoyo Denkai Co Ltd, which is followed by the EP or chemical polishing (CP) process to remove the surface layer by about 100 µm. Then, the samples were subjected to almost the same heat treatment as the cavity.

DEPTH PROFILE OF N-DOPE

The depth profile of the N-dope sample was measured by the GD-OES (HORIBA, Ltd GD-Profiler 2). The discharge gas was argon. The measured area was 4 mmΦ in the sample with a size of 50×50×3 mm^3. Figure 1 shows the depth profiles of the N-doped and the annealed samples for reference. As shown in Fig. 2 for the temperature and vacuum trend, the N-dope sample was first annealed at 800 °C in a vacuum of 1×10^{-4} Pa for 3 hours and then was doped in 3 Pa nitrogen for 20 minutes, which is followed by the diffusion process of nitrogen to the inner in a vacuum for 30 minutes. No additional EP was applied after heat treatment in both samples. From the data in Fig. 1, it is obvious that the nitrogen doping occurs at least up to 30 µm in depth for the N-dope sample. However, the carbon doping also seems to occur in both samples. We suspected the nitrogen purity in the furnace was poor because a small portable pump was used instead of the main pumps, which were off during nitrogen injection in order to avoid the failure of main pumps. The reached pressure of the small portable pump was 1×10^{-3} Pa. The surface distribution of the carbon can be also seen using the SEM (Hitachi High-Tech Corp., SU6600) in which EDS sensor can be insert from the horizontal axis to the sample surface with the large capture solid angle. Figure 3 shows the reference SEM and EDS image of another N-dope sample prepared in the KEK small furnace which is equipped with an oil diffusion pump. In this case, the carbon distribution is more clearly observed. The carbon seems to be absorbed to the grain boundary. However, the Q-value of the N-doped cavity using J-PARC furnace was improved after EP by several µm. We think that the effect of N-infusion is more sensitive to carbon pollution because the heat treatment affects the final surface.

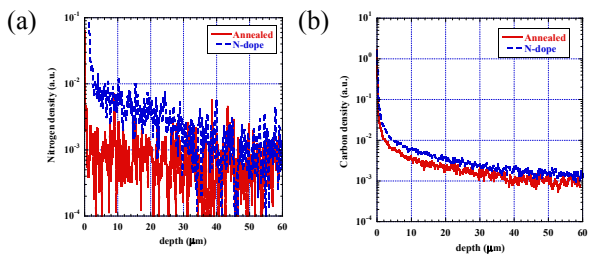


Figure 1: Depth profile of N-dope and annealed samples. (a) nitrogen, (b)carbon.

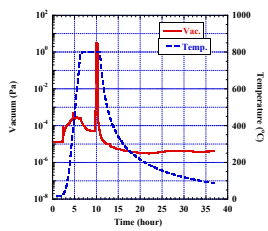


Figure 2: Heat treatment trend of the N-Dope.

† konomi@post.kek.jp.

Content from this work may be used under the terms of the CC BY 3.0 licence (© 2018). Any distribution of this work must maintain attribution to the author(s), title of the work, publisher, and DOI.

ISBN: 978-3-95450-194-6 ISSN: 2226-0366 doi:10.18429/JACoW-LINAC2018-TUPO074

DESIGN AND FABRICATION OF KEK SUPERCONDUCTING RF GUN #2

T. Konomi†, Y. Honda, E. Kako, Y. Kobayashi, S. Michizono, T. Miyajima, H. Sakai,
K. Umemori, S. Yamaguchi, M. Yamamoto
KEK/Sokendai, Tsukuba, Japan

Abstract

Superconducting RF gun can realize high acceleration voltage and high beam repetition. KEK has been developing the 1.3 GHz elliptical type 1.5 cell superconducting RF gun to investigate fundamental performance. A surface cleaning method and tools are developed by using KEK SRF GUN #1 and high surface peak gradient 75 MV/m was achieved without field emission. SRF GUN #2 equipped with the helium jacket and operable with electron beam was designed based on the SRF GUN #1. It can be operated with transmit type photocathode which include superconducting transparent material. The cathode rod is cooled by thermal conducting from the 2 K helium jacket and photocathode will be kept around 2K to maintain superconductivity. Bulk niobium photocathode rod, and substrate will used for the fundamental performance test. In parallel, the photocathode deposition chamber for multi-alkali photocathode will be prepared.

CAVITY DESIGN

The SRF GUN #2 cavity is 1.5 cell and 1.3 GHz shape designed based on SRF GUN #1. High gradient performance has demonstrated using SRF GUN #1. The maximum surface peak electric field (Esp) reached 75 MV/m [1]. The difference from #1 is that #2 has the helium jacket and the cathode rod size was changed for improving the cathode rod cooling. Figure 1 shows the #2 design. Table 1 shows the RF parameters of KEK SRF GUN#1. Yellow parts are made of niobium and green, blue parts are made of titanium and gray parts are made of stainless steel. Helium jacket can be connected by flanges with indium seal. The choke filter is placed as close to the accelerating cell as possible.

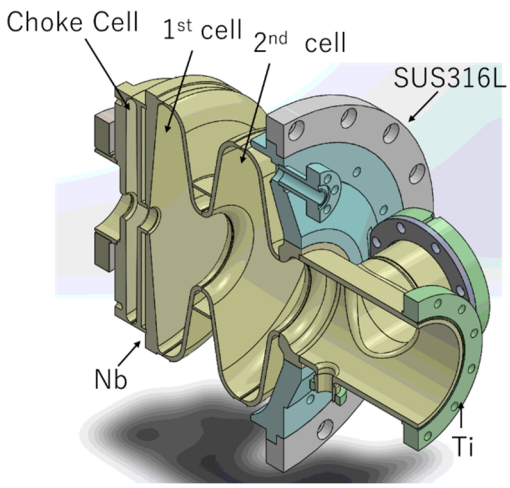


Figure 1: Design of KEK SRF GUN#2.

† konomi@post.kek.jp.

Table 1: RF Parameters of KEK SRF GUN#2

Parameter	Value
Frequency	1300 MHz
Geometrical factor	133.7 Ohm
Hsp/Esp	2.237 mT/(MV/m)
Z factor ($E_{sp} = Z\sqrt{Q_o P_{loss}}$)	234.04

RF leakage from the choke filter is simulated using SUPERFISH because the cathode rod length was shortened. Figure 2 shows the simulation condition. Rod head is made of niobium, niobium surface resistance is set to 10×10^{-9} Ω. Other cathode holder parts are made of oxide free copper (OFC). Electrical resistivity of OFC is set to 1.68×10^{-8} Ω·m. Figure 3 shows the Q value dependence on the choke diameter. When the all surface is made of niobium the Q value is 1.3×10^{10}. The best diameter is 186.6mm. If 1% degradation is tolerated, lose is diameter fabrication tolerance set to ±0.2 mm.

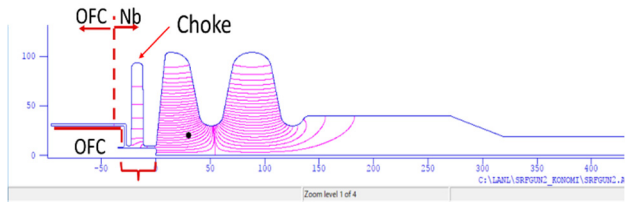


Figure 2: SUPERFISH simulation set up.

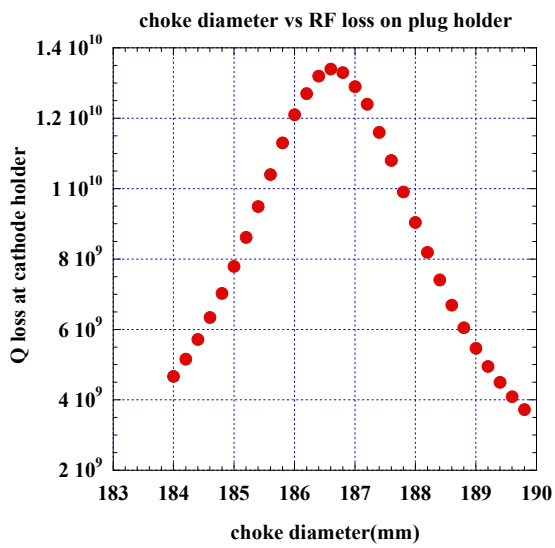


Figure 3: Q value dependence on choke diameter.

Content from this work may be used under the terms of the CC BY 3.0 licence (© 2018). Any distribution of this work must maintain attribution to the author(s), title of the work, publisher, and DOI.

ISBN: 978-3-95450-194-6 ISSN: 2226-0366 doi:10.18429/JACoW-LINAC2018-TUPO076

AN INNOVATIVE Nb_3Sn FILM APPROACH AND ITS POTENTIAL FOR SRF APPLICATIONS *

E. Barzi †, C. Ciaccia, S. Falletta, D. Turrioni, FNAL, Batavia, IL, USA
A. Kikuchi, NIMS, Tsukuba, Ibaraki, Japan
H. Hayano, T. Saeki, KEK, Tsukuba, Ibaraki, Japan
H. Ito, SOKENDAI, Hayama, Kanagawa, Japan
G. Eremeev, A.-M. Valente-Feliciano, R. L. Geng, R. Rimmer, JLAB, Newport News, VA, USA

Abstract

A novel electro-chemical technique to produce Nb_3Sn films on Nb substrates was developed and optimized at Fermilab. The Nb_3Sn phase is obtained in a two-electrode cell, by electrodeposition from aqueous solutions of Sn layers and Cu intermediate layers onto Nb substrates. Subsequent thermal treatments in inert atmosphere are realized at a maximum temperature of 700°C to obtain the Nb_3Sn superconducting phase. Several superconducting Nb_3Sn films were obtained on Nb substrates by studying and optimizing most parameters of the electro-plating process. Samples were characterized at Fermilab, NIMS, KEK and JLAB, including EPMA analyses, DC and inductive tests of critical temperature T_{c0}, and lower critical field $H_{c1}(4.2\ K)$ by SQUID. In parallel to sample development and fabrication at FNAL, at JLAB and KEK effort was put into etching and electro-polishing techniques adequate to remove the Cu and bronze phases from the samples' outer surface. This is necessary prior to measurements at JLAB of the surface impedance of flat samples in a setup that make use of an RF host cavity.

INTRODUCTION

The two most important aspects of SRF performance are the accelerating field E_{acc} and the cavity quality factor, Q_0. The accelerating gradient in SRF cavities is proportional to the peak magnetic field on the cavity wall. At RF frequencies the peak magnetic field is limited by the metastable superheating field, H_{sh} [1]. The maximum accelerating gradient expected for Nb cavities in the TESLA shape, for instance, is ~40 MV/m. Nb_3Sn is an attractive alternative because it has a higher T_{c0} of up to 18 K. With a theoretical H_{sh} of 0.42 T, as compared to a T_{c0} of 9 K and H_{sh} of 0.25 T for Nb [2], SRF cavities with a thin layer of Nb_3Sn coated onto their inner surface should produce larger accelerating gradients than Nb. The larger T_{c0} of Nb_3Sn allows for SRF cavities with a Q_0 at 4.2 K about 30 times larger than for Nb. It also has the advantage of allowing the cavities to operate at 4.5 K rather than at ~2 K that is used for Nb cavities to obtain a higher gradient. This means less expensive refrigeration and more cryogenic economy and reliability.

Nb_3Sn coated SRF cavities have been demonstrated to improve the cavity quality factor, but have not produced the theoretically expected gradient. Perhaps the longest standing Nb_3Sn technique for SRF is that of a vapor diffusion process followed by thermal reaction at high temperature to form the Nb_3Sn [3, 4]. It consists of five stages, including degassing at 100° to 200°C to remove moisture; nucleation at intermediate temperature; ramp up to and holding at a coating temperature between 1100°C and 1300°C for Nb_3Sn formation; and finally annealing to diffuse excess tin. This process has not produced so far full cavity assemblies because the scale-up from single cell is challenging. Nb_3Sn coating on 5-cell CEBAF-type cavities was achieved at JLAB [5].

In this paper an alternate process, that of chemical electrodeposition, followed by reaction in inert atmosphere, will be described. The electroplating is performed at near room temperature and at atmospheric pressure. The advantage of electrodeposition is its simplicity, accurate control, and low costs. Also, it can be performed on any 3D surface such as the inner surface of SRF cavities. Electrodeposition should be among the least expensive ways to produce SRF cavities. It should also provide a more uniform Nb_3Sn coating. Improving the quality of the Nb_3Sn could reduce the large gap between the theoretical and measured H_{sh}.

EXPERIMENTAL METHOD

An electro-chemical deposition technique, which had been collaboratively developed with Politecnico di Milano [6, 7] and is under patenting process, to produce superconducting Nb_3Sn films on Nb substrates, was reproduced at Fermilab. In the past year, the equipment and consumables were procured, and the complete electro-chemical system was commissioned.

In electroplating the metallic coating is deposited on another metal surface through an electrolyte solution. The metal to be plated acts as the cathode and when the appropriate current is applied, positively charged ions traveling from the anode into the solution will discharge and get deposited on the cathode until a film of desired thickness is formed. Fig. 1, top shows a schematic with two symmetric anodes for bilateral coating of flat samples. Fig. 1, bottom shows the concept for scale-up to 3D surfaces, such as internal coating of cylinders, as first step to the internal coating of SRF cavities.

Figure 2 shows the sequence of deposited layers. First, using the Nb as cathode and Cu anode, a thin seed layer of

* Work supported by U.S. DOE contract No. DE-AC02-07CH11359
† barzi@fnal.gov

Content from this work may be used under the terms of the CC BY 3.0 licence (© 2018). Any distribution of this work must maintain attribution to the author(s), title of the work, publisher, and DOI.

ISBN: 978-3-95450-194-6 ISSN: 2226-0366 doi:10.18429/JACoW-LINAC2018-TUPO078

EXTENSION OF BUSCH'S THEOREM TO PARTICLE BEAMS

L. Groening[1], M. Chung[2], and C. Xiao[1]
[1]Gesellschaft für Schwerionenforschung, Darmstadt, Germany
[2]Ulsan National Institute of Science and Technology, Ulsan 44919, Republic of Korea

Abstract

In 1926, H. Busch formulated a theorem for one single charged particle moving along a region with longitudinal magnetic field. The theorem relates particle angular momentum to the amount of field lines being enclosed by the particle cyclotron motion. It has been extended to accelerated particle beams. This contribution sketches the extension and applies the extended theorem to successfully performed emittance manipulations with electron and ion beams.

BUSCH'S THEOREM FOR SINGLE PARTICLE

In 1926, H. Busch applied the preservation of angular momentum for systems with cylindrical symmetry to a charged particle moving inside a region with magnetic field $\vec{B}$ [1]. Using conjugated momenta, the magnetic field strength is intrinsically included into the equations of motion. In linear systems, the normalized conjugated momenta p_x and p_y are related to the derivatives of the particle position coordinates (x, y) w.r.t. the main longitudinal direction of motion $\vec{s}$ through

$$p_x := x' + \frac{\mathcal{A}_x}{(B\rho)} = x' - \frac{yB_s}{2(B\rho)}, \quad (1)$$

$$p_y := y' + \frac{\mathcal{A}_y}{(B\rho)} = y' + \frac{xB_s}{2(B\rho)}, \quad (2)$$

where $\vec{\mathcal{A}}$ is the magnetic vector potential with $\vec{B} = \vec{\nabla}\times\vec{\mathcal{A}}$, B_s is the longitudinal component of the magnetic field, and $(B\rho)$ is the particle rigidity, i.e., its momentum per charge $p/(qe)$, with p as total momentum, q as charge number, and e as elementary charge. Busch's theorem states that the canonical angular momentum $\tilde{l} = xp_y - yp_x$ is a constant of motion that is written in cylindrical coordinates as

$$m\gamma r^2\dot{\theta} + \frac{eq}{2\pi}\psi = const\,. \quad (3)$$

A general formulation of Eq. (3) has been derived in [2], which is regarded as the generalized Busch theorem

$$\oint_C \vec{v}\cdot d\vec{C} + \frac{eq}{m\gamma}\psi = const\,, \quad (4)$$

i.e., the path integral around a stream of possible particle trajectories along a closed contour C, plus the magnetic flux through the area enclosed by C is an invariant of the motion. Figure 1 illustrates the first part of the left hand side of Eq. (4). Busch's theorem of Eq. (3) is the special case of this generalized form for C being a circle of radius r. It is emphasized that Eq. (4) is only valid for laminar motion.

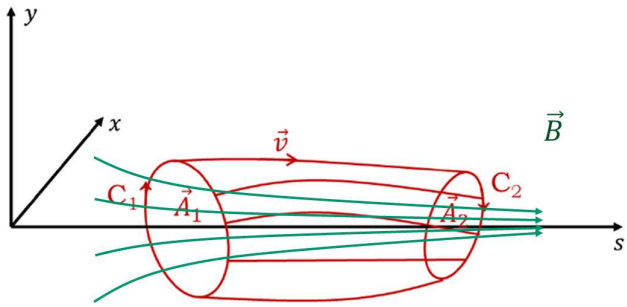


Figure 1: Fig. 3 from [3]: the contour C encloses possible streams of particle trajectories and encloses the area $\vec{A}$.

TRANSVERSE EIGEN EMITTANCES

The transverse eigen emittances were introduced by Dragt in 1992 [4] as the two transverse rms-emittances the beam acquires after all inter-plane correlations have been removed by appropriate linear beam line elements. They are calculated from the 2nd-moments beam matrix

$$\tilde{C} = \begin{bmatrix} \langle x^2\rangle & \langle xp_x\rangle & \langle xy\rangle & \langle xp_y\rangle \\ \langle xp_x\rangle & \langle p_x^2\rangle & \langle yp_x\rangle & \langle p_xp_y\rangle \\ \langle xy\rangle & \langle yp_x\rangle & \langle y^2\rangle & \langle yp_y\rangle \\ \langle xp_y\rangle & \langle p_xp_y\rangle & \langle yp_y\rangle & \langle p_y^2\rangle \end{bmatrix}, \quad (5)$$

together with

$$J = \begin{bmatrix} 0 & 1 & 0 & 0 \\ -1 & 0 & 0 & 0 \\ 0 & 0 & 0 & 1 \\ 0 & 0 & -1 & 0 \end{bmatrix}. \quad (6)$$

as [5]

$$\tilde{\varepsilon}_{1/2} = \frac{1}{2}\sqrt{-tr[(\tilde{C}J)^2] \pm \sqrt{tr^2[(\tilde{C}J)^2] - 16\,det(\tilde{C})}}\,. \quad (7)$$

The product of the two eigen emittances is equal to the 4d rms-emittance $\tilde{\varepsilon}_{4d}$ being in turn equal to the square root of the determinant of $\tilde{C}$. By definition $\tilde{\varepsilon}_{1/2/4d}$ are preserved by linear beam line elements as drifts, quadrupoles, dipoles, and solenoids even if they are tilted.

PRESERVATION OF EIGEN EMITTANCES

Busch's theorem was obtained from expressing preservation of axial angular momentum using conjugate momenta. Its extension to beams is achieved in analogue way by ex-

Content from this work may be used under the terms of the CC BY 3.0 licence (© 2018). Any distribution of this work must maintain attribution to the author(s), title of the work, publisher, and DOI.

ISBN: 978-3-95450-194-6 ISSN: 2226-0366 doi:10.18429/JACoW-LINAC2018-TUPO079

NUMERICAL AND EXPERIMENTAL STUDY OF H⁻ BEAM DYNAMICS IN J-PARC LEBT

T. Shibata†, K. Ikegami, Y. Liu, A. Miura, F. Naito, K. Nanmo, H. Oguri, K. Ohkoshi, M. Otani, K. Shinto, A. Takagi
J-PARC Center, Tokai, Japan

Abstract

Transport process of negative hydrogen ion (H^-) in LEBT (Low Energy Beam Transport) is investigated by comparison of experimental and numerical results. A three dimensional Particle-In-Cell (PIC) particle transport model has been developed in order to take into account (i) axial magnetic field by two solenoids in J-PARC LEBT and (ii) radial electric field by space charge (SC) effect. Ratio of H^- beam particles inside the RFQ (Radio Frequency Quadrupole) acceptance to the total particles at the RFQ entrance is calculated for different current conditions in LEBT solenoid 1 and 2. The results are compared with RFQ transmission rate measured in the J-PARC linac commissioning. The double peak of RFQ transmission rate to the solenoid applied current seen in the measurement is explained by the calculation results. The results indicate that presence of the LEBT orifice for differential pumping plays a role as a collimator to reduce emittance at RFQ entrance.

LEBT TUNING IN J-PARC LINAC COMMISSIONING

A schematic drawing of J-PARC ion source (IS) and LEBT is shown in Fig.1. In J-PARC Linac commissioning, negative hydrogen ion beam extracted from the IS is focused by two solenoids in LEBT. The focused beam is injected toward the RFQ. The resent commissioning parameter for IS and LEBT are shown in Table 1. In the IS, AMFC (Axial Magnetic Field Correction) coil current, extraction voltage, acceleration voltage and applied currents for horizontal/vertical steering electromagnets (STM) are the adjustment parameters in the commissioning.

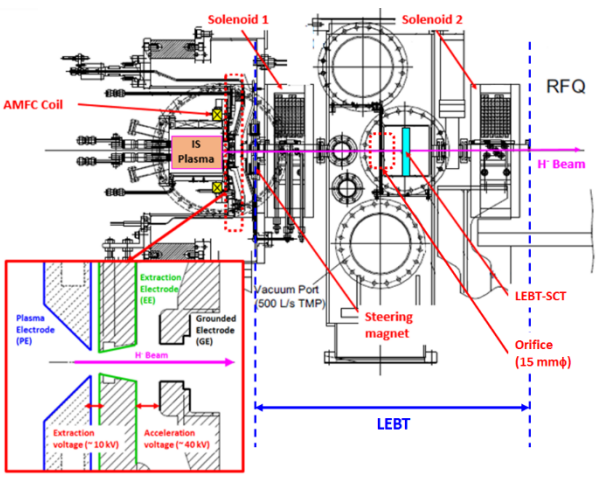


Figure 1: A schematic drawing of J-PARC IS and LEBT.

† email address:takanori.shibata@kek.jp

Table 1: Parameters for LEBT Tuning in J-PARC Linac Commissioning

Commissioning parameters	LI 30mA (2015)	LI 40 mA (2017)
AMFC coil (V)	0.0	2.0
Ext. voltage (kV)	9.9	9.8
Acc. Voltage (kV)	42.0	42.5
Hori. STM (A)	-1.0	-5.0
Vert. STM (A)	-5.5	-4.0
LEBT SOL1 (A)	495	500
LEBT SOL2 (A)	600	620

The AMFC and the extraction/acceleration voltages decide the initial divergence angle and beam energy of the H^- beam extracted from the IS. The beam energy is designed for 50 keV. Therefore, total value of extraction and acceleration voltages is 50 kV. However, recent results show that optimization of RFQ transmission rate is obtained for the total applied voltage up to around 51 – 52 keV while the beam intensity at LEBT increases monotonically with the applied voltage. The steering magnets are located in order to correct H^- beam bent by electron suppression magnets for reduction of co-extracted electron current.

In the LEBT, currents in two solenoid magnets are adjusted to obtain low emittance and Twiss parameter matching at the RFQ entrance. In the commissioning, current applied in the SOL 1 and 2 are set in ranges of 0 – 800 A to produce maximum 1.1 T at the solenoid center on beam axis. Optimization of the SOL currents are also shown in Table 1. At the center of the LEBT chamber, a 15 mm diameter orifice is located for differential pumping to prevent H_2 gas flow from the IS to the RFQ.

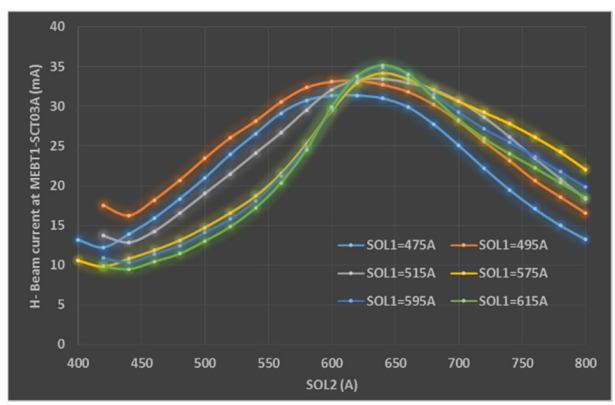


Figure 2: Dependence of H^- beam current measured at MEBT-SCT (just after RFQ exit) to the SOL1 and SOL2 currents in J-PARC Linac 30 mA operation.

Content from this work may be used under the terms of the CC BY 3.0 licence (© 2018). Any distribution of this work must maintain attribution to the author(s), title of the work, publisher, and DOI.

ISBN: 978-3-95450-194-6 ISSN: 2226-0366 doi:10.18429/JACoW-LINAC2018-TUPO083

BEAM DYNAMICS FOR THE FAIR P-LINAC LADDER RFQ*

M. Syha†, U. Ratzinger, M. Schütt
Institute of Applied Physics of Goethe University, 60438 Frankfurt, Germany

Abstract

After the successful measurements with a 0.8 m prototype the construction of a 3.3 m Ladder-RFQ at IAP, Goethe University Frankfurt, has been finished this summer. It is designed to accelerate protons from 95 keV to 3.0 MeV according to the design parameters of the p-Linac at FAIR. Along the acceleration section the parameters modulation, aperture and synchronous phase are linearly varied with cell number, which differs from former designs from IAP Frankfurt. The ratio of transversal vane curvature radius to mid-cell radial aperture and the vane radius itself are constant to support a flat voltage distribution along the RFQ. This was verified by implantation of the modulated vane geometry into MWS-CST RF field simulations. The development of adequate beam dynamics was done in close collaboration with the IAP resonator design team. The RFQGen-code was used for beam dynamics simulations. Among those were also error studies, that were performed to test the beam dynamic's stability against input Twiss parameter deviations to a degree indicated by the LEBT measurements performed in Q1/2018 at CEA[1] Saclay with participation of GSI's[2] Ion Source Group.

BEAM DYNAMICS DESIGN

The RFQGen-code was used for the beam dynamics calculations [1]. The beam dynamics design determined the mechanical design of the RFQ electrodes and was arrived at in consideration of the source beam as given by the Ion Source and LEBT Group of CEA Saclay and the design parameters of the Proton Linac at FAIR [2] (see Table 1). The current of the entrance cw beam was chosen rather high to 100 mA in order to have a large current margin. It was modeled in RFQGen with 10^5 (macro-)particles arranged in a 4D waterbag distribution. Other than slightly undershooting the final energy, slightly overshooting it poses no problem for the MEBT-section and the CH-DTL. For this reason and to provide a sufficient safety margin the final synchronous energy was set to 3.015 MeV. Figure 1 shows the plots of modulation parameter m, (minimum) radial aperture a and synchronous phase ϕ against the cell number. Their almost linear courses in the acceleration section result in higher acceleration efficiencies along the respective cells [3] and a therefore significantly reduced electrode length (compared to that generated by a more conservative design approach). This design was inspired by the beam dynamics design of CERN's Linac4-RFQ [4, 5].

Table 1: Beam Parameters at the RFQ Entrance and Electrode Design Parameters

Parameter	Value
Entrance Energy	95 keV
Beam Current	100 mA
Transversal $\varepsilon_{in,n,rms}$	0.3 π mm mrad
Twiss Parameter $\alpha_{x/y,in}$	0.7
Twiss Parameter $\beta_{x/y,in}$	0.04 mm/mrad
Frequency	325.224 MHz
Electrode Voltage	88.43 kV
ρ/r_0	0.85
Number of RM Cells	5

Table 2: Beam Parameters at the RFQ Wxit (10 mm behind the end of the electrodes)

Parameter	Value
$\varepsilon_{x,out,rms}$	0.33 π mm mrad
$\varepsilon_{y,out,rms}$	0.32 π mm mrad
$\varepsilon_{z,out,rms}$	0.21 MeV deg
Synchronous Exit Energy W_{syn}	3.015 MeV
Average Exit Energy W_{ave}	3.012 MeV
$W_{syn} - W_{ave}$	3 keV
$\frac{long.losses}{radial losses}$	59 %
Transmission	84.6 %

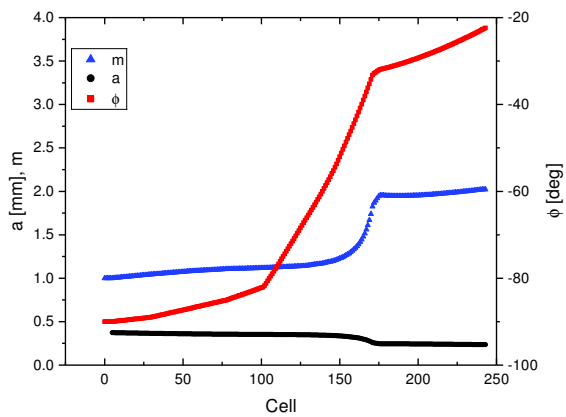


Figure 1: The modulation parameter, m, (minimum) radial aperture a and synchronous phase ϕ against the cell number.

Figure 2 shows the plots of the (macro-)particle losses per cell and the synchronous energy W_{syn} against the cell number as simulated by the RFQGen-Code. Most losses occur at the end of the gentle buncher section, i.e. at $W_{syn} = 0.67$ MeV. Here, the longitudinal losses reduce the longitudinal emittance, which did grow significantly during the earlier

* Work funded by BMBF 05P15RFRBA
† syha@iap.uni-frankfurt.de
[1] French Alternative Energies and Atomic Energy Commission
[2] Society for Heavy Ion Research (Gesellschaft fuer Schwerionenforschung)

Content from this work may be used under the terms of the CC BY 3.0 licence (© 2018). Any distribution of this work must maintain attribution to the author(s), title of the work, publisher, and DOI.

ISBN: 978-3-95450-194-6 ISSN: 2226-0366 doi:10.18429/JACoW-LINAC2018-TUPO084

BEAM DYNAMICS SIMULATIONS FOR THE NEW SUPERCONDUCTING CW HEAVY ION LINAC AT GSI*

M. Schwarz†[1], K. Aulenbacher[2,3], W. Barth[2,4], M. Basten[1], M. Busch[1], F. Dziuba[2], V. Gettmann[2], M. Heilmann[4], T. Kürzeder[2], M. Miski-Oglu[2], H. Podlech[1], A. Rubin[4], A. Schnase[4], S. Yaramyshev[4]
[1]IAP, Goethe University, Frankfurt am Main, Germany, [2]HIM, Mainz, Germany
[3]Johannes Gutenberg University, Mainz, Germany, [4]GSI Helmholtzzentrum, Darmstadt, Germany

Abstract

For future experiments with heavy ions near the coulomb barrier within the super-heavy element (SHE) research project a multi-stage R&D program of GSI/HIM and IAP is currently in progress. It aims at developing a superconducting (sc) continuous wave (CW) LINAC with multiple CH cavities as key components downstream the High Charge State Injector (HLI) at GSI. The LINAC design is challenging due to the requirement of intense beams in CW mode up to a mass-to-charge ratio of 6, while covering a broad output energy range from 3.5 to 7.3 MeV/u with the same minimum energy spread. Testing of the first CH-cavity in 2016 demonstrated a promising maximum accelerating gradient of $E_a = 9.6$ MV/m; the worldwide first beam test with a sc multi-gap CH-cavity in 2017 was a milestone in the R&D work of GSI/HIM and IAP. In the light of experience gained in this research so far, the beam dynamics layout for the entire LINAC has recently been updated and optimized.

INTRODUCTION

In the last decades the periodic table was essentially extended up to the nuclei with proton number $Z = 118$ and neutron number $N = 177$. It turned out, that the most successful methods for the laboratory synthesis of heavy elements are fusion-evaporation reactions using heavy-element targets, recoil-separation techniques and the identification of the nuclei by known daughter decays [1]. For the production of SHE, hot fusion reactions with ^{48}Ca projectiles and targets made of actinide elements ranging from ^{231}Pa to ^{254}Es are considered promising.

To sum it up, all of the experiments have the common challenge of very low cross sections and therefore require the separation of very rare events within weeks of beamtime from intense backgrounds [2]. Fortunately, the yield of SHE and therefore the number of events per unit time depends not only on the cross section but also on the projectile beam intensity, overall beam quality and target thickness. Thus, progress in SHE research is highly driven by technical developments in this fields [3]. Furthermore, the scientific fields of nuclear chemistry and spectroscopy as well as materials research and biology could benefit from these developments.

At GSI a comprehensive upgrade programme is performed. In this context, the UNILAC (Universal Linear Accelerator) is upgraded to the requirements of FAIR (Facility for Antiproton and Ion Research) and will be used as injector [4–9]. The duty factor will be relatively low (below 1 %). Conversely, for SHE experiments a high duty factor is required, which is why the presently available duty cycle of 25 % (5 ms pulse length @50 Hz) will be upgraded to CW-mode [10, 11]. Consequently a superconducting CW-LINAC was proposed [12] and is further investigated and developed [13–18].

BEAM DYNAMICS CONCEPT

Up to now, the reference design for the CW LINAC dates back to the publication of Minaev et al. in 2009 [12]. Meanwhile many experiences have been gained in design, fabrication and operation of superconducting CH-cavities and the associated components. In this context, a revision of the beam dynamics layout was recommended. Optimized cavity layouts resulted in modified voltage distributions. Furthermore, the cryomodule layout and intertank sections were specified in more details. Promising RF- and beam testing with the 15-gap CH0 showed, that higher accelerating gradients can be achieved [19], thus leading to a more efficient design approach. Consequently, extensive beam dynamics studies are carried out to fix the best layout with respect to the beam and all other RF and mechanical requirements. The beam dynamics concept for the CW-LINAC is based on multicell CH-type DTL-cavities operating at 216.816 MHz ($f_{HLI} = 108.408$ MHz) and focusing by superconducting solenoids. The main requirements and boundary conditions for the LINAC design are summarized in Table 1:

Table 1: Basic CW-LINAC Design Parameters

Parameter	Value
W_{in}	1.4 MeV/u
W_{out}	3.5–7.3 MeV/u
ΔW_{out}	±3 keV/u
I	≤ 1 mA
A/q	≤ 6

With a relatively low beam current, CW-operation and limited longitudinal space, this LINAC is predestined to be operated in the superconducting mode. Further thoughts on

* Work supported by BMBF contr. No. 05P15RFRBA, EU Framework Programme H2020 662186 (MYRTE) and HIC for FAIR
† schwarz@iap.uni-frankfurt.de

Content from this work may be used under the terms of the CC BY 3.0 licence (© 2018). Any distribution of this work must maintain attribution to the author(s), title of the work, publisher, and DOI.

ISBN: 978-3-95450-194-6 ISSN: 2226-0366 doi:10.18429/JACoW-LINAC2018-TUPO085

MODELLING OF BEAM PARAMETERS OF RF LINAC FOR GBS-ELI-NP

Piotr Tracz†
for the ELI-NP team
ELI-NP/IFIN-HH, RO-077125 Bucharest-Magurele, Romania

Abstract

The Gamma Beam System at the ELI-NP (Extreme Light Infrastructure – Nuclear Physics) currently being constructed in Magurele/Bucharest, Romania will be a high-brilliance advanced source of gamma rays based on laser Compton back-scattering. For a successful operation of the GBS a high brightness low emittance electron beam is of crucial importance. The warm RF linac is designed in two stages – one with the beam up to 300 MeV, and another one about 720 MeV. The S-band photo-injector is combined with a C-band linac. The beam is transported by transfer lines to the interaction points. In this paper we report the results of computer simulations of the electron beam transport in the low energy linac and transfer line up to the low energy interaction point (IP1). The simulation model makes it possible to predict the beam parameters to be recuperated in case of failure of any magnetic or accelerating elements as well as it enables to determine the optimal parameters of replaced components. It will be used for the development of the Gamma Beam System in the future.

INTRODUCTION

The Gamma Beam System was designed and is being constructed by the EuroGammaS Association – a consortium of European academic and research institutions and industrial partners, and it is hosted by the Horia Hulubei National Institute of Physics and Nuclear Engineering [1]. The technical design of GBS is described with details in [2], and several other publications like e.g. [3-5].

To perform the simulations we used the Elegant [6] code, and SDDS toolkit [7] for processing and graphing of the Elegant output data. The simulations of the beam transport in the injector and calculations of output beam parameters at the injector exit were done with use of the program Parmela [8, 9]. Currently we are studying beam optimization in the injector using the Astra [10] code.

Our study will be extended for the high energy linac. The aim is to provide means to re-optimize the linac settings to new working points in accordance to users' requirements.

S-band Injector

The GBS injector starts at the RF gun with photo-cathode. To suppress the beam loss by transverse spreading there are two focusing solenoid magnets with high gradient field starting very close to the gun exit. They focus the beam to minimum size and make the beam emittance low at the entrance of accelerating structure. The photo-cathode RF gun generates electron beam in the photoemission process. Ultraviolet laser pulses are incident on the copper photo cathode. The charge of the electron bunches depends on the laser power and the conversion efficiency of the photo-cathode material; in case of GBS it is 250pC. The 2D profile of the gun with electric field pattern designed in the electromagnetic code Superfish [11] is shown in Fig. 1. It will operate at π-mode with resonance frequency 2.856GHz with an input power sufficient to achieve 120MeV/m field gradient at cathode.

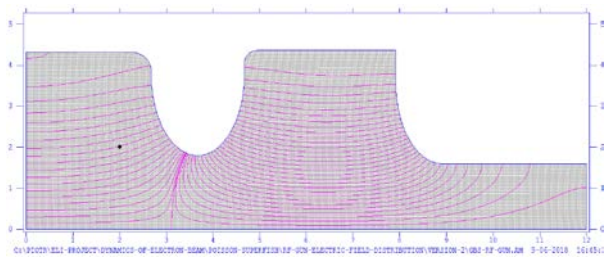


Figure 1: 2D profile of RF gun for GBS with electric field profile.

The RF gun is followed by two TW accelerating structures. These are constant gradient (22MV/m), and will operate in $2\pi/3$ mode. The first structure is surrounded by twelve independent coils. The purpose of them is to keep the radius of the beam from the entrance along the accelerating sections. Additionally the S-band sections will act as a bunch compressor.

Low Energy C-band Linac

The low energy linac that follows the injector is based on four C-band sections operating at 5.712 GHz. The length of each section is 1.78449m and the length of a single cell is 0.017495m. Each section is fed by 52MV RF voltage. The input RF phase of the first two sections is 82.5° and other two 115°. The dogleg type transport line transmits the beam to the interaction point. After the interaction point the beam is transported to the beam dump.

In addition to the accelerating sections the linac modules are completed by magnetic and diagnostic devices. There are two quadrupole triplets in the diagnostic sections. One after the first C-band structure and another one at the end of the low energy linac. They are used for emittance measurement and to provide the desired electron beam focusing. There are several beam profile monitors (screens) located at different positions along the linac to control the transverse profile of the beam. Figure 2 presents the distribution of the quadrupole magnets and the profile monitors in the low energy linac. Two S-band transverse deflecting structures will be used for measuring the longitudinal beam profile.

† email address: piotr.tracz@eli-np.ro

Content from this work may be used under the terms of the CC BY 3.0 licence (© 2018). Any distribution of this work must maintain attribution to the author(s), title of the work, publisher, and DOI.

ISBN: 978-3-95450-194-6 ISSN: 2226-0366 doi:10.18429/JACoW-LINAC2018-TUPO088

MEASUREMENT OF DIAGNOSTICS RESPONSE BY RF PARAMETERS FOR HARD X-RAY LINE IN PAL-XFEL*

H. Yang†, Pohang Accelerator Laboratory, 37673 Pohang, Korea

Abstract

PAL-XFEL is a hard x-ray (HX) and soft x-ray (SX) FEL machine to generate 2.5 – 15 keV FEL in the HX line and 0.28 – 1.2 keV FEL in the SX line. The HX line consists of an e-gun, a laser heater, S-band accelerators, an X-band linearizer, three bunch compressors (BC), and a dog-leg line. PAL-XFEL maintains the stable operation and FEL delivery with more than 98% availability due to machine stabilities including RF modules. In order to investigate the stable operation, we measure the diagnostics response for bunch charge monitors, energy beam position monitors, bunch length monitors, and a FEL intensity with a photon beam position monitor by RF parameters - RF amplitude and phase for an e-gun, accelerators, and a linearizer. In this paper, we present mainly corresponding RF parameters for e-beam and FEL jitters by this measurement and matrix analysis.

INTRODUCTION

PAL-XFEL is the third XFEL machine in the world using normal conducting linacs for e-beam accelerating. It is combined two lines - a Hard X-ray (HX) line generating 2.5 – 15 keV FEL and a soft x-ray (SX) line generating 0.28 – 1.2 keV FEL [1]. PAL-XFEL has been successfully operating and delivering XFEL since March 2017. The availability is more than 98% and the stability of beam parameters are under 0.02% for the e-beam energy, 7% for the peak current, and 10% for the FEL intensity. Especially, it has under 20 fs timing jitter - the most stable timing among XFEL machines in the world [2].

The HX line of PAL-XFEL consists of an e-gun, a Laser Heater (LH), S-band accelerators, an X-band Linearizer (XL), three Bunch Compressors (BC), and a Dog-Leg (DL) line (Fig. 1). The stable e-beam parameters are caused by the stability of RF devices in the injector and linac section, and magnet devices in bunch compressors and a dog-leg line. The stabilities from the error analysis with the ELEGANT simulation are applied for RF and magnet devices in PAL-XFEL [3]. The required stability of the magnet power supply system is few ten's ppm and it is easy to achieve by the developed technology. However, some stabilities for RF devices are challenging, for example, 0.01° phase jitter for the injector RF device and 0.05° phase jitter for the X-band linearizer. Since we use the RF timing system, there is phase drift in all RF devices by the drift of reference timing.

In order to investigate and quantify effects of jitters, we measured diagnostics responses by RF parameters. Bunch Charge Monitors (BCM), Energy Beam Position Monitors (EBPM), Bunch Length Monitors (BLM), and a Quadratic photon Beam Position Monitor (QBPM) were used in this measurement. The FEL pulse energy can be obtained from the sum value of the QBPM. The RF amplitude and phase of all RF modules were used. The response matrix was obtained from this measurement, and the main RF variables and modes for a FEL jitter were found by the method of Singular Value Decomposition (SVD) for the response matrix [4]

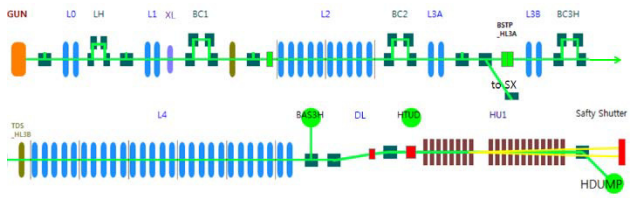


Figure 1: Layout of the HX line in PAL-XFEL.

LATTICE AND INITIAL SETTING

The HX line in PAL-XFEL consists of an injector, the LH, 4 linac sections, 3 BCs, and the DL line. The injector include S-band photo-cathode RF e-gun and 2 linacs with individual RF modules (L0). Electron bunches are generated with the 5-ps bunch length and longitudinally Gaussian distribution in the gun. The e-beam are accelerated to 140 MeV at the end of the injector. The slice energy spread of e-beam are heated in the LH. The linac sections are divided by BCs. We call those as L1, L2, L3, L4, BC1, BC2, and BC3H (Fig. 1). The XL is located between L1 and BC1. 20 undulators and a self-seeding region are in HU1 section. The undulator K-value can be adjusted by moving the undulator gap, but we normally use fixed K-value of 1.87. We set the machine for 9.7 keV FEL generation in this measurement. The detail parameters are in Table 1 and 2.

Table 1: Beam Parameters for Initial Setting

Parameters	Value
Initial charge	248 pC
Final charge	185 pC
Bunch energy at LH	0.14 GeV
Bunch energy at BC1	0.35 GeV
Bunch energy at BC2	2.50 GeV
Bunch energy at BC3H	3.50 GeV
Final bunch energy	8.70 GeV
Initial peak current	20 A
Peak current after BC1	87 A
Peak current after BC2	390 A
Peak current after BC3H	2000 A
FEL energy	9.7 keV
FEL Pulse Energy	1.0 mJ

Content from this work may be used under the terms of the CC BY 3.0 licence (© 2018). Any distribution of this work must maintain attribution to the author(s), title of the work, publisher, and DOI.

ISBN: 978-3-95450-194-6 ISSN: 2226-0366 doi:10.18429/JACoW-LINAC2018-TUPO090

ELECTRON-BEAM MATCHING TO SOLENOID MAGNETIC FIELD IN A KLYSTRON*

S. J. Park†, Y. J. Park, Pohang Accelerator Laboratory, POSTECH, 37673 Pohang, Korea
J. H. Hwang, S. G. Shin,
Division of Advanced Nuclear Engineering, POSTECH, 37673 Pohang, Korea
D. H. Yu, S. Y. Hyun, Vitzrotech Co., Ltd., 15603 Ansan City, Korea

Abstract

High-power klystrons for particle accelerators employ high-perveance electron guns which are usually focused by Solenoid magnets. The electron beam should be optically matched to the downstream magnetic field to prevent the beam from scalloping. The task usually requires a series of computer simulations with many design parameters, and therefore requires extensive(sometimes exhaustive) efforts if not aided by a priori experiences. In order to alleviate the difficulties we have developed a matching procedure which is systematic and reliable. In this article we describe the procedure with an example design of a 400 kV, 500 A electron beam with radius 8 - 11 mm.

MATCHING SCHEME

The focusing properties of the electron beam in a klystron is described by the envelope equation [1],

$$\ddot{r} + r\omega_L^2 \left[1 - \left(\frac{B_c}{B}\frac{r_c^2}{r^2}\right)\right]^2 - \frac{\eta I_B}{2\pi r \epsilon_0 u_0} = 0 \qquad (1)$$

where r is the radial position of an electron at a given longitudinal position, the dot denotes derivative with respect to time, $\eta = e/m$ is the charge to mass ratio, $\omega_L = \eta B/2$ is the Larmour frequency, B_c is the magnetic field strength at the cathode center, B is the magnetic field strength at a given longitudinal position, r_c is the cathode radius, I_B is the beam current, and u_0 is the average beam velocity.

Table 1: PAL Klystron Beam Parameters (Fine Tuned for the Beam Matching)

Parameter	Value
Beam Voltage, V_B	400 kV
Beam Current, I_B	500 A
Microperveance, uK	2 upervs
Cathode Radius, r_c	45 mm
Cathode Field, B_c	31 G
Equilibrium Beam Size, b	9.3 mm
Brillouin Field, B_B	735 G
Confinement Factor, m	1.609

Given beam parameters we can solve Eq. (1) numerically to obtain beam envelopes. With example parameters (for the linac klystrons in the Pohang Accelerator Laboratory (PAL)) presented in Table 1 we could obtain the so-called matched condition as shown in Fig. 1.

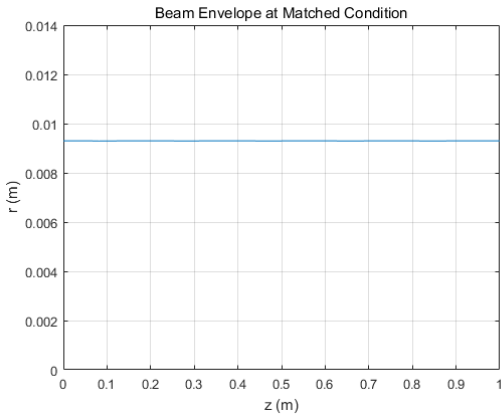


Figure 1: Matched beam envelope with parameters in Table 1.

If we deviate from the matched condition by changing some parameters we can obtain the family of envelopes from which the beam-matching methodology can be inferred. For example changing the B_c results in envelopes as shown in Fig. 2 in which the envelopes for B_c either higher or lower than the matched value (31 G) are quite symmetric. In contrast to this, changing the same parameter for a mismatched beam does not yield symmetric envelope families. Figure 3 is the envelope family for different B_c with a slightly detuned beam-injection angle ($\dot{b_0} = 0.01$) to make the beam mismatched.

From Figs. 2 and 3 it is evident that a scan for a properly chosen parameter for the matched beam results in a symmetric envelope family with its center envelope corresponding to the matched condition. Therefore the parameter scan and the resulting envelope family is a diagnostic tool for checking whether a beam is at the matched condition. It is interesting to see that, unlike the injection-angle detuning (as shown in Fig. 3), detuning the injection beam radius b_0 do not make the beam mismatched but shift the beam to a new matched condition. Figure 4 is the B_c-scanned envelope family for a injection-radius detuned beam. Comparing Figs. 2 and 4 we see that the beam is matched at a new condition of $B_c = 33$ G.

Here we note the importance of scan parameter selection. Figure 5 is the envelope family obtained by scanning the beam voltage V_B. Unlike the B_c-scanning (as shown in Fig. 2) the V_B-scanning does not yield a symmetric envelope

* Work supported by the Ministry of Science and ICT, Korea
† sjpark@postech.ac.kr

Content from this work may be used under the terms of the CC BY 3.0 licence (© 2018). Any distribution of this work must maintain attribution to the author(s), title of the work, publisher, and DOI.

ISBN: 978-3-95450-194-6 ISSN: 2226-0366 doi:10.18429/JACoW-LINAC2018-TUPO091

BEAM BREAK UP INSTABILITY ANALYSES FOR CAVITIES, LINACS, AND ENERGY RECOVERY LINACS*

V. Volkov†, V. M. Petrov, BINP SB RAS, Novosibirsk, Russia

Abstract

This analyze argue that *BBU* instability both in separate cavities and in Linacs or *ERLs* is going due to the consequence of fundamental property of dipole modes. "Head-tail" bunch instability has also the same nature. New BBU instability testing methods are described and analytically proved in the article.

INTRODUCTION

Beam Break Up (*BBU*) instability of a beam in a cavity begins to develop when the beam current value becomes higher than some threshold value. Then a transversal beam oscillation appears with avalanche growth that has the frequency of a one of dipole modes in the cavity. The dipole mode amplitude there also becomes to avalanche growth. As a role the process continues up to the beam hit to the channel wall (the tail particles in the first instance) if the beam current source duration is long enough or if the focusing system cannot limit this oscillation. If the growth increment is high enough to have time to pick up BBU instability for a single bunch so this is known as "head-tail" instability.

THRESHOLD CURRENT OF BBU INSTABILITY

The dipole mode growth is attended by transferring of a part of beam kinetic energy to saved dipole mode field energy. Incidentally, some part of this energy disappears in the cavity wall. This energy transferring process is going on due to beam space-modulation (transversal oscillation) appeared with the dipole mode frequency as a result of the beam interaction with the dipole mode. This occurred only for those dipole modes that applies the energy brake to the beam. Only approximately half of all dipole modes in a cavity can do it. Such a ratio of stable and instable dipole modes remind of equal probability of some stochastic process. The reason will be clear then later in the pillbox cavity example.

To be a stable process, the transferred average power (P_{BBU}) must be lower then disappeared power (P_{dis}), i.e. $P_{BBU} \le P_{dis}$. Such an approach has also considered by W.K.H. Panofsky in [1], but we have come to new conclusions.

On Fig.1 the example of the simplest dipole mode TM_{110} is shown in a pillbox cavity. Its resonance frequency (ω) is defined only by the cavity diameter (D) $\omega=0.82c\cdot D$ and is independent on its length (L).

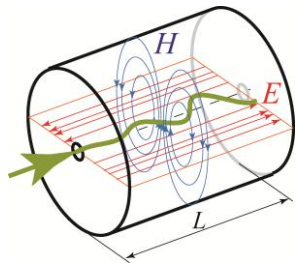


Figure 1: RF field distribution of TM_{110} dipole mode in a pillbox cavity with the view of a beam space-modulated trajectory.

We have to stress, only the average transferred power P_{BBU} plays a role in BBU instability. Each bunch separately hits to different phase of a dipole mode and so it can loss its energy or even to get it. So we can conclude that a bunch repetition frequency does not have an importance if dipole frequency is far enough from any harmonic of repetition frequency. Even any unbunched continuous beam can be instable.

BBU threshold current formula can be given if expressions for powers will be inserted to the above mentioned equation $P_{BBU} \le P_{dis}$: $P_{BBU} = -E_{BBU}\cdot I$, where E_{BBU} is average energy gain of beam particles in the dipole mode in Volts; I is the average beam current. $P_{dis}=\omega\cdot U/Q$, where ω is circular resonance frequency of the dipole mode; U is saved dipole mode energy; Q is loaded quality factor of the dipole mode. After the conversion we get

$$I \cdot Q \le I_Q = -\frac{\omega \cdot U}{E_{BBU}}. \quad (1)$$

The value of threshold current I_Q is the self-sufficing parameter for *BBU* instability as it follows from fundamental properties of dipole modes described further. Instability modes have positive value $I_Q>0$, for stability modes $I_Q<0$. Minus sign in *Eq.1* compensates the sign of energy loss of beam particles $E_{BBU}<0$.

BBU Fundamental Properties of Dipole Modes

One of unique property of dipole modes is the proportionality between values of average particle energy gain and dipole mode saved energy for beams propagating close enough to cavity axis:

$$E_{BBU} = -\frac{1}{I_Q}\cdot \omega U, \quad (2)$$

This proportionality is follows from the fact that rf longitudinal electric field of dipole modes (that caused the particle energy gain) is growth linearly with deviation (x) from

* Work supported by Russian Science Foundation (project N 14-50-00080)
† v.n.volkov@inp.nsk.su.

Content from this work may be used under the terms of the CC BY 3.0 licence (© 2018). Any distribution of this work must maintain attribution to the author(s), title of the work, publisher, and DOI.

ISBN: 978-3-95450-194-6 ISSN: 2226-0366 doi:10.18429/JACoW-LINAC2018-TUPO092

BEAM DYNAMICS AND COLLIMATION FOLLOWING MAGIX AT MESA

Ben Ledroit*, Kurt Aulenbacher, Johannes Gutenberg-Universität, 55128 Mainz, Germany

Abstract

The Mainz Energy-recovering Superconducting Accelerator (MESA) will be an electron accelerator allowing operation in energy-recovery linac (ERL) mode, where beam energy is recovered by decelerating the beam in linac cryomodules and transferring kinetic energy to the RF. The ERL mode provides the opportunity to operate experiments at peak energy with thin targets, combining high luminosities typical for storage rings and high beam brightness typical for linacs. The MESA Internal Gas Target Experiment (MAGIX) aims to operate jet targets at high luminosities with different gases up to Xenon. As scattering effects in the beam rise with the atomic number, investigations on the impact of the target on beam dynamics and beam losses are required for machine safety. The goal of this work is to understand target induced halo, track halo particles through downstream sections and protect the machine with a suitable collimation system and shielding from direct and indirect damage through beam losses and radiation. The present status of the investigations is presented.

MESA

An overview of MESA is given in [1]. MESA will supply the P2 experiment in external beam (EB) mode with a beam current of 150 µA at 155 MeV [1, 2]. In EB mode, the whole beam is dumped after interaction with the target. A second beamline is set up for the ERL mode, where the beam passes the MAGIX target and is then phase shifted 180° with respect to the RF and recirculated through the cryomodules for energy recovery. MESA will maintain a 1 mA beam current in the first stage and 10 mA after upgrade at 105 MeV.

MAGIX

ERL operation is possible since MAGIX provides a low density target and only a small fraction of the beam actually interacts with the gas. The target is designed as a gas jet of nearly homogenous density. The jet is of cylindrical shape with 4 mm in height and diameter [3] and is produced by accelerating gas to supersonic speeds in a Laval nozzle perpendicular to the beam axis. A gas catcher is set up opposite to the Laval nozzle to collect the major part of the injected gas in order to keep vacuum conditions at a tolerable level. MAGIX is designed to operate with various gases (H, He, O, Ar, Xe, CH_4) for fundamental physics experiments, e.g. the search for the dark photon as well as investigations on the proton form- and astrophysical S-factor [4]. The setup is shown in Fig. 1.

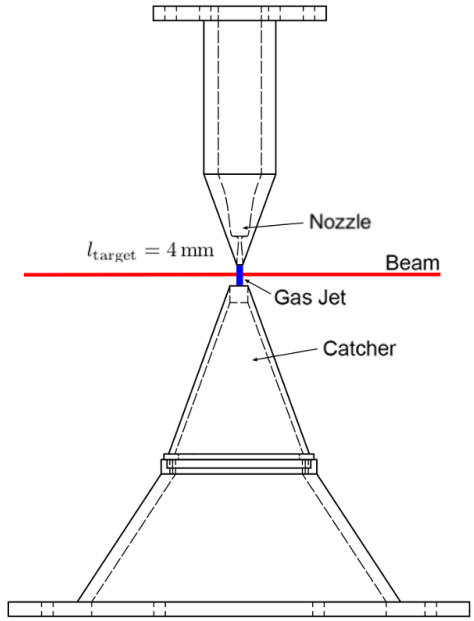


Figure 1: Schematic drawing of the MAGIX gas target [5].

Luminosity Limit Estimation

Target scattering and beam optics limit the luminosity of targets in ERL operation. Luminosity and target density limits for MAGIX can be estimated as presented in [6]. The luminosity limit then depends on beam and target properties. The necessities of radiation protection simultaneously set a limit to beam power losses outside adequately shielded areas. It is therefore important to examine these parameters to ensure reliable ERL operation.

TARGET INDUCED HALO

Scattering on the gas target widens the angle and energy distribution of the electron beam in a way that a halo forms around the original beam cross-sectional area as shown in Fig. 2. The halo is therefore called "Target Induced Halo" (TAIL). TAIL might cause malicious beam dynamical behavior when passing the cryomodules, such as inducing Higher Order Modes (HOMs) in the cavity, or directly damage machine parts when electrons get dumped in the cavities and beam pipes. Radiation produced by dumping electrons may further lead to damage especially to electronic components and generate background noise in the detectors of the experiments reducing measurement precision. It is therefore crucial to carefully investigate on the effects originating from the beam passage of MAGIX and formulate a collimation approach downstream the target to encounter impacts on machine operation safety and reliability.

* bledroi@uni-mainz.de

Content from this work may be used under the terms of the CC BY 3.0 licence (© 2018). Any distribution of this work must maintain attribution to the author(s), title of the work, publisher, and DOI.

ISBN: 978-3-95450-194-6 ISSN: 2226-0366 doi:10.18429/JACoW-LINAC2018-TUPO093

EXCITATION OF MILLIMETER WAVELENGTH CAVITY STRUCTURE

M. Arsentyeva†[1], A. Barnyakov, A. Levichev[1], D. Nikiforov, BINP, Novosibirsk, Russia
[1]also at Novosibirsk State University, Novosibirsk, Russia

Abstract

In this work excitation of W-band structure is studied. The structure consists of cylindrical cavities with the operating frequency of about 96 GHz. We plan to excite the structure by short bunches from the photocathode RF gun. In order to choose structure geometry and beam duration, we performed estimations and simulations; induced voltage was also estimated. Taking into account feasible parameters of the photocathode RF gun such as beam size and emittance, we studied exciting beam transverse dynamics to define its other characteristics (energy and charge). To lead the beam from the whole structure, focusing is needed. After estimation of required magnetic field, we considered possibility of focusing with help of permanent magnets.

INTRODUCTION

Accelerator facilities on the base of short beams for interdisciplinary research are being developed at research centers [1-3]. Radiofrequency (RF) photocathode gun is usually the source of short beams. Such a facility being developed at Budker Institute of Nuclear Physics (BINP) will provide electron beams of picosecond duration for different experimens that require short beams.

Excitation of W-band accelerating structure could be one of these experiments. Such structures are interesting from the point of view of high gradient [4] due to the higher frequency. Thus, length of the W-band accelerator may be significantly reduced compared to length of the S-band one.

Another motivation to develop W-band accelerating structures is connected with plasma excitation experiments where bunch required length is determined by the Langmuir wavelength

$$\sigma_t \sim c/\omega_p,$$

Here c is the speed of light, $\omega_p = \sqrt{4\pi n_p e^2/m}$, is the plasma frequency, e is the electron charge, n_p is the plasma density, m is the electron mass. With the plasma density of 10^{15} cm^{-3}, required bunch length is about 0.2 mm (0.6 ps). To obtain train of such short bunches, one can excite W-band structure by the "driver" beam from the photocathode gun, and then bunch there the secondary "long" beam. These bunches with spatial period of about mm are suitable for the plasma excitement and for the subsequent wakefield acceleration.

Thus, W-band structures are interesting not only in terms of accelerator fundamental physics but also for the industry where accelerator length may be significantly reduced.

RF PHOTOCATHODE GUN

After the photocathode RF gun (Fig. 1) beam is accelerated in the S-band disk-loaded accelerating structure up to tens MeV. After that it enters the W-band structure to excite it.

RF Photocathode Gun

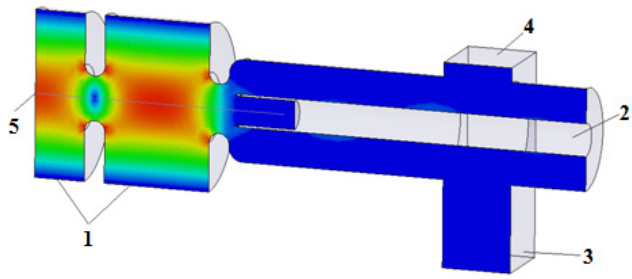


Figure 1: Layout of the photocathode gun with the electric field distribution: 1 — accelerating cavities, 2 — input for the laser beam, 3 — RF power input, 4 — vacuum pumping connection, 5 — photocathode.

Table 1: Photocathode Gun Specifications.

Parameter	Value
Operating frequency	2856 MHz
SWR at the operating mode	1.1
Unloaded quality factor of cavities	12000
Length of the first cavity	24.8 mm
Length of the second cavity	52.3 mm
Cavity diameter	82 mm
Beam duration	1-10 ps
Repetition rate	10 Hz
Beam charge	up to 2 nC
Transverse emittance	10 μm

Substantial feature of the photocathode guns is production of low emittance beams compared to conventional thermionic cathode guns [5]. Emittance evolution for the beam charge of 1nC and 2 nC at the BINP photocathode gun is shown at Fig. 2 (obtained during simulations at ASTRA [6]).

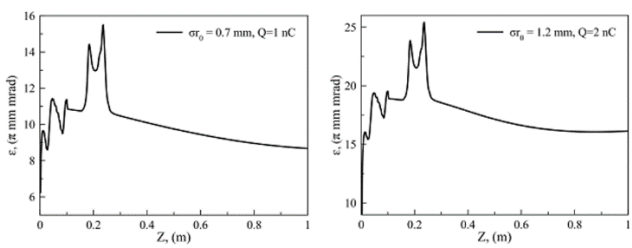


Figure 2: Emittance evolution for the beam from the photocathode gun with the charge of 1 nC (top) and 2 nC (bottom).

For the moment the gun is fabricated, measured and pumped (Fig. 3).

†mariemaltseva@yahoo.fr

Content from this work may be used under the terms of the CC BY 3.0 licence (© 2018). Any distribution of this work must maintain attribution to the author(s), title of the work, publisher, and DOI.

ISBN: 978-3-95450-194-6 ISSN: 2226-0366 doi:10.18429/JACoW-LINAC2018-TUPO095

BEAM LOADING WITH THE FIRST REBUNCHER OF SPIRAL2, FIRST MEASUREMENTS

M. Lechartier, J.F. Leyge, R. Ferdinand, GANIL, Caen, France

Abstract

The SPIRAL2 LINAC acceleration start with an RFQ (Radio Frequency Quadrupole). In the MEBT (Medium Energy Beam Transport) Line, the beam passes through rebunchers. The beam intensity is up to 5 mA. We need to take care of the beam loading as the RF (Radio Frequency) power in the cavity can give energy to the ion beam and also the ion beam can give energy to the cavity. This paper presents the effects of the beam on the rebuncher cavity

REBUNCHER CAVITY

Three identical rebunchers (see Figs. 1 and 2) are located in the MEBT Line. Only the first rebuncher is used today on the diagnostic plate to characterize the different beam parameters [1].

A solid-state amplifier is used with a 10 kW maximal output power. Actually, the power at the cavity entrance is 6-8% lower due to the losses in the circulator and RF transport lines. The maximum nominal voltage is 120 kV. The proton nominal value is 38 kV.

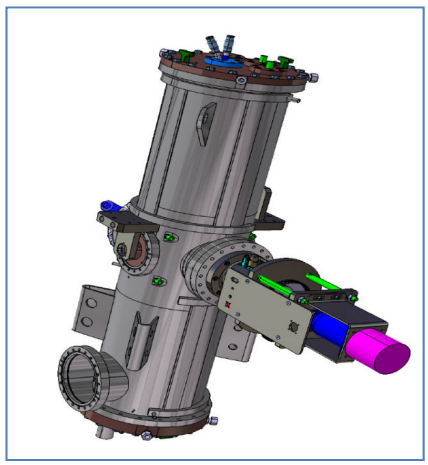


Figure 1: Cavity.

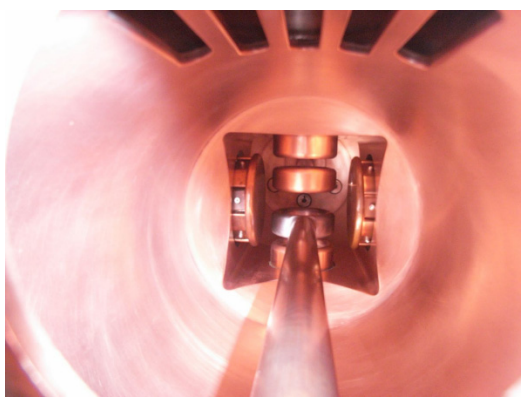


Figure 2: Inside the cavity.

Table 1: Parameters

Parameter	Value	Unit
Design voltage (continuous)	120	kV
Design voltage (50% DC)	190	kV
Beta	0.04	%
TTF	0,38	
Q_L	3335	
Power loss (@120 kV CW)	5.0	kW
Power loss (@190 kV)	12.2	kW
Tuning range	+/-300	kHz/mm
Cavity aperture diameter	60	mm
Gap distances	13 .30 .13	mm
Flange to flange distance	280	mm

RF REGULATION OF THE CAVITY

The RF system is regulated by a general LLRF (Low level radio Frequency) numerical system developed at Saclay. The regulation used in SPIRAL2 is a control feedback loop (see Fig. 3). The frequency choosed for the sample clock is 70.422 MHz (the RF is 88.0525 MHz). The signal reference and the cavity signal are sampled and compared. Then an equation is applied to model the loop filter. The loop filter is a P.I.D. (proportional, integrated, derivated) structure. Actually, we use only the P and I parameters to stabilize the RF voltage. The filtered error is then converted to analog signal and sent to an IQ (In phase and in Quadrature) modulator to correct the error. So, the amplitude and phase compensation cannot be separated.

Others classical systems used are often amplitude and phase separated loops. The goal values for the regulation are : amplitude error < 1% , phase error < 1° for the complete system. It contains a post mortem system which can be used as a precise monitoring system in the ns scale.

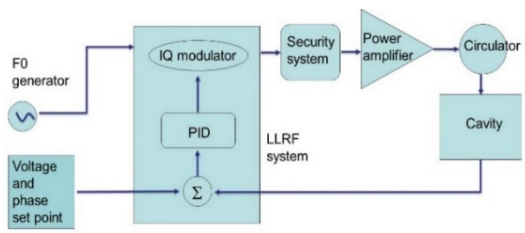


Figure 3: Regulation system.

EXPERIMENTS

The effects of the beam are evaluated when the rebuncher is in open loop regulation and in closed loop. The phase offset between RFQ (reference phase) and rebuncher is tuned from -180 to +180°. We record the phase offset and the voltage offset induced by the beam in both open and close loop regulation. This experience is made for different beam currents.

Content from this work may be used under the terms of the CC BY 3.0 licence (© 2018). Any distribution of this work must maintain attribution to the author(s), title of the work, publisher, and DOI.

ISBN: 978-3-95450-194-6 ISSN: 2226-0366 doi:10.18429/JACoW-LINAC2018-TUPO097

DESIGN OF C-BAND ELECTRON LINEAR ACCELERATOR FOR A COMPLEX OF RADIATION THERAPY*

L. Ovchinnikova†[1], V.I. Shvedunov[1], Skobeltsyn Institute of Nuclear Physics, Lomonosov Moscow State University (SINP MSU), 119991 Moscow, Russia
[1]also at Laboratory of Electron Accelerators MSU Ltd (LEA MSU), 119234 Moscow, Russia

Abstract

The report presents the design of the linear electron accelerator for a complex of radiation therapy. The three-electrode electron gun and C-band accelerating structure are optimised to produce a therapeutic electron beam with an energy of 6 MeV and a dose rate of 10 Gy/min and a beam with an energy of 2.5 MeV to obtain a portal image. The beam size at the bremsstrahlung target in both modes does not exceed 2 mm. The total length of the accelerating system with the electron gun does not exceed 330 mm. The accelerating structure is fed by RF power from a multibeam klystron at a frequency of 5,712 MHz with a maximum pulsed power of 3.5 MW.

INTRODUCTION

This work describes the results of beam dynamics calculation in the linear accelerator with the maximum energy of 6 MeV, intended for the complex of radiation therapy KLT6 [1].

The following requirements are specified for the linear accelerator KLT6:

- Accelerator length, i.e. distance from the bremsstrahlung target to the radiation shielding exterior part: maximum 350 mm.
- Minimum lateral dimensions of the accelerating structure to reduce the radiation shielding weight.
- Sequential operation at two values of the accelerated electron beam energy: 6 MeV in the therapeutic dose delivery mode and 2.5 MeV in the portal image acquisition mode.
- Maximum dose rate at the axis at the distance of 1 m from the bremsstrahlung target without a flattening filter with the energy of 6 MeV in the therapeutic dose delivery mode: at least 10 Gy/min.
- Electron beam diameter at the bremsstrahlung target: maximum 2 mm at half height of charge distribution.

The accelerator, we are developing, differs from those used in similar complexes by a possibility to switch energy of the accelerated electron beam within a broad band, as well as by small longitudinal and lateral dimensions of the accelerating structure.

In order to achieve the declared characteristics of KLT6, we have selected a 5-cm wavelength band of the accelerating field (C-band). As for a combination of a number of characteristic of the accelerating structures (in particular, value of the effective shunt impedance, maximum accelerating field strength, diameter of the beam hole, overall dimensions), the C-band is the most appropriate for the compact electron accelerators with a relatively low average accelerated beam power (no more than several kilowatts).

We plan to use as an RF source the multi-beam klystron KIU-273 with reversed permanent magnet focusing, operating at 5,712 MHz with maximum pulsed power 3.5 MW [2].

PARAMETERS OF THE ACCELERATING STRUCTURE

The basis of the accelerator is a bi-periodic accelerating structure with on-axis coupled cells, operating at the frequency of 5,712 MHz in the standing-wave mode, optimised for operation in a broad band of energies of the accelerating beam. The structure was developed earlier by Laboratory of Electron Accelerators MSU Ltd (LEA MSU) for the accelerator of the mobile cargo inspection system [3]. The distributions of the electric field of operating mode within the structure volume and along its axis are shown in Fig. 1(a) and 1(b), respectively.

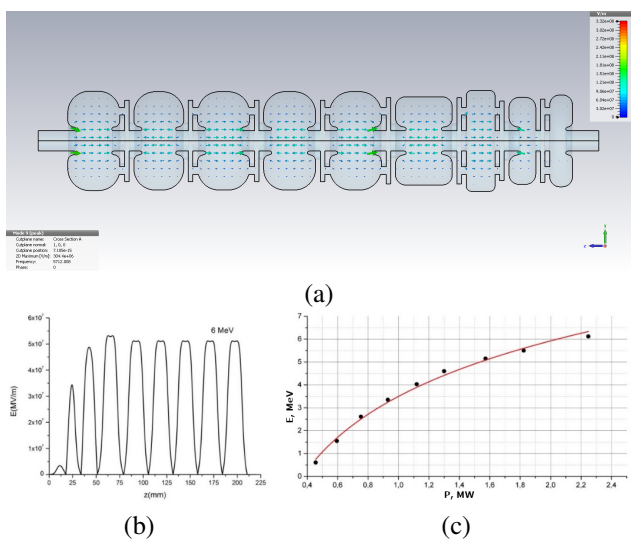


Figure 1: (a) Geometry of the accelerating structure with operating mode electric field distribution. (b) Distribution of the electric field along the axis. (c) Relationship between the output beam energy and the pulsed RF power loss in cavities walls.

* This material is based upon work supported by the Ministry of Education and Science of the Russian Federation, under Grant Agreement No. 14.582.21.0011, Grant Agreement Unique ID RFMEFI58217X0011.
† lub.ovch@yandex.ru

Content from this work may be used under the terms of the CC BY 3.0 licence (© 2018). Any distribution of this work must maintain attribution to the author(s), title of the work, publisher, and DOI.

ISBN: 978-3-95450-194-6 ISSN: 2226-0366 doi:10.18429/JACoW-LINAC2018-TUPO098

PROOF-OF-PRINCIPLE TESTS FOR SLIT-SCAN-BASED SLICE EMITTANCE MEASUREMENTS AT PITZ

R. Niemczyk*, H. Huck†, P. Boonpornprasert, Y. Chen, J. Good, M. Gross, I. Isaev, D. Kalantaryan, C. Koschitzki, M. Krasilnikov, X. Li, O. Lishilin, G. Loisch, D. Melkumyan, A. Oppelt, H. Qian, Y. Renier, C. Saisa-ard‡, F. Stephan, Q. Zhao§, DESY, 15738 Zeuthen, Germany
W. Hillert, University Hamburg, 22761 Hamburg, Germany

Abstract

Transverse slice emittance is one of the most important properties of high-brightness electron beams for free-electron lasers (FELs). The photo injector test facility at DESY in Zeuthen (PITZ) develops high-brightness electron sources for modern FELs. With a 23 MeV, 1 nC beam at PITZ the experimental slice emittance characterization with the quadrupole scan technique is complicated by strong space charge effects. Combining the slit scan technique with a transverse deflecting cavity (TDS) allows for time-resolved emittance measurements of such a space-charge-dominated beam. The first proof-of-principle results of slice emittance measurements at PITZ based on the 'TDS + slit scan'-technique are presented in this paper.

INTRODUCTION

At the Photo Injector Test facility at DESY in Zeuthen (PITZ) electron guns are developed and optimized for superconducting LINAC-based free-electron lasers (FELs) like FLASH and the European XFEL [1]. Besides gun development, plasma wakefield acceleration (PWFA) [2], accelerator-based THz generation [3] and electron diffraction [4] are also investigated at PITZ.

For FELs, emittance is one of the key parameters for the gain length [5]. Here, the properties of the central slices, i.e., the slices with the highest charges are important, since these slices will rather contribute to lasing than the low-charged head and tail of the bunch [6]. This motivates optimization of the photoinjector not only for projected, but also for slice emittance, especially since simulation results show that the optimum photoinjector setting for both might be different [7]. While a satisfying technique to measure slice emittance at intermediate electron energies exists [6], measurements of the slice emittance at low energies are heavily complicated by space charge forces. These lead to a deviation between the actual beam transport and the beam transport suggested by algorithms [7]. At PITZ, the standard technique to measure the projected emittance is the slit scan [8–10]. The information of the transverse slit position, together with the beamlet size, allows to reconstruct the transverse phase space, so that the normalized emittance can be calculated via

$$\epsilon_{n,x} = \beta\gamma\sqrt{\langle x^2\rangle\langle x'^2\rangle - \langle xx'\rangle^2}, \quad (1)$$

where $\beta = v/c$, with v the electron velocity, c the speed of light, γ the Lorentz factor and $\langle x^2\rangle$, $\langle x'^2\rangle$ and $\langle xx'\rangle$ the second-order beam moments. Employing an rf deflector (TDS) allows the measurement of the slice emittance. High-charge beams with low momenta are observed at photoinjector test facilities and energy recovery LINACs [11, 12], opening the demand for space-charge-resistive slice emittance diagnostics.

MEASUREMENT SET-UP

An overview of the PITZ beamline is given in Fig. 1. The electrons are generated with an UV laser at a Cs_2Te photocathode inside the rf gun, which accelerates the electrons to ~6 MeV. Up to 600 electron bunches are generated with a spacing of 1 µs inside a bunch train and a bunch train repetition rate of 10 Hz [1]. A booster further accelerates the electrons to an energy of ~23 MeV. A normalized emittance of the electron beam down to 0.7 µm for bunches with 1 nC has been obtained [1].

The PITZ beamline is equipped with three emittance measurement system (EMSY) stations, at which a slit mask is located. The mask has slits with 10 µm and 50 µm opening, while only the 10 µm-wide slit is used for measurement of the projected emittance at high charge [13]. During the here presented measurement the 50 µm-wide slit has been used to get a high signal-to-noise ration for the streaked beam. Two EMSY stations are located upstream the TDS, while the third one is upstream the dispersive section HEDA2. For the first slice emittance measurements the second EMSY station has been chosen as slit position to minimize the distance

* raffael.niemczyk@desy.de
† holger.huck@desy.de
‡ On leave from Chiang Mai University, Chiang Mai, Thailand
§ On leave from IMP/CAS, Lanzhou, China

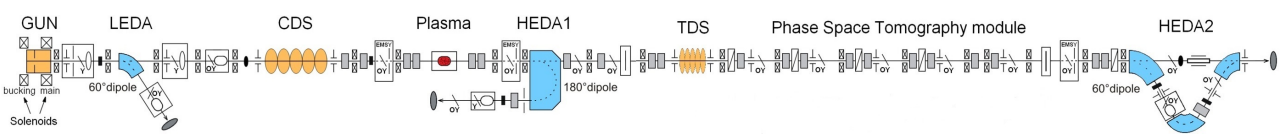


Figure 1: Schematic of the PITZ beamline. The electrons travel from left to right. The plasma cell was not mounted during the slice emittance measurement.

Content from this work may be used under the terms of the CC BY 3.0 licence (© 2018). Any distribution of this work must maintain attribution to the author(s), title of the work, publisher, and DOI.

ISBN: 978-3-95450-194-6 ISSN: 2226-0366 doi:10.18429/JACoW-LINAC2018-TUPO101

DESIGN OF PRACTICAL HSC TYPE INJECTOR FOR CANCER THERAPY

Chaochao Xing†, Liang Lu, Lei Yang[1], Tao He[1], Chenxing Li, Jia Li[1], Qianxu Xia[1], Zhichao Gao[1],
Institute of Modern Physics, Chinese Academy of Sciences, Lanzhou 730000, China
[1]also at University of Chinese Academy of Sciences, Beijing 100049, China

Abstract

We provided a compact linac injector, HSC (Hybrid single cavity), for cancer therapy. The HSC, operated in TE_{111} mode [1], consists of RFQ section and DTL section. This compact linac injector, running in frequency of 100 MHz, accelerates C^{6+} beams with 20 mA from 20keV/u up to 4 MeV/u [2]. The total length of HSC is designed less than 4 meters. We used RGQGen and PIMLOC to achieve the aims. More details will be given in the next parts.

INTRODUCTION

According to investigations, there are 6 people per minute suffering from cancer in china. Therefore, accelerators in medical applications have a great prospect. Unfortunately, the system of cancer therapy has a complex control system and huge injector. The factor resists the developments of accelerators in medical applications. The new type injector, HSC, has the ability to directly accelerate the high intensity C^{6+} ion beams. Compared with traditional types, HSC adopts DPIS (direct plasma injection scheme), which could easily supply enough C^{6+}ions to the linac. Secondly, RFQ section and DTL section share the operating system and feed system.

BEAM DYNAMICS

RFQ Design and DT Design

The section of RFQ, 4 rod IH type, was designed to accelerate C^{6+}ions to 0.6 MeV/u from 0.02 MeV/u. This RFQ section includes 90 cells. And the total length of RFQ is 1050 mm. The main parameters are listed in Fig. 1 and Table 1. Fig .2 gives the transmission efficiency, which almost over 95%, at last cell.

Table 1: The Main Parameters of the RFQ

Parameters	Value
Voltage	85 kV
B	7.1→9.76
m	1→2.11
ϕ	-90→-26 deg
Input energy	0.02 MeV/u
Output energy	0.6 MeV/u

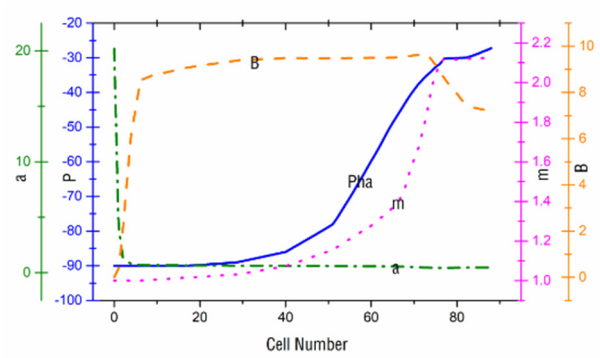


Figure 1: The dynamics parameters of RFQ design.

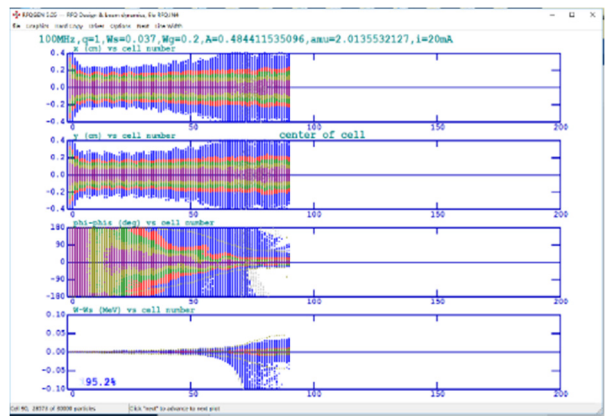


Figure 2: Transmission efficiency at last cell.

The output of RFQ are adopted convergent design for following DT injection. Therefore, the section of DT accelerates C^{6+}ions with 20 mA to 4 MeV/u from 0.6MeV/u. We used the PIMLOC to design the DT section. The most important theory in DT section is APF, Alternative Phase Focus. An APF linac is a modified version of usual drift tube linacs (DTL) and can achieve three-dimensional focusing without the installation of quadrupole lenses into the drift tubes. The phase in each gap was given in Fig. 3.

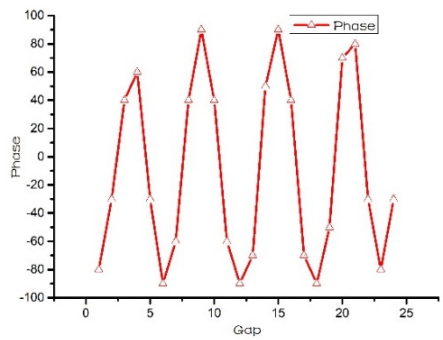


Figure 3: The phase in each gap.

†ccxing@impcas.ac.cn

Content from this work may be used under the terms of the CC BY 3.0 licence (© 2018). Any distribution of this work must maintain attribution to the author(s), title of the work, publisher, and DOI.

ISBN: 978-3-95450-194-6 ISSN: 2226-0366 doi:10.18429/JACoW-LINAC2018-TUPO106

MATHEMATICAL PRINCIPLE AND NUMERICAL RECONSTRUCTION IN REAL SPACE MEASUREMENT WITH A ROTATING BPM*

Peiyong Jiang†, Yuan He, Zhijun Wang
Institute of Modern Physics, Chinese Academy of Sciences, Lanzhou, China

Abstract

It is difficult to measure beam profiles and monitor the beam during beam supply for high intensity high power accelerators. Based on the button pick-ups, the mathematical principle of a rotating BPM is proposed. SVD method is used to reconstruct the beam in x-y real space, and the basic parameters used in beam reconstruction are argued. The beam distribution in x-y real space is reconstructed well and compared to the reference beam. The beam reconstruction is sensitive to the electrode radius. The meshing and the grid numbers in the solution window have an import effect on the beam reconstruction.

INTRODUCTION

It is difficult to measure beam profiles for high intensity high power accelerators. The wire scanner system is often used to measure beam profiles [1]. However, the stable operation of wire scanners has much to do with beam power [2]. The beam current has to decrease below a power limit in CIADS project to protect the wire scanners, bringing the difference in x-y real space between the low intensity and the high intensity beams. Besides, the slit and Faraday cup are used to measure beam profiles.

The two methods are invasive diagnostics, which cannot be applied to the high power accelerators with the high requirement of continuity in operation such as CIADS project [3]. Meanwhile, owing to the high requirement of stability and security of CIADS, it is necessary to monitor the beam including the beam profiles dynamically and to adjust the machine parameters properly. Thus, there is a strong need to use a non-invasive beam diagnostic component to measure beam profiles during beam supply, based on which a rotating BPM is proposed mathematically.

BPM PRINCIPLE

BPM is widely used in accelerators to measure the beam orbit, beam phase and beam emittance [4,5,6]. Button pick-ups, shoe box pick-ups and stripline pick-up are the three common kinds of BPM [7]. Figure 1 shows the theory of button pick-ups. There are 4 electrodes in the top, bottom, left and right of the pipe respectively. The electrodes induct the current while a charged beam line pass through the pipe. Considering a beam with current I(r,ϕ) in a straight wire of infinite length in a polar coordinate system, the current density j(a,θ,r, ϕ) on the pipe boundary induced by the straight wire current and its mirror current is

$$j(a,\theta,r,\phi)=\frac{I(r,\phi)}{2\pi a}\frac{a^2-r^2}{a^2+r^2-2\cos(\phi-\theta)} \qquad (1)$$

where (a,θ) is an arbitrary point on the pipe boundary in a polar coordinate system , while a is the pipe radius and θ is the angle pointed to the point. (r,ϕ) is an arbitrary point in the pipe while r is the distance between the beam and the pipe center, and ϕ is the angle pointed to the beam.

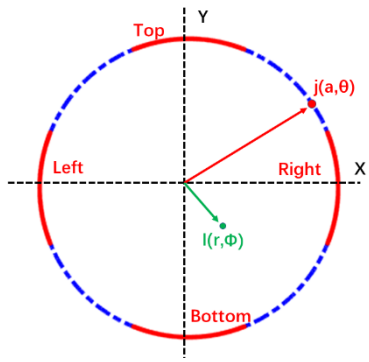


Figure 1: The theory of button pick-ups. The blue dashed circle is the pipe boundary. The red curves at top, bottom, left and right are the BPM electrodes respectively. I(r,ϕ) is the current of a straight wire of infinite length, and j(a,θ,r, ϕ) is the induced current at the point (a,θ) in a polar coordinate system.

As for a beam with a cross section, the total induced current J on the electrode with a flare angle β is an integral as follows:

$$J(a)=\int_{-\beta/2}^{\beta/2}\int\int j(a,\theta,r,\phi)drd\phi d\theta \qquad (2)$$

The integral J changes to be a product while beta is small:

$$J(a)=\beta\int\int j(a,\theta,r,\phi)drd\phi \qquad (3)$$

and the average induced current B is written as:

$$B(a)=\frac{J}{\beta}=\int\int j(a,\theta,r,\phi)drd\phi \qquad (4)$$

By substituting Eq.(1) into Eq.(4), the discrete form of Eq.(4) is obtained:

$$B=M\cdot I \qquad (5)$$

Where I and B are column vectors, and the lengths of I and B are corresponding to the number of straight wires of beam current and the number of BPM electrodes respectively. M is a matrix with

$$M_{b,i}=\frac{1}{2\pi a_b}\frac{{a_b}^2-{r_i}^2}{{a_b}^2+{r_i}^2-2\cos(\phi_i-\theta_b)} \qquad (6)$$

where b is the b[th] electrode, and the i is the i[th] straight wire of beam current.

RECONSTRUCTION

Mathematically, the reconstruction is to solve Eq.(5). However, the matrix is unknown in this equation. Thus during the solving, a solution window has to be assumed,

* Work supported by NSFC (Grant NO. 11605261)
† jiangpeiyong@impcas.ac.cn

Content from this work may be used under the terms of the CC BY 3.0 licence (© 2018). Any distribution of this work must maintain attribution to the author(s), title of the work, publisher, and DOI.

ISBN: 978-3-95450-194-6 ISSN: 2226-0366 doi:10.18429/JACoW-LINAC2018-TUPO109

ELECTRON CLOUD ESTIMATES FOR THE JEFFERSON LAB EIC

K. E. Deitrick*, V. S. Morozov, T. Satogata,
Thomas Jefferson National Accelerator Facility, Newport News, VA 23606, USA

Abstract

In this work, we present preliminary estimates for electron cloud build-up and saturation for the ion ring of the Jefferson Laboratory Electron-Ion Collider (JLEIC) currently under development. Using the baseline ion ring design, we study the impact of various operational parameters on the behavior of the electron cloud for a 100 GeV proton beam, including estimated tune shifts.

INTRODUCTION

The Jefferson Lab Electron-Ion Collider (JLEIC) [1], shown in Fig. 1, currently under development anticipates a high luminosity - which requires careful consideration of various collective effects, including electron cloud. The build up of the electron cloud in an ion machines is seeded by primary electrons, which typically originate from three causes - photoelectrons, ionization of residual gas, and electrons produced by collisions between the beam pipe and stray particles. This paper serves as a current evaluation of the severity of electron cloud in the current JLEIC design, using the simulation code PyECLOUD [2].

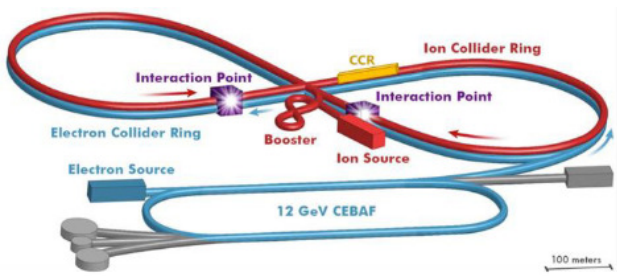


Figure 1: A conceptual layout of JLEIC.

SIMULATION SET UP

Using PyECLOUD, it is possible to observe the density of electrons over time for a given set of proton beam, vacuum, and secondary electron yield (SEY) parameters, which are given in Table 1. The SEY settings assume that the beam pipe is made from stainless steel [4]. These parameters were used to simulate the electron density for a number of cases, including dipoles, drifts, quadrupoles, and sextupoles. These cases are summarized in Table 2. For the quadrupoles and sextupoles, the highest field gradient outside of the interaction region (IR) magnets is used - these are not representative of the average field for these elements.

Table 1: Proton Beam and Vacuum Parameters Used in the simulations

Parameter	Symbol (Unit)	Value
Beam energy	E_b (GeV)	100
Circumference	C (m)	2230
Collision frequency	f_c (MHz)	476
Beam pipe cross-section	-	Circular [3]
Beam pipe radius	r_b (mm)	40 [3]
Number of bunches per train	K_B	1856
Bunch spacing	s_b (ns)	2.1
Bunch population	N_p (10^{10})	0.98
Bunch length	σ_l (cm)	1
Bunch profile	-	Gaussian
Empty bunches between trains	-	126
Normalized emittance	$\epsilon_x^N, \epsilon_y^N$ (μm-rad)	0.5, 0.1
Residual gas pressure	P (nTorr)	5
Temperature	T (K)	4.5
Peak SEY	$\delta_{max} \equiv \delta(E_{max})$	2.25
Ionization cross-section	σ_i (Mbarns)	2
Energy at peak SEY	E_{max} (eV)	300

Table 2: Magnetic Properties for Simulations

Element	Absolute Field Strength	Unit
Drift	-	-
Dipole	3.06	T
Quadrupole	85	T/m
Sextupole	450	T/m^2

RESULTS FOR DIFFERENT ELEMENTS

The electron cloud density for each magnetic element is shown in Fig. 2 over the time span of a single bunch train, which contains 1856 bunches separated by 2.1 ns. Simulations have been performed for multiple bunch trains in dipoles and drifts, separated by 126 empty buckets, and the electron cloud density behavior remains consistent despite the bunch train number - the electron cloud reaches saturation before the end of the bunch train and decreases in the gap between trains. For certain elements, like the sextupole, the preceding bunch train will mean that successive trains reach saturation more quickly. This behavior can be seen

* deitrick@jlab.org

Content from this work may be used under the terms of the CC BY 3.0 licence (© 2018). Any distribution of this work must maintain attribution to the author(s), title of the work, publisher, and DOI.

ISBN: 978-3-95450-194-6 ISSN: 2226-0366 doi:10.18429/JACoW-LINAC2018-TUPO112

CALCULATION OF ELECTRON BEAM DYNAMICS IN FOUR ACCELERATING STATIONS FOR JINR ELECTRON ACCELERATOR LINAC-200

A. S. Sledneva†, V. S. Aleksandrov, V. V. Kobets,
Joint Institute for Nuclear Research, Dubna, Moscow Region, Russian Federation

Abstract

In the Joint Institute for Nuclear Research a Test Stand with an electron beam generated by the linear accelerator LINAC-200 with the energy up to 200 MeV is being constructed to investigate properties of accelerating and semiconducting structures for advanced detectors, a radiation resistance of detectors based on gallium arsenide semiconductor, to study a free electron laser and to do other applied work. The technical characteristics of the LINAC-200 accelerator make it possible to create an advanced system of test beams for scientific and methodological studies of detectors on its basis.

Four accelerating stations with maximum beam energy up to 200 MeV are put into operation. The work is being carried out for experiments with electron test beams with energy up to 800 MeV

This work presents the calculation results of the magnetic field of the focusing solenoidal system and electron beam dynamics in accelerating stations A00 – A04. In addition, the results on the formation of the electron beam with optimal parameters to be captured in further accelerating sections.

DESCRIPTION OF LINAC-200

Linear electron accelerator LINAC-200 is created on the basis of the accelerator MEA (Medium Energy Accelerator), brought from Dutch National Institute for Subatomic Physics to Dubna in 1999-2000 [1].

Linac-200 consists of 4 accelerating stations A01 – A04 with the maximum energy of about 200 MeV.

Injection station A00 consists of injector, prebuncher and buncher. The buncher is a short acceleration section with the length 1.654 m.

The focusing and transporting systems along the accelerator path includes solenoids, quadruples and beam correction elements. The buncher and short acceleration sections (A0BB, A1AA, B2AA) with the length 3.67 m have a constant solenoidal magnetic field from 100 to 500 Gauss generated by lenses (L1, L2) and solenoidal. After exiting the gun, the beam is picked up by a thin solenoidal magnetic lens 1, which focuses the beam on the chopper collimator. The second thin solenoidal lens focuses the beam on the input to the buncher. The long sections (A3A, B4A, B5A, A6A) with the length 7.35 m have no magnetic field, it contains quadruples Q1 and Q2 (Fig. 1). All quadruple lenses are identical. The internal radius of the channel is 2.5 cm, the field gradient is 7.6 kGauss/m.

† sledneva@jinr.ru

THE RESULTS OF CALCULATIONS ON THE FORMARTION OF THE MAGNETIC FIELD

For calculations on the formation of the magnetic field was used POISSON program [2]. The layout of the magnetic system for accelerating stations A00 – A02 is illustrated In Figure 2. Figure 3 shows a distribution of longitudinal and radial components of the magnetic field in accelerating stations A00 – A02.

Summarizing the calculation results, a Table 1 with the optimum values of the magnetic field was made.

The obtained results are used for further beam dynamics calculations of the electron beam.

Table 1: Optimal magnetic field for different elements of the accelerator

Element	B_{max}, Gauss
Lens 1 (L1)	200
Lens 2 (L2)	100
Buncher	200
A0BB	300
A1AA	400
B2AA	500

THE RESULTS OF ELECTRON BEAM DYNAMICS CALCULATIONS USING PARMELA PROGRAM [3]

The initial distribution of the particles was determined according to the Vladimirsky-Kapchinskii. The number of particles: 10 – 1000.

The goal of a prebuncher and a buncher is to compress the length of the bunch to a value suitable for capturing in the first accelerating section A0BB. Preference was given to variants with phases with a maximum energy of the high-frequency field in the section A0BB. The final choice of the optimal variant was made according to the results of the analysis for the maximum number of particles in the required phase range.

Beam cross-sections along the accelerator are illustrated in Figure 4 (sizes are in cm). Figure 5 shows beam spot (on the left) and energy-phase distribution (on the right). Energy gain along the LINAC-200 is demonstrated in Figure 6.

Content from this work may be used under the terms of the CC BY 3.0 licence (© 2018). Any distribution of this work must maintain attribution to the author(s), title of the work, publisher, and DOI.

ISBN: 978-3-95450-194-6 ISSN: 2226-0366 doi:10.18429/JACoW-LINAC2018-TUPO113

BEAM DYNAMICS STUDIES THROUGH DIELECTRIC THZ ACCELERATING STRUCTURES

R. Apsimon*, G. Burt, , A. Healy, S. Jamison, Lancaster University, Bailrigg, UK
A. Latina, CERN, Geneva, Switzerland
R. B. Appleby, E. Smith, University of Manchester, UK

Abstract

As conventional RF accelerating schemes approach the physical limit of accelerating gradient, the accelerator community is increasingly looking at novel accelerating techniques to overcome these limitations. Moving from the RF to the THz frequency range, higher acceleration gradients of high energy beams can be achieved in compact structures. Beam dynamics studies are crucial as part of the design of novel accelerating structures to maximise the output beam current as well as the accelerating gradient. In this paper we present beam dynamics simulations through dielectric lined waveguide structures using novel techniques to simulate broadband signals for particle tracking studies in RF-Track. The beam parameters through the structure are optimised and we study the dynamics of general broadband accelerating structures.

INTRODUCTION

As conventional RF accelerating schemes approach the physical limit of accelerating gradient, the accelerator community is increasingly looking at novel accelerating techniques in the THz regime to overcome these limitations. Dielectric lined waveguides (DLWs) (Figure 1)are one such accelerating technique, favoured for its ability to produce high field gradients as well as its ease of fabrication.

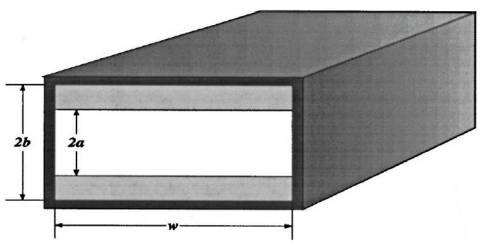


Figure 1: Diagram of a dielectric lined waveguide [1].

Due to the relative simplicity of the physical system for a DLW, a full analytical solution for the electromagnetic fields can be obtained [1]. In this paper, we only consider the LSM_{11} accelerating mode. LSM modes are equivalent to TM modes in a waveguide without any dielectric, but the LSM mode couples to the TM modes in both the vacuum and dielectric regions. If we define a as the half-height of the vacuum region, b as the half-height of the waveguide and w as the full width of the waveguide, as shown in Figure 1, then the dispersion relation for the LSM_{mn} mode is given as

$$k_{mn}^{(1)} \sin\left[k_{mn}^{(1)}(b-a)\right] \sin k_{mn}^{(0)} a - \varepsilon_r k_{mn}^{(1)} \cos\left[k_{mn}^{(1)}(b-a)\right] \cos k_{mn}^{(0)} a = 0 \quad , \tag{1}$$

where

$$k_{mn}^{(0)} = \sqrt{\left(\frac{\omega}{c}\right)^2 - \left(\frac{m\pi}{w}\right)^2 - \beta_{mn}^2}$$
$$k_{mn}^{(1)} = \sqrt{\varepsilon_r \left(\frac{\omega}{c}\right)^2 - \left(\frac{m\pi}{w}\right)^2 - \beta_{mn}^2} \quad . \tag{2}$$

This dispersion relation is a transcendental equation that needs to be evaluated numerically (Figure 2a), but provides a functional relationship between ω and β_{mn}, from which we can obtain the phase velocity, $v_p = \frac{\omega}{\beta_{mn}}$, and group velocity, $v_g = \frac{d\omega}{d\beta_{mn}}$ (Figure 2b). The electric and magnetic fields in the frequency domain within the vacuum region of the DLW respectively are given as

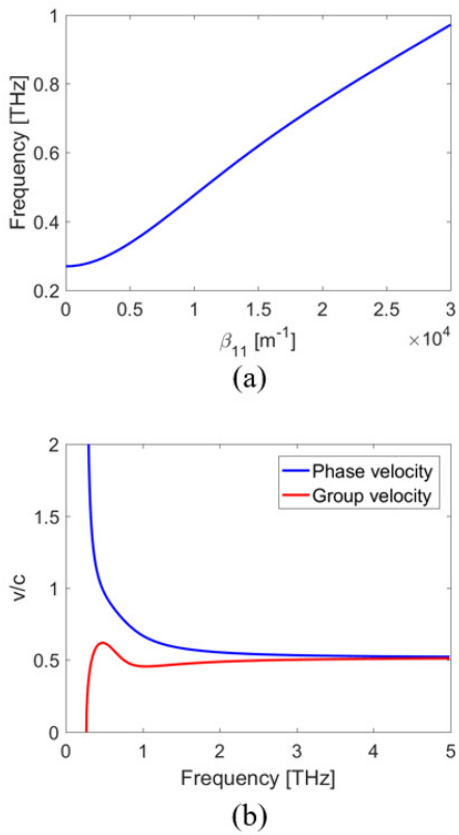


Figure 2: Dispersion relation (a) and phase (blue) and group (red) velocity (b) for a DLW for the LSM_{11} mode with a = 250 µm, b = 300 µm and w = 1200 µm.

* r.apsimon@lancaster.ac.uk

Content from this work may be used under the terms of the CC BY 3.0 licence (© 2018). Any distribution of this work must maintain attribution to the author(s), title of the work, publisher, and DOI.

ISBN: 978-3-95450-194-6 ISSN: 2226-0366 doi:10.18429/JACoW-LINAC2018-TUPO114

BEAM DYNAMICS STUDIES FOR THE CSNS DTL DUE TO A QUADRUPOLE FAULT

J. Peng†, Y.W. An, M.Y. Huang, L.S. Huang, Y. Li, M.T. Li, Z.P. Li, Y.D. Liu, X.H. Lu, X.B Luo
S.Y. Xu, Y. Yuan, S. Wang, S.N. Fu
Dongguan Campus, Institute of High Energy Physics, Dongguan, 523803 China

Abstract

The China Spallation Neutron Source(CSNS) accelerator systems is designed to deliver a 1.6GeV, 100kW proton beam to a solid metal target for neutron scattering research. It consists of a 50keV H- Ion Source, a 3 MeV Radio Frequency Quadrupole (RFQ), an 80MeV Drift Tube Linac (DTL), and a 1.6 GeV Rapid-cycling Synchrotron (RCS). The DTL consists of four tanks. In 2017, three of four tanks have been commissioned successfully, and beam has been accelerated to 61 MeV with nearly 100% transmission. However, in July 2017, one quadrupole contained in the drift tube was found fault, the beam transmission decreased to 80%. A new lattice has been designed and the 100% transmission has recovered. In January 2018, the last tank of the DTL has been commissioned and accelerated the H- beam to the design energy of 80MeV for the first time. The commissioning progress and the measurement results before and after lattice adjustment will be presented.

INTRODUCTION

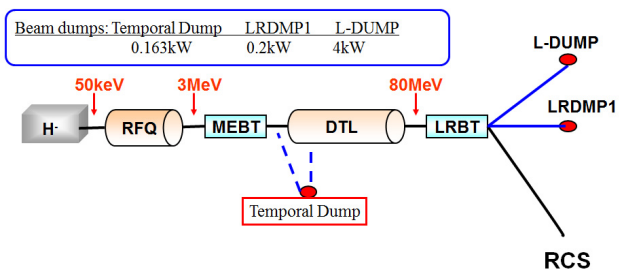


Figure 1: CSNS Linac layout.

The layout of the CSNS Linac is shown in Fig. 1. Details of the Linac design can be found in [1]. The DTL consists of four tanks and accelerates H- beam from 3MeV to 80MeV. Each tank is fed by a 324MHz, 3MW klystron. From 2016 to 2018, the DTL has been commissioned tank by tank. In 2017，since only three klystrons were available, DTL1to3 have been fed and the beam was successfully accelerated to 61 MeV [2]. The last tank has been used as a beam line. Figure 2 shows the CT signals along the Linac. Beam transmission from the DTL to the LRBT (Linac to RCS Beam Transport) was nearly 100%. In May 2017, the vacuum in DTL1 became worse. And one month later, the beam commissioning was interrupted for the DTL vacuum checking. We found that the cooling channel of the EMQ13 in the DTL1 was leaking [3]. So we had to turn off the EMQ13 which made the beam transmission decrease to about 80%. Due to the tough arrangement of the commissioning timetable, beam commissioning has continued. A temporary lattice was used, in which the EMQ13 and EMQ 14 were turned off and the other quadrupoles' setting remained unchangeable. The beam transmission has been fluctuating from 96% to 98% during commissioning. In November 2017, we had two month interval for testing the klystron and RF conditioning of the DTL4. A new lattice for the DTL has been designed. According to this new lattice, every 2 of 4 quadrupoles after the EMQ13 had to exchange the polarities by modifying the cable connection mode. In January 2018, the last tank of the DTL has been commissioned and the H- beam to the design energy of 80MeV for the first time. With the new transverse focusing lattice, the beam transmission has recovered to 100%. Figure3 shows the CT signals along the linac with the new lattice.

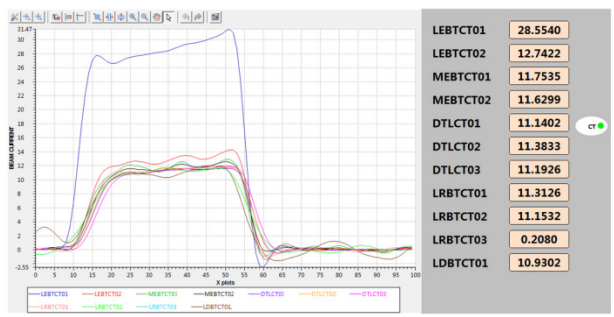


Figure 2: Current transform signals along the Linac with the old lattice.

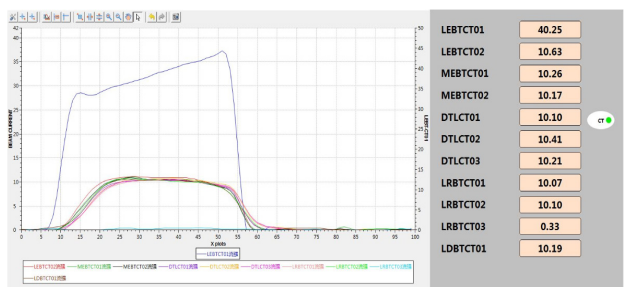


Figure 3: Current Transform signals along the Linac with the new lattice.

Old Lattice

The DTL uses Electrical Magnet Quadrupoles (EMQ) for transverse focusing and the focusing is done in a

*This work is supported by National Natural Science Foundation of China (11505101).
**E-mail:pengjun@ihep.ac.cn

Content from this work may be used under the terms of the CC BY 3.0 licence (© 2018). Any distribution of this work must maintain attribution to the author(s), title of the work, publisher, and DOI.

ISBN: 978-3-95450-194-6 ISSN: 2226-0366 doi:10.18429/JACoW-LINAC2018-TUPO115

BEAM PARAMETERS MEASUREMENT AND CORRECTION IN CSNS LINAC

Z.P. Li, J. Peng, Y. Li, Dongguan, 523803, China

Abstract

All the beam parameters of China Spallation Neutron Source (CSNS) linac had achieved the acceptance goals in January 2018 after a 2-year commissioning. Parameters of the H- beam were carefully studied and corrected. Beam energy was measured and the energy dispersion are reduced. Transverse emittance are obtained by different tools and methods. Linear optics measurements and corrections were carried out under varied beam energies and peak intensities.

INTRODUCTION

The linear accelerator of CSNS [1] mainly consists of a 50KeV H- ion source, a four-vane radio frequency quadrupole accelerator(RFQ)and a four-tank drift tube linac(DTL) working at RF frequency of 324 MHz. The low energy beam transport line (LEBT) and medium energy beam transport line (MEBT) connect and match the above three accelerating sections. The linac to ring beam transport line (LRBT) which transports the beam from DTL to the Rapid-cycling Synchrotron (RCS) reserves the space for linac upgrading in the further. The total length of the straight section is 200m. The layout of the CSNS linac is shown in Fig. 1.

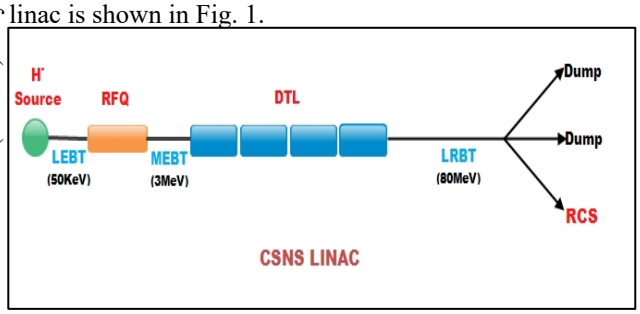


Figure 1: The CSNS Linac Layout.

The beam commissioning of linac started in April 2015 and was separated into 4 runs due to DTL tank installations and klystron failures. By January 2018, the beam peak current intensity reached 15mA and the beam energy achieved the design value of 80 MeV. The overall transport efficiency of DTL reached over 97%.

Beam parameters of CSNS linac were carefully measured and corrected during the commissioning. In this paper, the main beam parameters measurement and correction results will be displayed and discussed. The content includes: beam current intensity measurement and transport efficiency optimization, beam orbit correction, transverse emittance and twiss parameters measuring and matching, beam kinetic energy and momentum spread measurements .

BEAM PARAMETERS MEASUREMENT AND CORRECTION

Beam Current Intensity

The current beam power of CSNS linac is 1 KW with the peak current of 10 to 15 mA, the pulse width of 130 us, and the repetition rate of 25 Hz. Current transformers (CT) in linac beam line monitor the beam intensity and the transport efficiency. Figure 2 shows a set of CT signals along the linac.

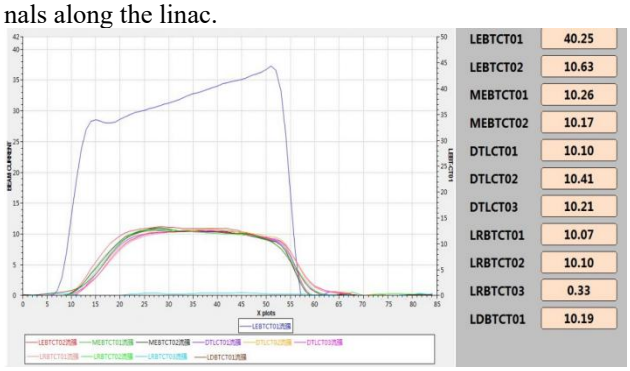


Figure 2: Current Transform Signals of CSNS Linac.

The transport efficiency is one of the most important parameters to be optimized in the linac beam commissioning. By beam orbit correction and operations of beam matching, transport efficiency is greatly improved thus the beam loss satisfies the design standard. The overall transport efficiency of DTL reached over 97%, there is still work to be done for further improvement.

Beam Orbit

Beam orbit is usually the first parameter to measure and correct in beam commissioning. The beam orbit distortion should be as small and as smooth as possible along the beam line, especially for CSNS linac with small aperture. Orbit correction application in XAL was adopted for the case of orbit manipulation in CSNS linac.

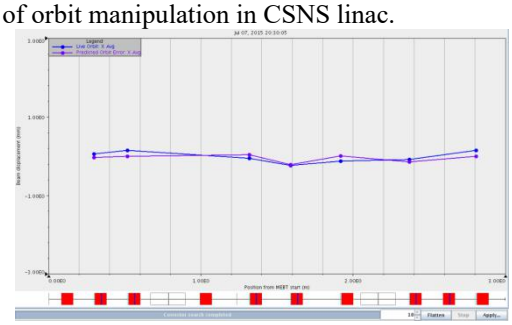


Figure 3: Beam Orbit of MEBT after Orbit Correction.

The Fig. 3 is the result of orbit correction for MEBT. The beam orbit of MEBT can be corrected from 1.5 mm

Content from this work may be used under the terms of the CC BY 3.0 licence (© 2018). Any distribution of this work must maintain attribution to the author(s), title of the work, publisher, and DOI.

ISBN: 978-3-95450-194-6 ISSN: 2226-0366 doi:10.18429/JACoW-LINAC2018-TUPO116

PARTICLE DYNAMICS OPTIMIZATION IN DTL

I. S. Skudnova†, Saint Petersburg University, 198504 Saint Petersburg, Russia

Abstract

The research concerns ion dynamics in linear accelerators with drift tubes (DTL). Permanent quadrupole magnets are placed inside some of the drift tubes. Frequency of the field is 432 MHz. Electromagnetic fields and particle dynamics in the cavity are calculated using Comsol Multiphysics software. The input energy of the beam is 6 MeV, output 10 MeV. Initial beam is assumed to come from Radio Frequency Quadrupole accelerator (RFQ). The considered parameters are drift tubes radii, cavity diameter, gradient of the magnetic field from quadrupoles inside drift tubes and focusing lattice. Effectiveness is estimated by the emittance growth.

INTRODUCTION

The initial part of the injection system of a large ion accelerator often consists of injector, radio-frequency quadrupole (RFQ), drift tube linear accelerator (DTL). This structure is used, for instance, in the Spallation neutron source (SNS) facility in USA [1]. In this study we consider a similar tank with 22 drift tubes mounted inside (Fig.1).

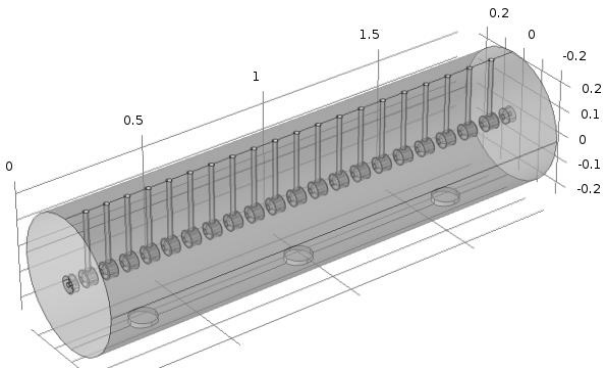


Figure 1: Tank model.

The parameters of the structure are listed in Table 1.

Table 1: DTL Parameters

Parameter	Value
Frequency	432 MHz
Particles	H^-
Input Energy	6 MeV
Output Energy	10 MeV
Cell length	βλ
Gap coefficient (L/L_{gap})	0.25
Drift tube number	22
Tank length	1.863 m
Channel diameter	16 mm

Tube walls are trapeze-shape in section with rounded corners to avoid breakdown. Focusing is provided by permanent magnet quadrupoles, placed inside some drift tubes. Some drift tubes are left empty without magnets. The configuration of the focusing lattice is discussed below. Magnets can be magnetized in two layouts which create focusing and defocusing field. 3 slug tuners are placed inside the cavity to adjust radio frequency.

DESIGN

The model of the tank is created using Comsol Multiphysics - a general-purpose software platform, based on advanced numerical methods, for modeling and simulating physics-based problems [2].

Field Distribution

In the model with preliminary calculated parameters, the first thing to adjust was a resonance frequency of the electric field. The working frequency is 432 MHz. To gain this value the following parameters were altered: cavity diameter, inner and outer diameter of drift tubes, slug tuners.

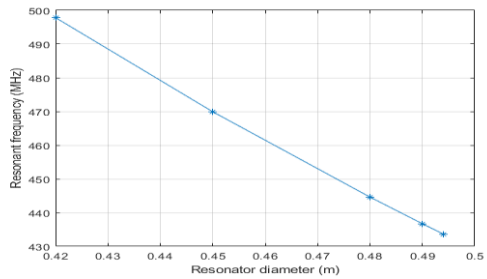


Figure 2: Dependence of the cavity resonant frequency on the cavity diameter.

At first, cavity diameter was estimated (Fig. 2). For the desired value of frequency the appropriate diameter was calculated as 49.6 cm.

To adjust the resonant frequency by means of drift tube diameter at first a constant value of inner and outer diameter was used. But the results were not satisfying. Later the drift tubes were divided into three parts of 11 drift tubes with increasing outer diameter value. Thus, the inner diameter of drift tubes is constant – 16 mm, and outer diameter is 58 mm for first part, 60 mm for second and 62 for third.

The calculation in Comsol Multiphysics of the resonant frequency of the structure uses finite element method. For this purpose the mesh of around 95000 tetrahedral elements was built. While solving eigenfrequency problem Comsol solver provide a number of eigenfrequencies nearest to the specified value. As for the case of desired 432 MHz nearest values were 422.57 MHz and 436 MHz. The gap between these values seems to be tolerable enough.

Three slug tuners are mounted inside, each one of 10 cm diameter. To make the field distribution more uniform slug tuners are set as 1 cm, 1 cm and 3 cm height. After adjusting cavity diameter, drift tubes radii and slug tuners, the

† email address st016313@student.spbu.ru.

Content from this work may be used under the terms of the CC BY 3.0 licence (© 2018). Any distribution of this work must maintain attribution to the author(s), title of the work, publisher, and DOI.

ISBN: 978-3-95450-194-6 ISSN: 2226-0366 doi:10.18429/JACoW-LINAC2018-TUPO119

A DIAGNOSTICS BOX FOR THE LINEAR ACCELERATOR OF INSTITUTE FOR RESEARCH IN FUNDAMENTAL SCIENCES (IPM)

Sh. Sanaye Hajari†, S. Ahmadiannamin, M. Bahrami, H. Behnamian, S. Kasaei, H. Shaker, School of Particles and Accelerators, Institute for Research in Fundamental Sciences (IPM), Tehran, Iran
F. Ghasemi, Nuclear Science and Technology Research Institute (NSTRI), Tehran, Iran

Abstract

The IPM linac is an 8 MeV (up gradable to 11 MeV) electron linear accelerator under development at Institute for Research in Fundamental Sciences, Tehran, Iran. The design and construction of the linac is nearly finished and it is in the commissioning stage. The commissioning is planned in several phase of different energy ranging from 50 keV to 8 MeV. At each phase, appropriate diagnostics is required in order to investigate the linac performance. A diagnostics box including a scintillator view screen, a dipole magnet, and a focusing solenoid is designed to diagnose the beam longitudinal and transverse parameters in wide range of energy. These parameters are the beam transverse profile, size, position, emittance and the energy spectrum.

INTRODUCTION

The IPM linac is an electron linear accelerator with an energy and current up to 8 MeV and 10 mA, respectively. The machine is developed at the Institute for Research in Fundamental Sciences, Tehran, Iran. Labled as Iran's first linear accelerator project, nearly all the components of the linac is designed and constructed within the country, in particular, the RF amplifier system (klystron and its modulator), RF cavities, magnets and beam diagnostics systems. The main aim of this research project is to provide the scientific foundations for the future accelerator projects at IPM.

The linac consists of a thermionic electron gun followed by a pre-buncher, a travelling wave (TW) tapered phase velocity buncher and two constant impedance TW accelerating tube (see Fig.1). The TW tubes are connected together via appropriate flanges and fed with a 2 MW RF power. The tubes are embedded in solenoidal magnetic fields for the focusing. The beam energy at the end of electron gun, TW buncher, first and second tube is 50 keV, 1.4 MeV, 4.8 MeV and 8 MeV, respectively. The design of the different parts of the linac is described in [1-3] and the construction process in [4-6]. The beam parameters at the end of linac are listed in Table 1.

The construction of the linac is nearly finished and it is in the commissioning stage. The commissioning is foreseen in phases of different energies – up to the end of pre-buncher, TW buncher, first and second accelerating tubes. At each phase appropriate beam diagnostics is demanded in order to investigate the linac performance. The parameters to be measured are the beam current, the transverse beam profile, size, divergence, emittance and the energy spectrum. In order to diagnose the mentioned parameter in a relatively large range of energy a flexible diagnostics system is required. For this purpose, according to Fig. 2 a diagnostics box has been designed based on a focusing solenoid and a dipole magnet followed by a movable scintillator view screen. Such an integrated diagnostics box is capable to measure the beam transverse parameters and the energy spectrum of the beam via the beam profile measurement when the dipole magnet is off and on, respectively. At each phase of the commissioning, the diagnostics box will be installed at the end of the structure. In the next sections we first describe the beam profile monitor system then we will present how the beam transverse parameters and its energy spectrum can be extracted from the transverse profile. Special attention has been paid to the resolution of the measurement. For each parameter the resolution of the measurement has been calculated and the corresponding diagnostics system has been designed with the aim of providing the best resolution in the whole range of the energy of interest.

Table 1: Beam Parameters at the End of the Linac

Parameter	Value
Beam energy	8 MeV
Beam current (peak)	10 mA
Rms energy spread	0.23 MeV
Rms bunch length	2.3 mm
Normalised emittance	3.8 mm-mrad

BEAM PROFILE MONITOR SYSTEM

The view screen consists of a 3 cm × 3 cm YAG:Ce scintillator of 30 μm thickness on an aluminium substrate. The substrate ensures the heat and charge transfer. The substrate as well can be connected to an electronics readout system to be used as a Faraday cup for the beam current measurement. The scintillator view screen should be placed at a 45 degree angle and the visible photons are detected with an optical system consists of an aluminium mirror, an achromatic lens and a CCD camera.

† sanayehajari@ipm.ir

Content from this work may be used under the terms of the CC BY 3.0 licence (© 2018). Any distribution of this work must maintain attribution to the author(s), title of the work, publisher, and DOI.

ISBN: 978-3-95450-194-6 ISSN: 2226-0366 doi:10.18429/JACoW-LINAC2018-TUPO120

THE STUDY OF THE LENGTH AND SHAPE OF BEAM IN A HIGH POWER ELECTRON ACCELERATOR

M. Salehi†, F. A. Davani, B. Ghasemi, Shahid Beheshti University, Tehran, Iran
F. Ghasemi, A. Poursaleh, Nuclear Science and Technology Research, Tehran, Iran

Abstract

The output beam of a high-power linear accelerator, used for industrial purposes, is irradiated on products and scanning them. In order to improve the dosimetry of radiation which products received and to prevent loss of the attacked- beams to the edge of products, the exact evaluation of scanning length is necessary. One of the other challenges of the scanning beam is the lack of uniformity in dosimetry of received radiation. The scanning beam does not collide in parallel to the products, which is also a challenge to accelerator efficiency. To improve dosimetry of received radiation, the use of trajectory correction magnets is suggested. These magnets correct the beams that do not scan in parallel. Also, using the Monte Carlo code, the dosing rate of received radiation to products is simulated and compared in two non-uniform and uniform modes (corrected by trajectory correction magnets).

INTRODUCTION

Various types of industrial accelerators have different applications in the industry by providing an electron beams with energy range of 0.5 to 10 mega electron volts. In these accelerators, the irradiation rate of the products depends on the current and the power of the electron beam. In these accelerators, the irradiation rate to the products depends on the current and the power of the electron beam. At the present, the use of industrial electron accelerators in Iran is restricted to the Yazd radiation monitoring center of the Atomic Energy Organization, which uses TT200 rhodotron accelerators to irradiate their products [1]. At the present, the use of industrial electron accelerators in Iran is restricted to the Yazd radiation monitoring center of the Atomic Energy Organization, which uses industrial accelerators to irradiate their products. In each industrial electron accelerator, the beam enters the extraction beam section after accelerating in the acceleration part. Figure 1 shows the components of the beam extraction system of the industrial accelerator in Yazd. The diameter of output electron beam of industrial accelerators such as linac accelerators is about 1 cm to 2 cm. Therefore, to irradiate it to the product, it is necessary, the beam enters the sweeping magnet. The sweeping magnet is placed at the beginning of the horn and swept the beam into the horn according to the required scan length. Therefore, in a static state the affected cross section has same dimension of beam diameter. Therefore, it is necessary to move the box in front of the beam at the appropriate speed, which is proportional to the amount of doses required. In Fig. 1, the effect of the sweeping magnet on the electron beam is obvious.

The Power supply of the sweeping magnet is such that it starts to sweep the beam linearly from a minimum magnet current and changes with the increase of the current of the scanning angle, so that the minimum and maximum flow rates are in accordance with the angles of the beam in the two corners of the horn. The beam extraction system horn in industrial accelerators is actually a vacuum chamber, which is maintained with a suitable foil of titanium, which is vacuumed relative to room air. Determining the exact length of the scan in Horn and the need to correct the path of the beam in it, are discussed in this article [2].

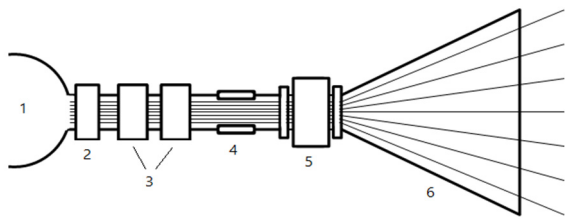


Figure 1: Components of extraction system and transmition of output beam of Linac accelerator. 1) accelerating structure, 2) control magnet, 3) quadrupole doublet, 4) diaphragm, 5) scanning electromagnet, 6) horn.

CHECK THE IMPORTANCE OF DETERMINING PRECISELY AND APPLYING SCAN LENGTH

In industrial accelerator of Yazd radiation center, the output beam of the accelerator at the beginning of the Horn are swept with a frequency of 100 Hz by a sweeper magnet in a way which some of the beams does not collide with the product, and part of the beams does not irradiate products completely and in fact part of power of input beam is wasted. This issue affects the irradiation efficiency.

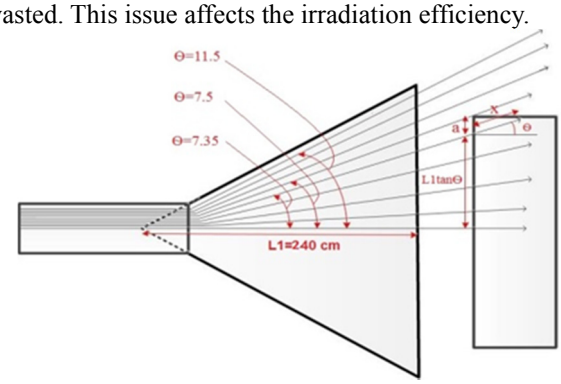


Figure 2: Geometrical parameters at the horn of the beam extraction system.

† Mohammad7salehi@yahoo.com

Content from this work may be used under the terms of the CC BY 3.0 licence (© 2018). Any distribution of this work must maintain attribution to the author(s), title of the work, publisher, and DOI.

ISBN: 978-3-95450-194-6 ISSN: 2226-0366 doi:10.18429/JACoW-LINAC2018-TUPO127

ACTIVITIES AT THE LINAC4 TEST STAND

J-B. Lallement†, V. Bencini, S. Bertolo, F. Di Lorenzo, J. Lettry, A. M. Lombardi,
C. Mastrostefano, D. Noll, M. O'Neil,
CERN, Geneva, Switzerland

Abstract

Linac4, the new CERN H- injector to the Proton Synchrotron Booster, has been commissioned and has delivered a beam intensity and quality calculated to be sufficient to produce the standard beams for LHC and the high intensity beams for ISOLDE when connected. The beam current is nevertheless half of what is foreseen and the problem has been identified at the low energy end, between the extraction and the matching to the RFQ. The Linac4 test stand is being used to address this issue by testing different extraction geometries and different plasma generators. A fast method to access the current in the RFQ acceptance has been put in place. This paper reports the results of the measurements obtained so far.

INTRODUCTION

Linac4 is a 160 MeV H- normal conducting linear accelerator that is about to replace the present Linac2 as injector to the whole CERN proton accelerator complex. After a staged commissioning successfully completed in fall 2016, the linac underwent several test runs in 2017 and 2018 during which its performance, reliability and availability were recorded and optimized [1]. Linac4 has met all the required beam quality parameters needed for creating the various beams that the PSB is currently producing from the LHC beams to the fixed-target experiments beams. This is possible with a beam intensity of 25 mA, which represents 60% of the nominal intensity (40 mA). Nevertheless, to open the door to higher intensity in the CERN complex a current of 40 mA is needed. The intensity limitation comes from the pre-injector because the emittance of a 50mA beam from the present source exceeds the RFQ acceptance. For the present source a maximum current of 25 mA falls in the RFQ acceptance. A dedicated test stand, in operation for source development since 2008, is now dedicated to addressing this issue.

THE LINAC4 TEST STAND

The Linac4 pre-injector is made of a RF source, which can provide a 600 µs, 50 mA H- beam at 45 keV with a maximum repetition rate of 2 Hz, and a 352MHz, 3 m long Radio Frequency Quadrupole, bunching and accelerating the beam to 3 MeV. Acceleration is loss-less from 3 MeV onwards and no emittance growth has been observed for peak currents up to 25 mA. The 45 keV beam extracted from the source is matched to the RFQ via a Low Energy Beam Transport line housing 2 magnetic solenoids, an electrostatic pre-chopper, two steerers, a mechanism to inject different gases to influence neutralisation and a beam current transformer and time resolved profile harps for diagnostics.

The Linac4 set-up is not suitable for in-depth studies and source tests. Therefore, a replica of the Low Energy Beam Transport has been assembled at a dedicated test stand, which is equipped with extra diagnostics including a slit-and-grid, time resolved emittance meter, a Faraday cup and profile harps. A very effective procedure to reconstruct a sample beam from emittance measurements has been described in [2] and it has been extensively used to estimate the number of particles falling into the RFQ acceptance and the matching conditions. In parallel a more rapid method has been put in place. This method is based on simulating the RFQ acceptance by a series of four transverse collimators (the mask) and obtaining the current into the RFQ acceptance by measuring the current with a Faraday cup placed downstream. This method, besides being faster, is more suitable for an automatic optimisation of the LEBT parameters (focusing and steering). The layout of the test stand is show in Fig. 1.

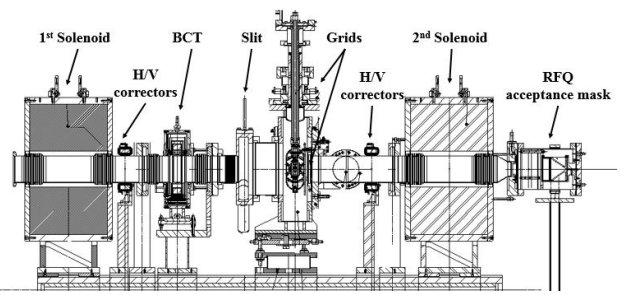


Figure 1: Linac4 test-stand layout.

The RFQ Acceptance Mask

The RFQ acceptance mask device is made of four intercepting plates with squared aperture restrictions. The aperture size and their relative distances are chosen such that only the particles within the RFQ acceptance can pass through all four aperture restrictions. Extensive calculation under different regimes of space charge distribution and intensity have been performed to validate this device.

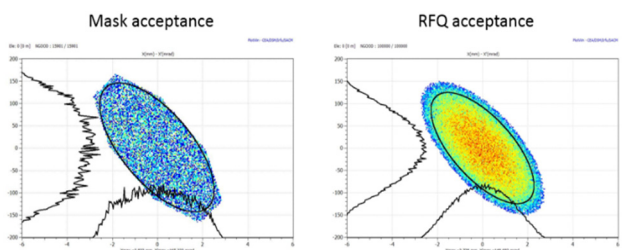


Figure 2: Comparison between the Linac4 RFQ and the mask transverse acceptances at zero current. Mask acceptance on the left, RFQ acceptance on right.

† jean-baptiste.lallement@cern.ch

Content from this work may be used under the terms of the CC BY 3.0 licence (© 2018). Any distribution of this work must maintain attribution to the author(s), title of the work, publisher, and DOI.

ISBN: 978-3-95450-194-6 ISSN: 2226-0366 doi:10.18429/JACoW-LINAC2018-TUPO130

THE DESIGN OF HEPS MAGNET DATABASE AND APPLICATIONS

Y. S. Qiao[1], P. Chu, F. S. Chen[1], Institute of High Energy Physics, 100049 Beijing, China
[1]also at University of Chinese Academy of Sciences, 100049 Beijing, China

Abstract

HEPS (High Energy Photon Source) is a planned ultra-bright and extremely low emittance synchrotron light source which will contain about 2500 magnets. The magnet related data including design, measurements, tests, and operation are typically scattered in various storages which can be hard to access for high-level purposes. For such a large number of magnets, it is very important to have essential magnet information systematically stored in relational databases for efficient management and applications. This paper outlines the conceptual and the functional design for the HEPS magnet database and its associated applications, mainly for design of the database schema and application software architecture. This database is developed with MySQL. To provide a better view and access function of magnet related data, a web-based management platform has been developed for data uploading, querying and data managing.

REQUIREMENTS ANALYSIS

Magnets are among the most important components for a charged particle accelerator. From physics and engineering design to online operation, many kinds of information will be generated. The HEPS magnet related data workflow is shown in Fig. 1. We would like to capture and store all essential data regarding a magnet. For the moment, the Magnet Database is focused on related needs of magnet data management, which includes support for a few particular magnet measurement methods. It should be easy to add more measurement method support at any time. Applications for this database will provide magnet operation curves for the control system [1].

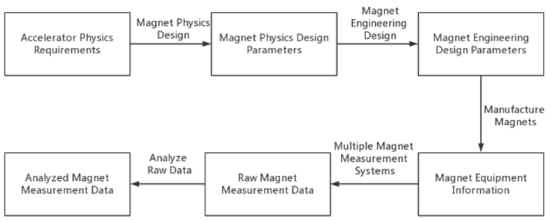


Figure 1: Magnet related data workflow.

Besides the magnet database mentioned here, it is also necessary to establish links for other related data. As magnets being installed and becoming part of the accelerator, the magnet operation data will then be collected and related to this magnet database. Again, the link between the Magnet Database and operation database is through the manufacture equipment ID tag.

DATABASE DESIGN

There are many magnets related data for an accelerator and various applications need to access a combination of these data. With an overall consideration, it is better to store such complicated data in a well-organized relational database like MySQL.

Conceptual Structure Design

The database schema design is implemented to MySQL database systems via MySQL Workbench. The schema holds the following data: magnet design data, magnet measurement data, magnet excitation curve data, and magnet operation or beam-based measurement data in the future. The complete database design schema generated by MySQL Workbench is shown in Fig. 2.

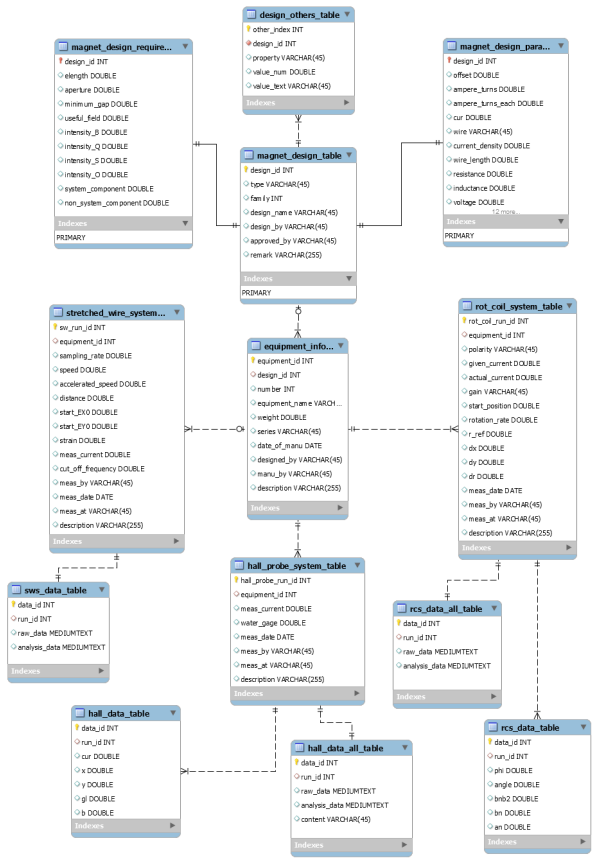


Figure 2: Magnet database schema.

Logical Structure Design

From conceptual design to the logical database design is an important part of the design process. EER (Enhanced entity–relationship) model concept design phase was to reflect the needs of the magnet data model, regardless of the specific DBMS. In order to establish the

Content from this work may be used under the terms of the CC BY 3.0 licence (© 2018). Any distribution of this work must maintain attribution to the author(s), title of the work, publisher, and DOI.

ISBN: 978-3-95450-194-6 ISSN: 2226-0366 doi:10.18429/JACoW-LINAC2018-TUPO132

IMPLEMENTATION OF THE BEAM LOADING COMPENSATION ALGORITHM IN THE LLRF SYSTEM OF THE EUROPEAN XFEL

L. Butkowski*, Julien Branlard, Mathieu Omet, Radoslaw Rybaniec,
Holger Schlarb, Christian Schmidt,
Deutsches Elektronen-Synchrotron DESY, Hamburg, Germany

Abstract

In the European XFEL, a maximum number of 2700 electron bunches per RF pulse with beam currents up to 4.5 mA can be accelerated. Such large beam currents can cause a significant drop of the accelerating gradients, which results in large energy changes across the macro-pulse. But, the electron bunch energies should not deviate from the nominal energy to guarantee stable and reproducible generation of photon pulses for the European XFEL users. To overcome this issue, the Low Level RF system (LLRF) compensates in real-time the beam perturbation using a Beam Loading Compensation algorithm (BLC) minimizing the transient gradient variations. The algorithm takes the charge information obtained from beam diagnostic systems e.g. Beam Position Monitors (BPM) and information from the timing system. The BLC is a part of the LLRF controller implemented in the FPGA. The article presents the implementation of the algorithm in the FPGA and shows the results achieved with the BLC in the European XFEL.

INTRODUCTION

The European X-Ray Free Electron Laser (XFEL) [1] is coherent light source providing laser pulses of tunable wavelength by the SASE process. It uses an electron beam accelerated to 17.5 GeV in 2 km long superconducting linac, which operates in a pulsed mode. The main superconducting linac in XFEL has been divided into 25 RF stations. Each of the RF stations consist of four cryogenics accelerating modules (CM), one klystron and a dedicated LLRF system that is split into master and slave subsystems [2].

The XFEL general bunch pattern consists of up to 2700 electron bunches with a variable charge distribution at a repetition rate of 4.5 MHz. To ensure highly reproducible and stable photon pulses for users, it is required to regulate precisely the RF filed inside the accelerating cavities, which should be ensured by the Low Level RF (LLRF) system.

The key element of the LLRF system is the digital feedback controller, which is a distributed system that has been implemented in Micro Telecommunications Computing Architecture (MTCA.4) [3]. Its main task is to compensate for field perturbations inside cavities using the feedback information about this field. However, high beam current can cause a significant drop of the accelerating gradient which cannot be compensated using a feedback controller i.a. due to its limited bandwidth. To overcome this issue it is required to use more complex algorithms like Beam Loading Compensation (BLC).

LLRF SYSTEM OVERVIEW

There are two MTCA.4 crates installed at each of the RF stations, one crate in the master and one crate in the slave LLRF subsystems. The simplified block diagram of a RF station is presented in Fig. 1.

One LLRF MTCA.4 crate is filled out with six pairs of down-converter (uDWC) - digitizer (uADC) boards, LLRF controller (uTC), CPU, crate management module (MCH), timing card (x2timer) and a vector modulator placed only in the master crate. Each LLRF subsystem processes RF signals from two cryo-modules while only the master system provides the drive signal to the klystron.

The uTC board in the master subsystem contains the main LLRF controller. It collects all the feedback data which are required to generate proper drive. All the algorithms are implemented in the FPGA chip located on the uTC board. The feedback data are transmitted over optical links or over differential lines within the crate and are received by the main controller using Multi-Gigabit Transceivers (MGTs).

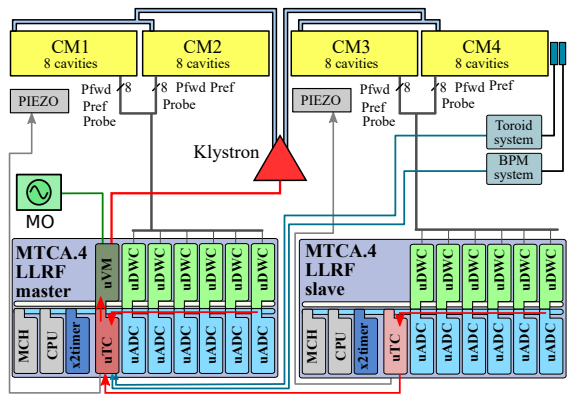


Figure 1: Simplified block diagram of the LLRF system installed at one RF station in XFEL.

BEAM CHARGE INFORMATION

The information about current beam charge can be obtained from the Beam Position Monitor (BPM) and toroid systems. They are located upstream the RF station [4]. Each of these systems sends the data in a real time to the main LLRF controller over a separate optical link working at 3.125 Gbps. A dedicated protocol has been settled, which defines packet of the data transmitted to the LLRF controller. The BPM data packet is presented in Fig. 2.

* lukasz.butkowski@desy.de

Content from this work may be used under the terms of the CC BY 3.0 licence (© 2018). Any distribution of this work must maintain attribution to the author(s), title of the work, publisher, and DOI.

ISBN: 978-3-95450-194-6 ISSN: 2226-0366 doi:10.18429/JACoW-LINAC2018-WE1A03

LATEST RESULTS OF CW 100 mA ELECTRON RF GUN FOR NOVOSIBIRSK ERL BASED FEL *

V. N. Volkov †, V. Arbuzov, E. Kenzhebulatov, E. Kolobanov, A. Kondakov, E. Kozyrev, S. Krutikhin, I. Kuptsov, G. Kurkin, S. Motygin, A. Murasev, V. Ovchar, V.M. Petrov, A. Pilan, V. Repkov, M. Scheglov, I. Sedlyarov, S. Serednyakov, O. Shevchenko, S. Tararyshkin, A. Tribendis, N. Vinokurov, BINP SB RAS, Novosibirsk, Russia

Abstract

Continuous wave (CW) 100 mA electron rf gun for injecting the high-quality 300-400 keV electron beam in Novosibirsk Energy Recovery Linac (ERL) and driving Free Electron Laser (FEL) was developed, built, and commissioned at BINP SB RAS. The RF gun consists of normal conducting 90 MHz rf cavity with a gridded thermionic cathode unit. Bench tests of rf gun is confirmed good results in strict accordance with our numerical calculations. The gun was tested up to the design specifications at a test bench that includes a diagnostics beam line. The rf gun stand testing showed reliable work, unpretentious for vacuum conditions and stable in long-term operation. The design features of different components of the rf gun are presented. Preparation and commissioning experience is discussed. The latest beam results are reported.

INTRODUCTION

Recent projects of advanced sources of electromagnetic radiation [1] are based on the new class of electron accelerators where the beam current is not limited by the power of rf system – energy recovery linacs (ERLs). Such accelerators require electron guns operating in continuous wave (cw) mode with high average current. The only solution is an rf gun, where the cathode is installed inside the rf cavity. RF guns have no problem with degradation of the cathode due to absence of back bombardment electrons so the vacuum condition is not important there. The most power Novosibirsk FEL [2] can be more powerful by one order on magnitude with this rf gun [3-5]. Measured rf gun characteristics are presented in Table 1.

RF GUN AND DIAGNOSTIC STAND

The rf gun and diagnostic stand are presented in Fig. 1.

The RF gun cavity is made on the base of standard bimetallic cavity of Novosibirsk ERL Detailed information can be found in [3-5]. Only the insert with the thermionic cathode-grid unit is built into the cavity. The gridded thermionic dispenser cathode is driven by special modulator with GaN rf transistor. The insert focusing electrode executes the strong rf focusing of the beam just near the cathode that ensures the beam emittance compensation at the relatively low electric field at the cathode. Also it ensures the absolute absence of dark currents in the beam.

There are in the stand: 30 kW water cooled beam dump with 5 cm lead radiation shield, wideband Wall Current Monitor (WCM2) inserted into the replaceable target, Transition Radiation Sensor, the pair of standard WCM, three focusing solenoids, and the testing cavity.

Table 1: Measured RF Gun Characteristics

Average beam current, mA	≤100
Cavity Frequency, MHz	90
Bunch energy, keV	100 ÷ 400
Bunch duration (FWHM), ns	0.06 ÷ 0.6
Bunch emittance, mm mrad	10
Bunch charge, nC	0.3 ÷ 1.12
Repetition frequency, MHz	0.01 ÷ 90
Radiation Doze Power, mR/h	100/2m
Operating pressure, Torr	10^{-9}…10^{-7}
Cavity RF loses, kW	20

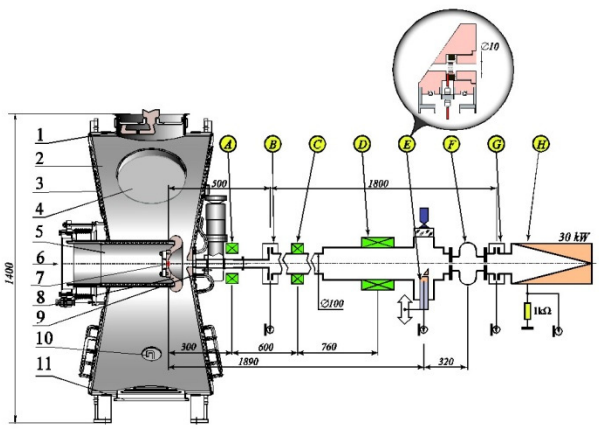


Figure 1: RF gun and stand layout: 1-Power input coupler; 2- Cavity shell; 3-Cavity back wall; 4-Sliding tuner; 5-Insert; 6-Cathode injection/extraction channel; 7-Thermionic cathode-grid unit; 8-Concave focusing electrode; 9-Cone like nose; 10-Loop coupler; 11-Vacuum pumping port; A-Emittance compensation solenoid; B-First Wall Current Monitor (WCM); C, D -Solenoids ; E-Wideband WCM and transition radiation target; F – Test Cavity; G-third WCM; H-Faraday cup and Water-cooled beam dump.

STAND TESTING RESULTS

Beam Current Regulation

There are some methods of beam current increasing: decreasing of the grid bias voltage (V_{bias}), increasing of the modulator pulse voltage (V_{puls}), and increasing of the

* Work supported by Russian Science Foundation (project N 14-50-00080)
† v.n.volkov@inp.nsk.su

Content from this work may be used under the terms of the CC BY 3.0 licence (© 2018). Any distribution of this work must maintain attribution to the author(s), title of the work, publisher, and DOI.

ISBN: 978-3-95450-194-6 ISSN: 2226-0366 doi:10.18429/JACoW-LINAC2018-WE1A04

THE HIGH POWER RF SYSTEM FOR THE EUROPEAN XFEL

S. Choroba, Deutsches Elektronen-Synchrotron, DESY, Hamburg, Germany
for the XFEL Work Package High Power RF

Abstract

The RF system for the European XFEL consists of 26 high power RF stations each capable of 10MW RF pulse power. This paper will report on the overall system layout, cover RF system components e.g. klystrons, modulators and high power RF waveguide distribution. It will also cover system modifications during construction phase and report on commissioning results.

DESCENT OF THE EUROPEAN XFEL

The European XFEL descends from the TESLA project, a linear collider with a center-of-mass-energy of 500GeV. In the early 1990s the TESLA collaboration was established and the TESLA Test Facility has been set up at DESY by the TESLA collaboration to develop all components required to construct a linear collider based on superconducting RF technology. A technical design report on the linear collider with integrated free electron laser was published in 2001 [1]. In 2006 it was decided to build the free electron laser as stand-alone facility at DESY. Construction started in 2007 and first X-rays were produced in 2017. The high power RF system components for the European XFEL have been developed to meet the requirements for the TESLA linear collider and have later been modified to meet the European XFEL demands.

The TELSA linear collider proposal served as the basis for the International Linear Collider, ILC, too. Since both, the ILC and the XFEL, descends from the TESLA linear collider, many of the high power RF systems components now in operation for the E-XFEL, might be used for ILC too.

EUROPEAN XFEL

The European XFEL produces X-rays of unprecedented properties in terms of brilliance, average brilliance, coherence, pulse duration and time structure.

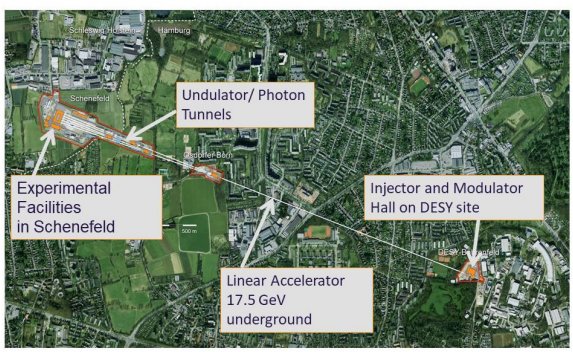


Figure 1: XFEL site.

The E-XFEL is located in Hamburg, with the injector on the DESY site, the experimental facilities in Schenefeld and the main linear accelerator in an underground tunnel in between. The E-XFEL site layout is shown in Figure 1. Electrons generated by a RF gun are accelerated in the superconducting cavities of the linac and are distributed to up to five beam lines for experiments. The total length of the facility is 3.4km. Details can be found in [2].

RF SYSTEM REQUIREMNTS

The linear accelerator of the E-XFEL is based on superconducting RF technology. Electrons are generated in a normal conducting RF gun and are accelerated in the superconducting cavities of the 1.9km long linac. The 2700 electron bunches are accelerated in 600µs long macro-pulses with a repetition rate of 10Hz up to 17.5GeV. The electron beam current is 5mA. The main linac consists of 96 cryogenic modules with 8 superconducting 9-cell Niobium-cavities each. The high power RF system (HPRF) provides RF power at 1.3GHz, at a RF pulse duration of 1.38ms with a repetition rate of 10Hz. The average accelerating gradient is 23.6MV/m.

In order to achieve this gradient 122kW per cavity are required. 32 cavities in 4 cryogenic modules are connected to one RF station. Taking into account losses and a regulation reserve 5.2MW of RF power per station are required in the main linac. The RF station for the RF gun in the injector provides 8MW up to 650µs pulse duration, the station for one single module in the injector up 1.3MW at 1.38ms. Table 1 summarizes the requirements.

Table 1: HPRF Requirements

Number of sc cavities	776
Power per cavity	122kW
Gradient at 17.5GeV	23.6MV/m
Power per 32 cavities (4 cryogenic modules)	3.9MW
Power per RF station main linac/RF gun/injector	5.2MW/8MW/1.3MW
Number of RF stations total/main linac/injector	26/24/2
RF pulse duration main linac/RF gun/injector	1.38ms/0.65ms/1.38ms
Repetition rate	10Hz

Content from this work may be used under the terms of the CC BY 3.0 licence (© 2018). Any distribution of this work must maintain attribution to the author(s), title of the work, publisher, and DOI.

ISBN: 978-3-95450-194-6 ISSN: 2226-0366 doi:10.18429/JACoW-LINAC2018-WE1A05

SwissFEL LINAC COMMISSIONING STATUS, CURRENT PERFORMANCE AND FUTURE PLANS

P. Craievich* on behalf of the SwissFEL team
Paul Scherrer Institut, 5232 Villigen PSI, Switzerland

Abstract

SwissFEL, the hard x-ray free-electron laser facility at PSI, is in an advanced commissioning phase. The commissioning of the 5.8 GeV Linac started in 2016 and the first FEL pilot-experiments were performed at a reduced beam energy in the end of 2017. In 2018, it is foreseen to progressively increase the electron beam energy and photon energy up to the maximum design values, interleaved by several FEL pilot experiments. This paper gives an overview of the commissioning progress including the achieved machine performance and first operational experience.

INTRODUCTION

The newest large research facility at the Paul Scherrer Institute, the hard-X-ray free-electron laser SwissFEL [1] has recently commenced its scientific program with a series of pilot experiments. SwissFEL aims at delivering ultrashort coherent photon pulses through two beam lines called Aramis (hard X-rays, 1-7 Å) and Athos (soft X-rays, 6.5-50 Å). So far only the Aramis beam line has been commissioned with two experimental stations in operation, called Alvra and Bernina. Alvra is a multipurpose pump-probe station focusing on ultrafast biology and chemistry, while Bernina specializes in pump-probe crystallography for the study of ultrafast dynamics in solid matter, in particular strongly correlated systems, as well as structural biology.

The SwissFEL accelerator consists of an electron source, an S-band (3 GHz) booster linac and a C-band (5.7 GHz) main linac (Fig. 1). The electron source is a laser driven 2.5-cell S-band RF photoinjector gun. The electron bunches, with charge ranging between 10 and 200 pC, are longitudinally compressed in two stages at nominal energies of 300 MeV and 2.1 GeV, respectively. A higher-harmonic cavity (X-band, 12 GHz) linearizes the electron phase space before the first compression stage. The accelerated and compressed electron bunches are sent into the Aramis undulator line comprising 13 in-vacuum undulator modules of 4 m length each. A second undulator line, Athos, is currently under construction. It will be driven by 3 GeV electrons extracted in a switchyard halfway along the main linac. Table 1 lists the most important parameters of the SwissFEL facility.

This paper is an updated version of the contribution presented at the IPAC'18 [2] since new important results are been achieved between May and September 2018. SwissFEL linac reached its nominal electron beam energy of 5.8 GeV, first lasing with an photon energy of 9 keV and in the summer period other four pilot experiments were performed.

* paolo.craievich@psi.ch

STATUS OF C-BAND LINAC

The C-band main linac is the centrepiece of the SwissFEL accelerator defining the available electron and hence photon energy. It consists of a total of 26 RF modules, each providing a nominal accelerating voltage of 240 MV with four tuning-free copper structures [3, 4]. Figure 2 shows a part of the tunnel with C-band accelerating structures. The effectively achieved accelerating voltages vary between 200 and 280 MV, depending on the conditioning states of the modules. In each station, an IGBT-switched solid-state modulator manufactured by Ampegon (first half of the linac) or ScandiNova (second half) drives an E37212 Toshiba klystron, which can furnish up to 50 MW for a duration of 3 µs. The RF pulse is compressed in a barrel-open-cavity (BOC) [5] before being delivered to the four structures via a precisely adjusted waveguide network. Currently 25 of the 26 stations are available for beam acceleration. One RF station in Linac 2 is currently used for the upgrade of the software system. In case of failure of one RF station in Linac 1 and/or Linac 3 there is enough RF power reserve in order to guarantee the operations. The delivered power is typically around to 80% of the maximum value.

Table 1: SwissFEL Main Parameters

Parameter	Value
Photon wavelength	0.1-5.0 nm
Photon energy	0.25-12.4 keV
Pulse duration	1-30 fs
Electron energy	5.8 GeV
Electron bunch charge	10-200 pC
Repetition rate	100 Hz

A campaign of measurements on the RF stations has been performed to characterize the actual stability of the klystron voltage. A high performance differential amplifier has been used for this scope. This implements a high stability low-noise voltage generator and a low overdrive recovery time comparator in order to accurately monitor the pulse-to-pulse reproducibility. The results of these measurements showed that pulse-to-pulse stability of the klystron high voltage are better than the specified value of 15 ppm.

After the conditioning periods dedicated for each RF station, typically from 3 to 4 weeks for RF stations, the SwissFEL Linac has reached the nominal electron bunch energy of 5.8 GeV required for Aramis beamline in September 2018. In the present configuration, the linac delivers 5.5 GeV for a total energy of 5.8 GeV (300 MeV from the injector linac). The beam energy is for a compressed bunch with off-crest op-

Content from this work may be used under the terms of the CC BY 3.0 licence (© 2018). Any distribution of this work must maintain attribution to the author(s), title of the work, publisher, and DOI.

ISBN: 978-3-95450-194-6 ISSN: 2226-0366 doi:10.18429/JACoW-LINAC2018-WE1A06

PLUSE-TO-PULSE BEAM MODULATION FOR 4 STORAGE RINGS WITH 64 PULSED MAGNETS

Y. Enomoto*, K. Furukawa, T. Kamitani, F. Miyahara, T. Natsui,
M. Satoh, K. Yokoyama, M. Yoshida, KEK, Tsukuba, Japan
S. Ushimoto, Mitsubishi Electric System & Service Co. Ltd. Tsukuba, Japan
H. Saotome, Kanto Information Service Tsukuba, Japan

Abstract

In 2017, sixty-four pulsed magnets (28 quadrupoles and 36 steerings) were installed in the KEK electron positron linac for simultaneous injection to four different rings. Since each ring requires different injection energy, magnetic field in the injector linac has to be changed shot by shot (every 20 ms) according to the destination of the beam. To realize such operation, novel pulsed power supplies and an EVENT timing system compatible PXI based control system were developed. Installation and commissioning of the system were successful and it has been working for one year without severe trouble.

INTRODUCTION

The KEK injector linac [1] has delivered electrons and positrons for particle physics and photon science experiments for more than 30 years. Figure 1 shows electron and positron accelerator complex in the KEK Tsukuba site. There are four storage rings, i.e. two rings for light source, PF and PF-AR, and two rings for electron positron collider, SuperKEKB [2] HER and LER. In addition to them, positron damping ring have been in operation since February 2018. All of the rings require full energy injection, 2.5 GeV for PF, 6.5 GeV for PF-AR, 4 GeV for SuperKEKB LER and 7 GeV for SuperKEKB HER as shown in the Fig. 1. To satisfy the requirement, 64 pulsed magnets were installed in 2017 and 32 more are planned to be installed in 2018. Using these magnets, magnetic field can be changed shot by shot in 20 ms and was optimized for each destination.

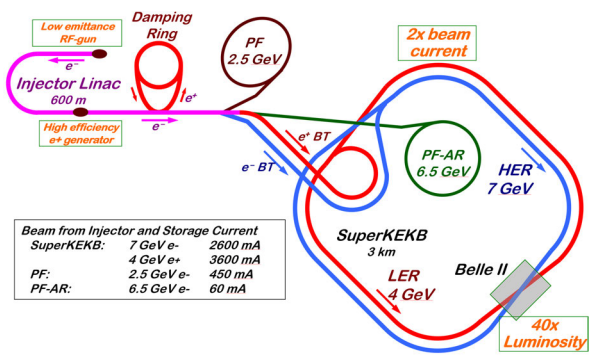


Figure 1: A schematic view of the electron and positron accelerator complex in the KEK.

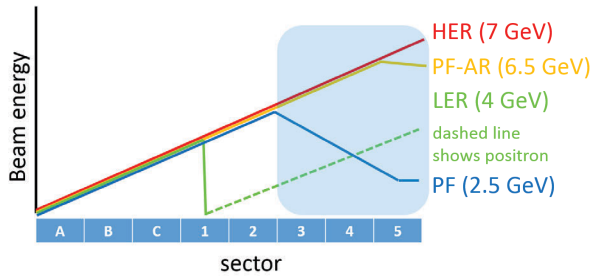


Figure 2: Beam energy along the beam line. Solid line shows electron beam dashed line shows positron beam respectively.

There are 8 (A-C, 1-5) sectors in the linac. Each sector is about 80 m long and the total length of the linac is about 650 m. Figure 2 schematically shows beam energy along the beam line. To minimize the installation of the pulsed magnets, acceleration scheme is carefully adjusted to minimize the length of the beam line where the beam with different energy pass through. The beam for the SuperKEKB HER, it is accelerated all of the sectors. The beam for the PF, it is accelerated in sector A to 2 and decelerated in sector 3 to 5. The beam for the SuperKEKB LER, electrons are accelerated in sector A to 1 and generate positrons at the target located in the middle of the sector 1. Positrons, shown in dashed line, are accelerated rest of the sectors. Since the beam energy is the same in the sector A to C and first half of the sector 1 regardless of the destination, it is not necessary to use pulsed magnets. On the other hand, in sector 3 to 5 shaded by light blue in the Fig. 2, beam with very different energy pass through, magnets in these sectors were completely replaced with pulsed magnets. In sector 2 and a part of sector 1, beam energy of the electron and positron is very different. Magnetic field optimized for the low energy positron beam affect the orbit of the high energy electron beam very little. In these section, DC magnets with compatible setting for both electron and positron beam are used except for several pulsed steering magnets at the moment.

MAGNET AND SUPPORT

Several types of magnets were installed in the beam lines as summarized in the Table 1. Appearance of these magnets are shown in Fig. 3. In sector 3 to 5, a common unit shown in Fig. 4, which consists of two quad magnets (PM_32_4), a horizontal steering magnet (PX_32_4), a vertical steering magnet (PY_32_4) and a beam position monitor located on a motor controlled movable support, was installed at 13 points.

* yoshinori.enomoto@kek.jp

Content from this work may be used under the terms of the CC BY 3.0 licence (© 2018). Any distribution of this work must maintain attribution to the author(s), title of the work, publisher, and DOI.

ISBN: 978-3-95450-194-6 ISSN: 2226-0366 doi:10.18429/JACoW-LINAC2018-WE2A01

FIRST ACCELERATION AT FRIB*

E. Pozdeyev†, H. Ao, J. Brandon, N. Bultman, F. Casagrande, S. Cogan, K. Davidson, E. Daykin, P. Gibson, W. Hartung, L. Hodges, K. Holland, M. Ikegami, D. Jager, S. Kim, M. Konrad, B. Kortum, T. Larter, Z. Li, S. Lidia, S. Lund, G. Machicoane, I. Malloch, H. Maniar, F. Marti, T. Maruta, C. Morton, D. Morris, D. Omitto, P. Ostroumov, A. Plastun, J. Popielarski, H. Ren, K. Saito, J. Stetson, D. Victory, Y. Yamazaki, T. Yoshimoto, J. Wei, J. Wong, M. Xu, T. Xu, S. Zhao, Q. Zhao,
Facility for Rare Isotope Beam, East Lansing, 48824, USA

Abstract

FRIB is now moving to commissioning interleaved with installation. The ECR, low energy transport and RFQ have been commissioned with beam. By the time of the conference the 4K cryogenic system and first three beta 0.041 QWR cryomodules will be commissioned with beam. The talk will focus on hardware and beam performance.

INTRODUCTION

The Facility for Rare Isotope Beams [1] is the premiere DOE-SC national user facility for nuclear physics research built on the campus of Michigan State University. The FRIB driver accelerator will accelerate ions with the mass up to Uranium to energies higher than 200 MeV and beam power on target higher than 400 kW. The main focus of the experimental program is rare isotope beams by fragmentation, gas stopping, and reacceleration.

Project commissioning performance requirements are defined by Key Performance Parameters (KPP) for CD-4:

1. Accelerate Argon beam with the energy larger than 200 Me/u and a beam current larger than 20 pnA
2. Detect 84Se in FRIB separator focal plane. The last KPP requirement for the experimental systems can be translated to the following requirement for the accelerator: accelerate 86Kr beam to produce 84Se by fragmentation.

Phased Beam Commissioning

FRIB has adopted a "paper-clip" design shown in Fig. 1. The FRIB Front End and RFQ are located on the east side of the project site (marked in red). The beam is accelerated in Linac Segment 1 (LS1) through three beta 0.041 (blue) and eleven 0.085 (yellow) 80.5 MHz QWR cryomodules to the energy of approximately 20 MeV/u. A lithium stripper will be installed at the end of LS1. The stripped beam is collimated in first folding segment (FS1) and accelerated by HWRs operating at 325 MHz in linac segments 2 (LS2, green) and 3 (LS3, grey) and sent towards experimental facilities through BDS. Another folding segment FS2 is used between LS2 and LS3 to reduce the footprint of the facility.

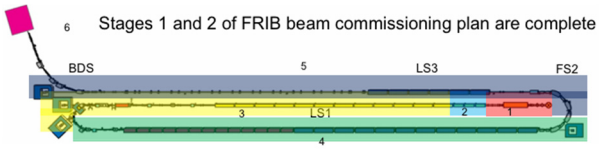


Figure 1: Paper-clip design of the FRIB accelerator. Colors and numbers mark commissioning stages: red - Front End, blue – three beta 0.041 cryomodules, yellow – eleven 0.085 cryomodules and part of FS1, green – LS2, and grey – FS2 and LS3.

FRIB beam commissioning is interleaved with installation and is approached in stages as show in Fig. 1. Commissioning follows installation of linac systems along the beam path starting from the Front End. In this article, we describe commissioning of the Front End, completed earlier in 2018, and the first beam acceleration in the first three beta 0.041 QWR cryomodules demonstrated in July 2018.

HIGHLIGHTS OF TECHNICAL SYSTEMS

Figure 2 shows the layout of the FRIB Front End [2] with the first three beta 0.041 QWR cryomodules and a temporary diagnostics station (D-Station). The front end is located on two levels to allow for maintaining one ion source while the other source is used for the program.

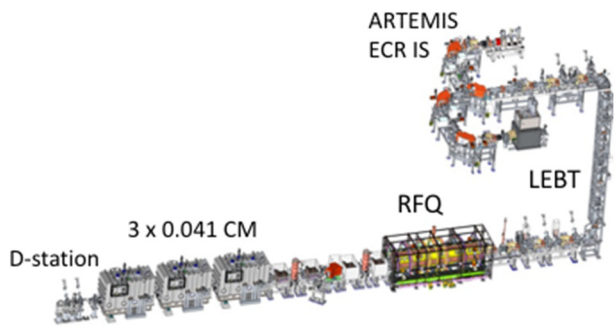


Figure 2: FRIB Front End with the first three 0.041 cryomodules and the temporary diagnostics station.

The front end includes

1. Two ECR sources on High Voltage (HV) platforms. 1) ARTEMIS is a 14 GHz ECR ion source. The source has been installed and commissioned in 2016. 2) The second source is a 28 GHz superconducting (SC) source based on VENUS (LBNL). The superconducting source is under construction, with planned delivery in 2019.

* Work supported by the U.S. Department of Energy Office of Science under Cooperative Agreement DE-SC0000661 and the National Science Foundation under Cooperative Agreement PHY-1102511, the State of Michigan and Michigan State University.
† pozdeyev@frib.msu.edu.

Content from this work may be used under the terms of the CC BY 3.0 licence (© 2018). Any distribution of this work must maintain attribution to the author(s), title of the work, publisher, and DOI.

ISBN: 978-3-95450-194-6 ISSN: 2226-0366 doi:10.18429/JACoW-LINAC2018-WE2A03

CONSTRUCTION STATUS OF THE SUPERCONDUCTING LINAC AT THE RIKEN RADIOACTIVE ISOTOPE BEAM FACILITY

N. Sakamoto*, M. Dantsuka, H. Imao, O. Kamigaito, K. Kusaka, H. Okuno, K. Ozeki, K. Suda, T. Watanabe, Y. Watanabe, K. Yamada, RIKEN Nishina Center, Saitama, Japan
E. Kako, H. Nakai, H. Sakai, K. Umemori, KEK, Ibaraki, Japan
H. Hara, K. Miyamoto, K. Sennyu, T. Yanagisawa,
Mitsubishi Heavy Industries Machinery Systems, Ltd. (MHI-MS), Kobe, Japan

Abstract

The RIKEN Heavy-Ion Linac (RILAC) is undergoing an upgrade to allow it to further investigate super-heavy elements. In this project, a new superconducting (SC) electron cyclotron resonance ion source and SC booster linac are being developed and constructed. The SC Linac consists of 10 TEM quarter-wavelength resonators that are operated at 73 MHz and contained in three cryomodules. The design and construction status of the Superconducting RILAC, including the medium-energy beam transport line, are given in this paper.

INTRODUCTION

The mission of the RIKEN Radioactive Isotope Beam Factory (RIBF) [1, 2] is to improve our understanding of the mechanism of synthesis of elements in the universe via experiments using intense heavy-ion beams. At the RIBF, heavy-ion beams with various energies are available from sub-coulomb energy levels for fusion reactions to intermediate energy levels for radioisotope beam production using fission reactions. Beams of ion species ranging from hydrogen to uranium are accelerated in accordance with experimental requirements.

The most important upgrades are designed to increase the beam intensity and acceleration voltage in order to synthesize super-heavy elements, because its reaction cross section is estimated to be as small as a femtobarn. The original RILAC [3] consists of six drift-tube-linac (DTL) tanks that are frequency-tunable from 17 to 45 MHz, and can accelerate heavy-ions to 2.9 MeV/u at 37.75 MHz. The new element Nh was synthesized by bombarding a ^{209}Bi target with an intense ^{70}Zn^{14+} beam with an energy of 5 MeV/u [4] accelerated by the RILAC, which was upgraded by adding a booster linac [5] comprising six DTLs. The first two DTLs of the booster, A1 and A2, are equipped with short-plate frequency tuning systems to have a frequency range from 36 to 76 MHz, which will expand the energy range of the beam injected to the RIKEN Ring Cyclotron, while the latter four DTLs have a fixed frequency.

The Superconducting RILAC (SRILAC) was proposed [6] in order to allow further experiments on super-heavy element synthesis. To preserve the versatility of the beams that are utilized for coupled operation of the RILAC and RRC, it was decided to upgrade the RILAC by replacing the latter 4 DTLs of the booster linac, which are fixed-frequency cavities, with a SC linac. The goals of the upgrade are listed in Table 1.

Table 1: Specifications of RILAC Before and After Upgrade

Upgrade	Before	After
No. of tanks	12 DTLs	8 DTLs, 3 CMs
Freq. (MHz)	37.75/75.5	36.5*/73.0
Total Acc. V (MV)	25 (A/q = 5)	39 (A/q = 6)

* 36.5 MHz is the fundamental frequency for the RF system of the RIBF accelerators.

The design of the SRILAC is based on the idea of increasing the intensity of the uranium beams and accelerating them to up to 11 MeV/u [7,8]. The original design of the SRILAC consists of 14 cryomodules (CMs), and each CM accommodates four quarter-wavelength resonators QWRs. The QWRs are optimized for a beta of 0.08 and an energy of about 3 MeV/um, which matches the energy of the beams provided by the RILAC. As shown in Fig. 1, the SRILAC consists of three CMs–CM1, CM2, and CM3–with a room-temperature medium-energy beam transport (MEBT) between them. The CMs do not contain superconducting magnets. The design of the CMs is a modification of a prototype CM developed at RIKEN [9–11] as a part of the ImPACT Program [12]. For the MEBT, a newly designed beam energy position monitor will be employed instead of traditional wire scanners. Since the SRILAC will be installed in the existing facility, it is important to have an isolation system to prevent contamination of the SC parts.

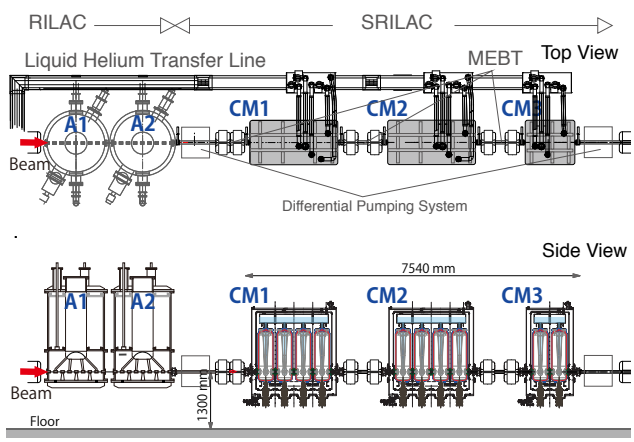


Figure 1: Layout of the Superconducting RILAC.

* nsakamot@ribf.riken.jp

Content from this work may be used under the terms of the CC BY 3.0 licence (© 2018). Any distribution of this work must maintain attribution to the author(s), title of the work, publisher, and DOI.

ISBN: 978-3-95450-194-6 ISSN: 2226-0366 doi:10.18429/JACoW-LINAC2018-WE2A04

COMISSIONING OF THE NEW SARAF RFQ AND DESIGN OF THE NEW LINAC

A. Perry, D. Berkovits, H. Dafna, B. Kaizer, Y. Luner, J. Rodnizki, A. Shor, I. Silverman, L. Weissman, Soreq Nuclear Research Center, Yavne, Israel
R. Duperrier, G. Ferrand, B. Gastineau, M. Jacquemet, S. Ladegaillerie, C. Madec, N. Pichoff, T. Plaisant, D. Uriot CEA/IRFU, Gif-sur-Yvette, France
A. Bechtold, P. Niewieczerzal Neue Technologien GmbH, Gelnhausen, Germany

Abstract

Soreq Nuclear Research Center (SNRC) and CEA collaborate for the upgrade of the existing Soreq Applied Research Accelerator Facility (SARAF) accelerator up to 5mA Continuous Wave (CW) 40 MeV deuteron and proton beams (Phase 2). SNRC is upgrading the injector: the ion source, the low energy beam transport line and the 4-rods Radio Frequency Quadrupole (RFQ). CEA is in charge of the development and commissioning of the medium energy beam transport line and the superconducting linac. This paper presents the status of the SARAF linac development by CEA and the installation and testing of a new set of rods electrodes in the SARAF RFQ.

INTRODUCTION

Soreq Applied Research Accelerator Facility (SARAF) is based on a high intensity proton/deuteron linac currently in operation at Soreq Nuclear Research Center (SNRC, Israel) [1]. SARAF-Phase 2 project aims to upgrade the existing capabilities and, in particular, increase the available beam energy and current up to 40MeV and 5mA respectively, in both pulsed and Continuous Wave (CW) modes.

Within the frameworks of the Phase 2 project, CEA (France) manages the SARAF-LINAC project [2]. This project includes the design, construction and commissioning of a new Medium Energy Beam Transport (MEBT) line and a new Superconducting Linac (SCL) made of 4 cryomodules (CM1-CM4). These will replace the existing MEBT and Prototype Superconducting Module (PSM) which are now in operation. The SARAF-LINAC project is now approaching the end of its third and final year of detailed design and prototyping, and is about to transition into the production stage. In preparation, several design reviews took place in 2018. The status of the SARAF-LINAC project will be presented in the second part of this paper.

The existing ion source, Low Energy Beam Transport (LEBT) line and Radio Frequency Quadrupole (RFQ) will serve as the injector to the Phase 2 linac. SNRC is modifying these components in order to reach the Phase 2 specifications. In particular, significant efforts have been devoted to improving the RFQ performance. The original SARAF RFQ, designed by the University of Frankfurt [3] and built by NTG GmbH and RI-ACCEL GmbH, has been able to accelerate high intensity (up to 4 mA) proton beams to 1.5 MeV. However, despite numerous conditioning campaigns, acceleration of CW deuteron beams in the RFQ was unachievable for a long time. Over the years a series of major modifications to the RFQ structure have led to a considerable improvement of the RFQ performance and, following the introduction of an additional RF power coupler, record results of high power operation were achieved in April 2016 [4]. Yet, reliable CW operation at the 250 kW power level which was required for CW deuteron acceleration was unachievable. It was therefore decided to re-design the rods modulation in order to enable deuteron acceleration at a slightly lower inter-electrode voltage [5]. Lowering of the applied RFQ voltage, while keeping the RFQ length and the entrance beam properties, has the unavoidable consequence of lowering the inter-rod separation and lowering the outgoing beam energy from 1.5 MeV/u to 1.27 MeV/u. Extensive beam dynamics simulations of the redesigned RFQ were performed using the GPT beam dynamics code [6] and showed that the beam quality in the transverse and longitudinal phase space should improve with the new modulation. Further simulations using the TraceWin code package [7] indicated that the beam emerging from the RFQ can be satisfactorily matched to the SCL. Electromagnetic simulations using CST [8] were performed as well to guarantee proper RF resonance frequency and to estimate the field homogeneity in the structure. Following this work the new rods fabrication was performed at Neue Technologien (NTG).

INSTALLATION OF THE NEW RODS

Installation of the electrodes was accomplished in two sessions utilizing a laser tracking system. The RFQ tank was opened and the old rods and tuning plates were disassembled and stored prior to the first laser tracker session, which focused on measurements of the stems heights. On the basis of these measurements and the metrology of the electrodes a set of precise shims spacers was manufactured to compensate for errors on stems and electrodes. The new electrodes were installed in their positions with the adapted shims during the second installation campaign (June 2017). The top and side positions of all electrode supports were measured. The measuring positions are indicated as red spots in Fig. 1. As seen in Fig. 1 the deviations of the measured and calculated positions are within ±40 and ±10 microns for the top and side surfaces respectively.

Content from this work may be used under the terms of the CC BY 3.0 licence (© 2018). Any distribution of this work must maintain attribution to the author(s), title of the work, publisher, and DOI.

ISBN: 978-3-95450-194-6 ISSN: 2226-0366 doi:10.18429/JACoW-LINAC2018-TH1A01

FIRST EVER IONIZATION COOLING DEMONSTRATION IN MICE

J. Y. Tang*, Institute of High Energy Physics, CAS, 100049 Beijing, China
on behalf of the MICE Collaboration

Abstract

The Muon Ionization Cooling Experiment (MICE) at RAL has studied the ionization cooling of muons. Approximately 350 million of individual particle tracks have been recorded passing through a series of focusing magnets in different configurations with a liquid hydrogen, lithium hydride or polyethylene (wedge) absorber. Measurements of the tracks upstream and downstream of the absorber have shown the expected effects of the 4D emittance reduction as a consequence of ionization cooling. This invited talk presents and discusses these results, and projects the future of ionization cooling.

INTRODUCTION

Muon cooling is one of the basic techniques required for a neutrino factory and muon collider [1]. The international Muon Ionization Cooling Experiment (MICE) at RAL was established to demonstrate the principle and relevant technology [2]. One way of producing high-intensity muons is to collide a high-power proton beam with a target, producing pions that then decay into muons. However, the tertiary muon beam has a very large emittance, typically between 15-20 πmm·rad. In order to optimize the muon yield and fit the beam into cost-effective apertures for further acceleration, one would need to reduce the beam emittance. The desired muon normalized beam emittance at the neutrino factory ranges between 2 and 5 πmm·rad. An initial muon collider needs further cooling with a desired normalized transverse emittance of 0.4 πmm·rad and normalized longitudinal emittance of 1 πmm·rad. Ionization cooling is the only beam cooling technique suitable for reducing the muon beam emittance within the short muon lifetime. MICE successfully demonstrated this technique for the first time.

BEAMLINE

The proton beam used for muon production in MICE is produced by the ISIS proton synchrotron at RAL [3], with a kinetic energy of 800 MeV in a parasitic mode to the operation of the ISIS spallation neutron source and muon source. As shown in Fig. 1, a triplet of quadrupole magnets (Q1, Q2, and Q3), two dipole magnets (D1 and D2), and one decay solenoid (DS) are used for pion transport and proper pion momentum selection, pion decay and muon momentum selection.

Two more triplets prepare the muon beam into the muon cooling channel [4]. As a result, the beam that enters MICE has a small pion content. To ensure further muon beam purity, these pions are tagged and rejected from the cooling measurement using a series of particle identification (PID) detectors (Fig. 2) [5].

* tangjy@ihep.ac.cn

MICE DETECTORS AND ABSORBERS

MICE detectors can be divided into PID and tracking detectors. The primary PID detectors are three Time of Flight (ToF) counters (ToF0, ToF1, and ToF2) made of scintillating slabs. Electrons and pions can be distinguished by their different flight times with the same momentum. In addition, two aerogel Cherenkov detectors help the rejection of pions and electrons. The KLOE-Light (KL) detector is a calorimeter and uses lead layers alternating with scintillating fibers to differentiate between particles based on their energy depositions. Electrons shower in KL and as a result have broader KL distributions compared to muons and pions. The most downstream calorimeter is the Electron Muon Ranger (EMR), made of planes of scintillator extrusions, which makes use of the differing particle track topologies. Electron showers in the EMR typically miss some planes as they travel along their paths (occupancy < 1) in contrast to muon tracks which consistently hit all planes (occupancy ≈ 1) [6].

MICE has two tracking detectors, upstream and downstream of the absorber [7]. Each tracker is composed of five planar scintillating-fiber stations, each with three doublet fiber layers, and is immersed in the solenoidal field of a Spectrometer Solenoid (SS). The upstream and downstream SS consist of five superconducting coils; two match the muon beam into and out of the absorber, and three produce constant fields inside the tracking volumes. For measurement of beam cooling, the input and output beam distributions are compared at the tracker stations immediately upstream and downstream of the absorber (tracker reference planes).

Three kinds of absorbers were used in the cooling experiments, first with lithium hydride (LiH), then liquid hydrogen (LH2) and a wedge type of polyethylene. LiH and LH2 were used to demonstrate the cooling effect in the transverse phase space, and the wedge polyethylene was to demonstrate the emittance exchange between the transverse space and the longitudinal space.

MEASUREMENT OF MUON IONIZATION COOLING

Ionization cooling occurs when muons travel through an absorbing material and undergo a “soft” inelastic collision. With the incoming muon energies significantly larger than the binding energies of the atomic electrons of the material, the atom ionizes, ejecting a valence electron [8]. Concurrent with the ionization energy loss process, elastic collisions with the atomic nuclei of the material can occur. Given the larger mass of the atomic nuclei compared with the incident muons, this process causes very small energy loss [2]. However, it is the driving force behind

Content from this work may be used under the terms of the CC BY 3.0 licence (© 2018). Any distribution of this work must maintain attribution to the author(s), title of the work, publisher, and DOI.

ISBN: 978-3-95450-194-6 ISSN: 2226-0366 doi:10.18429/JACoW-LINAC2018-TH1A03

HIGH BRIGHTNESS ELECTRON BEAMS FROM PLASMA-BASED ACCELERATION*

A. Marocchino†, E. Brentegani, A. Biagioni, E. Chiadroni, M. Ferrario,
A. Giribono, F. Filippi, R. Pompili, C. Vaccarezza INFN-LNF, Frascati, Italy
A. Cianchi, University of Rome Tor Vergata, Rome, Italy
A. Bacci, A. R. Rossi, INFN MIlano Milano, Italy
V. Petrillo, Università di Milano Milano, Italy

Abstract

Plasma Wakefield acceleration is a promising new acceleration technique that profits by a charged bunch, e.g. an electron bunch, to break the neutrality of a plasma channel to produce a wake where a trailing bunch (or witness) is eventually accelerated. The quest to achieve extreme gradient conserving high brightness has prompted to a variety of new approaches and techniques. Most of the proposed schemes are however limited to the only plasma channel, assuming in the vast majority of cases, ideal scenarios (e.g. ideal bi-gaussian bunches and uniform density plasma channels). Realistic start-to-end simulations, from the photo-cathode to FEL via a high gradient, emittance and energy spread preserving plasma section, are mandatory for paving the way towards plasma-based user facilities.

INTRODUCTION

Plasma-based accelerators (PBAs) represent, today, a new frontier for the development of compact advanced radiation sources and next generation linear colliders. High brightness electron beams are the future goal of such kind of accelerators, a new technology that is envisioned to compete with the RF technology. Since the very first conception [1] great effort (with equivalent progress) has been placed [2–8] to demonstrate the acceleration of electron beams with gradients of the order of several tens of GV/m, produced either by a laser drive (LWFA) or with a particle driven (PWFA). In PWFA the high gradient wakefield is induced by a high-energy charged particle beam (referred to as driver bunch) travelling through a pre-ionised plasma. The background electrons by shielding the charge breakup produced by the driver induce an accelerating field. The second bunch (referred to as trailing bunch or witness) placed on the right phase is so accelerated by the induced electric field [9–11].

The aforementioned publications indicate that either LWFA and PWFA are capable to produce strong accelerating gradients, but do not address the issue of beam acceleration with quality retention. In other words, the capability for a PWFA scheme to accelerate a trailing bunch with an acceptable quality for any scientific applications, such a Free Electron Laser (FEL) or a future particle-particle collider, or even for medical applications is still an open question.

The work presented in this proceeding tries to address the problem of quality bunch transport numerically for a PWFA scheme. The scheme proposed leverages on the well establish RF know-how to produce and manipulate the bunches to match the strict plasma matching requirements, so that, once injected into the plasma the trailing bunch is boosted to the desired energy. The scheme can thus be decoupled into two parts. A first stage aims in generating two electron bunches (the driver and the trailing bunch) with a given time-separation so that once injected into the plasma they will be at right phase to maximize acceleration. The generation, distance positioning and acceleration is achieved using the COMB [12] technique and an RF in the X-band regime, for a final particle energy of 500 MeV. The plasma with a 10^{16} cm^{-3} number density is confined by a millimeter diameter capillary and ionized with plasma discharges, accelerates the particles from 500 MeV to 1 GeV in about 30 cm. The particle extracted from the plasma accelerating section are then injecting into a FEL. The evolution of the beam, from the photo-injector to the FEL via the plasma cell, is performed with a *single* simulation by concatenating several codes used to addressed the different physics occurring in the different accelerating section. We refer to this single simulation as a *start-to-end* simulation. This work is part of EuPRAXIA [13, 14] (European Plasma Research Accelerator with eXcellence In Applications) European project whose final goal is to use PBA to seed a FEL for physical and biological applications. Specifically EuPRAXIA@SPARC_LAB [14] is the envisioned EuPRAXIA European Italian-located facility operating at 1-5 GeV for FEL experiments.

INJECTOR

A comb-like configuration for the electron beam is used to generate simultaneously a 200 pC driver followed by a 30 pC trailing bunch. The comb-like operation foresees the generation of two or more bunches within the same RF accelerating bucket through the so-called laser-comb technique [12, 15] consisting in a train of laser time-spaced pulses illuminating the photocathode. The witness arrives earlier than the driver on the photocathode and then they are reversed in time at the end of the velocity bunching process, during which the longitudinal phase space is rotated. Experimental results have been obtained at SPARC_LAB where the laser-comb technique is routinely used in order to produce trains of multiple electron bunches [16] for narrow-band

* Work supported by European Union Horizon 2020 research and innovation program, Grant Agreement No. 653782 (EuPRAXIA)
† alberto.marocchino@lnf.infn.it

Content from this work may be used under the terms of the CC BY 3.0 licence (© 2018). Any distribution of this work must maintain attribution to the author(s), title of the work, publisher, and DOI.

ISBN: 978-3-95450-194-6 ISSN: 2226-0366 doi:10.18429/JACoW-LINAC2018-TH1A04

THE PROTON DRIVEN ADVACED WAKE FIELD ACCELERATION EXPERIMENT (AWAKE) AT CERN*

S. Doebert on behalf of the AWAKE collaboration

Abstract

The Advanced Proton Driven Plasma Wakefield Acceleration Experiment (AWAKE) aims at studying plasma wake field generation and electron acceleration driven by proton bunches. It is a proof-of-principle R&D experiment at CERN and the world's first proton driven plasma wake field acceleration experiment. The experiment uses the 400 GeV proton beam from the super proton synchrotron (SPS) which travels through a 10 m long Rb-vapour plasma cell where it gets self-modulated and generates the plasma wake fields. An electron witness beam is injected externally to probe the wake-fields. AWAKE has completed several experimental campaigns, starting in 2016. Results from the initial characterization of the plasma cell and measurements of the seeded self-modulation of the proton beam will be presented. First results on electron witness beam acceleration using the proton driven plasma wake field have been obtained recently and are presented in this paper.

INTRODUCTION

The AWAKE experiment at CERN aims to study and demonstrate for the first time proton driven wakefield acceleration. Laser driven plasma wake field acceleration (LPWA) has been proposed almost 40 years ago [1] and impressive experimental results have been achieved in recent years, demonstrating several GeV electrons from a short plasma cell [2,3]. LPWA provides very high gradients over short, centimetre scale length. To reach particle energies suitable for high-energy physics many acceleration stages have to be coupled and therefore dephasing and energy depletion issues need to be solved.

A second well known and already demonstrated option is electron driven plasma wakefield acceleration, here gradients of the order of 50 GV/m over meter scale plasmas have been demonstrated [4,5]. This scheme suffers from a limited energy transfer from the drive bunch to the witness bunch [6] and therefore requires as well a large number of stages to reach TeV scale energies.

Proton driven wakefield acceleration has in principle the potential to overcome these challenges since high energy proton bunches carry enough energy to accelerate electrons to TeV scale energies in a single stage [7]. Readily available proton beams come from large synchrotrons and have therefore a long, centimetre scale, bunch length, prohibiting high wakefields when used as a driver. The AWAKE experiment therefore uses a seeding laser pulse to trigger a self modulation resulting in a micro-bunching of the long proton bunches [8]. These micro-bunches can then drive the plasma wake fields resonantly up to GV/m gradients. This process will be described below in more detail.

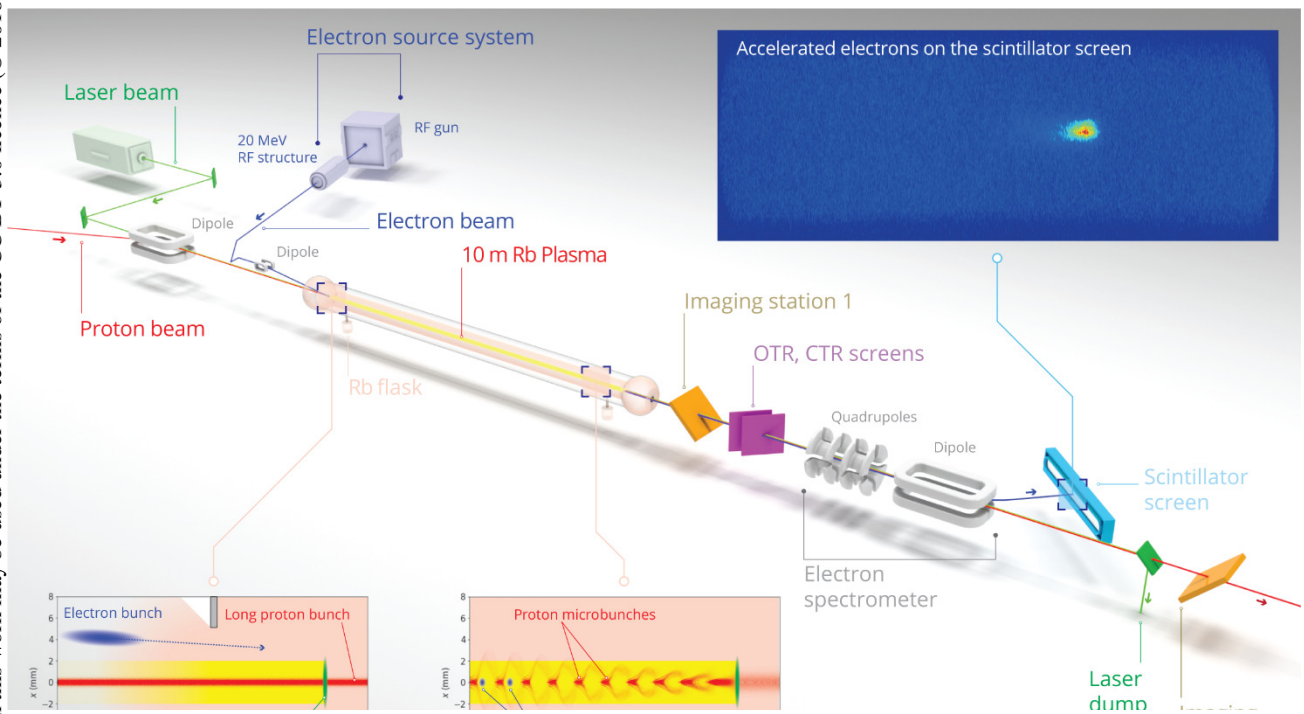


Figure 1: Schematic layout of the AWAKE experiment at CERN. A proton beam from the SPS (left) is focused into a plasma cell. A laser beam and an electron beam are injected synchronized to generate the plasma and probe the wakefileds. A diagnostic section (right) allows to observe the self-modulation process and the accelerated electrons.

Content from this work may be used under the terms of the CC BY 3.0 licence (© 2018). Any distribution of this work must maintain attribution to the author(s), title of the work, publisher, and DOI.

ISBN: 978-3-95450-194-6 ISSN: 2226-0366 doi:10.18429/JACoW-LINAC2018-TH1A05

JITTER STUDY FOR THE APS LINAC PHOTO-INJECTOR BEAM*

D. Hui[1, †], Y. Sun, M. Borland, J. Byrd
Advanced Photon Source, Argonne National Laboratory, Argonne, Chicago, USA
[1]also at Chinese Academy of Sciences, Beijing, China

Abstract

The APS Linac photo-injector can deliver high brightness electron beams to the Linac Extension Area (LEA) for beam experiments such as TESSA (Tapering Enhanced Stimulated Superradiant Amplification). Beam jitter in the device-under-test (DUT) area of the LEA can adversely affect the quality of data for such experiments. In this paper, a start-to-end simulation of jitter is studied. Sources of jitter include photo-cathode drive-laser arrival time, laser energy, and RF phases and voltages of the photo-cathode gun and accelerating cavities. It is found that at the DUT the relative mean energy jitter is the most significant concern, and that improvements in the Linac RF voltage stability can help to reduce it. RMS energy spread are more sensitive to the laser timing and charge jitter. The laser timing jitter itself can be compressed by the magnetic chicane by a factor of 5.6.

INTRODUCTION

The APS LEA, which is downstream of the APS injector Linac, is designed and being built at Argonne National Laboratory (ANL) to provide high brightness electron beams for advanced beam experiments such as Tapering Enhanced Stimulated Superradiant Amplification (TESSA) and dielectric wakefield accelerator [1-3]. The photo-injector, which is equipped with an upgraded LCLS style Photo-Cathode Gun (PCG), will deliver the high brightness electron beams through the injector Linac down to the LEA.

The high brightness beam in the LEA experiment chamber is dedicated to small aperture apparatuses. Beam jitters in the device-under-test (DUT) area of LEA result in the degradation of the beam quality (such as emittance and energy spread growth, bunch arrival time and bunch length jitters), which will adversely affect the quality of data for the experiments. Characterization of the beam jitter and knowledge about its possible origins are of great importance to compensate or reduce the jitters for future stability improvements of the system. In this paper, *Astra* [4] and *Elegant* [5] codes are combined to study the beam jitter and sensitivity to various jitter sources including photo-cathode drive-laser arrival time and energy (i.e. charge), gun and Linac RF phases and voltages. Beam parameters of particular interest are the relative mean energy, energy spread, bunch arrival time, bunch length etc. Firstly, the beam responses at the DUT to each jitter source are studied, and then the combined effects with jitter in all sources. Jitter correlations between all the studied jitter sources and key beam properties at the DUT are also studied.

APS LINAC AND LEA OVERVIEW

Figure 1 shows a schematic of the APS Linac down to LEA. There are two thermionic RF guns, RG1 and RG2, for usual injector operation (RG1 is a back-up). The PCG, with a maximum field gradient of 120 MV/m, is at the front end of the Linac. And a 3m S-band accelerating structure- "L1", is equipped downstream of it, delivering the PCG beam to an energy of approximately 40-45 MeV. Then three accelerating sectors known as Linac Two, Linac Four, and Linac Five ("L2", "L4" and "L5") is followed. Each sector uses a single SLEDed klystron to drive four S-band accelerating structures, accelerating the beam to a total energy up to 375-500 MeV at the end of L5. A bunch compressor chicane (R56=-65) is set behind the L2 to realize the bunch length compression with a given energy chirp [6], so that provide higher bunch brightness beam into the LEA experiment area. Three fast switching dipole magnets are set downstream of the Linac structure to ensure the interleaving operation for RG beam and PCG beam. During the RG beam operation, the three fast switching dipole magnets are turned on to inject the beam into and extract out of the PAR, and then send into the Booster. These magnets are all turned off during the PCG beam operation, so that the PCG beam will bypass the PAR and Booster, then go straight to the LEA [7]. The RG beam for APS storage ring and the PCG beam for LEA will be operated simultaneously though the Linac in an interleaved fashion. The experiment area in the LEA tunnel is where the DUT will be installed. It is sufficient to accommodate DUTs with up to 2m length. To measure the effect of the DUT on the electron beam, a magnetic spectrometer and several diagnostic YAG screens (not shown here) are also installed downstream of the DUT.

START-TO-END JITTER STUDY

In order to understand the beam properties in the DUT under various jitter sources and provide a guidance for the jitter tolerances of the global Linac, an elaborate beam jitter study using tracking codes has been performed. The simulations apply repeated 6D particle tracking for 150 times with 10k macro-particles per tracked beam pulse while varying machine parameters such as photo-cathode drive-laser arrival time and energy, gun and Linac RF phases and voltages. Also, a beam file with no errors is used as an ideal reference case. The reference bunch is

*Work supported by by the U.S. Department of Energy, Office of Science, under Contract No. DE-AC02-06CH11357.
† dhui@anl.gov

Content from this work may be used under the terms of the CC BY 3.0 licence (© 2018). Any distribution of this work must maintain attribution to the author(s), title of the work, publisher, and DOI.

ISBN: 978-3-95450-194-6 ISSN: 2226-0366 doi:10.18429/JACoW-LINAC2018-TH2A01

NITROGEN INFUSION R&D FOR CW OPERATION AT DESY

M. Wenskat[1*], C. Bate[1,2], T. F. Keller[1], A. Dangwal Pandey[1], B. Foster[1,2,3], D. Reschke[1], J. Schaffran[1], G. Dalla Lana Semione[1,2], S. Sievers[1], A. Stierle[1,2], N. Walker[1], H. Weise[1]
[1] Deutsches Elektronen-Synchrotron, 22607 Hamburg, Germany
[2] University of Hamburg, 20148 Hamburg, Germany
[3] Physics Dept., University of Oxford, Oxford, UK

Abstract

The European XFEL cw upgrade requires cavities with reduced surface resistance (high Q-values) for high duty cycle while maintaining high accelerating gradient for short-pulse operation. To improve on European XFEL performance, a recently discovered treatment is investigated: the so-called *nitrogen infusion*. The recent test results of the cavity-based R&D and the progress of the relevant infrastructure is presented. The aim of this approach is to establish a stable, reproducible recipe and to identify all key parameters for the process. Advanced surface analysis is carried out on cut-outs of cavities and samples treated together with cavities. Techniques used include SEM/EDX, TEM, XPS, XRR, GIXRD and TOF-SIMS. The aim of this approach is to establish a stable, reproducible recipe, to identify key parameters in the process and to understand the underlying processes of the material evolution, that result in the improved performance observed.

THE EUROPEAN XFEL

The successful construction of the 17.5 GeV European X-ray Free Electron Laser (XFEL) [1] represents the culmination of over 20 years of superconducting radio-frequency (SRF) R&D. The core high-gradient 1.3 GHz nine-cell niobium cavity and cryomodule technology was originally developed by an international collaboration coordinated by DESY for the TESLA (TeV-Energy Superconducting Linear Accelerator) project — a 500 GeV center-of-mass electron-positron linear collider and integrated X-ray FEL, proposed in 2003 [2].

A total of 102 cryomodules containing 816 cavities have been produced, of which 97 have been installed in the SRF linacs of the European XFEL, which represents by far the largest deployment of TESLA technology to date [3,4]. The cavities achieved an average usable accelerating field of 29.7 ± 5.1 MV/m and an average quality factor Q_0 of 1.2×10^{10} at the design field of 23.6 MV/m in the vertical acceptance test. The design energy of 17.5 GeV of the superconducting linac was met beginning of August 2018.

The design beam pattern for the user operation of the European XFEL has a duty factor of 1.4% with 2.7k bunches per second accelerated up to the maximum energy. As a future upgrade, more flexible beam patterns are planned, allowing 50k bunches per second and a duty factor of 10-50% up to 10 GeV or a continuous wave (cw) mode with 100k bunches per second up to 8 GeV are planned. In order to achieve these duty factors, higher quality factors of the cavities at medium gradients are necessary.

The current plan for the upgrade is to exchange the first 17 cryomodules (136 cavities) in the tunnel (injector plus section L1 and L2) and possibly lengthen L3 using the cryomodules removed which is otherwise kept unchanged, see Fig. 1. An installation of a SRF gun capable of cw operation, and one Klystrode (IOT) for each rf station of 4 modules is further necessary. This will allow the operation of the European XFEL with short pulses at high energies or with high duty cycles at moderate or low energies [5]. Two R&D topics have been identified to increase the Q_0 of the cavities: *large-grain* (lg) material and *nitrogen infusion* [6,7].

Large-grain niobium material has been studied during the European XFEL preparation phase and is characterized by an average grain size on the order of centimeters, which is several orders of magnitude larger than the standard grain size of $\approx$ 50 μm of the material (fine-grain or fg) for the European XFEL cavity production. Eleven nine-cell and several three- and single-cell cavities have been fabricated and showed on average a 25% higher quality-factor Q_0 compared to fine-grain material with the same surface treatment. Furthermore, a pre-series cryomodule called XM-3, consisting of seven lg and one fg cavities, shows excellent results in cw operation [8]. Recent module tests showed stable operation at 17 MV/m with a Q_0 of 2.3×10^{10} at 2K and long pulse operation with duty factors from 22 - 43% up to 22 MV/m.

The emphasis of this paper will be on the investigation and application of a process called *nitrogen infusion*, which was first presented by Fermilab [7]. Several laboratories including DESY are working on the understanding of the process and its influence on the cavity surface and the relation of the changed surface to the rf performance [9–11]. The current status and plans of DESY's efforts are presented here.

INFUSION R&D AT DESY

The R&D program at DESY has three approaches:

- treating cavities in a large furnace, together with samples as quality control, to reproduce the performance improvements
- treating samples in a UHV mobile chamber with in-situ surface characterization to observe and understand the surface evolution

* marc.wenskat@desy.de

Content from this work may be used under the terms of the CC BY 3.0 licence (© 2018). Any distribution of this work must maintain attribution to the author(s), title of the work, publisher, and DOI.

ISBN: 978-3-95450-194-6 ISSN: 2226-0366 doi:10.18429/JACoW-LINAC2018-TH1P01

LINAC4 COMMISSIONING

A.M. Lombardi for the Linac4 Team, CERN, Geneva, Switzerland

Abstract

This paper reviews the design, construction, and commissioning effort of CERN's new proton linear accelerator, Linac4, which has recently been commissioned and which is presently undergoing a reliability run. Linac4 will be connected to the LHC proton injector chain during the next long LHC shutdown (LS2) and will then replace the ageing Linac2.

MOTIVATION AND BEAM QUALITY REQUIREMENTS

In its June 2007 session the CERN Council approved the White Paper "Scientific Activities and Budget Estimates for 2007 and Provisional Projections for the Years 2008-2010 and Perspectives for Long-Term", which included construction of a 160 MeV H^- linear accelerator called Linac4, and the study of a 5 GeV, high beam power, superconducting proton Linac (SPL).

Since 2011 Linac4 became integrated in the framework of the LHC Injector Upgrade program [1] which includes modification to all CERN's LHC injectors to allow increasing of the beam brightness delivered to LHC and opens the way to the parameters needed for the High Luminosity LHC [2].

During the LHC Long Shutdown 2 (LS2) the Linac4 will be physically connected to the CERN PS Booster (PSB) and will inject via charge-stripping up to 1.3 10^{13} protons per ring at 160 MeV (e.g. an average current of 25 mA along the pulse before chopping, injection over 150 turns of 150 μs). The beam injected into each ring can be tailored to durations from 1 to 150 μsec, and its energy can be dynamically varied by ±0.8 MeV over 40 μs and the rms energy spread varied from 85 to 450 keV rms. The 352 MHz microstructure can be modified by a dedicated beam chopper that can impose patterns between 10 ns and 0.7 μs at the frequency of 1-20 MHz to match the shape of the bucket in the PSB and to further optimise the effect of the longitudinal painting [3]. This flexibility is meant to cover all possible beams needed from the PSB and will require a substantial commissioning and tuning period for the optimum working point once the Linac4 beam is injected into the PSB after LS2.

The Linac4 beam attained the final energy of 160 MeV in October 2016 with a peak current of 18 mA, i.e 70% of the minimum current for the high intensity users. Since then a series of dedicated beam runs lasting typically around three months have been scheduled to further access and optimise the beam quality, to test the injection and stripping mechanism and to access the beam availability and reliability. Before the connection to the PSB, two other beam runs are planned between September and December 2018 and between July and September 2019.

LAYOUT

Linac4 is a normal conducting linear accelerator operating at the frequency of 352 MHz. The first element of Linac4 is a RF ion source which can provide a 600 μsec 50 mA H^- beam at 45 keV with a maximum repetition rate of 2 Hz. The beam is then matched to the first stage of RF acceleration (from 45 keV to 3 MeV) in a 3 m long Radio Frequency Quadrupole. At 3 MeV the beam enters a 3.6 meter long Medium Energy Beam Line (MEBT), consisting of 11 quadrupoles, 3 bunchers and two sets of deflecting plates. The beam is "chopped" by removing selected micro-bunches in the 352 MHz sequence to match the beam to the distribution system (which delivers the beam to the 4 superimposed PSB rings) and to the 1 MHz CERN PSB RF bucket. Presently the preferred scheme envisages to chop 133 bunches out of 352 with a resulting average current reduced by 40%. The part described up to now, where the beam quality for the PSB is determined, goes under the name of pre-injector. After the pre-injector the beam is further accelerated to 50 MeV in a conventional Drift Tube Linac (DTL). The DTL, subdivided in 3 tanks, is 19 meters long in total. Each of the 111 drift tubes is equipped with a Permanent Magnet Quadrupole (PMQ). The acceleration from 50 to 100 MeV is provided by a Cell-Coupled Drift Tube Linac (CCDTL). The CCDTL is made of 21 tanks of 3 cells each for a total length of 25 meters. Three tanks are powered by the same klystron, and constitute a module. The focusing is provided by electromagnetic quadrupoles placed outside each module, with PMQs between coupled tanks. The acceleration from 100 to 160 MeV is done in a PI-Mode structure (PIMS). The PIMS is made of 12 tanks of 7 cells each for a total of 22 m. Focusing is provided by 12 Electromagnetic Quadrupoles (EMQ). A 70 m long transfer line, including 17 electromagnetic quadrupoles, 5 dipole bendings (3 horizontal and 2 vertical) and a PIMS-like debuncher cavity connects the Linac4 high energy end to the present injection line into the PSB. The existing line (110 m in length) will not be modified as it can accommodate and match the beam from Linac4 to the new H^- injection system. It contains 16 electromagnets to transport the beam and match the dispersion, two bending magnets and a distributor to send the beam in the 4 superimposed PSB rings.

A sketch of Linac4 is shown in Fig.1.

Content from this work may be used under the terms of the CC BY 3.0 licence (© 2018). Any distribution of this work must maintain attribution to the author(s), title of the work, publisher, and DOI.

ISBN: 978-3-95450-194-6 ISSN: 2226-0366 doi:10.18429/JACoW-LINAC2018-TH1P02

INJECTION COMPLEX DEVELOPMENT FOR THE NICA PROJECT

A.V. Butenko, A.I. Govorov, B.V. Golovenskiy,D.E. Donets, A.D. Kovalenko, ,K.A. Levterov, D.A. Lyuosev, A.A. Martynov, V.V. Mialkovsky, V.A. Monchinskiy , D.O. Ponkin, K.V. Shevchenko, A.O. Sidorin, I.V. Shirikov, A.V. Smirnov, G.V. Trubnikov
Joint Institute for Nuclear Research, Dubna, Moscow Region, Russia
T.V. Kulevoy
Institute of Theoretical and Experimental Physics NRC "Kurchatov Institute", Moscow, Russia
S.M. Polozov
National Research Nuclear University – Moscow Engineering Physics Institute, Moscow, Russia
H.Höltermann, U.Ratzinger, A.Schempp, H.Podlech
BEVATECH GmbH, Frankfurt, Germany

Abstract

Wide international collaboration is working on construction of NICA collider complex at JINR, Dubna. The main goal of new collider is investigation of the heavy ion collisions with center-of-mass energy up to about √s = 11 GeV/u. Injection complex of the project is under development, it consists of two synchrotron rings with two linear accelerators. Current status of the injection complex development and latest results are presented in this paper.

INTRODUCTION

Nuclotron-based Ion Collider fAcility (NICA) (Fig. 1.) is new accelerator complex developing and constructing at JINR [1] for ion collision and high-density matter study.

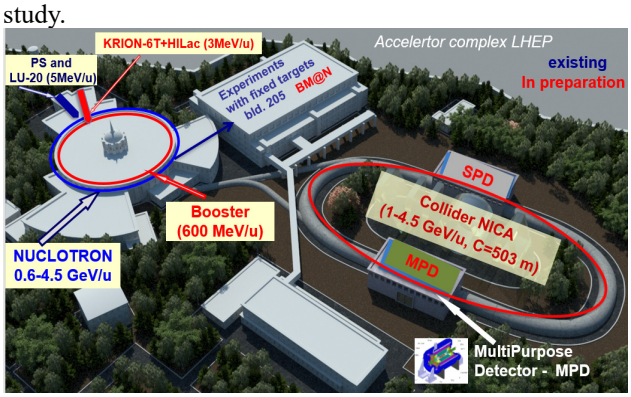


Figure 1: The NICA complex.

For the NICA collider ion beams from p to Au ions with energies from a few hundred MeV/u up to a few GeV/u will be provided by two injection LINACs and two superconducting synchrotrons: the Booster and the Nuclotron. The beams are generated by three new ion sources: SPI (Source of Polarized Ions), LIS (Laser Ion Source) and Krion (ESIS type heavy ion source). The ion sources feed two LINACs: the existing linac LU-20 with a new RFQ as pre-injector and the new heavy ion linac – HILAc. Design and development of RFQ, MEBT and two IH sections of the HILAc was performed by Bevatech GmbH (Frankfurt, Germany) [2] and described in detail in [3]. HILAc commissioning was performed with the C^{3+}, C^{2+} and Fe^{14+} beams from the laser ion source.

HILAC

The main parameters of the HILAc (Fig. 2) are given in the Table 1.

Table 1: HILac Parameters

A/q	6.25
Current	< 10 emA
Pulse length	10 μs – 30 μs
Rep. rate	< 10 Hz
LEBT energy	17 keV/u
RFQ energy	300 keV/u
IH1 energy	1.87 MeV/u
IH2/LINAC max. energy	3.2 MeV/u

The HILac RFQ is a 4-rod structure operating at 100.625 MHz.The RFQ tank is a 3.16 m stainless steel tank of 0.35 m in diameter which is copper-plated inside. The RFQ is powered by a 140 kW solid state amplifier.

The first IH tank contains an internal quadrupole triplet lens. The IH1 and IH2 have 2.42 m and 2.15 m outer length correspondingly. For the design A/q – value of 6.5 the sum voltage gain is 20.8 MV. Both IH cavities are powered by 340 kW solid state amplifiers, one for each cavity.

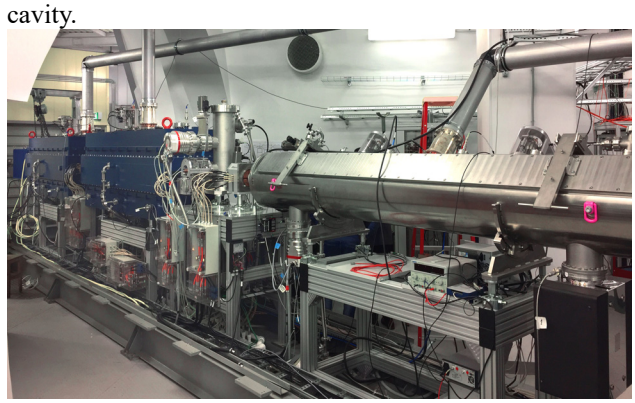


Figure 2: HILAC at JINR.

Before installing the IH cavities the RFQ has been tested with beam. The beam energy was measured with a

Content from this work may be used under the terms of the CC BY 3.0 licence (© 2018). Any distribution of this work must maintain attribution to the author(s), title of the work, publisher, and DOI.

ISBN: 978-3-95450-194-6 ISSN: 2226-0366 doi:10.18429/JACoW-LINAC2018-TH1P03

NEW TRENDS IN PROTON AND CARBON THERAPY LINACS

S. Benedetti*, CERN, Geneva, Switzerland

Abstract

In the last years, many developments have contributed to make feasible an all linac solution for proton and carbon ion therapy, with typical output energies of about 200 MeV and 400 MeV/u, respectively. The efficient beam matching of the source to the high-energy linacs, operating at 3 GHz, represents one of the major challenges. With the successful test of a 750 MHz RFQ at CERN, this possibility starts to be a reality. At the same time CERN is testing a high-gradient S-band cavity, successfully exceeding the accelerating gradient goal of 50 MV/m - more than twice what has been obtained before - and paving the way to more compact medical facilities. In this paper, some of the most significant projects involving linear accelerators for hadron therapy will be presented.

INTRODUCTION

The energy gain ΔW across a RF cavity is proportional to:

$$\Delta W \propto \sqrt{ZTT \cdot P_d \cdot L} \tag{1}$$

where ZTT is the effective Shunt impedance of the cavity, P_d is the dissipated power on the cavity walls and L the cavity length. Eq. (1) shows that, for a given energy gain and cavity design, one can either increase the power consumption P_d and decrease the cavity length L, or vice versa. At the same time, it can be shown that the cavity design, so its ZTT, is a function of the maximum accelerating gradient achievable, and in particular the higher the accelerating gradient, the lower is the ZTT achievable. Hadron therapy linacs can be thus divided into high-gradient and high-efficiency designs. Though arbitrary, the separation bar between the two approaches can be set at 30 MV/m accelerating gradient; linacs designed for values lower or equal than this threshold can be referred as high-efficiency designs.

Proton therapy linacs have been designed in both high-gradient and high-efficiency solutions. Carbon ions linacs have been predominantly designed in high-efficiency solutions, to limit the RF power consumption [1]. However in recent years a researchers are working on a high-gradient design for carbon ions [2]. The different projects are listed in Table 1.

Two of the most important developments of recent years have been started at CERN. Those are the construction and test of a 750 MHz RFQ [3,4] and of a 50 MV/m accelerating gradient 3 GHz cavity for a relativistic beta of 0.38 [5], corresponding to approximately 70 MeV/u. The 750 MHz RFQ solved the issue of the efficient low energy acceleration and control of the beam, bridging the gap between the ion source and the 3 GHz accelerating cavities. The 3 GHz cavity designed for 50 MV/m accelerating gradient showed that more compact linac designs can be conceived.

LOW ENERGY BEAM ACCELERATION

The low energy beam acceleration is probably the most difficult part in a linac design. Space charge does not affect a medical linac design thanks to the low beam current - average of few nA - needed. However, the need to reduce the footprint as much as possible makes the design challenging in many different ways.

A key aspect in this regard is the choice of the operating frequency f_{RF}. The scaling law $ZTT \propto \sqrt{f_{RF}}$ [6] relates the cavity effective Shunt impedance ZTT with the resonating frequency f_{RF}, and it is valid if the cavity beam aperture is scaled accordingly with the frequency. This is not always possible due to beam dynamics constraints, and in addition different geometries, as the drift tubes in drift tube linacs (DTL) or the septum thickness in coupled cavity linacs (CCL) are bounded in the minimum dimension by mechanical and thermal limitations. For these reasons, while in principle it would be ideal to increase the cavity operating frequency, in reality an optimum has to be found. For hadron therapy linacs it has been historically chosen a frequency of 3 GHz [7], in order to profit of the availability of relatively cost-effective power supplies developed for radiotherapy linacs. In [8] it has been showed that for a proton therapy linac design a 3 GHz solution has to be preferred over a 6 GHz one.

Before 2014, existing RFQs did not have high enough operating frequencies to efficiently inject the beam into the longitudinal acceptance of 3 GHz linacs. In the 2011 TOP-IMPLART project [9, 10] a 425 MHz commercial injector, composed by a 3 MeV RFQ and a 7 MeV DTL, inject into a 3 GHz side coupled DTL (SCDTL), with losses. Researchers proposed the so called cyclinac design [7], where a commercial cyclotron provides the beam acceleration up to 20 to 30 MeV for protons, and around 150 MeV/u for carbon ions, followed by the 3 GHz linac. In this case even higher losses occurred at the injection in the 3 GHz linacs.

The 750 MHz CERN RFQ was explicitly designed to inject into 3 GHz cavities, accepting losses in the RFQ itself but preserving full transmission and a good beam matching in the transition from 750 MHz to 3 GHz, thus maintaining constant the normalized beam emittance. The CERN 750 MHz RFQ is now successfully in operation [11] in the ADAM bunker in the CERN ALICE area.

For low energy beam acceleration, three different type of linear accelerators are usually considered: RFQs, SCDTLs and H-mode DTL cavities. A qualitative assessment of their advantages and disadvantages is proposed in Fig. 1. Each accelerator has been ranked from one to three considering four aspects: the RF efficiency, the maximum accelerating

* stefano.benedetti@cern.ch

Content from this work may be used under the terms of the CC BY 3.0 licence (© 2018). Any distribution of this work must maintain attribution to the author(s), title of the work, publisher, and DOI.

ISBN: 978-3-95450-194-6 ISSN: 2226-0366 doi:10.18429/JACoW-LINAC2018-THPO001

DESIGN STUDY ON CEPC POSITRON DAMPING RING SYSTEM*

D. Wang †, C. Meng, J. Gao, D. Gong, J. Zhang, G. Pei, Y. Chi, IHEP, Beijing 100049, China

Abstract

The primary purpose of CEPC damping ring is to reduce the transverse phase spaces of positron beam to suitably small value at the beginning of linac and hence reduce the beam loss in the booster. Before damping ring, an energy spread compression structure is designed to match the RF acceptance of damping ring. A longitudinal bunch length control is also necessary to meet the energy spread requirement in the linac by a bunch compressor system after the damping ring. Both designs for damping ring and energy/bunch compressors are discussed in this paper.

INTRODUCTION

So far, the whole CEPC system is composed of three parts: a linac, a booster, the collider ring [1]. The linac injector system is composed of a 10 GeV S-band linac with electron/positron source and a 1.1 GeV damping ring. The layout of CEPC accelerator chain is shown in Fig. 1.

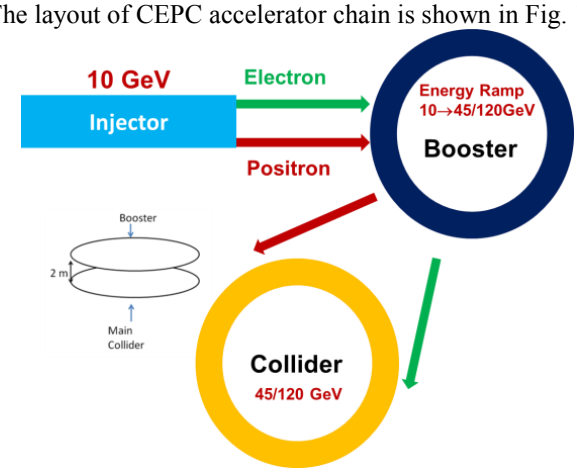


Figure 1: Sketch of CEPC accelerator chain.

The repetition rate of Linac is 100 Hz and one-bunch-per-pulse is considered. To achieve larger than 3 nC positron bunch, a 4 GeV primary electron beam with 10 nC hit tungsten target. The large transverse emittance of the positron beam emerging from the target is transformed to match pre-accelerating section with AMD flux concentrator. The captured positron beam will be pre-accelerated to 200 MeV. Each positron bunch is injected into damping ring every 10 ms and two bunches are stored in the ring so that the storage time for each bunch is 20 ms. The layout of CEPC Linac and damping ring is shown in Fig. 2.

* Work supported by the National Key Programme for S&T Research and Development (Grant NO. 2016YFA0400400) and the National Natural Science Foundation of China (11505198 and 11575218).
† wangd93@ihep.ac.cn

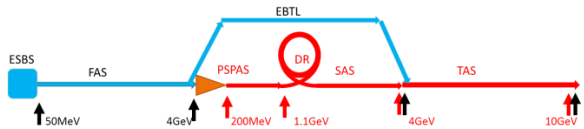


Figure 2: Sketch of CEPC Linac and damping ring.

DAMPING RING DESIGN

The energy of DR is 1.1 GeV and the circumference is 75.4 m. The DR has a racetrack shape and the arcs were designed with 60 degree FODO cell.

The injected emittance (normalized) for DR is 2500 mm·mrad and the injected energy spread is smaller than 0.2%. The positron beam will be stored in DR for 20 ms according to the 100 Hz repetition rate and two-bunch storage scheme. The extracted emittance is better to be smaller than one quarter of the injected emittance. Considering the issue of injection efficiency, the transverse acceptance of DR should be larger than five times of the injection beam size.

DR Parameter Design

The parameters of damping ring are calculated analytically based on the method in reference [2]. The layout of damping ring is shown in Fig. 3 and the main parameters are listed in Table 1.

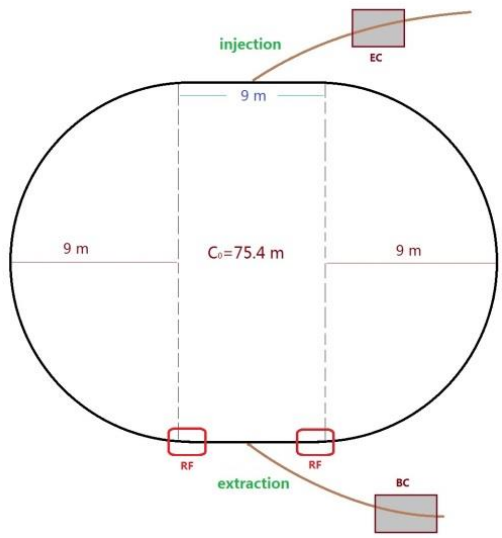


Figure 3: Layout of CEPC damping ring.

Table 1: Main Parameters of Damping Ring

	DR V2.0
Energy (Gev)	1.1
Circumference (m)	75.4
Bending radius (m)	3.6
Dipole strength B_0 (T)	1.03
U_0 (kev/turn)	36.3
Damping time x/y/z (ms)	15.2/15.2/7.6

Content from this work may be used under the terms of the CC BY 3.0 licence (© 2018). Any distribution of this work must maintain attribution to the author(s), title of the work, publisher, and DOI.

ISBN: 978-3-95450-194-6 ISSN: 2226-0366 doi:10.18429/JACoW-LINAC2018-THPO002

INVESTIGATION OF SRF ELLIPTICAL CAVITIES MADE BY NEW Nb MATERIALS IN KEK

T. Dohmae†, K. Umemori, Y. Watanabe, M. Yamanaka, KEK, Tsukuba, Japan
M.Okada, SOKENDAI, KEK, Tsukuba, Japan

Abstract

Two kinds of in-house 3-cell superconducting RF cavities were fabricated using two kinds of niobium in KEK. These materials are expected to reduce the cost for the cavity material since some processes in niobium production were skipped. Completed cavities were then RF tested in the vertical cryostat to measure their performance. One of them achieved maximum gradient of 40 MV/m with maximum Q_0 value of 1.87×10^{10}.

INTRODUCTION

The International Linear Collider (ILC) is now under contemplation in Japan. Reducing the cost for cavity fabrication is presently one of the main issue to realize ILC. The Cavity Fabrication Facility (CFF) at KEK which enables the entire process of cavity fabrication approached this issue in terms of cavity materials.

The ratio of tantalum in niobium was first focused on to reduce the material cost. An additional chemical process is generally necessary to remove tantalum from niobium. This process arises niobium production cost. Thus niobium which contains high tantalum is cheaper than one contains low tantalum. The production processes of niobium were also focused on for the cost reduction. Several processes such as melting, forging and rolling are necessary to produce niobium sheets and tubes used for cavity. Skipping some of these process can also reduce material production cost.

The main purpose of this study is evaluation of new niobium for cavity materials which are expected to reduce the cost. Several cavities were fabricated and RF tested using these materials.

FABRICATION

CFF fabricated two types (“type1” and “type2”) of cavities using different materials. The shape of these cavities are all 3-cell Tesla-like [1] shape and designed to be used in 1.3GHz RF operation. Two 3-cell cavities (“cavity1” and “cavity2”) were fabricated for each type respectively.

Type1 Cavity

Figure 1 shows fabricated type1 cavities. Niobium which residual resistance ratio (RRR) is low and containing higher ratio of tantalum was used as start material for type1 cavities. This material was then forged and rolled into niobium sheets and seamless tubes. Niobium sheets were used for stiffener rings and tubes were used for beam tubes. Rest of this material was melted two times by electron beam welding in the vacuum chamber to purify. This melting process is normally done five or more times. Thus, production cost of this material was also reduced. This melted niobium was forged and rolled into niobium sheets and used for cavity cells. RRR of start material was 60~108 (ingot), and it recovered up to 277~298 (ingot). RRR of the sheets (after forge and rolling) used for cells was 293. RRR of ingot varies widely since measured samples were taken from both edges of ingot. RRR are summarised in Table 1. Chemical components of these materials are summarised in Table 2. In Table 2, “Ingot1” represents the value of start materials, “Sheet” represents the value of niobium sheets used for stiffener rings and “Ingot2” represents the value of ingot after two times melting. The start material was supplied by CBMM, and melting, forge and rolling process were done by ULVAC

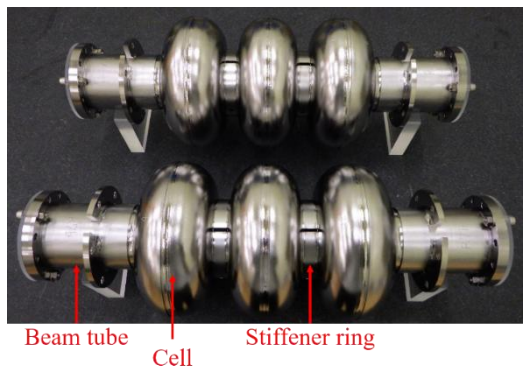


Figure 1: Fabricated type1 cavities and explanation of each parts.

Type2 Cavity

Figure 2 shows fabricated type2 cavities. Niobium sheets directly sliced from niobium ingot which is called large grain (LG) were used for this cavity. Production cost of LG niobium sheet is lower than normal sheet since forge and roll process are skipped. Used niobium sheet for type 2 cavity is shown in Figure 3. LG sheet has strong anisotropy as it has large crystal size which diameter is about 100~150 mm, as shown in Figure 3. This strong anisotropy leads some technical difficulties in fabrication. For example, the roundness of the inside equator is worse than one made of normal sheet due to large deformation after press forming. Hence, a special jig shown in Figure 4 which

Table 1: RRR Values of Materials Used for Each Part of Type1 and Type2 Cavities

	Type1	Type2
Cells	293	242~298
Beam tubes	60~108	60~108
Stiffener rings	60~108	-

Content from this work may be used under the terms of the CC BY 3.0 licence (© 2018). Any distribution of this work must maintain attribution to the author(s), title of the work, publisher, and DOI.

ISBN: 978-3-95450-194-6 ISSN: 2226-0366 doi:10.18429/JACoW-LINAC2018-THPO003

L-BAND RESONANT RING FOR TESTING RF WINDOWS FOR ILC

B.T. Du†,1, T. Matsumoto1,2, S. Michizono1,2, T. Miura1,2, F. Qiu1,2, N. Liu1
[1] SOKENDAI (The Graduate University for Advanced Studies), 240-0193, Hayama, Japan
[2]High Energy Accelerator Research Organization, 305-0801, Tsukuba, Japan

Abstract

A resonant ring is widely used for the breakdown test of RF components under high power. It can reach power gain of more than 10 dB, which is limited by the attenuation of the ring. An L-band resonant ring is constructed for testing RF components of International Linear Collider (ILC) which is based on an RF frequency of 1.3 GHz. The target of the high power test is 5 MW. We have finished the test of an input power of 500 W using a solid state amplifier, and the principle of the resonant ring is verified. The resonant ring is tuned to an optimal condition, which is preparation for high power operation. This paper details the principle, construction, and test of the L-band resonant ring.

INTRODUCTION

The International Linear Collider (ILC) is a 250 GeV linear electron-positron collider, based on the 1.3 GHz superconducting radio-frequency technology [1]. Figure 1 shows the power distribution system (PDS) for ILC. Every PDS contains one 10 MW multi-beam klystron and that drives 39 cavities. Based on Fig. 1, the power on RF window, which is next to the variable power divider, is 1.1 MW. Considering the maximal standing wave, the power on the RF window may be 4 times to theoretical value, which is 4.4 MW. Therefore, it is necessary to test the RF window under 5 MW using a long operating period.

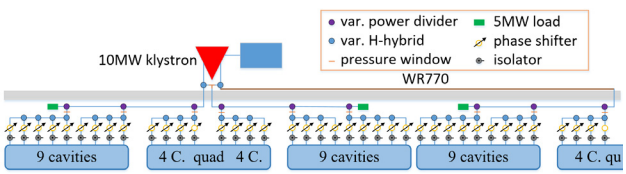


Figure 1: Power distribution system for ILC.

A resonant ring is a closed loop of a waveguide system that can amplify power, and it is widely used for the breakdown test of the RF components under high power [2]. In the superconducting RF test facility (STF), the variable hybrid, the phase shifter and the 500kW circulator have already been developed [3]. Moreover, the 800 kW modulated-anode klystron is developed in the STF, which is employed in the distributed RF system for the ILC [4].

Firstly, we a construct resonant ring with a variable hybrid, a phase shifter and a circulator at a low input power of 500 W from a solid state amplifier. The power gain is compared with one-turn phase of the ring and the coupling factor of the hybrid is tested [5]. The measured result shows that the maximum power gain can reach 10 ~13 dB, and is matched with simulation. A circular power of 5 MW can be achieved by the resonant ring with an input from an 800 kW klystron.

† baiting@post.kek.jp

Secondly, considering the high power test of 5 MW circular power, the ring is expected to be pressurized by SF_6 or N_2 for preventing high power breakdown. The variable hybrid and phase shifter cannot be worked as pressurized due to its construction. Therefore, a fixed 11 dB hybrid is used to replace the variable hybrid and the operating frequency is changed to adjust one-turn phase. Moreover, the 500 kW circulator cannot be used at 5 MW due to the power limit. Even a low reflection generated in the resonant ring will be accumulated in the high reflected power. A 3-stub tuner is inserted in the ring to reduce the reflection in the ring. After adjusting the depth of the stub, the reflection is reduced significantly and the resonant ring worked at an optimal condition with a higher forward power gain.

THEORY AND STRUCTURE

The structure of the resonant ring is shown in Fig. 2. It contains a signal generator, hybrid, dummy load, and certain length of the waveguide system.

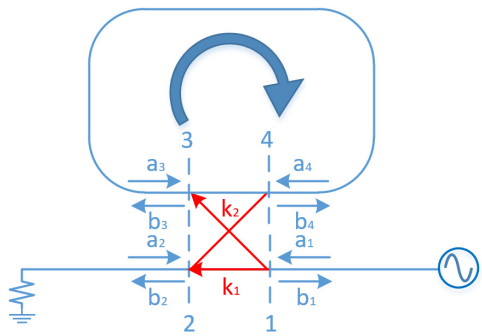


Figure 2: Schematic diagram of the resonant ring.

If the hybrid is assumed to be lossless and symmetrical, with no reflection, then the power gain (G) will be as given in equation (1), where k_1 and k_2 are transmitted and coupling coefficients of the hybrid at voltage respectively; α, β, and L are the attenuation coefficient, phase coefficient, and length of the resonant ring respectively.

$$G = \frac{|b_3|^2}{|a_1|^2} = \frac{k_2^2}{1 + k_1^2 e^{-2\alpha L} - 2k_1 e^{-\alpha L}\cos\beta L} \quad (1)$$

It is obvious that the power gain reaches a maximum when βL=2nπ, where n is an integer. This means that the wave in the ring will be superposed at an optimum condition [6].

$$G_{\max} = \frac{k_2^2}{1 + k_1^2 e^{-2\alpha L} - 2k_1 e^{-\alpha L}} = \frac{1 - k_1^2}{\left(1 - k_1 e^{-\alpha L}\right)^2} \quad (2)$$

Content from this work may be used under the terms of the CC BY 3.0 licence (© 2018). Any distribution of this work must maintain attribution to the author(s), title of the work, publisher, and DOI.

ISBN: 978-3-95450-194-6 ISSN: 2226-0366 doi:10.18429/JACoW-LINAC2018-THPO004

PULSED OPERATION OF CEBAF FOR JLEIC INJECTION*

J. Grames, J. Guo#, R. Kazimi, F. Lin, T. Plawski, R. Rimmer, H. Wang,
JLAB, Newport News, VA 23606, USA

Abstract

The JLab Electron-Ion Collider (JLEIC) proposed by Jefferson Lab is planning to use the 12 GeV CEBAF 1497 MHz SRF CW recirculating linac as a full-energy injector for the electron collider ring, which might be the first SRF electron linac to be used as a storage ring injector. The electron collider ring is proposed to reuse the 476MHz PEP-II RF system to achieve high installed voltage and high beam power. The JLEIC electron injection requires 3-10 (or 12) GeV beam in bunch trains <4μs long with low duty factor and high peak current, resulting strong transient beam loading for the CEBAF. In this paper, we present our recent studies on JLEIC electron injection scheme and CEBAF pulsed operation.

JLEIC ELECTRON INJECTION SCHEME

The propose JLEIC, as shown in Fig. 1, is a high luminosity electron-ion collider with 3 to 10 GeV electrons and 20 to 100 GeV protons (or up to 40 GeV per nucleon for heavy ions), with the possibility to upgrade to higher energy [1, 2]. The nominal beam current in the electron ring is 3 A, but the beam current is limited by 10 MW total synchrotron radiation power at energies higher than 7 GeV. The newly upgraded 12 GeV CEBAF linac is chosen as the full energy injector for the electron ring. The preliminary JLEIC injection scheme with CEBAF was initially developed in 2014 as published in [3], and has been evolved since then.

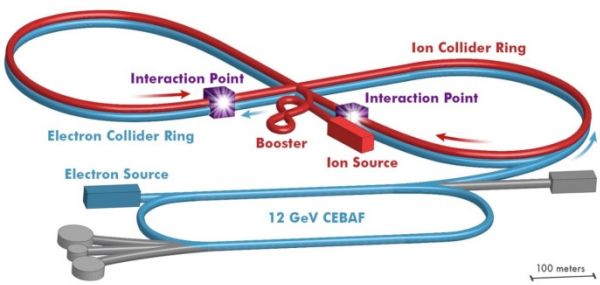


Figure 1: Conceptual layout of JLEIC.

The JLEIC electron injection uses 68.05 MHz bunch repetition rate (and possibly its sub-harmonics in circumstances) , which is 1/22 of the CEBAF RF frequency of 1497 MHz, and 1/7 of the slightly adjusted PEP-II RF system frequency 476.3 MHz. The electron ring has a harmonic number of 3584, with a circumference of around 2256 m and the revolution time of 7.52 μs.

One major capability of JLEIC is colliding polarized electrons with light ions. In this type of runs, the electron rings will provide two bunch trains with opposite spin polarization in the same ring, with two gaps of ~270 ns each in between. The gaps will match the ion ring abort gaps, and serve for the purposes of injection/abort kickers' rise/fall time as well as ion clearing.

The JLEIC electron ring uses transverse phase space injection with damping time τ_d ranges from 6 to 389 ms, depending on the beam energy and the use of damping wigglers. To maximize the total charge injected in one kicker cycle, we can inject a long polarized bunch train into half of the collider ring, with the bunch train length of ~3.5 μs, slightly shorter than the circumference of CEBAF of ~4.38 μs. The kicker cycle has a rise/fall time ~200 ns, and a flat top of 3.5 μs, comparable to the PEP-II abort kickers. At least $2\tau_d$ is needed to damp the injected portion of a bunch before the next kicker bump involving the same bucket; however we can arrange at least two kicker cycles bumping the two halves of the ring during $2\tau_d$. To arrange more than two injections during $2\tau_d$, more gaps might be needed.

CEBAF PULSED OPERATION

The beam in CEBAF can be accelerated during the 6

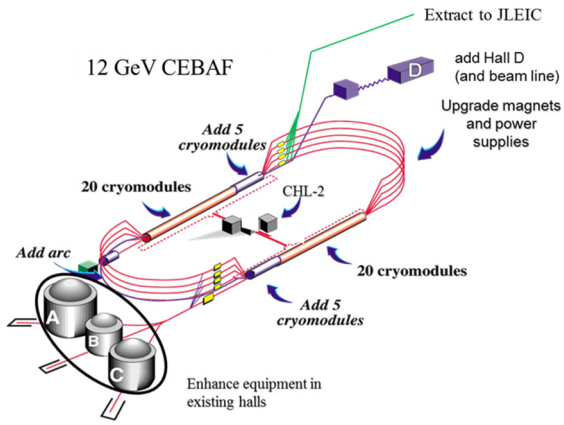


Figure 2: CEBAF after 12 GeV upgrade.

passes in the north linac (NL) and 5 passes in the south linac (SL), before it's extracted to Hall D or JLEIC. If CEBAF RF is operating in the usual CW mode, the major factor limiting the maximum charge in each bunch train is the energy droop along the bunch train caused by the transient beam loading in the SRF cavities. The maximum energy droop is limited by the ±0.2% momentum acceptance of CEBAF arc. If the bunch train is short enough compared to the cavity fill time and the RF feedback delay, and the cavity is operating on-crest on-resonance, the cavity gradient droop under CW RF is

* Authored by Jefferson Science Associates, LLC under U.S. DOE Contract No. DE-AC05-06OR23177
#jguo@jlab.org

Content from this work may be used under the terms of the CC BY 3.0 licence (© 2018). Any distribution of this work must maintain attribution to the author(s), title of the work, publisher, and DOI.

ISBN: 978-3-95450-194-6 ISSN: 2226-0366 doi:10.18429/JACoW-LINAC2018-THPO005

HIGH ASPECT RATIO BEAM GENERATION WITH THE PHASE-SPACE ROTATION TECHNIQUE FOR LINEAR COLLIDERS

Masao Kuriki*,Hiroshima University, Higashihiroshima, Japan
John Power, Argonne National Laboratory, Argonne, Illinois
Hitoshi Hayano, Xiuguang Jin, Taro Konomi, Yuji Seimiya, Naoto Yamamoto, KEK, Tsukuba, Japan
Philippe Piot,Northern Illinois University, Dekalib, Illinois
Shigeru Kashiwagi, Tohoku University, Sendai, Japan
Kazuyuki Sakaue, Masakazu Washio, Waseda University, Tokyo, Japan

Abstract

Linear colliders is the only way to realize e+ e- collision at higher energy beyond the limit of ring colliders by the huge synchrotron radiation energy loss. In the linear collider, the beam current should be much smaller comparing to the ring collider to save the required electricity. A way to realize an enough luminosity with the small beam current and less energy spread by Beamstrahlung, is collision in flat beam. This high aspect ratio beam can be made by phase-space rotation technique instead of the conventional way with DR (Damping Ring). We present a simulation of this technique and pilot experiments at KEK-STF and ANL WFA.

INTRODUCTION

Electron Positron Collider is the only way to realize annihilation of elementary particles with controlled conditions with the current technology. Because there has been no any significant evidence of Super-symmetry in LHC experiments, the significance of detail studies of Higgs boson and searching inconsistency in the standard model with electron positron collider is maximized. ILC (International Linear Collider) [1] is an e+e- linear collider based on superconducting accelerator with CME from 250 to 1000 GeV. It would be constructed in Iwate, Japan, as the main project of High energy physics.

Luminosity L is the index showing the performance of colliders. It can be expressed as

$$L = \frac{f n_b N^2}{4\pi\sigma_x\sigma_y}, \tag{1}$$

where f is repetition of pulse, n_b is number of bunches in a pulse, N is number of particles in a bunch, $\sigma_{x,y}$ is transverse beam size. In the linear collider, the beam after the collision is dumped. If we employ a large current beam in linear colliders as same as in ring colliders, the required wall plug power is huge and such machine is unrealistic. One way to enhance the luminosity is minimize $\sigma_{x,y}$, but it causes a large energy spread by Beamstrahlung as

$$\Delta E \propto \frac{1}{\sigma_z}\left(\frac{2}{\sigma_x+\sigma_y}\right)^2. \tag{2}$$

A practical way to enhance the luminosity and suppress Beamstrahlung simultaneously is squeezing the beam in one of the transverse direction, e.g. $\sigma_x \gg \sigma_y$. For ILC, The beam size at IP is 640 nm in horizontal direction and 5.7 nm in vertical direction. Emittances are 10 and 0.04 mm.mrad in horizontal and vertical directions, respectively [1]. This asymmetric emittance beam is made by radiation damping in a storage ring in the current design. We propose to generate the flat beam for ILC only with the injector by employing the emittance exchange technique.

* mkuriki@hiroshima-u.ac.jp

PHASE-SPACE ROTATION TECHNIQUES FOR LINEAR COLLIDERS

Emittance exchange technique is change the emittance partitioning among the degree of freedom, i.e. x, y, and z. Any partitioning is possible if 6D phase space volume (emittance) is conserved. There are two methods as the phase-space rotation for the re-partitioning. One is RFBT (Round to Flat Beam Transformation) [2] generating the flat beam from an angular-momentum dominated beam produced by beam emission in a solenoid field. Another is TLEX (Transverse to Longitudinal Exmittance eXchange) exchanging the phase-spaces between longitudinal and transverse directions by dipole mode cavity in a dispersive beam line [3]. These two techniques are experimentally demonstrated by P. Piot et al. [4] for RFBT and Y-E Sun et al. [5] for TLEX. The flat beam generation with RFBT and TLEX are explained in Ref. [6] for more detail.

As explained in the introduction, the flat beam is essential to enhance the beam luminosity for linear colliders. In the ILC current design, the emittance at IP are 10 mm.mrad for horizontal direction, 0.04 mm.mrad for vertical direction, and 8.4×10^5 mm.mrad for longitudinal direction. This beam is made up with radiation damping in 3 km DR in the current design [1]. Figure 1 shows the schematic drawing of the injector with DR.

By employing the emittance exchange techniques (RFBT and TLEX), the ILC compatible beam can be generated only with an injector lilac as shown in Fig. 2. 3.1 km DR can be omitted. The emittance budget is summarized in Table1. The first row is required emittance at IP for ILC. The second row is emittance at Gun when we employ only RFBT. In RFBT, the product of ε_x and ε_y is conserved. To make 10 mm.mrad and 0.04 mm.mrad with RFBT, the emittance from Gun should be 0.6 mm.mrad. This small emittance cause several problems. One is emission density. To make this

Content from this work may be used under the terms of the CC BY 3.0 licence (© 2018). Any distribution of this work must maintain attribution to the author(s), title of the work, publisher, and DOI.

ISBN: 978-3-95450-194-6 ISSN: 2226-0366 doi:10.18429/JACoW-LINAC2018-THPO006

STATUS OF 650 MHz SRF CAVITY FOR ERHIC SRF LINAC*

W. C. Xu†, [1], I. Ben-Zvi[1, 2], Y. Gao[1], D. Holmes[1], P. Kolb[1], G. McIntyre[1], R. Porqueddu[1], K. Smith[1], R. Than[1], F. Willeke[1], Q. Wu[1], A. Zaltsman[1],
[1]Collider-Accelerator Department, Brookhaven National Laboratory, Upton, NY, 11790, USA
[2]Physics & Astronomy Department, Stony Brook University, Stony Brook, NY, 11794, USA

Abstract

A 5-cell 650 MHz SRF cavity was design for eRHIC high current SRF linac. One Cu cavity was fabricated for HOM damping study, and one Nb cavity was fabricated for SRF performance study with various post-processing procedures. The SRF performance study includes both high Q-value study (at gradient of 15 ~ 18 MV/m) and high gradient study (> 26 MV/m). This paper reports the HOM measurements results on Cu cavity and first result of vertical test on the Nb cavity.

INTRODUCTION

Collider-Acceletaor Department at Brookhaven National Laboratory (BNL) has been actively working on R&D of an electron-ion collider for more than a decade. This collider, named eRHIC, aims to collide electron beam that is from a new electron accelertor, with proton beams that is provided by existing RHIC [1]. The new electron accelerator will be placed in the RHIC tunnel, and most of components of RHIC will be reused for eRHIC. The layout of eRHIC is shown in Figure 1. To make sure we get the best machine performance with reasonable cost, both ERL-Ring [2] and Ring-Ring eRHIC [3] were studied. However, either design requires high performance SRF cavities.

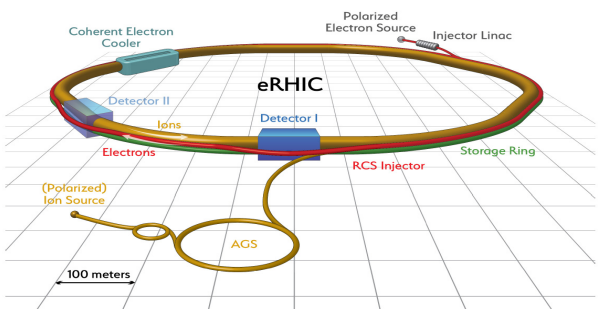


Figure 1: eRHIC layout.

Although the design of 5-cell 647 MHz cavity was aimed for high current ERL-Ring eRHIC[4-5], the cavity will be used for performance study for Ring-Ring SRF as well. A Cu prototype cavity was fabricated for HOM damping study, and an Nb cavity was fabricate for performance study. This paper will report the HOM measurement results, plan of the performance study, and first vertical test result.

* Work supported by LDRD program of Brookhaven Science Associates, LLC under Contract No. DE-AC02-98CH10886 with the U.S. DOE.
† wxu@bnl.gov

HOM MEASUREMENT ON CU CAVITY

The cavity fabrications contract was awarded to RI [6], which we have weekly telephone meeting to discuss the progress and resolve different issue during cavity fabrication. As we expect to have tons of R&D on the cavity, we asked for 4.5 mm cavity wall thickness. However, the geometry deformation tolerance is not allowed to be higher than +/- 0.3mm. To meet the tolerance, RI had to do at least once reshaping of each half cell. The beampipe of the cavity was design to be detachable so that we can study HOM damping in the future, as shown in Figure 2.

The spectrum measured in the Cu cavity matches very well with simulation results, which Figure 3 shows the spectrum comparision of the first HOM passband. This is also benefitted from tight geometry control during cavity fabrication. Due to the large cell-to-cell coupling and tight cavity shape tolerance, the cavity's field flatness is 89% as fabricated, and it required little tuning to reach 98.2% of field flatness.

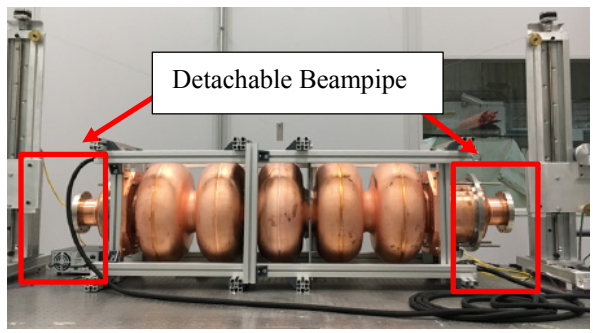


Figure 2: Bare 650 MHz Cu cavity with detachable beampipe.

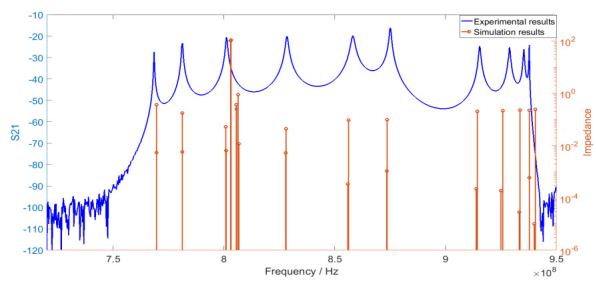


Figure 3: Simulated HOM spectrum and measured HOM spectrum.

NB CAVITY

Cavity fabrication and processing

Cu cavity is kind of a dry-run of the tooling for the Nb cavity fabrication, which made the Nb cavity fabrication much smoothly. However, a lot of dents and scratches were

Content from this work may be used under the terms of the CC BY 3.0 licence (© 2018). Any distribution of this work must maintain attribution to the author(s), title of the work, publisher, and DOI.

ISBN: 978-3-95450-194-6 ISSN: 2226-0366 doi:10.18429/JACoW-LINAC2018-THPO007

MESA - STATUS OF THE IMPLEMENTATION OF THE MicroTCA.4-BASED LLRF CONTROL SYSTEM

J. Bai*, K. Aulenbacher, F. Fichtner, R. Heine, J. Diefenbach
Institut für Kernphysik, Johannes Gutenberg-Universität Mainz, D-55099 Mainz, Germany

Abstract

The Mainz Energy-recovering Superconducting Accelerator (MESA) at the Institut für Kernphysik (KPH) at Johannes Gutenberg-Universität Mainz is a multi-turn Energy-Recovery-Linac (ERL), aiming to serve as user facility for particle physics experiments. The RF-accelerating systems of MESA consist of 12 cavities, four of them are 9-cell TESLA superconducting (SC) cavities. They operate in continuous wave (CW) mode. In order to control the radio frequency (RF) amplitude and phase within the 12 cavities with the required accuracy and stability better than 0.01% and 0.01°, the Micro Telecommunications Computing Architecture (MicroTCA.4) based digital low-level RF (LLRF) control system based on the development at DESY, Hamburg will be adapted for the MESA cavities. A Matlab/Simulink model was created to find the proper control parameters and to predict the system performance. In this paper, the simulation results, the progress of the implementation and the first tests of the LLRF system for MESA are presented.

INTRODUCTION

The MESA accelerator is a multi-turn ERL working at low energy and CW mode for particle physics experiments, which is currently under construction at KPH, Johannes Gutenberg-Universität Mainz. MESA has two different operation modes, the external beam (EB) mode and the energy recovery (ER) mode, which serve for two physics-experiments. The EB mode is mainly to measure the weak mixing angle with the highest accuracy. The polarized electron beam of 150 µA current at 155 MeV energy is dumped after being used with the external fixed target experiment P2. In the ER mode, MESA runs as an ERL, generating an unpolarised beam of 1 mA at 105 MeV. An internal fixed target experiment named MAGIX (MESA Gas Internal target eXperiment) is used in this mode. After a further upgrade of the cryomodules, MESA can achieve a beam current of 10 mA in the ER mode.

MESA CAVITIES

The MESA RF system topology includes four 9-cell TESLA SC cavities working at 1.3 GHz, four normal conducting (NC) pre-accelerator cavities at 1.3 GHz, two chopper cavities at 1.3 GHz, one buncher cavity at 1.3 GHz and the second buncher cavity at 2.6 GHz, which are illustrated in Fig. 1. All cavities will be driven by their own solid state power amplifier (SSPA). Due to the narrow bandwidth of 100 Hz, the SC cavity has tighter requirements for the amplitude and phase stability of the electrical field within the cavities. Tab. 1 shows the main parameters of the MESA SC cavity [1]. MESA requires an amplitude and phase stability better than 0.01% and 0.01°.

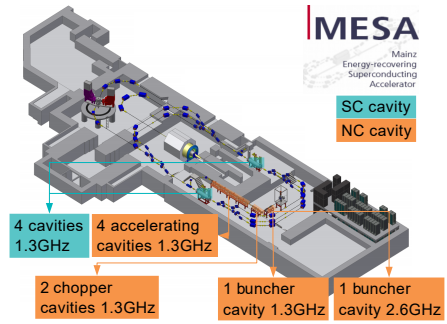


Figure 1: Overview of MESA RF system topology.

Table 1: Main Parameters of the MESA SC Cavity

Max E_{acc}	RF power	Q_L	Bandwidth
12.5 MV/cavity	15 kW	1.4×10^7	100 Hz

LLRF SYSTEM

MESA makes use of the MicroTCA.4 based LLRF system mainly developed by DESY [2]. All cavities are fed by their own RF power source, therefore we are implementing a single cavity LLRF control system [3]. The combination of a SIS8300-L Advanced Mezzanine Card (AMC) digitizer and a DWC8VM1 Rear Transition Module (RTM) analog boards purchased from Struck [4] offers a very compact solution for the single cavity control. The DWC8VM1 consists of 8 channel high frequency down-converters and one channel high frequency up-converter, which is the so-called vector modulator (VM) [5]. In the MESA project, the 1.3 GHz RF input signal picked up by the antenna will be down-converted to a 54 MHz intermediate frequency (IF) signal by means of a 1.354 GHz local oscillator (LO) signal and a low pass filter. The central components of the SIS8300-L are 10 125 MS/s 16-bit analog-digital converters (ADC), a Xilinx Virtex 6 FPGA and two 250 MS/s 16-bit digital-analog converters (DAC) [6]. The polar representation of an RF signal can be decomposed into its Cartesian representation by the so-called inphase (I) and quadrature (Q) components [7]. The advantage of this procedure is that phase and amplitude can be controlled simultaneously using setpoint values in I/Q description. The IF signal is sampled at the 81 MHz by ADCs. On the FPGA, the control deviation is calculated from the

* jibai@uni-mainz.de

Content from this work may be used under the terms of the CC BY 3.0 licence (© 2018). Any distribution of this work must maintain attribution to the author(s), title of the work, publisher, and DOI.

ISBN: 978-3-95450-194-6 ISSN: 2226-0366 doi:10.18429/JACoW-LINAC2018-THPO008

LONG-TERM OPERATION WITH BEAM AND CAVITY PERFORMANCE DEGRADATION IN COMPACT-ERL MAIN LINAC IN KEK

H. Sakai†, T. Furuya, E. Kako, T. Konomi, T. Miura, F. Qui, K. Umemori, KEK, Ibaraki, Japan

Abstract

We developed ERL main linac cryomodule for Compact ERL (cERL) in KEK. The module consists of two 9-cell 1.3 GHz superconducting cavities. After construction of cERL recirculation loop, beam operation was started in 2013 Dec. First electron beam of 20 MeV successfully passed the main linac cavities [1]. Beam current increased step by step and currently reached to 1 mA (CW) [2]. Energy recovery has successfully achieved. However, field emission was one of the problems for long term operation [3]. Therefore, the performance of the SRF cavities through long term beam operation has been investigated. In this paper, details of SRF beam operation, degradation, applied recovery methods are described.

INTRODUCTION FOR COMPACT ERL

Compact ERL Accelerator

Compact ERL (cERL) [1] is a test facility, which was constructed on the ERL Test Facility in KEK. Its aim was to demonstrate technologies needed for future multi GeV class ERL light source [4]. Recently, the future light source project in KEK was shifted to the high-performance ring accelerator. KEK directorates kept the importance of the R&D for industrial application based on ERL technologies like EUV-lithography [5] and so on. R&D of cERL was shifted to the industrial application from 2017.

cERL consists of 500 kV DC photocathode gun, which made high charge and low emittance electron beam, the injector cavities, the main linac cavity, which made energy recovery, recirculation loop and the beam dump. Detailed design beam parameters are shown in Table 1.

Table 1: Design Parameters of the cERL

Nominal beam energy	35 MeV
Nominal injection energy	5 MeV
Beam current	10 mA (initial goal) 100 mA (final goal)
Normalized emittance	0.1 – 1 mm-mrad
Bunch length (bunch compressed)	1-3 ps (usual) 100 fs (short bunch)

Main Linac Cryomodule

The left of Fig. 1 shows a schematic view of the main linac cryomodule [3], which contains two 9-cell KEK ERL model-2 cavities [6] mounted with He jackets. In order to achieve strong HOM damping for high-current ERL, iris diameter is increased to 80 mm. Epeak/Eacc becomes high and to be 3.0. Beampipe-type ferrite HOM absorbers [7] are connected at both sides of cavities, to strongly damp HOMs. The HOM absorbers are placed on 80 K region. Coaxial input couplers [8] with double ceramic windows feed RF power to the cavities. Frequency tuners [9] control cavity resonant frequencies. Cooling pipes of 80K, 5K and 2K are extended throughout the cryomodule. The 80K line was cooled by Nitrogen, and 5K and 2K lines were cooled by Helium. After filling with 4K liquid He, insides of the He jackets were pumped down and the cavities were cooled down to 2K. RF amplitude and phase on the main linac cavities are stabilized by the digital feedback system. RF stability of 0.01% R.M.S. for amplitude and 0.01 degree R.M.S. for phase were achieved [10].

Unfortunately, main linac cavity performance was not so good. Severe field emission was observed from low fields, for both cavities [3]. Operation voltage was limited to 8.6 MV for each cavity, to avoid the problem caused by the heavy radiation. Therefore operation energy of cERL beam was limited to 20 MeV; 2.9 MeV at injector part and 8.6 + 8.6 MeV at main linac part.

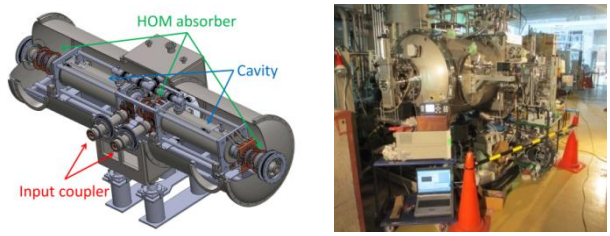


Figure 1: Schematic view of ERL main linac cryomodule (left) and the one placed inside the cERL radiation shielding room (right).

Beam Operation History until 2016

We briefly summarize our beam operation history. After first beam commissioning at December of 2013, we did the energy recovery with 6.5 μA. CW beam in 2nd and 3rd beam operation phase. In this phase, we learned the careful beam tuning without beam loss [11]. We started 100 μA current beam operation at 4th and 5th phase in 2015. During summer shutdown in 2014, we installed Laser Compton Scattering (LCS) beamline to demonstrate the future high-flux gamma-ray source and advanced X-ray imaging technology [12]. By using this high beam current, we successfully obtain clear narrow-band X-ray image come from LCS [13]. During summer shutdown in 2015, we upgraded the DC Gun and added the radiation shield to be operated for 1 mA energy recovery condition. In 2016, we started the 6th phase beam operation for 7 weeks. Finally, energy recovery has successfully achieved with about 1 mA (CW) beam [2].

Q-values of cavities were several times measured until 2016. Results are shown in Fig. 2. Main linac 1 (ML1) and Main linac 2 (ML2) represent the KEK-ERL model-2

† hiroshi.sakai.phys@kek.jp

Content from this work may be used under the terms of the CC BY 3.0 licence (© 2018). Any distribution of this work must maintain attribution to the author(s), title of the work, publisher, and DOI.

ISBN: 978-3-95450-194-6 ISSN: 2226-0366 doi:10.18429/JACoW-LINAC2018-THPO009

EVALUATION OF 60 pC BEAM PERFORMANCE AT cERL INJECTOR FOR ERL BASED EUV-FEL

T. Hotei*, SOKENDAI, Tsukuba, Ibaraki, Japan
T. Miyajima, R. Kato, KEK, Tsukuba, Ibaraki, Japan

Abstract

In order to compensate for the emittance which is increased by space charge in the low energy region, it is important to transport the beam as designed. Until now, we did not consider couplers in injector superconducting cavities in optics design. But in this study, to improve optics matching and emittance compensation conditions for space charge dominated beam in cERL at KEK, we introduced a new 3D cavity model. We first investigated the influence of the couplers on electromagnetic field distribution. As a result, it was found that an asymmetric focusing force is generated by the influence of the couplers. It also became clear that the influence of the coupler kick on the optics significantly devastated the emittance compensation condition from the calculating including space charge. Furthermore, it was found that by optimizing the optics in consideration of the coupler kick, it is possible to improve the beam control accuracy and reduce the emittance in beam commissioning.

INTRODUCTION

Energy recovery linac (ERL) is the linear accelerator which can supply high average current beam. ERL based EUV-FEL for semiconductor lithography is designed at KEK [1]. EUV-FEL requires a beam with a bunch charge of 60 pC, kinetic energy of 10 MeV, bunch length of 1 ps and emittance of 1 mm.mrad in the injector.

Since the emittance increases due to space charge in the low energy region, the increased emittance must be compensated. In order to compensate the emittance, it is important to transport the beam as well as the designed optics. But, in beam commissioning at cERL in KEK, we found that the influence on the optics caused by coupler kick of injector cavity can not be ignored [2, 3].

We analyzed numerically and experimentally to study the influence of coupler kick on optics and emittance compensation. In this proceedings, we report on these results.

ELECTROMAGNETIC FIELD ANALYSIS

In order to analyze the influence on the electromagnetic field distribution by the couplers, we created two models of cERL injector cavity [4]; model 1 does not have couplers (Fig. 1 top, 2D model), model 2 has couplers (Fig. 1 bottom, 3D model). The electromagnetic field for 2D model is calculated assuming cylinder symmetry by Poisson/Superfish [5], for 3D model is calculated by CST [6]. 3D model has no cylindrical symmetry.

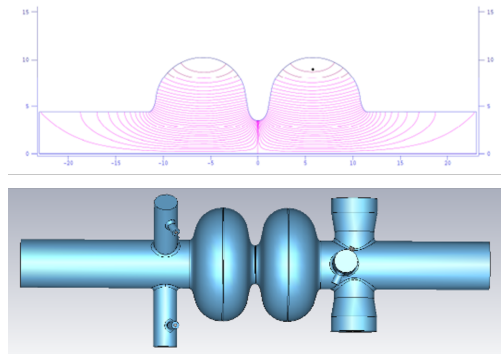


Figure 1: Two models of cERL injector cavity. Top is 2D cavity model and bottom is 3D cavity model.

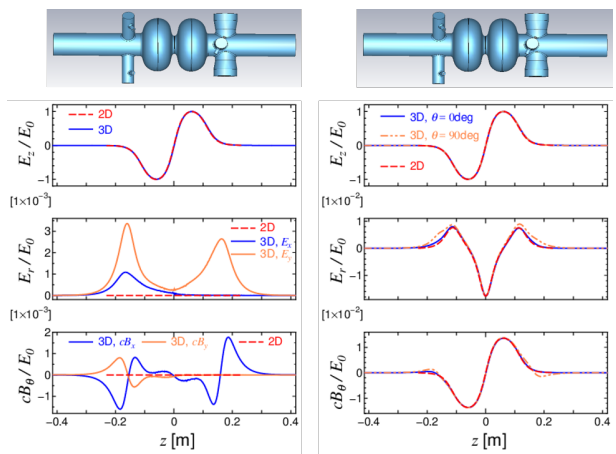


Figure 2: Comparison of electromagnetic field distribution (left: $r = 0$ mm, right: $r = 1$ mm). The red dotted line is the result of 2D model. The blue solid line is the result of 3D model with $\theta = 0$deg. The orange solid line is the result of 3D model with $\theta = 90$deg. The magnitude of the electromagnetic field is normalized by the maximum value of $E_z(r = 0, z)$.

Figure 2 shows the electromagnetic field distribution of $r = 0$ mm (left) and $r = 1$ mm (right) for each model. This indicates that the transverse electromagnetic field is generated on the central axis of the cavity by the couplers. In addition, it can be seen that the transverse electromagnetic field distribution becomes angle dependent by the coupler.

FOCUSING FORCE FROM CAVITY

In order to quantitatively evaluate the influence of coupler on beam dynamics, we tracked the single particle trajectory. The schematic layout is shown in Fig. 3. In this case, the lens whose focusing force is measured is a cavity. The kinetic

* hotei@post.kek.jp

Content from this work may be used under the terms of the CC BY 3.0 licence (© 2018). Any distribution of this work must maintain attribution to the author(s), title of the work, publisher, and DOI.

ISBN: 978-3-95450-194-6 ISSN: 2226-0366 doi:10.18429/JACoW-LINAC2018-THPO010

NOVEL "STRAIGHT" MERGER FOR ENERGY RECOVERY LINACS*

K. E. Deitrick†, A. Hutton‡
Thomas Jefferson National Accelerator Facility, Newport News, VA 23606, USA
S. Overstreet
Center for Accelerator Science, Old Dominion University, Norfolk, VA 23529, USA
A. C. Bartnik, C. M. Gulliford
Cornell Laboratory for Accelerator-Based Sciences and Education,
Cornell University, Ithaca, NY 14853, USA

Abstract

One of the most critical design considerations for an energy recovery linac (ERL) is how to merge the injected bunch onto the linac axis with minimal beam degradation. All merger designs in established and upcoming machines involve significant bending of the injected beam – even using a so-called straight merger bends the injected beam several degrees. We propose a merger which reduces the bending of the injected beam by an order of magnitude. By passing both beams through a septum magnet followed by an rf separator cavity with a superimposed dipole magnetic field, the injected beam bends minimally within the cavity, while the recirculated beam bends to align with the linac axis. Here we describe the concept in detail and present simulation results to demonstrate the advantages of such a design, particularly for magnetized beams or minimal energy separation between the injected and recirculated beams. Measurements from an experiment at CBETA evaluating the beam dynamics of the rf separator are presented and compared with simulation results.

INTRODUCTION

Mergers remain one of the most challenging design aspects of ERLs to date. While significant effort has gone into minimizing the beam degradation due to mergers over the years, all merger designs in established and upcoming machines bend the beam significantly, which is problematic when dealing with beams sensitive to transport asymmetries, such as magnetized beams [1]. As one of the components of the Jefferson Lab Electron Ion Collider (JLEIC) design is a magnetized electron beam to cool the ion beam, driven by an ERL, this is a critical topic in future design work [2]. Additionally, this merger concept works well for ERLs without significant energy separation between injected and recirculated beams, which is traditionally a challenging design prospect.

"STRAIGHT" MERGER

The layout of the "straight" merger concept is shown in Fig. 1. Both the injected and recirculated beams pass through a septum followed by an rf separator with a superimposed magnetic dipole field. The injected beam passes through the zero-field aperture of the septum before passing through the rf separator and magnetic dipole field assembly. When the injected beam passes through this assembly, the separator is on-crest and the dipole field is set to buck, or compensate, for the kick provided by the separator. To first order, the injected bunch is undeflected. The recirculated beam, on the other hand, is deflected by the septum magnet before passing through the cavity and coils assembly. As a consequence of the required 180° phase separation in an ERL between the bunches of the injected and recirculated beams, the separator cavity and dipole field deflect the recirculated beam in the same direction - leading to a deflection twice what either the cavity or magnetic field would provide alone. The combination of the fields in the cavity coil assembly is seen in Fig. 2.

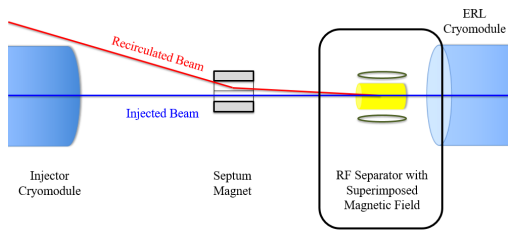


Figure 1: Layout of the "straight" merger concept, Fig. 1 from [3].

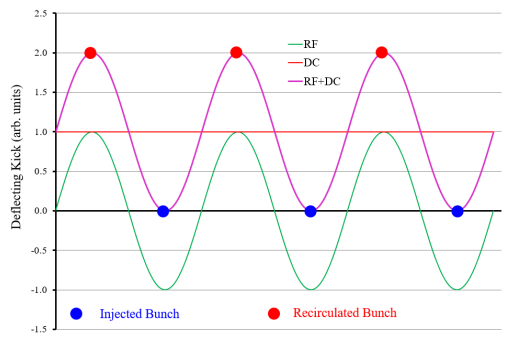


Figure 2: Kick in the rf separator with superimposed magnetic dipole, Fig. 2 from [3].

One of the anticipated higher order effects of this merger design is the "banana" effect. This effect is the deflection

* Authored by Jefferson Science Associates, LLC under U.S. DOE Contract No. DE-AC05-06OR23177.
† deitrick@jlab.org
‡ andrew@jlab.org

Content from this work may be used under the terms of the CC BY 3.0 licence (© 2018). Any distribution of this work must maintain attribution to the author(s), title of the work, publisher, and DOI.

ISBN: 978-3-95450-194-6 ISSN: 2226-0366 doi:10.18429/JACoW-LINAC2018-THPO011

FIRST ENERGY RECOVERY OPERATION AT THE S-DALINAC: RF CONTROL STABILITY MEASUREMENTS*

M. Steinhorst†, M. Arnold, N. Pietralla,
Institut für Kernphysik TU Darmstadt, 64289 Darmstadt, Germany
C. Burandt, Helmholtz-Institut Mainz, 55128 Mainz, Germany

Abstract

Energy recovery linacs (ERL) are used to overcome the rf power limits of rf amplifiers to further increase beam current at particle accelerators. Since the last major upgrade of the electron accelerator S-DALINAC it can be operated in ERL mode. To demonstrate the capability of a stable operation of the current rf control system during ERL operation, measurements regarding the rf control stability and the demand of rf power were done. This contribution is discussing this measurements and possible improvements for future energy recovery beamtimes.

INTRODUCTION

The recirculating superconducting linear accelerator S-DALINAC is one of the main research instruments at the institute for nuclear physics at the TU Darmstadt (see Fig. 1) [1]. Many improvements were implemented at the S-DALINAC since the first recirculated beam in 1991. One of the major enhancements is the upgrade from a twice to a thrice recirculating scheme in 2015/2016 [2]. With this upgrade the S-DALINAC can provide a beam with the same design energy of up to 130 MeV in cw operation at reduced accelerating gradients by using the main accelerator an additional time. Furthermore an rf phaseshift of the beam of up to 360° can be done due to a path length variation of the arcs in the new second recirculation. A phase shift of 180° changes the operation mode of the S-DALINAC between a conventional accelerating and an ERL mode. ERL operation was not possible when the rf control system for the superconducting structures was set up in 2010 [3]. Therefore it is not optimized for this task. The rf control system had to be tested during ERL operation in order to also demonstrate its capability of this mode.

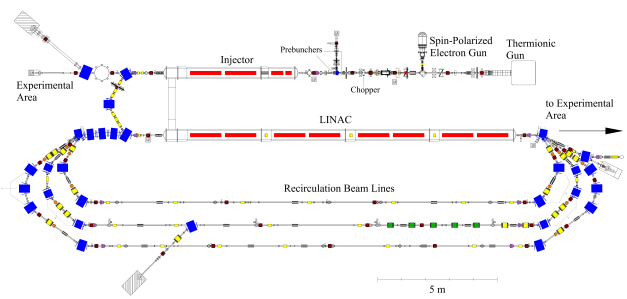


Figure 1: Current layout of the S-DALINAC.

Table 1: Design Specifications for the 20-cell Superconducting Cavities

Parameter	Design value
Material	Niobium, RRR = 280
R/Q	1995.2 Ω/m
Resonance f_0	2.997 GHz
Unloaded Q_0	3×10^9
Loaded Q_L	variable (typical 3×10^7)
Accelerating E_{acc}	5 MV/m

RF-CONTROL SYSTEM

The current low-level rf (LLRF) control system had to be tested to show its capability in terms of sufficient stability during the new ERL operation. In the following the current setup for LLRF control is briefly described. A design parameter overview of the used superconducting 20-cell structures is given in Table 1.

Hardware

The rf signal proccessing is done analog and digitally by an in-house developed board [3]. The rf signal is analog IQ-demodulated to baseband and for higher precision the amplitude of the rf signal is measured separately by an amplitude detector. Afterwards the analog signals are digitized by 18-bit ADCs with a 1 MS/s sampling rate. The further processing and control is done on an Xilinx Spartan-6 FPGA where a custom digital signal processor is implemented. This digital signal processor executes the control algorithm described in the next section. All data produced during signal processing on the FPGA can be streamed by an USB-2.0 interface at full ADC rate in 8 channels simultaneously. After the digital signal processor the signal is converted back by a DAC and is IQ-modulated to radiofrequency and sent to the cavity.

Control Algorithm

At the S-DALINAC two different control algorithms are used, both controlling the amplitude and phase of the rf signal. The bunching of the continuous beam after the thermionic electron source is done by normal conducting copper cavities with cylindrical geometry. For control of this low Q factor cavities with a resonance bandwidth in the MHz range a generator-driven resonator algorithm is used. The reference master oscillator is used to directly inject the

* Supported by DFG (GRK 2128)
† msteinhorst@ikp.tu-darmstadt.de

Content from this work may be used under the terms of the CC BY 3.0 licence (© 2018). Any distribution of this work must maintain attribution to the author(s), title of the work, publisher, and DOI.

ISBN: 978-3-95450-194-6 ISSN: 2226-0366 doi:10.18429/JACoW-LINAC2018-THPO012

ONCE RECIRCULATING ENERGY RECOVERY LINAC OPERATION OF S-DALINAC*

M. Arnold†, J. Birkhan, J. Pforr, N. Pietralla, F. Schließmann, M. Steinhorst
Technische Universität Darmstadt, Darmstadt, Germany
F. Hug, Johannes Gutenberg-Universität Mainz, Mainz, Germany

Abstract

The S-DALINAC is a thrice recirculating superconducting electron accelerator which can be either used in conventional accelerating operation or, since a major upgrade in 2015/2016 was installed, as an energy recovery linac (ERL) alternatively. A once or twice recirculating ERL operation is possible due to the layout of the accelerator. For both setups beam dynamics calculations have been performed or are under investigation at the moment. The once recirculating ERL mode was proven successfully in August 2017, which set the first German ERL into operation. The results will be discussed more in detail in this contribution.

INTRODUCTION

The superconducting linear electron accelerator S-DALINAC is in full operation since 1991 [1]. In the years 2015/2016 a major upgrade modified it to a thrice recirculating machine [2, 3]. Featuring the new recirculation beam line, a path length adjustment system was installed which enables a total phase shift of 360°. Thus the change between normal operation and an operation as an ERL is possible [4].

S-DALINAC

Figure 1 shows the floorplan of the thrice recirculating S-DALINAC. It houses two electron sources: A thermionic gun with a pre-acceleration of 250 keV and a spin-polarized source with a pre-acceleration of up to 125 keV. In the normal conducting chopper-prebuncher-section the beam is prepared for an acceleration with 3 GHz in the superconducting RF system. The injector accelerator is able to provide an energy gain of up to 10 MeV (7.6 MeV in case of recirculating operation) with currents of up to 60 µA. For recirculating operation the beam is bent into the main accelerator which then will provide an energy gain of up to 30.4 MeV. The beam can be recirculated up to three times, resulting in four passages through the main accelerator. A total energy of up to 130 MeV with currents of up to 20 µA can be reached.

Energy Recovery Linac Mode

The layout of the S-DALINAC allows a once recirculating or a twice recirculating ERL mode. In case of the once recirculating ERL operation, see Fig. 2, the beam is accelerated in the main linac and then directly bent into the second recirculation beam line. Therefore the ratio of injection energy and main linac energy gain needs to be set to 1:8. A

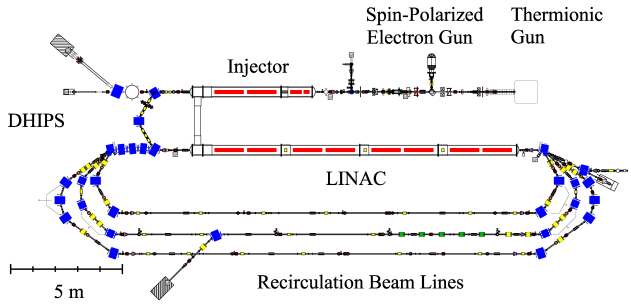


Figure 1: Floorplan of the S-DALINAC.

180° phase shift is done while travelling through the beam line. The beam is re-injected into the main accelerator at a decelerating phase so that it can be dumped at injection energy after leaving the main linac.

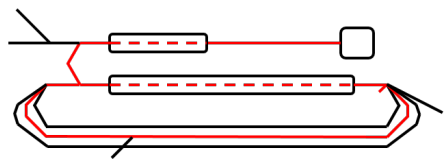


Figure 2: Scheme of the once recirculating ERL operation.

Figure 3 shows the path of the beam in case of the twice recirculating ERL mode. In contrast to the once recirculating mode the beam is first bent into the first recirculation beam line. After a second acceleration in the main linac, a 180° phase shift is performed in the second recirculation beam line. The beam is then guided through the first recirculation beam line a second time. Being twice decelerated in the end, the beam is dumped at injection energy after the last transition through the main linac. In this operation mode the ratio of injection and main linac energy gain is set to 1:4.

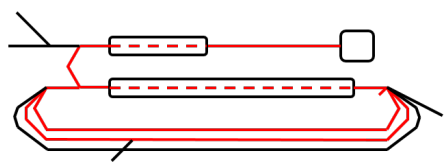


Figure 3: Scheme of the twice recirculating ERL operation.

BEAM DYNAMICS SIMULATION

To ensure the transportation of the beam, it is necessary to conduct dedicated beam dynamics simulations. During the design and installation of the thrice recirculating layout, the lattice was not optimized for ERL mode. Meanwhile

* Work supported by DFG through GRK 2128
† marnold@ikp.tu-darmstadt.de

Content from this work may be used under the terms of the CC BY 3.0 licence (© 2018). Any distribution of this work must maintain attribution to the author(s), title of the work, publisher, and DOI.

ISBN: 978-3-95450-194-6 ISSN: 2226-0366 doi:10.18429/JACoW-LINAC2018-THPO016

INVESTIGATION OF 2D PBG-WAVEGUIDES FOR THz DRIVEN ACCELERATION

A. Vint and R. Letizia, Cockcroft Institute/Lancaster University, WA4 4AD, Warrington, UK

Abstract

There is significant interest in novel accelerating techniques which can overcome the limitations of conventional radio-frequency (RF) based devices in terms of frequency, gradient, and footprint. Moving from the RF to the terahertz (THz) frequency range, higher accelerating-gradient of high-energy beams can be achieved, as well as structure miniaturisation. Furthermore, in respect to the optical frequency range, THz allows for larger structures and better beam quality. This work has been investigating the use of a 2D photonic-bandgap dielectric waveguide (PBG-W) for THz-driven electron acceleration which could potentially offer a good compromise between dispersion engineering, low losses and ease of parallel illumination. Dispersion characteristics of the accelerating mode are studied to achieve the best compromise between high accelerating field and effective accelerating bandwidth, assuming a ~10% bandwidth of the THz driving pulse.

INTRODUCTION

With current state-of-the-art particle accelerators reaching several kilometres in size, a paradigm shift is required for future technologies to prevent them becoming unattainable. Terahertz (THz) frequencies offer the opportunity to build micron-scale structures, and the use of dielectrics over metal offers the ability to push fields higher due to the increased breakdown resistance—or fluence threshold. Additional benefits over optical frequencies, which similarly exhibit the prior stated benefits of THz, is the larger aperture sizes allowed for the beam and the higher bunch charges THz affords beams to use.

In conventional RF-driven accelerators, sources are typically narrowband—usually on the order of a few percent. In the regime of ultrashort THz pulse, broad bandwidths are generated and require a more careful study of the beam-pulse interaction. Much of the current work investigating THz acceleration has focused on the use of corrugated and dielectric-loaded waveguides (DLWs), of both rectangular and cylindrical geometry. While these devices are effective, they are hindered by the use of metal walls—which at THz frequencies exhibit large ohmic losses. [1] Due to the wavelength scales of THz, employing photonic-crystal (PhC) theory for confinement instead of metal walls can offer low ohmic losses and high fluence threshold. Moreover, the design flexibility offered by PhCs can potentially aid the tailoring of the accelerating mode dispersion for the THz acceleration regime.

For comparison with other designs such as the DLW proposed in [2] and ease of realisation, a rectangular waveguide configuration is chosen. This work focuses on waveguides based on a 2D-PBG slab structure with a triangular lattice of air/vacuum holes, offering a good compromise between design flexibility and ease-of-manufacture.

PBG-WAVEGUIDE DESIGN

Using MPB [3], initial 2D simulations of the PhC unit cell were carried out to optimise the fill factor of the PBG structure for maximum bandgap around the central frequency of 1 THz. The dielectric material used was silicon with relative permittivity $\varepsilon_r \sim 11.6$. The maximum photonic bandgap (PBG) was found to be at a radius of $r = 0.445a$ yielding a bandgap of 50% in the normalised frequency region of 0.29-0.48 $\omega a/2\pi c$, where ω is the angular frequency, a is the PhC period, and c is the speed of light. The schematic of the proposed PBG-waveguide is shown in Fig. 1.

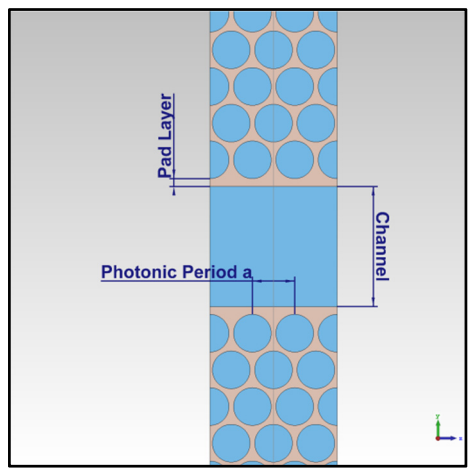


Figure 1: Schematic of three longitudinal unit cells of the PBG-W, with z-axis being direction of propagation.

The PBG-W is then realised by introducing a line defect along the longitudinal direction z across the PhC lattice for confinement of specific electromagnetic states (as propagating modes) within the PBG. In the case of DLWs, the modes can be described as a superposition of both TE and TM modes as the longitudinal-section magnetic (LSM) mode if either x or y components of the magnetic fields is set to 0, likewise longitudinal-section electric (LSE) if one of the transverse electric fields is set to 0 [4].

PBG-Ws such as shown in Fig. 1 are both nonhomogeneous and anisotropic—as such, they cannot support true LSE/LSM modes. At lower wavenumbers however, these modes serve as a good approximation for the PBG-W modes. Higher wavenumbers often exhibit higher levels of coupling to the dielectric over the waveguide channel which modifies the dispersion curve.

Content from this work may be used under the terms of the CC BY 3.0 licence (© 2018). Any distribution of this work must maintain attribution to the author(s), title of the work, publisher, and DOI.

ISBN: 978-3-95450-194-6 ISSN: 2226-0366 doi:10.18429/JACoW-LINAC2018-THPO017

PROGRESS OF THE NOVEL SPIRAL INJECTION TEST EXPERIMENT*

M. A. Rehman†, SOKENDAI (The Graduate University for Advanced Studies), Kanagawa 240-0193, Japan
H. Iinuma, Ibaraki University, Mito, Ibaraki, Japan
S. Ohsawa, H. Nakayama, H. Hisamatsu, K. Furukawa, T. Mibe, High Energy Accelerator Research Organization, 1-1 Oho, Tsukuba, Ibaraki 305-0801, Japan

Abstract

A new muon $g-2$/EDM experiment at J-PARC (E34) is under preparation in order to resolve a 3 σ discrepancy of muon anomalous magnetic dipole moment between the measurement and the standard model prediction. The E34 experiment will employ a unique three-dimensional spiral injection scheme in order to store the muon beam into a small storage orbit. In order to demonstrate the feasibility of this novel injection scheme, the Spiral Injection Test Experiment (SITE) with the electron beam is under construction at KEK Tsukuba campus. The goals of the SITE are divided into two phases. In the first phase of the SITE, 80 keV DC electron beam was injected and detected as a fluorescent light due to the de-excitation of the nitrogen gas into solenoidal storage magnet. In the second phase of the SITE, the pulsed electron beam, and a pulsed magnetic kicker are developed in order to keep the pulsed beam on the very midplane of the solenoidal storage magnet. This paper describes the achievements of the first phase of the SITE and progress towards the second phase.

INTRODUCTION

The muon's anomalous magnetic moment is one of most important measurement in elementary particle physics. The recent measurement of muon $g-2$ results a 3 σ [1] discrepancy with the equally precise standard model prediction. The new J-PARC muon $g-2$/EDM (E34) is under preparation to resolve current discrepancy. The E34 experiment is aiming to measure muon's $g-2$ to the precision of 0.1 ppm and EDM down to the sensitivity of 10^{-21} e.cm [2].

The key idea to measure muon $g-2$ is to store polarized muon beam in a magnetic field and measure the evolution of spin precession vector with respect to time. In E34 a low emittance muon beam of momentum 300 MeV/c from muon accelerator will be injected into a 3-T Magnetic Resonance Imaging(MRI)-type solenoid magnet in order to store the muon beam in 0.66-m diameter orbit. In order to enhance injection efficiency and overcome technical challenges related to small storage orbit, a new three-dimensional spiral injection scheme is under development to inject the muon beam into MRI type storage magnet. Figure 1 shows the basic concept of a three-dimensional spiral injection scheme. The details and recent updates of three-dimensional spiral injection scheme can be found in [3–5].

* Work supported by "Grant in Aid" for Scientific Research, JSPS (KAKENHI#26287055)
† rehman@post.kek.jp

The three-dimensional spiral injection scheme is an unproven idea, therefore, a demonstration experiment to prove the feasibility of this unique scheme is inevitable. A scale down Spiral Injection Test Experiment (SITE) by the use of electron beam is under development at KEK Tsukuba campus. This paper will describe the development of the spiral injection scheme test experiment (SITE).

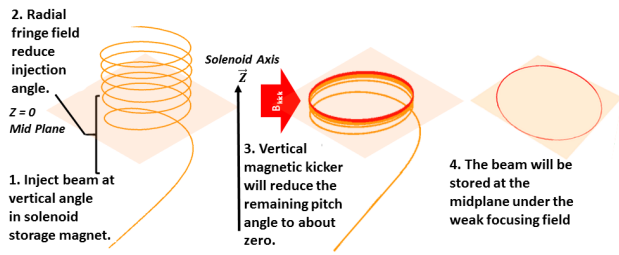


Figure 1: Layout of three-dimensional spiral injection scheme.

SPIRAL INJECTION TEST EXPERIMENT (SITE)

The SITE setup contains a 2 m long straight beamline, a solenoid storage magnet to store the electron beam and forty degrees bend section to guide the electron beam towards the storage magnet. A triode type thermionic electron gun with LaB_6 cathode is used to generate the DC electron beam of 80 keV with current in the range of few μA.

After the electron gun, a magnetic lens is placed to focus the low energy beam. A pair of steering coils also has been placed to control the transverse position of the beam. An electric chopper system has been placed after the electron gun to produce the pulsed beam. Details of the electric chopper can be found in [6]. A collimator of diameter 3 mm and depth 5 mm is placed after the electric chopper. The collimator is served as the beam dump for the chopper system and also used to create the differential vacuum system for the gas monitor in the storage magnet.

A bending magnet (BM1) is placed on the straight beamline to deflect the beam at forty degrees towards the storage magnet. A second bending magnet (BM2) is also placed near the injection point in order to control the injection angle slightly. Air core quadruple magnets have been placed on a bend section to create required beam phase space for the spiral injection.

A pulsed magnetic kicker is also under development in order to keep the beam to the very center of the storage

Content from this work may be used under the terms of the CC BY 3.0 licence (© 2018). Any distribution of this work must maintain attribution to the author(s), title of the work, publisher, and DOI.

ISBN: 978-3-95450-194-6 ISSN: 2226-0366 doi:10.18429/JACoW-LINAC2018-THPO018

BUILDING A 12 GHz TRAVELING WAVE ACCELERATING STRUCTURE BRAZED THROUGH IRISES

V. A. Dolgashev*, G. B. Bowden, M. Dal Forno, A. Haase, SLAC, Menlo Park, USA
H. Zha, Tsinghua University, Beijing, China
A. Grudiev, CERN, Geneva, Switzerland

Abstract

Accelerating structures are usually manufactured by precision turning of individual cells combined with precision milling for complex parts such as rf power couplers. These multiple parts are staked and brazed into a complete structure. We consider an alternative approach: precision milling of multiple cells and couplers into metal blocks that comprise halves or quadrants of the complete structure. We successfully produced a 12 GHz Compact Linear Collider (CLIC) main linac accelerating structure prototype using this method. A previous prototype was designed as an open structure with a gap between cell irises. Here we describe a different approach, an accelerating structure which is brazed through irises. It is based on a multi-cell traveling wave structure designed at CERN for PSI, so called *T24 PSI 12 GHz*. This brazed-through irises structure was built at SLAC for high power tests at CERN. Here we describe the details of this process.

INTRODUCTION AND MOTIVATION

Accelerating structures of normal conducting linacs are typically built from a multitude of precisely machined cells. Examples are X-band structures of linear colliders [1] or S-band cavities of medical accelerators [2]. The cells are joined using high-temperature brazing or diffusion bonding into a complete structure. An alternative approach has been used for making structures from two halves at W-band [3–6] and X-band [7–10], quadrants [11, 12] or octants [13]. These halves, *etc.* are made by precision milling and then joined together either by clamping [11, 13] or brazing [7, 8, 12]. All these structures were designed with gaps between irises: a small, difficult to control gap [11]; small, controlled gap [12]; and a large gap on the order of a millimeter [3–10, 13]. High power tests of these structures have shown that structures with controlled gaps performed satisfactorily [9, 12].

Here we present an alternative approach to build a constant gradient traveling wave accelerating structure from halves [14]. We braze the halves through irises thus eliminating both rf field enhancement caused by a controlled gap between irises and degradation of high gradient performance attributed to uncontrolled gaps. The geometry of this structure is practically identical to a structure made of discs but with several advantages. In the case of halves, the machined surface area is smaller and number of precision parts to handle is fewer thus reducing fabrication costs.

* dolgash@slac.stanford.edu

More advantages come from the absence of rf current flow through the joints between the halves. This makes pre-brazing rf cold test practical and useful, and reduces risk of arcing or erosion in small, uncontrolled gaps between cells. In cases of structures made from stacked cells rf currents cross these gaps. The gaps could be caused by joints starved for alloy in brazed structures or uneven bonding pressure in diffusion-bonded structures.

DESIGN AND MANUFACTURING

Design

The geometry of our structure is based on the so called *T24 PSI 12 GHz* which was designed at CERN for PSI [15] and was successfully built and high power tested [16]. The rf parameters of this structure are presented in [16] and should be practically identical to our structure. The original structure is made out of symmetric cells with rounded outer diameter. This cells geometry is suitable for manufacturing by milling into halves. Meanwhile the rf couplers (mode launchers) of the *T24 PSI 12 GHz* were brazed of separate milled parts and had to be re-designed both electrically and mechanically. We report this work in [17]. We show a solid model of the mode launcher from [17] in Fig. 1b). With a new coupler the electrical re-design was complete.

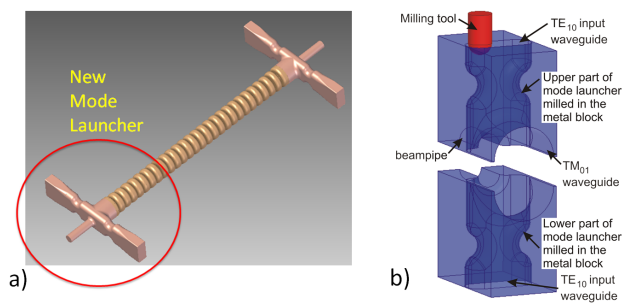


Figure 1: a) Solid model of RF envelope with re-designed mode launcher as imported into Solid Edge from HFSS [18], and b) solid model of the mode launcher, with detail of 8 mm diameter milling tool [17].

Manufacturing

In manufacturing of previous, open structure made of halves [7] we have validated an approach where we built a solid model directly from the electrical model. This electrical model was imported into Solid Edge [19] from HFSS [18]. After mechanical design was finished, the resulting solid model was used to generate the milling machine control program. No interim drawings were utilized for the

Content from this work may be used under the terms of the CC BY 3.0 licence (© 2018). Any distribution of this work must maintain attribution to the author(s), title of the work, publisher, and DOI.

ISBN: 978-3-95450-194-6 ISSN: 2226-0366 doi:10.18429/JACoW-LINAC2018-THPO020

DYNAMIC BEHAVIOUR OF ELECTRON BEAM UNDER RF FIELD AND STATIC MAGNETIC FIELD IN CYCLOTRON AUTO RESONANCE ACCELERATOR*

Yating Yuan, Kuanjun Fan†, State Key Laboratory of Advanced Electromagnetic and Technology, Huazhong University of Science and Technology, 430074, Wuhan, China
Yong Jiang‡, Yale University, 06520, New Haven, USA

Abstract

The cyclotron auto-resonance accelerator (CARA) is a novel concept of accelerating continuous gyrating charged-particle beams to moderately or highly relativistic energies, which can be used as the high power microwave source and applied in environment improvement area, particularly in the flue gas pollution remediation. In CARA, the continuous-wave (CW) electron beam follows a gyrating trajectory while undergoing the interaction with the rotating TE-mode rf field and tapered static magnetic field. Simulation models are constructed to study the effect of rf field and static magnetic field on electron beam in CARA, where the beam energy, trajectory and velocity component are analysed. The simulation results match reasonably well with theoretical predication, which sets up a solid foundation for future designs of CARA.

INTRODUCTION

The CARA may have application as a compact, low-energy injector for a multimegawatt gyroharmonic converter [1, 2] or for use in a source of radiation that requires low-energy electrons [3, 4]. An alternative technology to combat environmental pollution, electron beam dry scrubbing (EBDS), was introduced in 1970, and subsequently demonstrated in several manifestations [4]. CARA is an efficient process for converting rf energy into electron beam energy [4, 5]. The accelerated beam produced in CARA follows a gyrating trajectory, thus the beam is "self-scanning", requiring no other deflecting device or external field to sweep across a gas stream. So CARA is suitable for environmental applications include sterilization, flue gas and waste water treatment.

BASIC THEORY

When the static magnetic field satisfies a certain resonance condition in CARA, the gyrating electrons are maintained in phase synchronism with a rotating TE_{11} waveguide field, then electron beam can be continuously accelerated [2, 4].

The electron beam will gyrate under guiding magnetic field B_z. The rest electron gyration frequency is

$$\Omega_0 = eB_z / m_0 . \quad (1)$$

where e, m_o are the electron charge and rest mass respectively.

The synchronous axial guiding magnetic field is

$$B_z = m_0 \omega \gamma (1 - n\beta_z) / e . \quad (2)$$

where β_z, γ and ω are normalized axial velocity, relativistic factor and rf field frequency respectively. Refractive index n is expressed by

$$n = k_z c / \omega = c\sqrt{(\frac{2\pi f}{c})^2 - (\frac{1.841}{a})^2} / 2\pi f . \quad (3)$$

The relationship between the β_z and γ can be given

$$\beta_{z1} = \frac{1}{\gamma_1}[n_1(\gamma_1 - \gamma_0) + D^{1/2}] \quad (\gamma_1 > \gamma_0, \beta_{z1} > 0) . \quad (4)$$

where $D = (\gamma_0^2 - 1) - (1 - n_1^2)(\gamma_1 - \gamma_0)^2$, γ_0 is the beam's initial relativistic factor, β_{z1}, γ_1 and n_1 denote the output parameters in CARA.

The maximum acceleration energy [2] in CARA is

$$\gamma_{1\max} = \gamma_0 + \left(\frac{\gamma_0^2 - 1}{1 - n_1^2}\right)^{1/2} . \quad (5)$$

Then the normalized transverse velocity β_T can be expressed by γ and β_z

$$\beta_T = \sqrt{1 - \frac{1}{\gamma^2} - \beta_z^2} . \quad (6)$$

There are many challenges in CARA:

(i) The maximum acceleration energy is related to n according to Eq. (5), so it is important to get a large n (close to 1) in order to achieve high energy electron beam. But n->1 implies large waveguide radius according to Eq. (3).

(ii) In order to achieve an effective acceleration, it is essential to find the appropriate rf field power and axial magnetic field to maintain the resonance condition.

(iii) The rf field strength and the slope of guiding magnetic field always have perturbations in practice, so the effect of the perturbation is of great significance.

SIMULATION MODEL

For simplicity, a cylindrical waveguide is modelled. In order to achieve a high refractive index, the related parameters of this model are showed in Table 1. The simulation indicates that the rf field distribution in the cylindrical waveguide is the $TE_{11\text{-}35}$ mode of standing wave

* Work supported by the National Natural Science Foundation of China
† kjfan@hust.edu.cn
‡ yong.jiang@yale.edu

Content from this work may be used under the terms of the CC BY 3.0 licence (© 2018). Any distribution of this work must maintain attribution to the author(s), title of the work, publisher, and DOI.

ISBN: 978-3-95450-194-6 ISSN: 2226-0366 doi:10.18429/JACoW-LINAC2018-THPO021

RESEARCH ON X RAY CHARACTERISTICS PRODUCED BY HIGHENERGY PICOSECOND ELECTRON BEAM SHOOTING*

X. D. Zhang†, X. P. Ouyang, X. F.Weng, X. J. Tan, B.Sun
State Key Laboratory of Intense Pulsed Radiation Simulation and Effect (Northwest Institute of Nuclear Technology), Xi'an, China

Abstract

The X ray sources based on electron linac can produce X-rays with high energy, concentrated directions, and strong penetrating power, which have been widely applied in various fields.An electronic linear accelerator which has been built at present can provide an electron beam with energy of 120 MeV and pulse width of picoseconds. The electron beam shooting at the metal targets can produce ultra-fast pulsed X-rays in the order of picoseconds. In this paper, the pulse X ray characteristics are studied through simulating electron beam shooting at four metal targets with different thickness of Au, Ta, U, W and Pb by Monte Carlo methods. The calculation shows that the X-rays can reach about 10^{10} /pulse and the pulse width can reach about picoseconds level, when the pulsed electron beams with energy of 120 MeV, charge of 0.5 nC and pulse width of picoseconds shooting at Ta targets. The yield and time width of pulsed X-rays are related to the diameter and thickness of the target.

INTRODUCTIONS

Since the discovery of X-rays, various types of X-rays generating devices have been developed, among which the most widely used one is the X-ray source devices used in electron linac, such as industrial irradiation electron linac, medical treatment accelerator and so on. These kinds of accelerators produce high energy electron beams，which can produce X-rays with high energy, concentrated direction and strong penetration. They have been widely used in irradiation processing, nondestructive testing, medical and other fields. The generation rate and time characteristic of X-ray are related to the beam energy, beam length, material and thickness of the target. The X-ray produced by this kind of linear accelerator is either DC or pulse, and the pulse width is mostly more than ns.

The electronic linear accelerator currently being built by Northwest Institute of Nuclear Technology can produce energy of 120 MeV and pulse width of 1ps to 3ps and electron beam with diameter of 15 μm. Using this electron beam to shoot target can produce ultrafast X-ray with high intensity and pulse width of picosecond magnitude, which can provide experimental basis for studying nuclear data and ultrafast ray measurement technology. Therefore, it is of great significance to study the target shooting by picosecond electron beam for designing the parameters of electron linac and target. In this paper, Monte Carlo method is used to calculate the X-ray characteristics produced by electron beam shooting, and the relationship between X-ray characteristics and target parameters, beam parameters.

CONVERSION TARGET SELECTION AND BEAM PARAMETERS

According to classical electrodynamics, charged particles accompany electromagnetic radiation when they are accelerated or decelerated. When a high-speed moving charged particle collides with an atom or a nucleus, under the action of the Coulomb potential, it will be deflected and decelerated while emitting x-rays, which is also called bremsstrahlung. In the electromagnetic theory, the intensity of bremsstrahlung is proportional to the square of the target nuclear charge and inversely proportional to the square of the mass of charged particles. Therefore, high-speed electrons are usually used to bombard the target nuclei to obtain high-intensity X-rays, and electrons are radiated in the target material. The energy loss of the electron can be expressed by the following formula [1]:

$$(-\frac{dE}{dx})_r = \frac{z(z+1)e^4 NE}{137 m_0^2 c^4}(4\ln\frac{2E}{m_0c^2} - \frac{4}{3}) \quad (1)$$

Where E is the energy of the incident electron; N is the number density of atoms of the target substance; m_0 is the electron mass; c is the speed of light; and e is the unit charge.

From the electromagnetic theory [2], we can know that bremsstrahlung radiation has the following characteristics: 1) the greater the atomic number, the higher the intensity of X-ray produced by the element; 2) the continuous change of energy; 3) the existence of short-wave limit, short-wave limit $\lambda_{min}=E/(hc)$, in which E is the energy of the incident electron; 4) when the incident electron energy is low, the momentum of the photon is small, the photon is emitted in all directions, and when the incident electron energy is high, the photon tends to emit forward. Therefore, in actual use, an element having a large atomic number and a high energy electron beam are usually selected.

Table 1: Electron Beam Parameters

Parameters	Values	Units
Energy	60～120	MeV
Charges	0.1～0.5	nC
Energy dispersion	0.3%(rms)	
Beam length	1～3(rms)	ps
Beam diameter	~15(rms)	μm
Emittance	<1@0.5nC	mm·mrad

Electron linac is generally used to produce high energy electrons. The electron linac we are currently developing consists of photocathode microwave gun, two acceleration tubes, three microwave power sources, a three-in-one

Content from this work may be used under the terms of the CC BY 3.0 licence (© 2018). Any distribution of this work must maintain attribution to the author(s), title of the work, publisher, and DOI.

ISBN: 978-3-95450-194-6 ISSN: 2226-0366 doi:10.18429/JACoW-LINAC2018-THPO022

DEVELOPMENT PROGRESS OF THE H+/H- LINEAR ACCELERATORS AT TSINGHUA UNIVERSITY*

Q.Z. Xing, X.D. Yu, C. Cheng, T.B. Du, X.L. Guan, H.Y. Zhang, S.X. Zheng, Y. Lei, R. Tang, P.F. Ma, S. Wang, C.B. Bi, C.T. Du, Q.K. Guo, X.W. Wang†, Key Laboratory of Particle & Radiation Imaging (Tsinghua University), Ministry of Education, Beijing 100084, China
also at Laboratory for Advanced Radiation Sources and Application, Tsinghua University, Beijing 100084, China
also at Department of Engineering Physics, Tsinghua University, Beijing 100084, China
B.C. Wang, W.L. Liu, M.W. Wang, Y. Yang, C. Zhao, Z.M. Wang, State Key Laboratory of Intense Pulsed Radiation Simulation and Effect (Northwest Institute of Nuclear Technology), Xi'an, 710024, China
W.Q. Guan, Y. He, J. Li, NUCTECH Co. Ltd., Beijing 100084, China

Abstract

We present, in this paper, the development progress of the 13MeV proton linac for the Compact Pulsed Hadron Source (CPHS), and the 7MeV H- linac injector for the synchrotron of the Xi'an 200MeV Proton Application Facility (XiPAF).

INTRODUCTION

One proton and one H- linear accelerators are being constructed. The Compact Pulsed Hadron Source (CPHS) project is aimed at becoming an experimental platform for education, research, and innovative applications at Tsinghua University. The facility will provide the proton beam, together with the neutron beam by delivering the proton beam to bombard the beryllium target. The designed parameters for the proton beam is 13 MeV/50 mA with the pulse length of 500 μs and repetition rate of 50 Hz [1][2]. The Xi'an 200MeV Proton Application Facility (XiPAF) project was launched in the year of 2014 for the research of the single event effect. The facility is mainly composed of one 7 MeV H- linac injector, one 200 MeV six-fold synchrotron and two experimental stations. The designed parameters for the H- beam of the linac injector is 7 MeV/5 mA with the pulse length of 10-40 μs and maximum repetition rate of 0.5 Hz [3].

13 MeV PROTON LINAC FOR CPHS

CPHS project consists of a high-current proton linac (13 MeV, 16 kW, peak current 50 mA, 0.5 ms pulse width at 50 Hz), a neutron target station, a small-angle neutron scattering instrument and a neutron imaging/radiology station. The accelerator system consists of the 50 keV ECR Ion Source (IS), Low Energy Beam Transport line (LEBT), 3MeV four-vane Radio Frequency Quadrupole (RFQ) accelerator, 13 MeV Alvarez-type Drift Tube Linac (DTL), RF power supply and distributor, and High Energy Beam Transport line (HEBT). Figure 1 presents the latest layout of the linac of the compact pulsed hadron source.

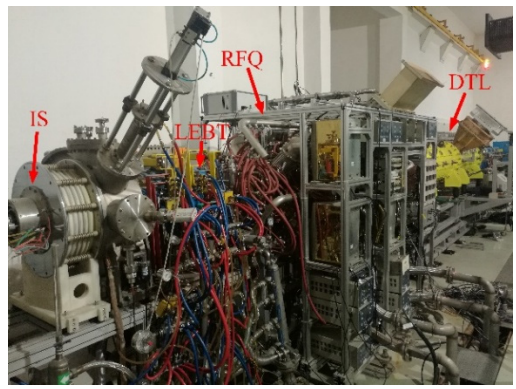


Figure 1: Layout of the linac of the compact pulsed hadron source.

CPHS has provided ~2000 hrs beam time since 2013 to the users with the neutrons produced by the 3 MeV proton beam from the RFQ bombarding on the beryllium target [4]. The application of the neutrons mainly consists of the neutron imaging [5], and the test of the neutron detectors including the B_4C-coated straw-tube [6] and the gadolinium-doped micro-channel plate (MCP) [7].

DTL

The 4.3-meter-long Alvarez-type DTL accelerates the 3 MeV proton beam to 13 MeV. The final tuning of the DTL cavity is completed and it is being installed in the beam line (Fig. 2).

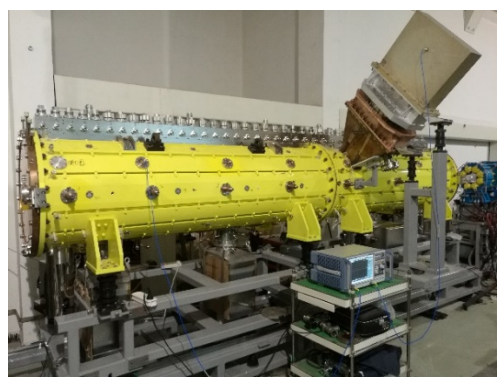


Figure 2: Assembled CPHS DTL for RF measurement.

* Work supported by National Natural Science Foundation of China (Project 11575098 and 11275106).
† wangxuewu@tsinghua.edu.cn

Content from this work may be used under the terms of the CC BY 3.0 licence (© 2018). Any distribution of this work must maintain attribution to the author(s), title of the work, publisher, and DOI.

ISBN: 978-3-95450-194-6 ISSN: 2226-0366 doi:10.18429/JACoW-LINAC2018-THPO026

THE MULTI-PHYSICS ANALYSIS OF DUAL-BEAM DRIFT TUBE LINAC *

Tao He[1,2], Liang Lu[1], Wei Ma[1], Lei Yang[1], Xianbo Xu[1], Liepeng Sun[1], Chaochao Xing[1],
[1]Institute of Modern Physics, Chinese Academy of Science, Lanzhou 730000, China
[2]also at University of Chinese Academy of Sciences, Beijing 100049, China

Abstract

The dual-beam drift tube linac (DB-DTL) prototype has been designed for verification of feasibility of multi-beam accelerator in middle energy region [1] [2]. The DB-DTL will accelerate 1 mA proton from 0.56MeV to 2.5MeV in pulse model. The DB-DTL operates at 81.25MHz, room temperature. The power dissipated on the surface on the DB-DTL internal surface will increase cavity temperature, which cause structure deformation and resonant frequency shifting. It is important to simulate the temperature rise, deformation and frequency shifting of DB-DTL cavity. The detailed three-dimensional multi-physics field analysis of DB-TL will be presented in this paper.

INTRODUCTION

The DB-DTL prototype is proposed to validate the feasibility of multi-beam accelerator in middle energy region. The main parameters are listed in Table. 1. The DB-DTL will operate as pulse injector with the capacity of accelerating proton from 0.56 MeV to 2.5 MeV [3]. The 35.83 kW normalized power dissipation of DB-DTL dissipated on the cavity internal surface will heat the cavity and cause cavity temperature rise and structural deformation, which will lead to resonant frequency shifting. The cooling water takes away the power to resolve this problem. In this paper, detailed multi-physics field simulation of DB-DTL is performed by using ANSYS multi-physics, which is a coupled electromagnetic, thermal and structural analysis.

Table 1: DB-DTL Prototype Main Parameters

Parameters	Value
Particle	H^+
Operation	pulsed
Frequency (MHz)	81.25
Current (mA)	1
Input/output energy (MeV/u)	0.56/2.56
Maximum gap voltage (kV)	387.50
Transmission efficiency (%)	35.0
Power dissipation (MW)	35.83
Kilpatrick factor	2.10
Shunt impedance (MΩ/m)	200.02

MULTI-PHYSICS ANALYSIS

As shown in Fig. 1 [4], the multi-physics analysis is a coupled electromagnetic, thermal, structural and frequency shifting analysis. The ANSYS workbench [5] and CST Microwave Studio (MWS) [6] are employed in the simulation. The total cavity power loss is firstly calculated with the MWS and the distribution of RF thermal loss on the cavity internal surface is simulated with the ANSYS High Frequency Structure Simulator (HFSS), which will be coupled to the next thermal analysis. The thermal solution will generate cavity temperature map based on cavity internal surface heat flux, which is applied to calculate the structural stresses and deformations. The last step is to calculate the resonant frequency shift according to the deformations. Through multi-physics analysis, appropriate parameter of cooling-water is chosen to satisfy the requirement for cavity operation of DB-DTL. The deformation and stress of cavity and corresponding resonant frequency shifting should be within a proper range.

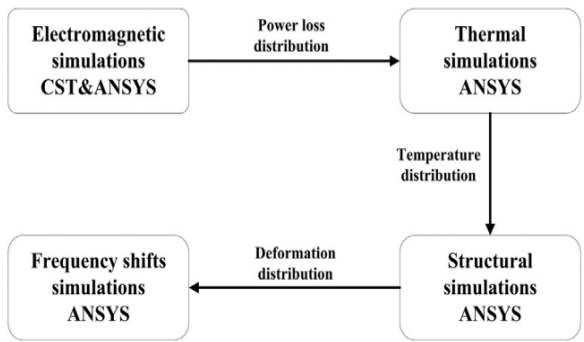


Figure 1: Multi-physics analysis scheme with CST and ANSYS.

The electromagnetic simulation results in MWS show that cavity resonant frequency is 81.24993 MHz. The normalized power dissipation is 35.83 kW and the shunt impedance is 100.01 MΩ/m. Then, verification of electromagnetic calculation by using ANSYS HFSS is performed. Table. 2 gives a comparison of electromagnetic simulation between the MWS and ANSYS, which indicates the difference is enough small to ignore. As shown in Fig. 2, the octahedron cavity shape model is chosen for easily assembling, which includes 8 ridge waterways and 5 wall waterways. The parameter of cooling-water is plotted in Table. 3. Figure 3 shows the distribution of the cavity power dissipation, which will be applied to following thermal simulation. The power dissipated on cavity internal surface will increase temperature rise of DB-DTL cavity. It is important to simulate the temperature distribution of DB-DTL, which is couple to next structural analysis in ANSYS Static Structural code for simulating the deformation and stress distribution of DB-DTL cavity.

The simulation results of multi-physics analysis show that the temperature rise, deformation， stress and resonant frequency are beyond a proper range, which indicate the

* Work supported by NSFC and CAS through Grant Nos. 11475232 and 11535016.
† email address: hetao0216@impcas.ac.cn

Content from this work may be used under the terms of the CC BY 3.0 licence (© 2018). Any distribution of this work must maintain attribution to the author(s), title of the work, publisher, and DOI.

ISBN: 978-3-95450-194-6 ISSN: 2226-0366 doi:10.18429/JACoW-LINAC2018-THPO028

MAGNETIC FIELD MEASUREMENT AND ANALYSIS FOR DRIFT TUBE LINAC OF CSNS*

B. Li[1,†], H. C. Liu[1], Q. Chen[1], X. L. Wu[1], K. Y. Gong, A. H. Li[1], M. X. Fan[1], Y. Wang[1], P. H. Qu[1], J. X. Zhou, W. Kang, China Spallation Neutron Source, Institute of High Energy Physics, China Academy of Sciences, 523803, Dongguan, P. R. China,
[1]also at Dongguan Neutron Science Center, 523808, Dongguan, P. R. China

Abstract

A 324MHz Alvarez-type Drift Tube Linac (DTL) is used to accelerate the H- ion beam from 3 to 80 MeV with peak current 15mA for China Spallation Neutron Source (CSNS). DTL is composed by 36 meters cavity and 161 DTs, the DT magnet coil adopted SAKAE structure with compact, smaller aperture. Magnetic field is measured by self-developed high precision rotating coil measurement system. This paper introduces the rotating coil measurement system simply and presents the 161 DTs magnetic field measurement results comprehensively, include magnetic field center offset, integral magnetic field, higher-order harmonics. In addition, cooling test result of magnet coil is also presented.

INTRODUCTION

Drift Tube Linac of CSNS which accelerating an H- ion beam from 3 MeV to 80 MeV has been designed as 4 tanks with a total length of approximately 36 m [1, 2]. The electromagnetic quadrupoles (EMQs) are used in DTL accelerator for transverse focusing since the magnetic field gradient can be adjusted by varying the current flow in the conductors. The major parameters of the designed DTL quadrupole (DTLQ) are presented in Table 1.

DRIFT TUBE AND ROTATING COIL MEASUREMENT SYSTEM

The structure of Alvarez-type Drift Tube is show in Fig. 1. We adopted an electroformed hollow coil- SAKAE type coil which has no bending radius, for its compact structure. The wire cutting and the Periodic Reverse copper electroforming method are applied to the coil manufacture process. The DT shell and stem are made of oxygen free copper and cooled via the supporting stem. The fabrication process is complex and time consuming accompanied with a series of tests. All joints of the DT and the stem are welded by the electron beam welding (EBW). The space around the magnet in the DT is filled with the epoxy resin by a vacuum impregnation method.

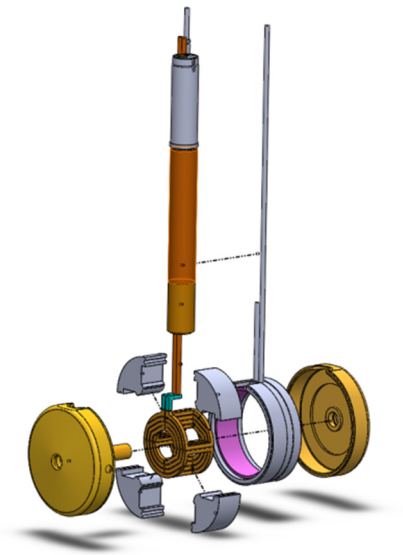


Figure 1: Drift tube structure.

Table 1: Design Parameters of DTL Quadrupole Magnets

Cavity number	Cavity 1		Cavity 2&3	Cavity 4
Magnet type	DTL-QA	DTL-QB	DTL-QC	DTL-QD
Quantity	26	39	69	27
Outer radius(mm)	108	108	108	108
Inner radius(mm)	19	19	23	27
Good field region(mm)	14	14	18	22
Higher-order harmonics(Bn/B2)	$<3.0\times10^{-3}$	$<3.0\times10^{-3}$	$<3.0\times10^{-3}$	$<3.5\times10^{-3}$
Effective length(mm)	40	50	75	70
Field gradient(T/m)$_{max}$	55	55	17	13.5
Integral field(T)	2.2	2.75	1.275	0.945
Field gradient(T/m)$_{min}$	40	25	12	12

† libo0910@ihep.ac.cn

Content from this work may be used under the terms of the CC BY 3.0 licence (© 2018). Any distribution of this work must maintain attribution to the author(s), title of the work, publisher, and DOI.

ISBN: 978-3-95450-194-6 ISSN: 2226-0366 doi:10.18429/JACoW-LINAC2018-THPO029

QUALITY FACTOR AND POWER LOSS OF THE CSNS DTL*

P.H Qu†, H.C Liu, A.H Li, M.X Fan, B. Li , J. Peng, Y. Wang, X.L Wu, Q. Chen, K.Y Gong Institute of High Energy Physics, Chinese Academy of Science, Beijing, China, Dongguan Neutron Science Center, Dongguan, China

Abstract

An Alvarez-type Drift tube linac (DTL) was utilized to accelerate the H- ion beam of up to 15mA peak current from 3 to 80MeV of China Spallation neutron source (CSNS). For ease of manufacturing and measurement, the CSNS DTL was divided into four independent cavities. The Q factor of four cavities were given, including the measurement results of low-power [1] and high-power [2], and several reasons for the low Q factor of the cavity in the measurement process were analysed. During the operation of the DTL, the frequent alarm of the water flow switch causes the power of the cavity to fall to 0. Estimate the power loss of each component, under the circumstances of ensuring adequate water flow, reduce the alarm threshold of the water flow switch of some components to improve the stability of the system.

INTRODUCTION

Injectors for CSNS include a 50KeV H- ion, a LEBT, a 3MeV Radio Frequency Quadrupole (RFQ), a MEBT and an 80MeV Drift Tube Linac (DTL) as shown in Fig. 1. The Q factor is an important parameter in the DTL cavity design specifications. The Q factor of the hollow cavity reaches more than 89% of the theoretical value, and the cavity copper plating process meets the high-frequency requirement. The hollow cavity does not include stems, drift tubes (DTs), post couplers (PCs) and slug tuners. Each DTL cavity was powered by a 3MW klystron, the Q factor of total cavity which includes stems, DTs, PCs and slug tuners reached more than 75% of the theoretical value, the power loss of each cavity is within the working range of the klystron. In the course of cavity running, the water flow switch warning question becomes prominent day by day. Through two methods of experimental measurement and CST software simulation [3] to estimate the power loss of each component, especially the PCs and slug tuners. Optimized water cooling system, reducing the system failure rate.

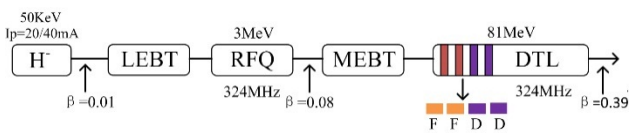


Figure: 1: CSNS Linac injectors.

* Work supported by National Natural Science Foundation of China (11105166), and Youth Innovation Promotion Association of CAS (2015011).
† Email: quph@ihep.ac.cn

Q FACTOR OF HOLLOW CAVITY

The length of first tank DTL1 is 8.5 meters, a total of three units. The first unit DTL1-1 has a length of about 2.8 meters. The unloaded Q factor which called Q_0 of the DTL1-1 hollow cavity which shown in Fig. 2(a) was tested. Hollow cavity of DTL1-1 has no stems, DTs, PCs and slug tuners. The openings of the cavity were sealed with copper plugs as shown in Fig. 2(b) and (c).

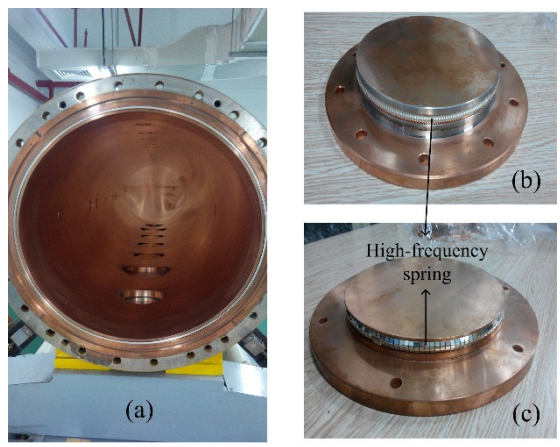


Figure 2: Hollow cavity of DTL1-1 and copper plugs.

Table 1 shows the results of Q_0 of DTL1-1. The final Q_0 was taken as the average of 89.88% of the theoretical value. It shows that the inner wall copper plating process meets the high-frequency requirements. The loaded Q factor Q_L was measured by a vector network analyser using the two-port network method [1]. The Q_0 can be calculated by Q_L, and the formula is shown in Eq. (1).

$$Q_0 = Q_L \cdot (1 + \beta_1 + \beta_2) = Q_L \cdot \left(1 + 1/VSR_1 + 1/VSR_2\right) \quad (1)$$

The factors that influence the measurement result of Q_0 are as follows. The better the high-frequency spring (shown in Fig. 2) seal of copper plugs, the larger the Q_0 measurement. Partial copper plug diameter is too large to install, milling part of the copper layer, bare iron exposed as shown in Fig. 2 (b), due to a part of the material from copper to iron, which makes a little drop in the measured value of Q_0. During the measurement, the standing wave ratio is reduced, which makes the received signal relatively strong. The three results in table 1 are not much different and the measured Q_0 is more accurate.

Content from this work may be used under the terms of the CC BY 3.0 licence (© 2018). Any distribution of this work must maintain attribution to the author(s), title of the work, publisher, and DOI.

ISBN: 978-3-95450-194-6 ISSN: 2226-0366 doi:10.18429/JACoW-LINAC2018-THPO030

OPERATION EXPERIENCE OF THE CSNS DTL*

Huachang Liu[1,2,3†], Jun Peng[1,2,3], Keyun Gong[1,2],Ahong Li[1,2,3], Bo Li[1,2], Qiang Chen[1,2], Xiaolei Wu[1,2] ,Mengxu Fan[1,2], Yun Wang[1,2] , Peihua Qu[1,2], Shinian Fu[1,2,3]

[1] Institute of High Energy Physics, Chinese Academy of Sciences (CAS), Beijing, China
[2] Dongguan Neutron Science Center, Dongguan 523803, China
[3] University of Chinese Academy of Sciences, Beijing, 100049, China

Abstract

The China Spallation Neutron Source (CSNS) Drift tube linac (DTL) accelerates H- beam from 3 to 80MeV with 4 independent tanks. The 80MeV beam acceleration was achieved in January 2018. The linac is a key to the reliability of the whole CSNS facility since all the beams stop when these upstream facilities fail. Many efforts have been made for DTL reliable operation. This paper presents the operation experience learned in DTL commissioning.

INTRODUCTION

The China Spallation Neutron Source (CSNS) is an accelerator-based multidisciplinary user facility constructed in Dongguan, Guangdong, China [1]. The CSNS complex consists of an H- linear accelerator, a rapid cycling synchrotron (RCS) accelerating the beam to 1.6 GeV, a solid-tungsten target station, and instruments for spallation neutron applications. Construction and commissioning has been completed so far. The facility operates at 25 Hz repetition rate with an initial beam power of approximately 20 kW on target. It can be foreseen that the beam power on target will reach 100kW within 2~3 years. The facility will provide scientists with a world-leading platform for studies in fields such as materials science and technology, life sciences, and new energy, etc.

The 324MHz drift tube linac (DTL) is the main part of CSNS accelerator linac complex (Fig.1). It can provide 15mA peak current beam with energy gain from 3 to 80MeV [2]. It consists of four independent tanks with ~9m in length. Each tank is divided into three short unit sections for ease of fabrication and assembly. A hollow coil based electromagnet is accommodated in each drift tube for its compact structure. The main design parameters of DTL are listed in table 1.

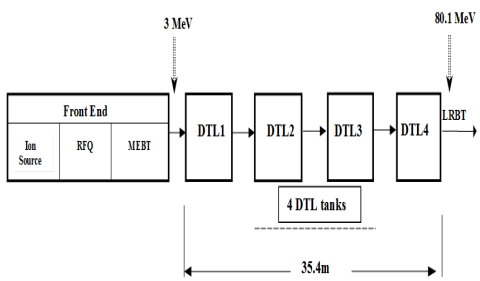


Figure 1: Layout of the CSNS LINAC.

The commissioning of the first DTL tank started in January 2016. The first 20MeV@18mA beam was achieved within ten days. Based on the experience of DTL1 commissioning, the three successive DTL tanks were progressively installed and commissioned. Final 80 MeV acceleration was successfully obtained in January 2018. During the commissioning and operation, the performance of DTL gradually improved owing to a series of prompt action to the troubles.

Table 1: Major Parameters of CSNS DTL

Tank number	1	2	3	4	total
Output energy (MeV)	21.67	41.41	61.07	80.1	80.1
Length (m)	8.51	8.56	8.78	8.8	
Number of cells	64	37	30	26	157
RF driving power (MW)	1.35	1.32	1.32	1.34	5.33
Total RF power (MW)@30mA	1.91	1.92	1.92	1.93	7.68
Accelerating field (MV/m)	2.86	2.96	2.96	3.0	
Synchronous phase (degree)	-35 to -25	-25	-25	-25	
RF frequency(MHz)	324	324	324	324	324
Max. repetition rate(Hz)	25	25	25	25	25
Peak surface field(Kilpatrick)	/	/	/	/	<1.3

BEAM COMMISSIONING

The DTL consists of four accelerating tanks with final output energy 80MeV. The transverse focusing was arranged in a FFDD lattice utilizing electric-magnet quadrupoles. Because no drift tube is empty, diagnostics have to be imbedded between tanks. After each tank, a FCT and a CT were installed to monitor beam phase and current. Between DTL 3 and DTL 4, a Beam Position Monitor (BPM) was added for monitoring beam orbit.

For DTL tanks, it is essential to find the correct tank RF field amplitude and phase to minimize energy spread and mismatch, which are highly required by the following

*Work supported by Youth Innovation Promotion Association of CAS (2015011)
† email address:liuhc@ihep.ac.cn

Content from this work may be used under the terms of the CC BY 3.0 licence (© 2018). Any distribution of this work must maintain attribution to the author(s), title of the work, publisher, and DOI.

ISBN: 978-3-95450-194-6 ISSN: 2226-0366 doi:10.18429/JACoW-LINAC2018-THPO031

RF CONDITIONING AND BEAM COMMISSIONING STATUS OF CSNS DTL

Y. Wang[1,†], H. Liu[1], B. Li[1], M. Fan[1], A. Li[1], P. Qu[1], K. Gong[1], X. Wu[1], Q. Chen[1], J.Peng[1]
Institute of High Energy Physics, Chinese Academy of Sciences, 100049 Beijing, China
[1]also at Dongguan Institute of Neutron Science, 523803 Dongguan, China

Abstract

The high power RF conditioning of CSNS DTL was finished in April 2017 with peak input power 1.6 MW, 650 us pulse width, 25 Hz repetition frequency. With careful tuning of RF amplitude and phase, beam was accelerated to 80 MeV successfully with maximum peak beam current 12 mA and about 98% transmission efficiency. DTL operate stably at full power level with several trips per day without beam interruption after six months commissioning. The whole RF conditioning process was presented and some details of beam commissioning were described in this paper.

INTRODUCTION

The CSNS DTL is a Alvarez-type Linac, consists of four cavities, accelerate H^- particle from 3 to 80 MeV [1]. Each cavity is powered by individual klystron with 324 MHz operation resonant frequency. The Lattice structure made up of electromagnets inside every drift tube provide transverse focus force for the beam [2]. The main parameters of the CSNS DTL are listed in Table 1.

Table 1: Main Parameters of the CSNS DTL

Tank number	1	2	3	4	total
Output energy (MeV)	21.67	41.41	61.07	80.09	80.09
Number of cell	64	37	30	26	157
RF driving power (MW)	1.35	1.32	1.32	1.34	5.33
Total RF power (MW) (I=30 mA)	1.91	1.92	1.92	1.93	7.68
Accelerating field (MV/m)	2.86	2.96	2.96	3.0	
Synchronous phase (degree)	-35 to -25	-25	-25	-25	

RF CONDITIONONGING

The high power conditioning started in December 2015, and finished in February 2017. Due to time limitation, the couplers and ceramic windows of all four cavities were not previously conditioned. The actual effective aging time is about 106 days, the DTL-1 cavity took about 61days due to high frequently arcing and poor vacuum condition. After DTL-1 conditioning process, the first beam had been successfully accelerated to design energy 21.6 MeV by deliberately adjusting of input power amplitude and phase. The rest three cavities took about 45 days finishing conditioning process with 700 us, 25 Hz, peak input power 1.6 MW. The RF conditioning parameters are presented as Table 2.

Table 2: RF Conditioning Parameters

Operation Frequency	324 MHz
Repeation Frequency	25 Hz
Power Width	650 us
Input Power	1.5 MW

Figure 1 shows the whole DTL structure. Before conditioning, the interlock protection systems, include temperature sensors mounted on outside wall, vacuum system read from Cold Cathode Gauges, water cooling system which monitors cooling water flow and VSWR protection system used to shut down RF power when severe arc occurs, are rechecked to ensure cavity operation normally.



Figure 1: The CSNS DTL in tunnel.

The high power conditioning process is illustrated as following,

Firstly, 5~10 kW(650 us, 25 Hz) input power is fed in cavity to see whether cavity operation correctly. The ceramic window is sensitive with the increase of input power, which is almost fully reflected back during initial conditioning process. Half of hour later, power is smoothly transferred into cavity, clear signal can be seen in the oscilloscope captured by pickup.

Secondly, as power comes into cavity, the vacuum fluctuation is big due to outgas from internal wall. Input power was increased gradually according vacuum condition changing, which should rebalance to a stable situation after new high power level. If vacuum condition continues to deteriorate because of arcing inside cavity, then input power amplitude should be reduced until vacuum condition getting stable again. Generally, 5~10 kW increasing power per step is reasonable below 1 MW. For keeping high conditioning efficiency, the klystron fre-

* Work supported by Youth Innovation Promotion Association of CAS (2015011)
† wangyun@ihep.ac.cn

Content from this work may be used under the terms of the CC BY 3.0 licence (© 2018). Any distribution of this work must maintain attribution to the author(s), title of the work, publisher, and DOI.

ISBN: 978-3-95450-194-6 ISSN: 2226-0366 doi:10.18429/JACoW-LINAC2018-THPO032

CSNS LINAC BEAM COMMISSIONING TOOLS AND EXPERIENCE

Y. Li, J. Peng, Z.P. Li, S. Wang DINS/IHEP, Dongguan, 523803, China

Abstract

The China Spallation Neutron Source (CSNS) successfully accelerated the H- beam to 80 MeV in January 2018, marking a key progress in the beam commissioning. One of the keys to success is the development and use of software tools. XAL, a Java-based software infrastructure originally developed by SNS was applied for CSNS beam commissioning. We have developed and transplanted many applications based on XAL. Some of the applications for the LINAC are described, and some experiences are shared.

INTRODUCTION

The CSNS [1] accelerator complex consists of an H- injector, a linear accelerator, a RCS ring and associated beam transport lines. The LINAC is 200m with the output energy of 80 MeV in CSNS-I and 250 MeV in CSNS-II. The LINAC commissioning initiated April 2015 and completed in January 2018, was performed in 4 discrete runs with interruption of DTL tank installation and the faults of CPI klystron and DTL vacuum. The beam commissioning for the Front-End to MEBT was form April 2015 to July. The beam transmission of the RFQ is more than 90% and the parameters of MEBT are also accurately measured. DTL-1 beam commissioning was completed in January 2016. The beam transmission is 100% and the peak current is 18 mA, which is higher than the design value of 15 mA. In April 2017, the DTL-2 and DTL-3 beam commissioning was completed, and the beam energy reached 60MeV. In January 2018, the beam commissioning for DTL-4 was finished. The beam energy reached the design value of 80 MeV with the error of $\pm$0.01 MeV, and the overall beam transmission of DTL reached over 97%.

Beam commissioning for LINAC is generally smooth regardless of hardware installation and the major faults. The software tools play an important role for this successful beam commissioning. The XAL [2, 3] and Open XAL were selected as our software development platform. XAL was originally developed and used by SNS for accelerator physics commissioning. It consists of upper applications, physics model of the beam and other toolkit. The XAL was confirmed as our tuning software development platform at the end of 2012, and a large number of physical applications were developed based on the SNS / XAL version between 2014 and 2015 and officially used in April 2015. A lot of useful applications have been developed in subsequent beam commissioning. OPEN XAL is an upgrade of XAL, which is a collaboration among several laboratories, including CSNS. XAL and OPEN-XAL are used simultaneously in our control room now and XAL is used more.

In this paper, the physical applications used in LINAC beam commissioning including longitudinal and transverse were introduced firstly. Then the problems and solutions during the development and use of the software tools will be shown later.

THE APPLICATIONS

Applications for LINAC beam commissioning are mainly divided into three aspects: longitudinal、 transverse and machine management related applications.

RF Phase Scan and Tuning Application

The longitudinal tuning is the first and the most important step for LINAC beam commissioning. To achieve the design value, accurate RF phase and amplitude settings are required. A software application called PASTA [4] in XAL has been written to perform RF phase setting using the signature matching method. The PASTA of CSNS version has been modified in two ways. First, SNS uses Beam Position Monitor (BPM) to measure the phase of the beam, but we use Fast Current Transforms (FCTs), so the corresponding components are replaced. In addition, due to the great difference between CSNS-DTL and SNS-DTL in the relationship between the transition time factor and Beta, we also revised the underlying energy calculation code to make it consistent with the CSNS-DTL acceleration characteristics. Figure 1 is the analysis panel of the PASTA application with the result of DTL-4 tank. It shows the error is very small in the range of 70 degrees and the calculated energy is very close to the design energy. The energy of LINAC is also measured using the Time-of-Flight (TOF) method, which is also close to the design value and the maximum difference is less than 0.5%.

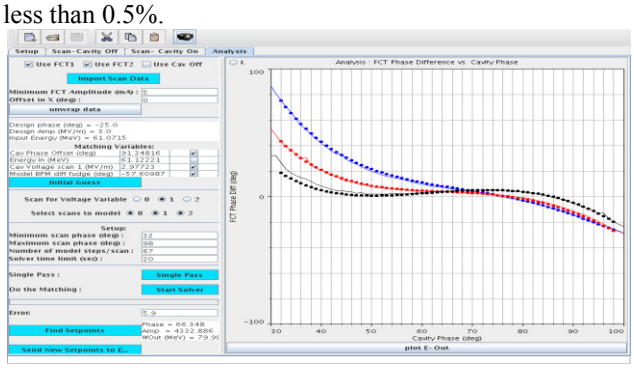


Figure 1: The analysis panel of the PASTA application.

Orbit Correction

Due to the small aperture of the vacuum beam pipe in LINAC, the beam orbit distortion should be small and smooth. The “orbit correction” application in XAL can realize orbit distortion measurement and correction [5]. Based on the response matrix of BPM to corrector (theoretical or measurement response matrix), the Solver calculation module was used to fit the measured orbit and predicted orbit. After repeated iterations, the correspond-

Content from this work may be used under the terms of the CC BY 3.0 licence (© 2018). Any distribution of this work must maintain attribution to the author(s), title of the work, publisher, and DOI.

ISBN: 978-3-95450-194-6 ISSN: 2226-0366 doi:10.18429/JACoW-LINAC2018-THPO033

THE DEVELOPMENT OF PERMANENT MAGNET QUADRUPOLES FOR XiPAF DTL

B. C. Wang, Z. M. Wang, M. T. Qiu, C. Y. Wei, State Key Laboratory of Intense Pulsed Radiation Simulation and Effect (Northwest Institute of Nuclear Technology), 710024 Xi'an, China
S. X. Zheng[1], Q. Z. Xing[1], Q. K. Guo[1], C. T. Du[1], X. W. Wang[1], Department of Engineering Physics, Tsinghua University, 100084 Beijing, China
[1]also at Key Laboratory of Particle & Radiation Imaging (Tsinghua University), Ministry of Education, 100084 Beijing, China; Laboratory for Advanced Radiation Sources and Application, Tsinghua University, 100084 Beijing, China

Abstract

Permanent magnet quadrupoles (PMQs) are developed for the DTL of Xi'an 200 MeV Proton Application Facility (XiPAF). In this paper, we describe the fabrication and measurements for the Halbach-type PMQs. The main procedure of the PMQ manufacture is presented. And the magnetic measurements of PMQs are carried out with the help of vibrating wire, Hall probe and rotating coil respectively. The results show the PMQs are able to meet the requirements of XiPAF DTL.

INTRODUCTION

The Alvarez-type DTL is being built to accelerate the H- beam from 3 MeV to 7 MeV for Xi'an 200 MeV Proton Application Facility (XiPAF). The permanent magnet quadrupoles (PMQs) are adopted for focusing the beam. The Halbach-type PMQ is developed by our team to meet the requirements obtained by beam dynamics calculations. All the PMQs are fabricated and measured.

The main parameters and requirements of the PMQs are listed in Table 1 and Table 2. The gradient of the PMQ is about 80 ~ 90 T/m. It is worth noting that the integrated gradient *Gl* makes more sense in accelerators. Therefore, *Gl* is listed in the requirements rather than the gradient.

Table 1: Main Parameters of the PMQs

Parameter	Symbol	Values
Inner diameter	*DI*	22 mm
Outer diameter	*DO*	60 mm
Length	*l*	40 mm
Integradient gradient deviation	Δ*Gl*/*Gl*	1.5%

Table 2: Integrated Gradient Requirements of the PMQs

Type	Integrated Gradient *Gl* (T)	Quantity
A	3.293	1
B	3.540	1
C	3.570	1
D	3.587	1
E	3.336	19

PMQ DEVELOPMENT

The 16-segment type PMQ is adopted in our facility. Figure 1 illustrates the cross section of a PMQ consisting 16 SmCo segments wherein the arrows indicate the easy axis orientation of each segment.

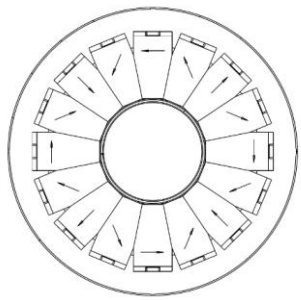


Figure 1: Cross section of the PMQ.

The fabrication procedure of the PMQs can be summarized as follows. Firstly, a number of SmCo segment blocks, which are shown in Figure 2, are produced in order to achieve enough qualified PMQs. Secondly, all the blocks are aged for 12 hours at 180 degrees Celsius. Thirdly, the magnetic field direction and strength of each blocks are measured and screened. Fourthly, the qualified blocks are then sorted by the strength and direction. Lastly, the blocks are assembled together with specified accuracy. Figure 3 and Figure 4 show one PMQ being assembled and after assembling respectively.

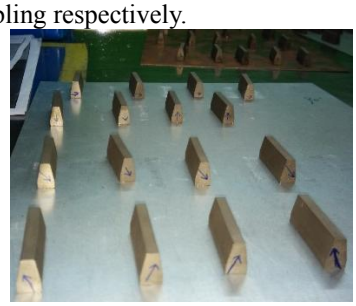


Figure 2: The aged blocks.



Figure 3: One PMQ being assembled.

Content from this work may be used under the terms of the CC BY 3.0 licence (© 2018). Any distribution of this work must maintain attribution to the author(s), title of the work, publisher, and DOI.

ISBN: 978-3-95450-194-6 ISSN: 2226-0366 doi:10.18429/JACoW-LINAC2018-THPO034

EXPERIMENTAL STUDY OF TUNING METHOD ON A MODEL ALVAREZ DTL CAVITY FOR CPHS PROJECT

Y. Lei[1,2], S. X. Zheng[1,2], Q. Z. Xing[1,2†], R. Tang[1,2], X. L. Guan[1,2], X. W. Wang[1,2], Key Laboratory of Particle & Radiation Imaging (Tsinghua University), Ministry of Education, Beijing 100084, China
[1]also at Laboratory for Advanced Radiation Sources and Application, Tsinghua University, Beijing 100084, China
[2]also at Department of Engineering Physics, Tsinghua University, Beijing 100084, China

Abstract

This article is devoted to the experimental study of tuning method for an Alvarez-type drift tube linac (DTL) of the Compact Pulse Hadron Source (CPHS) project at Tsinghua University. The biperiodic structure based on the post couplers are introduced to overcome the instability of the Alvarez DTL tank which is used to operate in 0 (or 2π) mode. The experimental method and results are presented, and the tuning scheme for the formal CPHS DTL is summarized from the tuning experiment.

INTRODUCTION

The effective shunt impedance of the Alvarez-type DTL is typically high when it operates in a typical 0 (or 2π) mode with the group velocity of 0. But the structure is very susceptible to perturbation such as the beam loading, mechanical and installation error, because of the narrow space near the adjacent modes on the TM dispersion curve. The post couplers, which are the resonant-coupling elements constitutionally, are mounted on the wall of the DTL cavity oppositely and alternatively to introduce a new PCs (post couplers) dispersion curve. When the stopband between the two passbands of the dispersion curves disappears by adjusting the slugging length of the post couplers, the lowest frequency of the TM passband will be moved to the π/2 mode point of the new dispersion curve. Therefore the new stable biperiodic structure of the DTL will be achieved [1].

To verify the tuning method, one model cavity has been machined and the turning experiment is carried out based on the cavity. The cavity is designed and manufactured for verifying the mechanical design and undertaking some low-power experiment. The model cavity consists of ten full drift tubes, two half drift tubes mounted on the end flanges, three post couplers and two tuners [2]. The end of the post couplers is designed to be eccentric to facilitate the tuning of the local field distribution by rotating the post.

TUNING EXPERIMENTAL CONFIGURATION

On the experimental stand as shown in Fig. 1, the measurement based on the bead-pull method is executed. According to the perturbation theory, when the bead is pulled into the field between the two adjacent drift tubes, the resonant frequency changes. Then the corresponding phase shift can be detected by a vector network analyzer (VNA) and the electric field along the beam-axis can be deduced [3].

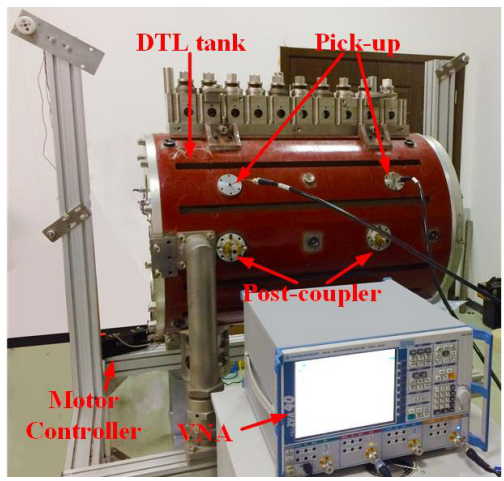


Figure: 1 Tuning experimental stand.

A stepping motor is adopted to pull a fine nylon line on which the small perturbation bead is fixed. The size of the bead shall be rather appropriate, so that the responsive signal caused by the bead is big enough compared with the background noise and at the same time within the linear range of the phase around the resonant frequency. It depends on the Q factor of the cavity. The Q factor of this model cavity is measured as 17796 which is about 44% of the designed value. It is because that the surfaces of the interior copper-plated cavity wall and the aluminous end flanges are oxidic. With the value of the Q factor, the radius of the bead is determined as 0.7 mm by estimation.

To ensure the accuracy of the measurement, the peak field is employed to represent the field distribution instead of the integral one due to its further advantages [4]. Before the measurement, the reproducibility is checked. The reproducibility R_{ij} is defined by Eq. (1).

$$R_{ij} = \frac{E_{ij}}{\left(\sum_{j=1}^{n} E_{ij}\right)/n} . \quad (1)$$

where E_{ij} is the measured electric field strength of the ith cell for the jth time, and n is the number of times of the measurements. Ten sequential measurement is analyzed by this definition, and the reproducibility is better than ±0.15% as shown in Fig. 2.

† xqz@tsinghua.edu.cn

Content from this work may be used under the terms of the CC BY 3.0 licence (© 2018). Any distribution of this work must maintain attribution to the author(s), title of the work, publisher, and DOI.

ISBN: 978-3-95450-194-6 ISSN: 2226-0366 doi:10.18429/JACoW-LINAC2018-THPO035

TUNING AND LOW POWER TEST OF THE 325 MHz IH-DTL AT TSINGHUA UNIVERSITY

R. Tang[1,2], W.B. Ye[1,2], P.F. Ma[1,2], Y. Lei[1,2], S. X. Zheng[1,2†], Q. Z. Xing[1,2], H.Y. Zhang[1,2], C. T. Du[1,2], K. D. Man[1,2], X. L. Guan[1,2], X. W. Wang[1,2],
C. X. Tang[1,2], Key Laboratory of Particle & Radiation Imaging (Tsinghua University), Ministry of Education, Beijing 100084, China
[1]also at Laboratory for Advanced Radiation Sources and Application, Tsinghua University, Beijing 100084, China
[2]also at Department of Engineering Physics, Tsinghua University, Beijing 100084, China
J. Li, NUTECH Co.Ltd, Beijing 100084,China

Abstract

An interdigital H-mode drift tube linac (IH-DTL), which accelerates proton beam from 3 MeV to 7 MeV has been designed and assembled at Tsinghua University. There are 8 plungers in the 1 m tank and one coaxial coupler is used to feed the power. The frequency is tuned to 325 MHz. The field distribution is measured by the bead perturbation method. Finally, the gap voltage error has been tuned to be within ±3.0%, which satisfies the design requirement. The Q factor of the tank is 7000 while the power dissipation is 244 kW. Details of the low power test is presented.

INTRODUCTION

Since 1950s, IH DTL was firstly proposed by J.P. Blewett, it has been carefully studied and been adopted as the heavy ion accelerators. Because of its high shunt impedance and high accelerating field, IH DTL is adopted widely for the injection of the synchrotron-based medical facilities [1-3]. A 325 MHz IH DTL has been designed, fabricated and assembled at Tsinghua University for the medical purpose [4,5]. The length of the IH DTL is about 1 m and the 3 MeV proton from the RFQ can be accelerated to 7 MeV. A modified KONUS beam dynamics has been adopted in the design [5]. There are no magnets in the tank. The RF characteristics has been studied with the 3D microwave studio. The Q_0 factor is 11300 and the power dissipation is 151 kW. The designed parameters of the IH DTL are listed in Table. 1.

The tuning method of the IH DTL has been carefully studied. Several kinds of the IH tank has been tuned and reported [2,3,6]. The relative error between the measurement and the design is within ±3% mostly. For the 325 MHz IH DTL, 8 symmetric plungers are adopted for the tuning. The tuning range of the frequency is about 10 MHz. After the error analysis of the beam dynamics, the requirement of the error between the measurement and the design is≤±3.0%, which is consistent with the other IH DTLs. Details of the low power test and the tuning will be presented.

Table 1: Parameters of the IH-DTL

Parameters	Value
Particle species	Proton
Frequency	325 MHz
Injection energy	3 MeV
Output energy	7 MeV
Tank length	1.14 m
Number of cells	21
Frequency	325 MHz
Q_0	11300
Power	151 kW
Z [MΩ/m]	193 MΩ/m
$ZTT\times\cos^2(\phi)$ [MΩ/m]	107 MΩ/m
E_{peak}	2.3 Kp

LOW POWER TEST PLATFORM

The low power test plat form is composed of a stepped motor with the controller, a vector network analyser, and a co-axial coupler. The electric field is much smaller at the both ends of the tank while the magnetic field is much bigger. Thus, an insulated bead is adopted for the bead perturbation measurement [7]. The bead is pulled by the stepped motor with constant velocity and S21 signal of the VNA is used to measure the phase variation.

The low power test has been divided into two stages. The first stage of low power test is performed at Tsinghua University before the paint. The frequency is tuned to 325 MHz and the relative gap voltage error is within ±3.0% with the adjustable aluminium plungers. The high power operation will be performed at site where is one thousand kilometres far from Tsinghua University. The performance of the tank is worried after the long-distance transportation, therefore the second low power test is performed. Figure 1 shows the platform at both sites. There is no difference between the two measurement. Thus, the result shows that the long-distance transportation causes little influence on the tank.

Content from this work may be used under the terms of the CC BY 3.0 licence (© 2018). Any distribution of this work must maintain attribution to the author(s), title of the work, publisher, and DOI.

ISBN: 978-3-95450-194-6 ISSN: 2226-0366 doi:10.18429/JACoW-LINAC2018-THPO036

ERROR STUDY OF CPHS DTL AFTER ASSEMBLY

P.F. Ma[1,2], Q.Z. Xing*[,1,2], R. Tang[1,2], Y. Lei[1,2], Q.K. Guo[1,2], C.T. Du[1,2], S.X. Zheng[1,2], X.L. Guan[1,2], X.W. Wang[1,2], Key Laboratory of Particle and Radiation Imaging, Tsinghua University, Ministry of Education, Beijing 100084, China
B.C. Wang, State Key Laboratory of Intense Pulsed Radiation Simulation and Effect, Northwest Institute of Nuclear Technology, Xi'an, 710024, China
[1]also at Laboratory for Advanced Radiation Sources and Application, Tsinghua University, Beijing 100084, China
[2]also at Department of Engineering Physics, Tsinghua University, Beijing 100084, China

Abstract

The Compact Pulsed Hadron Source (CPHS) at Tsinghua University is one multi-purpose pulsed neutron source. The injector of the CPHS is a linac, which mainly consists of a source, a low-energy beam transport line (LEBT), a radio frequency quadrupole (RFQ) and a drift tube linac (DTL). The error study of the DTL for CPHS is presented in this paper. The error study can provide the field tolerances in the DTL cavity and the alignment tolerance between the RFQ and DTL.

INTRODUCTION

Compact Pulsed Hadron Source (CPHS) at Tsinghua University is a pulsed hadron-source scientific facility based on one high-intensity proton linac. The linac mainly consists of an electron cyclotron resonance (ECR) source, a low-energy beam transport line (LEBT), a radio frequency quadrupole (RFQ) and a drift tube linac (DTL). The construction was launched in 2009 [1]. In July 2013, the 3 MeV RFQ was built, the proton beam was accelerated to 3 MeV [2, 3] and the neutron beam was produced [4]. So far, the 13 MeV DTL cavity is assembled [5]. The DTL will be commissioned and the neutron beam will be produced by the 13 MeV proton beam bombarding the Beryllium target.

PARAMETERS OF DTL

The DTL will accelerate 50 mA proton beams from 3 MeV to 13 MeV to bombard the target [6,7]. The permanent magnet quadrupoles (PMQs) are used to focus the beam downstream of the RFQ. The PMQs are mounted in the drift tubes with an FD lattice. Besides, no MEBT is used to match the beam between the RFQ and the DTL as the phase advance in the RFQ and DTL are optimized to be continuous.

The total length of the DTL is 4.4 m. The bore radius is 10 mm. The DTL cavity is presented in Fig. 1 [8].

The main design parameters of the DTL are listed in Table 1 [7].

BEAM DYNAMICS

The alignment of the drift tubes has been finished [5]. The alignment results of the DTL, including the displacements and the rotation around the z-axis of the PMQs, are presented in Fig. 2. The RMS value of the displacements of the PMQs is 0.13 mm (x)/ 0.10 mm (y), which is slightly larger than the required value (0.1 mm) [7].

The emittance measured is different from the designed value. According to the result of the emittance meter at the downstream of the RFQ, the normalized RMS emittance is 0.34 π mm·mrad (x)/ 0.35 π mm·mrad (y) [9], which is much larger than the designed value. We can assume that the normalized RMS emittance at the entrance of the DTL is the same on the basis of Liouville's theorem.

As the PMQs are difficult to rectify in the drift tubes, it is necessary to figure out the tolerances of other parameters after the alignment.

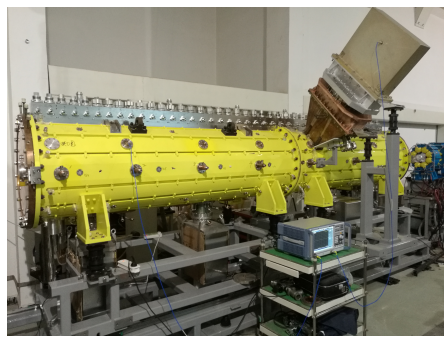


Figure 1: CPHS DTL cavity.

Table 1: DTL Design Parameters

Parameter	Value
Ion type	Proton
Input beam energy	3 MeV
Output beam energy	13 MeV
Input Norm. RMS emit.	0.25 π mm·mrad
Peak current	50 mA
RF frequency	325 MHz
Pulse length	0.2 ms
Pulse repetition rate	50 Hz
Cell number	40
Accelerating field	2.2 to 3.8 MV/m
Total RF peak power	1.2 MW
Total length	4.4 m

* xqz@tsinghua.edu.cn

Content from this work may be used under the terms of the CC BY 3.0 licence (© 2018). Any distribution of this work must maintain attribution to the author(s), title of the work, publisher, and DOI.

ISBN: 978-3-95450-194-6 ISSN: 2226-0366 doi:10.18429/JACoW-LINAC2018-THPO038

STATUS OF THE POWER COUPLERS FOR THE CSNS DTL*

M. X. Fan†, H. C. Liu, K. Y. Gong, P. H. Qu, B. Li, X. L. Wu, Y. Wang, A. H. Li, Q. Chen
Institute of High Energy Physics, Chinese Academy of Sciences (CAS), Beijing, China
also at Dongguan Neutron Science Center, Dongguan, China

Abstract

There are four Drift Tube Linac (DTL) tanks in China Spallation Neutron Source (CSNS) Project. Each DTL tank requires a power coupler with a peak power of 2 MW and a duty cycle of 1.5% for beam operation. After approximately two years machining, all four couplers were already installed in the tunnel before year 2017. Up to now, the first phase of beam tuning has been completed, the maximum transmission power of the coupler exceeds 1.7 MW with a pulse width of 650 μs and a repetition rate of 25 Hz, meanwhile, the vacuum is maintained on the order of 10^{-6} Pa during the operation and no breakdown was observed. This paper describes the architecture, the fabrication, the low power test results and the high power conditioning process of the coupler. Some problems encountered are also presented.

INTRODUCTION

The Accelerator system of China Spallation Neutron Source (CSNS) Project contains a 50 keV H^- Ion Source, a 3 MeV Radio Frequency Quadrupole (RFQ), a 80 MeV Drift Tube Linac (DTL) and a 1.6 GeV Rapid-cycling Synchrotron (RCS) successfully passed the technology acceptance test with a beam power over 10 kW in March 2018. The DTL section is 34.67 m long and is divided into 4 physical tanks. Each DTL tank has a similar design and is equipped with the same size power coupler in the center position. The type of half-height WR2300 ridge waveguide power coupler is chosen for DTL, design parameters of the coupler are shown in Table 1. Preliminary design of the coupler was quite early before 2012, and a cold model was manufactured to determine the dimension

Table 1: Parameters of the Coupler

Type	Waveguide
Frequency	324 MHz
Peak RF power	2 MW
Average RF power	30.2 kW
Pulse width	650 μs
Repetition rate	25 Hz
Maximum duty factor	1.625%
Coupling coefficient	1.3±0.1

of the coupler. Measurement of the cold model was made in 2015, and some dimensions were modified to optimize the coupling coefficient. Finish machining, installation and high power conditioning of the power couplers were executed between December 2015 and March 2017. The coupler has been in operation for most of the time since April 2017.

DESIGN AND SIMULATION OF THE COUPLER

Preliminary design of the power coupler draws on the successful experience of America Spallation Neutron Source (SNS) and Korea Proton Engineering Frontier Project (PEFP). It uses a dog-bone shaped coupler iris to connect the tapered ridge waveguide with a constant ridge width and the DTL cavity. The size near the side of the ceramic window is designed to be the size of half-height WR2300 waveguide, the size close to the cavity side is given by optimizing the return loss (s11). To improve the simulation efficiency, a simplified model-a pillbox loaded with two symmetrical dog-bone shaped couplers is used. According to the simulation, the size of the hole diameter is determined to be 25.5 mm [1].

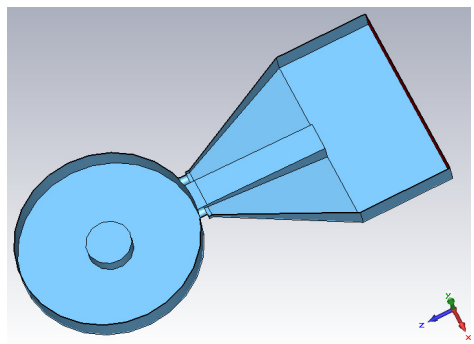


Figure 1: A cutplane of the new simulation model.

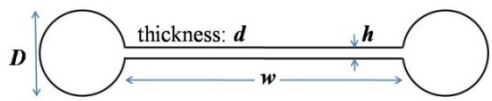


Figure 2a: Geometry of the dog-bone shaped aperture.

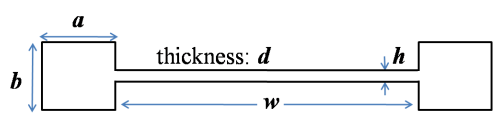


Figure 2b: Geometry of the modified dog-bone shaped aperture.

On the basis of preliminary design, a cold model is manufactured. Measurement of the cold model was taken in August 2015, and the results were far from the simulation. Considering that the dimensions of the hole diameter and ridge waveguide have an impact on matching, a new simulation model closer to the real situation is proposed,

* This work was supported by Youth Innovation Promotion Association of CAS (2015011)
† fanmx@ihep.ac.cn

Content from this work may be used under the terms of the CC BY 3.0 licence (© 2018). Any distribution of this work must maintain attribution to the author(s), title of the work, publisher, and DOI.

ISBN: 978-3-95450-194-6 ISSN: 2226-0366 doi:10.18429/JACoW-LINAC2018-THPO039

THE STATUS OF CSNS FRONT END*

H. Li, H. F. Ouyang†, X. Cao, W. Chen, S. Fu, T. Huang, S. Liu, Y. J. Lv, Y. C. Xiao, K. Xue, China Spallation Neutron Source (CSNS), Institute of High Energy Physics (IHEP), Chinese Academy of Sciences (CAS), 523803 Dongguan, China

Abstract

The commissioning and improvement of front end as well as the laboratory construction are summarized. The improvement as well as its effects mainly focuses on a low energy beam transport line (LEBT) and a 3.0MeV four-vane type radio frequency quadrupole (RFQ). In addition, the constitution, significance and construction of laboratory are mentioned.

INTRODUCTION

The China Spallation Neutron Source (CSNS) is an accelerator-based high power project with multipurpose currently under commissioning. The accelerator complex consists of an 81MeV H- linear accelerator as the injector and a 1.6GeV rapid cycling proton synchrotron (RCS). The linear accelerator consists of a 50keV H- penning surface plasma ion source (IS), a low energy beam transport line (LEBT), a 3.0MeV four-vane type radio frequency quadrupole (RFQ) accelerator, a medium energy beam transport line (MEBT), a 81MeV drift tube linear accelerator (DTL) and a high energy beam transport line (HEBT).

As shown in Figure 1, the front end means the front part of linac that includes IS, LEBT, RFQ and MEBT. As the start point of CSNS, the condition of front end is one of key factors which influence the stable operation of CSNS. Based on the beam requirement of CSNS phase I, the front end should provide a stable H- beam with energy of 3.0MeV, a maximum pulsed peak current up to 15mA, a beam duty factor 1.0% at a repetition of 25Hz and beam pulse width of 400us before chopping. The installation of CSNS front end was completed in 2015. Although the front end satisfies the beam requirement of CSNS phase I, the stability of the front end is not satisfactory during beam commissioning. The instability mainly comes from the ion source and RFQ sparking. After last 3 years commissioning and improvements, now the stability of CSNS front end was improved a lot.

PENNING IS

The main design parameters of penning IS for CSNS phase I are listed in Table 1.

Table 1: Main Design Parameters of IS for CSNS Phase I

Parameter	Value
Ion source	H-
Output Energy (keV)	50
Output Current (mA)	>20
Emittance $\varepsilon_{n,rms}$ (π mm · mrad)	<0.20
Repetition Rate (Hz)	25
Beam Duty Factor (%)	1.3
Lifetime (month)	>1

During the last 3 years commissioning and operation of CSNS, there are in total used about 20 sets of ion source discharge chamber. In general, for each set of discharge chamber, the ion source can produce up to 50mA H- ion beam with a beam duty factor about 1.25% (500us & 25Hz) and a normalized rms. emittance about 0.8π mm·mrad. Although the emittance is much larger than the acceptance of RFQ (0.2π mm·mrad), the H- ion beam current is still larger than 20mA within the acceptance of RFQ, which satisfies the current requirement of CSNS phase I. The average expected lifetime of CSNS IS, mainly limited by the discharge chamber, is about 1 month, which satisfies the requirement of CSNS phase I. The longest operation time for one of the 20 discharge chambers is near to 50 days.

Since the ion source was installed in CSNS tunnel in Oct. 2014, many improvements have been made for the ion source. Firstly, the electric penning magnet, which was integrated with the bending magnet before, was replaced by an independent permanent magnet that has the same electric potential as the discharge chamber; Sec ondly, the extraction power supply was moved into tunnel where was much closer to the source to decrease the induced voltage by the cable; Thirdly, the post acceleration

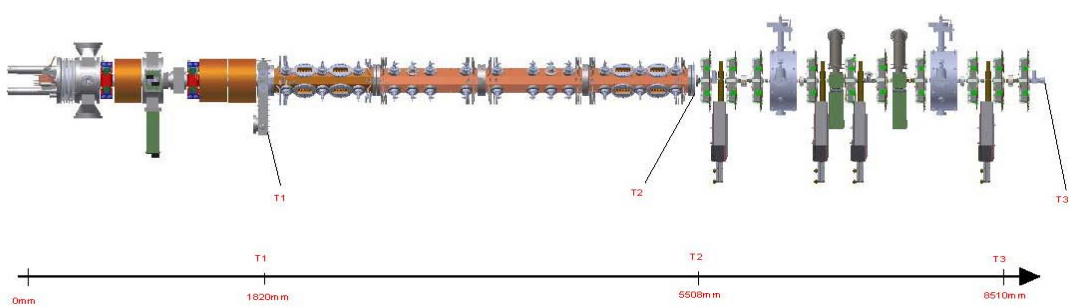


Figure 1: The beam line of CSNS Front End.

Content from this work may be used under the terms of the CC BY 3.0 licence (© 2018). Any distribution of this work must maintain attribution to the author(s), title of the work, publisher, and DOI.

ISBN: 978-3-95450-194-6 ISSN: 2226-0366 doi:10.18429/JACoW-LINAC2018-THPO040

OPERATION EXPERIENCES OF THE J-PARC LINAC

Kazuo Hasegawa*, for the J-PARC Linac group, J-PARC, JAEA/KEK, Tokai-mura, Japan

Abstract

The J-PARC linac has delivered beam to users since 2008. As of 2018, the linac provides a 40 mA beam at an energy of 400 MeV to the following Rapid Cycling Synchrotron. We have had many issues that impede high availability during the operation. One of them was troubles of high voltage power supply of klystrons. The other category is related to vacuum property in accelerating cavities. The cleaning of the inside surface of some acceleration cavities were performed after the big earthquake in 2011. The cooling water flow rate drop had been a long-time issue. We modified a cooling system to take better flow balances. As a result of these improvements, the availability is approximately 93% or more in these days. The operation experiences and availability improvement at the J-PARC linac are presented.

INTRODUCTION

The J-PARC facility consists of a linac, a 3-GeV Rapid Cycling Synchrotron (RCS), a 30-GeV Main Ring synchrotron (MR) and three experimental facilities[1]. The linac consists of a negative hydrogen ion source, a 3-MeV RFQ, a 50-MeV DTL (Drift Tube Linac), a 191-MeV SDTL (Separated-type DTL) and a 400-MeV ACS (after the upgrade) as shown in Fig. 1. RF frequencies are 324 MHz and 972 MHz for the low energy section (RFQ, DTL and SDTL) and for the high energy section (ACS), respectively. A proton beam from the RCS is injected to the Materials and Life Science Experimental Facility (MLF) for neutron and muon experiments. The MR has two beam extraction modes; a fast extraction (FX) for the neutrino beam line (NU) for the Tokai-to-Kamioka (T2K) experiment, and a slow extraction (SX) for the Hadron Experimental Facility (HD).

The goal of the J-PARC project is to deliver a 1-MW beam from the RCS and a 0.75-MW beam from the MR-FX. To achieve the goal, the linac have had big upgrade work such as peak current and energy upgrade[2]. On the way of the beam operation, we have had many issues that impede high availability and also have taken countermeasures.

BEAM HISTORY

The history of the beam power from the RCS to the MLF is shown in Fig. 2. User operation was started in 2008. At that time, trip rate of the RFQ was high and operation days and power ramp-up were limited. The beam current was low at 5 mA, and the RCS beam power was 20 kW. This was mostly settled by the vacuum improvement work during the summer shutdown of 2009 [3]. The progress of beam power of the J-PARC linac by 2015 is described in Ref[4].

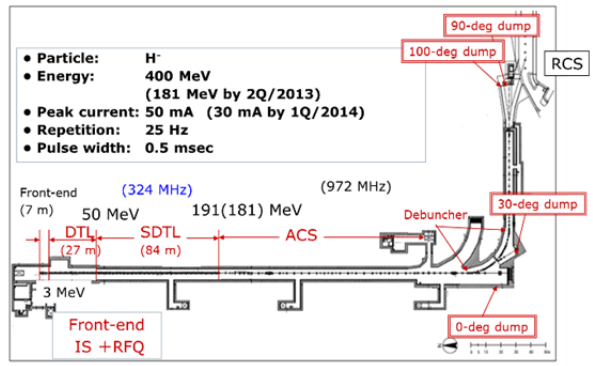


Figure 1: Configuration and main parameters of the J-PARC Linac

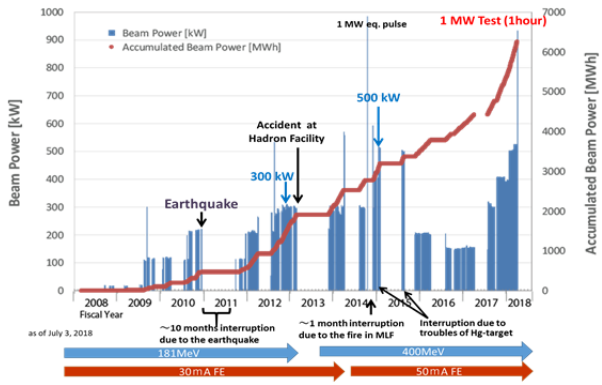


Figure 2: Beam power history for the MLF. (by courtesy of the MLF group, modified).

We had a crisis of the Great Earthquake in March 2011 and the J-PARC facilities were severely damaged. We resumed beam operation in December and user operation in January 2012[5]. We started beam operation sooner, but several aftereffects were left. The number of trips in the RFQ and some of the SDTL cavities was serious. As conditioning and operation days continued for half a year, the number of trips decreased as vacuum conditions went better. As described later, the SDTL remained issues.

We have steadily increased a beam power after the energy upgrade (from 181 to 400 MeV) in 2013 and beam current upgrade (ion source and RFQ replacement, from 30 to 50 mA) in 2014. As a result of these upgrade, we demonstrated a 1-MW-equivalent single shot beam from the RCS successfully. For continuous operation, we need to mitigate beam losses and to consolidate some power supplies, but this was a great milestone to perform the potential of accelerators.

We have steadily increased the beam power up to 500 kW at the MLF. But we had two neutron production target failures in April and November 2015[6]. After that, we used a spare target and the power was limited to 200-150 kW. During the maintenance period of summer 2017, we exchanged for a target with a new design[7]. Then we have gradually increased the power from 300 kW, 400

* hasegawa.kazuo@jaea.go.jp

Content from this work may be used under the terms of the CC BY 3.0 licence (© 2018). Any distribution of this work must maintain attribution to the author(s), title of the work, publisher, and DOI.

ISBN: 978-3-95450-194-6 ISSN: 2226-0366 doi:10.18429/JACoW-LINAC2018-THPO042

AN OPTIMIZATION METHOD OF THE NOSE-CONE BUNCHER CAVITY

W. L. Liu, P. T. Cong, Z. M. Wang, State Key Laboratory of Intense Pulsed Radiation Simulation and Effect (Northwest Institute of Nuclear Technology), Xi'an 710024, China
S. X. Zheng[1,2], H. P. Jiang[3], Department of Engineering Physics, Tsinghua University, Beijing 100084, China
[1]also at Key Laboratory of Particle & Radiation Imaging (Tsinghua University), Ministry of Education, Beijing 100084, China
[2]also at Laboratory for Advanced Radiation Sources and Application, Tsinghua University, Beijing 100084, China
[3]also at Space Environment Simulation Research Infrastructure, Harbin Institute of Technology, Harbin 150001, China

Abstract

The nose-cone buncher cavity is widely used on proton accelerators. It's important to properly optimize the cavity geometry for fine RF performance. However, currently the optimization is usually carried out manually and the criteria are not objective enough. In this paper, an optimization method using the multi-objective, multi-variable optimization approach is presented. The geometry and RF parameters are considered as the variables and objectives respectively. The goal function is defined as the weighted sum of multiple RF parameters. The multi-variable functions are approximately derived from the single-variable functions based on electromagnetic simulation. And an optimization code is developed accordingly which has been applied to the XiPAF debuncher optimization.

INTRODUCTION

The Xi'an proton application facility (XiPAF) is a synchrotron proton accelerator built for radiation effects research. There's a debuncher on the medium energy transport line (MEBT) to reduce the beam energy spread. The nose-cone buncher cavity is adopted, which has been widely used on proton accelerators as bunchers or debunchers [1, 2]. Since the RF performance depends on the cavity geometry, the optimization of the cavity geometry is a vital procedure of debuncher design. The optimization aims for optimized RF performance like low probability of RF breakdown and high shunt impedance and Q factor while keeps the resonance frequency exactly equal to the RF frequency, which is 325 MHz in the case of XiPAF.

A lot of optimization work of nose-cone buncher cavities has been carried out, in which, the manual way that determining the geometry parameters by evaluating their effects on the RF parameters based on electromagnetic (EM) simulation is adopted accordantly [1-4]. However, since multiple RF parameters should be optimized synchronously while their values are decided by multiple geometry parameters, the criteria of the manual optimization approach are not objective enough and the results mostly rely on experience. Therefore, a common optimization method which could automatically accomplish the nose-cone buncher cavity optimization under specific demands is in need.

An optimization method using the multi-objective, multi-variable optimization approach is presented in this paper. By treating geometry parameters and RF parameters as the variables and objectives respectively, the optimized cavity geometry would be obtained mathematically via optimization algorithm.

APPROXIMATE FUNCTION

Relation Between RF and Geometry Parameters

The function between variables and objectives are the footstone of multi-objective, multi-variable optimization. The RF and geometry parameters considered as the variables, objectives and constraint in the optimization are shown in Table 1. Three geometry parameters that affect the cavity geometry most intensely are adopted as the optimization variables primarily.

Using EM simulation software CST a parametric model of the nose-cone cavity is established as shown in Fig. 1, based on which the relation between the RF and geometry parameters is studied by parameter sweep. The effective cavity voltage VT is 160 kV and the beam energy E_{beam} is 7 MeV while calculating the bravery factor b and the transient time factor T.

Applying polynomial fit to the simulation data, one-dimensional approximate functions between RF and geometry parameters are acquired.

Table 1: Variables, Objectives and Constraint

roles	parameters	symbol
objective	effective shunt impedance	R
	Q factor	Q
	bravery factor	b
variable	cavity radium	r
	gap length	g
	nose cone angle	t
constraint	resonance frequency	f

Approximate Function between RF and Geometry Parameters

The multidimensional functions that contain all variables for each objective are in need to accomplish the optimization. It can be approximately derived from the one dimension functions acquired via EM simulation.

Content from this work may be used under the terms of the CC BY 3.0 licence (© 2018). Any distribution of this work must maintain attribution to the author(s), title of the work, publisher, and DOI.

ISBN: 978-3-95450-194-6 ISSN: 2226-0366 doi:10.18429/JACoW-LINAC2018-THPO043

ESS NORMAL CONDUCTING LINAC STATUS AND PLANS

E. Sargsyan†, H. Danared, F. Hellström, G. Hulla, Ø. Midttun, J. S. Schmidt, European Spallation Source ERIC, Lund, Sweden
L. Celona, S. Gammino, L. Neri, INFN-LNS, Catania, Italy
A-C. Chauveau, B. Pottin, CEA/IRFU, Gif-sur-Yvette, France
I. Bustinduy, N. Garmendia, J. L. Muñoz, ESS-Bilbao, Bilbao, Spain
F. Grespan, A. Pisent, INFN-LNL, Legnaro, Italy
P. Mereu, INFN-Torino, Torino, Italy

Abstract

The European Spallation Source (ESS) uses a linear accelerator to deliver the high intensity proton beam to the target station for producing intense beams of neutrons. The average beam power is 5 MW with a peak beam power at the target of 125 MW. The normal conducting linear accelerator (linac) operating at 352.21 MHz accelerates a proton beam of 62.5 mA from 0.075 to 90 MeV. It consists of an ion source, Low Energy Beam Transport (LEBT), Radio Frequency Quadrupole (RFQ), Medium Energy Beam Transport (MEBT), and Drift Tube Linac (DTL). The design, construction and testing of those structures is done by European partner labs as an in-kind contribution to the ESS project. This paper presents the status and plans for the ESS normal conducting linac.

INTRODUCTION

The ESS linear accelerator (linac) generates and accelerates protons to 2 GeV energy, delivering them onto a rotating tungsten target to create neutrons, via the spallation process, for use by research instruments [1]. The linac is composed of normal conducting structures followed by superconducting spoke and elliptical cavities. The layout of the ESS linac is shown in Fig. 1. The normal conducting linac (NCL) consists of an ion source, Low Energy Beam transport (LEBT), Radio Frequency Quadrupole (RFQ), Medium Energy Beam Transport (MEBT) and Drift Tube Linac (DTL). The NCL operates at 352.21 MHz frequency, 14 Hz repetition rate, with 62.5 mA peak beam current and 2.86 ms beam pulse length.

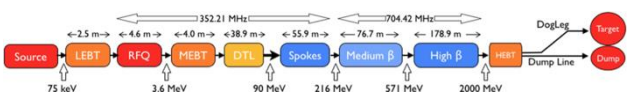


Figure 1: Layout of the ESS linac.

STATUS AND PLANS

The ESS facility is currently under construction, with the start of the user programme planned for 2023. The installation of the utilities and accelerator components in the accelerator tunnel and the klystron gallery is ongoing at ESS. All sections of the ESS NCL are presently under construction, while the ion source and LEBT are already delivered and installed at ESS. A brief description, status and plans for the ESS NCL are presented below.

† edgar.sargsyan@esss.se

Ion Source and LEBT

The ion source and LEBT are in-kind contribution from INFN-LNS, Catania, Italy. The source is a 2.45 GHz microwave discharge ion source with a flexible magnetic system [2]. The requirements include proton beam current of 74 mA, normalised rms emittance of 0.25 π.mm.mrad at the RFQ entrance, proton fraction of >75%, intra-pulse beam current stability of ±2%, pulse to pulse stability of ±3.5%, repetition rate of 14 Hz, beam pulse length of 6 ms from the source and 2.86 ms in the LEBT. The LEBT consists of two solenoid magnets with embedded steerers, and beam diagnostics to measure the beam current, emittance, position, and fraction. It also contains a fast electrostatic chopper to remove the first part of the beam pulse during which the plasma needs to stabilise. An iris with six movable blades reduces the beam current for running the linac in low-power mode.

The ion source and LEBT were installed and commissioned in Catania prior to the delivery to ESS. The range of possible extracted beam currents and stability were measured during the spring 2017 [3]. The current range with stable beam was 40-120 mA. With the nominal ion source settings, the fractions of the different ion species were 85%, 12% and 3% for protons, H_2^+ and H_3^+ respectively. With this proton fraction, the proton beam current was 85 mA. The measured stability was ±1.5% inside the beam flat top, and ±3% among pulses as shown in Fig. 2.

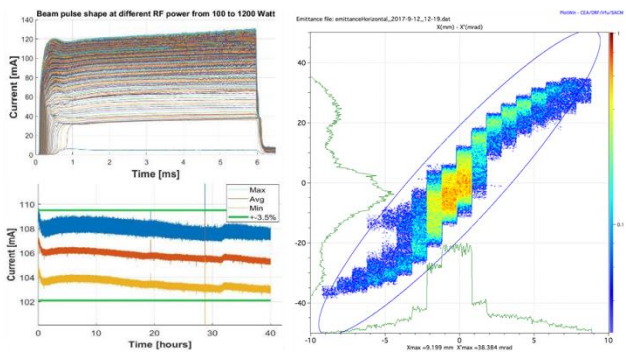


Figure 2: Ion source intra-pulse beam stability (top left), pulse-to-pulse stability (bottom left), and emittance at the RFQ entrance (right).

The ion source produced the nominal time structure of 6 ms pulse length and 14 Hz repetition rate, with the first 3 ms removed by the chopper. Beams with flat top pulse

Content from this work may be used under the terms of the CC BY 3.0 licence (© 2018). Any distribution of this work must maintain attribution to the author(s), title of the work, publisher, and DOI.

ISBN: 978-3-95450-194-6 ISSN: 2226-0366 doi:10.18429/JACoW-LINAC2018-THPO045

TUNING ESPERIENCE ON THE ESS DTL COLD MODEL

F. Grespan, A. Baldo, P. Bottin, G. S. Mauro, A. Palmieri, A. Pisent INFN-LNL, Legnaro (PD), Italy
P. Mereu, M. Mezzano, INFN-Turin, Turin, Italy

Abstract

An aluminum mock-up of the ESS DTL tank 2 was produced to INFN-LNL in December 2017. The tank is 7.1 m long, equipped with movable tuners and movable post couplers. The purpose of this DTL model is to verify the RF design choices (in particular on the first 2 tanks where the Post coupler distribution is irregular) as well as to implement and to debug algorithms and procedure for stabilization and tuning. The preparatory simulation work and the results of measurements campaign are presented here.

INTRODUCTION

The 5 tanks of the ESS DTL are equipped with post couplers (PCs) for field stabilization [1]. The number of post couplers of each DTL tank was fixed following the criterion of the minimum number of PCs per unit length which guarantees to keep the accelerating field E_0 within specifications (±2%) in case of perturbation [2]. The distribution must be compliant with the increasing cell length as well as with the 2 m tank modulation. As a consequence of these boundaries, the distribution of post couplers per number of cells changes along Tank 1 and Tank 2, while it is regular in Tank 3, 4 and 5, as listed in Table 1.

Table 1: PCs Distribution of ESS DTL Tanks

	T1	T2	T3	T4	T5
N Cells	61	34	29	26	23
N DTs	60	33	28	25	22
N.PCs	24	23	28	25	22
PCs/DT	-up to DT 14th: 1/4 -up to DT 32nd: 1/3 -up to end: 1/2	-up to DT 21st: 1/2 -up to end: 1/1	1/1	1/1	1/1

The distance between post couplers is then gradually increasing as βλ in the last three tanks, while is jumping from 4 βλ to 3 βλ to 2 βλ in Tank 1 and from 2 βλ to 1 βλ in Tank 2.

In particular, in Tank 2, looking to the PCs as the second chain of resonators, this is equivalent to say that the period of the PC chain is suddenly changing from 43 cm to 21.5 cm. For this reason – along with the opportunity to test and define hardware and procedures for DTL tuning - it was decided to produce an aluminium model of DTL tank 2, to demonstrate the proper stabilization of a DTL with such irregular post coupler distribution (Fig. 1).

ALUMINUM DTL AND BEAD-PULL APPARATUS

The purpose of the aluminum mock-up is to provide a valid test bench for the bead pulling activities, without duplicating a real DTL tank, for cost and time optimization. The mock-up is geometrically identical to the actual DTL Tank 2; thus the cavity internal diameter, the modularity (i.e. the length of each module), distribution and positioning of the ports for the corresponding components (Drift Tubes, Pick-Ups, Tuners and Post Couplers) are the same as in the real DTL Tank; the vacuum ports and the RF coupler ports were not realized, as they are irrelevant for bead pulling purposes.

The structure is made of a 2-mm-thick aluminum skin bended with 521 mm internal diameter. The proper form of the aluminum skin is given by four ribs, evenly placed along each module. Each rib is machined by milling from a 20 mm-thick solid aluminum sheet. The flexural stiffness of the module is provided by 5 struts made of structural steel beams with rectangular hollow section. The struts provide also the housing for the interfaces of the ports. The module is supported at each rib by a welded structure, which is coupled to a corresponding carriage with longitudinal skid. An isostatic alignment system is provided between the welded structure and the carriage for the proper relative positioning of the modules. The pair of rails for the longitudinal movement during the coupling of the modules is fixed to a substructure made of four aluminum profile beam support, fixed to the ground. The tank is terminated by two covers, which integrate the corresponding half Drift Tube, with a central hole for the passage of the bead. In Fig. 2 an internal view of the DTL mock-up is shown

The alignment of the dummy Drift Tube is reached using a Laser Tracker and is made with an isostatic regulation on top of the upper strut, which permit a complete spatial regulation (6 DOF) of each Drift Tube. The final alignment reached has been with a spatial error from the nominal position less than 0,1 mm.

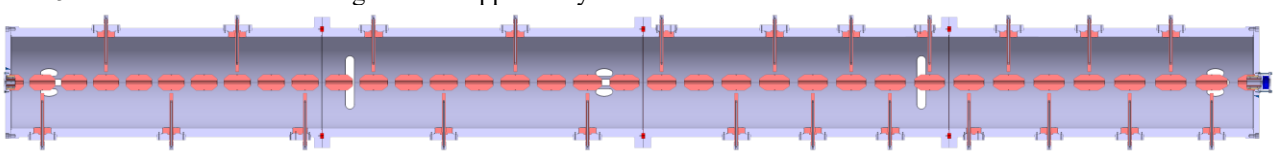


Figure 1: The ESS DTL Tank 2: it is possible to notice the tank subdivision as well as the PC distribution change.

Content from this work may be used under the terms of the CC BY 3.0 licence (© 2018). Any distribution of this work must maintain attribution to the author(s), title of the work, publisher, and DOI.

ISBN: 978-3-95450-194-6 ISSN: 2226-0366 doi:10.18429/JACoW-LINAC2018-THPO046

STATUS OF THE FAIR PROTON LINAC

C. Kleffner, S. Appel, R. Berezov, J. Fils, P. Forck, M. Kaiser, K. Knie, C. Muehle, S. Puetz, A. Schnase,G. Schreiber, A. Seibel, T. Sieber, V. Srinivasan, J. Trueller, W. Vinzenz, C. Will, GSI, Darmstadt
A. M. Almomani, H. Hähnel, U. Ratzinger, M. Schuett, M. Syha, IAP, Frankfurt am Main, Germany

Abstract

As part of the accelerator chain for antiproton production of the FAIR facility, a special high-intensity short pulsed 325 MHz Proton Linac is being developed [1], [2]. The Proton Linac is designed to deliver a beam current of 70 mA with an energy of 68 MeV. A 2.45 GHz ECR source designed for the generation of 100 mA beams with an energy of 95 keV is currently being tested at CEA/Saclay. The production of the structure of the IAP ladder RFQ is nearly completed. All parts of the RFQ vacuum chambers have been successfully copperplated at the GSI. Seven Thales Klystrons have been delivered to GSI at the beginning of 2018 and are nearly ready for use. The completion of the setup of the HV modulator is expected mid of the year 2019. The state of procurement and development of further accelerator components will be presented.

OVERVIEW

Figure. 1 and Table 1. shows main properties and the structure of the Proton Linac. A 2.45 GHz ECR source generating 100 mA of 95 keV protons is followed by a Low-Energy Beam Transport line (LEBT) based on two sole-noid magnetic lenses enclosing a diagnostics chamber. A ladder 4-Rod RFQ will be built behind the LEBT, which is followed by a chopper and a beam conus in front of the RFQ entrance. Six normal conducting crossbar cavities of CCH and CH type arranged in two sections accelerate the beam to the final energy of 68 MeV.

The construction work on the Proton Linac beam dump and the eight meter thick radiation safety wall as seen in fig. 2 has been build up alongside the existing TK tunnel. This work has been executed as part of the GAF project in the first quarter of 2018.

PROTON LINAC BUILDING

After submission of the building application for the Proton Linac building in October 2017 the execution planning of the technical infrastructure started.



Figure 2: Proton Linac Interface Wall with the construction area for the Proton Linac in front.

ION SOURCE AND LEBT

The commissioning of the Proton source takes place at CEA, Saclay [3]. The 100 kV/150 mA high voltage power supply of the source has been commissioned successfully. By means of AC current transformer, fast current transformer FC, Wien filter (beam proportion) and Alison Scanner (emittance measurements) the extracted Proton beam has been characterized, see fig.3.

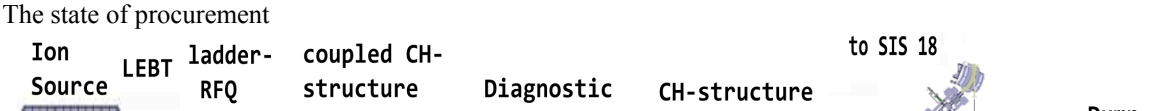


Figure 1: Layout of the FAIR Proton Linac.

Table 1: Proton Linac Main Parameters

Particle	Proton (H^{+})
Ion source	95 keV
MEBT energy	3 MeV
CCH section	33 MeV
Final energy	68 MeV
Pulse current	70 mA
RF-frequency	325.224 MHz
Rep. rate	2,7 Hz

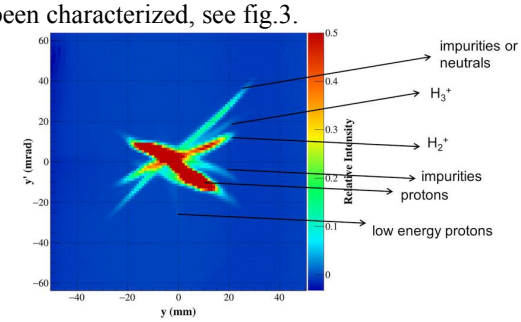


Figure 3: Typical emittance measurement taken at the diagnostic section within the LEBT.

Content from this work may be used under the terms of the CC BY 3.0 licence (© 2018). Any distribution of this work must maintain attribution to the author(s), title of the work, publisher, and DOI.

ISBN: 978-3-95450-194-6 ISSN: 2226-0366 doi:10.18429/JACoW-LINAC2018-THPO047

SPIRAL2 INJECTOR COMMISSIONING

R. Ferdinand†, M. Di Giacomo Marco, H. Franberg, O. Kamalou, J-M. Lagniel, G. Normand, A. Savalle, F. Varenne GANIL, Caen, France
D. Uriot, DRF/IRFU/DACM, Saclay, France

Abstract

The SPIRAL2 injector is composed of two ion sources (p/d and heavy ions up to A/Q=3) followed by a 730 keV/u RFQ. Beam commissioning has started in 2014 in parallel with the superconducting linac and HEBT installations. The RFQ beam commissioning started soon after the first RF conditioning done in October 2015. This paper describes the RFQ beam measurements done on the diagnostic plate for the reference particles (H^+, $^4He^{2+}$ and recently $^{18}O^{6+}$) and the difficulties encountered for the RFQ commissioning at the A/Q=3 field level.

INTRODUCTION

The layout of the SPIRAL2 driver takes into account a wide variety of beams to fulfill the physics requests [1]. It is a high power CW superconducting linac delivering up to 5 mA proton or deuteron beams or 1 mA ion beams for Q/A > 1/3 (Table 1). Our major challenges are to handle the large variety of different beams due to their different characteristics (in terms of particle type, beam currents – from a few µA to a few mA - and/or beam energy), a high beam power (200 kW, CW) and to answer correctly to the safety issues, especially with the deuteron beam.

Table 1: Beam Specifications

Particles	H^+	D^+	ions	option
A/Q	1	2	3	6
Max I (mA)	5	5	1	1
Max energy (MeV/A)	33	20	15	8.5
Max beam power (kW)	165	200	45	51

We do not have yet the authorization to accelerate deuteron beams or to inject in the LINAC. A test bench, the Diagnostic-plate (D-plate), is used after the RFQ to validate the RFQ performances, to tests various diagnostics and to measure the beam characteristics for the future Linac injection.

BEAMS FOR COMMISSIONING

Three beams have been selected to demonstrate the injector performances.

The 5 mA proton beam requires only 40 kV on the RFQ vane voltage. It is the easiest to produce, requires little RF in the RFQ cavity but is the most difficult to transport in the LEBT because of space charge forces.

The $^4He^{2+}$ was selected in order to mimic the future deuteron beam. It allows to test the A/Q=3 ECR source and LEBT and requires a little higher RFQ vane voltage (80 kV).

The ultimate injector performances require an A/Q=3 beam up to 1 mA. The $^{18}O^{6+}$ has been selected. The RFQ vane voltage rise to 114 kV (1.65 Kilpatrick). We were not able to achieve stable operation of the RFQ and associated RF system at such set point until recently. 105 kV was easier to achieve and $^{16}O^{6+}$ beam (A/Q=2.67) was used as backup for performance measurement. Recent improvement in the cavity conditioning and LLRF tuning allow a much better cavity operation, leading to an availability of about 75% at nominal voltage (114 kV). The merit of this is that the measurement results for both oxygen beams can be compared, and $^{18}O^{6+}$ can be measured à 105 and 114 kV.

D-PLATE DESCRIPTION

The D-Plate is installed in the Medium Energy Beam Transport Line (MEBT, Fig. 1). It allows to measure:

- Intensity with Faraday cups, ACCT and DCCT
- Transverse profiles with classical multi wire profilers and ionisation gas monitor (MIGR in the text)
- H and V transverse emittance with Allison type scanners
- Energy with a Time of Flight (TOF) monitor
- Phase with the TOF and the 2 BPMs
- Longitudinal profile with a Fast Faraday Cup (FFC), and a Beam Extension Monitor (BEM)
- Beam position and ellipticity ($\sigma_x^2 - \sigma_y^2$), with the BPMs.

The diagnostics performances are given in [2,3,4]

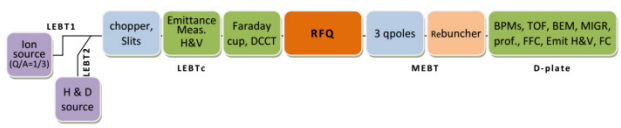


Figure 1: Injector scheme up to Diagnostic Plate.

RFQ RF CONDITIONING

The RFQ RF conditioning improved during the past few months with a better control of the RF chains and better conditioning methods. At first, the RF conditioning was managed in pulse mode with a Duty Cycle (DC) low enough to avoid copper heating. It allows to burn the dusts and spikes. We were quickly able to reach 125 kV (240 kW), 500 µs/100 ms, ending with operation without sparks. The LLRF is then switched in CW mode, integrating a PLL. In both cases (pulsed, CW with PLL), the cavity frequency tuning is manual using the temperature control. In CW mode, the cavity starts to spark at 105 kV, much lower than the level achieved just before in pulse mode. The copper heating in CW mode increases an outgassing inducing sparks at lower voltage. The RF conditioning is greatly improved increasing the copper temperature up to 55°C with RF for few weeks. Coming back to the normal LLRF operation, unfortunately without PLL during the

Content from this work may be used under the terms of the CC BY 3.0 licence (© 2018). Any distribution of this work must maintain attribution to the author(s), title of the work, publisher, and DOI.

ISBN: 978-3-95450-194-6 ISSN: 2226-0366 doi:10.18429/JACoW-LINAC2018-THPO048

LOW POWER MEASUREMENT OF A 1300-MHz RFQ COLD MODEL

Y. Kondo*, T. Morishita, J. Tamura, JAEA, 319-1195, Tokai, Japan
M. Otani, KEK, 305-0801, Tsukuba, Japan

Abstract

A muon linac development for a new muon g-2 experiment is now going on at J-PARC. Muons from the muon beam line (H line) at the J-PARC muon science facility are once stopped in a silica-aerogel target, and room temperature muoniums are evaporated from the aerogel. They are dissociated with lasers, then accelerated up to 212 MeV using a linear accelerator. In the current reference design, a 324-MHz radio frequency quadrupole (RFQ) and an interdigital H-mode drift tube linac (IH-DTL) are used for the low beta acceleration. We propose a 1300 MHz (L band) RFQ instead of the 324 MHz RFQ and IH-DTL as an alternative to simplify the configuration of the muon linac. In this paper, the present status of the design and the measurement of a cold model of this world first 1300-MHz RFQ is described.

INTRODUCTION

The muon anomalous magnetic moment $(g-2)_\mu$ is one of the most promising probe to explore the elementary particle physics beyond the standard model (SM). Currently, the most precise $(g-2)_\mu$ experiment is E821 of Brookhaven national laboratory [1]. The precision is 0.54 ppm and the measured value indicates approximately three standard deviations from the SM prediction. The J-PARC E34 experiment aims to measure the $(g-2)_\mu$ with a precision of 0.1 ppm. In addition, the electric dipole moment (EDM) also can be measured with a precision of $1 \times 10^{-21}\, e\cdot$cm [2]. The experimental method of E34 is completely different from that of the previous experiments. The previous experiments directory used decay muons from the secondary pions generated on the production target. The emittance of such muon beam is very large (typically, 1000π mm mrad); this is a major source of uncertainty of the measurement. On the other hand, E34 will use a low emittance muon beam to improve the precision. The required beam divergence $\Delta p_t/p$ is less than 10^{-5}, and assumed transverse emittance is 1.5π mm mrad. To satisfy this requirement, we are planning to use ultra-slow muons (USMs) generated by laser-dissociation of thermal muoniums (Mu: μ^+e^-) form a silica-aerogel target [3]. The room temperature USMs (25 meV) should be accelerated to 212 MeV to obtain the required $\Delta p_t/p$. A linac realizes rapid acceleration required to accelerate muons, whose lifetime is very short (2.2 µs). Figure 1 shows the configuration of the muon linac [4].

The muon linac will be constructed at the H line [5] of the J-PARC muon science facility. The USMs are bunched and accelerated to 340 MeV by a radio frequency quadrupole linac (RFQ). Following the RFQ, an interdigital H-mode drift tube linac (IH-DTL) [6] is used to accelerate to 4.5 MeV.

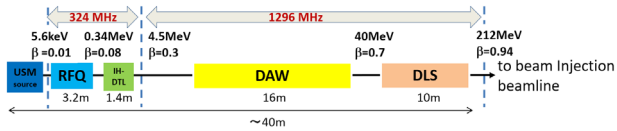


Figure 1: Configuration of the muon linac.

Then, muons are accelerated to 40 MeV through a disk and washer (DAW) coupled cavity linac section, and finally, accelerated to 212 MeV using disk loaded traveling wave structures (DLS) [7].

To reduce the development costs, a spare RFQ for the J-PARC linac will be used, therefore, the resonant frequency is 324 MHz. Removing the restriction to use the J-PARC RFQ, if the same frequency of the following linac, which is 1.3 GHz (L-band), can be used, is becomes reasonable because only one type of the RF source should be prepared. In case of the proton acceleration, the cell length for 50 keV, which is typical injection energy to the RFQ, is $\beta\lambda/2 =$ 1.2 mm: this is too short to fabricate. On the other hand, for muon acceleration it becomes a feasible length of 3.5 mm. Therefore, we propose to replace the 324-MHz RFQ and IH-DTL by an 1300-MHz RFQ shown in Table 1bl:requirement as an alternative of the muon linac baseline design. In this paper, the present status of the design of the 1300-MHz RFQ and low-power measurement of a cold model.

Table 1: Requirements for the 1300-MHz RFQ

Parameter	Value
Beam species	μ^+
Resonant frequency	1296 MHz
Injection energy	30 keV
Extraction energy	5.2 MeV
Peak beam intensity	1×10^6
Transverse emittance (normalized rms)	$< 0.25\pi$ mm mrad
Repetition rate	25 Hz
RF pulse length	20 µs
RF duty factor	0.05%

DESIGN OF THE 1300-MHz RFQ

The beamdynamics design of the 1300-MHz RFQ has been done using RFQGEN [8]. Figure 2 shows the cell parameters, and the obtained design parameters are listed in Table 2. In this design, the average bore radius r_0 is kept same as that of the 324 MHz RFQ to be acceptable the present injection muon beam. Due to this design concept, the power dissipation is rather high. The matching between the RFQ and injection design is an issue from now on.

* yasuhiro.kondo@j-parc.jp

Content from this work may be used under the terms of the CC BY 3.0 licence (© 2018). Any distribution of this work must maintain attribution to the author(s), title of the work, publisher, and DOI.

ISBN: 978-3-95450-194-6 ISSN: 2226-0366 doi:10.18429/JACoW-LINAC2018-THPO049

FIELD TUNING OF A RADIO-FREQUENCY QUADRUPOLE USING FULL 3D MODELING

T. Morishita†, Y. Kondo, H. Oguri, K. Hasegawa, JAEA, 319-1195, Tokai, Japan
M. Otani, KEK, 305-0801, Tsukuba, Japan

Abstract

The radio-frequency quadrupole (RFQ) is operating in the frontend of the J-PARC linac to accelerates 50-mA negative hydrogen beams from 0.05 MeV to 3 MeV. As a backup, the spare RFQ has been fabricated in 2018. The vane-voltage ramping is adopted to improve the acceleration efficiency so that the cross-sectional shape is adjusted longitudinally to produce the designed voltage distribution. Then, the three-dimensional cavity models including modulations and cutbacks were created in CST Micro-Wave Studio. The vane-base widths and cutback depths were optimized to produce the desired vane-voltage distribution. In the final tuning, the insertion depths of the stub turners were also determined based on the tuner responses obtained from the full 3D models.

INTRODUCTION

The J-PARC (Japan Proton Accelerator Research Complex) is a complex research facility consisting of high-intensity proton accelerators and experimental facilities. The accelerator comprises an injector linac, a 3-GeV Rapid-Cycling Synchrotron and a Main Ring. The front end of the linac consists of a negative hydrogen ion source and an RFQ with an output energy of 3 MeV. For the beam current upgrade, the new frontend (RF ion source, RFQ, chopping system) is installed in summer 2014. Since then, the beam current was increased to 30 mA, and to 40 mA from January 2016. We continued operation without major trouble, however, the spare RFQ was fabricated in 2018 in preparation for unexpected trouble. In this paper, the detailed design process of the cavity dimensions and the result of the low-power measurements are described.

RFQ PARAMETERS

The major parameters of the spare RFQ are shown in Table 1. The vane voltage distribution of the operating RFQ in J-PARC is taken to be uniform in the longitudinal direction [1], but in the new RFQ, the vane voltage distribution is designed to make the ramping on the downstream side of the cavity to improve the acceleration efficiency. Figure 1 show the longitudinal variation of the vane voltage, the average bore radius, and the maximum surface field. The average bore radius increases smoothly toward the downstream so that the maximum surface field is almost constant. Figure 2 shows the test pieces of a vane tip. From left to right, the modulations for the longitudinally centre, entrance, and exit of the vane, respectively. Prior to the fabrication, the machining conditions of the vane-tip modulations using the ball-end mill were confirmed based on this prototype.

Table 1: Major Parameters

Frequency [MHz]	324
Cavity type	Four vane
Vane length [m]	3.1
Inter-vane voltage[kV]	61.3 ~ 143
Max. surface field [MV/m]	29.8(1.67 Kilpatrick)
Average bore radius [mm]	2.6 ~ 6.2
Vane-tip curvature [mm]	$0.75r_0$

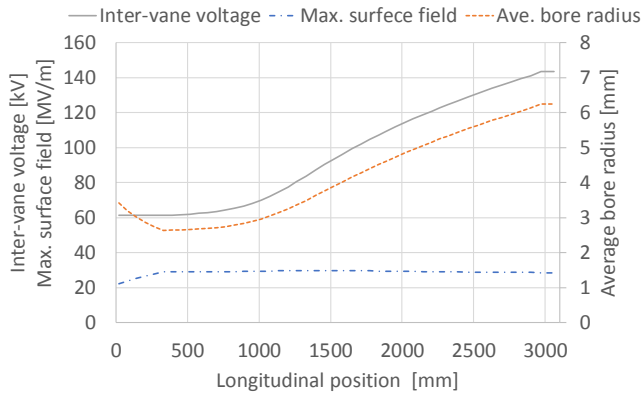


Figure 1: Longitudinal variation of the vane voltage and the average bore radius.

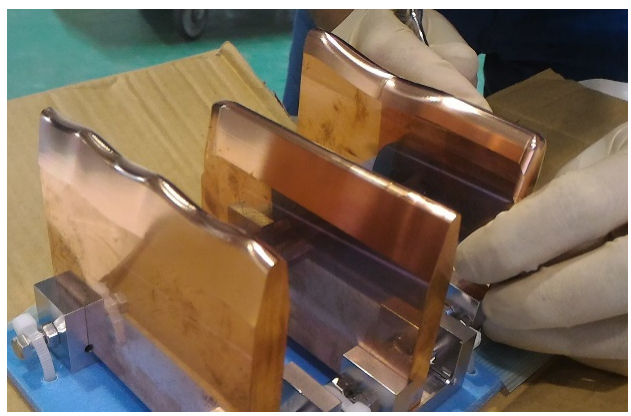


Figure 2: Test piece of the vane tip for checking the surface roughness with the machining conditions.

RF DESIGN

To make the vane-voltage distribution in the longitudinal direction, the vane-base width was adjusted. Cross sectional shape of the cavity is shown in Fig. 3.

† takatoshi.morishita@j-parc.jp

Content from this work may be used under the terms of the CC BY 3.0 licence (© 2018). Any distribution of this work must maintain attribution to the author(s), title of the work, publisher, and DOI.

ISBN: 978-3-95450-194-6 ISSN: 2226-0366 doi:10.18429/JACoW-LINAC2018-THPO050

RESEARCH ON THE NEW CAVITY STRUCTURE OF RFQ ACCELERATOR WITH BENT VANES AT IMP *

Lei Yang † [1], Liang Lu, Zhouli Zhang,
Liepeng Sun, Chenxing Li, Tao He[1], ChaoChao Xing[1], Yaun He
Institute of Modern Physics, Chinese Academy of Sciences, Lanzhou 730000, China
[1]also at University of Chinese Academy of Sciences, Beijing 100049, China

Abstract

A new cavity structure of RFQ accelerator with bent vanes has been proposed at IMP. The new structure can reduce the lateral dimension of the cavity and possesses simple cooling structure in the low frequency field. In this paper, the dynamics of an 81.25 MHz bent-vane RFQ has been designed as a prototype device of the bent-vane RFQ. The 2D EM simulation of the bent-vane RFQ has been performed. Detailed description is presented in this paper.

INTRODUCTION

Four-vane type and four-rod type are commonly used in radio frequency quadrupole (RFQ) linac structure. Four-vane type RFQ is mainly used in the high frequency field and four-rod type RFQ applies to the low frequency field prevailingly [1]. In continuous wave (CW) operating mode, it is necessary that RFQ structure should have a complete cooling structure so that it can fully cool the RFQ cavity to ensure stable operation with a large amount of heat generated by the cavity during CW mode. The CW four-rod type RFQ cooling structure is quite complicated, which makes it difficult to design and machine the cavity, which limits the application and development of four-rod type RFQ in CW condition. Although the four-vane type RFQ is suitable for working in CW condition with single cooling structure and sufficient cooling efficiency，in the low frequency field, its lateral dimension is large, and the lower the frequency, the larger the lateral dimension, which increases machining difficulty and cost.

In order to overcome the disadvantages of four-rod and four-vane RFQ in the CW condition and the low frequency band, we put forward a kind of new RFQ accelerator structure called bent-vane type RFQ at Institute of Modern Physics (IMP),Chinese Academy of Sciences. The bent-vane type RFQ combines the advantages of four-rod type RFQ and four-vane type RFQ. It significantly reduces the lateral dimension of the cavity in the low frequency field and has a water-cooled system with a simple structure and sufficient cooling efficiency. In this paper, we present an 81.25 MHz bent-vane RFQ beam dynamics design and two-dimensional electromagnetic field (2D EM) simulation.

RFQ BEAM DYNAMICS DESIGN

The beam dynamics design of the bent-vane RFQ is simulated by the code RFQGen [2]. Taking into account research requirements and cost, the design parameters of the bent-vane RFQ are listed in Table 1.

The bent-vane RFQ accelerates He^+ (q/A=1/4) from 4 keV/u to 42.5 keV/u. In order to decrease the cavity length, the maximum peak surface electric field is 18.23 MV/m, which is 1.73 times higher than the Kilpatrick limit. The transverse focusing strength (B) keeps constant to decrease the cavity machining difficulty. The simulation results of beam transmission are shown in Fig. 1. The transmission efficiency is 96.9 % at 5 mA.

Table 1: The Design Parameters of the Bent-vane RFQ

Parameter	Value
Particle	He^+(q/A=1/4)
Frequency(MHz)	81.25
Beam current(mA)	5
Input energy(keV/u)	4
Output energy(keV/u)	42.5
Vane voltage(kV)	70
Vane length(mm)	533.76
Kilpatrick factor	1.73
Transmission efficiency(%)	96.9

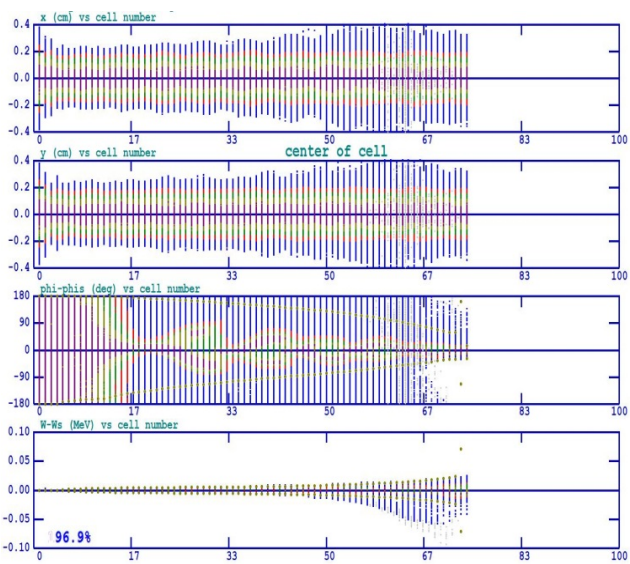


Figure 1: Beam dynamics simulation of the bent-vane RFQ (RFQGen).

2D EM SIMULATION

The cross-section profile is important in the bent-vane RFQ EM design, which is shown in Fig. 2. The cross-

* Work supported by Natural Science Foundation of China (Grant No. 11675236, 11475232 and 11535016)
† email address: yanglei@impcas.ac.cn

Content from this work may be used under the terms of the CC BY 3.0 licence (© 2018). Any distribution of this work must maintain attribution to the author(s), title of the work, publisher, and DOI.

ISBN: 978-3-95450-194-6 ISSN: 2226-0366 doi:10.18429/JACoW-LINAC2018-THPO051

THE MULTI-PHYSICS ANALYSIS OF LEAF RFQ

X. Xu, L. Lu, W. Ma, L. Sun, C. Li, L. Shi, T. He, L. Yang, C. Xing, A. Shi, Y. He, H. Zhao,
Institute of Modern Physics, CAS, Lanzhou, China

Abstract

The 81.25 MHz CW RFQ is designed to accelerate heavy ions with Q/A from 1/7 to 1/2 at 0.5 MeV/u for the Low Energy Accelerator Facility (LEAF) at the Institute of Modern Physics (IMP) of the Chinese Academy of Science (CAS). The four-vane RFQ consists of six modules with a total length of 5.95 meters, For the CW operating mode, thermal management will be a very important issue, Therefore a multi-physics analysis is necessary to ensure that the cavity can stably operate at the high RF power . The multi-physics analysis process includes RF electromagnetic analysis, thermal analysis, mechanical analysis, and the frequency shift, the cooling water system is used for frequency tunning by the temperature adjustment, and also analyze RFQ undercuts, fixed tuners, and pi-mode rods, the results show that the thermal and structural design of this RFQ is reasonable.

INTRODUCTION

The LEAF project is being developed at the Institute of Modern Physics(IMP), composed of superconducting ECR ion source, low energy beam transport line (LEBT), CW radio frequency quadrupole accelerator (RFQ), medium energy beam transport line(MEBT) and an experimental platform [1], the layout of the LEAF project is shown in Fig. 1.

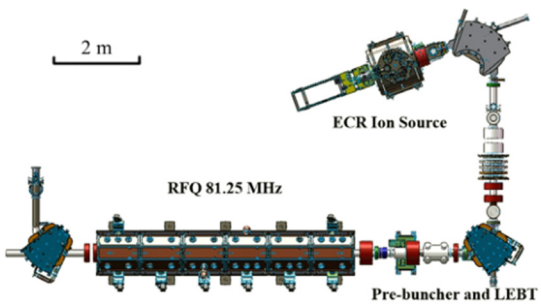


Figure 1: The layout of the LEAF project.

The four-vane RFQ will accelerate heavy ions beams from from 14 keV/u up to 500 keV/u. The operating frequency is 81.25 MHz. The PI-mode rods are used for frequency separation. The cavity will be divided into six segments about 5.95m long. The oxygen-free high-conductivity copper (OFHC) is adopted because of its good heat conduction performance and. An octagon cavity structure is chosen for its structural stability to avoid cavity deformation and convenient design of water cooling system [2].

For high power CW RFQ, the thermal issue will cause structure deformation, frequency shift, and other harmonics. So it's very important to calculate the deformation and evaluate its influence to the electromagnetic field in theory. The thermal and structural distortion of the cavity is calculated by ANSYS code [3], both the temperature rise and the frequency shift can be controlled in an acceptable level according to the optimization of the cooling water design.

The main parameters of the RFQ are listed in Table 1.

Table 1: The Main Parameters of the RFQ

Parameters	Value
Frequency (MHz)	81.25
Injection/Output energy (keV/u)	14/500
Design charge-to-mass ratio	1/7-1/2
Inter-vane voltage (kV)	70
Kilpatrick factor	1.55
Peak current (emA)	2
Transmission efficiency (%)	97.2
Length of the vane (mm)	5946.92
Average radius of the aperture (mm)	5.805

THIN SLICE MODEL SIMULATION

The multi-physics analysis procedure include RF electromagnetic, thermal and mechanical analysis [4], A 1/4 part of the cross section is used for simulation due to symmetry, thin slice model with water cooling channels are shown in Fig. 2.

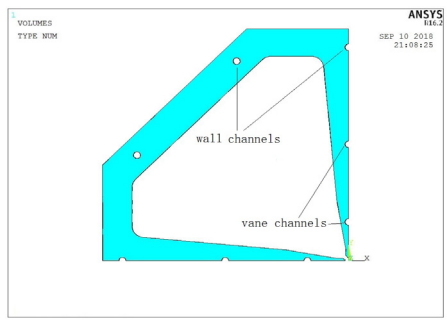


Figure 2: Thin slice model with water cooling channels.

The RF analysis has been carried out with ANSYS code, the result gives RF power losses in cavity in order to obtain a temperature map.

Content from this work may be used under the terms of the CC BY 3.0 licence (© 2018). Any distribution of this work must maintain attribution to the author(s), title of the work, publisher, and DOI.

ISBN: 978-3-95450-194-6 ISSN: 2226-0366 doi:10.18429/JACoW-LINAC2018-THPO052

HIGH POWER TEST OF THE LEAF-RFQ*

L. LU†, W. MA, Y. H. ZHAI, Y. YANG, L.P. Sun, L. B. Shi, L.T. Sun, Y. He, H.W. Zhao
Institute of Modern Physics (IMP), CAS
509 Nanchang Rd., Lanzhou, Gansu, China

Abstract

An 81.25 MHz continuous wave (CW) radio frequency quadrupole (RFQ) accelerator has been designed and fabricated for the Low Energy Accelerator Facility (LEAF) by the Institute of Modern Physics (IMP) of the Chinese Academy of Science (CAS). The operation frequency is 81.25 MHz and the inter-vane voltage is a constant of 70 kV. It took about 44 hours continuous conditioning to reach RF power of 75 kW which is 1.1 time of the maximum designed operation power, and the successful CW acceleration of 150 eμA He^+ beam to the designed energy of 0.5 MeV/u. Both the results of the high power test and the beam test will be reported in this paper.

INTRODUCTION

The LEAF project was launched as a pre-research facility for the high intensity Heavy Ion Accelerator Facility (HIAF) project and a heavy ion irradiation facility for material research at IMP [1, 2]. The LEAF will consist of a 2 mA U^{34+} electron cyclotron resonance ion source, a low energy beam transport line, a CW 81.25MHz RFQ accelerator [3], a medium energy beam transport and an experimental platform for nuclear physics. The layout of the LEAF project is shown in Fig. 1. The LEAF-RFQ shown in Fig. 2 will operate as a CW injector with the capability of accelerating all ion species from proton to uranium from 14 keV/u up to 500 keV/u. The design goal is to design a compact type cavity with lower power loss and high operation stability. Considering the LEAF-RFQ will operate in CW mode, a four-vane structure is a better choice than four-rod type, because the four-vane structure is a more stable structure for water cooling. The PISLs structure is adopted to suppress the dipole effect. In addition, tuners and undercuts are used for frequency tuning and field flatness. The main parameters of the LEAF-RFQ are listed in the Table 1. In this paper, we report the results of the low power test and the high power test.

Table 1: Main Parameters of the LEAF-RFQ

Parameters	Value
A/q	7
Operation	CW/pulsed
Vane type	Four vane
Frequency (MHz)	81.25
Input energy (keV/u)	14
Output energy (MeV/u)	0.5
Inter-vane voltage (kV)	70
Kilpatrick factor	1.55
Peak current (emA)	2
Transmission efficiency (%)	97.2
Acceleration efficiency (%)	81.7
Length of vane (mm)	5946.92
Average radius of aperture (mm)	5.805

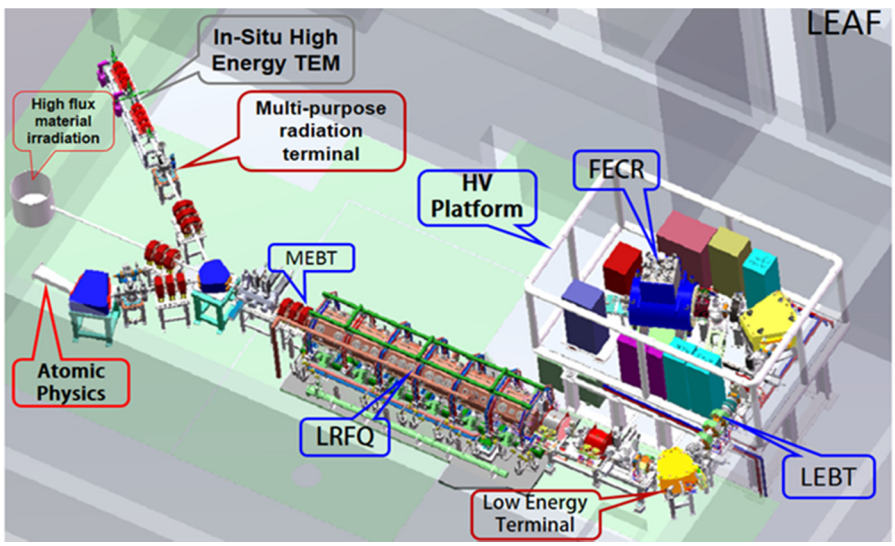


Figure 1: Layout of LEAF facility.

*Work supported by the NSFC under Grant No. 11427904, No. 11475232 and No. 11535016.
†luliang@impcas.ac.cn

Content from this work may be used under the terms of the CC BY 3.0 licence (© 2018). Any distribution of this work must maintain attribution to the author(s), title of the work, publisher, and DOI.

ISBN: 978-3-95450-194-6 ISSN: 2226-0366 doi:10.18429/JACoW-LINAC2018-THPO053

STATUS OF THE CHINA MATERIAL IRRADIATION FACILITY RFQ*

Chenxing Li †, Weiping Dou[1], Weilong Chen[1], Zheng Gao, Yuan He, Guirong Huang, Chunlong Li, Liang Lu, Aimin Shi, Longbo Shi, Liepeng Sun, Fengfeng Wang, Wenbin Wang, Zhijun Wang, Qi Wu, Xianbo Xu, Lei Yang[1], Peiyan Yu[1], Bin Zhang, Junhui Zhang, Peng Zhang, Tieming Zhu
Institute of Modern Physics, CAS, Lanzhou, China
[1]also at University of Chinese Academy of Sciences, Beijing, China

Abstract

The pulsed high power test and beam test of the China Material Irradiation Facility RFQ have been implemented. Before this, the radio frequency measurements and tuning are performed. In this paper, the processes and results of the radio frequency measurements, tuning, pulsed high power test and beam test will be presented. The results of tests are in good agreement with the design.

INTRODUCTION

Material study is important for the fusion energy utilization. It is important to construct accelerator-based neutron sources for verification of materials candidate to fusion reactor. The IFMIF project is a part of ITER project for this purpose. As counterpart to CFTER, the CMIF project is proposed. As a key equipment of CMIF, the RFQ is designed to accelerate 10 mA CW deuteron beam from 20 keV/u to 1.5 MeV/u. The design procedure is expatiated in references [1] and [2]. The key parameters are listed in Table1.

Table 1: Parameters of CMIF RFQ

Parameters	Values
Particle	D+
Frequency (MHz)	162.5
Energy (I/O, MeV/u)	0.02/1.55
Beam current (mA)	10
Cavity length (m)	5.34
Inter-vane Voltage(kV)	65
Kilpatrick factor	1.4
Transmission efficiency (%)	98.9

TUNING OF CMIF RFQ

Fabrications of single modules were completed May 2017. And assembly of whole length cavity is completed during July 2017. Rf measurements and tuning of the RFQ was carried out during July and August. The tuning process was expatiated in references [3]. The tuning was implemented by utilizing 100 slug tuners. Owe to the utilization of PISLs, the dipole perturbative components are below 1% during tuning, so there is no need for tuning of dipole perturbative components. Therefore, the lengths of tuners with same longitudinal position will be set to the same length. The evolution of the lengths of tuners is plot in Fig. 1. The quadrupole perturbative component during tuning is measured and plot in Fig. 2.

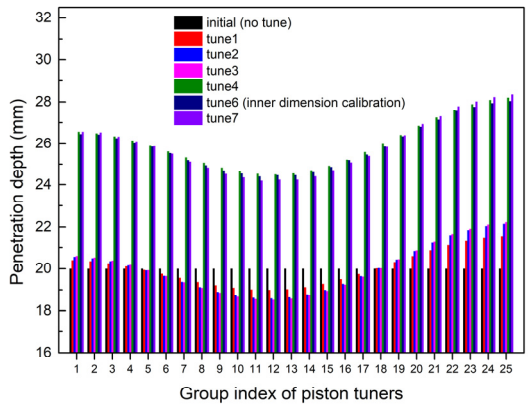


Figure 1: Evolution of lengths of slug tuner groups.

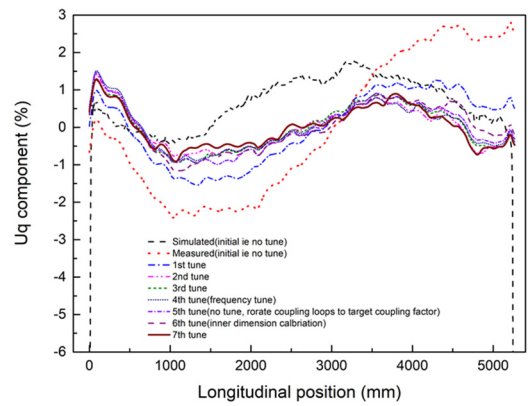


Figure 2: Evolution of the quadrupole perturbative component during tuning.

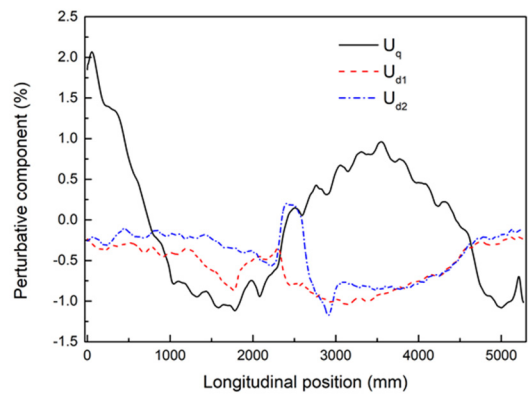


Figure 3: The measured perturbative components after the assembly of copper slug tuners.

* Work supported by the National Magnetic Confinement Fusion Science Program of China (Grant No. 2014GB104001) and the National Natural Science Foundation of China (Grant No. 91426303).
† email address: lichenxing@impcas.ac.cn

Content from this work may be used under the terms of the CC BY 3.0 licence (© 2018). Any distribution of this work must maintain attribution to the author(s), title of the work, publisher, and DOI.

ISBN: 978-3-95450-194-6 ISSN: 2226-0366 doi:10.18429/JACoW-LINAC2018-THPO054

RECENT PROGRESS OF A CW 4-ROD RFQ FOR THE SSC-LINAC*

Z. S. Li[1], J. W. Xia[1], Y. J. Yuan, J. C. Yang, Y. He, Y. Q. Yang, Z. Xu, Y. Cong, J. Meng, L. Jing, H. Du[1], Z. J. Wang, Y. Zhang, X. N. Li[1], K. D. Wang[1], W. J. Xie, Y. Wei, H. M. Xie[1], G. D. Shen[1], Q. Y. Kong[1], X. J. Yin[1, †], J. X. Wu[1, ‡],
Institute of Modern Physics of Chinese Academy of Sciences, 730000 Lanzhou, China
Y. R. Lu[§],
State Key Lab of Nuclear Physics and Technology, Peking University, 100871 Beijing, China
[1]also at Huizhou Research Center of Ion Sciences, 516003 Huizhou, China

Abstract

The SSC-LINAC is under design and construction as a linear injector for the Separated-Sector Cyclotron (SSC) of the Heavy Ion Research Facility at Lanzhou (HIRFL). The continuous-wave (CW) 4-rod radio-frequency quadrupole (RFQ) of the SSC-LINAC has important progress in past years. In the autumn of 2016, the cavity has been operated with 35 kW on CW mode in automatic RF controlled mode during RF power commissioning, which is needed to accelerate $^{238}U^{34+}$ beams. The beam transmission efficiency, transverse emittance and energy spread has been obtained in beam commissioning. In this paper, the results of experiments will be presented and discussed in detail.

INTRODUCTION

To achieve excellent performance in nuclear and atomic physics, the Heavy Ion Research Facility in Lanzhou (HIRFL) was upgraded with a multifunctional Cooler Storage Ring (CSR) at the end of 2007 [1]. As the only injector of the HIRFL, the Sector Focusing Cyclotron (SFC) is needed to provide ion beams for the Separated Sector Cyclotron (SSC) and the CSR. The SSC has to be shut down when the SFC provides the beams to the CSR, which results in the low utilization of the HIRFL. Furthermore, several new experiment such as the Super Heavy Elements (SHE) and precise mass measurement experiments have a higher beam current requirement, which cannot be satisfied by the SFC. To solve these problems, a room-temperature heavy ion linac called SSC-LINAC was proposed as a new injector of the SSC to replace the SFC [2], as shown in Fig. 1. The SSC-LINAC mainly consists of a superconducting high-charge-state electron cyclotron resonance (ECR) ion source, a low energy beam transport (LEBT) system, a CW 4-rod RFQ, a medium energy beam transport (MEBT) system, three IH-DTLs and a high energy beam transport (HEBT) section [3].

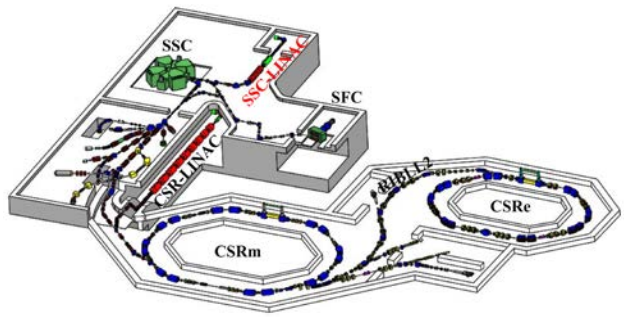


Figure 1: Layout of the HIRFL with the SSC-LINAC.

As a critical component of the SSC-LINAC, the RFQ is required to accelerate intense beams and operate in CW mode, which was the greatest challenge. In beam dynamics, a quasi-equipartitioning design strategy was applied to control the emittance growth and beam losses caused by intense beams [4]. The main parameters of the RFQ are listed in Table 1. The thermal analysis and cooling design have been done carefully by the CST [5] code. A bottom plate, 12 stems and 4 mini-vanes are all cooled by deionized water to ensure security and reliability of the CW mode operation [6].

Table 1: Main Parameters of the SSC-LINAC RFQ [4]

Parameters	US Letter Paper
Frequency	53.667 MHz
Ratio of Charge to Mass	1/3~1/7
Beam Current	0.5 pmA
Duty Factor	100%
Input Energy	3.728 keV/u
Output Energy	143 keV/u
Inter-Vane Voltage	70 kV
Vane Length	2.508
Transmission efficiency	94.1%

The SSC-LINAC has important progress in past years. The cavity was delivered to the Institute of Modern Physics (IMP) in the first season of 2013. The RF performance measurement, including the frequency, quality factor Q_0 and the electric field distribution, was finished in 2014. Then, the commissioning with high RF power and ion beams has been finished. In this paper, the RF power and beam commissioning are reported. The experimental setup for the RFQ test is depicted in Fig. 2.

* This work was supported by the National Natural Science Foundation of China (Nos. 11375243, 11405237, and 11475235) and the Guangdong Innovative and Entrepreneurial Research Team Program (No. 2016ZT06G373).
† yinxj@impcas.ac.cn
‡ wujx@impcas.ac.cn
§ yrlu@pku.edu.cn

Content from this work may be used under the terms of the CC BY 3.0 licence (© 2018). Any distribution of this work must maintain attribution to the author(s), title of the work, publisher, and DOI.

ISBN: 978-3-95450-194-6 ISSN: 2226-0366 doi:10.18429/JACoW-LINAC2018-THPO057

REDESIGN OF CERN LINAC3 RFQ FOR LEAD 29+

S. Benedetti *, A.M. Lombardi, G. Bellodi, J.B. Lallement, CERN, Geneva, Switzerland

Abstract

CERN Linac3 is at the heart of the CERN Heavy Ion Facility, providing 4.2 MeV/u ion beams to the Low Energy Ion Ring (LEIR). It mostly accelerates $^{208}Pb^{29+}$, though in recent years runs were performed with $^{40}Ar^{11+}$ and $^{129}Xe^{22+}$, in view of the raising interest of the physics community towards lighter ions experiments. In the framework of the LHC Injectors Upgrade (LIU) project, measurements and beam dynamics simulations showed that a transmission bottleneck of Linac3 is represented by the RFQ. As this accelerator was originally designed for $^{208}Pb^{25+}$, the lower beam rigidity of the heavy ions currently in used – and planned to be used – permits a redesign of the RFQ aimed at increasing its transverse acceptance, and thus the transmitted beam current. The methodology adopted and the results of this study are presented.

INTRODUCTION

Linac3 [1] is composed by an Electron Cyclotron Resonance (ECR) source producing heavy ion beams at 2.5 keV/u. The desired charge state is filtered by a Low Energy Beam Transport (LEBT) line and further accelerated by a 101.28 MHz RFQ to 250 keV/u. A Medium Energy Beam Transport (MEBT) line matches the beam, both longitudinally and transversally to an Interdigital H-type (IH) linac, which boosts the beam to 4.2 MeV/u. After the IH linac, the beam is stripped to a higher charge state and transported to LEIR. The layout of Linac3 is shown in Fig. 1.

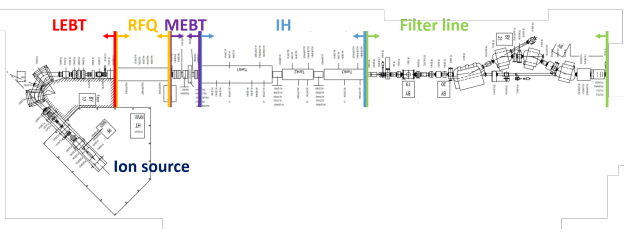


Figure 1: Linac3 layout, with the different sections marked.

In 2005, the original Linac3 ion source was replaced by a higher intensity 14.5 GHz room temperature ECR ion source (GTS-LHC) [2]. This source operates mostly in afterglow mode to produce $^{208}Pb^{29+}$, and in recent years, $^{40}Ar^{11+}$ and $^{129}Xe^{22+}$. This change called for a new study of the beam dynamics in Linac3 [3]. A major result is that the RFQ represents a bottleneck of the line, with transmission of 70 % or lower, depending on the accelerated ion species, while originally the transmission was higher than 90 %. The phase space orientation of the beam emittance appears to be reasonably well matched at the RFQ input, with the losses due to the input emittance larger than the acceptance (Fig. 2).

* stefano.benedetti@cern.ch

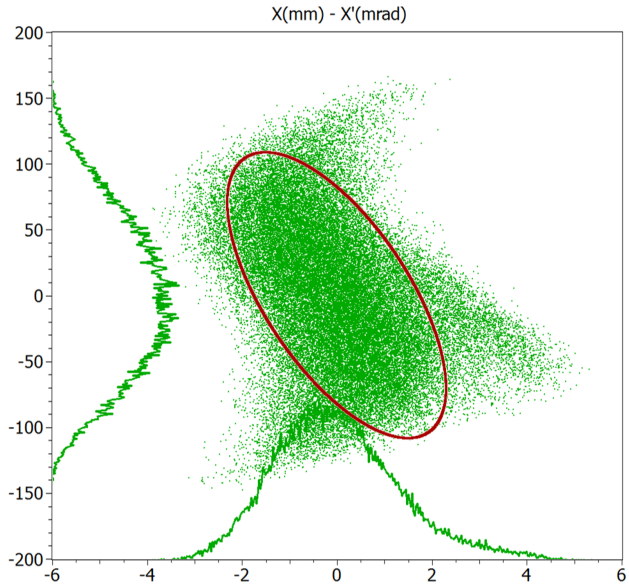


Figure 2: RFQ acceptance in red (0.45 mm.mrad 95 % beam) and simulated beam in green dots (0.97 mm.mrad 95 % beam) at the RFQ input for the the x-x' plane.

The lower beam rigidity of the currently accelerated ions with respect to the originally considered $^{208}Pb^{25+}$ permits to redesign the RFQ increasing its transverse acceptance. The redesign shall meet the constraints discussed in the following section.

CONSTRAINTS OF THE REDESIGN

The RFQ redesign had to meet three constraints: to maintain the same cavity length – 2.5 m – and operating frequency – 101.28 MHz, to maintain the same vane voltage V_0 – 71 kV – and maximum surface electric field – 23.9 MV/m, to maintain or decrease the output longitudinal emittance, 39 π.deg.keV/u for 95 % of the particles.

The first constraint guarantees a minimal change of the line, as only the rod modulation and aperture will change, while the outer tank and power supply would not be replaced. The second point ensures that the redesigned has the same Break-Down (BD) rate of the current one. Operating at 101.28 MHz, with a maximum surface electric field of nearly 24 MV/m, the cavity Kilpatrick factor is 2.1.

The last constraint – to maintain or decrease the output longitudinal emittance – is a consequence of the small longitudinal acceptance of the IH linac that follows the RFQ.

The transmission through the IH cavities was measured as a function of the phase of the input beam. This was achieved by changing the RFQ RF phase, which accepts a continuous input beam and it is thus unaffected by this modification. The phase of the buncher cavities between the RFQ and the IH were also changed accordingly, in order to guarantee

Content from this work may be used under the terms of the CC BY 3.0 licence (© 2018). Any distribution of this work must maintain attribution to the author(s), title of the work, publisher, and DOI.

ISBN: 978-3-95450-194-6 ISSN: 2226-0366 doi:10.18429/JACoW-LINAC2018-THPO058

RF DESIGN OF A HIGH-FREQUENCY RFQ LINAC FOR PIXE ANALYSIS*

H. W. Pommerenke†,1,2, A. Bilton[1], A. Grudiev[1], A. M. Lombardi[1], S. Mathot[1], E. Montesinos[1], M. Timmins[1], M. Vretenar[1], U. van Rienen[2]
[1] CERN, Geneva, Switzerland
[2] University of Rostock, Germany

Abstract

Protons with an energy of few MeV are commonly used for Ion Beam Analysis of materials, in particular with the Proton Induced X-ray Emission technique (PIXE). Because of its non-damaging character, PIXE is used in a variety of fields, in particular for the diagnosis of cultural heritage artwork. A compact accelerator based on a high frequency RFQ (Radio Frequency Quadrupole) linac has been designed and is being built at CERN. The length of the RFQ is only one meter and it allows the acceleration of a proton beam up to an energy of 2 MeV. The complete system is conceived to be transportable, allowing PIXE analysis almost anywhere. This paper covers the RF design of the compact RFQ operating at 750 MHz. We present general accelerator parameters and the current state of the RF design, which includes RFQ geometry and coupler design, thermal simulation and first particle tracking results.

INTRODUCTION

The Proton Induced X-Ray Emission (PIXE) [1] is a widely used method for cultural heritage material characterization (among others). It allows for a non-damaging and highly sensitive quantitative analysis by stimulating specimen atoms using 2 to 4 MeV proton beams and measuring the emitted X-ray spectrum.

Conventional electrostatic PIXE accelerators require significant space and infrastructure and are thus installed in dedicated centres. Contrarily, an RFQ operating at 750 MHz is able to provide 2 MeV protons over the length of just one meter, as proposed in [2]. The PIXE RFQ is developed within the context of the MACHINA project [3], whose aim is to build the first transportable system for *in situ* ion beam analysis. The RFQ design is based on the high-frequency RFQ for medical applications [2, 4, 5], adapted to the requirements of PIXE analysis. A selection of design parameters is presented in Table 1.

RF DESIGN

In general, all geometries are optimised to a resonant frequency of $f_0 = 749.48$ MHz, as well as minimum surface losses expressed by a maximum Q_0 factor. While a circular shape of the four quadrants would be the optimum in this regard, a planar back side surface is used to simplify the machining (Fig. 1). The cavity geometries of the two RFQ modules are slightly different to account for the changing vane modulation.

Table 1: Design Parameters of the PIXE RFQ

Input energy	$\mathcal{E}_{in}$	20	keV
Output energy	$\mathcal{E}_{out}$	2	MeV
RF frequency	f_0	749.48	MHz
RFQ length		1072.938	mm
Vane voltage	V	35	kV
Min. aperture		0.7	mm
Vane tip radius		1.439	mm
Peak current		200	nA
Transmission	T	30	%
Max. duty cycle	d_{max}	2.5	%

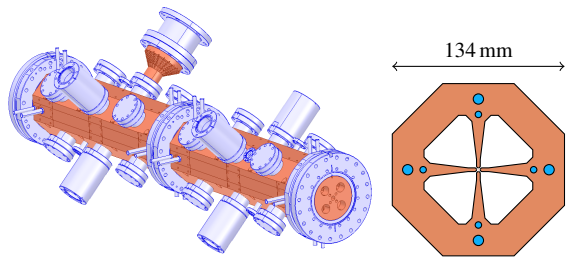


Figure 1: CAD model of the PIXE RFQ. (a) Accelerator with equipped tuners, pumping ports, and coupler. (b) 2D cavity cross section with water cooling channels.

The RFQ is terminated by two end plates with holes in each quadrant that allow for bead-pull measurement access. Further, four dipole stabilization rods on each end plate are used to give the maximum possible spectral margin of ±12 MHz from the quadrupole operating mode (TE_{210}) to the next closest higher order modes (TE_{211} and TE_{111}).

Figure 2 shows the surface electric field E_s at the vane tip. The overall maximum $E_s = 39.1$ MV/m occurs at the gap between the two RFQ modules (Fig. 2b). Excluding this effect, the maximum surface field is located in the bunching section of the RFQ with $E_s = 36.5$ MV/m (Fig. 2a).

The shapes of tuners and pumping ports are similarly optimised for minimum losses. The tuners are copper slugs with a conic tip (Fig. 3a). The pumping ports end with crossbars that help conducting the surface currents (Fig. 3b).

The total RF power P_0 dissipated through surface losses can be estimated by longitudinally decomposing the RFQ

* This work has been sponsored by the Wolfgang Gentner Programme of the German Federal Ministry of Education and Research (grant no. 05E15CHA).
† hermann.winrich.pommerenke@cern.ch

Content from this work may be used under the terms of the CC BY 3.0 licence (© 2018). Any distribution of this work must maintain attribution to the author(s), title of the work, publisher, and DOI.

ISBN: 978-3-95450-194-6 ISSN: 2226-0366 doi:10.18429/JACoW-LINAC2018-THPO060

FIRST RF MEASUREMENTS OF THE 325 MHz LADDER-RFQ

M. Schuett*, U. Ratzinger and M. Syha
Institute for Applied Physics, Goethe University, Frankfurt, Germany

Abstract

Based on the positive results of the 0.63 m unmodulated 325 MHz Ladder-RFQ prototype from 2013 to 2016 [1], a modulated 3.3 m Ladder-RFQ (see Fig. 1) has been designed and built. In this paper, we will show the results of manufacturing as well as first low level RF measurements of the Ladder-RFQ.

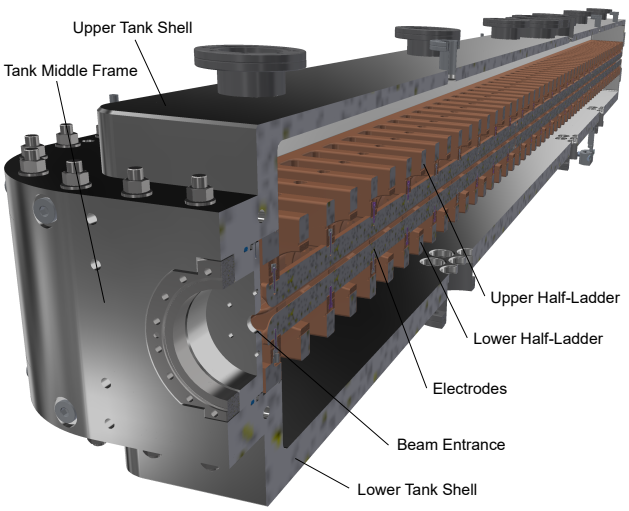


Figure 1: Isometric view of the 3.3 m modulated Ladder-RFQ. Copper carrier-rings guarantee the electrode positioning as well as the RF contact. The ladder structure consists of bulk copper components. Any brazing or welding processes were avoided for the assembly of the main components.

INTRODUCTION

The idea of the Ladder type RFQ firstly came up in the late eighties [2, 3] and was realized successfully for the CERN Linac3 operating at 101 MHz [4] and for the CERN antiproton decelerator ASACUSA at 202 MHz [5].

Due to its high symmetry, this Ladder-RFQ features a very constant voltage along the axis. The Ladder-RFQ prototype was high power tested at the GSI test stand. It accepted 3 times the RF power level needed in operation [6]. That level corresponds to a Kilpatrick factor of 3.1 with a pulse length of 200 µs. The 325 MHz RFQ is designed to accelerate protons from 95 keV to 3.0 MeV according to the design parameters of the proton linac within the FAIR project. This particular high frequency creates difficulties for a 4-ROD type RFQ, which triggered the development of a Ladder-RFQ with its higher symmetry. The results of the unmodulated prototype have shown, that the Ladder-RFQ is a suitable candidate for that frequency. For the present design duty cycles are feasible up to 5%. The basic design and tendering of the RFQ has been successfully completed in 2016 [7]. Manufacturing of the large components has been completed in September 2018.

Table 1: Main RF and Geometric Parameters of the Modulated Ladder-RFQ

Parameter	Value
No. of RF cells	55
Q-Value (simulated)	6800
Loss (with sim. Q)	675 kW
Shunt Impedance (sim.)	45 kΩm
Vane-Vane Voltage	88.43 kV
Frequency	325.224 MHz
Repetition Rate	4 Hz
Pulse Duration	200 µs
Total Length	3410 mm
Cell Length	40 mm
Spoke Height	280 mm
Spoke Width	150 mm
Electrode Length	3327 mm

DESIGN AND MANUFACTURING

The mechanical design consists of an inner copper ladder structure mounted into an outer stainless steel tank. The tank is divided into three parts - the lower and upper shells and a middle frame.

The lower shell of the tank carries and fixes the position of the inner resonating ladder structure. Due to manufacturing reasons, the ladder structure is divided into two lower and two upper half-ladder elements, which are precisely aligned via guide pins. The half-ladders themselves are machined from solid copper blocks. Between the half-ladder elements, the electrodes are precisely fixed via carrier-rings [8]. Those carrier-rings furthermore guarantee a seamless RF connection between the electrodes and the ladder structure.

The RF features are mainly determined by the resonating structure, while the dimensions of the tank have no significant influence on the frequency. Based on the successful high power tests of the unmodulated prototype, we decided to develop a new beam dynamics for a vane-vane voltage of 88.4 kV [9]. For details of the final beam dynamics see [10]. The basic physical and mechanical parameters of the Ladder-RFQ results are shown in Table 1. Furthermore, the thickness of the tank walls inside the entrance and exit flange of the RFQ have been reduced to 10 mm within the flange diameter of 100 mm (CF100). That allows an integration of preceding and following components like a cone or steerer to reduce an emittance growth caused by an additional drift. The next step, beginning in 2019, is the development of

* schuett@iap.uni-frankfurt.de

Content from this work may be used under the terms of the CC BY 3.0 licence (© 2018). Any distribution of this work must maintain attribution to the author(s), title of the work, publisher, and DOI.

ISBN: 978-3-95450-194-6 ISSN: 2226-0366 doi:10.18429/JACoW-LINAC2018-THPO061

BEAM CHARACTERIZATION OF THE MYRRHA-RFQ*

P. P. Schneider†, Martin Droba, Oliver Meusel, Holger Podlech, Alwin Schempp
Institute for Applied Physics (IAP), Goethe-University, Frankfurt am Main, Germany
D. Noll, European Organization for Nuclear Research (CERN), Geneva, Switzerland

Abstract

The Linear Accelerator for the MYRRHA project [1] is under construction. In a first step, the linac up to 100 MeV will be realized. The LEBT section has been set into operation in Belgium and the RFQ is installed in summer 2018. A system to analyze the ion beam consisting of a slit-grid emittance scanner, a beam dump and a momentum spectrometer, called diagnostic train descripted in [2], will be set on the rails to characterize the beam at the RFQ injection point. The results will be used to adjust the optimal matching for the RFQ. After the measurements downstream the LEBT, the diagnostic train begins its journey along the beam line and at the first station the RFQ is installed. The accelerated beam of the RFQ is then analyzed and optimized. In addition to optimization of transmission the artificial production of beam offsets in the LEBT is of special interest. These will be measured at the injection point to estimate the range of possible offsets. In the following measurements these offsets will be used to study the influence of the offsets on the RFQ performance. Furthermore, the RFQ parameters are varied to see their influence on the beam transport, transmission and beam quality.

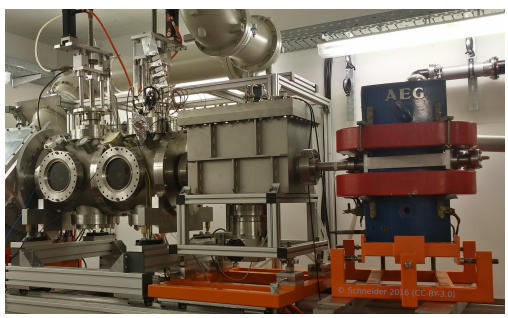


Figure 1: The diagnostic train in operation (left to right): emittance meter – beam dump – momentum spectrometer.

INTRODUCTION

In order to optimize the transport of an ion beam in an accelerator, it is important that each component is tested and optimized as independently as possible after its installation. For this purpose, the installation of the MYRRHA injector includes a measurement of the ion beam after the installation of each individual acceleration component. A flexible diagnostic train was developed to measure the ion beam at different stations along the accelerator chain using the same components for comparable results.

Based on the experiences in [2] numerical evaluations were performed to prepare and optimize the beam and its measurements.

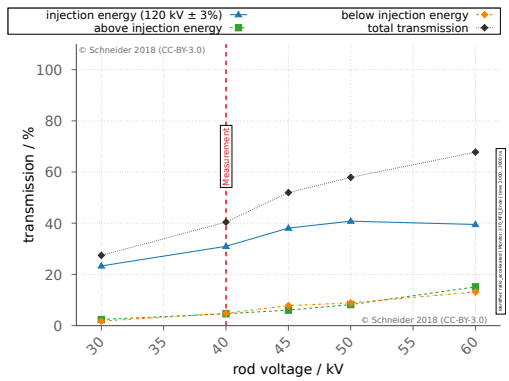


Figure 2: Influence of the rod voltage on the transmission of a Helium beam (120 keV, 1 mA) at rod voltages of $U_{\mathrm{Rod}} = 30\,\mathrm{kV}...60\,\mathrm{kV}$, operating the RFQ in transport mode. The beam remains unaccelerated. The measurements of [2] were performed at $U_{\mathrm{Rod}} \approx 40\,\mathrm{kV}$.

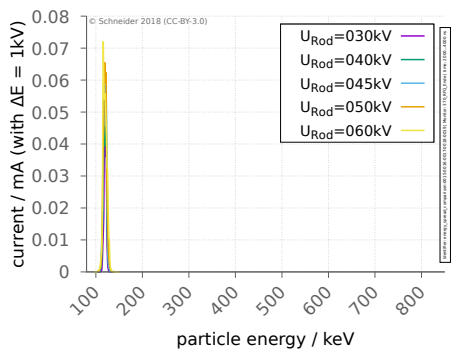


Figure 3: Energy histogram for a Helium beam (120 keV, 1 mA) at various rod voltages of the RFQ in transport mode. The beam remains unaccelerated and the energy spread is very narrow. This makes it perfect for the calibration of a momentum spectrometer.

Diagnostic Train

The diagnostic train as seen in Fig. 1 consists of an emittance meter followed by a beam dump with an 1 mm aperture and a trailing momentum spectrometer.

It was set up for measurements at the Frankfurt Neutron Source and is now calibrated for the upcoming measurements at the MYRRHA injector in Louvain-la-Neuve, Belgium.

* This work is supported by the German Federal Ministry of Education and Research (BMBF) #05P15RFRBA and HORIZON 2020 for the MYRRHA project #662186 and HIC for FAIR.
† schneider@iap.uni-frankfurt.de

Content from this work may be used under the terms of the CC BY 3.0 licence (© 2018). Any distribution of this work must maintain attribution to the author(s), title of the work, publisher, and DOI.

ISBN: 978-3-95450-194-6 ISSN: 2226-0366 doi:10.18429/JACoW-LINAC2018-THPO062

IFMIF/EVEDA RFQ PRELIMINARY BEAM CHARACTERIZATION

E. Fagotti, L. Antoniazzi, L. Bellan, M. Comunian, F. Grespan†, M. Montis, A. Palmieri, A. Pisent, F. Scantamburlo, INFN-LNL, 35020 Legnaro, Italy
T. Akagi, K. Kondo, T. Shinya, M. Sugimoto, K. Sakamoto, QST, Aomori, Japan
P. Cara, IFMIF/EVEDA Project Team, Aomori, Japan
H. Dzitko, R. Heidinger, A. Marqueta, I Moya, F4E, Garching, Germany
I. Podadera, CIEMAT, Madrid, Spain

Abstract

The IFMIF/EVEDA RFQ is the longest and powerful operated. Therefore, it requires a careful characterization from several aspects: beam dynamics, RF, mechanics, installation and commissioning. Due to the very large power handling, the preliminary beam operation was decided to be performed with a low proton beam current at one half of the voltage needed for deuteron acceleration, i.e. from 8 mA to 30 mA at 2.5 MeV in pulsed mode, with respect to the nominal 130-mA deuteron beam at 5 MeV in CW. In this framework, it will be presented the characterization of the RFQ in terms of simulation and measurements.

INTRODUCTION

The Linear IFMIF Prototype Accelerator (LIPAc) is composed of an ion source, a LEBT, a RFQ, a MEBT and a SC linac and HEBT, with a final energy of 9 MeV [1].

This paper is mainly focalized on Normal Conducting linac performance. In particular RFQ is a CW linac capable of delivering 125 mA of D^+ beam at 5 MeV. The 10-m-long, 175-MHz RFQ structure is designed to accelerate the DC 100 keV, 130 mA D^+ beam from the injector with more than 90% transmission [2].

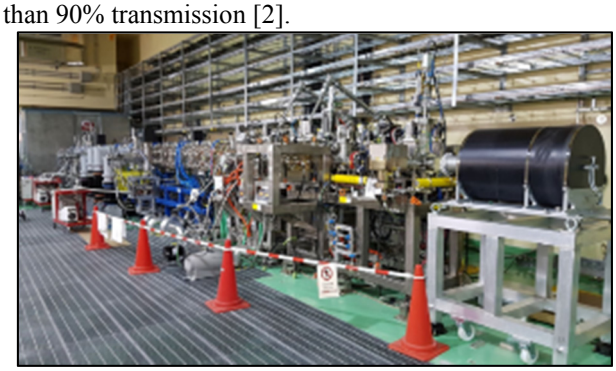


Figure 1: IFMIF/EVEDA LIPAc in Rokkasho (Japan).

RFQ is installed in IFMIF site in Rokkasho (Fig. 1) since April 2016. The low power RF characterization (bead pulling and tuning) was concluded in September 2016. We installed the 8 power couplers in December 2016, checking the field by pick-up reading. After baking and connection to the cooling system and to the 8 RF systems, RF conditioning started in July 2017. Some problems slowed down hardware conditioning and integration: the 132 kV max nominal voltage for D^+ beam was reached on January 2018 with very short RF pulses (20 μs/125 ms). Maximum power reached in CW was 60 kW. Until now the RFQ did not show any problem in terms of RF performances [3].

These partial results were nevertheless enough to start RFQ beam commissioning phase B1, consisting in the acceleration of a pulsed proton beam up to 2.5 MeV. On June 13th first proton beam was successfully accelerated through the RFQ. Beam operation continued until August 10th despite some trouble in one RF power supply which was then bypassed by operating with 7 over 8 RF chains only.

LIPAC CONFIGURATION

The accelerator configuration for beam commissioning of LIPAc RFQ is shown in Fig. 2. LEBT optics includes two solenoids (Sol#) with integrated steering magnet pairs (ST#). Diagnostics include Doppler-Shift Spectroscopy, a 4 grid analyser, an Allison-Scanner, a beam stop, two CCD beam profile monitors. Three cm before RFQ matching point, there is LEBT-ACCT. RFQ input plate includes an electron repeller (-3 kV). Cavity is maintained at 10^{-8} mbar vacuum level by 10 cryo-pumps. For RFQ beam characterization, MEBT is equipped with an ACCT just after the gate valve separating it from the RFQ, a Fast Current Transformer (FCT) and 4 BPM's. Diagnostic-Plate next to MEBT includes 3 BPM's, 2 Slits combined with SEM-Grids for profile and emittance measurement, an ACCT-DCCT, a Residual Gas Bunch Length Monitor (RGBLM), a Fluorescence Profile Monitor (FPM) and an Ionization Profile Monitor (IPM). Lastly, a Low Power Beam Dump (LPBD) is used as Faraday Cup.

In this first beam commissioning period, profile diagnostics and Doppler-Shift diagnostic were not operational yet. Hence, results presented in the following are based on the ACCTs, LPBD and BPMs diagnostics.

COMMISSIONING PLAN AND SIMULATIONS

Beam operation represents the first integrated test of LIPAc systems. In the followed approach, beam intensity was gradually increased while verifying and debugging each sub-system and their interfaces. This constitutes a safe operation mode with respect to starting directly at nominal proton current (65 mA). Low current and so low power beam operation allows using interceptive diagnostics while increasing RFQ acceptance with respect to the input mismatch.

For a better extraction conditions at low currents, injector was equipped with a 3 mm radius extraction hole instead of the original 6 mm.

* The views and opinions expressed herein do not necessarily reflect those of the author's home institutions or research funders.

† francesco.grespan@lnl.infn.it

Content from this work may be used under the terms of the CC BY 3.0 licence (© 2018). Any distribution of this work must maintain attribution to the author(s), title of the work, publisher, and DOI.

ISBN: 978-3-95450-194-6 ISSN: 2226-0366 doi:10.18429/JACoW-LINAC2018-THPO064

TUNING OF A FOUR-VANE RFQ FOR XI'AN 200 MeV PROTON APPLICATION FACILITY

X.D. Yu†, Q.Z. Xing, Q.K. Guo, P.F. Ma, Y. Lei, S.X. Zheng, Y. Li, S. Wang, K. Liu, X.L. Guan, X.W. Wang, Key Laboratory of Particle & Radiation Imaging (Tsinghua University), Ministry of Education, 100084 Beijing, China
also at Laboratory for Advanced Radiation Sources and Application, Tsinghua University, 100084 Beijing, China
also at Department of Engineering Physics, Tsinghua University, 100084 Beijing, China
B.C. Wang, C. Zhao, Z.M. Wang, State Key Laboratory of Intense Pulsed Radiation Simulation and Effect (Northwest Institute of Nuclear Technology), 710024 Xi'an, China

Abstract

This paper mainly describes the procedures and results of tuning a four-vane Radio Frequency Quadrupole (RFQ) accelerator for the Xi'an 200 MeV Proton Application Facility (XiPAF) project. The 3-meter-long RFQ will accelerate a 50 keV H^- beam from the ECR source to 3 MeV, and deliver it to the downstream drift tube linac (DTL) with a peak current of 5 mA, pulse length of 10-40 μs and maximum repetition rate of 0.5. The machining, assembly, and RF tuning of the RFQ cavity has been completed successfully. After tuning, the relative error of the operating quadrupole mode field is within ±2.7%, and the dipole mode component is within ±1.9% of the quadrupole mode. The RFQ now is ready for high-power RF conditioning.

INTRODUCTION

The four-vane Radio Frequency Quadrupole (RFQ) accelerator will be used as a component of the linac injector for the Xi'an 200 MeV Proton Application Facility (XiPAF) project, a facility capable of providing single-event effect test of semiconductor devices in spacecraft electronic systems. The main function of this RFQ is to bunch, focus and accelerate low-speed H^- beam and finally match the beam to the DTL. To make this RFQ compact, the inter-vane voltage of XiPAF RFQ rises from the low-energy end to high-energy end.

Tuning plays an important role for the operation of an RFQ. Due to the deviation of undercut design and machining error, the actual field distribution of RFQ is always different from the designed one. The relatively large error of the field distribution can lead to changes in the synchronous energy, twiss parameters, and transmission efficiency of the beam at the RFQ exit. In order to adjust the field distribution, 48 tuners are equipped on this RFQ.

The main objectives of tuning the XiPAF RFQ are as follows: 1) Reduce the field distribution difference between the measured and designed quadrupole field; 2) decrease the dipole mode field component; 3) tune the frequency to the desired value; 4) adjust the coupling coefficient of the power coupler to the desired value; 5) enlarge the frequency separation between the operating quadrupole mode and the nearest dipole modes to enhance the field stability. In order to ensure that the final field distribution can meet the requirements, the RFQ has been tuned twice, including the pre-braze tuning and final tuning.

†yxd17@mails.tsinghua.edu.cn

XIPAF RFQ

Main parameters of the XiPAF RFQ are shown in Table 1 [1].

Table 1: Main Design Parameters of XiPAF RFQ

Parameters	Value	Unit
Particle	H^-	
Input energy	50	keV
Output energy	3	MeV
Frequency	325	MHz
Peak current intensity	5	mA
Maximum reputation rate	0.5	Hz
Beam pulse length	10-40	μs
Peak wall power	388	kW
Q_0	8600	

Assembled XiPAF RFQ is shown in Fig. 1. This RFQ consists of three segments. A total of 48 tuners are equipped in the four quadrants of the cavity. Each segment is about 1 meter long and contains 16 tuners. Four dipole-mode stabilizer rods [2] are mounted on each of the two flanges in order to adjust the frequency separation between the quadrupole mode and adjacent dipole modes. Undercuts [3] are separately designed for each end of the RFQ in order to help achieve the field distribution close to the designed one. The RFQ is fed by only one power coupler and the coupler is located in the first quadrant in the middle of the RFQ. Power is fed into the cavity by loop coupling [4] and the coupling coefficient can be adjusted by rotating the coaxial coupler.

EXPERIMENTAL SETUP

The magnetic field distribution near the outer wall is obtained by the bead-pull method. Main measuring device is a vector network analyser. One port of the network analyser is connected to power coupler and the other port is connected to a field probe. The probe is inserted into the cavity through a vacuum port to measure the S12 signal. A hollow metal bead with a diameter of 11.5 mm is used for a perturbation. The bead passes through the four quadrants under the drive of a stepper motor.

Content from this work may be used under the terms of the CC BY 3.0 licence (© 2018). Any distribution of this work must maintain attribution to the author(s), title of the work, publisher, and DOI.

ISBN: 978-3-95450-194-6 ISSN: 2226-0366 doi:10.18429/JACoW-LINAC2018-THPO066

FIRST HIGH POWER TEST OF THE ESS HIGH BETA ELLIPTICAL CAVITY

H. Li, M. Jobs, R. Santiago Kern, L. Hermansson, R. Ruber
FREIA Lab, Uppsala University, Sweden,
G. Devanz, T. Hamelin, CEA, France

Abstract

ESS, the European Spallation Source, will adopt elliptical multi-cell superconducting cavities with a beta value of 0.86 to accelerate the proton beam up to 2 GeV at the last section of the linac. A 5-cell high-beta cavity for ESS project was tested with high power at FREIA Laboratory. A pulse mode test stand based on a self-excited loop was used in this test. The qualification of the cavity package involved a 5-cell elliptical cavity, a fundamental power coupler, a cold tuning system, LLRF system and a RF station. These tests represented an important verification before the series production. This paper presents the test configuration, RF conditioning history, first high power performance and experience of this cavity package.

INTRODUCTION

The ESS elliptical SRF linac section is composed of two types of state-of-the-art 704.42 MHz cavities, medium-beta (MB) of 0.67 and high-beta (HB) of 0.86, to accelerate the proton beam from the spoke superconducting linac up to full energy [1]. A total of 84 5-cell HB elliptical cavities are designed at CEA and will be grouped by 4 in 21 cryomodules [2]. Figure 1 shows the layout of the ESS accelerator.

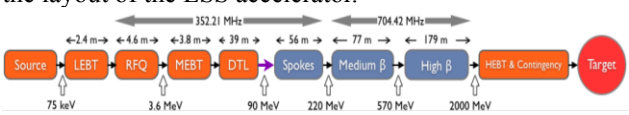


Figure 1: The layout of the ESS accelerator.

The nominal operation parameters of HB section are shown in Table 1 [3].

Table 1: Main Parameters of 5-cell HB Cavities

Frequency [MHz]	704.42
Beta_optimum	0.86
Operating gradient [MV/m]	19.9
Temperature [K]	2
G [Ohm]	241
R/Q [Ohm]	435
Lacc [m]	0.915
Bpk/Eacc [mT/MV/m]	4.3
Epk/Eacc	2.2
Qext	7.6×10^5
π and 4π/5 mode separation [MHz]	1.2

FREIA, at Uppsala University, was established in order to support the development of instrumentation and accelerator technology and started high power test of ESS double spoke cavity tests in 2015 [4, 5]. In 2018, FREIA laboratory also implemented the first high power test of overall HB elliptical cavity package. A power conditioning stand for klystron and a RF test system were commissioned in this test. An optimal procedure for both klystron and power coupler conditioning was used to reduce the time and effort of overall power conditioning. The object of this test thus became the validation of the complete chain as used in ESS: klystron, high power circulator, RF load, high power RF distribution, fundamental power coupler (FPC), HB elliptical cavity, cold tuning system (CTS) and low level RF system (LLRF).

RF CONDITIONING

The warm coupler conditioning was completed with an effective conditioning time of 20 hours and finally achieved 1 MW peak power with a standing wave regime at 14 Hz repetition rate @ 500 μs and 300 kW peak power with 14 Hz repetition rate @ 2600 μs. Lots of outgassing happened at low power with short pulses, as shown in Fig. 2 (a). At the first phase of 50 μs @ 1Hz, the first arcing occurred in the FPC at about 600 kW, afterward it was very hard to increase the RF power without severe outgassing. Half of the total warm conditioning time (10 hours) was taken to reach 1 MW and completed the first phase. Figure 2 (b) shows all following phases which went smoothly through. The conditioning procedure was finally finished by 2 hours power sweeping from 15 kW to 300 kW with 2.6 ms and 14 Hz repetition rate. The choice of pulse duration is limited by the capacity of the modulator prototype. In order to condition and sweep as much area as possible in the FPC, the cold conditioning of the FPC was carried out by the same system but at two different frequencies, with one slightly higher and one slightly lower than the cavity resonant frequency. Each frequency was about 100 kHz away from the cavity resonant frequency of 704.08 MHz at 2K (with free end), in order to make sure there was no RF coupled in to build a field in the cavity.

Compared to the FPC conditioning, the RF conditioning of the cavity with its power coupler, so-called cavity package, is done by a self-excited loop (SEl) at resonant frequency. Since the tuner feedback controller is still under development, SEL naturally becomes a substitute for following the cavity resonant frequency without feedback. In order to produce pulses in the SEL, a RF switch controlled by a programmable trigger signal is introduced. In the vertical test, this cavity showed high performance but unfortunately quenched at 18 MV/m,

Content from this work may be used under the terms of the CC BY 3.0 licence (© 2018). Any distribution of this work must maintain attribution to the author(s), title of the work, publisher, and DOI.

ISBN: 978-3-95450-194-6 ISSN: 2226-0366 doi:10.18429/JACoW-LINAC2018-THPO067

CONTROL SYSTEM AND EXPERIMENT FOR RAON HWR CRYOMODULES*

Heetae Kim†, Moo Sang Kim, Min Ki Lee, Yong Woo Jo, Jong Wan Choi, Youngkwon Kim, Juwan Kim, Sangbeen Lee, Yoochul Jung, Kitaek Son, Doyoon Lee, Ohryong Choi, Kyungtae Seol, Hyojae Jang and Hoechun Jung
Rare Isotope Science Project, Institute for Basic Science, Daejeon 34047, Republic of Korea

Abstract

A prototype of half-wave resonator (HWR) cryomodules is fabricated and tested. Cables and tray are installed for horizontal test. The design and the piping and instrumentation diagram (P&ID) of the HWR cryomodule are presented. The HWR cryomodule is tested with developed programmable logic controller (PLC) and experimental physics and industrial control system (EPICS) control systems. The heat loads of the HWR cryomodule for static and dynamic are measured.

INTRODUCTION

Cryogenic system is required to construct a linear accelerator when superconducting cavities are used to accelerate ion beams. The coolants of cryogenic systems are liquid helium, supercritical helium, liquid nitrogen, etc.

The Stefan-Boltzmann constant for n-dimensional blackbody radiation [1] and the size effect of thermal radiation were studied [2]. The effective temperature was investigated for non-uniform temperature distribution [3, 4]. RAON accelerator system was designed [5], QWR and HWR cryomodules were developed [6] and superconducting radio frequency (SRF) test facility was constructed [7]. The SRF test facility consists of cleanroom, cryogenic system, vertical test site and horizontal test site. Cavity processes and cavity assembles are performed in the cleanroom. Temperature measurement techniques was introduced for RAON cryomodules [8] and RF power couplers for half wave resonator (HWR) were designed [9]. In this research we design, fabricate and test a HWR cryomodule with developed PLC control system. Tray and cable information are shown for horizontal test. Design, feedthrough and radio frequency (RF) amplifier information are presented for the HWR cryomodule. The HWR cryomodule is tested, so static and the dynamic heat loads of the cryomodule are measured.

TRAY AND CABLE INSTALLATION

In order to perform the horizontal test, we develop the programmable logic controller (PLC) for cryomodules. To operate the PLC, tray and cables are installed in the horizontal test site. Figure 1 shows the pictures of tray and cables for the horizontal test. The PLC racks are located outside of the horizontal test bunker. All of the cables are connected with the PLC and the cables come to the local box as shown in Figure 1(c). Cables come out of the local box and are connected to the feedthroughs of cryomodules with connectors. The bunker consists of tray, local box, cables with connectors, compressed air distributors, RF power lines and helium transfer lines.

The cable of 1.5SQ is used for the power line of turbo pumps, dry pumps and heaters. Solenoid valves are used with 20AWG shielded pair cable. 22AWG shielded pair cable is used for gate valves, vacuum gauges, turbo pumps, dry pumps, control valves, temperature sensors and liquid helium level sensors. The connectors of 32 PIN are used for temperature sensors and the connectors of 10 PIN are used for heaters, pressure gauges and level sensors. Specific plastic connectors are used for pumps, display control units (DCUs), gate valves, vacuum valves, vacuum gauges, heaters, etc. The display control unit (DCU) is a universal operating unit for the monitoring and control the Pfeiffer turbo pumps.

Tray sizes are 300X100 (mm^2) and 500X100 (mm^2) which depend on the number of cables.

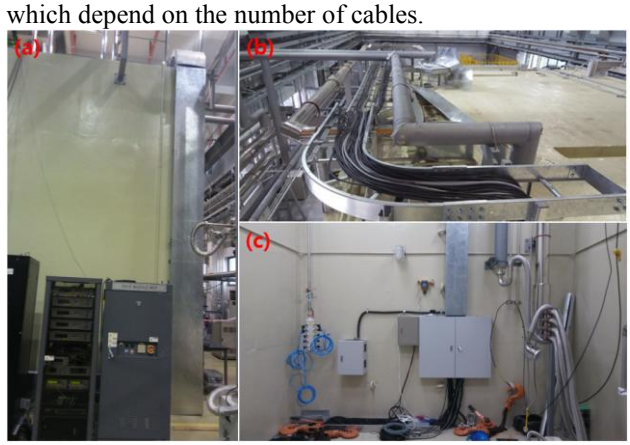


Figure 1: Pictures of tray and cables for horizontal test. (a) PLC rack and tray, (b) cables in tray on the roof of the horizontal test bunkers and (c) cables with connectors, tray, local box, compressed air distributors, RF power lines and helium transfer lines inside of the bunker.

HWR CRYOMODULE

A prototype of a HWR cryomodule is designed. Figure 2 represents the design of the HWR cryomodule. The HWR cryomodule consists of two liquid helium reservoirs, two cavities, two couplers, two tuners, thermal shield, magnetic shield, etc. The operation frequency and temperature of the HWR cryomodule at RAON accelerator

* Work supported by by the Rare Isotope Science Project of Institute for Basic Science funded by the Ministry of Science, ICT and Future Planning (MSIP) and by the National Research Foundation (NRF) of the Republic of Korea under Contract 2013M7A1A1075764. …
† kimht7@ibs.re.kr

Content from this work may be used under the terms of the CC BY 3.0 licence (© 2018). Any distribution of this work must maintain attribution to the author(s), title of the work, publisher, and DOI.

ISBN: 978-3-95450-194-6 ISSN: 2226-0366 doi:10.18429/JACoW-LINAC2018-THPO068

AN EFFECT OF FIELD EMISSION ON LOW BETA SUPERCONDUCTING CAVITIES*

Xinmeng Liu†, Yuan He , Guirong Huang,Zheng Gao
Institute of Modern Physics, Chinese Academy of Sciences 730000, Lanzhou, China

Abstract

Superconducting RF (SRF) technology is widely applied in particle accelerators to shorten the accelerator length and lower the construction price due to its high acceleration gradients with low rf losses. Field emission is the chief limitation associated with the surface electric field which will finally determine the cavity performance during the operation. The pickup-drop signal caused by field emission seriously affect the stable operation of the superconducting linac in the Chinese initiative Accelerator-Driven Sub-critical System (CiADS) demon facility. Simulations of the field emission effect and experimental measurements of the pickup-drop signal have been performed on the half wavelength resonator (HWR) cavity. And a modified design of the pickup antenna will be discussed to solve the pickup-drop problem.

INTRODUCTION

The Chinese initiative Accelerator Driven Sub-critical System (CiADS) project is based on a 10 mA, 1.5 GeV CW proton linac for nuclear waste transmutation. CiADS project needs a high stability linac to demonstrate the technology of 10 mA CW beam of superconducting front-end linac for ADS technology. The first cryo-module of this demon SRF linac includes six 162.5 MHz HWR010 cavities working at 4K with optimum beta equal to 0.1.

In one of coulping ports of the cavity, a power transmission antenna rooted in a RF ceramic window to pick up the RF field power. We measured the pickup-drop signal of HWR010 PT and showed in Fig. 1. The frequently deviant signal result to the irregular responses of LLRF control system and limit the stable operation of the SRF linac.

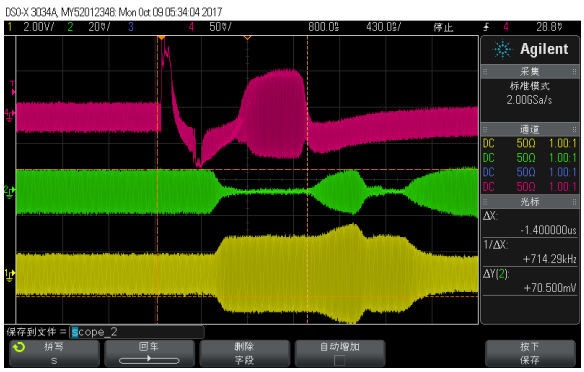


Figure 1: The signal with pickup-drop on oscilloscope.

In Fig. 1, the pink signal is pick up power (Pt) from cavity, the green one is forward RF power (Pf) and the yellow one is reflected RF power (Pr). The pick up signal shows that there is discharge happened on the surface of RF ceramic window , which is called flashover[1]. What's behind it is should be the effect of continuous field emission electron beam hit on the surface of ceramic window[2].

SIMULATION OF FE PARTICAL

This simulation was performed in CST Microwave Studio. The simulation results of electromagnetic field of the cavity is showed in Fig. 2 and Fig. 3.

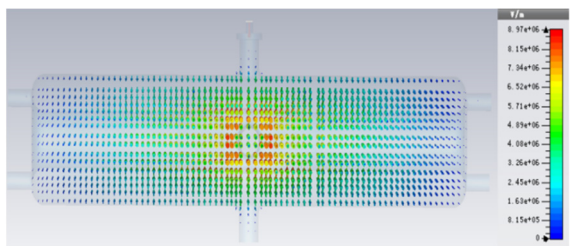


Figure 2: The electric field in HWR010 SRF cavities.

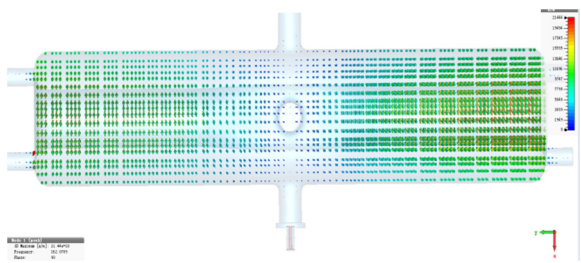


Figure 3: The magnetic field in HWR010 SRF cavities.

The electric field is strongest in the middle of the cavity and is weakest at the ends. The magnetic field is weakest in the middle and strongest at the ends. FE particles were attached to the cavity surface with the high electric field area.

The particles movement in electromagnetic field shows in Fig. 4. From Fig. 4, The particles movements straightly alone the electric field line for the movements were dominated by the electric field, and the weak magnetic field has little effect on their direction of motions. These particles will finally hit on the PT antenna and ceramic window, as shown in Fig. 4 (d). Electrons constantly accumulated on the surface of ceramic window due to the electric property of ceramics, flashover happened when the accumulation to the limit.

* This work was supported by National Natural Science Foundation for Young Scientists of China (Grant NO. 11505255)
† liuinmeng@impcas.ac.cn

Content from this work may be used under the terms of the CC BY 3.0 licence (© 2018). Any distribution of this work must maintain attribution to the author(s), title of the work, publisher, and DOI.

ISBN: 978-3-95450-194-6 ISSN: 2226-0366 doi:10.18429/JACoW-LINAC2018-THPO069

THE DEVELOPMENT OF TE-SAMPLE HOST CAVITY AT IMP*

Shichun Huang†, Yuan He, T. Tan, shengxue Zhang, Institute of Modern Physics, Chinese Academy of Sciences, 73000 Lanzhou, China

Abstract

As a part of the research and development work of thin-film materials for superconducting radio frequency(SRF) application in future accelerator projects at Institute of Modern Physics, CAS, such as Heavy Ion Accelerator Facility(HIAF) and the SRF proton Linac for Chinese Accelerator Driven System etc., a 3.9GHz sample host cavity is being developed for the purpose of characterizing the RF property and the loss mechanism of the superconducting thin-film materials (e.g., Nb/Cu, Nb3Sn and MgB2 etc.). The cavity operates in the TE011 mode and accommodates disk sample with 110mm diameter, theoretically, the maximum magnetic field on sample surface can go up to 100mT, the resolution of surface resistance on sample can reach nOhm scale by using thermometry technique(T-Mapping). In this paper, the electromagnetic optimization result of TE-sample host cavity will be presented, and the design consideration of coupler and T-mapping system are also discussed.

INTRODUCTION

SRF technology has long been adopted in many particle accelerators world-wide in the past, such as Continuous Electron Beam Accelerator Facility(CEBAF) at Jefferson Lab and Spallation Neutron Source(SNS) at Oak Ridge National Lab, will be also used in future accelerator projects, such as FRIB at MSU, LCLS-II at SLAC, ESS and XFEL in Europe, Heavy Ion Accelerator Facility (HIAF) and the proton Linac for Chinese Accelerator Driven System at IMP, CAS, Light Source at IHEP, CAS, FEL at SINAP, CAS etc.. The key components in SRF accelerators are SRF cavities, which have been routinely fabricated by Niobium material. The performance of SRF cavity made out of niobium is mainly determined by the superheating magnetic field Hsh of niobium material (Hsh~=240mT (T=0K)). After more than half a century development in SRF science and technology (the optimization of cavity structure and the advance in cavity surface processing techniques etc.) [1]. For the high beta cavities (beta=v/c, v: the velocity of beam, c: the speed of light), its performance is approaching its material limit (Corresponding accelerating gradient Eacc~=60MV/m) [2]. However, the performance of low beta (0.01-0.3) cavities is still below its material limit, which is mainly determined by electron-loading effect inside the cavities (e.g., field emission effect and multipacting effect etc.) [1], and the cost of niobium bulk technique is still expensive.

* Work supported by National Natural Science Foundation for Young Scientists of China (Grant NO. 11505255).
†huangshichun@impcas.ac.cn.

In order to further reduce the total cost of the SRF cavities system in accelerator (i.e., the cost of SRF cavities and the cryogenic plant) and/or improve the accelerating field of the SRF cavities. One of the solutions is to use superconducting materials thin film technology for the fabrication of the cavity. Niobium thin film on copper substrate technology is attractive due to the high thermal conductivity of copper substrate. Other materials such as MgB2 and Nb3Sn etc. have great potential because of their higher critical temperature and superheating field (i.e. for MgB2: Tc=40K, Hsh=430mT (T=0K); for Nb3Sn: Tc=18.3K, Hsh=540mT (T=0K)) [3,4]. Many laboratory around the world are developing thin film technology for accelerator application.

At IMP, Our accelerator projects, HIAF and CiADS proton Linac both will use SRF technology as mentioned above. Therefore, we started our thin film study two year ago. Both niobium thin film on copper substrate and Nb3Sn on niobium substrate technology are being developed. Normally, the RF properties of thin film can be obtained by low temperature testing of the cavity coated with material thin film. But the results are averaged over the whole cavity surface, local loss mechanism cannot be precisely characterized. And coating the cavity with material thin film is complex and time-consuming. Another way to measure the RF properties of material thin film is to test the thin film sample, where the sample is set as part of the host cavity. To date, there are two methods to characterize the sample, i, end-plate replacement method; ii, RF-DC calorimetric method; the details of above methods are described in reference [5,6]. The measurement apparatus of method two is much complex in comparison with that of method one, because it needs to thermal decouple between host cavity and sample. In order to make host cavity structure simpler and easy to attach sample, reduce the testing period of each sample. Therefore we adopted the end-plate replacement method for the characterization of sample, the sample host cavity will operating in TE011 mode, For perfect TE011 mode, there will be no electric field perpendicular to cavity surface, to ease the electric related effect, such as mulptipacting and field emission effect. And no RF current cross the joints between host cavity and sample disk, to obtain high resolution of RF surface resistance.

In this paper, the electromagnetic optimization of the TE- sample host cavity will be presented, and the design consideration of coupler and T-mapping system will also be discussed.

CAVITY DESIGN

In the end-plate replacement methods, the host cavity resonates in the TE0mn mode, where the sample is one of the end-plates of the host cavity. By measuring the un-

Content from this work may be used under the terms of the CC BY 3.0 licence (© 2018). Any distribution of this work must maintain attribution to the author(s), title of the work, publisher, and DOI.

ISBN: 978-3-95450-194-6 ISSN: 2226-0366 doi:10.18429/JACoW-LINAC2018-THPO072

CRYOGENIC TESTS OF THE SUPERCONDUCTING BETA=0.069 CH-CAVITIES FOR THE HELIAC-PROJECT*

M. Basten[1,†], K. Aulenbacher[3,4], W. Barth[2,3], M. Busch[1], F. Dziuba[3], V. Gettmann[3], M. Heilmann[2], T. Kürzeder[3], M. Miski-Oglu[3], H. Podlech[1], M. Schwarz[1], S. Yaramyshev[2]

[1]IAP University of Frankfurt, 60438 Frankfurt am Main, Germany
[2]GSI Helmholtz-Centre, 64291 Darmstadt, Germany
[3]HIM Helmholtz-Institute Mainz, 55099 Mainz, Germany
[4]KPH Mainz University, 55128 Mainz, Germany

Abstract

In the future the existing UNILAC (UNIversal Linear Accelerator) at GSI will be most exclusively used as an injector for FAIR to provide short pulse high intensity heavy ion beams at low repetition rates [1]. A new superconducting (sc) continuous wave (cw) high intensity heavy ion Linac should provide ion beams with max. duty factor above the coulomb barrier for the Super Heavy Element (SHE) program at GSI. The fundamental Linac design comprises a low energy beam transport (LEBT)-section followed by a sc Drift Tube Linac (DTL) consisting of sc Crossbar-H-mode (CH) structures for acceleration up to 7.3 MeV/u [2, 3]. After the successful test and commissioning of the first demonstrator section with heavy ion beam from the HLI in 2017 [4], the next two sc CH-structures have been constructed and the first one has been extensively tested at cryogenic temperatures at the Institute for Applied Physics (IAP) at Goethe University Frankfurt (GUF). The results of the final cold test of the first CH-structure as well as the next steps realizing a new sc cw heavy ion LINAC at GSI will be presented.

INTRODUCTION

The construction of two sc 217 MHz CH-cavities (CH 1 and CH 2) for the new advanced demonstrator started in December 2016 and was finished in March (CH1) and September 2018 (CH2). During the construction phase several factory side measurements have been performed to monitor crucial parameters like frequency and the tuning concept [5, 6]. Both cavities have the same geometry and the same constant beta profile. Compared to recent sc CH-cavities both cavities are designed without girders and with stiffening brackets on each inclined end cap (see Fig. 1) aiming for increased mechanical stiffness and reduced pressure sensitivity. Each cavity is equipped with two dynamic bellow tuners to adjust the frequency accordingly during operation. The design gradient is 5.5 MV/m, which has to be achieved by eight accelerating cells. In Table 1 the main parameters of the first two 217 MHz CH-cavities are depicted.

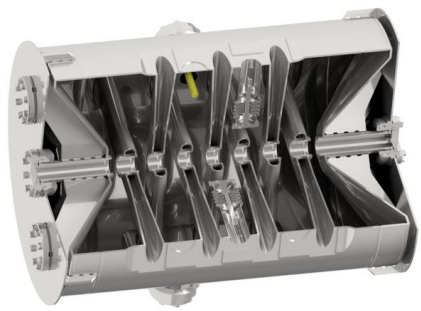


Figure 1: Layout of the sc 217 MHz CH-cavity CH1/CH2.

Table 1: Main Parameters of CH-cavity CH1/CH2

Parameter	Unit	Value
β		0.069
Frequency	MHz	216.816
Accelerating cells		8
Length ($\beta\lambda$-definition)	mm	381.6
Cavity diameter (inner)	mm	400
Cell length	mm	47.7
Aperture diameter	mm	30
Static tuner		3
Dynamic bellow tuner		2
Wall thickness	mm	3-4
Design Accelerating gradient	MV/m	5.5
E_p/E_a		6
B_p/E_a	mT/(MV/m)	<10
G	Ω	50
R_a/Q_0	Ω	1070

EXPERIMENTAL SETUP

After the delivery of CH1 to GUF in March 2018, cavity preparations have been started for the first test at 4.2 K in a vertical cryostat at IAP. The cavity has been equipped with eight temperature probes, 60 Thermo-Luminescence-Dosimeters (TLD's) and two piezo elements (see Fig. 2). The TLD's around the cavity surface record the x-ray-spectra generated inside the cavity during high field levels to observe possible sources of field emission. The piezo elements can be used as actuator and sensor to analyze the mechanical eigenfrequencies of the cavity. The RF measurement setup

* Work supported by BMBF Contr. No. 05P15RFRBA and the EU Framework Programme H2020 662186 (MYRTE)
† Basten@iap.uni-frankfurt.de

Content from this work may be used under the terms of the CC BY 3.0 licence (© 2018). Any distribution of this work must maintain attribution to the author(s), title of the work, publisher, and DOI.

ISBN: 978-3-95450-194-6 ISSN: 2226-0366 doi:10.18429/JACoW-LINAC2018-THPO073

RF COMMISSIONING OF THE SUPERCONDUCTING 217 MHz CH CAVITY FOR HEAVY IONS AND FIRST BEAM OPERATION

F. Dziuba[1,*], K. Aulenbacher[1,4], W. Barth[1,2], M. Basten[3], M. Busch[3], V. Gettmann[1], M. Heilmann[2], J. Salvatore[2], T. Kürzeder[1], M. Miski-Oglu[1], H. Podlech[3], A. Schnase[2], M. Schwarz[3], S. Yaramyshev[2]

[1]HIM Helmholtz Institute Mainz, 55099 Mainz, Germany
[2]GSI Helmholtzzentrum für Schwerionenforschung GmbH, 64291 Darmstadt, Germany
[3]IAP Goethe University Frankfurt, 60438 Frankfurt am Main, Germany
[4]KPH Johannes Gutenberg University Mainz, 55128 Mainz, Germany

Abstract

Future research programs at GSI in the field of super heavy element (SHE) synthesis require high intense heavy ion beams above the coulomb barrier and high average particle currents. The upcoming demands exceed the technical opportunities of the existing UNIversal Linear ACcelerator (UNILAC). Furthermore, the existing machine will be exclusively used as an injector for FAIR (Facility for Antiproton and Ion Research) providing high power heavy ion beams at a low repetition rate. Consequently, a new dedicated superconducting (sc) continuous wave (cw) linac is crucial to keep the SHE research program at GSI competitive on a high level. Recently the first linac section, serving as a prototype to demonstrate the reliable operability of 217 MHz multi gap crossbar-H-mode (CH) cavities under a realistic accelerator environment, has been extensively tested with heavy ion beams delivered from the GSI High Charge State Injector (HLI). Fulfilling its role as a key component of the whole demonstrator setup, the first sc 217 MHz CH cavity (CH-0) successfully accelerated heavy ions up to the design beam energy and even beyond at high beam intensities and full transmission. In this contribution the RF commissioning and the first beam operation of the cavity is presented.

INTRODUCTION

Regarding the future construction of a sc cw linac at GSI an R&D program has been initiated in collaboration with the Institute of Applied Physics (IAP) of Goethe University Frankfurt. In a first step realizing the proposed HElmholtz LInear ACcelerator (HELIAC) it was intended to build and test the first linac section with beam as a demonstrator at the GSI High Charge State injector (HLI) [1, 2]. The demonstrator setup is directly located behind the HLI as shown in Fig. 1. As a key component it contains a 850 mm long 15 gap sc CH cavity (CH-0) [3] operated at 217 MHz (see Fig. 2). Three dynamic bellow tuners inside the cavity allow slow and fast frequency adjustment during operation [4]. The beam dynamics concept of the cavity is based on the EQUidistant mUlti-gap Structure (EQUUS) layout [5, 6]. For beam tests with strong input coupling a 2 kW cw coaxial power coupler is available. Furthermore, the cavity is embedded by two sc 9.3 T solenoids providing the required transverse beam focusing. All components are mounted on a common support frame suspended inside a horizontal cryomodule. After final surface preparation steps and assembly of the helium jacket, the cavity has been extensively tested with low level RF power at 4.2 K followed by a successful full performance test with heavy ion beams.

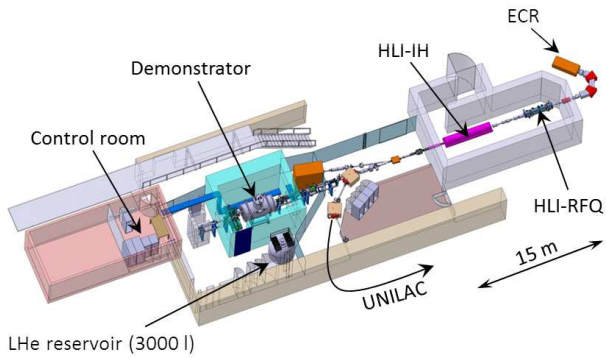


Figure 1: Demonstrator test environment at GSI.



Figure 2: 3D model of the sc 217 MHz CH cavity [7].

RF COMMISSIONING

A first cold test of the CH-0 cavity with low level RF power has been performed in a vertical bath cryostat without helium jacket at IAP beginning of 2016 [7]. During this test the cavity performance was strongly limited by field emission due to an insufficient surface preparation. Nevertheless,

* f.dziuba@gsi.de

Content from this work may be used under the terms of the CC BY 3.0 licence (© 2018). Any distribution of this work must maintain attribution to the author(s), title of the work, publisher, and DOI.

ISBN: 978-3-95450-194-6 ISSN: 2226-0366 doi:10.18429/JACoW-LINAC2018-THPO076

MULTI-PHYSCIS DESIGN STUDIES OF A SUPERCONDUCTING QUARTER-WAVE RESONATOR AT PEKING UNIVERSITY*

Meng Chen, Feng Zhu†, Shengwen Quan‡, Jiankui Hao, Wei Cheng, Shu Chen, Anqi Cheng
Institute of Heavy Ion Physics & State Key Laboratory of Nuclear Physics and Technology, Peking University, Beijing, 100871, China

Abstract

A 81.25MHz, geometric beta=0.046 quarter-wave resonator has been designed and analysed at Peking University. This paper mainly presents the multi-physics studies of this cavity, include electromagnetic design, mechanical analysis and multipacting simulation, to predict its behaviour under practical operating process. Various transverse vibration modes of inner conductor were found under different fixed conditions and an asymmetric shorting plate was adopted to avoid high possibility of multipacting.

INTRODUCTION

There's presently a growing amount of CW high current heavy-ion linear accelerator facilities based on superconducting technology to better support various field of science [1]. Based on that, we designed a quarter-wave resonator for the demand of low beta high current cavity. Structural design is an important aspect overall cavity and cryomodule implementation. Because of the asymmetric geometry of the cavity and usually a long pendulous inner conductor, the thin-wall structure of QWR cavity can be easily deformed by the impact of various fluctuations, causing resonant frequency shift. Excessive frequency shift require additional RF power to control the RF amplitude and phase [2]. Thus a stable resonant frequency is required. We did a sequential coupled field simulations to predict the behaviour of the naked cavity under practical operation, several coupled field analysis were carried out. For the issue of multipacting, an asymmetric shorting plate was adopted to lower the possibility of multipacting.

RF DESIGN

The model of 81.25 MHz QWR is shown in Fig. 1, it is designed and optimized in CST MWS [3]. Taper-shape inner and outer conductors can improve the RF performance relative to using straight cylinders [4]. The top and bottom four ports are used for rinse and the bottom two are also used for power coupler and pick up. All ports are located at a proper position that the water pipes can go deep into the cavity, at the meanwhile they won't influence the surface peak electromagnetic field as shown in Fig. 1. In addition, donut-shaped drift tube was adopted to reduce the magnetic field in the gap [5]. Additional methods to supress the beam steering effect have been studied.

The main geometry and RF parameters of this cavity are summarized in Table 1.

* supported by National Basic Research Project (2014CB845504)
† zhufeng7726@pku.edu.cn
‡ qsw@pku.edu.cn

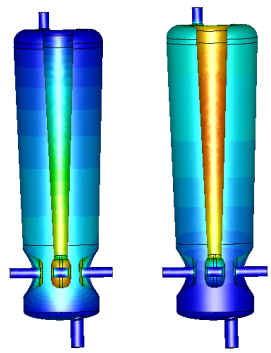


Figure 1: Magnetic field distribution (left) and electric field distribution (right) for the 81.25 MHz mode.

Table 1: The Main Parameters of 81.25 MHz QWR. Surface Resistance was Assumed to be 25nΩ @4.5K in the Calculation

Frequency[MHz]	81.25
β_g	0.046
G[Ω]	21
R_{sh}/Q[Ω]	592
Q_0	8.4e8
Epk/Eacc	4.9
Bpk/Eacc[mT/(MV/m)]	6.4
Beam aperture[mm]	34
Cavity height[mm]	980
Cavity diameter[mm]	270

MECHANICAL SIMULATION

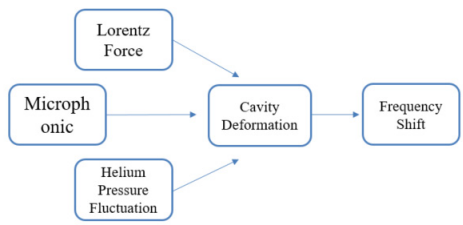


Figure 2: Multi-physics field coupling with cavity.

As shown in Fig. 2, cavity deformations from cooling down, Lorentz force, Helium Pressure Fluctuations (HPF) and microphonics can lead to resonant frequency change, the prediction of the resonant frequency change depends on the accuracy of the calculated electromagnetic fields as well as the calculated mechanical deformation. Due to the asymmetric structure with four ports, we used the whole structure to do the simulation.

Content from this work may be used under the terms of the CC BY 3.0 licence (© 2018). Any distribution of this work must maintain attribution to the author(s), title of the work, publisher, and DOI.

ISBN: 978-3-95450-194-6 ISSN: 2226-0366 doi:10.18429/JACoW-LINAC2018-THPO079

RF TEST OF STANDING WAVE DEFLECTING CAVITY WITH MINIMIZED LEVEL OF ABERRATIONS

V. Paramonov*, INR of the RAS, Moscow, Russia
K. Floettmann, DESY, Hamburg, Germany

Abstract

For diagnostics of longitudinal distribution of electrons in the unique REGAE bunches a specially developed deflecting structure with a minimized level of aberrations in the field distribution and improved RF efficiency is applied. A short deflecting cavity has been constructed and installed on the REGAE beam line. The cavity is tested at the operational level of RF power. The main distinctive features of the cavity are mentioned and the obtained results are reported.

INTRODUCTION

The periodical Deflecting Structures (DSs) were introduced for charged particle deflection and separation. The bunch crosses the DS synchronously with the deflecting field Ed, which corresponds to the phase $\phi = 0$ in the DS and all the particles get the similar increment in the transverse momentum p_t.

Now DSs find new applications in bunch rotation for the purpose of diagnostics of the longitudinal distribution, the emittance exchange and the luminosity improvements in colliders. For these applications a DS operates in another mode - the central particle of the bunch crosses the DS at a zero E_d value, $\phi = 90^o$. Downstream and upstream particles get opposite increments in p_t. In applications for bunch rotation a DS should produce the minimum possible own distortions in the original distributions of particles in the 6D phase space.

METHODOLOGICAL AND PHYSICAL BASIS

The concept of DSs with a minimized level of own aberrations in E_d distribution, preferred for bunch rotation, was introduced in [1]. The equivalent deflecting field E_d is defined by transverse components of RF field as:

$$E_d = E_x - \beta Z_0 H_y, \quad Z_0 = \sqrt{\frac{\mu_0}{\epsilon_0}}, \tag{1}$$

where β is the relative velocity of particles. The reasons for the transverse emittance growth during bunch rotation are the aberrations - the nonlinear additives in the E_d distribution, which take place due to non relativistic energy of particles, additions from higher multipole modes and the higher spatial harmonics in the distribution of the dipole deflecting field. The analysis of the deflecting field distributionwas performed [2] using the basis of hybrid waves HE and HM [3].

* paramono@inr.ru

Both for travelling wave and standing wave DS operations, the deflecting field distribution can be represented [2] as an equivalent travelling wave. The main attention should be drawn to the higher spatial harmonics in E_d distribution [2, 4].

To estimate the level of higher spatial harmonics in E_d distribution and as a criterion for DS shape optimization parameters $\delta\psi_j(z)$ and Ψ_j at the DS axis are introduced:

$$\delta\psi_d(z) = \psi_d(z) + \frac{\Theta_0 z}{d}, \quad \Psi_d = max(|\delta\psi_d(z)|), \tag{2}$$

in the physical sense as the deviation and the maximal deviation in phase of the equivalent travelling wave E_d distribution from the synchronous harmonic. Here Θ_0 is the operating phase advance, d is the DS period length and $\psi_d(z)$ is the phase distribution for the equivalent travelling E_d wave. During bunch deflection or bunch rotation, the central particle in the bunch sees the field:

$$E_{def}(z) = E_{d0} cos(\psi_d(z)) \sim E_{d0}(1 - \frac{\Psi_d^2}{2}), \tag{3}$$
$$E_{rot}(z) = E_{d0} sin(\psi_d(z)) \sim E_{d0}\Psi_d,$$

where E_{d0} is the deflecting field amplitude. With DS shape optimization we can change the ratio $\frac{E_x}{Z_0 H_y}$ in E_d distribution, Eq. 1. Minimizing Ψ_d we keep the bunch close to the DS axis, where the nonlinear field of higher spatial harmonics is not large. Simultaneously the level of higher spatial harmonics in E_d will be reduced - the spatial harmonics in E_x compensate the spatial harmonics in $Z_0 H_y$. As a result, we have in orders smaller transverse emittance growth during bunch rotation [4].

For conventional DSs [3] Ψ_d minimization is an additional limitation and can be achieved only at the expense of reduction in the effective shunt impedance value Z_e. To combine the requirements for high RF efficiency and high field quality we need more freedom in the structure design. Based on promising parameters of the DS with a 'TE-like' operating mode [5] a decoupled DS was proposed with separated control on the RF efficiency and on the field quality. Possible solutions with decoupled DS are introduced in [6]. Later on the decoupled DS was investigated and optimized more thoroughly, showing very high rates in RF efficiency together with high field quality. A variety of possible attractive combinations in parameters of the developed DSs is described in [7].

CAVITY DESIGN PARAMETERS

For implementation in the deflecting cavity for diagnostics of longitudinal particles distribution in the REGAE (Rela-

Content from this work may be used under the terms of the CC BY 3.0 licence (© 2018). Any distribution of this work must maintain attribution to the author(s), title of the work, publisher, and DOI.

ISBN: 978-3-95450-194-6 ISSN: 2226-0366 doi:10.18429/JACoW-LINAC2018-THPO080

DESIGN VALIDATION OF A CHOPPING AND DEFLECTING SYSTEM FOR THE HIGH CURRENT INJECTOR AT IUAC

Sanjay Kumar Kedia[1, 2*], Rajeev Mehta[1], Rajesh Kumar[1], Rajeev Ahuja[1]
[1]Inter-University Accelerator Centre, Aruna Asaf Ali Marg, New Delhi-110067
[2]Department of Physics, Indian Institute of Technology Delhi, New Delhi-110016

Abstract

A chopping and deflecting system (CDS) has been designed and developed to provide the chopped beam with various repetition rates to the experimental facilities at the Inter-University Accelerator Centre (IUAC). The CDS consists of four pairs of deflecting plates with increasing gap from 15 mm to 21 mm to provide the maximum effective electric field and to achieve the maximum current within the same voltage conditions. The design of CDS has been validated with various simulation codes including CST MWS, Solid Works, Python and TRACE 3D etc. The deflecting plates, bushes and spacer have been fabricated and assembled within the accuracy of 100 microns. The mechanical measurements were carried out using a slip gauge and Coordinate Measuring Machine. A high vacuum chamber has been designed and developed to incorporate the entire inner assembly. The whole assembly has been installed in the high vacuum chamber and aligned using theodolite. The assembly has been leak tested using helium leak detector in the range of $1x10^{-9}$ mbar.liter/sec. The electrical design of CDS has been validated by installing and testing in the Low Energy Ion Beam Facility (LEIBF) at IUAC. A slit has been introduced to cut the undesired particles, and a beam profile monitor and Faraday cup has been installed to measure the amount of deflection and beam current respectively. The DC voltage has been applied across the four pairs of deflecting plates and amount of deflection was measured accordingly. The design, development, and DC beam test will be discussed in the article.

INTRODUCTION

The accelerator-based experimental facilities at the Inter-University Accelerator Centre (IUAC) depend on the 15 UD Pelletron [1] accelerator and the niobium superconducting quarter wave resonator based superconducting linear accelerator operating (SC-LINAC) at 97 MHz [2]. The ion beams delivered by Pelletron accelerator can be used directly for the experiments or injected into the superconducting linear accelerator for further energy gain. An alternative injector was felt to be necessary due to the limitation of the existing Pelletron accelerator. The High Current Injector (HCI) [3] accelerator has been designed to overcome the limitation of the existing Pelletron accelerator and to provide the high current with varieties of the ion species including inert gases etc. which are not feasible with the existing 15 UD Pelletron accelerator. The HCI was proposed as an alternative injector to the SC-LINAC, and the current Pelletron accelerator will serve as a standalone facility.

The HCI consists of various normal conducting RF cavities including Radio Frequency Quadrupole [4], Six IH type Drift Tube Linear Accelerator [5], Spiral Buncher [6] and low beta cavity. The nuclear physics experimental facilities at IUAC require a clean pulsed beam without dark current at various repetition rates. A requirement of a chopper and deflector was found to be necessary to provide a chopped beam with multiple repetition rates to the IUAC experimental facilities. The LEBT section was found to be the most suitable section for CDS since it needs lower voltage to deflect the undesired charged particles. Due to space constraint, both chopper and travelling wave deflector (TWD) has to combine, and a single device has been designed called chopping and deflecting system [7]. The CDS has been designed within 220 mm space along the beam direction (see Fig. 1).

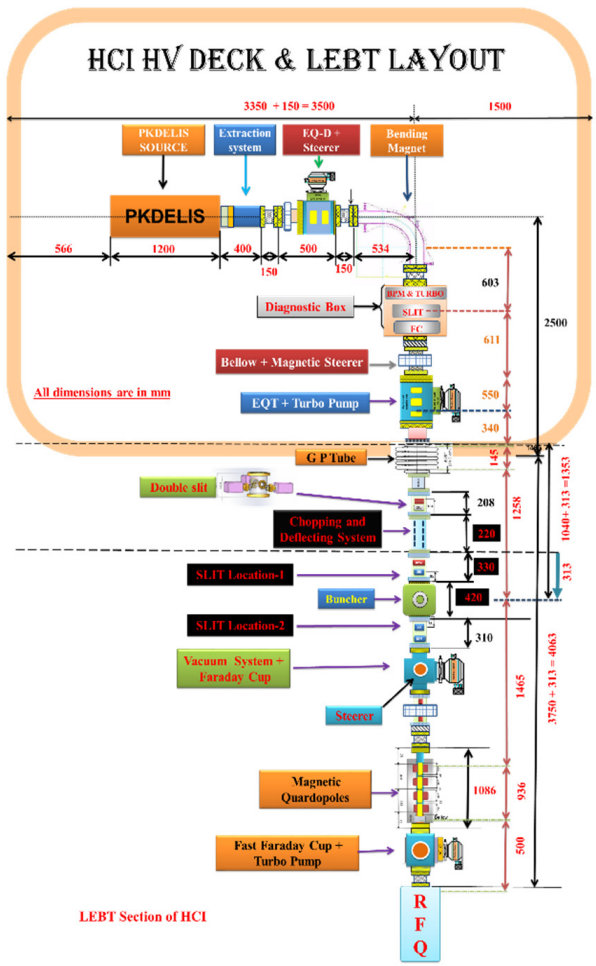


Figure 1: The location of CDS has been depicted in the layout of the LEBT section of the High Current Injector.

Content from this work may be used under the terms of the CC BY 3.0 licence (© 2018). Any distribution of this work must maintain attribution to the author(s), title of the work, publisher, and DOI.

ISBN: 978-3-95450-194-6 ISSN: 2226-0366 doi:10.18429/JACoW-LINAC2018-THPO082

PHYSICAL DESIGN OF A RECTANGULAR RF-DEFLECTOR FOR ULTRA-SHORT BUNCH LENGTH MEASUREMENT*

J. Bai, Q. Chen, K. Fan†, State Key Laboratory of Advanced Electromagnetic and Technology, Huazhong University of Science and Technology (HUST), [430074] Wuhan, China

Abstract

Cylindrical deflectors which are now widely used for bunch length measurement suffer from the degeneration of polarization, while rectangular deflectors can separate polarization mode easily. This paper is focused on the study of a one-cell rectangular deflector, which is considerably different from cylindrical structure or multi-cell structure. A one-cell structure is free of π mode restriction and can achieve higher deflection efficiency per unit length. The proposed scheme is expected to achieve time resolution better than 200fs with the driving power less than 1MW. Cavity optimization and beam dynamic simulation are introduced in this paper.

INTRODUCTION

The linac-based terahertz free-electron laser (THz-FEL) facility with an independent tunable cavity (ITC) RF gun built in Huazhong University of Science and Technology (HUST) has undergone a long term beam commissioning [1]. One important reason is that there is no adequate beam diagnostic instruments due to the ultra-compact structure. In FEL, bunch length that defines the peak current is a critical parameter for the amplification process, but we still have not had an effective method to measure it accurately. Using RF deflector is an attractive method to measure bunch length in sub-picosecond level, while conventional cylindrical cavities suffer from degeneration of polarization due to their axial symmetry [2]. So we propose to use a rectangular structure with an aspect ratio not equal to 1. For 10 MeV electron beams and 1 MW driving power, the rectangular RF deflector system is targeted to be shorter than 1 m and is supposed to achieve time resolution better than 200 fs.

THEORY OF RF-DEFLECTOR SYSTEM

An RF-deflector imparts a transverse momentum on the bunch and directly relates the longitudinal bunch distribution into transverse one. The bunch length can then be inferred after measuring the downstream beam profile. According to the Panofsky-Wenzel theorem [3], the deflecting voltage is:

$$V_d = \int_h [E_\perp + (v \times B)_\perp] dz \,. \qquad (1)$$

Where h is cavity length along the beam direction (z-axis).

Considering a simple case in which there is only a drift between the deflector and the downstream screen, the bunch length can be computed as:

$$\sigma_t = \frac{p_z c}{q V_d L \omega} \sqrt{\sigma_{ys}^2 - \sigma_{yso}^2} \,. \qquad (2)$$

Where p_z is the longitudinal momentum of the electron bunch, L is the drift distance from the center of the RF-deflector to the downstream screen, c is the velocity of the light, σ_{ys} and σ_{yso} are the beam size on the screen with the deflector on and off, respectively. Temporal resolution σ_{t_res} is defined as:

$$\sigma_{t_res} = \frac{p_z c}{q V_d L \omega} \sigma_{ys0} \,. \qquad (3)$$

For a specific electron beam and power source, higher deflecting voltage will result in better time resolution [4] The goal of the cavity design optimization is to find a cell geometry to maximize the deflecting voltage.

OPTIMIZATION OF THE CELL GEOMETRY

For the TM_{120} mode, there is no transverse electric field. According to Eq. (1), the analytical form of V_d can be expressed by,

$$V_d = \sqrt{\frac{2PQ\omega\varepsilon}{a^3 b h}} \frac{8\pi\mu_0 c}{k_c^3} \sin(\frac{\omega h}{2v_z}) \,. \qquad (4)$$

Where a and b are the horizontal and vertical dimensions of the cavity, P is the power loss on the inner wall, Q is the quality factor of the cavity in TM_{120} mode, ε is the dielectric constant, k_c is the wave number, v_z is the particle velocity along the z axis. Eq. (4) is assumed as the basis for optimizing the cavity in this paper.

As for a rectangular cavity operated in the TM_{120} mode, the quality factor is determined by its geometry:

$$Q = \frac{2}{\delta} \frac{\int_v |H^2| dv}{\oint_s |H_\tau^2| ds} = \frac{1}{\delta} \frac{abh(a^2 + 4b^2)}{a^3(b+2h) + 4b^3(a+2h)} \,. \qquad (5)$$

Where δ is the skin depth, H_τ is the tangential magnetic field of the cavity surface.

According to Eq. (5), Eq. (4) can be re-written as:

$$V_d = A \sqrt{\frac{(a^2 + 4b^2)}{a^5(b+2h) + 4a^2 b^3 (a+2h)}} \sin(\frac{\omega h}{2v_z}) \,. \qquad (6)$$

* Work supported by the National Natural Science Foundation of China (No. 11705062) and the China Postdoctoral Science Foundation (No. 2018T110763).
† Email address: kjfan@hust.edu.cn

Content from this work may be used under the terms of the CC BY 3.0 licence (© 2018). Any distribution of this work must maintain attribution to the author(s), title of the work, publisher, and DOI.

ISBN: 978-3-95450-194-6 ISSN: 2226-0366 doi:10.18429/JACoW-LINAC2018-THPO083

TRANSVERSE DEFLECTING CAVITY FOR LONGITUDINAL BEAM DIAGNOSTICS AT bERLinPro

G. Kourkafas*, T. Kamps, A. Neumann, Helmholtz-Zentrum Berlin, Berlin, Germany
B. Keune, RI Research Instruments GmbH, Bergisch Gladbach, Germany

Abstract

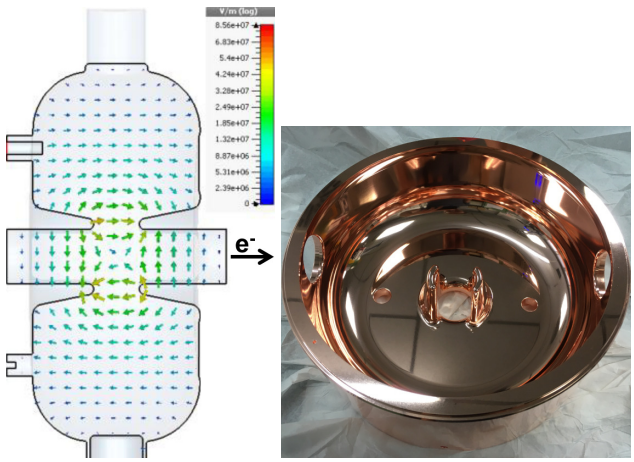
The Berlin Energy Recovery Linac Prototype (bERLinPro) at Helmholtz Zentrum Berlin (HZB) aims to deliver a continuous-wave electron beam of high average current (100 mA) and brilliance (normalized emittance below 1 mm·mrad). The achievement of these ambitious goals necessitates a thorough determination of the bunch parameters after the first acceleration stages, namely the photoinjector and the succeeding booster module. For the measurement of primarily the bunch duration and subsequently the longitudinal phase space and transverse slice emittance, a single-cell 1.3-GHz TM110-like mode vertically deflecting cavity was manufactured by RI Research Instruments GmbH, following the respective design developed for the Cornell ERL injector. This article summarizes the design parameters, manufacturing procedure and testing of this pulsed RF resonator, together with the expected temporal measurement resolution for the nominal beam energies at the initial acceleration stages of bERLinPro.

MOTIVATION AND DESIGN

A new Energy Recovery Linac (ERL) is being constructed at Helmholtz Zentrum Berlin (HZB) under the name Berlin Energy Recovery Linac Prototype (bERLinPro). The goal of this project is to develop the ERL operation principle towards user-oriented applications. The design of bERLinPro is that of a single-pass electron ERL which utilizes superconducting radiofrequency (SRF) technology to deliver a continuous-wave operation of high average current (100 mA) and brilliance (normalized emittance below 1 mm·mrad) [1]. The longitudinal beam properties at the initial acceleration stages (up to 6.5 MeV kinetic energy) will be diagnosed by a transverse deflecting cavity (TCAV).

A TCAV offers a straightforward way of measuring the electron bunch duration, or even the complete longitudinal phase space when combined with a spectrometer dipole, as well as the transverse slice emittance with the help of a quadrupole magnet [2]. It consists of an RF resonator operated in the TM_{110} mode (Fig. 1a), which when phased properly, transversely deflects the head and tail of the bunch in opposite directions. As a result, the longitudinal plane is projected into the transverse after some drift. Due to the damage threshold of the projection viewscreens, TCAV will be operated only in a special diagnostics mode of bERLinPro with reduced repetition rate which allows up to 0.5 μA average current. When passive, the cavity will not interfere with high beam currents as long as it is detuned from its resonant frequency (up to 75 mA demonstrated at Cornell ERL [3]).

The design of the cavity followed closely the one developed for the Cornell ERL injector, due to the resemblance of requirements for both applications [4]. In short, this design features a single-cell copper RF resonator with a transverse impedance of more than 5 MΩ and a resonance frequency of 1.3 GHz, tunable by a motorized plunger. Necessary adjustments were made to accommodate the available interfaces of HZB (Fig. 2): a) coaxial power feedthrough with 50 Ω matched impedance, 100 W average power rating and 2.7 kV_{rms} tolerance, b) coaxial 50 Ω RF pickup coupled at -51 dB to the input power, providing a mW signal level after cable attenuation (-13dB) at nominal operation, c) UHV-compatible linear stage for the adjustment of the plunger position up to ±25 mm, positioned at the bottom of the structure for improved particulate-free conditions, d) ion getter pump at the top of the structure.



(a) Electric field map. (b) Pot of TCAV after machining.

Figure 1: Inner contour of TCAV. Protrusion cones improve the vertical impedance and orientation of the dipole mode.

Two cavities were manufactured by RI Research Instruments GmbH according to these specifications. The manufacturing procedure, the results of the RF and vacuum testing and conditioning as well as the estimated resolution of the e-beam measurements at bERLinPro are described below.

CAVITY MANUFACTURING

The most significant adjustment from the original Cornell configuration was building the cavity out of two pieces, namely pot and lid, instead of two lids and a center ring. This increased the manufacturing precision, while minimizing the process time and risk. Each cavity part was milled from

* georgios.kourkafas@helmholtz-berlin.de

Content from this work may be used under the terms of the CC BY 3.0 licence (© 2018). Any distribution of this work must maintain attribution to the author(s), title of the work, publisher, and DOI.

ISBN: 978-3-95450-194-6 ISSN: 2226-0366 doi:10.18429/JACoW-LINAC2018-THPO084

BPM TIME OF FLIGHT MEASUREMENTS FOR SETTING-UP THE RF CAVITIES OF THE CERN LINAC4

M. Bozzolan†, CERN, 1211 Geneva 23, Switzerland

Abstract

The newly constructed H- LINAC4 at CERN has recently completed its first extended reliability run. It is equipped with Beam Position Monitors (BPMs) based on shorted-stripline pick-up electrodes to measure both position and Time of Flight (ToF). The ToF, in turn used to calculate the kinetic energy of the beam, is determined through signal phase shift measurements between pairs of BPMs. ToF measurements are performed by scanning of the phase of the RF injected into the cavities to find the nominal RF settings for optimal beam acceleration. This paper focuses on the technical aspects of the ToF measurement as well as on the results obtained during beam commissioning and their comparison with beam dynamics simulations.

INTRODUCTION

At the restart of the CERN accelerator complex in 2020, following a long shutdown (LS2), the CERN LINAC4 will be the first stage in the LHC injector chain for protons, replacing the ageing LINAC2. It is a normal conducting 80 m long H- LINAC which will supply beam pulses up to 600 μs long with an initial peak current of 25 mA, later to be increased to 40 mA [1].

The nominal output energy of 160 MeV is reached after a sequence of RF cavities, which include a Radio Frequency Quadrupole (RFQ), 3 Drift Tube Linac Tanks (DTL), 7 Cell Coupled DTL modules (CCDTL) and 12 Pi-mode Structures (PIMS) operating at f_{RF}=352.2 MHz

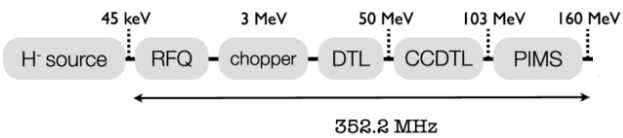


Figure 1: LINAC 4 accelerating structure – not to scale.

There are 15 BPMs installed inside the LINAC between the DTL (12 MeV) and the last PIMS module (see Fig. 1) and another 27 in the transfer line which connects LINAC4 with the PS booster [2].

Each BPM stripline electrode is directly connected to a 50—Ω cable, with lengths of the order of 100 m. These feeds the first analog stage of the acquisition system located in the instrumentation rack outside the tunnel, where the signals are amplified, downconverted to an intermediate frequency (IF) of 22.0125 MHz, filtered and digitized individually.

A ToF-based beam energy measurement is performed by measuring the time delay of the beam between two BPMs in a drift space (Fig. 2). As the distance between BPMs *L* is known the kinetic energy of the beam can be calculated by mean of the relativistic formulas

$$\beta = \frac{L}{TOF \cdot c}$$

$$E_{KIN} = \frac{m_0 \cdot c^2}{\sqrt{1-\beta^2}} - m_0 \cdot c^2$$

The electrode output signal, bandpass filtered at the LINAC bunching frequency f_{RF}, for the two BPM locations can be written as

$$y_{BPM1}(t) = A_1(t) * \sin(\omega_{RF} * t + \varphi_1)$$

$$y_{BPM2}(t) = A_2(t) * \sin(\omega_{RF} * t + \varphi_2)$$

Bunch shape, and therefore the amplitude modulation *A(t)* is not conserved, so a calculation of the time delay by cross correlation is not an option and only phase shift Δφ is used.

Since the phase wrap around every 360 °, we know only the fractional part **δ** of the ToF

$$TOF = NT + \delta = \frac{1}{f_{RF}}\left(N + \frac{\Delta\varphi}{360°}\right)$$

while the integer number *N* of RF periods (i.e. the number of bunches between the two BPMs) cannot be measured.

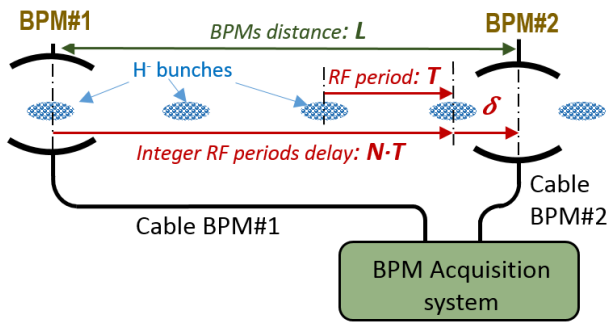


Figure 2: ToF principle.

PHASE MEASUREMENT & CALIBRATION

The sampling clocks at 4 times the IF frequency are phase locked to the linac RF, so that amplitude and phase of the signals can be recovered as

$$A = \sqrt{I^2 + Q^2}$$

$$\varphi = arctg\left(\frac{Q}{I}\right)$$

where I and Q are two consecutive samples.

For an operational system a precise phase (and amplitude for position measurement) calibration is needed

† michele.bozzolan@cern.ch

Content from this work may be used under the terms of the CC BY 3.0 licence (© 2018). Any distribution of this work must maintain attribution to the author(s), title of the work, publisher, and DOI.

ISBN: 978-3-95450-194-6 ISSN: 2226-0366 doi:10.18429/JACoW-LINAC2018-THPO086

BEAM LOSS AND AVERAGE BEAM CURRENT MEASUREMENTS USING A CWCT

F. Stulle*, H. Bayle, J. Bergoz, T. Delaviere, L. Dupuy
Bergoz Instrumentation, Saint Genis Pouilly, France
P. Forck, M. Witthaus, GSI Helmholtzzentrum für Schwerionenforschung, Darmstadt, Germany
D. Vandeplassche, Belgian Nuclear Research Centre SCK-CEN, Mol, Belgium
J. Wu, Institute of Modern Physics, Chinese Academy of Sciences, Lanzhou, China

Abstract

The CWCT is a novel instrument adapted to an accurate average current determination of bunched CW beams or macro pulses. By combining a high-droop current transformer with novel electronics for signal analysis, an output signal bandwidth of DC to about 500 kHz and a current resolution down to the micro-ampere level are achieved. Beam current fluctuations are followed within microseconds, permitting fast detection of beam loss. These characteristics render the CWCT an ideal instrument for HPPAs, for example ADS linacs, and other proton or ion accelerators. We present the CWCT principle and the CWCT performance achieved in beam experiments at UNILAC, GSI.

INTRODUCTION

New trends in accelerators are driven by the society to better and faster serve its needs in medicine, energy and materials studies:

- Accelerators for proton-hadron therapy and medical isotopes production,
- High-power proton accelerators (HPPA) for accelerator driven systems (ADS), e.g. nuclear waste transmutation or subcritical reactors, and spallation neutron sources (SNS),
- Accelerators for materials studies.

Additional background information can be found in [1].

These accelerators, initially developed to produce macropulses at low repetition rate, began to evolve towards CW beam accelerators, which hinders the use of ACCTs and introduces beam instrumentation challenges interfering with the use of DCCTs:

- Beam power damages equipment, rendering fast loss detection mandatory.
- Temperature variations are large.
- In low to medium energy sections, magnetic stray-fields are high due to compact designs.
- Space for instrumentation is scarce.

Moreover, longitudinal bunch profiles vary during the energy ramp further complicating average current measurements and accurate beam loss detection.

In response, Bergoz Instrumentation developed a novel system for average beam current measurements. It consists of a current transformer (CWCT) and analog electronics (BCM-CW-E) to process the CWCT's output signal. CWCT and BCM-CW-E are an alternative to ACCTs and DCCTs, well suited in many cases where those cannot be used.

Their characteristics were optimized for CW proton and ion accelerators, e.g. the injectors of the China ADS project [2] or the MYRRHA ADS project [3]. Though they can be used for macropulse measurements and in other types of accelerators. Table 1 summarizes CWCT and BCM-CW-E design specifications. Fig. 1 shows photographs.

Table 1: CWCT and BCM-RF-E Design Specifications

Bunch repetition rate	50 MHz … 500 MHz
Current measurement range	10 µA ... 200 mA
Reaction time (full bandwidth)	1 µs (10% ... 90%)
Output noise (10 kHz bandwidth)	1 µArms
Output noise (100 Hz bandwidth)	0.5 µArms
Output voltage (in 1 MΩ)	–4 V ... +4 V
Controlled via TTL or USB	

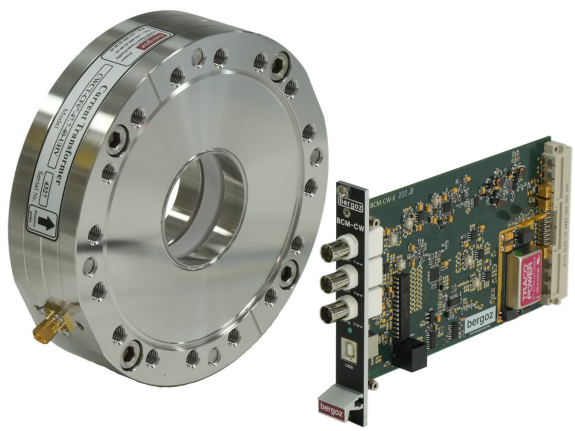


Figure 1: CWCT and BCM-CW-E.

CWCT and BCM-CW-E electronics were installed at UNILAC, GSI [4] for beam measurements. UNILAC can accelerate a wide variety of ions at different charge states up to several MeV/u kinetic energy. It is capable of fast switching between two different ion sources and sets of accelerator parameters. Like this, changing the macropulse current and its position as well as changing length and width of the individual pulses could be done with little impact on other beam users.

CWCT / BCM-CW-E PRINCIPLE

Passive current transformers (CT) are only capable of measuring AC currents down to a certain minimum

* stulle@bergoz.com

Content from this work may be used under the terms of the CC BY 3.0 licence (© 2018). Any distribution of this work must maintain attribution to the author(s), title of the work, publisher, and DOI.

ISBN: 978-3-95450-194-6 ISSN: 2226-0366 doi:10.18429/JACoW-LINAC2018-THPO090

THE ANALYSIS OF MODULES FAILURE IN SOLID-STATE AMPLIFIER FOR HIGH CURRENT RFQ

Liepeng Sun#, Longbo Shi, Guirong Huang, Xianbo Xu,
Chenxing Li, Liang Lu, Aimin Shi, Yuan He, Hongwei Zhao
Institute of Modern Physics, Chinese Academy of Sciences, Lanzhou 730000, China

Abstract

The new RF system of Radio Frequency Quadrupole accelerator (RFQ) in ADS project at IMP was upgraded in the beginning of 2017, the original tetrode amplifier was replaced by two new solid-state amplifiers (SSA) for proton acceleration, they are the same 80kW rated power to combine at least 120kW inside the cavity through two uniform couplers. But for SSA, since too many power modules were set on the amplitude and phase for power combination, one or some damaged circulator (including sink loads) may lead to high risk of whole RF system fail. Especially, according to experiments and simulation, when the transmission line between two different level combiners meets a specific condition, the scattering parameter of system would have a great fluctuation, even cut-off, if some problems happen in circulators or sink loads. In this paper, the simulated methods aiming at simulating the multi-level synthetic amplifying were introduced in detail, the failure analysis and related experiments focusing on amplifying links of SSA under the special circumstances was also presented simultaneously.

INTRODUCTION

Since the old 200kW tetrode amplifier was operated in high current beam without a circulator, two new SSAs was considered to replace it on site due to their specialties of stable, sustainable and reliable, whose cavity operates in 162.5MHz, the dissipated power reaches up to approximate 90kW, and especially, the beam power has also 21kW while 10mA beam current was applied [1]. thus, some special technologies of new generation SSA were developed for this kind of high intensity accelerator in BBEF, such as two types of reflection power experiments on module including long-term continuous wave power and four times pulsed power. Due to too high power, the design of power module and combiner need to be considered the scattering parameters in the situation of mismatch resulting from the multi-port balance [2].



Figure 1: The four-vane RFQ cavity with two couplers.

sunlp@impcas.ac.cn

SSA MODULES FAILURE

In our case, over 120 power modules are integrated through several level synthesizers for full power output, which shows in Fig. 1, and every module can provide maximum 850W RF power for 80kW power output even when one pre-amplifier fails. Last June, 19 power modules were burned at the same time, within them, almost all power transistors, circulators and sink loads (connected directly with the circulators) were damaged on the same time only to be replaced. When failure happened, the power values was recorded from many directional couplers in the screen of control system, the specific values were presented in Fig. 2.

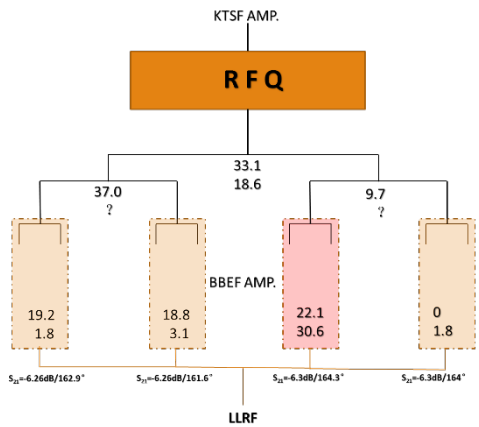


Figure 2: The screenshot of failure situation.

From it, our SSA was consisted of four 20kW sections to integrate gradually for providing 50 or 60kW RF power (without beam or 10mA beam) for separate coupler simultaneously. And after basic analysis and check on the machine, one most possible reason for accident should be too sensitive of driving signal interlock in 3# section comparing other three sections, the input signal of 3# section was shut down suddenly because of abnormal interlock during the operation, other three sections were influenced to increase rapidly power at that time due to LLRF close loop on the amplitude modulation. Furthermore, the weird location of all injured modules indicate that some inappropriate RF configuration need to be removed and optimized.

In this dangerous situation, more than half transistors, circulators and sink loads in 3# section were burnt severely. However, it is very difficult to explain clearly the phenomenon which the broken modules are all belong to 3# section, especially on the left side.

Content from this work may be used under the terms of the CC BY 3.0 licence (© 2018). Any distribution of this work must maintain attribution to the author(s), title of the work, publisher, and DOI.

ISBN: 978-3-95450-194-6 ISSN: 2226-0366 doi:10.18429/JACoW-LINAC2018-THPO091

90 kW SOLID-STATE RF AMPLIFIER WITH A TE011-MODE CAVITY POWER-COMBINER AT 476 MHz

Yuji Otake†, Takao Asaka and Takahiro Inagaki, RIKEN SPring-8 Center, RIKEN, 1-1-1 Kouto, Sayo-cho, Sayo-gun, Hyogo, Japan
Hiroto Yamada, Tsuneyuki Okuyama, Kenji Nagatsuka, Shuichi Aizawa, Kazuyuki Sato, Nihon koshuha Co., Ltd, 1119 Nakayama-cho, Midori-ku, Yokohama, Japan

Abstract

Solid-state rf amplifiers, which have long lifetimes and small failures, are the recent trend as reliable and stable high-power rf sources for particle accelerators. Hence, we designed a 90kW solid-state amplifier with an extreme low-loss TE011 mode cavity (Q0=100,000) power-combiner operated at 476 MHz and a 50 us pulse width. Developing this amplifier is for replacement of an IOT rf amplifier, at the X-ray free-electron laser, SACLA. In SACLA, highly RF phase and amplitude stabilities of less than 0.02 deg and 10^{-4} in rms are necessary in order to obtain stable lasing within a 10 % intensity fluctuation. The amplifier comprises a drive amplifier, a reentrant cavity rf power divider, 100 final amplifiers with a 1 kW output each and a TE011 mode cavity combiner. Water-cooling with precise temperature regulation at 10 mK and a DC power supply with a noise of less than -100 dBV at 10 Hz for the amplifier are necessary in order to realize the previously mentioned stabilities. Based on the test results of the amplifier, the above-mentioned specifications with the extreme low-loss are confirmed. The amplifier also allows us to operate in pulsed and CW rfs for linacs and ring accelerators.

INTRODUCTION

Medium-power rf sources comprising vacuum tubes, such as triodes, tetrodes [1] and an induction output tube (IOT, klystrodes) [2] based on the traditional rf technology, usually drive acceleration cavities for proton and injectors. These medium rf-output powers are form 10 kW to 100 kW, if it is compared with the output power of a high-power klystron over mega-watts. In the case of an X-ray free-electron laser (XFEL), SACLA [3], a 476 MHz IOT having a 100 kW rf-output power with a 50 μs pulse width is unexceptionally used to drive a booster cavity, which accelerates an electron beam up to 1 MeV [4]. We recently decided to replace from our IOT to a solid-state amplifier, since the IOT had some troubles, such as the end of its lifetime, shortage of its supply.The reference [5], which mentions the design of this amplifier, describes the detail reason of the replacement.

Based on the design concept described in the reference [5], we developed a 90 kW, 476MHz rf solid-state amplifier with a pulse width of 50 μs using a field effect transistor (FET) with a 1 kW output each [6]. Therefore, this amplifier used these 100 FETs in order to generate 90 kW. Furthermore, because of this FET could work in a continuous wave (CW) mode, we also aimed for diverting this amplifier to ring accelerator rf sources. This CW operation mode is one of the development concepts [5]. Concerning use of this amplifier as the CW rf source, an extreme low-loss rf cavity combiner using a TE011 resonant mode (Q0=100,000) was employed. Since the rf combing loss exactly corresponded to many of the output power of the FETs, in order to reduce the costs of the solid-state amplifier, reducing loss by an rf-combining method is important. The intended combing loss of the rf power combiner including the loses of rf connectors and cables is 0.1 dB [5]. On the other hand, since SACLA is going to use this amplifier, ultra-stable rf-output is also indispensable feature in order to realize stable XFEL intensity [3]. Highly rf phase and amplitude stabilities of less than 10^{-4} and 0.02 deg. in rms are necessary for stable lasing within a 10 % intensity fluctuation. An ultra-low noise DC power supply technique for realizing the rf stability already established in SACLA [7] is also needed. Realization of the 90 KW, 476 MHz amplifier had great possibility in the design stage in order to obtain the demanded XFEL intensity stability, since, in the design stage, we already obtained a 1kW rf output of the final amplifier module [5]. Furthermore, because of environmental temperature change largely affected the rf phase and amplitude changes of the amplifier, counter measures in order to reduce the temperature change are crucial. Hence, to employ a precise temperature controller originally developed for SACLA [8] having a temperature regulation within 10 mK is a big candidate. In addition to the above-mentioned requirements, because the SACLA building did not have a sufficient-big space for installing the amplifier instead of the IOT, the compactness of the amplifier was also important.

We have finally built a 90 kW, 476 MHz pulse solid-state amplifier with an extreme low-loss rf-power combining method using a TE011 mode rf-cavity. In this paper, we describe the test results and the final characteristics of the amplifier.

CONFIGURATION OF AMPLIFIER

In this summer, we finished to build the 100 kW, 476 MHz pulse solid-state amplifier. Table 1 tablets the specifications of the amplifier. Figure 1 shows electrical configuration of the amplifier using the FET described in Table 2. The amplifier comprises a 20 W amplifier in order to drive the final stage amplifier modules through a re-entrant type cavity power divider. Following the driving amplifier, there are 100 final stage amplifier modules

† email address otake@spring8.or.jp

Content from this work may be used under the terms of the CC BY 3.0 licence (© 2018). Any distribution of this work must maintain attribution to the author(s), title of the work, publisher, and DOI.

ISBN: 978-3-95450-194-6 ISSN: 2226-0366 doi:10.18429/JACoW-LINAC2018-THPO092

LCLS II FUNDAMENTAL POWER COUPLER MANUFACTURING STATUS AND LESSONS LEARNED

S. Sierra†, C. Lievin, I. Yao Leclerc, THALES, Vélizy, France
G. Garcin, G. Vignette, THALES, Thonon les Bains, France
M. Knaak, M. Pekeler, R.I. Research Instruments Gmbh, Bergisch Gladbach, Germany

Abstract

Thales and RI Research Instrument have manufactured and assembled half of the Power Couplers for the LCLSII Project,. This paper remains main characteristics of these couplers, main challenges overcomed and among them thickness of copper coating on Warm Internal Conductor (WIC) at 150 µm. It also proposes some possible optimization for a future mass production and parameters which could be relevant for a better understanding link to statistic results obtained from this production and the one from XFEL production.

MAIN CHARACTERISTICS AND COUPLERS DESCRIPTION

The design of these couplers (Fig. 1) is an adaptation of the TTF3/XFEL Fundamental Power Coupler (FPC) [1].

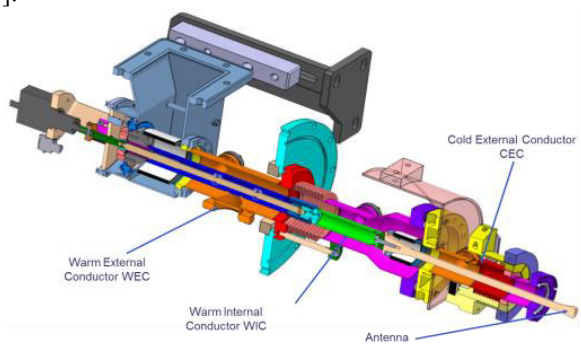


Figure 1: General Layout of the Coupler.

Main parameters of the coupler are:
- RF frequency: 1.3 GHz
- Power up to 7 kW CW
- Tuning: ± 10 mm
- Two ceramics windows

Main modifications in respect to the XFEL/TTF3 design are:
- Antenna profile in order to be adapted to the cavities performances
- Copper coating thickness of the WIC defined at a thickness of 150 µm, compared to 30 µm for E-XFEL, in order to avoid too large temperature heating when operating at full power of 7 kW.
- Residual Gas Analysis (RGA) is made during baking operation at 150°C.

† serge.sierra@thalesgroup.com

MANUFACTURING

Main metallic sub-assemblies: Warm External Conductor (WEC), Warm Internal Conductor (WIC), Cold External Conductor (CEC) and antenna (Fig. 2) were manufactured and copper coated at Thonon factory then sent to RI factory. Ceramics are TiN coated and then the coupler is assembled by Electron Beam Welding (EBW) at RI factory.

After cleaning and assembly on the test stand, they are sent to JLAB/Fermilab for integration on cryomodules.



Figure 2: CEC, Antenna and WEC.

Overview on Manufacturing Difficulties:

Due to the XFEL manufacturing experience [2] (where more than 670 couplers were manufactured at a rate up to more than 10 couplers a week) there were not a lot of difficulties for the manufacturing of LCLSII FPC.

The copper plating process is the trickiest step for the coupler manufacturing which also have been developed during XFEL production except for the WIC where the thickness of 150 µm had been obtained. During the manufacturing of all couplers, check of coating thickness (Fig. 3) and Residual Resistivity Ratio (RRR) have been done

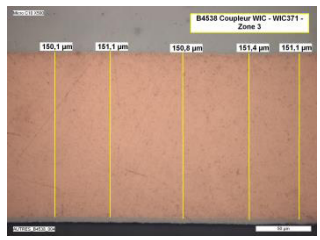


Figure 3: Example on Copper Coating Measurement

This was done also statistically on parts of main components (Figs. 4 and 5).

Content from this work may be used under the terms of the CC BY 3.0 licence (© 2018). Any distribution of this work must maintain attribution to the author(s), title of the work, publisher, and DOI.

ISBN: 978-3-95450-194-6 ISSN: 2226-0366 doi:10.18429/JACoW-LINAC2018-THPO093

STATUS AND RESULTS OBTAINED ON A RF CONDITIONING TEST BENCH FOR 704 MHz COUPLERS IN THE FRAME OF ESS PROJECT

S. Sierra†, Y. Amal, C. Lievin, I. Yao Leclerc, THALES, Vélizy, France
M. Chahbazian, J.De Oliviera, A. Goeury, L. Nenning, S. Petitjean,
GERAC Thales, Le Barp, France

Abstract

Thales and GERAC are developing a test bench able to make the RF conditioning of the Fundamental Power Couplers at 704 MHz in the frame of the ESS project for CEA. The status of the development of the test bench is described, including the modulator, klystron and all relative equipment. We describe also the results obtained at this date.

OVERVIEW OF THE TEST BENCH

The RF test bench consists of a fully integrated power station including:

- RF power station,
- High power modulator,
- A 1.5 MW klystron TH2182A at 704 MHz,
- Interlocks and acquisition system
- RF power network including High power circulator.

KLYSTRON

The TH2182A klystron has been designed to comply with ESS specification [1]. Main characteristics of the klystron are:

- Built-in electromagnet (water cooled)
- Built-in X-ray shielding (easily removable)
- Built-in oil tank with heater transformer
- Diode gun
- 6 cavities with 3rd one on second harmonic
- Coaxial window and cross-bar coax to waveguide transition
- Low cathode loading
- Low DC gradient on beam forming electrode

The 3D model (Fig. 1) shows the disposition of klystrons sub-assemblies, from the diode gun to the collector.

This Klystron has been design with a low beam perveance of 0.6 $\mu A/V^{1.5}$ generated by a diode gun, at an operating point of 108 kV and 21.4 A. In order to have a safe value at the operating point, the electrical gradient on the beam forming electrode remains below 4.7 kV/mm. Due to the large cathode size, the cathode loading is low (< 2A/mm²), with low temperature cathode for a long lifetime, more than 100.000 hours and low Barium evaporation rate.

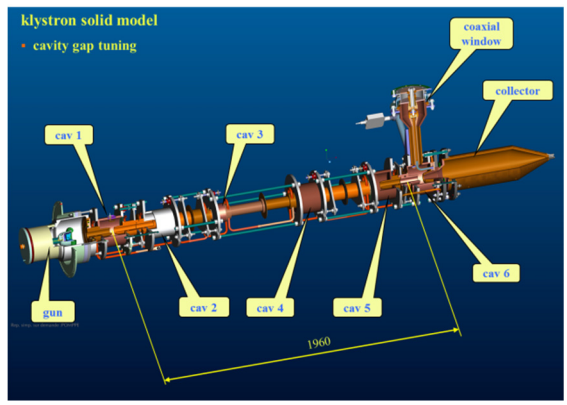


Figure 1: klystron.

The klystron is mounted in a built-in electromagnet water cooled (Fig. 2) composed of 14 independent coils on a supporting frame which allow to install X-ray shielding which could be easily removed.



Figure 2: assembly of the Klystron.

MODULATOR

Modulator is composed of an AC/DC power supply charging the capacitor bank up to 2 kV. Then RF converters at 25 kHz allow setting the pulse shape at the primary of pulse transformers. At the secondary of these pulse transformers, addition of redressed voltages allows to give the desired voltage and current to the Klystron (Fig. 3).

† serge.sierra@thalesgroup.com

Content from this work may be used under the terms of the CC BY 3.0 licence (© 2018). Any distribution of this work must maintain attribution to the author(s), title of the work, publisher, and DOI.

ISBN: 978-3-95450-194-6 ISSN: 2226-0366 doi:10.18429/JACoW-LINAC2018-THPO095

PRESENT STATUS OF CAPACITOR-CHARGING POWER SUPPLIES FOR KLYSTRON MODULATORS IN SuperKEKB INJECTOR LINAC

M. Kawamura†, M. Akemoto, H. Nakajima, T. Natsui, T. Shidara, S. Fukuda, H. Honma,
S Michizono, KEK, 305-0801 Tsukuba, Japan
O. Endo, H. Akikawa, K. Sato, Nihon Koshuha Co., Ltd., 226-0011 Yokohama, Japan

Abstract

Capacitor charging power supplies (CCPSs) have been used in compact klystron modulators. Two main types of CCPSs, the normal model and highly precise model, have been developed by Nihon Koshuha Co. in collaboration with KEK since JFY2012. In the KEK, regarding the output voltage stability of normal model, almost the same characteristic as the specification 0.2 %p-p was measured. After some repairs for the discharge problems, the CCPSs in the SuperKEKB injector linac were operated without important breakdown for about 6,000 h from autumn in 2017 to summer in 2018.

INTRODUCTION

The SuperKEKB injector linac has delivered electrons and positrons for particle physics and photon science experiments since 1982 [1]. At present, 59 S-band (2856 MHz) klystrons are used as RF sources in the injector.

One klystron modulator supplies pulsed high-power to one klystron. All klystron modulators have pulse-forming networks (PFNs). Thirteen compact klystron modulators [2-5] and 46 conventional klystron modulators [6] are now used. Regarding the charging method of PFN capacitors, compact modulator is a switching charging type using a capacitor-charging power supply (CCPS) [2-5,7-11], and conventional modulator is the resonant charging type. Further, the former is almost 1/3 the size of the latter.

Compact modulators and CCPSs have been developed since JFY2002 [3-5]. At first, the CCPSs were developed by Toshiba Electro-Wave Products Co. [3-5,7], and since JFY2012, they have been mainly developed by Nihon Koshuha Co. (NIKOHA) [8-11], in collaboration with KEK.

This article describes the present status of the CCPSs developed by NIKOHA. It includes the specifications, the difference between the normal model and the highly precise one, the measured results, and operation conditions in KEK.

OUTLINE OF NIKOHA CCPS

At present, 18 normal model CCPSs, two highly precise models and one exclusive model for the flux concentrator modulator [12] have been developed [11].

Figure 1 shows the outward appearances of the normal model and highly precise model, and Table 1 shows their specifications [8-11].

† masato.kawamura@kek.jp



Figure 1: Outward appearances of the normal model (left) and highly precise model (right) of Nikoha CCPSs [11].

Figure 2 shows the schematic diagram of the 30 kJ/s normal model [8]. The normal model consists of three sections; the rectifier section,

Table 1: Specifications of the normal model and highly precise model of Nikoha CCPSs (for 0.62 μF load)

	Normal [8]	Highly Precise [9]
Input voltage	AC 420V±5% (3-phase)	
Charging power	30 kJ/s	35 kJ/s (Main: 30 kJ/s, Sub: 5kJ/s)
Output voltage	43 kV	
Average output current	1.6 A	1.8 A (Main:1.6 A, Sub:0.2 A)
Repetition rate	50 pps	50 pps
Output voltage stability	0.2 %p-p (at 43 kV)	0.03 %p-p (at 43 kV)
Efficiency	More than 80%	
Cooling	Water 5 L/min.	Water 5 L/min. (Main) Air (Sub)
Size (mm^3)	480×760×680	480×760×980

inverter section, and HV section.

The rectifier section converts 3-phase 420 V AC input to 600 V DC output. The inverter section is an IGBT-switched 20 kHz inverter, and it is constructed by two se-

Content from this work may be used under the terms of the CC BY 3.0 licence (© 2018). Any distribution of this work must maintain attribution to the author(s), title of the work, publisher, and DOI.

ISBN: 978-3-95450-194-6 ISSN: 2226-0366 doi:10.18429/JACoW-LINAC2018-THPO096

DESIGN STUDY OF A HIGH EFFICIENCY KLYSTRON FOR SuperKEKB LINAC

F. Qiu, S. Fukuda, S. Matsumoto, T. Matsumoto, T. Miura, T. Natsui
Accelerator Laboratory, KEK, Tsukuba, Japan

Abstract

The injector linear accelerator (linac) for the SuperKEKB particle accelerator requires a higher efficiency klystron than the currently used 50 MW, S-band, pulsed unit (PV3050/E3730), which operates at the same voltage, to increase the power redundancy. The efficiency is expected to improve from the currently observed 45% to more than 60%. We propose a type of high efficiency klystron using novel bunching mechanisms. The 1-D disk model based code is used for preliminary optimization of the tube parameters; these parameters are further checked by 2-D codes known as field charge interaction (FCI) and MAGIC. In this paper, the design consideration of the high efficiency klystron is presented.

INTRODUCTION

The KEKB electron–positron (e-/e+) collider is being upgraded to the SuperKEKB to achieve a 40-times higher luminosity [1]. As shown in Fig. 1, the linac consists of eight sectors (A–C and 1–5). The black squares in each sector represent the accelerating units that provide an energy gain of approximately 160 MeV each [1-2]. A total of 60 accelerating units are mounted in the SuperKEKB injector.

The klystron drive line for each unit is shown in Figure 2 (left). The low-level radio frequency (LLRF) system generates 4 μs RF pulses at first, and the phase of the RF pulse is reversed by 180° during the last 1 μs. The RF pulse is then amplified by the 600 W solid state amplifier (SSA). In the next step, the output of the SSA drives an S-band 50 MW klystron (PV3050/E3730A). A SLAC energy doubler (SLED) compresses the 4 μs pulse from the klystron output and generates a shorter 1 μs pulse with high peak power, thus powering four 2-m accelerating structures with an accelerating field of 21 MV/m. The picture and specifications of the klystron PV3050 are shown in Figure 2 (right) and Table 1, respectively [3].

High efficiency klystrons have become popular in recent years owing to their benefits of reducing the operating costs of the accelerators as well as increasing the operating margins. In cooperation with MELCO (Mitsubishi Electric Corporation), KEK has a plan to develop a type of high efficiency klystron (PV3064) to replace the current PV3050 tubes [4]. Several methods have been proposed to increase the efficiency of a klystron. These methods can be divided into two main categories: The first kind is a multi-beam klystron (MBK) which has several low perveance beam-lets because lower perveance usually corresponding to higher efficiency [5]. Each beamlet carries a small amount of current, but the total current can be large. The other kind focuses on novel bunching mechanisms. Based on this idea, the core oscillation method (COM) [6], bunching-alignment-collection (BAC) [7], and core stabilization method (CSM) [8] are proposed. It would be useful if we can develop a compatible tube of the existing PV3050 with minor modifications by following the recent trends in efficiency improvement. These techniques can also be extended to other projects such as the international linear collider (ILC). In this paper, based on the existing PV3050, we present a compatible BAC-based tube. To achieve higher efficiency, the cavity parameters are first optimized, and the focusing magnet and tube length are modified slightly. The RF window would need to be redesigned because of the increment in the output power; however, this is not considered in the current work.

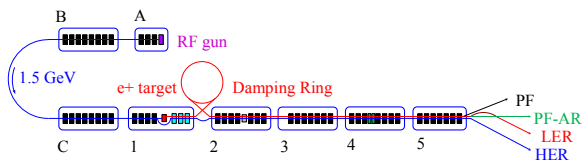


Figure 1: Layout of SuperKEKB injector linac.

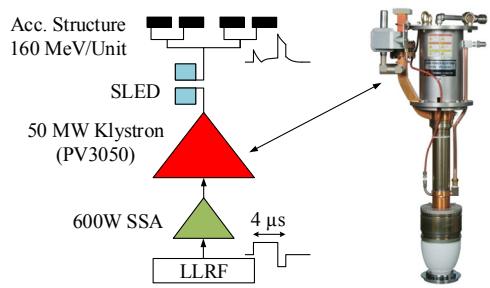


Figure 2: Klystron drive line (left), and the 50 MV klystron PV3050 (right).

Table 1: Specifications of PV3050

	Value	Unit
Frequency	2856	MHz
Peak RF power	50	MW
Repetition rate	50	Hz
Efficiency	45	%
RF pulse duration	4	μs
Beam voltage	310	kV
Gain	50	dB

Content from this work may be used under the terms of the CC BY 3.0 licence (© 2018). Any distribution of this work must maintain attribution to the author(s), title of the work, publisher, and DOI.

ISBN: 978-3-95450-194-6 ISSN: 2226-0366 doi:10.18429/JACoW-LINAC2018-THPO097

RECENT RESULTS FOR STUDY OF CERAMIC AND COPPER PLATING FOR POWER COUPLERS

Y. Yamamoto†, E. Kako, S. Michizono, KEK, Tsukuba, Japan
Y. Okii, Nomura plating Co., Ltd., Osaka, Japan
E. Cenni, F. Aurelien, IRFU/CEA, Gif-sur-Yvette Cedex, France

Abstract

KEK has conducted a survey to select an optimum ceramic after withdrawal by a domestic manufacturing company two years ago. For this selection, there are four important items on the properties of ceramic; that is, relative permittivity, dielectric loss tangent, surface and volume resistance, and secondary electron emission coefficient. For measurements of these parameters, ten kinds of ceramic samples supplied from five companies were measured using three kinds of measurement systems. For measurement of secondary electron emission, scanning electron microscope (SEM) with beam blanking system was used. On the other hand, residual resistivity ratio (RRR) for copper plating, which is the most important item for quality control, has also been carried out by collaboration with KEK-CEA. In this report, the recent results for these studies will be presented in detailed.

INTRODUCTION

In the E-XFEL, ESS, LCLS-II, etc. which have been constructed (or under construction) in recent years, several hundred superconducting cavities are used, and the quality control of the power coupler has become important. In particular, the manufacturing cost of copper plating covering the inner surface of the power coupler, ceramics used for RF windows, and titanium nitride coating (TiN coating) deposited on the surface of ceramic is also a large proportion of cost, which are the main items for this R&D. R&D for power coupler is also included in the framework of cost reduction R&D for the International Linear Collider (ILC) concluded between KEK and the US Fermi National Laboratory (FNAL) in 2017. Currently, various investigations and studies under the cooperation with affiliated companies, are being advanced at KEK [1].

SURVEY AND RESEARCH ON COPPER PLATING

The quality control of copper plating is an item which became a problem frequently also in E-XFEL [2], which is still an important matter in the other projects under construction. The quality control is generally evaluated by RRR measurement. RRR measurement has been carried out in KEK/COI by using small refrigerator with conduction cooling method. Figure 1 shows the measurement system (upper) including the small cryostat in the COI building in KEK, and the stage (lower) for placing the sample. Four samples can be mounted at the same time and can be measured with different electric current values (for example, three stages such as 1 mA, 10 mA, 100 mA). The electric current is bi-directionally loaded and the average resistance value is calculated. After the preliminary tests, the optimum electric current value was found to be 1 to 10 mA. And, the optimum sample size is fixed to 150 mm x 5 mm x 0.5 mm, because this system uses the conduction cooling method, and too large sample cannot be cooled.

As a way of evaluating the RRR of the copper plating, after measuring the resistance to a copper plating sample, the copper plating is peeled off and returned to the base material SUS316L, and resistance measurement is performed again. As the final step, by estimating with the ratio of the two measured values of room temperature and low temperature, the net RRR for copper plating is obtained. With respect to the SUS316L material, it is not necessary to peel off for all the copper plating samples in order to take almost the same resistance values.

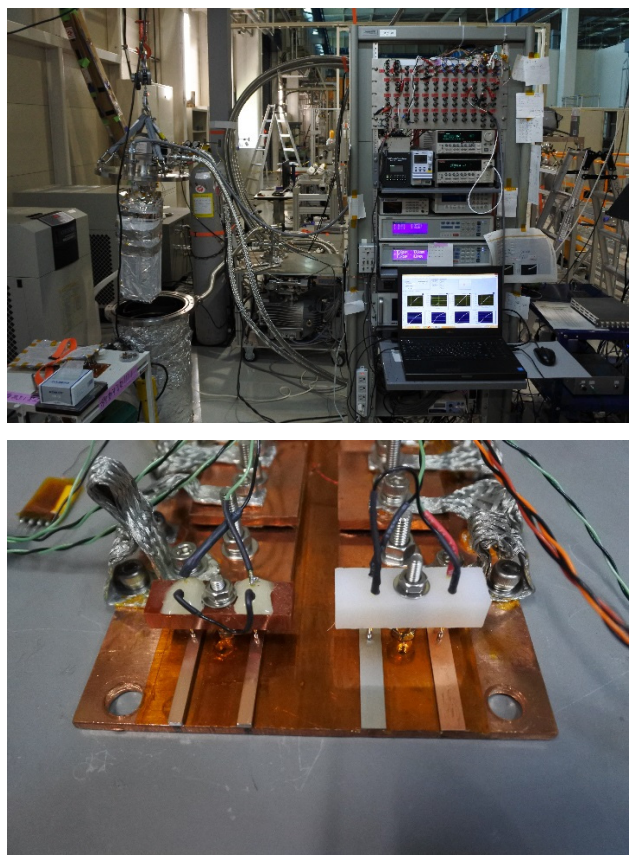


Figure 1: Residual Resistivity Ratio (RRR) measurement system (top) and four samples on the stage (bottom) in KEK/COI.

† yasuchika.yamamoto@kek.jp

Content from this work may be used under the terms of the CC BY 3.0 licence (© 2018). Any distribution of this work must maintain attribution to the author(s), title of the work, publisher, and DOI.

ISBN: 978-3-95450-194-6 ISSN: 2226-0366 doi:10.18429/JACoW-LINAC2018-THPO100

DEVELOPMENT OF A 1.5GHz HIGH-POWER CW MAGNETRON FOR SRF ACCELERATOR

Li Wenliang[1], Liu Youchun[2], Sun Lingbin[2], Zhou Bowen[1], Zhang Pengjiao[1], Ke Yijing[1], Zhao Lei[3], Hou Rui[3], Li Junzhou[3], Zhang Liping[3], Sun An[1,3]
[1]PLAI, Nanjing University, Nanjing 210046, China
[2]Nanjing Sanle Electronic Information Industry Group Co., Ltd., Nanjing 211899, China
[3]Andesun Technology Group Co., Ltd., Nanjing 210046, China

Abstract

An 1.5 GHz, 13.5 KW CW high-power magnetron for a superconducting RF accelerator has been developed by Andesun Technology Group Co., Ltd. with Nanjing Sanle Electronic Information Industry Group Co., Ltd., in order to replace the klystron, that could reduce the power source cost to about one-third. The cavity, output power antenna and coupling door-nob have been optimized by using CST Studio. Testing results have shown that the resonance frequency and output power have met the requirements, and the efficiency of the magnetron is higher that 78.45%.

INTRODUCTION

At present, the microwave energy of the RF superconducting accelerator is mainly provided by the klystron internationally. However, the klystron as a microwave source is characterized by low efficiency and high cost, which increases operating costs of the entire accelerator system. So the magnetron with a cost of one-third of the klystron is the best choice for the replacement of the original SRF accelerator microwave source. In order to meet the urgent need of microwave sources for SRF accelerator, a 1.5 GHz、13.5 kW CW magnetron for SRF accelerator is researched and developed by Andesun Technology Group Co., Ltd. with Nanjing Sanle Electronic Information Industry Group Co., Ltd.

The development of this magnetron is based on the 2450 MHz magnetron. First, the frequency of magnetron is reduced from 2450 MHz to 1500 MHz by increasing the radius of the cavity and so on. The CST Studio is used to optimize the coupling output part of the magnetron and gets the best parameter of the coupled antenna [1]. The electronic simulation of the magnetron is completed by the Particle-in-cell solver, which gains a general understanding of the performance of the magnetron [2]. The prototype measurement shows that the output power of the magnetron reached the requirement, the whole tube efficiency is 78.45%, and the tuning range is 10 MHz.

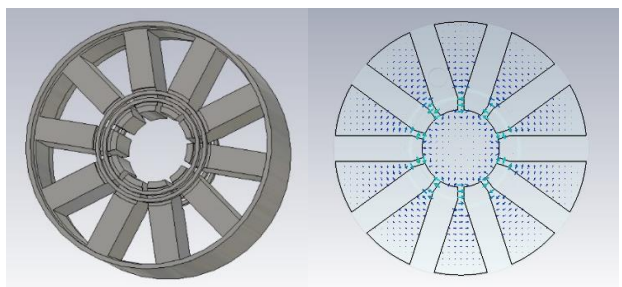
DESIGN OF THE MAGNETRON

According to the working parameters of the SRF accelerator, the performance parameters of this magnetron are as follows:

(1) Working frequency: 1.5 GHz
(2) Average output power: 13.5 kW
(3) Peak power: 17 kW
(4) Efficiency: ≥70%
(5) VSWR: ＜1.4
(6) Way of working: CW

Cavity Design

The anode cavity of the magnetron adopts a fan-slot type co-cavity resonance system with a diaphragm belt. A total of 10 cavities were used and the blade-to-slot ratio is 3.01. Figure 1 shows the simulation model and the electric field distribution of the π mode which is the magnetron operating mode. Cavity simulation with strips gains that the mode separation is 84.6%.



(a) (b)

Figure 1: (a) The simulation model. (b) The electric field distribution of the π mode.

Output Structure Design

The magnetron uses an axial energy extraction device. The design of the excitation cavity is based on the WR-650 standard waveguide. The semi-cylindrical short-circuit surface is used, and the output part of the antenna is designed as a bullet type. The parameters of the bullet antenna are decided by simulation with the excitation cavity. The simulation result shows that the S_{11} curve is lower than -70 dB at 1.5 GHz and lower than -40 dB within 20 MHz bandwidth. Figure 2 shows the simulation curve of S_{11}. Figures 3 shows the finished excitation chamber and output coupling antenna.

Content from this work may be used under the terms of the CC BY 3.0 licence (© 2018). Any distribution of this work must maintain attribution to the author(s), title of the work, publisher, and DOI.

ISBN: 978-3-95450-194-6 ISSN: 2226-0366 doi:10.18429/JACoW-LINAC2018-THPO102

DESIGN STUDIES OF OUTPUT WINDOW FOR CEPC KLYSTRON

Z. J. Lu[1,2,4], S. Fukuda[1,3],Z. S. Zhou[1,4], S. C. Wang[1,4], O. Z. Xiao[1,4], Zaib-un-Nisa[1,4], G. X. Pei[1,4], Y.L.Chi[1,4]

[1]Institute of High Energy Physics, Chinese Academy of Sciences, Beijing 100049, China
[2]University of Chinese Academy of Sciences, Beijing 100049, China
[3]High Energy Accelerator Research Organization (KEK), Tsukuba 305-0801, Japan
[4]Key Laboratory of Particle Acceleration Physics and Technology, Institute of High Energy Physics, Chinese Academy of Sciences, Beijing 100049, China

Abstract

A high power and high efficiency klystron for the Circular Electron Positron Collider (CEPC) is developed at IHEP. This paper presents the design and simulation for a high-power coaxial window of the 650MHz, 800kW CW klystron, and the coupler design for high power test of window are also included. CST, ANSYS and Multipac 2.1 are used for design of window microwave performance, thermal analysis and multipacting effect. The simulation results of the coaxial window S-parameter analysis, shows a low reflection at the desire frequency of 650 MHz after optimized. The E-field and thermal simulation shown a good temperature distribution and maximum temperature has been found to be 36 Celsius degree at ceramic with water cooling in the inner and outer conductor. And the multipacting simulation for the window shows that multipacting has less chance to occur on the surface of ceramic.

INTRODUCTION

The Institute of High Energy Physics (IHEP), Chinese Academy of Sciences (CAS), has proposed a future plan of Circular Electron-Positron Collider (CEPC), which will be the biggest electron-positron collider in the world. Klystron is a critical component for an operation of accelerator. As RF power sources, more than 200 high efficiency klystrons with a frequency of 650 MHz and CW 800 kW output power are required. Those klystrons are designed at IHEP and the first prototype klystron is going to manufacture in China. The specifications of CEPC klystron are listed at Table 1 [1], we aim at more than 65 percent of the efficiency for the first klystron and more than 80 percent for the future plan to reduce the operation cost.

Table 1: CEPC Klystron Design Parameters

Frequency(MHz)	650
Output Power(kW)	800
Beam Voltage(kV)	81.5
Beam Current(A)	15.1
Efficiency (%)	>65

For successful operation of CEPC, the stable operation of klystrons is crucial, and an output window used in the klystron is one of the key components. Output window is a critical part of transmitting high RF power from klystron vacuum side to the external atmosphere, therefore a low power dissipation and no breakdown is important for window.

We had made a strategy to manufacture a reusable klystron with two steps or more as shown in Fig. 1. Before build the tube, the window itself must be manufactured and evaluated by using the existing RF power source to ensure the power handling capability.

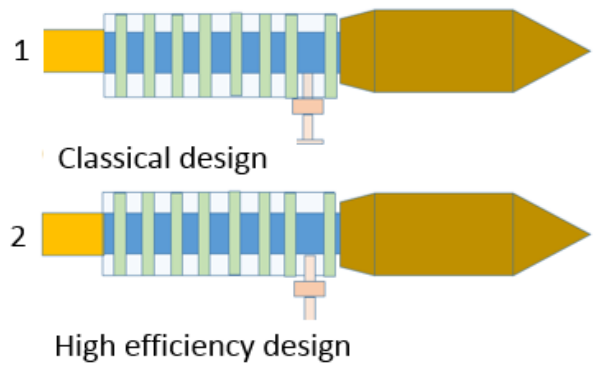


Figure 1: Klystron development strategy.

WINDOW DESIGN

WR1500 (381 mm×190.5 mm) waveguide is used to transmit 650 MHz RF power from klystron to accelerator, but it is difficult to use the pill-box window with rectangular waveguide to the klystron output cavity because of its big size. The pill-box window has a difficulty in cooling the center of ceramic so the high temperature may cause a high thermal stress that possibly may cause ceramic window breakdown.

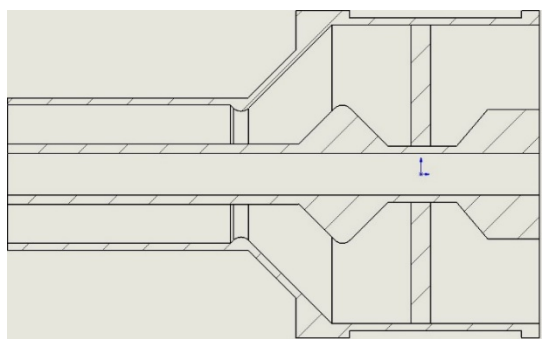


Figure 2: Schematic drawing of CEPC klystron output window.

Content from this work may be used under the terms of the CC BY 3.0 licence (© 2018). Any distribution of this work must maintain attribution to the author(s), title of the work, publisher, and DOI.

ISBN: 978-3-95450-194-6 ISSN: 2226-0366 doi:10.18429/JACoW-LINAC2018-THPO103

APPLICATION OF SOLID STATE AMPLIFIERS IN ADS PROJECT AT IHEP*

O. Z. Xiao†, 1,2), Z. S. Zhou1,2), X. P. Ma1,2), N. Gan1,2), Y. L. Chi1,2)
1) Institute of High Energy Physics, Chinese Academy of Sciences, Beijing 100049, China
2) Key Laboratory of Particle Acceleration Physics and Technology, Institute of High Energy Physics, Chinese Academy of Sciences, Beijing 100049, China

Abstract

The solid state amplifier is an important part of the RF power source system of ADS project at IHEP. Three kinds of solid state amplifier with different power and frequency have been applied. In this paper, the specifications of solid state amplifier are presented. In addition, the principle of breakdown of power modules during the high power test of coupler are analyzed.

INTRODUCTION

With the progress of transistor technology, the output power and efficiency of a single transistor has been greatly improved. The high power can be obtained by combination of numerous transistors. Recently the power capability of solid state amplifier (SSA) can extend from a few kW to several hundred kW, and the operating frequency from less than 100 MHz to above several GHz[1 - 4]. Compared with vacuum tube, there are many advantages for SSA such as high reliability for redundancy design, high flexibility for module design, high stability, absence of warm-up time and reasonable efficiency [5]. So the SSA is a priority RF power source for injector I of accelerator driven subcritical transmutation system (ADS). Three kinds of solid state amplifier with different power and frequency have been used to feed the cavities or test high power coupler in injector I of ADS at institute of high energy and physics (IHEP), whose performance and detailed parameters are presented in this paper.

325 MHz/10 kW SSA

The 325 MHz/10 kW SSA is used to feed bunchers and spoke cavities of injector I of ADS. The one cavity per source is chosen to simplify the LLRF control and RF distribution system. The bandwidth of SSA needs more than 2 MHz for LLRF control requirement. The nominal maximum power of 10 kW is achieved with less than 1 dB compression, and the harmonic output power is less than -30 dBc. The AC to RF efficiency goal for the SSA at the rated power is at least 50%. The single power module must include circulator and absorbing load to ensure isolation between modules and withstand the full reflection power. Each SSA must monitor the status data of every power module such as voltage, current and temperature. Ethernet port is required to communicate with control system. Also, interlock is necessary for external faults like water leaks. The mean time between failures (MTBF) should be larger than 20,000 hours, and less than 5% of the power modules fail per year. The failure of one power module can still run. The output port is 3-1/8 inch rigid coaxial line. The 325 MHz/10 kW SSA specifications are shown in Table 1.

In July 2012, the first 325 MHz/10 kW SSA was delivered to IHEP by BBEF, which was used to build a workbench for the high power test of the coupler of spoke cavity. In September 2013, another one was delivered for the horizontal test of spoke cavity. In April 2014, 14 SSAs were installed and commissioned in power supply hall. In 2015, 9 SSAs were put into operation. In March 2016, another two SSAs were delivered by the 38th institute of CETC. In the end of 2016, 16 325 MHz/10 kW SSAs were used in injector I, as shown in Fig. 1.

Table 1: 325 MHz/10 kW SSA Specifications

Parameters	Value
Frequency(MHz)	325
Output Power(kW)	10
Gain(dB)	≥65
Bandwidth(MHz)	≥ 2
Amplitude stability	≤1%
Phase stability	≤1°
Harmonic(dBc)	< -30
Spurious(dBc)	< -65
MTBF(h)	20000
Efficiency at 10 kW	≥50%



Figure 1: 325 MHz/10 kW SSA.

* Work supported by ADS Injector I solid state RF power system
† email address xiaooz@ihep.ac.cn

Content from this work may be used under the terms of the CC BY 3.0 licence (© 2018). Any distribution of this work must maintain attribution to the author(s), title of the work, publisher, and DOI.

ISBN: 978-3-95450-194-6 ISSN: 2226-0366 doi:10.18429/JACoW-LINAC2018-THPO104

DEVELOPMENT OF 150.4MHz CW SOLID-STATE AMPLIFIER

Zhao Lei [1], Sun An[2,3], Zhou Bowen[2], Li Wenliang[2], Zhang Pengjiao[2], Ke Yijing[2]
[1]School of Materials Science and Technology, Nanjing University of Aeronautics and Astronautics, Nanjing 211146, China
[2]PLAI, Nanjing University, Nanjing 210046, China
[3]Andesun Technology Group Co., Ltd., Nanjing 210046, China

Abstract

A 150.4MHz to 155.4MHz, 300W continuous wave solid-state amplifier as an accelerator power source has been developed by us. In order to increase the lifetime of MOSFET and meet the requirements of every parameters, Drain voltage and quiescent current is set at a better point with a well-designed heat dissipation structure, we make the solid state amplifier stable in performance. Taking the microwave leakage into account, the chassis structure is optimized and designed, and the microwave absorption device is adopted to make the structure compact, protect other parts not affected by the microwave leakage. After the assembly is completed, the working parameters meet the design requirements very well. The MOSFET flange temperature and output parameters meet the design requirements.

INTRODUCTION

RF power amplifier is a traditional key component in the field of microwave technology. It is an important part of the microwave system and is still in the process of continuous development. Currently solid-state amplifiers are the most active part of microwave power sources. With the development of semiconductors, the development of solid-state amplifiers has entered a new climax [1].

Many years ago, electric vacuum tubes as the microwave source in the accelerator system. They output different energies. We can see in the Table 1 [2].

Table 1: Different Power Device in Common use in Accelerator

Device	Frequent	Mode	Power
Electric vacuum tubes	30~300 MHz	CW and pulse	~2.5 MW
IOT	500~1500 Mhz	CW and pulse	100 kW
Klystron	300~10 GHz	CW and pulse	2 MW
FET		CW and pulse	1250 W

In recent years, solid-state amplifiers are used more and more in accelerator system. Some of them as exciting source to provide incentives to the klystron, some of them as RF sources to the excitation cavity.

In this paper, a high power CW solid-state amplifier is designed for superconducting cavity power source. MOSFET has many advantages such as small size, voltage control, low heat generation and so on, therefore, NXP's MOSFET - MRFE6VP61K25H is selected by us as the core to design the final amplifier module. The 10W small power amplifier module with the gain is 35 dB is used as the boosting stage, combine with the power supply system, the power monitoring system, the cooling system, and the control system, we completed the solid-state amplifier.

CIRCUIT DESIGN

The Overall Circuit Design

The overall principle is shown in Figure 1. The low-power RF signal enters the push-level amplifier module through the input coupler and the RF switch. The push-level module inputs the amplified RF signal to the final amplifier module, and the final output high-power signal is output through the output coupler. The coupler coupling ends are connected to the corresponding power detection module to detect input, output, and reflected power in real time. The signal of detection modules are input to the control system to protect the amplifier modules and display power on the screen. Table 2 shows insertion loss.

Table 2: Insertion Loss in the RF Circuit

Item	Insertion Loss
The coaxial cables of input	0.6 dB;
RF switch	0.4 dB
The coaxial cable between pusher amplifier and final amplifier	0.2 dB
The coaxial cables of output	0.4 dB
Isolator of output	0.4 dB

Considering that the maximum input power is 0dBm, we could calculate and get:

P(the input power of pusher amplifier)≤-1 dBm;
P(the output power of pusher amplifier)≤34 dBm;
P(the input power of final amplifier)≤33.8 dBm.

Content from this work may be used under the terms of the CC BY 3.0 licence (© 2018). Any distribution of this work must maintain attribution to the author(s), title of the work, publisher, and DOI.

ISBN: 978-3-95450-194-6 ISSN: 2226-0366 doi:10.18429/JACoW-LINAC2018-THPO107

HIGH POWER COUPLER R&D FOR SUPERCONDUCTING CH-CAVITIES

J. List*[1], K. Aulenbacher[1,4], W. Barth[1,2], M. Basten[3], M. Busch[3], F. Dziuba[1], V. Gettmann[1], M. Heilmann[2], T. Kürzeder[1], M. Miski-Oglu[1], H. Podlech[3], J. Salvatore[2], A. Schnase[2], M. Schwarz[3], and S. Yaramyshev[2]

[1]HIM, Helmholtzinstitute Mainz, 55099 Mainz, Germany
[2]GSI Helmholtzzentrum, 64291 Darmstadt, Germany
[3]IAP, Goethe-University Frankfurt, 60438 Frankfurt am Main, Germany
[4]IKP, Johannes Gutenberg-University Mainz, 55128 Mainz, Germany

Abstract

The upcoming demands of the future research programs at GSI exceed the technical opportunities of the existing GSI UNIversal Linear ACcelerator (UNILAC). Besides, the existing machine will be exclusively used as an injector for FAIR (Facility for Antiproton and Ion Research) providing high power heavy ion beams at a low repetition rate for injection into a heavy ion synchrotron. A new dedicated superconducting (sc) continuous wave (cw) linac is crucial to keep the GSI research program competitive. The first part of the cw-linac, comprising a 217 MHz multi gap Crossbar-H-mode (CH) cavity surrounded by two sc solenoids inside a cryostat, already served as a prototype demonstrating reliable operability in a realistic accelerator environment. A sufficient high power RF-coupling concept is needed to feed this newly developed cw-RF cavity with up to 5 kW of RF-power in cw-mode. A high power coupler test stand was recently built to provide for a testing environment; further upgrade measures of this test area are foreseen in the next future. This contribution deals with the recent coupler R&D for the demonstrator set up. Besides that simulations of thermal losses at the coupler (inside the RF-cavity) will be shown as well.

INTRODUCTION

The 13 m superconducting continuous wave linac proposed to be built at the GSI, comprises Crossbars-H-mode (CH) RF-cavities, to accelerate heavy ions up to 7.3 MeV/u [1]. The first part of the accelerator, called 'Demonstrator', comprises one CH-cavity and two 9.3 T solenoids in a cryostat. This structure was already successfully tested with beam in summer 2017 [2–4]. It was the first sc CH-cavity in the world running with beam. In the next stage an advanced module consisting of three CH-cavities [5], a rebuncher and two solenoids will be set up for further testing. This module will be the prototype for three following similar modules (Fig. 1) to complete the entire cw-LINAC. Recent beam dynamics studies indicate, that only 2 of the modules need a rebuncher [6]. The heavy ion beam is provided by the GSI - High Charge State injector (HLI).

* j.list@gsi.de

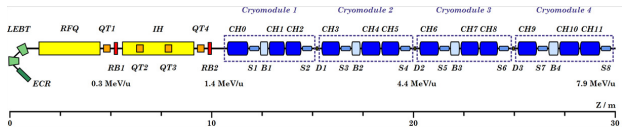


Figure 1: Recent desing of the cw-LINAC at GSI made with four standard cryo modules [7].

HIGH POWER COUPLER FOR CH-CAVITIES

For suitable coupling the RF-cavities are equipped with a capacitive, coaxial power coupler [8]. The design is a modification of an existing Fermilab power coupler [9]. Noteworthy is a diameter jump from a $3\frac{1}{8}''$ rigid line to a CF-40 line since the space at the cavities coupler port is strongly limited. The reflection caused by a parasitic capacitance due to the changing diameters is canceled out by a shift between the diameter jump the of inner and outer conductor, called "gap" (see Fig. 2). The two RF-windows of the coupler are coated with TiN for a lower secondary electron yield.

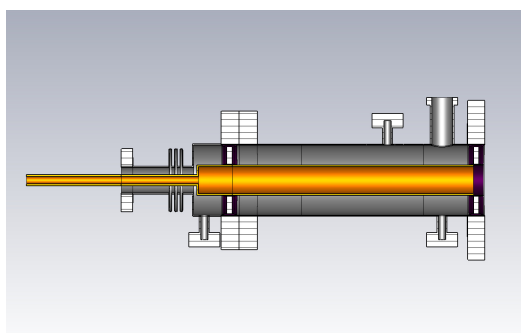


Figure 2: Cross section of the CST Microwave Studio [10] - coupler model.

COUPLER TEST STAND

A coupler test stand was established at GSI, where two couplers can be tested and conditioned in paralell. It features a quarter wave resonator (QWR)-type cavity (see Fig. 3) with an extended center-tube, presented in [11]. It has a broadband RF-transmission of ± 10 MHz. A 5 kW cw solid

Content from this work may be used under the terms of the CC BY 3.0 licence (© 2018). Any distribution of this work must maintain attribution to the author(s), title of the work, publisher, and DOI.

ISBN: 978-3-95450-194-6 ISSN: 2226-0366 doi:10.18429/JACoW-LINAC2018-THPO108

DEVELOPMENT OF AN HIGH GRADIENT SIDE COUPLED CAVITY FOR PROBE

S. Pitman, R. Apsimon, G. Burt, Cockcroft Institute/Lancaster University, Lancaster, UK
W. Wuensch, N. Catalan-Lasheras, A. Grudiev, CERN, Geneva, Switzerland
H. Owen, Cockcroft Institute/University of Manchester, Manchester, UK

The PROBE project aims to develop a high gradient proton accelerator for protons with energies from 250-350 MeV for proton radiography. Detailed studies have shown that the optimum design is a side-coupled cavity at S-band. With an aperture of 8 mm a gradient of 54 MV/m can be obtained with 13 MW of RF power in a 30 cm structure. A prototype cavity has been machined by VDL and will be diffusion bonded by Bodycote. We present initial measurements of the prototype.

INTRODUCTION

The use of proton therapy is increasing with the expected number of centres offering protons reaching over 50 worldwide [1]. The advantage of protons compared to photons is the precision to which the dose can be delivered, providing lower doses to healthy tissue and organs. However to make full use of this precision we need to ensure that we can target the dose with sufficient accuracy, which requires knowledge of the proton stopping power of the imaged patient. Currently patients are imaged using CT scans and the Hounsfield units are converted to proton stopping power, but this method employs approximations limiting the accuracy of the dose placement. Recent studies have shown that using proton CT (pCT) scans can provide better estimates of proton stopping power. The limitation in pCT is that the protons should not be stopped in the patient but rather in the detector, hence this technique is only useful for children or head imaging using a 250 MeV beam. In order to do full-body scanning of adults higher energy protons are required, up to perhaps 330-350 MeV. The PRoton BOosting Extension (PROBE) project aims to provide a linac that can be retrofitted to an existing proton therapy cyclotron, in order to boost the proton energy for pCT. The linac should fit in a 3 meter space based on available space at the Christie Proton Therapy centre.

BEAM TRANSPORT

While the beam current required for pCT is small (~3 pA) compared to treatment, the linac will have a minimum duty cycle meaning the beam losses may still be a concern. For example, one requires 2% beam transmission for a 50 Hz repetition rate and a 5 μs pulse; however, lower transmission or a shorter RF pulse only results in a longer imaging time so is not a strict limit. As the protons will be delivered from a cyclotron the longitudinal and transverse phase space of the input beam is relatively large hence focussing is required to keep the beam losses to 2%. The project specification was to achieve 100 MV in 3 meters of linac length, however as we require focussing between the cavities this implies a higher gradient than 33.3 MV/m. We believe the minimum feasible drift length between two cavities will be around 135 mm, so having a larger number of shorter cavities will have more drift spaces and hence a higher gradient would be required, while with longer cavities it may be difficult to keep the losses on the aperture within limits. In addition we expect losses both on the aperture and on the energy selection system due to the cyclotron proton bunch being significantly longer than the RF period. Hence we set the energy selection system to collimate particles outside ±1% of the desired beam energy. After the first cavity we can select the synchronous phase of subsequent cavities to either provide more gradient or more capture. In this study we choose a synchronous phase of -20 degrees as this gives only a 6% drop in gradient from the peak while capturing almost 14% of the beam.

A study was performed of the maximum gradient reach of a re-entrant standing wave cavity as a function of beam aperture; in reality the requirement for coupling between cells will reduce this but it is a useful starting point. For a given cavity length we reduce the aperture (using an analytical estimate) until we reach 2% transmission; we increase the aperture by a factor 1.3 as a safety factor. We then in CST optimise a single-cell S-band cavity without side coupling for that cavity length and aperture to see the maximum gradient, and compare this to the required gradient using a 10% safety margin. In this study we limit the peak surface electric field to 200 MV/m, the modified Poynting vector to 2 W/sq-μm [2] and the input power to 100 MW for the 3 meter linac, based on scaling results obtained by other groups [3,4].

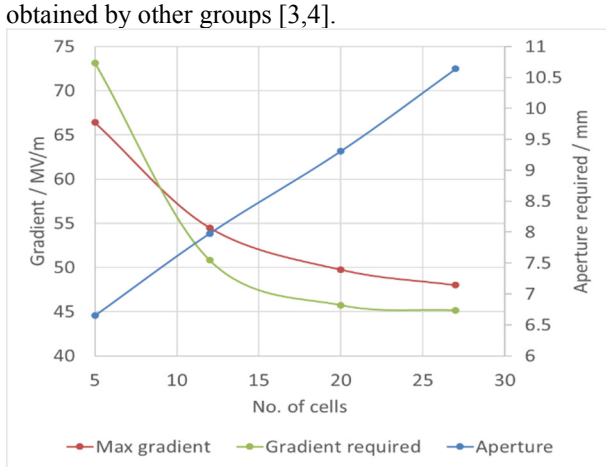


Figure 1: Required and achievable gradients as a function of number of cells per cavity, and the aperture required to meet transmission targets.

Content from this work may be used under the terms of the CC BY 3.0 licence (© 2018). Any distribution of this work must maintain attribution to the author(s), title of the work, publisher, and DOI.

ISBN: 978-3-95450-194-6 ISSN: 2226-0366 doi:10.18429/JACoW-LINAC2018-THPO109

A NEW SPHERICAL PULSE COMPRESSOR WORKING WITH DEGENERATED "WHISPERING GALLERY" MODE*

Z. Li[1], W. Fang[#], Q. Gu, Z. Zhao[†], SINAP, CAS, Shanghai, China
A. Grudiev, CERN, Geneva, Switzerland
[1]also at UCAS, Beijing, China

Abstract

This paper introduces a new design concept of spherical pulse compressor. The main characteristics of this new design can be described as: spherical storage cavity, degenerated "Whispering Gallery" mode and a compact mode launcher.

INTRODUCTION

CLIC is focusing on the Compact Linear Collider. To obtain a relatively high accelerating gradient, CLIC utilizes Pulse Compressors to increase the input power of accelerators. This work is to make an alternative design for CLIC pulse compression scheme. There are several kinds of pulse compressor: SLED, BOC, SLED-II, spherical pulse compressor and so on. Usually, a spherical cavity, including BOC, can offer a higher Q factor compared with a cylindrical cavity. This design utilizes a spherical cavity working with degenerated "Whispering Gallery" mode.

THEORY OF BOC

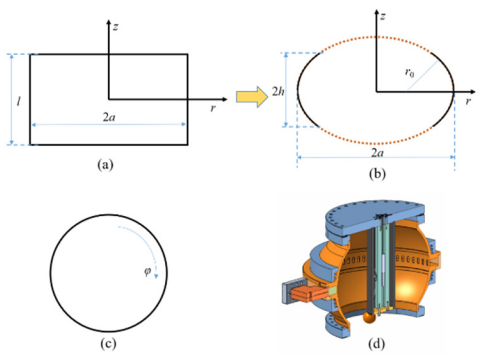


Figure 1: Cylindrical cavity (a), BOC (b), Top-view of BOC (c) and 3D-view of BOC (d).

BOC [1,2] is short for *Barrel-shaped Open Cavity*. This cavity and its theory can be derived from a cylindrical cavity by removing the two ends of a CC (cylindrical cavity) and bending the boundary inside like shown in Fig. 1(a) and Fig. 1(b). The definitions of TE and TM mode in BOC are the same as in CC: z is the longitudinal direction, and φ [Fig. 2(c)] and r are the transverse directions. The definitions of mode indexes m, n, p are also the same as in CC respectively. Fig. 1(d) shows a typical BOC.

The cavity profile of BOC is an ellipse. But it is not a perfect cavity. There's no cavity wall where the red dotted line shows in Fig. 1(b), which indicates the name "Open Cavity". The analytical formula of the ellipse is:

$$\frac{z^2}{ar_0}+\frac{r^2}{a^2}=1, \tag{1}$$

where a is the major axis of the ellipse, and r_0 is the curvature radius.

This kind of cavity shape allows the existence of the modes only those who have large number of azimuthal variations (so called "Whispering Gallery" modes), while the other modes that have weak azimuthal dependence cannot be formed. Because of the reflection of the cavity walls, the electromagnetic field of "Whispering Gallery" mode is concentrated in a relatively small area close to the cavity surface around the equator plane, like shown in Fig. 2.

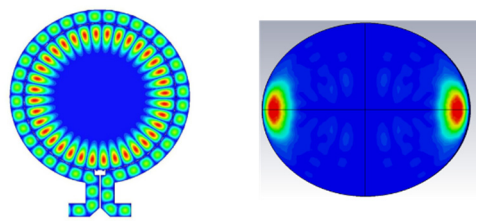


Figure 2: Top-view and side-view of "Whispering Gallery" mode.

According to its field distribution, the "Whispering Gallery" mode is a TM mode. The resonant frequency of a TM mode in BOC is:

$$ka=\upsilon_{mn}+\frac{(p-1/2)\alpha}{\sin\theta}, \tag{2}$$

where k is the wavenumber in the free space, m and p are the azimuthal and longitudinal indexes of the mode, respectively. For TM modes, υ_{mn} is the n-th positive root of Bessel function of order m and its derivative for TE modes. Angle α is defined as: $\sin\alpha=(a/r_0)^{1/2}\sin\theta$, where θ can be calculated from $\cos\theta=m/\upsilon_{mn}$.

For "Whispering Gallery" mode, the indexes n=1, p=1, and m is determined by the required Q factor and the working frequency. The Q factor is:

* Work supported by the National Natural Science Foundation of China (No. 11675249)
fangwencheng@sinap.ac.cn
† zhaozt@sinap.ac.cn

Content from this work may be used under the terms of the CC BY 3.0 licence (© 2018). Any distribution of this work must maintain attribution to the author(s), title of the work, publisher, and DOI.

ISBN: 978-3-95450-194-6 ISSN: 2226-0366 doi:10.18429/JACoW-LINAC2018-THPO111

THE TEST OF RF BREAKDOWNS OF CPHS RFQ

W.B.Ye, S.X.Zheng†, J.R.Shi, C.Cheng, Q.Z.Xing, X.L.Guan, X.W.Wang, Key Laboratory of Particle & Radiation Imaging (Tsinghua University), Ministry of Education, Beijing 100084, China
also at Laboratory for Advanced Radiation Sources and Application, Tsinghua University, Beijing 100084, China
also at Department of Engineering Physics, Tsinghua University, Beijing 100084, China
M.C.Wang, State Key Laboratory of Intense Pulsed Radiation Simulation and Effect (Northwest Institute of Nuclear Technology), Xi'an, 710024, China

Abstract

The high accelerating gradient is significant for a compact linear accelerator, and RF breakdowns is a limitation for the high gradient. This work aims to research RF breakdowns of a 325 MHz proton Radio Frequency Quadrupole (RFQ) accelerator of the Compact Pulsed Hadron Source（CPHS）. The breakdown rate (BDR) of the RFQ has been measured. Breakdown waveforms have been recorded, which have been used for counting breakdown time distribution and analyzing the location of RF breakdowns.

INTRODUCTION

Linear accelerator (linac) is an important component of the wide family of accelerators. Since charged particles pass accelerating structures only once in a linac, high accelerating gradient is significant for a compact linac to achieve high energy. The accelerating gradient of a linac is mainly limited by RF breakdown. Up to now, numerous studies have been conducted to research the mechanism of RF breakdown. However, most of them concern about electron linacs whose frequency is usually GHz [1,2]. There has been very little research on RF breakdown of proton linac with much lower frequency. The purpose of this study is to research RF breakdown of a 325 MHz proton Radio Frequency Quadrupole (RFQ) accelerator.

The Compact Pulsed Hadron Source（CPHS）project at Tsinghua University is a university-based proton accelerator platform for multidisciplinary and proton application. The CPHS accelerator consists of an ECR proton source, a low-energy beam transport line (LEBT), a radio frequency quadrupole (RFQ) and a drift tube linac (DTL). The breakdown test was conducted on RFQ of the CPHS project. The main design parameters of the CPHS RFQ are listed in Table 1 [3].

EXPERIMENTAL SETUP

Figure 1 shows the experimental setup. There have three pickups on RFQ cavity so that we can get the RFQ cavity field signal from these pickups. From the directional coupler, we can get the reflected wave. An oscilloscope is used to record these waveforms. Control system help us record some other parameters, like RF power, pulses width, repetition rate, number of breakdowns, and vacuum of RFQ. During the conditioning and beam commissioning of the RFQ, when an RF breakdown happened, the reflected wave amplitude increased and then the breakdown would be detected and the waveforms would be recorded by the oscilloscope.

Table 1: Main Design Parameters of CPHS RFQ

Parameters	Value
Species	Proton
Type	Four-vane
Frequency	325 MHz
Input beam energy	50 keV
Output beam energy	3.0 MeV
Peak beam current	50 mA
Emittance (norm. rms)	0.2 π mm mrad
Maximum surface field	32.1 MV/m
Pulse length	0.5 ms
Pulse repetition rate	50 Hz
RF peak power	537 kW
Beam duty factor	2.5%

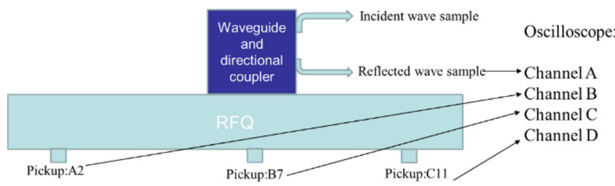


Figure 1: Experimental setup layout.

DATA AND ANALYSIS

Figure 2 is the operation history of CPHS RFQ. The left part and the right of Fig. 2 are corresponding to the conditioning and beam commissioning history of CPHS RFQ respectively. This figure shows the power loss of RFQ and accumulated number of breakdowns with respect to the accumulated number of pulses.

In previous work, CERN has proposed a scaling law to describe the relationship of breakdown rate, accelerating gradient and pulse length for the accelerating structures with very high frequency (usually several GHz) [1]:

$$\frac{E_0^{30}\tau^5}{BDR} = const \quad (1)$$

where E_0 indicates the accelerating gradient (depend on power loss of the structure) and τ the rf pulse length.

† zhengsx@tsinghua.edu.cn

Content from this work may be used under the terms of the CC BY 3.0 licence (© 2018). Any distribution of this work must maintain attribution to the author(s), title of the work, publisher, and DOI.

ISBN: 978-3-95450-194-6 ISSN: 2226-0366 doi:10.18429/JACoW-LINAC2018-THPO113

DESIGN OF 4 AMPERE S-BAND LINAC USING SLOTTED IRIS STRUCTURE FOR HOM DAMPING*

J. Pang†, X. He, S. Chen, Institute of Fluid Physics, CAEP, Mianyang, China
S. Pei, J. Zhang, H. Shi, Institute of High Energy Physics, CAS, Beijing, China

Abstract

An S-band LINAC with the operating frequency of 2856 MHz and beam current of 4 A was designed for flash X-ray radiography for hydrodynamic test. The optimization of the parameters of the LINAC was processed to obtain the minimum beam radius and the maximum energy efficiency. For the purpose of reducing the beam orbits offset at the exit of LINAC, a slotted iris accelerating structure would be employed to suppress the transverse Higher Order Modes (HOMs) by cutting four radial slots in the iris to couple the HOMs to SiC loads. In this paper, we present the design of the LINAC and the results of beam dynamic analysis.

INTRODUCTION

Linear induction accelerators were used in large-size or full-size radiographic hydrodynamic test with dose of hundreds of Rad by accelerating several-kA electron beam to tens of MeV. In addition, small machine, such as pulsed X-ray machine with several hundred kV and anode-pinch diode, was used in small-size hydrodynamic subdivision experiments for dynamic material characteristic study, micro jetting diagnosis, et al. Figure 1 shows a typical layout of flash X-ray radiography system.

In the past twenty years, intense-beam normal conducting RF accelerator has been developed with great achievement due to the development of large collider technology. The CLIC Test Facility, CTF3, has accelerated the beam with current of up to 5A to150MeV with full beam loading [1-2]. The HOM was damped by using slotted iris constant aperture (SICA) accelerating structures. The 100 MeV/100 kW LINAC, constructed by IHEP and used as a driver of a neutron source in KIPT, Ukraine, has accelerated a beam of 2 A to 100 MeV by using detuning accelerating tubes [3-5].

The great progress in intense-beam linac motivates the compact radiographic facility driven by a 4 A 30 MeV linac, which might be utilized for multi-pulse radiographic with the material planar density of several to tens g/cm2. The most considered parameter, FWHM of transverse distribution of electron beam, should be limited less than 1 mm. A radiographic system has been discussed in [6]. Simulation results showed that the exposure dose 1 m away from the target right ahead was about 9.1 R and the X-ray spot sizes were not increased with the increment of the thickness of target material. The results also showed that pulse number was limited up to 8 when using a fixed target

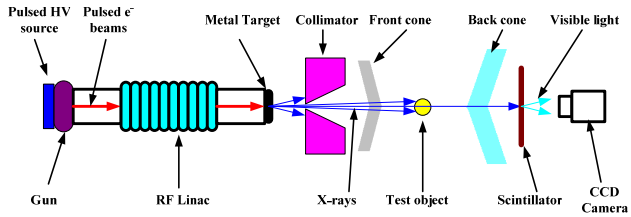


Figure 1: Layout of a typical flash X-ray radiography system using RF accelerator.

when FWHM of transverse size was about 1 mm with bunch charge of 400 nC.

In this paper, the design of accelerator was described. A beam dynamic analysis was carried out with the primary design of the accelerating structure. BBU effect calculation was also carried out.

GENERAL DESCRIPTION OF THE ACCELERATOR

Layout of the accelerator, which consists of a DC gun, 3 accelerating tube, a chicane and matching beam line, was shown in Fig. 2. The total length is about 14 m and could be reduced by farther optimization. Table 1 lists main parameters.

Table 1: Main Linac Parameters

Parameter	Value	Unit
RF frequency	2856	MHz
Energy	>30	MeV
Beam current (max)	4	A
Energy spread (FWHM)	<0.01	
Emittance (RMS)	<50	mm mrad
Beam pulse length	100	ns
Number of pulses in a train	4-8	
RF pulse duration	10	μs
Pulse repetition rate	10	Hz
Number of ACC. structure	3	
Gun voltage	~120	kV

ACCELERATING STRUCTURE

General Design

The goal of the design of accelerating structure is to achieve a high RF-beam power efficiency with short length as much as possible. Two type of structure was considered: the conventional disk-load structure and constant-aperture structure. Both of them should be slotted on the iris to suppress the HOM modes, which would be introduced by

* Work supported by Key Laboratory of Pulsed Power, CAEP (Contract NO. PPLF2014PZ05) and Key Laboratory of Particle Acceleration Physics &Technology, IHEP, CAS (Contract NO. Y5294109TD)
† jpang@caep.cn

Content from this work may be used under the terms of the CC BY 3.0 licence (© 2018). Any distribution of this work must maintain attribution to the author(s), title of the work, publisher, and DOI.

ISBN: 978-3-95450-194-6 ISSN: 2226-0366 doi:10.18429/JACoW-LINAC2018-THPO115

CONSOLIDATION AND EXTENSION OF THE HIGH-GRADIENT LINAC RF TECHNOLOGY AT PSI

P. Craievich*, M. Bopp, H. Braun, A. Citterio, H. Fitze, T. Garvey, T. Kleeb,
F. Loehl, F. Marcellini, M. Pedrozzi, J.-Y. Raguin, L. Rivkin, K. Rolli, R. Zennaro
Paul Scherrer Institut, 5232 Villigen PSI, Switzerland

Abstract

For SwissFEL a novel production process for high-gradient, high-precision C-band accelerating structures had been developed at PSI and was implemented for series production in collaboration with industry. The copper parts of the structures are machined and brazed relying on a ultra-high precision manufacturing process and tight mechanical tolerances; no RF tuning methods are applied during or after production. So far none of the structures of the series production failed during RF power conditioning and operation in the SwissFEL facility. After completing the series production for SwissFEL PSI started collaborations with CERN, ELETTRA and DESY for applying the production process and related know-how to other frequencies, namely S-band (3 GHz) and X-band (12 GHz). This paper gives an overview on the ongoing and planned R&D activities and results obtained so far.

INTRODUCTION

The SwissFEL project [1], presently under commissioning at the Paul Scherrer Institut (PSI), produces FEL radiation for hard X-rays with pulse durations ranging from a few to several tens of femtoseconds. The SwissFEL accelerator consists of an electron source, an S-band (3 GHz) booster Linac and a C-band (5.7 GHz) main Linac. A total of 26 C-band modules are installed in the C-band Linac and each module consists of four 2-m long C-band structures that are mounted onto two granite girders (see [2] for a schematic and [3] for further information). The C-band structures [4] are stacked and brazed at PSI out of copper cells that were produced at VDL ETG (J-couplers) and VDL ETG Switzerland (regular cells) with micrometer precision using ultra-precision diamond milling and turning. These structures do not undergo any tuning steps from cup production to installation into the bunker. The target precision of a single copper cup is less than ±2 µm with a surface finish Ra of 25 nm and concentricity of less than 50 µm before and after brazing of a stack of 111 copper regular cells and two couplers. Bead pull measurements have confirmed the high precision machining of the cups and couplers and thus validated the choice to produce the structures without implementing mechanical tuning on the cups, i.e., any push-pull technique. Furthermore, the measurement of the Q-factor was within 1% of the simulated one and the rms phase advance error was less than 2° over the whole structure which has a negligible effect on the energy gain. The manufacturing process of the individual cup was developed and tested at PSI before transferring the technology to the industry for the series production. It consists of an initial raw-cut and then pre-turned on a conventional and numerical lathe to a precision of about 10 µm while the finishing of the cups is performed on a sturdy and pneumatically stabilized slanted bed lathe using poly and mono-crystalline diamond (PCD, MCD) tools in a temperature and humidity controlled machining compartment of the lathe itself. Metrology measurements on the copper cells have shown a turning precision better than ±0.5 µm. The copper is oxygen free, high-conductivity and forged in three dimensions to have a homogeneous distribution of the small pores, a stress-free and intrinsically stable material. In order to assure the required concentricity, a robot with an action radius of 2 m and a tridimensional accuracy of 5 µm is used for the stacking of the cups before brazing [5]. This production process allows one to avoid any tuning steps while still achieving excellent field flatness and phase advance errors. In addition to the four structures, each Linac module also comprises a barrel open cavity (BOC) pulse compressor [6], and these were machined and brazed at PSI [7]. A picture of the C-band module is shown in Figure 1. A module is fed by a single RF source with up to 50 MW. The achieved straightness of the structures is excellent, the maximum measured deviations from a straight line are typically below 25 µm. The RF properties of the C-band structures have been measured using the bead-pull technique and an example result is shown in Fig. 2. All structures achieved an excellent electric field profile along the longitudinal coordinate of the

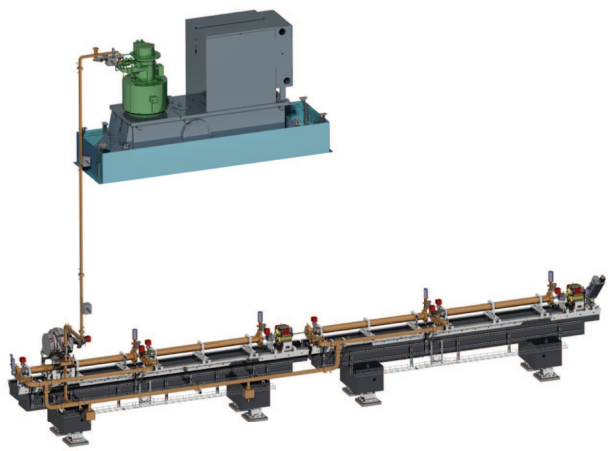


Figure 1: C-band module composed from four C-band accelerating structures, a pulse compressor and 50 MW Toshiba klystron.

* paolo.craievch@psi.ch

Content from this work may be used under the terms of the CC BY 3.0 licence (© 2018). Any distribution of this work must maintain attribution to the author(s), title of the work, publisher, and DOI.

ISBN: 978-3-95450-194-6 ISSN: 2226-0366 doi:10.18429/JACoW-LINAC2018-THPO116

SPACE-CHARGE DOMINATED PHOTOEMISSION IN HIGH GRADIENT PHOTOCATHODE RF GUNS

Y. Chen*[a], P. Boonpornprasert[a], H. Chen[b], H. De Gersem[c], M. Dohlus[d], Y. C. Du†[b], E. Gjonaj[c], J. D. Good[a], M. Gross[a], W. H. Huang[b], H. Huck[a], I. Isaev[a], D. Kalantaryan[a], C. Koschitzki[a], M. Krasilnikov‡[a], O. Lishilin[a], G. Loisch[a], D. Melkumyan[a], R. Niemczyk[a], A. Oppelt[a], H. J. Qian§[a], Y. Renier[a], S. Schmid[c], F. Stephan[a], C. X. Tang[b], Q. L. Tian[b], L. X. Yan[b]
[a]DESY, 15738 Zeuthen, Germany; [b]Tsinghua University, 100084 Beijing, China
[c]TEMF, 64289 Darmstadt, Germany; [d]DESY, 22607 Hamburg, Germany

Abstract

The cathode emission physics plays a crucial role in the overall beam dynamics in an RF gun. Interplays between intricate emission mechanisms in the cathode vicinity strongly influence the cathode quantum efficiency (QE) and the intrinsic emittance. The presence of strong space-charge effects in high gradient RF guns further complicates the emission process. A proper modeling of photoemission and a careful treatment of the space-charge contribution is thus of great necessity to understanding the formation of the beam slice emittance. In this article, emission measurements are carried out using the L-band cesium-telluride photocathode RF gun at the Photo Injector Test Facility at DESY in Zeuthen (PITZ) and the S-band copper photocathode RF gun at Tsinghua University. Following the Dowell model a simple so-called space-charge iteration approach is developed and used to determine the QE through temporal- and spatial-dependent electromagnetic fields. An impact of the space-charge cooling on the intrinsic emittance is presented. Measurement data are shown and discussed in comparisons to preliminary simulation results.

INTRODUCTION

High gradient photocathode RF guns provide high brightness electron beams for coherent light sources [1–3]. Such applications require rather high bunch charge and very small transverse normalized emittance from the injector. Optimization of the injector performance to fulfill the beam requirements is essentially a trade-off between multiple machine operation parameters. Experimental results at PITZ [2, 4, 5] have revealed optimum injector parameters from which the space-charge dominated photoemission at the cathode is identified. A detailed understanding of the contribution of the strong space-charge effects present in the cathode vicinity onto the emission process is, therefore, a prerequisite to characterize crucial beam properties at extraction, such as the thermal emittance which occupies a major part of the overall emittance budget [6].

In this article, the photoemission characterization is performed at two gun facilities, the L-band cesium-telluride photocathode RF gun at PITZ whose copies are in use at the European XFEL and FLASH, and the S-band copper photocathode RF gun at Tsinghua University [3, 7] which has been used, for example, as the electron source for the compact Tsinghua Thomson Scattering X-ray Source [8] and many other research programs [9].

* ye.lining.chen@desy.de
† dych@mail.tsinghua.edu.cn
‡ mikhail.krasilnikov@desy.de
§ houjun.qian@desy.de

BEAM DYNAMICS

Figure 1 shows the extracted bunch charge (Q) from a cesium-telluride photocathode in the PITZ gun scanned over the full range of the emission phase (ϕ) and the applied cathode drive UV laser pulse energy (E_{las}). An 11 ps (FWHM) temporal Gaussian laser pulse with a transverse spot size of 1.2 mm in diameter is used for these measurements. The gun is operated at a maximum electric field gradient of 60 MV/m. The zero-crossing phase is at about 45°. The maximum mean momentum gain (MMMG) phase is at 6°. The charge is collected with a Faraday cup which is 0.78 m downstream of the cathode. The so-called Schottky scans (Q vs. ϕ) using different laser pulse energies and the emission curves (Q vs. E_{las}) at various RF phases are also shown in the 2D projections. In the Schottky scans, the increase of the bunch charge around 45° essentially relates to the pulse shape of the drive laser and the sharpness of the rising edge is limited by the space-charge effects as the laser pulse energy is increased. The slow increase of the charge in the middle of these curves reveals the Schottky-like effect. For the emission phases far away from the MMMG, a major part of the emitted electrons gets lost during beam transportation due to strong RF phase slippage (see [5, 10] for more details).

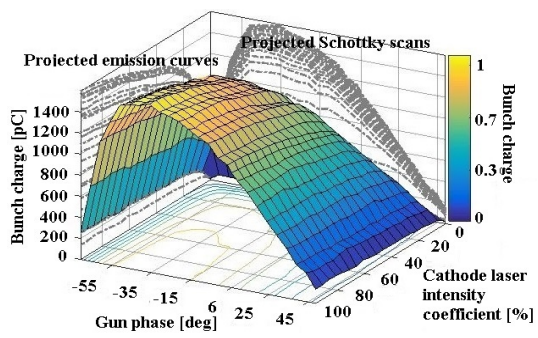


Figure 1: 3D reconstruction of a characterized photoemission distribution obtained from the experiments at PITZ. Note that the laser pulse energy is represented by the laser intensity coefficient following a linear correlation.

Content from this work may be used under the terms of the CC BY 3.0 licence (© 2018). Any distribution of this work must maintain attribution to the author(s), title of the work, publisher, and DOI.

ISBN: 978-3-95450-194-6 ISSN: 2226-0366 doi:10.18429/JACoW-LINAC2018-THPO118

BEAM TRANSVERSE COUPLING AND 4D EMITTANCE MEASUREMENT SIMULATION STUDIES FOR PITZ

Q. Zhao†, [1], M. Krasilnikov, H. Qian, F. Stephan, DESY, Zeuthen, Germany
[1]now at Institute of Modern Physics, Chinese Academy of Sciences, Lanzhou, China

Abstract

The Photo Injector Test Facility at DESY, Zeuthen site (PITZ) was built to test and optimize high brightness electron sources for Free Electron Lasers (FELs) like FLASH and the European XFEL. Although the beam emittance has been optimized and experimentally demonstrated to meet the requirements of FLASH and XFEL, transverse beam asymmetries were observed during operation of the RF guns. Based on previous studies [1], the beam asymmetries most probably stem from beam transverse coupling by quadrupole field errors in the gun section. A pair of normal and skew gun quadrupoles was successfully used for reducing the beam asymmetries in experiment. In this paper, we discuss the beam transverse coupling between X and Y planes due to quadrupole field errors and its impact onto horizontal and vertical rms emittance. Multi-quads scan and two quads with rotated slits scan were proposed to measure the 4D beam matrix for PITZ and tested by simulation, which will give the residual beam coupling after gun quadrupoles compensation and would be helpful for minimizing the 2D rms emittance experimentally.

INTRODUCTION

During several years of operation with different generations of guns, the transverse beam asymmetry was always observed from experiments in PITZ [1-3]. From previous studies [4-5], a PITZ gun RF coupler kick was found from RF field simulations. In the transition region from the coupler to the gun, the RF field distribution is not circularly symmetric. The RF coupler kick optics can be modelled as a rotated quadrupole and a rotated quadrupole near the coupler is effective at compensating for the coupler kicks, cancelling both the coupling emittance and the astigmatic focusing [6-7]. Another source of the beam asymmetries may come from solenoid field imperfections [8]. The feature of the beam transverse coupling from rotated quadrupoles can be observed from beam transverse distributions in experiment. These effects will result in an increase of the 2D rms emittances. For FELs this would imply a deterioration of the laser performance. Linear coupling can be compensated in principle by additional rotated quadrupoles [9-10].

† zhaoquantang@impcas.ac.cn

QUADRUPOLE FIELD ERRORS EFFECT ON THE 4D EMITTANCE AND COUPLING TERMS SIMULATION STUDIES

4D Emittance and Coupling Factor

In order to know the compensation quadrupoles strength and how much the coupling is decoupled, a full four-dimensional (4D) beam matrix measurement becomes necessary to measure precisely and possibly further correct the transverse coupling.

The 4D beam matrix, shown in formula (1) describes the transverse statistical properties of the beam:

$$\sigma^{4D} = \begin{bmatrix} <xx> & <xx'> & <xy> & <xy'> \\ <x'x> & <x'x'> & <x'y> & <x'y'> \\ <yx> & <yx'> & <yy> & <yy'> \\ <y'x> & <y'x'> & <y'y> & <y'y'> \end{bmatrix} = \begin{bmatrix} \sigma_{xx} & \sigma_{xy} \\ \sigma_{xy}^{T} & \sigma_{yy} \end{bmatrix} \quad (1)$$

And the 4D emittance is determined by (2):

$$\varepsilon_{4D} = \varepsilon_1 \varepsilon_2 = \sqrt{\det(\sigma^{4D})} \quad (2)$$

where x and y are the horizontal and vertical coordinates, respectively, x' and y' are their derivatives with respect to the longitudinal coordinate, and the ε_1, ε_2.are intrinsic emittance [11-12]. The matrices σ_{xx} and σ_{yy} describe the 2D horizontal and vertical motions, and σ_{xy} describes the cross-plane coupling. If one or more elements of σ_{xy} are nonzero, the beam is x-y coupled and the projections onto the x and y planes exhibit an increase of the observed emittance values. The transverse coupling contribution to the 2D rms emittances can be quantified by the coupling factor (3),

$$t = \frac{\varepsilon_x \varepsilon_y}{\varepsilon_1 \varepsilon_2} - 1 \geq 0 \quad (3)$$

Where ε_x, ε_y are the x and y plane 2D rms emittance. For t = 0 the beam is decoupled and for t > 0 the beam is transversely coupled.

Quadrupole Field Errors Effect on the Coupling Simulation Studies

Based on quadrupole field errors model [3], it is possible to study these kinds of field errors effect on the coupling factor t and to show how the 2D rms emittance increases by the quadrupole field errors. The simulation was done by ASTRA [13] and the machine settings are as follows: gun gradient is 51.36 MV/m, solenoid current is 350 A (arbitrary one, not the optimized current), bunch charge is 500 pC, and laser rms size is 0.3 mm with longitudinal Gaussian distribution. Beam momentum after gun is 5.8 MeV/c and after the booster is 20.8 MeV/c. A pair of normal and skew quadrupole field errors are modelled and added in the simulation and placed in the correspond-

Content from this work may be used under the terms of the CC BY 3.0 licence (© 2018). Any distribution of this work must maintain attribution to the author(s), title of the work, publisher, and DOI.

ISBN: 978-3-95450-194-6 ISSN: 2226-0366 doi:10.18429/JACoW-LINAC2018-THPO124

DESIGN OF PULSED HV AND RF COMBINED GUN SYSTEM USING GRIDDED THERMIONIC-CATHODE

T. Asaka†, H. Tanaka, RIKEN SPring-8 Center, Hyogo 679-5148, Japan
T. Taniuchi, Y. Otake, JASRI/SPring-8, Hyogo 679-5198, Japan

Abstract

We propose a simple and compact electron gun system with a control grid, which can provide a low emittance of a few mm mrad. The system is composed of a 50-kV thermionic-gun with a gridded cathode and a 238-MHz rf cavity, each of which is manufactured by extending the well-established technology. The rf cavity accelerates the extracted electrons from the thermionic-gun up to 500 keV to preserve the low emittance. Using the CST and PARMELA particle tracking simulation codes, the proposed system can generate a beam with a low emittance of 2 mm mrad by an extraction charge of 0.6 nC by optimizing voltage parameters of the 50-keV thermionic-gun and the 238-MHz rf cavity.

INTRODUCTION

As a low emittance electron source, a photocathode rf gun [1], or a 500-kV thermionic-gun with a single crystal cathode [2] are usually used. Each electron gun system has own strong and weak points. The rf gun system is rather compact but it requires a large and complicated laser system to obtain highly stable beam. On the other hand, the 500-kV thermionic-gun is almost maintenance-free. However, the weak point of the thermionic-gun is to prepare the large and difficult high voltage system.

In order to remove the above-mentioned weak point, one of the authors (Otake) proposed a robust, compact and low-cost electron gun system, while keeping the low emittance and an electron energy above 500 keV. The system comprises of a thermionic-gun with a charging voltage of 50-kV and a 238-MHz rf cavity in order to increase beam energy up to 500 keV. This system adopts a commercially available gridded cathode. An electron pulse length of less than 1 ns extracted from the cathode is sufficiently short to be captured by the phase space of the following acceleration rf. These combining instruments can eliminate the laser system.

Concern in the above-mentioned idea is an emittance growth by the distorted electric field (lens effect) in the grid [3]. It is well-known effect depends on the electric potential shape and strength on the grid wire and the space-charge field strength of the beam [4]. There is the cancelling point of both electric field strengths between the lens effect and the space charge effect. In order to improve this emittance deterioration, we have investigated the optimum condition of this cancellation by using computer simulation. In this paper, we describe basic design of the gun system and the optimized parameters of a beam transport to keep the low emittance.

† asaka@spring8.or.jp

DESIGN OF PULSED HV AND RF COMBINED GUN SYSTEM

The low-emittance pulsed HV and rf combined gun system just consists of extension of the established technology. To generate the pulsed beam without the laser system, the 50-kV thermionic-gun with a gridded cathode is employed. The gridded cathode is Y845, which is manufactured by CPI Corporation. To extract beam with a pulse length of 600 ps from the Y845, a fast pulser drives a voltage between a cathode and a grid mesh. Furthermore, the 238-MHz rf cavity is placed as close as possible to its acceleration gap and just behind of the 50-kV thermionic-gun for obtaining a relativistic beam energy of over 500 keV. This positioning is indispensable to reduce the emittance growth by the space charge effect, as which means quickly accelerating to a high β the electron. Furthermore, we consider rf leakage from the rf cavity to the grid and the cathode surface. The acceleration phase space of the 238-MHz rf cavity can capture the pulsed beam, which is beam acceleration scheme similar to a rf gun. In this case, nonlinearity of a rf voltage curvature is one of cause of the emittance growth. When the energy spread of the beam caused by the rf nonlinearity is less than a few percent, there is slight the emittance growth. It is acceptable for our design.

In the 50-kV thermionic-gun, a high-voltage instruments can operate in the atmosphere without insulation oil. Furthermore, a solid-state device can be handle this voltage for a pulser and a power supply. On the other hand, the device installed in a rf amplifier, which has long lifetime and lower failure, and can also drive the 238-MHz for the rf cavity. These are advantage of the gun system. This advantage is not only cost saving, but also improving maintainability.

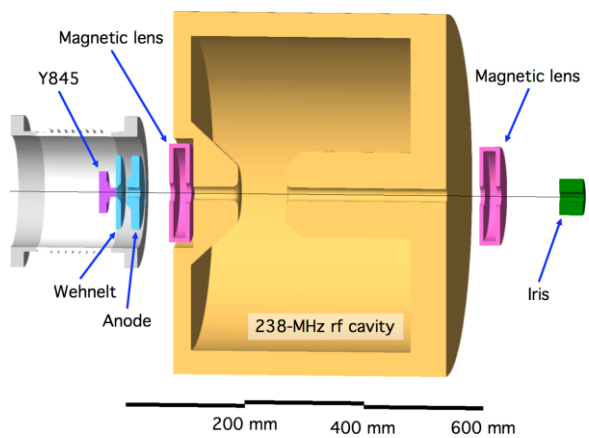


Figure 1: Schematic drawing of the low-emittance pulsed HV and rf combined gun system.

Content from this work may be used under the terms of the CC BY 3.0 licence (© 2018). Any distribution of this work must maintain attribution to the author(s), title of the work, publisher, and DOI.

ISBN: 978-3-95450-194-6 ISSN: 2226-0366 doi:10.18429/JACoW-LINAC2018-THPO125

RUNNING STATUS OF SRF GUN-II AT ELBE CENTER*

R. Xiang†[1], A. Arnold[1], P. Lu[1,2], P. Murcek[1], J. Schaber[1], J. Teichert[1], H. Vennekate[1,3], P. Zwartek[1]
[1]Helmholtz-Zentrum Dresden-Rossendorf, 01328 Dresden, Germany

Abstract

As a new electron source with higher brilliance, the second version of the superconducting RF photoinjector (SRF Gun-II) has been successfully commissioned at the ELBE Center for high power radiation sources since 2014. SRF Gun-II features an improved 3.5-cell niobium cavity as well as a superconducting solenoid in the same cryomodule. With Mg photocathode SRF Gun-II can provide high current beam with bunch charge up to 300 pC at 100 kHz repetition rate. For user operation the SRF Gun-II successfully generated stable beam with 200 pC in CW mode and sub-ps bunch length. In this presentation the gun's status and beam parameters will be presented.

INTRODUCTION

The unique feature of the ELBE accelerator is its ability to operate in continuous wave (CW) mode for high average power output. Hence, a flexible CW electron source is required. An rf photoinjector based on superconducting technology represents the ideal solution for this task. It produces high field gradients causing enhanced beam parameters and large beam currents due to increased repetition rates.

The ELBE SRF Gun project is the R&D effort to provide such an injector. Commissioning with further improvements and optimization of components as well as our operational experience has increased the performance and reliability so that the SRF Gun-II is now applied for user operation.

SRF GUN-II

SRF Gun-II has been installed in the accelerator hall since May 2014 [1]. The main design is based on the first SRF Gun [2] with a modified 1.3 GHz Nb cavity and a superconducting solenoid at about 70 cm from the cathode [3]. The combination of 258nm laser and Mg cathode allows to provide beam with bunch charge up to 300 pC, which is limited by the space charge effect in the gun with an acceleration gradient of 8 MV/m (20.5 MV/m peak field on axis).

SRF Cavity and RF Performance

The 1.3 GHz Nb cavity was built, treated and tested at JLab [4]. It consists of three TESLA like cells, a specially designed half-cell and a choke filter. This filter is surrounding the cathode, preventing RF leakage into the cathode support system (see Fig. 1).

The performance of cavity has been measured regularly in the gun cryomodule without or with cathodes. Compared to the last vertical test at Jlab the cavity lost about 30% of its performance. A serious contamination was caused by particles sputtered from cathode surface onto the first iris of the cavity. Nevertheless, the remaining gradient is still higher than that of SRF gun-I. The safe gradient for the routine operation is 7 MV/m, with field on cathode 10.7 MV/m, and the main drawback is the field emission under higher field.

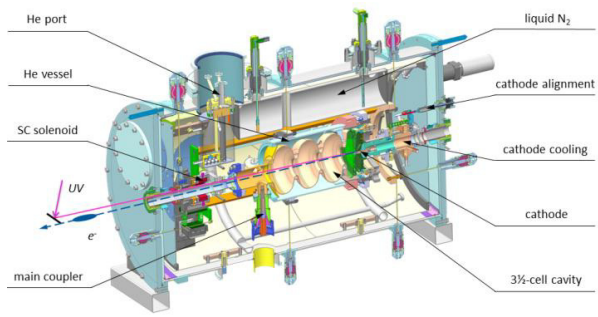


Figure 1: Cross section of the ELBE SRF gun II cryomodule, holding a 3.5 cell gun cavity and a superconducting solenoid at about 70 cm from the cathode.

Photocathode and Laser

In the first SRF gun at ELBE operating until 2014, the main problem caused by Cs_2Te photocathodes was multipacting in the gap of cathode hole, but the lifetime was not a problem [5]. In SRF Gun-II, the life time of Cs_2Te photocathodes was only two weeks. The possible reason of its degradation is the overheating of the cathode plugs during the operation. Further detailed studies and technical modifications are going on.

Mg cathodes made of bulk magnesium and cleaned with focused UV laser beam are working for the regular ELBE user operation with the SRF gun. Magnesium has a low work function of 3.6 eV. Illuminating with UV laser light at 258 nm, the expected quantum efficiency (QE) of Mg can be as good as 0.6 %, which is the best QE ever reported in rf guns. The UV drive laser can deliver pulses with up to 3 µJ at 100 kHz repetition rate, which is enough to produce bunches up to 300 pC with a Mg photocathode. The laser spot size on photocathode is about ϕ 4 mm. The temporal profile is Gaussian with an rms pulse length of about 2 ps.

Figure 2 shows the measured Faraday cup current (and bunch charge) versus drive laser phase for different laser power. The laser phase of the SRF gun in operation is indicated by the vertical zone between 40° to 60°. One

† email address: r.xiang@hzdr.de
2 present address: RI Research Instruments GmbH, Bergisch Gladbach
3 present address: KLA-Tencor, Shanghai

Content from this work may be used under the terms of the CC BY 3.0 licence (© 2018). Any distribution of this work must maintain attribution to the author(s), title of the work, publisher, and DOI.

ISBN: 978-3-95450-194-6 ISSN: 2226-0366 doi:10.18429/JACoW-LINAC2018-THPO126

COMPACT H+ ECR ION SOURCE WITH PULSE GAS VALVE

Y. Takeuchi*, H. Tongu, Y. Iwashita, Kyoto University, Uji, Kyoto 611-0011 Japan

Abstract

We are developing a compact ECR H+ ion source with a fast pulse gas valve. In the case of high current ion linac, the distance between the ion source and the first accelerating tube such as RFQ must be as short as possible to reduce the space charge effect, while operation in a high electric field a good vacuum condition is desirable. Since hydrogen gas always flows out from ion sources when the plasma chamber is filled with the gas, vacuum pumping systems have to evacuate the gas enough before the first accelerating tube. The quick pulse gas injection system achieved by a fast piezoelectric gas valve can reduce the gas load to the vacuum evacuation system and is suitable for installing the ion source close to RFQ. In order to optimize the operating parameter of the ion source, a multi-collector mass analyzing system is developed. The current status is reported together with the preliminary measurement data of the quick mass analysis and spectroscopy of the emitted lights from the plasma.

INTRODUCTION

In an ion source using gas discharge, not only ion beam but also neutral gas flows out from extraction hole. Most of the neutral gas is pumped out by the vacuum pumping system in the Low Energy Beam Transport (LEBT), and a part of the gas diffuses to the accelerating tube. Conventionally, even in the case of a pulsed ion source, neutral gas is constantly supplied and ion beam is extracted from the ion source during the pulse period, while neutral gas continues to flow out of the plasma chamber. In a high-intensity ion accelerator, it is desirable that the length of the LEBT is as short as possible in order to reduce the adverse effect of the space charge effect. However, if the LEBT is short, the effect of the inflow neutral gas to the acceleration tube increases. Then, frequent discharges in the accelerating tube may happen, which may interrupt operation. Chopping the supply of the gas into the plasma can reduce the gas flow. Therefore, we have developed ECR ion source with less gas load [1].

COMPACT H+ ECR ION SOURCE WITH PULSE GAS VALVE

Currently, we have developed a compact ECR H+ ion source with pulse gas valve and test its performance. Since it is assumed to be used for small neutron sources based on proton linac, H+ was chosen as the ion species. In order to achieve high H+ ratio in the extracted beam, the ECR method was adopted. The pulse gas injection system achieved by a fast piezoelectric gas valve can reduce the gas load to the vacuum evacuation system and is suitable for a close installation of the ion source to RFQ.

* takeuchi.yusuke.64z@st.kyoto-u.ac.jp

Desgin

The source is build on a ICF203 flange. There are two radial permanent magnet rings at the upstream and downstream of the chamber. Each magnet ring consists of twelve trapezoidal pieces and their magnetic holder. The extraction system consists of a plasma electrode and a set of three electrodes with a negative potential inserted between the two grounded electrodes, and up to 25 kV can be applied to the plasma electrode. The high voltage assembly is insulated and supported from ground potential by polyethylene insulators. The ion source unit is covered by an iron magnetic return yoke that reduces the stray magnetic field around the ion source. The structure of the ion source is shown in Fig. 1.

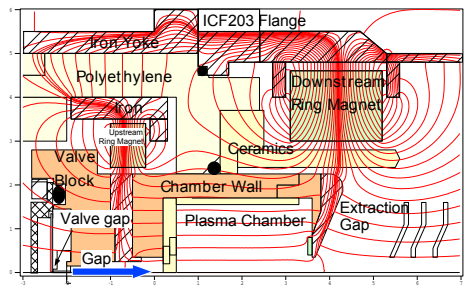


Figure 1: Schematic drawing of the ion source structure. Red lines indicate magnetic flux.

Gas Valve

We developed a fast pulse gas valve using a piezoelectric element KBS-27DA-5A to chop gas supply to ion source [2]. If positive voltage is applied to the piezoelectric element, the gas entrance into the chamber is blocked by the piezoelectric element, so that the gas does not flow into the chamber. However, when negative voltage is applied to the piezoelectric element, the piezoelectric element curves oppositely to open the flow path, and the gas flows into the chamber. By applying a quick pulse voltage to the piezoelectric element, it is possible to inject and chop gas quickly. Figure 2 shows a schematic diagram of the operating principle of the pulse gas valve using the piezoelectric element.

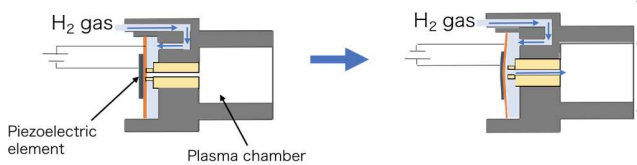


Figure 2: Operating principle of the pulse gas valve.

Magnetic Field

The magnetic field strength satisfying the ECR condition at 6 GHz is about 220 mT. For the generation of the magnetic

Content from this work may be used under the terms of the CC BY 3.0 licence (© 2018). Any distribution of this work must maintain attribution to the author(s), title of the work, publisher, and DOI.

ISBN: 978-3-95450-194-6 ISSN: 2226-0366 doi:10.18429/JACoW-LINAC2018-THPO127

THE EFFECT OF ENERGY FLUCTUATION ON THE MULTI-BUNCH ACCELERATION IN E-DRIVEN ILC POSITRON SOURCE

Masao Kuriki,* Hisayasu Nagoshi, Tohru Tahakashi, Hiroshima University, Higashihiroshima, Japan
Kentaro Negishi, Iwate University, Morioka, Japan
Toshiyuki Okugi, Tsunehiko Omori, KEK, Tsukuba, Japan
Masashi Satoh, Yuji Seimiya, Junji Urakawa, Kaoru Yokoya, Shigeru Kashiwagi,
Tohoku University, Sendai, Japan

Abstract

E-Driven method is a technical backup for positron source for ILC. In the positron source, the positron is generated and accelerated in a multi-bunch format with gaps in a macro-pulse. We employ AM (Amplitude Modulation) to suppress the transient beam-loading, but a small fluctuation is still expected, depending on the compensation accuracy. In this article, the positron yield which is ratio of numbers of positrons over electrons, is evaluated as a function of the compensation accuracy. With this result and the detail investigation of the beam loading compensation accuracy by AM, the positron yield of E-Driven Positron source for ILC is evaluated.

INTRODUCTION

ILC (International Linear Collider) [1] is an e+e- linear collider with CME from 250 to 1000 GeV. It would be constructed in Iwate, Japan, as the main project of High energy physics. In the E-driven ILC positron source, the positron is generated in a macro-pulse with 6.15 ns bunch spacing [2]. Schematic drawing of the E-Driven ILC positron source is shown in Fig. 1 3.0 GeV electrons hit W-Re(26) alloy target to generate positrons through pair creation process. At the downstream of the target, AMD (Adiabatic Matching Device) is placed [3] to suppress the transverse momentum. Thereafter, it is accelerated up to 250 MeV by 36 of 11-cell normal conducting L-Band Standing Wave (SW) cavities [4] surrounded by 0.5 T solenoid field. After a chicane removing electrons from the bunch, the positron booster composed from L-Band and S-Band Traveling Wave (TW) cavities accelerates the positron up to 5 GeV. After the booster, the positrons are injected to DR (Damping Ring) for radiation damping through ECS (Energy Compressor Section) for better phase-space matching. In ILC, positrons of 3.2 nC per bunch are required at the collision point. In the DR, the required bunch charge is 4.8 nC including 50% margin. The design criteria for the E-driven ILC positron source is to obtain a sufficient amount of positron in DR acceptance defined in a phase space [3]. The condition in the longitudinal phase-space is 70 mm in z and 1.5% in energy (full width).

Because the macro pulse is a copy of a part of DR (Damping Ring) fill pattern, there is a gap as shown in Fig. 2. This is an example and number of gaps depends on DR fill pattern. Seimiya performed a start-to-end simulation of the E-Driven ILC positron source without the beam loading effect [3].

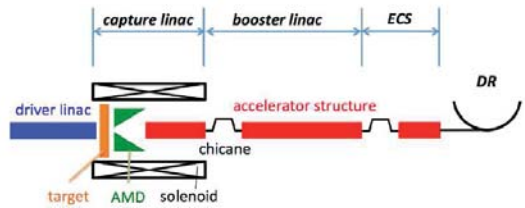


Figure 1: Schematic view of ILC E-driven Positron source.

Kuriki perform the simulation with the beam loading effect, but it is only for the injector part (up to 250 MeV) [4]. To accelerate the beam in such format, the transient beam loading effect which varies the accelerating field at the macro pulse and every mini-train heads, has to be compensated.

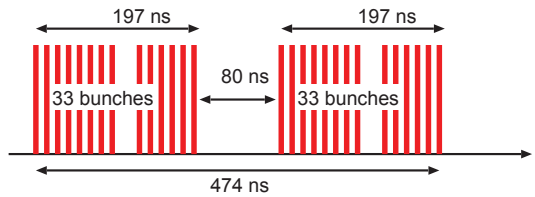


Figure 2: An example of macro-pulse structure in E-Driven ILC positron source. The macro pulse is composed from two mini-trains of 33 bunches with 6.15 ns bunch spacing. There is a gap of 80 ns.

M. Kuriki [5] shows that the energy variation by the beam loading with this beam format can be compensated by controlling timing and RF envelope in standing wave accelerator. H. Nagoshi et al. [6] shows that amplitude modulation [5] is effective to compensate the beam loading in travelling wave accelerator. The compensation can be perfect, but it requires a high peak RF input. The compensation have some imperfection if we limit the peak RF power [6] and an energy variation in pulse due to this imperfection is expected. In this article, we evaluate the yield variation of the positron source by the energy variation in pulse.

RESULT AND DISCUSSION

The transient beam loading effect should be compensated in the macro-pulse acceleration for ILC E-Driven positron source. Otherwise, we will have a large variation on the positron bunch intensity in DR. The large fluctuation causes a difficulty on the acceleration in the main linac, because the beam loading in a macro-pulse will be varied and we will

* mkuriki@hiroshima-u.ac.jp

Content from this work may be used under the terms of the CC BY 3.0 licence (© 2018). Any distribution of this work must maintain attribution to the author(s), title of the work, publisher, and DOI.

ISBN: 978-3-95450-194-6 ISSN: 2226-0366 doi:10.18429/JACoW-LINAC2018-THPO132

STUDY OF THE ELECTRON BEAM TRANSFER LINE FOR THE AWAKE RUN II EXPERIMENT AT CERN*

Seong-Yeol Kim[1], Moses Chung[1†], UNIST, 44919 Ulsan, Republic of Korea
Mohsen Dayyani[2], Institute For Research in Fundamental Sciences, 19395-5531, Tehran, Iran
Steffen Doebert[3‡], CERN, CH-1211, Geneva, Switzerland

Abstract

Proton Beam-Driven Plasma Wakefield Accelerator (PBD-PWFA) has been actively investigated at CERN within the AWAKE experiments to study the electron beam acceleration using plasma wake fields of the order of GV/m. In the AWAKE RUN 1 experiments an electron beam with an energy of 19 MeV and a bunch length of 2.2 ps rms has been used for the first demonstration of electron beam acceleration in the plasma wake fields. It has been observed that the energy gain of the electron beam is up to 2 GeV, and electron capture efficiency is few percent. Higher capturing efficiency and emittance preservation could be achieved by making the electron beam short enough to be injected only into the acceleration and focusing phase of the plasma wake fields. The electron accelerator needs to be upgraded for AWAKE RUN 2 experiments to obtain a bunch length less than 100 fs which corresponds to a quarter of the plasma wavelength. Planned electron beam parameters for the AWAKE RUN 2 are a beam charge of 100 pC, and a beam energy larger than 50 MeV. In this paper, we show the electron beam parameters for RUN 2, and the parameters of the transfer line such as Twiss parameters, beam envelope, and emittance.

INTRODUCTION

In the first run of the AWAKE to demonstrate the acceleration of 19 MeV electron beam through the PBD-PWFA, it has been observed that the energy gain of the electron beam is in the order of GeV [1]. Furthermore, a new experimental setup is now under study for the next run of AWAKE starting from 2021 to study electron acceleration with high energy and emittance preservation. For the RUN 2 experiments, target parameters have been determined from the simulation [2]. The beam size and length are less than 50 μm and 100 fs, respectively to increase capturing efficiency to more than 90 %. In addition, while a single Rb-Vapor plasma cell has been used for both Seeded Self-Modulation (SSM) and accelerating of the electron beam In RUN 1, it is considered for RUN 2 experiment that an additionally introduced 4 m plasma cell is used only for SSM to generate the micro-bunches of the proton beam. Then, the modulated proton beam propagates to another 10 m of plasma to generate the plasma wake fields, which are going to be used to accelerate the electron beam. The electron beam has to be injected in between the two plasma cells.

* Work supported by NRF
† mchung@unist.ac.kr
‡ steffen.doebert@cern.ch

In this paper, studies on electron beamline optimization using RUN 2 beam parameters are shown, and a new beamline is briefly proposed. For the beamline simulation, ASTRA [3], MAD-X [4] and ELEGANT [5] codes are used to simulate the beam, and for the optimization of the beam parameters along the beamline.

ELECTRON BEAMLINE AND OPTIMIZATION

The beam parameters considered for RUN 2 are obtained from a new injector combining S- and X-band electron accelerator [6]. Apart from a S-band RF gun, it consists of X-band buncher and a traveling wave structure to reduce the bunch length out of the linac section. Beam parameters at the end of the injector are shown in Table 1.

Table 1: Beam Parameters Out of the Linac Section

Parameters	Values
E_k	85 MeV
σ_E	0.33 %
σ_r	0.14 mm
σ_z	82.57 fs
$\epsilon_{nx,ny}$	0.5 mm mrad

Conventional Electron Beamline Optics

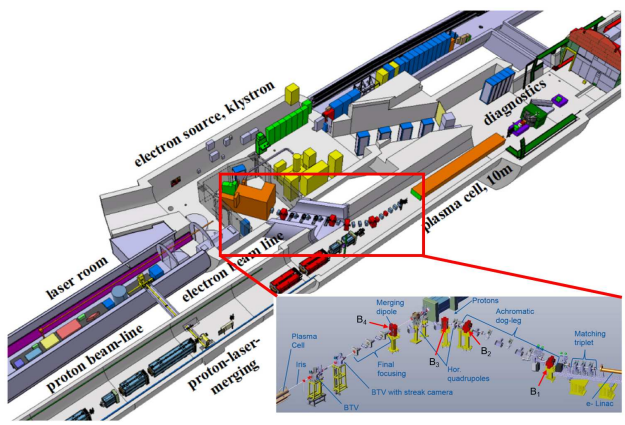


Figure 1: AWAKE tunnel and current electron beamline.

First, it has been studied whether the existing electron beamline for RUN 1 can be used also for the RUN 2 experiments with the initial beam parameters described in Table 1. The current electron beamline is depicted in Fig. 1 [7, 8].

Content from this work may be used under the terms of the CC BY 3.0 licence (© 2018). Any distribution of this work must maintain attribution to the author(s), title of the work, publisher, and DOI.

ISBN: 978-3-95450-194-6 ISSN: 2226-0366 doi:10.18429/JACoW-LINAC2018-FR1A01

RESULTS FROM THE 6D DIAGNOSTICS TEST BENCH AT SNS

B. Cathey, A. Aleksandrov, S. Cousineau, A. Zhukov
Oak Ridge National Laboratory, Oak Ridge, TN, USA

Abstract

This paper presents the method and results for measuring the full six-dimensional phase space of a low energy, high intensity hadron beam. This was done by combining four-dimensional emittance measurement techniques along with dispersion measurement and a beam shape monitor to provide the energy and arrival time components. The measurements were performed on the new Beam Test Facility (BTF) at the Spallation Neutron Source (SNS), a 2.5 MeV functional duplicate of the SNS accelerator front end. The results include a correlation the had not previously been observed.

INTRODUCTION

For high power, high intensity accelerators, beam loss is one of the limiting factors for performance and achievable beam power [1]. Today's state-of-the-art simulation codes provide accurate tracking for the RMS values of the beam through the beam line for many cases, and in principle should also be able to accurately track the beam halo formation and beam loss through the accelerator. However, successful simulation of beam halo and beam loss have yet to be accomplished. As the capabilities of the simulations should be sufficient, the problem may then lie in an incorrect initial assumption, and the most likely candidate is the initial particle distribution, as it is generally approximated [2].

In order to determine the initial particle distribution, the beam must be measured over all six independent spatial and momentum parameters in such a way that correlations between parameters can be seen. The Beam Test Facility at SNS is a small-scale accelerator that can accomplish this task [3].

EMITTANCE MEASUREMENT

Typically, three separate two dimensional phase space measurements are combined to create a six dimensional distribution. However, because the un-measured cross-terms are assumed to be zero in this reconstruction, this distribution may not be identical the actual six dimensional distribution. In order to determine true six dimensional distributions, all six degrees of freedom must be directly measured together. The technique used here is a generalization of the two-dimensional phase space measurement method using slits and a charge collector for the complete six-dimensional phase space.

The particles go through a series of five apertures and a Beam Shape Monitor (BSM). Each aperture allows particles through at the coordinate being measured. By combining two pairs of apertures, one pair being horizontal slits and the other pair vertical slits, the four-dimensional transverse phase space is measured.

To select the longitudinal momentum, we use a 90-degree bending magnet. During the turn, the beam spreads as higher momentum and lower momentum particles separate horizontally due to dispersion. This creates a correlation between the horizontal position and the longitudinal momentum of a particle allowing the selection of particles with certain momentum based on their horizontal position. This selection is executed using a third movable vertical slit.

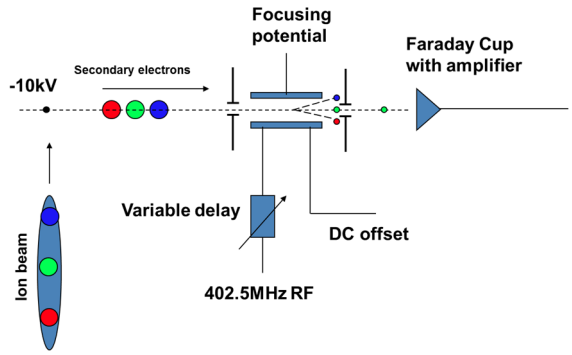


Figure 1: A diagram of the basic concept behind the BSM for measuring the longitudinal phase distribution in the beam.

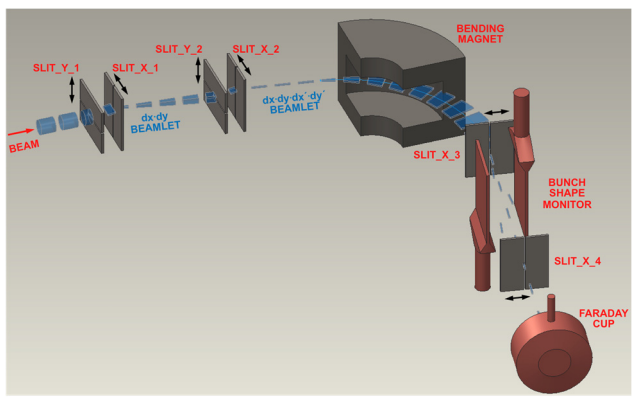


Figure 2: A diagram showing the concept of a full six-dimensional emittance scan.

The longitudinal measurement is conducted with a Beam Shape Monitor (BSM). The BSM contains a suspended wire with a potential in the beam pipe. When the hadron beam hits the wire, electrons are emitted which travel through a RF field and final aperture. See Fig. 1 and [3] for more details. These electrons then hit a detector and are measured as current. This final current measurement reflects the number of particles in the beam with the six measurements described above, particles with a specific horizontal, vertical, and longitudinal position and momentum. Figure 2 shows the full conceptual schematic for the six-dimensional measurement. After a measurement is made for a specified arrangement of apertures, one aperture is moved to the next position. This

Content from this work may be used under the terms of the CC BY 3.0 licence (© 2018). Any distribution of this work must maintain attribution to the author(s), title of the work, publisher, and DOI.

ISBN: 978-3-95450-194-6 ISSN: 2226-0366 doi:10.18429/JACoW-LINAC2018-FR1A02

BUNCH LENGTH MEASUREMENTS USING TRANSVERSE DEFLECTING SYSTEMS

M. Hüning†, DESY, Hamburg, Germany

Abstract

Shorter and shorter bunch lengths (some 10 fs) require sophisticated bunch length measurement devices. Free electron lasers - but not only - use transverse deflecting systems. Employing suitable diagnostic tools measurements are not limited to bunch lengths but can be extended to longitudinal profiles and phase-space distributions, and slice emittances. Not only do successfully operated systems aid the commissioning and operation of FELs but they allow control over more sophisticated phase-space manipulations. The design and construction of such systems, actually operated at different RF frequencies, includes cavity design and fabrication, powerful RF systems, low level RF control, beam lines, diagnostics, and data analysis.

INTRODUCTION

Many applications for electron beams require very short bunchlengths in the order of a few 10 fs and below. These applications range from FEL and electron diffraction to experiments towards novel accelerator schemes. Often the electron bunches are created with a considerably longer pulse length and only later they are compressed to their ultimate length. During the acceleration and compression process several non-linear effects can occur. Also coherent effects excited by the short intense bunches may occur. For a well-controlled operation of such accelerators longitudinal beam diagnostics with sufficiently low time resolution is required. Streak cameras which are used for diagnosing bunch lengths in the picosecond range are limited at resolutions of approximately 100 fs [1, 2]. Other diagnostic methods have been developed like spectroscopy of coherent radiation from the beam [3, 4, 5] or electro-optic sampling of the self-field of the beam [6]. Often these measurement techniques suffer from frequency cut-off, resonances or loss of phase information. Furthermore they are limited to diagnosing the current profile only. Another possibility is longitudinal phase space tomography by energy-modulating the bunches, which suffers from an uncomplete rotation in phase-space [7].

A much more straightforward method for measuring the longitudinal phase space is by streaking the original bunches with a transverse deflecting structure [8].

LAYOUT OF TDS BEAM DIAGNOSTICS

The most basic layout of a TDS beam diagnostics system is the combination of a high frequency deflector with a viewscreen after a short drift. By injecting the beam into the deflector at the zerocrossing of the RF the electrons in receive a transverse kick depending on their relative position within the bunch. The beam size on the viewscreen is given by the square sum of the streaked and un-streaked beam size [9]:

$$\sigma_y = \sqrt{\sigma_{y0}^2 + \sigma_{ys}^2},$$

with

$$\sigma_{ys} = \omega\sigma_t \frac{eV_0}{E} \cos\varphi \sqrt{\beta_d \beta_s} \sin\Delta\psi, \quad (1)$$

with ω the angular frequency and V_0 the effective deflecting voltage of the RF and E the beam energy, β_d, β_s the beta function at the deflector and screen, respectively, and $\Delta\psi$ the betatron phase advance between deflector and screen. The RF phase φ is zero at the zerocrossing of the field. The lower limit for the resolution may be defined as the point when the streak equals the natural beam size on the screen. This condition results in the following expression for the minimum achievable resolution [10]

$$\frac{1}{\sigma_{t0}} = \omega \frac{eV_0}{E} \cos\varphi \sqrt{\beta_d/\varepsilon} \sin\Delta\psi. \quad (2)$$

It is interesting to note that the resolution does not depend on the beta function at the location of the screen.

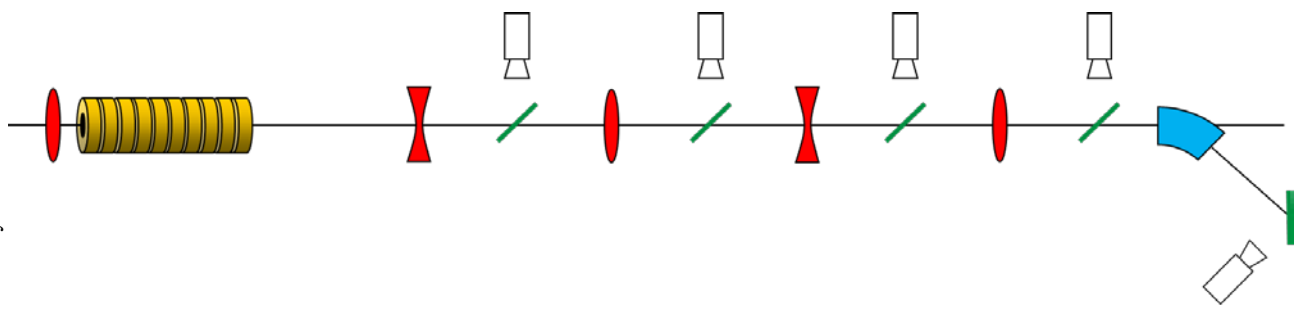


Figure 1: Typical setup of a TDS beam diagnostic system. The minimal system consists of a structure and a viewscreen. A spectrometer magnet allows to image the longitudinal phase-space. A series of screens along a FODO structure serves to measure slice emittances easily.

† markus.huening@desy.de

Content from this work may be used under the terms of the CC BY 3.0 licence (© 2018). Any distribution of this work must maintain attribution to the author(s), title of the work, publisher, and DOI.

ISBN: 978-3-95450-194-6 ISSN: 2226-0366 doi:10.18429/JACoW-LINAC2018-FR1A03

FRONTIERS OF BEAM DIAGNOSTICS IN PLASMA ACCELERATORS*

A. Cianchi†, University of Rome Tor Vergata, 00133 Rome, Italy
D. Alesini, M. P. Anania, M. Bellaveglia, F. Bisesto, M. Castellano, E. Chiadroni
G. Costa, M. Ferrario, F. Filippi, A. Giribono, A. Marocchino, R. Pompili, V. Shpakov,
C. Vaccarezza, F. Villa, INFN-LNF, 00044 Frascati, Italy
A. Mostacci, Sapienza University of Rome, 00185 Rome, Italy

Abstract

Advanced diagnostics tools are crucial in the development of plasma-based accelerators. Accurate measurements of the beam quality at the exit of the plasma channel are mandatory for the optimization of the plasma accelerator. 6D electron beam diagnostics will be reviewed with emphasis on emittance measurement, which is particularly complex due to the peculiarity of the emerging beams.

INTRODUCTION

High energy particles physics has driven for a long time the accelerators to reach higher energy or intensity. However, nowadays accelerators are also widely used in very different fields, covering a huge range of applications, including light sources for medical and industrial applications. Compared to other novel scheme, like high-frequency W-band metallic RF structures [1], dielectric wakefield structures [2] or direct laser acceleration [3], the plasma acceleration offers the highest gradient and compactness. It paves the way to use compact and cost affordable accelerators in universities, medical centers and small laboratories, with a lot of possible applications.

Laser beams (laser wakefield accelerator, LWFA) or charged particle beams (particle wakefield accelerator, PWFA) may be used to excite space-charge oscillations in plasma. They produce both accelerating and focusing fields.

The EuPRAXIA [4] (European Plasma Research Accelerator with eXcellence In Applications) project is expected to be the first Research Infrastructure devoted to establish the scientific and technological basis required to build a compact and cost effective high energy (up to 5 GeV) machine based on plasma accelerator technology.

While there is not yet a final decision about the acceleration scheme to be used, we noticed that in term of beam diagnostics there is not so much difference between different solutions. In all cases the driver must be removed, being a high power laser or an electron beam, because it prevents to put diagnostics downstream of the plasma interaction. In all cases the high beam divergence and large energy spread will force to capture the beam as soon as possible after the plasma stage. So, it is difficult to put diagnostics between the plasma and the capture optics.

In addition to the complications inherent to the plasma acceleration, as driver removal, shot by shot pointing or timing instabilities, large energy spread, there are specific issues about the resolution in measuring the 6D phase space. Time resolution must be in order of few fs, transverse emittance resolution better than 1 mm-mrad, the charge must be discriminate at the level of pC and the trajectory must be known at μm level. Sometimes it is forgiven that if the accelerator must be compact, the diagnostics have to be compact as well, resulting in a complete redesign of even conventional diagnostics.

At the same time in INFN-LNF Frascati a satellite project has been started [5] showing about the same problems in term of beam diagnostics.

This paper, starting from the state of the art, wants to emphasize the peculiarity of the plasma acceleration, and the challenges in measuring such kind of beams, giving also information about our developments still in progress. Longitudinal diagnostics will be the argument of Section I, while we will focus on transverse diagnostics in Section II, giving also more details about our work.

SECTION I:LONGITUDINAL DIAGNOSTICS

In a compact machine a longitudinal compressor is more appealing that a magnetic chicane, due to the shorter path required for its implementation. However, to set the correct compression phase in the velocity bunching and to recover the correlated energy spread induced in this way, a longitudinal diagnostics is mandatory. Longitudinal phase space measurement can be performed with a X-band RF deflector (RFD), i.e a RF cavity with a transverse deflecting mode, combined with a magnetic dipole. While the fs resolution is state-of-the-art for these devices, so far only one X-band RFD is operating, at SLAC [6], for an energy one order of magnitude greater than our case. It means that the design must be reconsidered and particular attention must be put in several details that usually are neglected. For instance the reduced iris aperture and the possibility that the beam goes inside out of the center must be evaluated with simulations. Particular attention must be put also in RF time jitter and the structure temperature stability, tailoring this requirements to the beam energy and the available beam line. As a rule of thumb, for GeV level beam, a temperature stability in the order of tens of mK and time stability in the order of tens of femtoseconds are required.

In a plasma accelerator, especially during the commission phase, a one to one correlation between the longitudinal properties of the beam sent into the plasma and the beam

* Work supported by European Union Horizon 2020 research and innovation program, Grant Agreement No. 653782 (EuPRAXIA)
† alessandro.cianchi@uniroma2.it

Content from this work may be used under the terms of the CC BY 3.0 licence (© 2018). Any distribution of this work must maintain attribution to the author(s), title of the work, publisher, and DOI.

ISBN: 978-3-95450-194-6 ISSN: 2226-0366 doi:10.18429/JACoW-LINAC2018-FR1A05

DEVELOPMENT OF PULSED GAS STRIPPERS FOR INTENSE BEAMS OF HEAVY AND INTERMEDIATE MASS IONS

P. Gerhard*[1], W. Barth[1,2], M. Bevcic[1], Ch. E. Düllmann[1,2,3], L. Groening[1], K. P. Horn[1], E. Jäger[1], J. Khuyagbaatar[1,2], J. Krier[1], M. Maier[1], P. Scharrer[1], A. Yakushev[1]
[1]GSI Helmholtzzentrum für Schwerionenforschung GmbH, 64291 Darmstadt, Germany
[2]Helmholtz-Institut Mainz, 55099 Mainz, Germany
[3]Johannes Gutenberg-Universität Mainz, 55099 Mainz, Germany

Abstract

The GSI UNILAC together with SIS18 will serve as a high current, heavy ion injector for the future FAIR. It has to deliver high beam brilliance at a low duty factor. A modified 1.4 MeV/u gas stripper setup has been developed, aiming at an increased yield into the particular desired charge state. The setup delivers short pulses of high gas density in synchronization with the beam pulse. This provides a higher gas density and at the same time reduces the gas load for the differential pumping system. Different gases as stripping targets were tested for optimum stripping results under operational conditions. Measurements with various isotopes and gas densities were conducted to investigate the stripping properties. High intensity beams of $^{238}U^{4+}$ were successfully stripped and separated using hydrogen as stripping gas. The stripping efficiency into the desired 28+ charge state was significantly increased by up to 60% while the beam quality remained suitable. The new stripper setup and major results achieved during the development are presented, including a comparison to the present gas stripper based on a N_2-gas jet.

During the last tests in 2016 problems with the fast valves arose while they were used at high back pressures for a longer duration for the first time. This triggered another revision of the setup and led to an exchange of the valves. In parallel, the installation of the required infrastructure for regular operation of the gas stripper using hydrogen was planned. These recent developments are reported in the last part.

INTRODUCTION

The UNIversal Linear ACcelerator (UNILAC) will serve as part of the heavy ion injector chain for the Facility for Antiproton and Ion Research (FAIR), currently under construction at GSI, Darmstadt, Germany. The reference projectile for FAIR is the heavy ion ^{238}U [1]. To meet the beam requirements for FAIR, an upgrade program of the UNILAC has been started to increase the delivered beam intensities especially for U. The task is to deliver $\approx 3 \cdot 10^{11}$ U^{28+} ions within 100 µs pulse length and adequate emittance at repetition rates of up to 2.7 Hz to the subsequent heavy ion synchrotron SIS18.

All ion beams for the UNILAC are delivered by three different ion sources in a time sharing mode. For the production of heavy ions like ^{238}U, a Vacuum ARc Ion Source [2] is used, which is one of the two sources located at the high current injector (HSI). The HSI comprises of a Radio Frequency Quadrupole (RFQ) structure and an Interdigital H-(IH-)structure Drift Tube Linac (DTL) [3]. After charge state and isotope separation in the LEBT ions with $A/q \leq 65$ are accelerated to 1.4 MeV/u by the HSI before they enter the gas stripper section (Fig. 1).

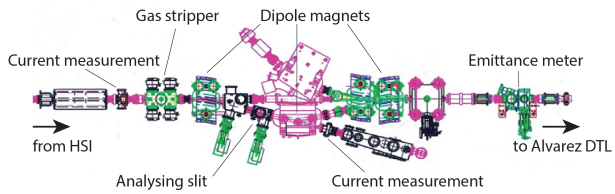


Figure 1: The UNILAC gas stripper section between the high current injector and the Alvarez DTL.

HEAVY ION STRIPPER

After the HSI, a gas stripper is used to increase the charge state of the ions. At this stage, the ions are stripped at an energy of 1.4 MeV/u, so far by a supersonic N_2-jet as a target, created by a Laval nozzle with a back pressure of up to 0.45 MPa [4]. In the gas stripper, the charge state of the ions is increased by charge changing processes occurring in the collisions between beam ions and neutral gas particles. After passing through the gas target, the ion beam is deflected by a fast switchable dipole magnet with a nominal deflection angle of 15°. Thereby the ions are separated according to their charge state, forming multiple beamlets. These are focused onto a charge analysing slit, which only ions having the desired charge state can pass. The remaining beam is then transported by two more fast switchable dipole magnets, matched and injected into the subsequent Alvarez DTL.

To reach the target beam parameters for FAIR injection, a development program for the gas stripper was conducted, aiming at increasing the stripping efficiency, e. g. into the 28+ charge state for uranium. Improving the performance of the gas stripper has proved difficult in the past especially for uranium operation. The main reason was the high gas load for the differential pumping system due to the continuous gas flow of the jet type stripper used [5]. With the existing N_2-jet stripper, the stripping efficiency into the U^{28+} charge state is about 12.7%, and the average charge state of the corresponding distribution is about 26.8 [6].

* p.gerhard@gsi.de

Content from this work may be used under the terms of the CC BY 3.0 licence (© 2018). Any distribution of this work must maintain attribution to the author(s), title of the work, publisher, and DOI.

ISBN: 978-3-95450-194-6 ISSN: 2226-0366 doi:10.18429/JACoW-LINAC2018-FR1A06

PULSE-BY-PULSE BEAM PARAMETER SWITCHING OF HIGH-QUALITY BEAMS FOR MULTI-BEAMLINE OPERATION AT SACLA

H. Maesaka†, T. Fukui, T. Hara, RIKEN SPring-8 Center, 679-5148 Sayo, Hyogo, Japan
N. Hosoda, C. Kondo[1], S. Matsubara, T. Ohshima[1], M. Yamaga, Y. Otake,
Japan Synchrotron Radiation Research Institute 679-5198 Sayo, Hyogo, Japan
T. Hasegawa, O. Morimoto, Y. Tajiri, S. Tanaka, M. Yoshioka,
SPring-8 Service Co., Ltd. 679-5165 Tatsuno, Hyogo, Japan
[1]also at RIKEN SPring-8 Center, 679-5148 Sayo, Hyogo, Japan

Abstract

Since the number of beamlines in a linac-based X-ray free-electron laser (XFEL) facility is limited, it is quite important to increase the machine time for user experiments. In the XFEL facility, SACLA, a new XFEL beamline, BL2, was constructed in addition to the existing beamline, BL3, and a kicker magnet was installed into the beam switchyard to distribute a 60 Hz electron beam to both beamlines one after another. Since a beam energy and an optimum bunch length are usually different for each beamline, we developed a beam route and parameter switching software to change beam parameters pulse-by-pulse. The switching system successfully distributed high quality electron beams to both beamlines and XFEL performance for each beamline was individually optimized. When a high-quality electron beam having less than 1 mm mrad normalized emittance, 10 fs FWHM bunch length, 10 kA peak current, etc. was injected into BL2, however, the XFEL intensity of BL2 was significantly smaller than BL3 due to the growth of the emittance and pointing jitter coming from coherent synchrotron radiation (CSR). Therefore, we rearranged the optics of the transport line to mitigate the CSR effect and the XFEL intensity comparable to BL3 was achieved. We are also developing an on-demand beam route and parameter switching system needed for the beam injection from SACLA to the SPring-8 storage ring. The on-demand system also showed a sufficient performance and it will be used for the user operation in the near future.

INTRODUCTION

Linac-based X-ray free-electron laser (XFEL) facilities were constructed for the past decade or so and they have contributed for various breakthroughs about microscopic phenomena. However, the number beamlines of an XFEL facility is much smaller than a ring-based light source. Therefore, increasing opportunities to use XFEL is quite important to maximize scientific outcomes.

The XFEL facility, SACLA, has been providing brilliant X-ray laser pulses since 2011 in a photon energy region from 4 keV to 20 keV [1]. SACLA mainly consists of a low-emittance thermionic electron gun [2] followed by sub-harmonic accelerators [3], C-band main accelerators up to 8 GeV [4] and XFEL beamlines with in-vacuum undulators, as shown in Fig. 1. The user operation of SACLA started with one XFEL beamline, BL3, with a maximum repetition rate of 60 Hz. An additional XFEL beamline, BL2, was constructed in 2014 to double the user time effectively and a kicker magnet was also installed into the switchyard to switch the beam route pulse-by-pulse [5]. In addition, the SCSS test accelerator [6] was moved to SACLA-BL1 in 2014, the maximum beam energy was upgraded to 0.8 GeV in 2016, and it has been providing soft-XFEL in the photon energy region around 0.1 keV [7]. Thus, SACLA is now providing three XFELs in parallel and the experimental opportunity of SACLA is increased substantially.

Furthermore, SACLA has a beam transport line to the SPring-8 storage ring (XSBT) and the beam injection from SACLA to SPring-8 is planned in the near future. This is because the low-emittance upgrade of the SPring-8 storage ring was proposed [8] and the upgraded ring requires a low-emittance injection beam from SACLA. Therefore, a flexible beam route switching system is necessary to provide electron beams to both XFEL beamlines and the SPring-8 storage ring in parallel.

Since the XFEL photon energy is different for each experimental user, the electron beam energy for each beamline must be changed pulse-by-pulse. In addition, the optimum bunch length is different for each beamline [5], since the optics of each electron beam transport line is significantly different. Therefore, we are developing a flexible rf parameter switching system of each accelerator unit to change the beam parameter pulse-by-pulse.

In fact, we encountered an instability problem that the horizontal emittance and the horizontal pointing stability deteriorated after the dogleg beam transport line of BL2 [5]. Since this instability was suppressed for a longer bunch beam with a lower peak current, the cause of the instability was considered to be a coherent synchrotron radiation (CSR) effect. The rf parameter switching system helped the suppression of the CSR effect by stretching the bunch length for BL2. However, the XFEL intensity of BL2 was significantly smaller than BL3 in case of a longer bunch length. Therefore, an improvement of the optics of the BL2 dogleg part was necessary for the mitigation of the CSR effect to generate XFEL comparable to BL3.

In this article, we describe the design and operation status of the pulse-by-pulse beam route and parameter control system of SACLA. We also discuss the mitigation of the instability due to the CSR effect in the dogleg part of BL2.

† maesaka@spring8.or.jp

Content from this work may be used under the terms of the CC BY 3.0 licence (© 2018). Any distribution of this work must maintain attribution to the author(s), title of the work, publisher, and DOI.

ISBN: 978-3-95450-194-6 ISSN: 2226-0366 doi:10.18429/JACoW-LINAC2018-FR2A02

COMMISSIONING OF THE EUROPEAN XFEL*

D. Nölle†, Deutsches Elektronen-Synchrotron DESY, Hamburg, Germany
on behalf of the European XFEL Commissioning Team

Abstract

The European X-ray Free-Electron Laser (EUROPEAN XFEL) in Hamburg, Northern Germany, was built to produce X-rays in the range from 0.25 up to 25 keV out of three undulators that can be operated simultaneously with up to 27,000 pulses per second. The EUROPEAN XFEL is driven by a 17.5 GeV superconducting linac. This linac is the worldwide largest installation based on superconducting radio-frequency acceleration, using the so-called TESLA technology which was developed for the superconducting version of an international electron positron linear collider. The construction of the European XFEL has been finished at the end of 2016 and commissioning has been started. Meanwhile the entire facility, driving 3 Free-Electron-Lasers in the hard and soft X-ray regime, is in operation. This contribution will report on commissioning and the transition to user operation.

INTRODUCTION

The European XFEL aims at delivering X-rays from 0.25 to up to 25 keV out of three SASE undulators [1, 2]. The FELs are driven by a superconducting linear accelerator based on TESLA technology [3]. The accelerator operates in 10 Hz pulsed mode and can deliver up to 2,700 bunches per RF-pulse. Electron beams can be distributed to three different beamlines within a RF-pulse allowing for simultaneous operation of three FELs.

Construction of the European XFEL started in early 2009. The beam commissioning of the facility began end of 2015 with a ½ year long operation of the injector [4]. End of 2016 the installation of the main linac was ready, and commissioning started with the cool-down of the superconducting accelerator. Now, 23 months after the first beam was injected in the beginning of 2017, the accelerator is operational, all three FELs are lasing and the experimental program has started for one hard X-ray beamline with the experimental stations FXE and SPB [5, 6]. The other two photon beamlines are in the commissioning process, and will start operation within a few months.

FACILITY LAYOUT

The complete facility is constructed underground, in a 5.2 m diameter tunnel about 25 to 6 m below the surface level and fully immersed in the ground water. The 50 m long injector is installed at the lowest level of a 7 stories underground building whose downstream end also serves as the entry shaft to the main linac tunnel. Next access to the tunnel is only about 2 km downstream, at the bifurcation point into the beam distribution lines. The beam distribution provides space for in total 5 undulators - 3 being initially installed. Each undulator is feeding a separate beamline so that a fan of 5 almost parallel tunnels, separated each by about 17 m, enters the experimental hall located 3.3 km away from the electron source. The schematic layout of the accelerator is shown in Fig. 1.

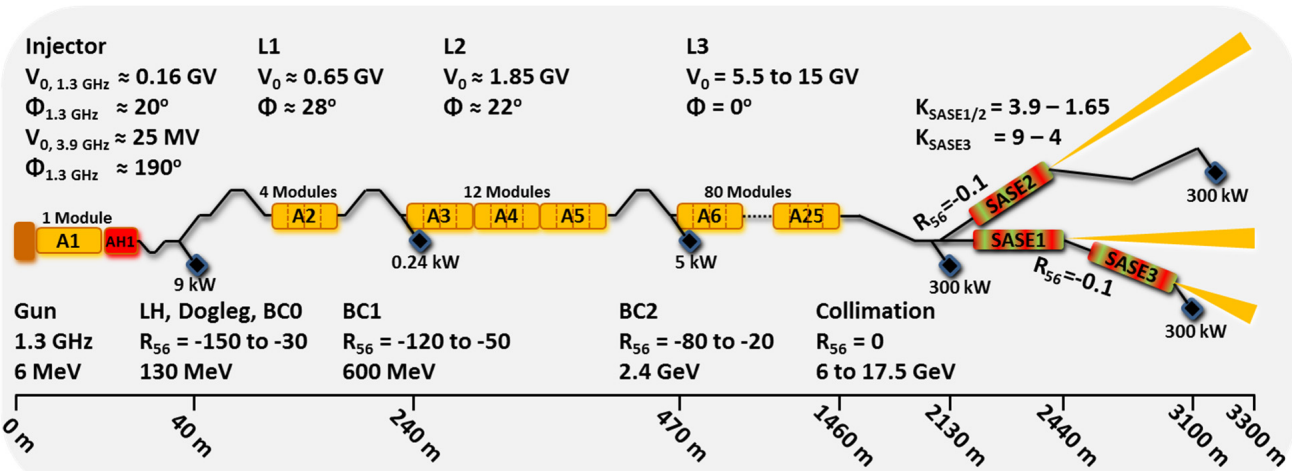


Figure 1: Schematic overview of the European XFEL accelerator. Single RF stations are named A*n* and feed either one module (A1) or 4 modules (A2-A25). R_{56} ranges for the bunch compressors are given in mm, and the phases of the different linac sections refer to typical compression set-ups. The maximum allowed beam power of the three commissioning dumps after the injector and the 2nd and 3rd bunch compressor (BC1 and BC2) as well as of the main dumps after the linac and each beam distribution line is given.

* Work supported by the respective funding agencies of the contributing institutes; for details please see http:\\www.xfel.eu
† dirk.noelle@desy.de

Content from this work may be used under the terms of the CC BY 3.0 licence (© 2018). Any distribution of this work must maintain attribution to the author(s), title of the work, publisher, and DOI.